

Volume 131 No. 6 Pp. 1199–1373

ANESTHESIOLOGY

DECEMBER 2019

ANESTHESIOLOGY

2019
December

Trusted Evidence: Discovery to Practice™

Population Pharmacokinetics of Propofol and Sevoflurane

Volume 131
Number 6
anesthesiology.org

The Journal of the American Society of Anesthesiologists, Inc.

Stay Ahead of Hypotension

with the Acumen Software Suite for Predictive Decision Support

Smart. Innovation.



Acumen Hypotension Prediction Index (HPI) Software

See whether your patient is trending toward a hypotensive event.*

Acumen Analytics Software

Retrospectively view and analyze hypotension duration, frequency, and severity.



Downloaded from /anesthesiology/issue/131/6 by guest on 16 April 2024

Learn more at [Edwards.com/Acumen](https://www.edwards.com/Acumen)

*A hypotensive event is defined as MAP <65 mmHg for a duration of at least one minute.

CAUTION: Federal (United States) law restricts this device to sale by or on the order of a physician. See instructions for use for full prescribing information, including indications, contraindications, warnings, precautions, and adverse events.

Edwards, Edwards Lifesciences, the stylized E logo, Acumen, Acumen Analytics, Acumen HPI, Acumen IQ, HemoSphere, HPI, and Hypotension Prediction Index are trademarks of Edwards Lifesciences Corporation or its affiliates. All other trademarks are the property of their respective owners.

© 2019 Edwards Lifesciences Corporation. All rights reserved. PP--US-4190 v1.0

Edwards Lifesciences • One Edwards Way, Irvine CA 92614 USA • [edwards.com](https://www.edwards.com)



NACOR: Where Data Becomes Value

KNOW EXACTLY WHERE YOU STAND AMONG YOUR PEERS

Get the evidence you need to move ahead in today's competitive environment. AQI's NACOR® registry helps you identify strengths and opportunities to improve patient safety across a wide range of clinical and administrative metrics. Don't enter another negotiation without NACOR.

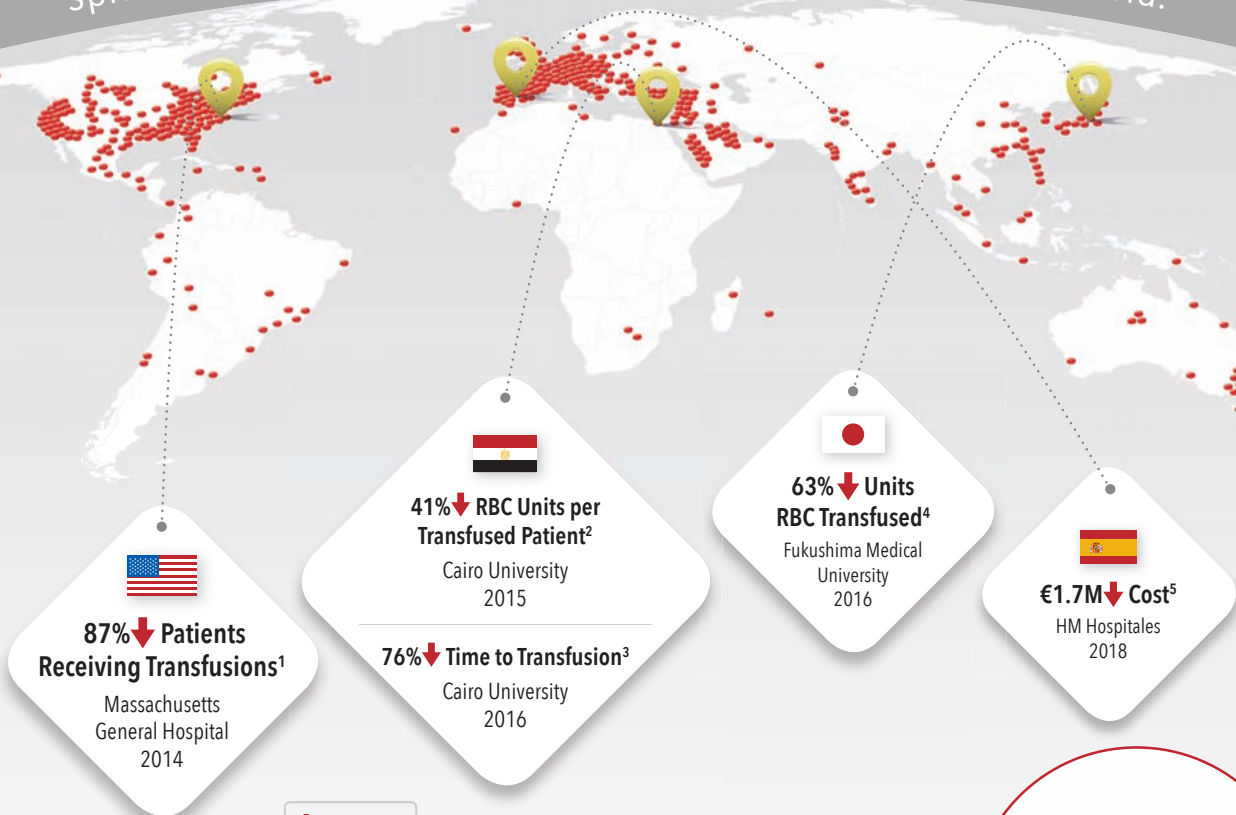
Get started now
asahq.org/improvement



Are You Improving Outcomes with SpHb®?

Five studies across four continents have found that noninvasive and continuous hemoglobin (SpHb) monitoring can help improve outcomes¹⁻⁵

SpHb is supporting clinicians in over 75 countries around the world.*



Improve Your Outcomes with SpHb

Visit www.masimo.com/sphb



Caution: Federal (USA) law restricts this device to sale by or on the order of a physician. See instructions for use for full prescribing information, including indications, contraindications, warnings, and precautions.

Clinical decisions regarding red blood cell transfusions should be based on the clinician's judgment considering among other factors: patient condition, continuous SpHb monitoring, and laboratory diagnostic tests using blood samples. SpHb monitoring is not intended to replace laboratory blood testing. Blood samples should be analyzed by laboratory instruments prior to clinical decision making.

¹Ehrenfeld et al. *J Blood Disorders Transf.* 2014. 5:9. ²Awada WN et al. *J Clin Monit Comput.* DOI 10.1007/s10877-015-9660-4. Study Protocol: In each group, if researchers noted SpHb trended downward below 10 g/dL, a red blood cell transfusion was started and continued until SpHb trended upward above 10 g/dL. The transfusion threshold of 10 g/dL was predetermined by the study protocol and may not be appropriate for all patients. Blood sampling was the same for the control and test group. Arterial blood was drawn from a 20 gauge radial artery cannula into 2 mL EDTA collection tubes, mixed and sent for analysis by a Coulter GEN-S Hematology Analyzer. ³Kamal A, et al. *Open J of Anesth.* 2016 Mar; 6, 13-19. ⁴Imaizumi et al. *Proceedings from the 16th World Congress of Anaesthesiologists*, Hong Kong. Abstract #PR607. ⁵Ribed-Sánchez B, et al. *Sensors* (Basel). 2018 Apr 27;18(5). pii: E1367. Estimated national savings derived from hospital savings extrapolated nationwide. * Data on file.

THIS MONTH IN ANESTHESIOLOGY



1223 Population Pharmacodynamics of Propofol and Sevoflurane in Healthy Volunteers Using a Clinical Score and the Patient State Index: A Crossover Study

Hypnotic drug effects can be assessed as the presence or absence of standard clinical endpoints, such as response to calling the person by name and tolerance to shake and shout. Antinociceptive drug effects can be assessed as the presence or absence of tolerance to tetanic stimulus. The Patient State Index is a processed, electroencephalographic-derived index that is considered by some to be a drug-independent representation of the depth of sedation and anesthesia. A four-period randomized sequence crossover study determined the concentration-effect relationships for both propofol and sevoflurane, both with and without remifentanyl coadministration, with effects measured as tolerance to standard stimuli and by the Patient State Index. The sevoflurane Patient State Index values associated with a 50% probability of tolerance to the standard stimuli were higher than those for propofol. Adding a $2 \text{ ng} \cdot \text{ml}^{-1}$ predicted effect-site remifentanyl concentration increased all Patient State Index values associated with a 50% probability of tolerance to the standard stimuli but $4 \text{ ng} \cdot \text{ml}^{-1}$ produced additional effects only during propofol administration. See the accompanying Editorial View on [page 1199](#). (Summary: M. J. Avram. Photo: J. P. Rathmell. Illustration: S. M. Jarret, M.F.A., C.M.I.)



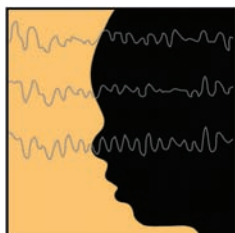
1254 Peripheral Nerve Blocks for Ambulatory Shoulder Surgery: A Population-based Cohort Study of Outcomes and Resource Utilization

Recent systematic reviews suggest that nerve blocks provide the highest degree of acute postoperative pain relief in ambulatory shoulder surgery patients. This retrospective study examined the association between nerve blocks and health system outcomes after ambulatory shoulder surgery by testing the hypothesis that receipt of a nerve block would reduce the odds of unplanned day of surgery admissions, emergency department visits, hospital readmissions, or deaths within 7 days of surgery (combined as a composite primary outcome). In the total cohort, 6,234 of 59,644 patients (10.4%) experienced the primary outcome; no patients died in the 30 days after surgery. Of the 31,073 patients with a nerve block, 2,808 (9.0%) had an admission, readmission, or emergency department visit within 7 days of surgery compared to 3,424 of the 28,571 patients (12.0%) without a nerve block (unadjusted odds ratio 0.73; 95% CI, 0.69 to 0.77). After multilevel, multivariable adjustment, no significant difference remained (odds ratio 0.96; 95% CI, 0.89 to 1.03). See the accompanying Editorial View on [page 1205](#). (Summary: M. J. Avram. Image: J. P. Rathmell.)



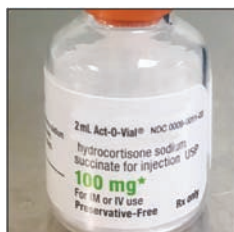
1316 Superior Trunk Block Provides Noninferior Analgesia Compared with Interscalene Brachial Plexus Block in Arthroscopic Shoulder Surgery

The conventional ultrasound-guided interscalene brachial plexus block provides highly effective postoperative analgesia after arthroscopic shoulder surgery but almost always produces hemidiaphragmatic paresis. A randomized, double-blinded, noninferiority clinical trial tested the hypothesis that superior trunk block would provide postoperative analgesia that is noninferior to that provided by interscalene brachial plexus block while reducing hemidiaphragmatic paresis in 78 patients undergoing arthroscopic shoulder surgery. The mean pain score at 24 h postoperatively was 1.4 ± 1.0 (mean \pm SD) and 1.2 ± 1.0 in the superior trunk block and interscalene block groups, respectively. The mean difference in pain scores was 0.1 (95% CI, -0.3 to 0.6). As the upper limit of the 95% CI was less than the prespecified noninferiority margin ($\delta = 1$), noninferiority was established. Twenty-nine patients (72.5%) in the interscalene block group and 2 (5.3%) in the superior trunk block group had complete hemidiaphragmatic paresis. Ten patients (25%) in the interscalene block group and 27 (71.1%) in the superior trunk block group had partial hemidiaphragmatic paresis. See the accompanying Editorial View on [page 1207](#). (Summary: M. J. Avram. Image: J. P. Rathmell.)



1239 δ -Oscillation Correlates of Anesthesia-induced Unconsciousness in Large-scale Brain Networks of Human Infants

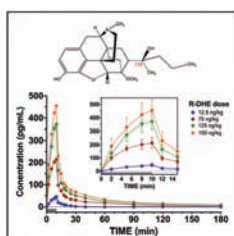
Differences in functional brain connectivity have been observed during general anesthesia and at different stages of brain development. Deeper stages of anesthesia in adults are characterized by reduced functional connectivity in higher-order brain networks, such as the default mode network and the frontoparietal network. Overall, α -oscillation functional connectivity in the anesthetized adult brain is less globally efficient and more segregated due to attenuated connectivity between higher-order networks. The hypothesis that infant brain networks during maintenance of general anesthesia would display less complex and more fragmented connectivity was tested using continuous multichannel electroencephalograph recordings collected during maintenance of anesthesia and at emergence in 20 subjects ages 0 to 3.9 months. Electroencephalograph functional connectivity was determined retrospectively using cross-spectral coherence between sensor signals or region of interest source reconstructed signals. Infant general anesthesia is potentially driven: by connectivity changes in key default mode network and frontoparietal regions; associated with more segregation (increase in δ -oscillation modularity); and related to reduction in δ -oscillation complexity at both the sensor and source levels. See the accompanying Editorial View on [page 1202](#). (Summary: M. J. Avram. Image: J. P. Rathmell.)



1292 Hydrocortisone Compared with Placebo in Patients with Septic Shock Satisfying the Sepsis-3 Diagnostic Criteria and APROCCHSS Study Inclusion Criteria: A *Post Hoc* Analysis of the ADRENAL Trial

Two recent large randomized controlled trials of the use of corticosteroids in patients with septic shock, the Adjunctive Glucocorticoid Therapy in Patients with Septic Shock (ADRENAL) trial and the Activated Protein C and Corticosteroids for Human Septic Shock (APROCCHSS) trial, reported different treatment effects on 90-day mortality. Although both trials enrolled patients who met the criteria for septic shock using Sepsis-2 definitions, the APROCCHSS trial used greater severity of shock as an inclusion criterion and reported improved 90-day mortality in the steroid group. The ADRENAL trial reported no difference in 90-day mortality between groups. The hypothesis that hydrocortisone may have beneficial effects on mortality in the sicker cohort of patients was tested by conducting *post hoc* subgroup analyses of the ADRENAL trial.

In ADRENAL trial participants who fulfilled either an updated consensus definition of sepsis and septic shock, termed Sepsis-3, or the APROCCHSS inclusion criteria, a continuous infusion of hydrocortisone did not result in a significantly lower 90-day mortality than placebo in septic shock. (Summary: M. J. Avram. Image: J. P. Rathmell.)



1327 Analgesic and Respiratory Depressant Effects of R-dihydroetorphine: A Pharmacokinetic–Pharmacodynamic Analysis in Healthy Male Volunteers

Opioid agonists acting at the nociception/orphanin FQ, δ -opioid, and κ -opioid receptors may counteract respiratory depression induced by activation of the μ -opioid receptor. R-dihydroetorphine is an opioid with full agonism and high affinity for the μ -opioid, κ -opioid, and δ -opioid receptors and low affinity for the nociception/orphanin FQ receptor. The hypothesis that, given its receptor profile, R-dihydroetorphine would produce an apparent plateau in respiratory depression but not in antinociception was tested by determining the effects of four R-dihydroetorphine doses (12.5, 75, 125, and 150 ng/kg) on isohypercapnic ventilation and antinociception in 40 healthy male volunteers. Over the dose range tested, an apparent maximum in respiratory depression to

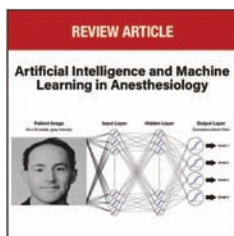
33% of baseline ventilation was identified but a maximum in antinociception was not reached. At an R-dihydroetorphine effect-site concentration of 20 pg/ml, the probability of analgesia was 60%, while the probability of analgesia without respiratory depression was 45%. The probability of analgesia increased to 95% at 100 pg/ml, but the probability of analgesia without respiratory depression was reduced to 20%. (Summary: M. J. Avram. Image: From original article.)



1276 Drug-selective Anesthetic Insensitivity of Zebrafish Lacking γ -Aminobutyric Acid Type A Receptor $\beta 3$ Subunits

Studies in transgenic mice indicate major actions of etomidate, propofol, and pentobarbital are mediated by a subset of γ -aminobutyric acid type A (GABA_A) receptor isoforms containing $\beta 3$ subunits. Compared to wild-type mice, global $\beta 3$ knockout ($\beta 3^{-/-}$) mice are resistant to the sedative-hypnotic effects of etomidate and propofol, but have unchanged sensitivity to pentobarbital and ethanol. Zebrafish larvae represent another vertebrate species for assessing the role of $\beta 3$ -containing GABA_A receptors in anesthetic mechanisms. To test the hypothesis that global $\beta 3^{-/-}$ zebrafish would have a pattern of anesthetic sensitivities similar to those of global $\beta 3^{-/-}$ mice, the effects of nine drugs, each at seven or more concentrations, were assessed in up to 18 animals per

condition, in both wild-type and $\beta 3^{-/-}$ zebrafish. The drug sensitivity profile of $\beta 3^{-/-}$ zebrafish larvae more closely resembled that of homozygous $\beta 3N265M$ knock-in mice than of $\beta 3^{-/-}$ mice. Compared to their wild-type controls, both $\beta 3^{-/-}$ zebrafish and $\beta 3N265M$ mice had reduced sensitivities to etomidate, propofol, and pentobarbital, but similar sensitivity to alphaxalone. The only notable difference among drug sensitivities was for ethanol. (Summary: M. J. Avram. Image: ©gettyimages.)



1346 Artificial Intelligence and Machine Learning in Anesthesiology (Review Article)

The present review introduces the theory underlying classical and modern approaches to artificial intelligence and machine learning and surveys current empirical and clinical areas to which these techniques are being applied. Basic concepts of artificial intelligence and machine learning are introduced incrementally. Creating a classical artificial intelligence algorithm begins by defining a set of possible solutions that the algorithm can produce using what is known about the problem, proceeds to progressively evaluating and searching possible solutions trying to find the optimal one, then the algorithm is terminated and a result presented. Logistic regression is a powerful machine-learning technique that fits a weighted linear combination of physiologic variables to an

outcome. Augmented linear regression allows certain nonlinear relationships between outcomes and physiologic variables to be discerned, even in the absence of a defined physiologic model. Neural networks provide a mechanism to establish a relationship between input variables and an output without defining a logical representation of the problem or defining transformations of the inputs in advance. (Summary: M. J. Avram. Image: From original article.)

TABLE OF CONTENTS

ANESTHESIOLOGY

◇ This Month in ANESTHESIOLOGY	1A
Science, Medicine, and the Anesthesiologist.....	13A
Infographics in Anesthesiology	17A
◆ Editorial Views	

The Art of General Anesthesia: Juggling in a Multidimensional Space
J. W. Sleight.....1199

Are There Common Network-level Correlates of the Anesthetized Brain in Infants and Adults?
M. P. Puglia, G. A. Mashour1202

Regional Anesthesia: A Silver Bullet, Red Herring, or Neither?
E. C. Sun, S. G. Memtsoudis, E. R. Mariano1205

Aiming to Refine the Interscalene Block: Another Bullseye or Missing the Mark?
N. M. Elkassabany, E. R. Mariano.....1207

Special Article

Etymology of *Letheon*: Nineteenth-century Linguistic Effervescence
R. P. Haridas, M. Gionfriddo, G. S. Bause.....1210

In 1846, William T. G. Morton chose *Letheon* as a commercial name for his preparation containing sulfuric ether. The adjective *Lethean* may have influenced the coinage of the name.

Perioperative Medicine

CLINICAL SCIENCE

◆ ◆ ◆ Population Pharmacodynamics of Propofol and Sevoflurane in Healthy Volunteers Using a Clinical Score and the Patient State Index: A Crossover Study

M. H. Kuizenga, P. J. Collin, K. M. E. M. Reyntjens, D. J. Touw, H. Nalbat, F. H. Knotnerus, H. E. M. Vereecke, M. M. R. F. Struys1223

A four-period randomized sequence crossover study determined the concentration–effect relationships for both propofol and sevoflurane, both with and without remifentanyl coadministration, with effects measured as tolerance to standard stimuli and by the Patient State Index. The sevoflurane Patient State Index values associated with a 50% probability of tolerance to the standard stimuli were higher for than those for propofol. Adding a 2 ng · ml⁻¹ predicted effect-site remifentanyl concentration increased all Patient State Index values associated with a 50% probability of tolerance to the standard stimuli, but 4 ng · ml⁻¹ produced additional effects only during propofol administration.

◆ ◆ ◆ δ-Oscillation Correlates of Anesthesia-induced Unconsciousness in Large-scale Brain Networks of Human Infants

I. Pappas, L. Cornelissen, D. K. Menon, C. B. Berde, E. A. Stamatakis1239

In infants younger than four months, slow-wave functional connectivity breaks down during general anesthesia and brain networks are less integrated. Functional disconnections in the cortex might be a common marker of anesthesia-induced unconsciousness in infants and adults.

◆ ◆ ◆ Peripheral Nerve Blocks for Ambulatory Shoulder Surgery: A Population-based Cohort Study of Outcomes and Resource Utilization

G. M. Hamilton, R. Ramlogan, A. Lui, C. J. L. McCartney, F. Abdallah, J. McVicar, D. I. McIsaac1254

Peripheral nerve blocks are associated with a decrease in unplanned admissions after ambulatory shoulder surgery. There is no associated improvement in other postoperative outcomes such as emergency department visits, readmissions, mortality, or costs.

◆ Refers to This Month in ANESTHESIOLOGY

◆ Refers to Editorial Views

 This article has an Audio Podcast

 See Supplemental Digital Content

 CME Article

 This article has a Video Abstract

 Part of the Letheon writing competition

 This article has a Visual Abstract

 Readers' Toolbox



ON THE COVER: It remains unclear how to quantitatively compare the pharmacodynamics of propofol and sevoflurane in the absence or presence of opioids during anesthesia. In this issue of ANESTHESIOLOGY, Kuizenga *et al.* assessed the population pharmacodynamics of propofol and sevoflurane with or without opioids in healthy volunteers. In an accompanying Editorial View, Sleight puts the new findings into the context of clinical practice where anesthesiologists commonly—and effectively—use more complex combinations of volatile agent, opioid, and infusions of propofol, dexmedetomidine, lidocaine, or ketamine. Cover photo: J. P. Rathmell. Cover illustration: S. M. Jarret, M.F.A., C.M.I.

- Kuizenga *et al.*: Population Pharmacodynamics of Propofol and Sevoflurane in Healthy Volunteers Using a Clinical Score and the Patient State Index: A Crossover Study, p. 1223
- Sleight: The Art of General Anesthesia: Juggling in a Multidimensional Space, p. 1199

Next Generation SedLine® Brain Function Monitoring and O3® Regional Oximetry

Available Together on the Root® Platform



Root with Next Generation SedLine and O3 provides a more complete picture of the brain through an instantly interpretable and adaptable display.

- > Next Generation SedLine helps clinicians monitor the state of the brain under anesthesia with an enhanced signal processing engine and four leads of bilateral EEG
- > O3 helps clinicians monitor cerebral oxygenation in situations where pulse oximetry alone may not be fully indicative of the oxygen in the brain

www.masimo.com/O3

© 2019 Masimo. All rights reserved.

Caution: Federal (USA) law restricts this device to sale by or on the order of a physician. See instructions for use for full prescribing information, including indications, contraindications, warnings, and precautions.



An Automated Software Application Reduces Controlled Substance Discrepancies in Perioperative Areas

N. Shah, A. Sinha, A. Thompson, K. Tremper, A. Meka,
S. Kheterpal1264

In a large number of patients studied, a software application that tracks perioperative controlled substance use that is integrated into the electronic health and pharmacy records and database systems is associated with a decrease in management errors.

BASIC SCIENCE

Drug-selective Anesthetic Insensitivity of Zebrafish Lacking γ -Aminobutyric Acid Type A Receptor $\beta 3$ Subunits

X. Yang, Y. Jounaidi, K. Mukherjee, R. J. Fantasia, E. C. Liao,
B. Yu, S. A. Forman1276

Zebrafish larvae lacking functional $\beta 3$ subunits of the γ -aminobutyric acid type A (GABA_A) receptor displayed selective insensitivity to the same anesthetic drugs (etomidate, propofol, and pentobarbital) as transgenic mice with mutated GABA_A receptor $\beta 3$ subunits. These experiments indicate phylogenetic conservation of $\beta 3$ subunit-containing GABA_A receptors between zebrafish and mice in mediating hypnotic and sedative components of general anesthesia. These observations also suggest that zebrafish can be a valuable experimental model for mechanisms of anesthesia research.

Critical Care Medicine

CLINICAL SCIENCE

Hydrocortisone Compared with Placebo in Patients with Septic Shock Satisfying the Sepsis-3 Diagnostic Criteria and APROCCHSS Study Inclusion Criteria: A Post Hoc Analysis of the ADRENAL Trial

B. Venkatesh, S. Finfer, J. Cohen, D. Rajbhandari, Y. Arabi,
R. Bellomo, L. Billot, P. Glass, C. Joyce, Q. Li, C. McArthur,
A. Perner, A. Rhodes, K. Thompson, S. Webb, J. Myburgh1292

In a *post hoc* analysis of the Adjunctive Glucocorticoid Therapy in Patients with Septic Shock (ADRENAL) trial, in participants who fulfilled either the Sepsis-3 or -2 inclusion criteria or those with severe septic shock, a continuous infusion of hydrocortisone did not result in a lower 90-day mortality than placebo.

BASIC SCIENCE

Sevoflurane Promotes Bactericidal Properties of Macrophages through Enhanced Inducible Nitric Oxide Synthase Expression in Male Mice

T. J. Gerber, V. C. O. Fehr, S. D. S. Oliveira, G. Hu, R. Dull,
M. G. Bonini, B. Beck-Schimmer, R. D. Minshall1301

In a lipopolysaccharide model of inflammation, sevoflurane increased mouse macrophage nitric oxide synthase activity and bacteria phagocytosis *in vitro* and *in vivo*. These effects were abolished by pharmacologically inhibiting nitric oxide synthase expression. In endotoxemia in mice, sevoflurane had bactericidal effects.

Pain Medicine

CLINICAL SCIENCE

Superior Trunk Block Provides Noninferior Analgesia Compared with Interscalene Brachial Plexus Block in Arthroscopic Shoulder Surgery

R. Kang, J. S. Jeong, K. J. Chin, J. C. Yoo, J. H. Lee,
S. J. Choi, M. S. Gwak, T. S. Hahm, J. S. Ko1316

When interscalene block was compared with superior trunk block, less frequent hemidiaphragmatic paralysis was seen in the superior trunk block group. Superior trunk block was noninferior to interscalene block in terms of pain scores for up to 24 h postoperatively, and superior trunk block patients were no less satisfied.

Analgesic and Respiratory Depressant Effects of R-dihydroetorphine: A Pharmacokinetic–Pharmacodynamic Analysis in Healthy Male Volunteers

E. Olofson, M. Boom, E. Sarton, M. van Velzen, P. Baily,
K. J. Smith, A. Oksche, A. Dahan, M. Niesters1327

The effects of four R-dihydroetorphine doses (12.5, 75, 125, and 150 ng/kg) on isohypercapnic ventilation and antinociception were studied in 40 healthy male volunteers. Over the dose range tested, an apparent maximum in respiratory depression to 33% of baseline ventilation was identified, but a maximum in antinociception was not reached. At an R-dihydroetorphine effect-site concentration of 20 pg/ml, the probability of analgesia was 60%, while the probability of analgesia without respiratory depression was 45%. The probability of analgesia increased to 95% at 100 pg/ml, but the probability of analgesia without respiratory depression was reduced to 20%.

Education

IMAGES IN ANESTHESIOLOGY

Holodiastolic Flow Reversal in Descending Aorta with Right Coronary Artery to Coronary Sinus Fistula

Z. Merchant, A. Alfievic1340

Spinal Epidural Hematoma after Interlaminar Cervical Epidural Steroid Injection

R. K. Banik, C. C. Chen Chen1342

Drug Label Ribbons to Improve Patient Safety in Low-resource Environments

M. Prin, C. E. Algeo, L. Kalonga, C. Mkwesalamba1344

Seeing Double: The Clinical Conundrum of the Double-barrel Coronary Sinus

S. J. Hankins1345

ASA + YOUR EDUCATION

Provide more effective treatment, improve patient outcomes and implement cost-effective practices with ASA best-sellers and complimentary courses – developed and extensively vetted by practicing physician anesthesiologists.

Start earning your credits today!



Choose from more than 150 courses conveniently suited to your learning style, including:

ACE ●

SEE ●

Safe Sedation Training – Moderate (SSTmoderate) ●

ANESTHESIOLOGY Annual Meeting OnDemand ●

PRACTICE MANAGEMENT™ OnDemand ●

Anesthesia SimSTAT ●●●

Fundamentals of Patient Safety 2018 ●●

Patient Safety Highlights ●

Patient Safety Modules ●

Understanding the Relationship between Intraoperative Hypotension and Clinical Outcomes in Surgical Patients ●

NMB Reversal with Sugammadex ●

ASA best-seller ●

Meets ABA MOCA 2.0® Part 2 Patient Safety Requirements ●

Meets ABA MOCA 2.0® Part 4 Requirements ●

Maintenance of Certification in Anesthesiology Program® and MOCA® are registered certification marks of The American Board of Anesthesiology®

MOCA 2.0® is a trademark of The American Board of Anesthesiology.



American Society of
Anesthesiologists™

Advance your knowledge
asahq.org/education

REVIEW ARTICLE

- ◇ **Artificial Intelligence and Machine Learning in Anesthesiology**
C. W. Connor 1346

Anesthesiologists synthesize data from disparate sources, of varying precision and prognostic value, making life-critical decisions under time pressure. This review describes the evolution of artificial intelligence and machine learning through application to this challenging environment.

MIND TO MIND

-  **So Many**
M. Dowd 1360

- Ganesh Furtado, M.D., ... My Cat**
I. F. Furtado, G. Furtado 1362

Correspondence

- Preload Dependence and Microcirculation Relationship: Comment**
J. Bakker, G. Hernandez 1366

- Preload Dependence and Microcirculation Relationship: Reply**
J. Duranteau 1367

- IV Fluids for Major Surgery: Comment**
H. Bahlmann, R. G. Hahn 1367

- IV Fluids for Major Surgery: Reply**
P. S. Myles, T. E. Miller 1368

Acknowledgment 1370

Erratum 1373

Careers & Events 19A

INSTRUCTIONS FOR AUTHORS

The most recently updated version of the Instructions for Authors is available at www.anesthesiology.org. Please refer to the Instructions for the preparation of any material for submission to ANESTHESIOLOGY.

Manuscripts submitted for consideration for publication must be submitted in electronic format. The preferred method is via the Journal's Web site (<http://www.anesthesiology.org>). Detailed directions for submissions and the most recent version of the Instructions for Authors can be found on the Web site (<http://www.anesthesiology.org>). Books and educational materials should be sent to Alan Jay Schwartz, M.D., M.S.Ed., Director of Education, Department of Anesthesiology and Critical Care Medicine, The

Children's Hospital of Philadelphia, 34th Street and Civic Center Blvd., Room 9327, Philadelphia, Pennsylvania 19104-4399. Article-specific permission requests are managed with Copyright Clearance Center's Rightslink service. Information can be accessed directly from articles on the journal Web site. More information is available at <http://anesthesiology.pubs.asahq.org/public/rightsandpermissions.aspx>. For questions about the Rightslink service, e-mail customer care@copyright.com or call 877-622-5543 (U.S. only) or 978-777-9929. Advertising and related correspondence should be addressed to Advertising Manager, ANESTHESIOLOGY, Wolters Kluwer Health, Inc., Two Commerce Square, 2001 Market Street, Philadelphia, Pennsylvania 19103 (Web site: <http://www.wkcenter.com>). Publication of an advertisement in ANESTHESIOLOGY does not constitute endorsement by the Society or Wolters Kluwer Health, Inc. of the product or service described therein or of any representations made by the advertiser with respect to the product or service.

ANESTHESIOLOGY (ISSN 0003-3022) is published monthly by Wolters Kluwer Health, Inc., 14700 Citicorp Drive, Bldg 3, Hagerstown, MD 21742. Business office: Two Commerce Square, 2001 Market Street, Philadelphia, PA 19103. Periodicals postage paid at Hagerstown, MD, and at additional mailing offices. Copyright © 2019, the American Society of Anesthesiologists, Inc. All Rights Reserved.

Annual Subscription Rates: *United States*—\$977 Individual, \$2249 Institution, \$393 In-training. *Rest of World*—\$1030 Individual, \$2497 Institution, \$393 In-training. Single copy rate \$230. Subscriptions outside of North America must add \$56 for airfreight delivery. Add state sales tax, where applicable. The GST tax of 7% must be added to all orders shipped to Canada (Wolters Kluwer Health, Inc.'s GST Identification #895524239, Publications Mail Agreement #1119672). Indicate in-training status and name of institution. Institution rates apply to libraries, hospitals, corporations, and partnerships of three or more individuals. Subscription prices outside the United States must be prepaid. Prices subject to change without notice. Subscriptions will begin with currently available issue unless otherwise requested. Visit us online at www.lww.com.

Individual and in-training subscription rates include print and access to the online version. Online-only subscriptions for individuals (\$323) and persons in training (\$323) are available to nonmembers and may be ordered by downloading a copy of the Online Subscription FAXback Form from the Web site, completing the information requested, and faxing the completed form to 301-223-2400. Institutional rates are for print only; online subscriptions are available via Ovid. Institutions can choose to purchase a print and online subscription together for a discounted rate. Institutions that wish to purchase a print subscription, please contact Wolters Kluwer Health, Inc., 14700 Citicorp Drive, Bldg 3, Hagerstown, MD 21742; phone: 800-638-3030; fax: 301-223-2400. Institutions

that wish to purchase an online subscription or online with print, please contact the Ovid Regional Sales Office near you or visit www.ovid.com/site/index.jsp and select Contact and Locations.

Address for non-member subscription information, orders, or change of address (except Japan): Wolters Kluwer Health, Inc., 14700 Citicorp Drive, Bldg 3, Hagerstown, MD 21742; phone: 800-638-3030; fax: 301-223-2400. In Japan, contact Wolters Kluwer Health Japan Co., Ltd., Foreca Mita Building 5th floor, 1-3-31 Mita Minato-ku, Tokyo, Japan 108-0073; phone: +81 3 5427 1969; e-mail: journal@wkjapan.co.jp.

Address for member subscription information, orders, or change of address: Members of the American Society of Anesthesiologists receive the print and online journal with their membership. To become a member or provide a change of address, please contact the American Society of Anesthesiologists, 1061 American Lane, Schaumburg, Illinois 60173-4973; phone: 847-825-5586; fax: 847-825-1692; e-mail: membership@ASAhq.org. For all other membership inquiries, contact Wolters Kluwer Health, Inc., Customer Service Department, P.O. Box 1610, Hagerstown, MD 21740; phone: 800-638-3030; fax: 301-223-2400.

Postmaster: Send address changes to ANESTHESIOLOGY, P.O. BOX 1610, Hagerstown, MD 21740.

Advertising: Please contact Hilary Druker, Advertising Field Sales Representative, Health Learning, Research & Practice, Medical Journals, Wolters Kluwer Health, Inc.; phone: 609-304-9187; e-mail: Hilary.Druker@wolterskluwer.com. For classified advertising: Dave Wiegand, Recruitment Advertising Representative, Wolters Kluwer Health, Inc., Two Commerce Square, 2001 Market Street, Philadelphia, PA 19103; phone: 847-361-6128; e-mail: Dave.Wiegand@wolterskluwer.com.

ASA + YOU



ASA + YOUR MEMBERSHIP

5 Important Reasons to Renew Today!

- 1 Every information-packed issue of *ASA Monitor*® and *Anesthesiology*®, the specialty's highest-rated peer-reviewed journal.
- 2 Powerful advocacy protecting physician-led team-based care, developing solutions for surprise medical bills and defeating state-level bills that could negatively impact patient care.
- 3 Complimentary credit-bearing education and deep savings on courses, events and other member-only benefits.
- 4 Resources and opportunities that develop your skills and advance your career through every stage.
- 5 **Your membership expires at midnight on December 31. Don't miss a thing in 2020!**

ANESTHESIOLOGY

Trusted Evidence: Discovery to Practice™

The Journal of the American Society of Anesthesiologists, Inc. anesthesiology.org

Mission: Promoting scientific discovery and knowledge in perioperative, critical care, and pain medicine to advance patient care.

EDITOR-IN-CHIEF

Evan D. Kharasch, M.D., Ph.D.
Editor-in-Chief, ANESTHESIOLOGY
Department of Anesthesiology
Duke University
Durham, North Carolina
Tel: 1-800-260-5631
E-mail: editorial-office@anesthesiology.org

PAST EDITORS-IN-CHIEF

Henry S. Ruth, M.D., 1940–1955
Ralph M. Tovell, M.D., 1956–1958
James E. Eckenhoff, M.D., 1959–1962
Leroy D. Vandam, M.D., 1963–1970
Arthur S. Keats, M.D., 1971–1973
Nicholas M. Greene, M.D., 1974–1976
C. Philip Larson, Jr., M.D., 1977–1979
John D. Michenfelder, M.D., 1980–1985
Lawrence J. Saidman, M.D., 1986–1996
Michael M. Todd, M.D., 1997–2006
James C. Eisenach, M.D., 2007–2016

COVER ART

James P. Rathmell, M.D., Boston, Massachusetts
Annemarie B. Johnson, C.M.I.
Medical Illustrator, Winston-Salem, North Carolina
Sara M. Jarret, M.F.A., C.M.I.
Medical Illustrator, North Wales, Pennsylvania

For reprint inquiries and purchases, please contact
reprintsolutions@wolterskluwer.com in North America, and
healthlicensing@wolterskluwer.com for rest of world.

Anesthesiology is abstracted or indexed in Index Medicus/MEDLINE, Science Citation Index/SciSearch, Current Contents/Clinical Medicine, Current Contents/Life Sciences, Reference Update, EMBASE/Excerpta Medica, Biological Abstracts (BIOSIS), Chemical Abstracts, Hospital Literature Index, and Comprehensive Index to Nursing and Allied Health Literature (CINAHL).

The affiliations, areas of expertise, and conflict-of-interest disclosure statements for each Editor and Associate Editor can be found on the Journal's Web site (www.anesthesiology.org).

CME EDITORS

Leslie C. Jameson, M.D.
Dan J. Kopacz, M.D.

EDITORIAL OFFICE

Ryan Walther, Managing Editor
E-mail: managing-editor@anesthesiology.org
Jennifer Workman, Peer Review Supervisor
Phil Jackson
Caitlin Washburn
ANESTHESIOLOGY Journal
1061 American Lane
Schaumburg, IL 60173-4973
Tel: 1-800-260-5631
E-mail: editorial-office@anesthesiology.org
Vicki Tedeschi, Digital Communications Director
E-mail: v.tedeschi@anesthesiology.org

WOLTERS KLUWER HEALTH PUBLICATION STAFF

Miranda Walker, Publisher
Sara Cleary, Senior Journal Production Editor/Team Leader
Emily Moore, Journal Production Editor
Colette Lind, Journal Production Associate
Hilary Druker, Advertising Field Sales Representative

ASA OFFICERS

Mary Dale Peterson, M.D., President
Beverly K. Philip, M.D., President-Elect
Linda J. Mason, M.D., Immediate Past President
Randall Clark, M.D., First Vice-President

All articles accepted for publication are done so with the understanding that they are contributed exclusively to this Journal and become the property of the American Society of Anesthesiologists, Inc. Statements or opinions expressed in the Journal reflect the views of the author(s) and do not represent official policy of the American Society of Anesthesiologists unless so stated.

ANESTHESIOLOGY

Trusted Evidence: Discovery to Practice™

The Journal of the American Society of Anesthesiologists, Inc. anesthesiology.org

Mission: Promoting scientific discovery and knowledge in perioperative, critical care, and pain medicine to advance patient care.

EDITOR-IN-CHIEF

Evan D. Kharasch, M.D., Ph.D., Durham, North Carolina

ASSISTANT EDITOR-IN-CHIEF

Michael J. Avram, Ph.D., Chicago, Illinois

EXECUTIVE EDITORS

Deborah J. Culley, M.D., Boston, Massachusetts

Brian P. Kavanagh,* M.B., F.R.C.P.C., Toronto, Canada

Jerrold H. Levy, M.D., F.A.H.A., F.C.C.M., Durham,
North Carolina

James P. Rathmell, M.D., Boston, Massachusetts

EDITORS

J. David Clark, M.D., Ph.D., Palo Alto, California

Andrew Davidson, M.B.B.S., M.D., F.A.N.Z.C.A.,
Victoria, Australia

Amanda A. Fox, M.D., M.P.H., Dallas, Texas

Yandong Jiang, M.D., Ph.D., Houston, Texas

Sachin Kheterpal, M.D., M.B.A., Ann Arbor, Michigan

Martin J. London, M.D., San Francisco, California

George A. Mashour, M.D., Ph.D., Ann Arbor, Michigan

Daniel I. Sessler, M.D., Cleveland, Ohio

Laszlo Vutskits, M.D., Geneva, Switzerland

STATISTICAL EDITOR

Timothy T. Houle, Ph.D., Boston, Massachusetts

ASSOCIATE EDITORS

Takashi Asai, M.D., Ph.D., Osaka, Japan

Brian Thomas Bateman, M.D., Boston, Massachusetts

George S. Bause, M.D., M.P.H., Cleveland, Ohio

Beatrice Beck-Schimmer, M.D., Zurich, Switzerland

James M. Blum, M.D., F.C.C.M., Atlanta, Georgia

Chad Michael Brummett, M.D., Ann Arbor, Michigan

John Butterworth, M.D., Richmond, Virginia

Vincent W. S. Chan, M.D., F.R.C.P.C., F.R.C.A., Toronto, Canada

Steven P. Cohen, M.D., Baltimore, Maryland

Albert Dahan, M.D., Ph.D., Leiden, The Netherlands

Douglas Eleveld, M.D., Groningen, The Netherlands

Holger K. Eltzschig, M.D., Ph.D., Houston, Texas

Charles W. Emala, Sr., M.D., M.S., New York, New York

David Faraoni, M.D., Ph.D., F.C.C.P., F.A.H.A., Toronto, Canada

Jorge A. Galvez, M.D., Philadelphia, Pennsylvania

Laurent Gance, M.D., Rochester, New York

Stephen T. Harvey, M.D., Nashville, Tennessee

Harriet W. Hopf, M.D., Salt Lake City, Utah

Vesna Jevtovic-Todorovic, M.D., Ph.D., M.B.A., Aurora,
Colorado

Ru-Rong Ji, Ph.D., Durham, North Carolina

Cor J. Kalkman, M.D., Utrecht, The Netherlands

Meghan Lane-Fall, M.D., M.H.S.P., Philadelphia, Pennsylvania

Adam B. Lerner, M.D., Boston, Massachusetts

Kate Leslie, M.B.B.S., M.D., M.Epi., F.A.N.Z.C.A., Parkville,
Australia

Jochen D. Muehlschlegel, M.D., M.M.Sc., Boston,
Massachusetts

Paul S. Myles, M.B., B.S., M.P.H., M.D., F.F.A.R.C.S.I.,
F.A.N.Z.C.A., Melbourne, Australia

Peter Nagele, M.D., M.Sc., Chicago, Illinois

Mark D. Neuman, M.D., M.Sc., Philadelphia, Pennsylvania

Craig Palmer, M.D., Tucson, Arizona

Cyril Rivat, M.D., Montpellier, France

Jeffrey Sall, M.D., Ph.D., San Francisco, California

Warren S. Sandberg, M.D., Ph.D., Nashville, Tennessee

Alan Jay Schwartz, M.D., M.S.Ed., Philadelphia, Pennsylvania

Allan F. Simpao, M.D., Philadelphia, Pennsylvania

Nikolaos J. Skubas, M.D., Cleveland, Ohio

Jamie W. Sleight, M.D., Hamilton, New Zealand

Ken Solt, M.D., Boston, Massachusetts

Michel Struys, M.D., Groningen, The Netherlands

Eric Sun, M.D., Ph.D., Palo Alto, California

BobbieJean Sweitzer, M.D., F.A.C.P., Chicago, Illinois

Marcos F. Vidal Melo, M.D., Ph.D., Boston, Massachusetts

David S. Warner, M.D., Durham, North Carolina

Duminda N. Wijeyesundera, M.D., Ph.D., F.R.C.P.C.,
Toronto, Canada

Hannah Wunsch, M.D., M.Sc., Toronto, Canada

*Deceased.

Instructions for Obtaining ANESTHESIOLOGY Continuing Medical Education (CME) Credit

CME Editors: Leslie C. Jameson, M.D., and Dan J. Kopacz, M.D.

ANESTHESIOLOGY's Journal CME is open to all readers. To take part in ANESTHESIOLOGY Journal-based CME, complete the following steps:

1. Read the accreditation information presented on this page.
2. Read this month's articles designated for credit (listed below) in either the print or online edition.
3. Register at <http://www.asahq.org/shop-asa>. In the category, search for Journal CME. Nonmembers will need to provide payment.
4. Achieve a score of at least 50% correct on the six-question online journal quiz and complete the evaluation.
5. Claim credit in 15-minute increments, for a maximum of 1 *AMA PRA Category 1 Credit™* per journal article.

Accreditation Information

Purpose: The focus of ANESTHESIOLOGY Journal-based CME is to educate readers on current developments in the science and clinical practice of anesthesiology.

Target Audience: ANESTHESIOLOGY Journal-based CME is intended for anesthesiologists. Researchers and other health care professionals with an interest in anesthesiology may also participate.

Accreditation and Designation Statements: The American Society of Anesthesiologists designates this journal-based activity for a maximum of 1 *AMA PRA Category 1 Credit™*. Physicians should claim only the credit commensurate with the extent of their participation in the activity.

Maintenance of Certification in Anesthesiology™ program and MOCA® are registered trademarks of The American Board of Anesthesiology®. MOCA 2.0® is a trademark of the American Board of Anesthesiology®.

This activity contributes to the CME component of the American Board of Anesthesiology's redesigned Maintenance of Certification in Anesthesiology™ (MOCA®) program, known as MOCA 2.0®. Please consult the ABA website, <http://www.theABA.org>, for a list of all MOCA 2.0 requirements.

Rates

Two options are available:

	ASA Member	Non-member
Annual Fee	\$0	\$120
Per Issue	\$0	\$20

Payment may be made using Visa or MasterCard.

Please direct any questions about Journal-based CME to: EducationCenter@asahq.org

Date of Release: November 2019

Expiration Date: November 2022

This Month's ANESTHESIOLOGY Journal-based CME Articles

Read the article by Hamilton *et al.* entitled "Peripheral Nerve Blocks for Ambulatory Shoulder Surgery: A

Population-based Cohort Study of Outcomes and Resource Utilization" on page 1254, and the article by Kang *et al.* entitled "Superior Trunk Block Provides Noninferior Analgesia Compared with Interscalene Brachial Plexus Block in Arthroscopic Shoulder Surgery" on page 1316.

Learning Objectives

After successfully completing this activity, the learner will be able to describe the association of nerve blocks for ambulatory shoulder surgery with postoperative outcomes, identify the sonographic location of the superior trunk of the brachial plexus, and recognize the differences between interscalene and superior trunk blockade for shoulder surgery.

Disclosures

These journal articles have been selected for and planned as a journal CME activity, which is designated for *AMA PRA Category 1 Credit™*. The authors disclosed relationships in keeping with ANESTHESIOLOGY's requirements for all journal submissions. All relationships journal authors disclosed to ANESTHESIOLOGY are disclosed to learners, even those relationships that are not relevant financial relationships, per the ACCME's requirements for CME activities.

Editor-in-Chief: Evan D. Kharasch, M.D., Ph.D., has reported receiving consulting fees from TEN Healthcare.

CME Editors: Leslie C. Jameson, M.D., has disclosed no relevant financial relationships with commercial interests. Dan J. Kopacz, M.D., has disclosed holding an equity position with SoloDex, LLC.

ASA Staff: Kari Lee and Anne Farace have disclosed no relevant financial relationships with commercial interests.

Authors: Gavin M. Hamilton, M.D., M.Sc., Reva Ramlogan, M.D., B.Sc., Anne Lui, M.D., M.Sc., Colin J. L. McCartney, M.B., Ch.B., Ph.D., Faraj Abdallah, M.D., M.Sc., Jason McVicar, M.D., Daniel I. McIsaac, M.D., M.P.H., RyungA Kang, M.D., Ph.D., Ji Seon Jeong, M.D., Ph.D., Ki Jinn Chin, M.B.B.S., F.R.C.P.C., Jae Chul Yoo, M.D., Ph.D., Jong Hwan Lee, M.D., Ph.D., Soo Joo Choi, M.D., Ph.D., Mi Sook Gwak, M.D., Ph.D., Tae Soo Hahm, M.D., Ph.D., and Justin Sangwook Ko, M.D., Ph.D., have disclosed no relevant financial relationships with commercial interests.

Disclaimer

The information provided in this activity is for continuing education purposes only and is not meant to substitute for the independent medical judgment of a health care provider relative to diagnostic and treatment options of a specific patient's medical condition.

DOI: 10.1097/ALN.0000000000003051

Getting Published is a Process.

We're Here to Help.



Get started today!

authors.lww.com



Wolters Kluwer

Key Papers from the Most Recent Literature Relevant to Anesthesiologists



Conserved cell types with divergent features in human versus mouse cortex. *Nature* 2019; 573:61–8.

An understanding of the cellular scheme of the cortex is essential to our understanding of cognitive function and susceptibility to neuronal disease. This study used single-nucleus RNA sequencing to classify cell types to reveal preserved and contrasting features between mouse and the human brain. The authors identified 75 transcriptomically distinct cell types, 45 of which were inhibitory. Among the excitatory neurons the authors noted that they were not restricted to single cortical layers but rather that they were often distributed between layers. When the author compared transcriptomic cell types in humans to those in mice, they found divergence in expression between the species. More specifically, two thirds of the 9,748 genes evaluated

were divergently expressed between the two species with the greatest differences noted among nonneuronal cells. These results suggest significant species differences in gene expression between mouse and human brain that may influence function and add to our understanding of why preclinical studies using mice are often not translatable to humans. (Article Selection: Evan D. Kharasch. Image: ©Adobe Stock.)

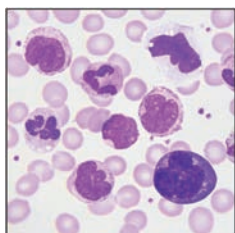
Take home message: There are significant differences between the human and mouse brain that may explain why preclinical studies using mice often do not translate to humans.



Is disruptive behavior inherent to the surgeon or the environment? Analysis of 314 events at a single academic medical center. *Ann Surg* 2019; 270:463–72.

Disruptive behavior is thought to disrupt a culture of safety. This study compared accounts of a reporter and the involved individual responses to an episode of disruptive behavior to evaluate whether the hospital environment may contribute and whether disruptive behavior is associated with patient harm. The authors identified 314 reports among 204 involved individuals. Surgical specialties had the highest percentage of involved individuals (43%) and 56% of the events occurred in high-intensity environments such as the operating room or intensive care unit ($P < 0.001$). Logistic regression analysis identified that unclear hospital policies (odds ratio 3.0; 95% CI, 1.7 to 5.6; $P < 0.001$), a surgeon being the involved individual (odds ratio 2.4; 95% CI, 1.4 to 4.1; $P < 0.001$), and urgent competing responsibilities (odds ratio 1.9; 95% CI, 1.1 to 3.2; $P = 0.02$) were associated with potential harm to patients. Interestingly, events involving members of nonsurgical services were more likely to be associated with insensitivity to patients (odds ratio 2.8; 95% CI, 1.6 to 4.8; $P < 0.001$). (Article Selection: Deborah J. Culley. Image: ©gettyimages.)

Take home message: Disruptive behavior that may be associated with harm to patients is related to unclear hospital policies, being a surgeon, and the presence of urgent competing responsibilities.



Dietary intake regulates the circulating inflammatory monocyte pool. *Cell* 2019; 178:1102–14.

Caloric restriction has been shown to be beneficial for inflammatory and autoimmune diseases. This study investigated the effect of fasting on monocytes in mice and humans. The authors found that fasting reduced the pool of circulating monocytes not because the cells are dying but rather due to decreased release of monocytes from the bone marrow to the periphery. This decrease in monocytes release from the bone marrow pool may be partially mediated by a reduction in CCL2, as CCL2 administration was shown to enhance monocyte migration from the bone marrow in fasted animals. The authors also demonstrated that fasting was associated with changes in monocyte metabolic activity as the expression of more than 2,700 genes

were differentially expressed after 20 h of fasting. Perhaps the most interesting finding of these studies was that while fasting can lead to improvements in chronic inflammatory diseases, it does not affect the ability of monocytes to mobilize during acute inflammation at least in normal weight individuals. (Article Selection: Martin J. London. Image: ©gettyimages.)

Take home message: Fasting has a major effect on monocyte egress to the periphery and gene expression yet allows monocytes to maintain their ability to mobilize in the setting of an acute immune response.



Sustained efficacy of kangaroo care for repeated painful procedures over neonatal intensive care unit hospitalization: A single-blind randomized controlled trial. *Pain* 2019; 160:2580–8.

Painful procedures are frequently performed on preterm neonates in intensive care units. A body of data suggests that maternal contact and sweet-tasting liquids reduce pain from a single procedure. This study evaluated whether maternal kangaroo care (infants placed upright on their mother's bare chest) with or without sucrose were equally efficacious in repeated procedural-related pain in neonates admitted to a neonatal intensive care unit. Preterm infants were randomized to kangaroo care plus water, kangaroo care plus sucrose, or sucrose alone before a medically indicated heel lance. A total of 242 patients were randomly assigned to one of the three groups. Premature Infant Pain Profiles were measured at 30, 60, and 90 s after each of three heel lances. Maternal kangaroo care and sucrose were equally efficacious as pain-relieving interventions over time. There was no additional benefit of providing both maternal kangaroo care and sucrose (all P values greater than 0.3). (Article Selection: J. David Clark. Image: L. Gray.)

Take home message: Maternal kangaroo care was as effective as sucrose during a medically indicated heel lance in neonates.



Effect of professional background and gender on residents' perceptions of leadership. *Acad Med* 2019 Jul 30 [Epub ahead of print].

Questions persist about how professional background and gender influence a resident's perception of leadership skills. This study used identically scripted, simulated, video-recorded resuscitation scenarios with either a male or female leader identified as either a nurse practitioner or physician to determine the effects of gender and profession on the perception of leadership skills. One hundred and sixty resident volunteers subsequently rated the leader's performance using the Ottawa Crisis Resource Management Global Rating Scale. Female leaders received lower scores in the areas of leadership and communication skills when compared to male leaders ($P < 0.01$) but the sexes were equivalent in their overall performance

and in the domains of problem solving, situational awareness, and resource utilization skills. There was no effect of professional background on any of the scores. (Article Selection: Cathleen Peterson-Layne. Image: ©gettyimages.)

Take home message: On identically scripted video recordings, females were perceived to have lower leadership and communication skills when compared to males despite identical performances. Interestingly, their overall scores were similar.



Persistent opioid use is associated with worse survival after lobectomy for stage I non-small cell lung cancer. *Pain* 2019; 160:2365–73.

A large percentage of patients have persistent opioid use after thoracic surgical procedures. This study used a national cancer registry linked with Medicare claims to identify whether persistent opioid use 3 to 6 months after lung resection in 2,884 patients with non-small cell lung cancer was associated with worse survival. Twenty-seven percent of patients had persistent opioid use between 3 and 6 months after their surgical procedure. On multivariate analysis, predictors of mortality included higher opioid utilization, age, male sex, not being married, larger tumors, open procedures, radiation therapy, lack of chemotherapy, higher tumor grade, and higher Charleston Comorbidity score. While the title highlights

that persistent opioid use is associated with worse survival after lobectomy, the multivariate analysis suggests that there are multiple indicators for early mortality after surgery for lung cancer that may be associated with increased opioid utilization. (Article Selection: J. David Clark. Image: ©gettyimages.)

Take home message: Higher opioid utilization, age, male sex, not being married, larger tumors, open procedures, radiation therapy, lack of chemotherapy, higher tumor grade, and higher Charleston Comorbidity score are independently associated with mortality in patients with lung cancer.



Donor simvastatin treatment in heart transplantation. *Circulation* 2019; 140:627–40.

Data suggest that the administration of simvastatin to organ donors may inhibit allograft ischemia-reperfusion injury. This prospective, randomized, double-blinded study evaluated the effect of administering simvastatin to heart donors on ischemia-reperfusion injury after heart transplantation in 84 heart donors. Primary outcome measures included plasma concentrations of troponin T, troponin I, or creatine kinase MB subunit in the recipient in the first 24 h after organ reperfusion. Administration of simvastatin to organ donors had no effect on creatine kinase MB concentrations and troponin T levels but did reduce concentrations of troponin I from $171,000 \pm 151,000$ to $103,000 \pm 109,000$ ng/l ($P = 0.04$) in

organ recipients. There was no effect of simvastatin on the incidence or severity of transplant rejections between the groups. (Article Selection: Martin J. London. Image: ©Adobe Stock.)

Take home message: Administration of simvastatin to heart donors may be associated with decreased concentrations of troponin I in organ recipients.



Improving operating room efficiency: Machine learning approach to predict case-time duration. *J Am Coll Surg* 2019; 229:346–54.

Operating room case duration estimates are important for optimizing operating room utilization. This study evaluated whether the use of supervised artificial intelligence and linear regression analyses to statistically predict case-time duration were accurate. Data were derived from 46,986 scheduled surgical procedures. Eighty percent of the data was used for training and 20% for validation of the model and comparison using average historical times and surgeon estimates. The historical times and surgeon estimate models accurately predicted case-time duration within a 10% tolerance threshold in 31% of cases. In 27% of cases this model overpredicted the case duration and in 41% of cases this model underpredicted the

case duration. The most accurate artificial intelligence model could predict case duration within a 10% tolerance threshold 50% of the time with the least accurate models being similar to the utilization of historical times and surgeon estimates. (Article Selection: Deborah J. Culley. Image: ©Adobe Stock.)

Take home message: Artificial intelligence may be useful in predicting surgical case time and may make it easier to optimize operating room utilization.

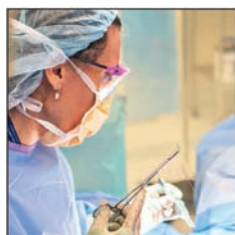


Mechanical and oral antibiotic bowel preparation versus no bowel preparation for elective colectomy (MOBILE): A multicentre, randomised, parallel, single-blinded trial. *Lancet* 2019; 394:840–8.

A growing body of data is suggesting that mechanical and oral antibiotic bowel preparation may lead to a decrease in surgical site infections and subsequent morbidity. This multicenter, parallel, single-blinded trial included 417 patients having elective colon surgery and randomized them to no bowel preparation or mechanical and oral antibiotic bowel preparation with a primary outcome of surgical site infection within 30 days after surgery. The final analysis included the 396 patients that completed the study. Surgical site infections within 30 days of surgery occurred in 13 of 196 patients receiving

mechanical and oral antibiotic bowel preparation (7%) and in 21 of 200 patients who did not undergo bowel preparation (11%, effect size 1.65; 95% CI, 0.80 to 3.40; $P = 0.17$). There were also no differences in any of the secondary outcomes including Comprehensive Complication Index score within 30 days of surgery, anastomotic dehiscence, reoperation, readmission, hospital length of stay, mortality at 30 or 90 days, and adverse effects of antibiotic administration. (Article Selection: Martin J. London. Image: ©Adobe Stock.)

Take home message: Mechanical and oral antibiotic bowel preparation does not appear to have benefit over no bowel preparation in patients having elective colectomy.



Association of domestic responsibilities with career satisfaction for physician mothers in procedural vs nonprocedural fields. JAMA Surg 2019 Apr 10 [Epub ahead of print].

Challenges between career goals and domestic responsibilities are common among mothers who are physicians. This study surveyed female physicians to investigate associations between increased domestic workload and career satisfaction among physician mothers in procedural and nonprocedural specialties. The majority of the 1,712 participants were married (99%). Interestingly, there were no differences between proceduralists and nonproceduralists in perceiving that they held sole responsibility for the majority of domestic tasks. Despite this similarity, physician mothers in procedural specialties

responsible for five or more domestic tasks had a greater interest in changing careers to a less demanding specialty when compared to those with fewer than five domestic tasks (odds ratio 1.5; 95% CI, 1.0 to 2.2; $P = 0.05$) on multivariate analysis. This difference was not noted for those in nonprocedural fields. Interestingly, there were a number of differences between proceduralists and nonproceduralists identified in this study that may be related to some of these differences. See the accompanying editorial, "Domestic Responsibilities of Physician Mothers: Chores, Catsup Sandwiches, and Snacks" (JAMA Surg 2019 Apr 10 [Epub ahead of print]), for creative examples of how one proceduralist mother reduced chores and parental guilt for not being that "perfect mom." (Article Selection: Deborah J. Culley. Image: J. P. Rathmell.)

Take home message: This study found an association between domestic chores and an interest in moving to a less demanding specialty among proceduralist but not nonprocedural physician mothers.



Mortality after discontinuation of primary care-based chronic opioid therapy for pain: A retrospective cohort study. J Gen Intern Med 2019 Aug 29 [Epub ahead of print].

The risks of discontinuing chronic opioid therapy for the treatment of chronic pain are relatively unknown. This retrospective cohort study was designed to evaluate mortality, use of prescription opioids, and stability of primary care in patients who had been on chronic opioid therapy that was stopped. This study included 572 patients on chronic opioid therapy from a clinic opioid registry. In 60% of these patients, chronic opioid therapy was discontinued. The reasons for discontinuation included a transfer of care or behavioral and safety concerns. In 18% of the patients where chronic opioid therapy was

discontinued, there were patient-initiated reasons for discontinuation; in 77% of cases there was at least one provider-initiated reason for discontinuation of chronic opioid therapy. Discontinuation of chronic opioid therapy was not associated with an increase in the overall death rate, although the overall death rate was high ($P = 0.12$, 21%), but was associated with an increased in overdose deaths (hazard ratio 2.9; 95% CI, 1.0 to 8.6; $P < 0.05$). (Article Selection: Evan D. Kharasch. Image: J. P. Rathmell.)

Take home message: Discontinuation of chronic opioid therapy may increase the risk of death by overdose.



Permanent percutaneous carotid artery filter to prevent stroke in atrial fibrillation patients: The CAPTURE trial. J Am Coll Cardiol 2019; 74:829–39.

Some patients who are at high risk of stroke, including those with atrial fibrillation, have contraindications to anticoagulation therapy. This study assessed the feasibility and safety of placing bilateral common carotid artery filters for the prevention of stroke in 25 patients from three centers. The primary feasibility endpoint was two properly positioned filters and the primary safety endpoints included absence of device- or procedure-related death, stroke, major bleeding, more than 70% common carotid artery stenosis, common carotid artery thrombus, or common carotid artery complication requiring endovascular treatment or surgery to repair at 30 days postprocedure. For the majority of the patients (92%), the investigators were able

to properly place the filters bilaterally and satisfied the safety endpoints. On follow-up there were four patients where thrombi were found in the filter on ultrasound. These patients were treated with subcutaneous heparin with resolution of the clot. (Article Selection: Martin J. London. Image: J. P. Rathmell.)

Take home message: Placement of a permanent carotid coil filter may be safe and feasible for the capture of thromboembolism in patients deemed unsuitable for anticoagulation therapy.

INFOGRAPHICS IN ANESTHESIOLOGY

Complex Information for Anesthesiologists Presented Quickly and Clearly

MULTI-DIMENSIONAL ANESTHESIA

The Effects of Sevoflurane or Propofol with Remifentanyl

Kuizenga *et al.*¹ studied 36 subjects, using sevoflurane or propofol +/- remifentanyl, measuring 3 endpoints and the Patient State Index*

Calling by Name



Shake & Shout



Tetanic Stimulus



Remifentanyl and Response

Propofol
With low-dose propofol (<2.5 ug/ml), remifentanyl reduces response rate from 50% to <1%, when increased from 0 to 4 ng/ml.

Remifentanyl and Patient State Index

With propofol, remifentanyl has little effect on the Patient State Index when increased from 0 to 4 ng/ml.

Patient State Index and Response

With propofol, most respond at a Patient State Index of 60, few at 30; remifentanyl reduces the response.

Propofol

Sevoflurane

With low-dose sevoflurane (<1.5%), remifentanyl reduces response rate, with diminishing returns above 2 ng/ml.

With sevoflurane, remifentanyl has no effect on the Patient State Index.

With sevoflurane, most **do not** respond at a Patient State Index of 60, almost none at 30; remifentanyl reduces this further.

*The Patient State Index (Masimo, USA) is a quantitative measure of anesthetic drug effect using processed EEG-derived indices.



These multidimensional interactions demonstrate the interplay between two hypnotics and one opioid; more research is needed to scale this understanding to include medications such as dexmedetomidine, ketamine, and lidocaine.²

EEG, electroencephalography.

Infographic created by Jonathan P. Wanderer, Vanderbilt University Medical Center, and James P. Rathmell, Brigham and Women's Health Care/Harvard Medical School.

Illustration by Annemarie Johnson, Vivo Visuals. Address correspondence to Dr. Wanderer: jonathan.p.wanderer@vanderbilt.edu.

1. Kuizenga MH, Colin PJ, Reyntjens KMEM, Touw DJ, Nalbat H, Knotnerus FH, Vereecke HEM, Struys MMRF: Population pharmacodynamics of propofol and sevoflurane in healthy volunteers using a clinical score and the Patient State Index: A crossover study. *ANESTHESIOLOGY* 2019; 131:1223–38
2. Sleight JW: The art of general anesthesia: Juggling in a multidimensional space. *ANESTHESIOLOGY* 2019; 131:1199–201

ANESTHESIOLOGY® Annual Meeting OnDemand



Downloaded from /anesthesiology/issue/131/6 by guest on 16 April 2024

Learn anytime, anywhere, from any device!

Access approximately 350 hours of content and earn continuing education credits!



Online access
from any device



Downloadable
PDFs and MP3s



Earn CME credits
with online testing



Portable Hard Drive
for offline learning

Order today and get a \$500 gift card with your purchase!

Order Online:

[ASA.OnDemand.org/GiftCard](https://asa.ondemand.org/giftcard)

Order by Phone:

(800) 501-2303 (U.S. Only)

or (818) 844-3299

Monday – Friday 6 a.m. – 5 p.m. PT



American Society of
Anesthesiologists™

The Art of General Anesthesia

Juggling in a Multidimensional Space

Jamie W. Sleight, M.D.

The art of general anesthesia involves making intuitive predictions of how a particular patient will respond to anesthetic drugs and to the noxious stimuli of surgery. Patient responses might consist of somatic movements, various autonomic nervous system effects (including tachycardia, bradycardia, hypertension, sweating, mydriasis), return of consciousness and memory, and endocrine and immune activation. To suppress these responses we use many different classes of anesthetic drugs or adjuncts. Clearly the delivery of anesthesia requires an appreciation of a multiplicity of dimensions. In this issue of *ANESTHESIOLOGY*, an article by Kuizenga *et al.*¹ attempts to bring some scientific quantification to the question of hypnotic–opioid interactions. They investigated how the addition of an opioid drug (remifentanyl) alters responses to two commonly used hypnotic drugs (propofol and sevoflurane). This sort of study has been done previously,^{2–4} but the novelty of the present study was the use of a within-subject design to formally compare the effects of remifentanyl on propofol head-to-head with sevoflurane. Thus they studied three input variables (two hypnotic drugs and one analgesic drug) and two output variables (the resting state of the cortical activity as measured by the Patient State Index [a processed electroencephalographic measure], and the probability of behavioral response to graded external stimulation). Because they were looking at perhaps five dimensions, it is hard to represent the totality of their results graphically in a single diagram. Instead we follow the conventional methods of reductive science, and ask separate, tractable (but two-dimensional) questions.



“[How does] the addition of an opioid drug (remifentanyl) alter responses to...propofol and sevoflurane?”

1. How does remifentanyl affect the relationship between hypnotic drug concentrations and the probability of quantal behavioral response to stimuli? (and ignore the cortical state)
2. Does remifentanyl alter the state of cortical activity at each concentration of hypnotic drug? (and ignore the behavioral response)
3. How does remifentanyl affect the relationship between the unstimulated resting cortical state and the probability of behavioral response to stimuli? (and ignore the hypnotic drug concentrations)

To answer the first question we find that the addition of even a low concentration of remifentanyl dramatically reduces the responses

to stimuli for propofol; furthermore, the effects are more marked for the more painful stimulus. This comes as no surprise to any clinician. Because it is one of the standard descriptive parameters estimated in the mathematical model, the remifentanyl effect is usually reported as a left shift in the concentration of propofol required to prevent a response in 50% of the population (EC₅₀; shown as a horizontal black arrow in fig. 1A). However the practicing clinician is more interested in the probability that a patient—when given at a particular propofol effect site concentration—will move in response to surgery. With this perspective, the effect of adding some remifentanyl is shown by the vertical black arrows in figure 1. We can see that, for low and moderate concentrations of hypnotic (less than 3 µg/ml propofol and less than 1.5% sevoflurane), the addition of remifentanyl causes dramatic reductions in probability of response. For example, at the

Image: J. P. Rathmell.

This editorial accompanies the article on p. 1223. This editorial has a related Infographic on p. 17A.

Accepted for publication January 27, 2019. From the Department of Anaesthesia and Pain Medicine, Waikato Clinical School, University of Auckland, Hamilton, New Zealand.

Copyright © 2019, the American Society of Anesthesiologists, Inc. All Rights Reserved. *Anesthesiology* 2019; 131:1199–201. DOI: 10.1097/ALN.0000000000002709

EC50 propofol concentration of 2.8 $\mu\text{g}/\text{ml}$, even 2 ng/ml of remifentanyl (equivalent to a steady-state infusion of about 0.1 $\text{ng}/\text{kg}/\text{min}$) reduces the probability of response from 50% to less than 5%. The lesser leftward shift of the EC50 for sevoflurane suggests a lesser additive remifentanyl effect. This conclusion is illusory. Because the slope of the sevoflurane curves are steeper than those for propofol, the clinical beneficial hypnotic-sparing effect of remifentanyl for sevoflurane is actually comparable with that of propofol (*i.e.*, both vertical black arrows in fig. 1 are similar in length). With the proviso that the tetanic stimulus is less than that of a surgical incision, these figures would suggest that giving concentrations of remifentanyl greater than 2 ng/ml has diminishing benefit for preventing patient movement.

For the second question: does the addition of remifentanyl have a direct effect on the relationship between the hypnotic drugs and resting state cortical activity? The answer seems to be: “a little effect with propofol at these concentrations of remifentanyl” and “no effect on sevoflurane.” The propofol–Patient State Index curve is slightly shifted to the left, and the effect on the sevoflurane–Patient State Index relationship is almost nil. Other work⁵ suggests that the EC50 of the remifentanyl sigmoid dose–electroencephalogram response curve—which is in turn acting to shift the propofol–electroencephalogram sigmoid curve—is higher (5 to 10 ng/ml of remifentanyl) than the 4 ng/ml achieved in the present study.

The third question looks at whether the preexisting unstimulated state of cortical activity (the Patient State Index value) has any correlation with the probability of subsequent behavioral response to stimulus. This question

lies at the core of the unending misunderstanding about the role of electroencephalographic monitors in clinical anesthesia. As is clearly shown in figure 5 of their article, the curves for response to verbal command are quite steep; for propofol, most patients will respond at a Patient State Index of 60, and most will not respond at 30. The curve is shifted 20 points to the left by using sevoflurane or adding remifentanyl. Again, no clinical surprises here. You can easily give a sevoflurane-only anesthetic, but it is hard to give a propofol-only anesthetic for any serious surgery. Sevoflurane is clearly better than propofol at blocking responses to sensory input. The curves of the probability of behavioral response to a painful stimulus are quite different; the flat slopes of these curves indicate that cortical state is a poor predictor of the probability of subsequent movement in response to pain. Any individual patient could move at almost any value of Patient State Index. Interestingly the addition of remifentanyl shifts the curves markedly up and to the left but does not make the slopes any steeper in this study. Somatic movement is largely driven by spinal cord responses. You cannot expect to accurately monitor spinal cord function by looking at the signal from electrodes on the forehead.

The article by Kuizenga *et al.*¹ essentially looks piecemeal at bivariate opioid–hypnotic combinations. In clinical practice we commonly—and effectively—use more complex (multidimensional) combinations consisting of volatile agent, opioid, and infusions of propofol, dexmedetomidine, lidocaine, or ketamine. How do we objectively quantify these multiple simultaneous interactions at an individual patient level? The art of anesthesia is progressing rapidly; can the science keep up?

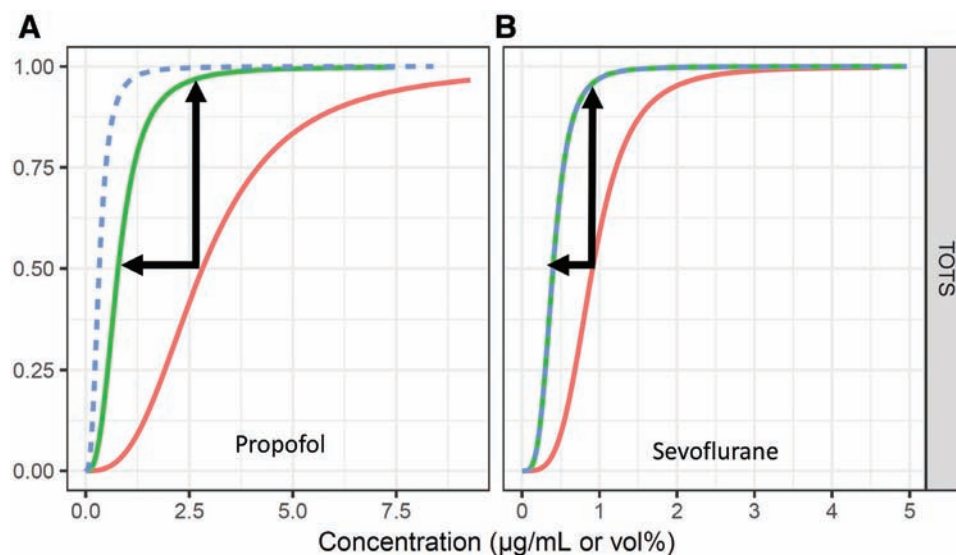


Fig. 1. Effect of addition of remifentanyl to probability of response to noxious stimulus, at different concentrations of propofol (A) and sevoflurane (B). Red lines, remifentanyl 0 ng/ml ; green, 2 ng/ml ; dashed blue, 4 ng/ml . Reproduced with permission from figure 2 of Kuizenga *et al.*¹

Acknowledgments

The author acknowledges interesting discussions with Dr. Ben Simpson, FANZCA, Department of Anaesthesia, Waikato Hospital, Hamilton, New Zealand.

Competing Interests

The author is not supported by, nor maintains any financial interest in, any commercial activity that may be associated with the topic of this article.

Correspondence

Address correspondence to Dr. Sleigh: Jamie.sleigh@waikatodhb.health.nz

References

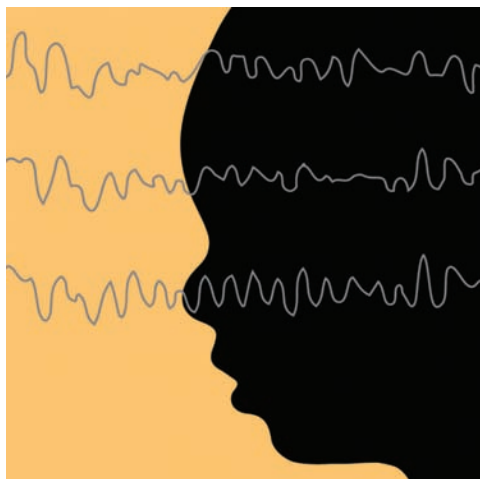
1. Kuizenga MH, Colin PJ, Reyntjens KMEM, Touw DJ, Nalbat H, Knotnerus FH, Vereecke HEM, Struys MMRF: Population pharmacodynamics of propofol and sevoflurane in healthy volunteers using a clinical score and the Patient State Index. *ANESTHESIOLOGY* 2019; 131:1223–38
2. Bouillon TW, Bruhn J, Radulescu L, Andresen C, Shafer TJ, Cohane C, Shafer SL: Pharmacodynamic interaction between propofol and remifentanyl regarding hypnosis, tolerance of laryngoscopy, bispectral index, and electroencephalographic approximate entropy. *ANESTHESIOLOGY* 2004; 100:1353–72
3. Katoh T, Ikeda K: The effects of fentanyl on sevoflurane requirements for loss of consciousness and skin incision. *ANESTHESIOLOGY* 1998; 88:18–24
4. Short TG, Hannam JA, Laurent S, Campbell D, Misur M, Merry AF, Tam YH: Refining target-controlled infusion: An assessment of pharmacodynamic target-controlled infusion of propofol and remifentanyl using a response surface model of their combined effects on bispectral index. *Anesth Analg* 2016; 122:90–7
5. Wiczling P, Bieda K, Przybyłowski K, Hartmann-Sobczyńska R, Borsuk A, Matysiak J, Kokot ZJ, Sobczyński P, Grześkowiak E, Bienert A: Pharmacokinetics and pharmacodynamics of propofol and fentanyl in patients undergoing abdominal aortic surgery: A study of pharmacodynamic drug-drug interactions. *Biopharm Drug Dispos* 2016; 37:252–63

Are There Common Network-level Correlates of the Anesthetized Brain in Infants and Adults?

Michael P. Puglia, M.D., Ph.D., George A. Mashour, M.D., Ph.D.

Anesthetic care of infants and children has evolved considerably over the last four decades. In the mid-1980s, infants were undergoing invasive procedures with either no or “light” anesthesia supplemented with a neuromuscular blocking agent. Parents became appalled, which motivated a public outcry and sparked an intense discussion among anesthesia providers on how best to anesthetize infants.¹ This led to a paradigm shift in pediatric anesthesiology, with providers recognizing the possibility and consequences of pain in infants undergoing surgery and reconsidering anesthetic regimens accordingly. The pendulum has now swung in the opposite direction, as the conversation in pediatric anesthesia over the last decade has been dominated

by neurotoxicity and the potentially detrimental effects of anesthetics in the developing brain, brought into public view by a recent Food and Drug Administration black box warning on anesthetic medications for young children and pregnant women. As every pediatric anesthesia provider will attest, infants and children are not just “little adults,” yet in accomplishing one of the fundamental goals of anesthetic care, methods of titrating anesthetics in infants are based on the same variables used in adult patients (*i.e.*, minimum alveolar concentration values, patient movement, and hemodynamic changes). This is, in part, due to an incomplete understanding of the neurobiologic mechanisms of anesthesia and lack of surrogate markers of unconsciousness in the developing brain. In this issue of *ANESTHESIOLOGY*, Pappas *et al.*² present an elegant study that begins to inform this current gap in knowledge.



“[The] emerging network-level picture of general anesthesia in infants is remarkably consistent with that of adults...”

cephalographic electrode/recording location (sensor) and (2) a mathematical transformation of the electroencephalographic data that estimates the neural origin of the signal in the brain (source). Both analyses yielded similar results. During the maintenance phase, functional connectivity was found to be decreased across several locations, including the frontal–parietal region. The breakdown of frontal–parietal connectivity has been postulated to be a neural correlate of unconsciousness and mechanism of disrupted long-range information transfer in adults,³ although this connectivity pattern is dynamic during anesthesia.^{4,5} The authors interpreted the finding of functional cortical disconnection as a potential mechanism for the loss of consciousness in infants. Additionally, Pappas *et al.*² used network science methods to explore how infant brain network architecture (in this case, modularity, or the degree to which functional networks are characterized by individual modules or an integrated

The study was a retrospective cohort analysis of multichannel electroencephalographic recordings of 20 infants, aged 0 to 3.9 months old, who underwent sevoflurane anesthesia for elective surgical procedures. The goals of the study were to identify changes in functional connectivity and network properties in the infant brain during two time points: the maintenance phase (end-tidal sevoflurane, 1.8 to 2.5%) and emergence (end-tidal sevoflurane, 0 to 0.3%). First, the investigators used a measure of functional connectivity, *i.e.*, the statistical covariation of activities across different brain regions. Their electroencephalographic analysis was limited to the slow-wave or δ bandwidth (1 to 4 Hz) and analyzed in two ways: (1) directly from the electroen-

Image: J. P. Rathmell.

This editorial accompanies the article on p. 1239.

Accepted for publication August 19, 2019. From the Department of Anesthesiology (M.P.P., G.A.M.), the Center for Consciousness Science (M.P.P., G.A.M.), and the Neuroscience Graduate Program (G.A.M.), University of Michigan Medical School, Ann Arbor, Michigan.

Copyright © 2019, the American Society of Anesthesiologists, Inc. All Rights Reserved. *Anesthesiology* 2019; 131:1202–4. DOI: 10.1097/ALN.0000000000002993

whole) and whole-brain dynamic patterns (complexity) changed during these two periods in the δ frequency band. They found that brain networks were more fragmented and less complex during general anesthesia, supporting the hypothesis of impaired integration and a constrained repertoire of states.

These findings are striking because this emerging network-level picture of general anesthesia in infants is remarkably consistent with that of adults, despite substantial differences in the properties of the electroencephalogram. Collectively, the past studies of anesthetized adults and these new data in anesthetized infants suggest the remarkable possibility that there might be a common network-level mechanism and marker of anesthetic-induced unconsciousness that is age-invariant. This heralds the possibility of a monitor that, in contrast to current commercial options, is effective even in the very young. The finding that networks appear to be less integrated during general anesthesia is also consistent with leading theories of consciousness.⁶

In adults, hypercoherent frontal α oscillations,⁷ breakdown in functional brain connectivity,⁸ reduced complexity in brain oscillatory patterns, and changes in network properties⁸ have all been consistently identified. In infants undergoing general anesthesia, there is a lack of clear electroencephalographic markers of unconsciousness, and the relevance of adult connectivity and network-based markers has been previously unexplored. To highlight the differences between infants and adults, figure 1 shows example spectrograms (*i.e.*, plots of electroencephalogram frequency by time, with color indicating power) and coherograms (*i.e.*, plots of synchrony between two signals at the same frequency, with color indicating strength) during the maintenance phase of sevoflurane anesthesia. Note, for example, the lack of coherent frontal α oscillations in the infant,^{9,10} which can be clearly identified in adults during anesthesia. Additionally, in figure 2A presented in the article by Pappas *et al.*,² notice the striking similarity between maintenance and emergence from general anesthesia in infants. It is remarkable that, despite these differences in infants and

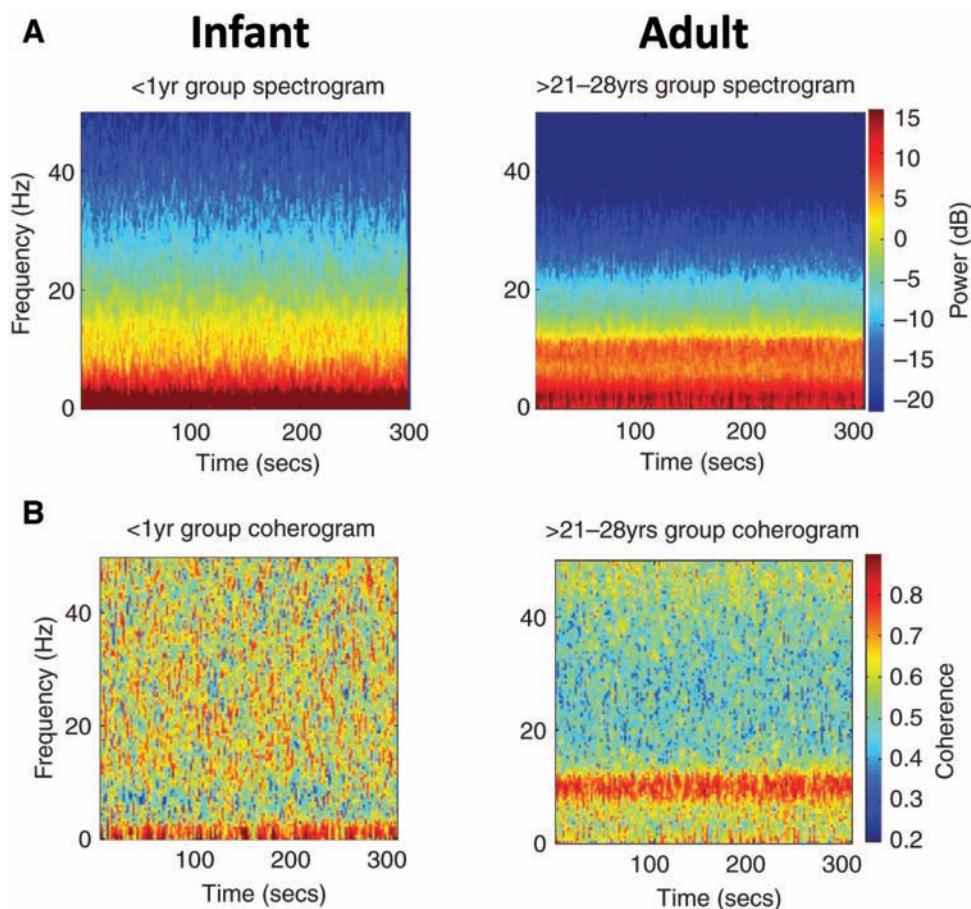


Fig. 1. Electroencephalographic and network property differences between infants and adults. Spectrograms (A) and coherograms (B) of infants (less than 1 yr old) and adults (21 to 28 yr old) during the maintenance phase of general anesthesia with sevoflurane (reproduced from the work of Akeju *et al.*,⁹ with permission from Elsevier).

adults, common patterns emerge when examining the network level.

Although these results are exciting, the study was relatively small, with the possibility of anesthetic and surgical stimulus heterogeneity. Additionally, although slow waves are the most prominent brain oscillation during this developmental period, additional frequency bands should be characterized in the future, as should different recording time points (such as baseline measurements) and different ages or stages of development. Finally, the possibility of dynamic transitions in these connectivity patterns, as has been shown in adults,^{4,5} should be explored.

In conclusion, the study by Pappas *et al.*² shows us that general anesthetics alter functional brain networks in infants in a way that is similar to adults. This establishes an important foundation for future work that can systematically identify age-invariant markers of anesthetic-induced consciousness.

Research Support

This work was supported by National Institutes of Health grant No. R01GM098578 (Bethesda, Maryland; to Dr. Mashour) and funds from the Department of Anesthesiology, University of Michigan Medical School, Ann Arbor, Michigan.

Competing Interests

The authors are not supported by, nor maintain any financial interest in, any commercial activity that may be associated with the topic of this article.

Correspondence

Address correspondence to Dr. Mashour: gmashour@umich.edu

References

1. Costarino AT Jr, Downes JJ: Pediatric anesthesia historical perspective. *Anesthesiol Clin North Am* 2005; 23:573–95, vii
2. Pappas I, Cornelissen L, Menon DK, Berde CB, Stamatakis EA: δ -Oscillation correlates of anesthesia-induced unconsciousness in large-scale brain networks of human infants. *ANESTHESIOLOGY* 2019; 131:1239–53
3. Hudetz AG, Mashour GA: Disconnecting consciousness: Is there a common anesthetic end point? *Anesth Analg* 2016; 123:1228–40
4. Li D, Vlisides PE, Kelz MB, Avidan MS, Mashour GA; ReCCognition Study Group: Dynamic cortical connectivity during general anesthesia in healthy volunteers. *ANESTHESIOLOGY* 2019; 130:870–84
5. Vlisides PE, Li D, Zierau M, Lapointe AP, Ip KI, McKinney AM, Mashour GA: Dynamic cortical connectivity during general anesthesia in surgical patients. *ANESTHESIOLOGY* 2019; 130:885–97
6. Koch C, Massimini M, Boly M, Tononi G: Neural correlates of consciousness: Progress and problems. *Nat Rev Neurosci* 2016; 17:307–21
7. Purdon PL, Pierce ET, Mukamel EA, Prerau MJ, Walsh JL, Wong KF, Salazar-Gomez AF, Harrell PG, Sampson AL, Cimenser A, Ching S, Kopell NJ, Tavares-Stoeckel C, Habeeb K, Merhar R, Brown EN: Electroencephalogram signatures of loss and recovery of consciousness from propofol. *Proc Natl Acad Sci USA* 2013; 110:E1142–51
8. Mashour GA, Hudetz AG: Neural correlates of unconsciousness in large-scale brain networks. *Trends Neurosci* 2018; 41:150–60
9. Akeju O, Pavone KJ, Thum JA, Firth PG, Westover MB, Puglia M, Shank ES, Brown EN, Purdon PL: Age-dependency of sevoflurane-induced electroencephalogram dynamics in children. *Br J Anaesth* 2015; 115:i66–76
10. Cornelissen L, Kim SE, Lee JM, Brown EN, Purdon PL, Berde CB: Electroencephalographic markers of brain development during sevoflurane anaesthesia in children up to 3 years old. *Br J Anaesth* 2018; 120:1274–86

Regional Anesthesia

A Silver Bullet, Red Herring, or Neither?

Eric C. Sun, M.D., Ph.D., Stavros G. Memtsoudis, M.D., Ph.D., M.B.A., Edward R. Mariano, M.D., M.A.S.

Today, clinicians in the perioperative realm are faced with increasing pressure from payers and policymakers to improve longer-term postoperative outcomes such as resource utilization (*i.e.*, reduced readmission rates) and persistent opioid use after surgery. Many anesthesiologists believe that nerve blockade can play an important role in achieving these aims. This belief is fairly intuitive; a large body of literature has established that regional anesthesia is associated with increased mobility and decreased risk for many short-term complications.¹ Moreover, the evidence strongly suggests that regional anesthesia is associated with improved pain control, which provides a basis for the assumption that it could reduce the risk of persistent postoperative opioid use. However, although widespread, is this belief actually true? In this issue of *ANESTHESIOLOGY*, Hamilton *et al.*² address this issue by comparing longer-term outcomes (*i.e.*, readmission rates and costs within 7 days of surgery as a primary outcome and within 30 days as a secondary outcome) among ambulatory shoulder surgery patients who received peripheral nerve blockade to those who did not. Overall, these researchers found that nerve blockade was not associated with any difference in a composite outcome measure, although it was associated with a small increase in costs (which may largely reflect the costs of the block itself), and—in a secondary analysis—a modestly reduced readmission rate.

The study has many strengths, such as the large size (59,644 patients from 118 hospitals), and careful statistical approach that adjusted for many possible confounders. As with any observational study, there is the concern of selection



“[A]lthough clinical intuition and a fairly robust literature suggest that nerve blockade is associated with improvements in short-term outcomes...the current state of nerve blockade has little impact on longer-term outcomes.”

and indication bias because patients who received blocks and the anesthesiologists who performed them may be different from those who did not. Irrespectively, it is worth noting that patients who received a block had generally similar characteristics compared with those who did not, although important patient and practitioner-related covariates may not have been available.

Although this study was limited to ambulatory shoulder surgery, other studies have found no association between nerve blockade and longer-term outcomes in a variety of settings.^{3–5} Thus, we are left with a dilemma: although clinical intuition and a fairly robust literature suggest that nerve blockade is associated with improvements in short-term outcomes, ultimately, the findings of this study—in line with others—suggest that the current state of nerve blockade has little impact on longer-term outcomes. This dilemma raises two important questions. First, given the lack of evidence that it impacts longer-term outcomes, should nerve blockade be abandoned in routine practice? Our opinion is that it should not: Anesthesiologists should still advance the science and clinical practice of regional anesthesia based on the well-demonstrated short-term benefits of nerve blocks, while realizing that the literature to date is at best equivocal in suggesting a longer-term benefit.

The second question is why is there a discrepancy between studies examining short-term outcomes, which have generally found better outcomes with nerve blockade, and studies that have examined longer-term outcomes, which generally have not? An easy answer is that this simply reflects the reality of the situation, but there are several other possibilities with important

Image: J. P. Rathmell.

This editorial accompanies the article on p. 1254.

Accepted for publication July 26, 2019. From the Department of Anesthesiology, Perioperative and Pain Medicine (E.C.S., E.R.M.) and Department of Health Research and Policy (E.C.S.), Stanford University School of Medicine, Stanford, California; Department of Anesthesiology, Hospital for Special Surgery, Weill Medical College of Cornell University, New York, New York (S.G.M.); Anesthesiology and Perioperative Care Service, Veterans Affairs Palo Alto Health Care System, Palo Alto, California (E.R.M.).

Copyright © 2019, the American Society of Anesthesiologists, Inc. All Rights Reserved. *Anesthesiology* 2019; 131:1205–6. DOI: 10.1097/ALN.0000000000002964

implications for research and clinical practice. The first possibility concerns variations in clinical practice. In this study, single-injection and continuous catheter approaches were grouped together as nerve blockade. Moreover, neither this study nor any other studies to date have considered factors such as dosing and length of infusion (in the case of continuous catheters). Intuitively, it may very well be the case that, for nerve blockade techniques to demonstrate longer-term benefits, the block must last for a longer time (*i.e.*, continuous infusion for several days). However, as demonstrated by this study and others,⁶ continuous catheters represent a small fraction of the nerve blocks that are placed in clinical practice. A second factor is the possibility of effect dilution. Half of the patients in the study by Hamilton *et al.*² received a block. If we assume that the block would only be beneficial in a minority of these patients (*i.e.*, those with severe comorbidities), the benefits of the block for this subpopulation would be diluted or averaged out by the majority of patients for whom the block had little benefit. A final factor is the simple fact that long-term outcomes, particularly opioid use, represent the sum of a patient's long-term interactions with the healthcare system (*i.e.*, the patient's surgeon and primary care physician). In this context, it may make sense that a nerve block, as one of many other perioperative interventions, would, at least by itself, have limited effect on longer-term outcomes.

In light of these factors, perhaps one key takeaway from this study is that anesthesiologists should focus on the use of continuous nerve catheters and/or other modalities that extend analgesia to match the trajectory of pain resolution. Moreover, this study suggests that further research should focus on identifying who is likely to benefit from a block, and that in clinical practice, anesthesiologists should expend efforts on making sure that blocks are offered—and made available—to the right patients (*i.e.*, those who will benefit most). Finally, because long-term outcomes are determined in large part by the patient's longer-term interaction with the healthcare system, anesthesiologists—as part of our desire to be holistic perioperative physicians—may need to consider how we can impact these interactions (*i.e.*, through healthcare system changes) to improve these outcomes.

Ultimately, given its benefits in the short term, nerve blockade should continue to be an important part of anesthesiology practice and considered as a first-line approach for many patients. However, at least for now, anesthesiologists should recognize that the evidence for longer-term benefit is mixed at best. Going forward, research and clinical practice should be aimed at identifying and addressing factors that may limit the ability of nerve blockade to improve long-term outcomes.

Research Support

Dr. Sun acknowledges support from the National Institute on Drug Abuse (Bethesda, Maryland; grant No. K08DA042314).

Competing Interests

Dr. Sun reports receiving consulting fees from Egalet, Inc. (Wayne, Pennsylvania), and the Mission Lisa Foundation

(Tampa, Florida) that are unrelated to this work. Dr. Memtsoudis reports consulting fees from Teikoku (San Jose, California) and Sandoz (Princeton, New Jersey). He is a medical advisory board member for HATH (Bedford Hills, New York) and has a pending patent application for a multi-catheter infusion system. He is the owner of SGM Consulting, LLC (Rumson, New Jersey). None of these relationships are related to this work. Dr. Mariano is not supported by, nor maintains any financial interest in, any commercial activity that may be associated with the topic of this article.

Correspondence

Address correspondence to Dr. Sun: esun1@stanford.edu

References

1. Memtsoudis S, Cozowicz C, Bekeris J, Bekere D, Liu J, Soffin E, Mariano E, Johnson R, Hargett M, Lee B, Wendel P, Brouillette M, Go G, Kim S, Baaklini L, Wetmore D, Hong G, Goto1 R, Jivanelli B, Argyra E, Barrington M, Borgeat S, Andres JD, Elkassabany N, Gautier P, Gerner P, Valle AD, Goytizolo E, Kessler P, Kopp S, Lavand'Homme P, MacLean C, Mantilla C, MacIsaac D, McLawhorn A, Neal J, Parks M, Parvizi J, Pichler L, Poeran J, Poultides L, Sites B, Stundner O, Sun E, Viscusi E, Votta-Velis E, Wu C, Deau JY, Sharrock N: Anaesthetic care of patients undergoing primary hip and knee arthroplasty: Recommendations from the International Consensus on Anaesthesia Related Outcomes after Surgery (ICAROS) Group based on a systematic review and meta-analysis of the literature. *Br J Anaesth* 2019; 123:269–87
2. Hamilton GM, Ramlogan R, Lui A, McCartney CJL, Abdallah F, McVicar J, McIsaac DI: Peripheral nerve blocks for ambulatory shoulder surgery: A population-based cohort study of outcomes and resource utilization. *ANESTHESIOLOGY* 2019; 131:1254–63
3. Mueller KG, Memtsoudis SG, Mariano ER, Baker LC, Mackey S, Sun EC: Lack of association between the use of nerve blockade and the risk of persistent opioid use among patients undergoing shoulder arthroplasty: Evidence from the Marketscan Database. *Anesth Analg* 2017; 125:1014–20
4. Chi D, Mariano ER, Memtsoudis SG, Baker LC, Sun EC: Regional anesthesia and readmission rates after total knee arthroplasty. *Anesth Analg* 2019; 128:1319–27
5. Ladha KS, Patorno E, Liu J, Bateman BT: Impact of perioperative epidural placement on postdischarge opioid use in patients undergoing abdominal surgery. *ANESTHESIOLOGY* 2016; 124:396–403
6. Gabriel RA, Ilfeld BM: Use of regional anesthesia for outpatient surgery within the United States: A prevalence study using a nationwide database. *Anesth Analg* 2018; 126:2078–84

Aiming to Refine the Interscalene Block

Another Bullseye or Missing the Mark?

Nabil M. Elkassabany, M.D., M.S.C.E., Edward R. Mariano, M.D., M.A.S.

In this issue of *ANESTHESIOLOGY*, Kang *et al.*¹ present the results of a randomized clinical trial in arthroscopic shoulder surgery patients which compares interscalene brachial plexus block with a more selective superior trunk block. The authors conclude that a superior trunk block results in noninferior analgesia and a lower risk of hemidiaphragmatic paresis (76%) when compared with interscalene block (98%). According to the authors, the superior trunk block represents “a refinement of the conventional interscalene block technique.”¹ This begs the question: Why does the interscalene block need to be refined?

One way to address this question is to use a quality improvement model.² One such model asks: (1) What are we trying to accomplish?; (2) How will we know that a change is an improvement?; and (3) What change can we make that will result in an improvement? Underlying all improvement models is general acceptance of the following concept: all improvement requires change, but not all change represents improvement.²

First, we will determine what the authors are trying to accomplish. The primary concern raised by Kang *et al.* with regard to the interscalene block is the risk of ipsilateral phrenic nerve block and subsequent temporary hemidiaphragmatic paresis. This has been a well-known side effect of interscalene block,³ and numerous alternative interventions have been proposed to avoid phrenic nerve block (table 1).⁴ Although effects on pulmonary function associated with hemidiaphragmatic paresis have been measured and reported by the authors of the current study and others,^{4,5} these measurements are typically limited to the immediate periprocedural episode, and data on downstream clinical and healthcare utilization outcomes (*e.g.*, unplanned admissions, emergency department visits) specifically



“[D]oes the interscalene block need to be refined?”

attributable to side effects of regional anesthesia are lacking. In a national database study including more than 15,000 patients who underwent arthroscopic shoulder surgery, the overall readmission rate was approximately 1%, and the primary associated risks were surgical factors and patient comorbidities.⁶ A larger study using a New York state database reported the rate of emergency department visits after arthroscopic shoulder surgery to be less than 2%, with pain being the most common reason, and use of regional anesthesia was associated with lower odds of requiring postoperative acute care.⁷ In a Veterans Affairs cohort study of ambulatory peripheral nerve block catheter patients, 6 of 185 patients (3%) who received an interscalene perineural catheter reported any subjective respiratory symptoms; 4 sought medical care, and all 6 resolved with discontinuing the local anesthetic infusion.⁸ In the study by Kang *et al.*, one patient in each group “developed symptomatic dyspnea without desaturation” and required no interventions.¹ Given these statistics, the risk of temporary asymptomatic hemidiaphragmatic paresis does not appear to be the highest priority problem worth solving in the general population of shoulder surgery patients, although we acknowledge that this side effect may be an important consideration for patients with severe pulmonary disease.

Next, we will assess whether or not the change is an improvement. The rates of complete hemidiaphragmatic paresis reported by Kang *et al.*¹ clearly favor superior trunk block over interscalene block (5% *vs.* 72%, respectively), but the difference in rates of any hemidiaphragmatic paresis is less dramatic (76% *vs.* 98%).¹ The primary outcome of 24-hour pain score at rest was noninferior between groups. All arthroscopic shoulder surgery patients in this study were

Image: J. P. Rathmell.

This editorial accompanies the article on p. 1316.

Accepted for publication August 14, 2019. From the Department of Anesthesiology and Critical Care, University of Pennsylvania, Philadelphia, Pennsylvania (N.M.E.); Department of Anesthesiology, Perioperative and Pain Medicine, Stanford University School of Medicine, Stanford, California (E.R.M.); Anesthesiology and Perioperative Care Service, Veterans Affairs Palo Alto Health Care System, Palo Alto, California (E.R.M.).

Copyright © 2019, the American Society of Anesthesiologists, Inc. All Rights Reserved. *Anesthesiology* 2019; 131:1207–9. DOI: 10.1097/ALN.0000000000002985

Table 1. Alternative Regional Analgesic Techniques to Standard Interscalene Brachial Plexus Block that May Decrease the Incidence of Hemidiaphragmatic Paresis

Interscalene block “light”	• Interscalene block but with lower doses of local anesthetic
Interscalene block catheter	• Continuous interscalene block using lower rates of infusion
Superior trunk block	• Block distal to interscalene location but before branching of suprascapular nerve
Supraclavicular block	• Distal brachial plexus block approximately at the level of divisions
	• Can perform superior trunk block at this level although suprascapular nerve may be spared
Distal peripheral nerve block(s)	• Isolated suprascapular nerve block
	• Combined suprascapular and axillary nerve blocks (also known as “shoulder block”)

admitted for 3 days after surgery, although they would have been discharged the same day from nearly all facilities in the United States. The multimodal analgesic regimen consisted of scheduled oral acetaminophen, celecoxib, and opioids as well as an IV fentanyl patient-controlled analgesia and as-needed IV boluses of morphine.¹ Not surprisingly, the pain scores in both groups were low and did not differ. What was surprising to us was the average opioid consumption in both groups: 61 IV morphine milligram equivalents for interscalene and 58 IV morphine milligram equivalent for superior trunk block (which convert to 183 and 176 oral morphine milligram equivalent for interscalene block and superior trunk block, respectively).¹ With these doses of opioids and in the context of other analgesic modalities, we would find it difficult to hypothesize a difference between any two regional analgesic interventions for any surgical indication. Based on the outcomes of hemidiaphragmatic paresis and analgesia in 24h, we cannot definitively conclude that superior trunk block represents a clinically relevant improvement over interscalene block.

Finally, we will explore what kind of change will result in real improvement. When evaluating new techniques, it may be useful to apply pragmatic criteria.⁹ We can rate both blocks on the following categories: improving access to regional analgesia for surgery patients, enhancing efficiency, decreasing disparities, and improving outcomes.⁹ Because outcomes have been addressed previously, we can focus on access, efficiency, and disparities. All blocks for the study were performed by a single expert regional anesthesiologist; all 40 interscalene block participants received their assigned block, but 2 of the 40 participants assigned to superior trunk block could not receive their assigned procedure.¹ In one participant, the transverse cervical artery prevented access to the superior trunk; in the other, the branching point of the suprascapular nerve could not be identified.¹ Both of these patients received an interscalene block for their surgeries instead. Careful identification of these detailed anatomic findings during superior trunk block will require expert-level ultrasound skills, and perhaps more scanning time. This level of expertise may not be available at the average hospital or surgery center. Therefore, we can safely conclude that superior trunk block may not improve access (experts already doing interscalene block may change to superior trunk block), may decrease efficiency (more scanning time),

and may increase disparities (only centers with advanced sonographic expertise may be able to perform superior trunk block).

If changing from interscalene to superior trunk block does not represent meaningful improvement, where else can we improve the clinical practice of regional analgesia for shoulder surgery? Although the development of new advanced techniques in regional anesthesia and analgesia is exciting for experts in the subspecialty, many patients everyday are not receiving any regional anesthesia.¹⁰ Using a nationwide anesthesia database with more than three million outpatient surgical cases that would have been amenable to regional analgesia, Gabriel and Ilfeld¹⁰ found that only 3% of those cases received a block. Looking specifically at arthroscopic shoulder surgery cases, regional analgesia was used in only 41% of them.¹⁰ Increasing patient access to regional anesthesia may represent the most meaningful improvement. A starting point for improvement is establishing a core set of regional anesthesia procedures that every new board-certified anesthesiologist can perform competently and safely for eligible surgical patients. Fellowship-trained regional anesthesiologists and acute pain medicine specialists will serve as the experts in the clinical setting and advocates for system-wide improvements in perioperative pain management, but we will need graduating residents in anesthesiology comfortable with basic regional anesthesia techniques for common surgeries like shoulder arthroscopy to be the frontline agents of change and increase patient access.

Competing Interests

The authors are not supported by, nor maintain any financial interest in, any commercial activity that may be associated with the topic of this article.

Correspondence

Address correspondence to Dr. Elkassabany: Nabil. Elkassabany@pennmedicine.upenn.edu

References

1. Kang R, Jeong JS, Chin KJ, Yoo JC, Lee LH, Choi SJ, Gwak MS, Halm TS, Ko JS: Superior trunk block provides noninferior analgesia compared with interscalene

- brachial plexus block in arthroscopic shoulder surgery. *ANESTHESIOLOGY* 2019; 131:1316–26
2. Silver SA, Harel Z, McQuillan R, Weizman AV, Thomas A, Chertow GM, Nesrallah G, Bell CM, Chan CT: How to begin a quality improvement project. *Clin J Am Soc Nephrol* 2016; 11:893–900
 3. Urmey WF, Talts KH, Sharrock NE: One hundred percent incidence of hemidiaphragmatic paresis associated with interscalene brachial plexus anesthesia as diagnosed by ultrasonography. *Anesth Analg* 1991; 72:498–503
 4. Tran DQ, Elgueta MF, Aliste J, Finlayson RJ: Diaphragm-sparing nerve blocks for shoulder surgery. *Reg Anesth Pain Med* 2017; 42:32–8
 5. Wong AK, Keeney LG, Chen L, Williams R, Liu J, Elkassabany NM: Effect of local anesthetic concentration (0.2% vs 0.1% ropivacaine) on pulmonary function, and analgesia after ultrasound-guided interscalene brachial plexus block: A randomized controlled study. *Pain Med* 2016; 17:2397–403
 6. Hill JR, McKnight B, Pannell WC, Heckmann N, Sivasundaram L, Mostofi A, Omid R, Rick Hatch GF 3rd: Risk factors for 30-day readmission following shoulder arthroscopy. *Arthroscopy* 2017; 33:55–61
 7. Liu J, Flynn DN, Liu WM, Fleisher LA, Elkassabany NM: Hospital-based acute care within 7 days of discharge after outpatient arthroscopic shoulder surgery. *Anesth Analg* 2018; 126:600–5
 8. King R, Mariano ER, Yajnik M, Kou A, Kim TE, Hunter OO, Howard SK, Mudumbai SC: Outcomes of ambulatory upper extremity surgery patients discharged home with perineural catheters from a Veterans Health Administration medical center. *Pain Med* 2019 Mar 11 [Epub ahead of print]
 9. Mudumbai SC, Auyong DB, Memtsoudis SG, Mariano ER: A pragmatic approach to evaluating new techniques in regional anesthesia and acute pain medicine. *Pain Manag* 2018; 8:475–85
 10. Gabriel RA, Ilfeld BM: Use of regional anesthesia for outpatient surgery within the United States: A prevalence study using a nationwide database. *Anesth Analg* 2018; 126:2078–84

ANESTHESIOLOGY

Etymology of *Letheon*

Nineteenth-century Linguistic Effervescence

Rajesh P. Haridas, M.B.Ch.B., F.A.N.Z.C.A.,
Michael Gionfriddo, B.A., George S. Bause, M.D., M.P.H.

ANESTHESIOLOGY 2019; 131:1210–22

Speed on the ship! But let her bear
No merchandise of sin,
No groaning cargo of despair
Her roomy hold within;
No Lethean drug for Eastern lands,
Nor poison-draught for ours;
But honest fruits of toiling hands
And Nature's sun and showers.

—“The Ship-Builders” (1846), by John Greenleaf
Whittier (1807–1892).

Seeking to commercialize the discovery of etherization in 1846, Boston dentist William T. G. Morton (1819–1868; fig. 1)¹ applied for a patent and then selected the trade name *Letheon* for his narcotic preparation. *Letheon* was essentially sulfuric (diethyl) ether, with a fragrance and a coloring agent. Almost from the outset, questions arose about the validity of Morton's patent and whether he should profit from it.

Historians have focused a good deal on Morton's character, his patent, and his disputes with dentists and physicians. Relatively little has been written about the coinage of the word *Letheon* itself, probably because its easy derivation from the Greek *lēthē* (forgetfulness, oblivion) has long been assumed. But who actually coined the name, when, and under what circumstances? What lay behind this particular linguistic tease? In fact, the mid-19th century was alive with language study, wordplay, neologisms, and inquiries into the origins of language itself. When Morton sought to advertise his discovery to a surprised and curious public, he welcomed the help of physicians who were trained in the classical canon. They presented Morton with a signature term designed to turn heads and arrest attention. We offer here an examination of the

ABSTRACT

In late 1846, following his successful public demonstrations of surgical anesthesia, Boston dentist William T. G. Morton selected *Letheon* as the commercial name for the ether-based “preparation” he had used to produce insensibility to pain. We have not identified a first-hand account of the coinage of *Letheon*. Although the name ultimately derives from the Greek *lēthē*, the adjective *Lethean*, much in use in the mid-19th century, may have influenced Morton and those he called on to assist in finding a commercial name. By one unverified account, the name *Letheon* might have been coined independently by both Augustus Addison Gould, M.D., and Henry Jacob Bigelow, M.D.

(*ANESTHESIOLOGY* 2019; 131:1210–22)

etymology of *Letheon* in light of 19th-century notions of verbal play and linguistic inquiries.

Boston, Massachusetts: October 1846

On October 16, 1846, Morton administered his then-undisclosed anesthetic preparation to a surgical patient at the Massachusetts General Hospital, Boston, Massachusetts. The hospital's senior visiting surgeon, John Collins Warren, M.D. (1778–1856; Hersey Professor of Anatomy and Surgery, Harvard Medical School, Boston, Massachusetts), operated on a congenital vascular malformation in the neck of his patient, Edward Gilbert Abbott.² According to Henry Jacob Bigelow, M.D. (1818–1890), a recently appointed surgeon at the hospital, the patient “muttered, as in a semi-conscious state,” afterward stating that “the pain was considerable, though mitigated...as though the skin had been scratched with a hoe.”³ The etherization for this relatively minor operation was nevertheless considered a partial success. This was the first public demonstration of surgical etherization.

Although some observers of Morton's historic demonstration had detected the smell of sulfuric ether, they were not certain that it was the active ingredient in Morton's preparation. Most would have known, of course, that ether was a widely used chemical solvent. Bigelow reported he himself “undertook a number of experiments, with the view of ascertaining the nature of this new agent,” going on to say the “first experiment was with sulphuric ether, the odor of which was readily recognized in the preparation employed by Dr. Morton.”³ We should note, though, that Bigelow's article on etherization was published in mid-November when the surgeons at the Massachusetts General Hospital were aware of the identity of Morton's preparation.

On October 27, just eleven days after Morton's demonstration, a joint patent application was signed by Morton and

Submitted for publication February 21, 2019. Accepted for publication August 7, 2019. From the Harry Daly Museum and Richard Bailey Library, Australian Society of Anaesthetists, North Sydney, New South Wales, Australia (R.P.H.); Departments of Anesthesiology and Perioperative Medicine and Oral and Maxillofacial Surgery, Case Western Reserve University School of Medicine, Cleveland, Ohio (G.S.B.); Wood Library-Museum of Anesthesiology, Schaumburg, Illinois (G.S.B.).

Copyright © 2019, the American Society of Anesthesiologists, Inc. All Rights Reserved. *Anesthesiology* 2019; 131:1210–22. DOI: 10.1097/ALN.00000000000029692019

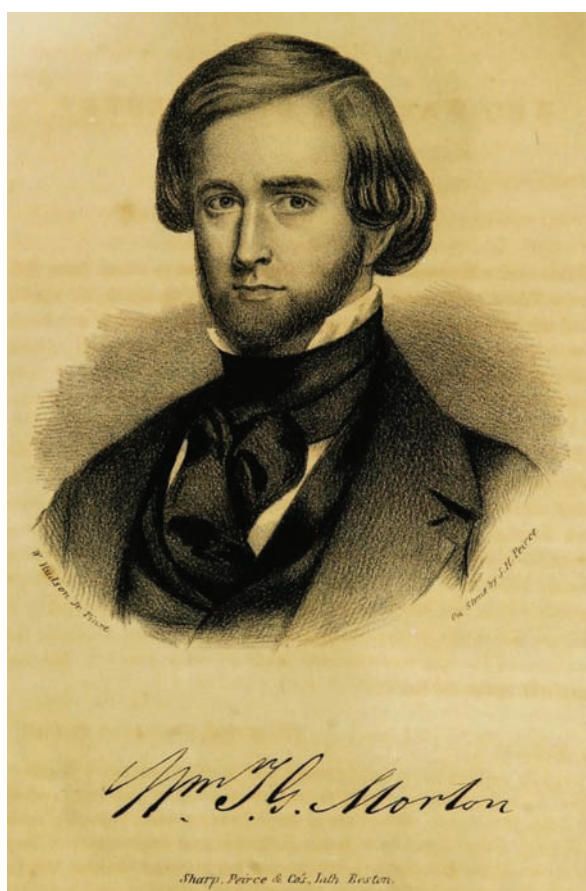


Fig. 1. William T. G. Morton, M.D. (1819–1868). An engraved portrait published in 1847 in the first edition of Edward Warren's pamphlet *Some Account of the Letheon; Or, Who was the Discoverer?*¹ Image reproduced with the permission of Yale University, Harvey Cushing/John Hay Whitney Medical Library, New Haven, Connecticut.

Charles T. Jackson, M.D. (1805–1880; Boston physician, chemist, and geologist). Immediately thereafter, Jackson assigned his financial rights in the patent to Morton. Although Jackson was no longer working as a physician (he had ceased practicing medicine a decade earlier), he continued to instruct medical students. As a member of the Massachusetts Medical Society, Jackson was not permitted to deal in secret remedies or profit from medical inventions. The initial agreement was for Morton to pay Jackson \$500 for assistance and advice rendered.⁴

Boston, Massachusetts: November 1846

Contrary to claims in some historical accounts, Morton did not attempt to disguise the preparation he used on October 16, 1846, by calling it *Letheon*. The word *Letheon* does not appear in United States Patent No. 4848 ("Improvement in Surgical Operations"), which was granted to Jackson and Morton on November 12, 1846. This suggests that the

name was adopted after the patent application had been signed on October 27, 1846.

Morton's patent lawyer, Robert H. Eddy (1812–1887), received official notice of the granting of the patent on Saturday, November 14, 1846.⁴ The next day, Eddy attended a meeting at the Tremont Street home of Augustus Addison Gould, M.D. (1805–1866; Boston physician, entomologist, and conchologist). Also present were Bigelow, Morton, and Jackson.⁴ Bigelow's manuscript, "Insensibility During Surgical Operations Produced by Inhalation," which he intended to place in *The Boston Medical and Surgical Journal*, received the approval of both Morton and Jackson; the manuscript would be published three days later.³ As in the patent application, the name *Letheon* does not appear in Bigelow's article. Eddy commented that Bigelow, even at this late date, did make some changes "particularly at the latter part of the article"⁴; presumably, he could have included the name *Letheon* at that point had the name been decided. In fact, Bigelow skirts mentioning any particular name, saying only that the "application of the process to the performance of surgical operations, is, it will be conceded, new" before entering into a defense of patent rights and "the actual position of this invention as regards the public."³ Speaking to the testy relationship between Morton and Jackson, Eddy reported departing with Jackson, leaving Gould, Morton, and Bigelow behind. Though there is nothing to indicate that they discussed a name for Morton's new preparation, the possibility exists that Morton, Bigelow, or Gould might have broached the subject after Eddy and Jackson departed.

Soon thereafter, hoping to advertise the success of his endeavors, Morton enlisted the help of physician friends to come up with a commercial name for his preparation. He approached Bigelow and Gould, and probably consulted Oliver Wendell Holmes, M.D. (1809–1894), a Boston physician, poet, and author. In their published accounts of Morton's activities, neither Edward Warren (*Some Account of the Letheon*, 1847) nor Nathan P. Rice, M.D. (*Trials of a Public Benefactor*, 1859) recorded the date on which Morton selected the name *Letheon*. The two accounts differ in some particulars and neither hints at the full list of names that might have been proposed for Morton's new preparation. Later reminiscences penned by Gould's daughter⁵ and Morton's wife⁶ do little to illuminate the matter. Regardless, though, of who might have proposed or advanced one name or another, all were willing to participate in what would essentially be a commercial venture, even if no one other than Morton might actually profit from it. Further, all would have known by then that the prime constituent of Morton's preparation was sulfuric ether.

By the month's end, readers of *The Boston Medical and Surgical Journal* would see a short notice posted by Morton advising that "a name for this new operation" (*i.e.*, the administration of his "compound" to produce insensibility to pain) would shortly be forthcoming. Moreover, Morton would enter a short-lived partnership with the esteemed Boston physician and dentist Nathan C. Keep, M.D., D.D.S.

(1800–1875). Both Morton's notice and his alliance with Keep bear on our present inquiries.

The Origin of the Name *Letheon*

It is by now a critical commonplace to note that the name *Letheon* derives from the Greek word *Λήθη*, transliterated as *Lēthē* (pronounced *LEE-thee*) or simply *Lethe*, the name in Greek mythology of both the river of forgetfulness (fig. 2) and the goddess of forgetfulness. Such a notion suffices well enough. But while *Lēthē* was undoubtedly the foundational root of *Letheon*, other factors might have informed the 19th-century coinage, chief among them the common adjective *Lethean* (inducing forgetfulness and oblivion), a word that enjoyed great currency at the time but is largely forgotten today.

Lethe: The River, a Goddess, and a Butterfly

Lethe is defined by Liddell and Scott (1889, p. 889) as “a forgetting, forgetfulness” and, in the post-Homeric period, “a place of oblivion in the lower world.” A Greek fragment sometimes attributed to Simonides of Cos (ca. 556–467 B.C.E.) refers to “the house of Lethe” (www.attalus.org/poetry/simonides.html) near the Acheron, the underworld River of Pain or Woe. The concluding section of Plato's *Republic* (ca. 400 B.C.E.), sometimes referred to as the Myth of Er (Book 10, parts 614a–621d), identifies Lethe as the plain of forgetfulness through which flowed the river of Lethe or *Ameles potamos*, the river of “unmindfulness” (forgetfulness). The well-sourced online “Theoi Project” (www.theoi.com) notes that “LETHE was the underworld river of oblivion and its goddess. The shades of the dead drank of its waters to forget their mortal lives. . . . The river-goddess Lethe was sometimes identified with the daimona [or ‘spirit’] Lethe, forgetfulness personified.” Louise H. Pratt, Professor of Classics at Emory University, usefully extends the discussion, observing how, besides amnesia, Lethe can be associated more broadly with “an absence of awareness.”⁷⁷ But keeping within the groupings of Greek gods and goddesses, Lethe (a child of Eris, or Strife) came to be associated with the minor Olympian god Nyx (Night), the latter's consort Erebus (Darkness), and their children Hypnos (Sleep) and Thanatos (Death). In a well-known engraving for Homer's *Iliad* prepared by Tommaso Piroli (ca. 1752–1824) after the design by British sculptor and illustrator John Flaxman (1755–1826), Hypnos and Thanatos convey the body of the slain Sarpedon, son of Zeus and distinguished protector of Troy, to his homeland of Lycia (fig. 3).

The works of Greek and Roman writers, with which 19th-century literati like Drs. Gould, Bigelow, and Holmes would have been more than familiar, refer more to the river Lethe than to the goddess. The Roman poet Ovid (43 B.C.E. to 17/18 C.E.), for instance, finds the river flowing through the cave of Hypnos, god of sleep: “There silence dwells: only the lazy stream / Of Lethe. . . / O'er pebbly shallows trickling lulls to sleep.” (*Metamorphoses*, Bk. XI, lines 604–606, trans. Melville, 1986). The reference is echoed by



Fig. 2. Dante submerged in the River Lethe by Matilda. Illustration by Gustave Doré (1832–1883) for Dante's *The Divine Comedy: Purgatory*, Canto XXXI. From: *Purgatory and Paradise*. Translated by Henry Francis Cary. Edited by Henry C. Walsh. Philadelphia: Henry Altemus, [no publication or copyright date; ca. 1889], opp. p. 148. Image source Internet Archive. Book source University of Illinois at Urbana-Champaign, Illinois.

Geoffrey Chaucer (ca. 1343–1400), who, in his poem, “The House of Fame” (“Hous of Fame”, ca. 1379), invokes “the god of slepe anon, / That dwelleth in a cave of stoon / Upon a streem that comth fro Lete, / That is a flood of helle unswete;” (Bk.1, lines 69–72, ed. Walter W. Skeat, 1899).

The reading public would more likely have encountered allusions to Lethe in everything from Shakespearean plays to homespun stories and poems. William Shakespeare (1564–1616) used the word at least half a dozen times, playing on its meaning to gain a richly lyrical quality as he moves from mention of “a Lethe'd dullness” (*Anthony and Cleopatra* 2.1.27) to “the Lethe of thy angry soul” in which to drown one's sad remembrance (*Richard III* 4.4.252) to “duller shouldst thou be than the fat weed / That roots itself in ease on Lethe wharf” (*Hamlet* 1.5.32–33). The celebrated Washington Irving (1783–1859), in *Abbotsford and Newstead Abbey* (1835), includes a character who implores, “Away! away! my early dream / Remembrance never must awake: / Oh! where is Lethe's fabled stream?” Nathaniel Hawthorne (1804–1864), in his tale, “A Select Party,” from the popular *Mosses from an Old Manse* (1846), describes how, at the behest



Fig. 3. Sleep [Hypnos] and Death [Thanatos] conveying the body of Sarpedon to Lycia. Engraved by Tommaso Piroli (ca. 1752–1824) from a drawing by John Flaxman (1755–1826) for Homer's *Iliad*. From: Church AJ. *Stories from Homer*. London: Seeley, Jackson and Halliday, 1878, opp. p. 116. Image source Hathi Trust. Book source University of California Libraries. Digitized by Internet Archive.

of a congenial host, “the love-lorn, the care-worn, and the sorrow-stricken, were supplied with brimming goblets of Lethe.” The narrator of a poem by Edgar Allan Poe (1809–1849) sketches a typically dark landscape while standing “beneath the mystic moon”: “Looking like Lethe, see! the lake / A conscious slumber seems to take, / And would not, for the world, awake. / All Beauty sleeps!” (“The Sleeper,” 1845 version). Not all references were as innocent. A bit of dully feather-brained erotica, the comic novel entitled *A Voyage to Lethe* (1741), authored by the redoubtable “Capt. Samuel Cock, sometime commander of the good ship the Charming Sally,” and published in London by “J. Conybeare in Smock-Ally near Petticoat Lane in Spittlefields,” appropriated the word as a simple place name, its meaning implied but unimportant, just one stop on a tour of sexual shenanigans disguised as all-but-impenetrable metaphors.

Nathan P. Rice, M.D., Morton’s authorized biographer, had written in *Trials of a Public Benefactor* that the provenance of the word *Letheon* was the Greek *Lēthē*.⁸ “The term,” Rice noted, “was derived from the name of the river Lethe, said in mythology to be one of the rivers in the infernal regions,” going on to note the association of the waters of the river with forgetfulness and oblivion.⁸ Perhaps Rice was relying on received wisdom or perhaps he simply assumed the derivation based on his own familiarity with mythologic associations. Such associations, however, did not stop with the forgetfulness and benign oblivion of anesthesia.

The coinage could not play on the Greek *Lēthē* without at least a sidelong glance at its Latin cognate *lētum*, meaning “death” (which more directly gives us our word *lethal*). But it did so in a way that emphasized a more benign state, not Chaucer’s “helle unswete,” but Shakespeare’s “Lethe’d dullness” stirred up from Hawthorne’s “brimming goblets.” A near-cadaveric repose, properly managed and contrary to anyone’s experience to date, was now a consummation devoutly to be wished. In his “Ode on Melancholy” (1819, published 1820), the English poet John Keats (1795–1821) had warned off readers with the striking “No, no, go not to Lethe, neither twist / Wolf’s-bane, tight-rooted, for its poisonous wine,” proceeding to a litany of images equally associated with death (toxic nightshade and yew-berries, the beetle, and the owl): “Nor let the beetle,” he wrote, “nor the death-moth be / Your mournful Psyche... / For shade to shade will come too drowsily, / And drown the wakeful anguish of the soul.” He argues here against the melancholy afforded by contemplation of a too-easy death, and he does so in terms that Gould, Holmes, and Bigelow, for instance, might readily have embraced. With *Letheon*, we proceed across or *on* Lethe (“Lethe” + “on”), appearing insensate, dead, but tricking perception by overturning it. Proceed, they might have been thinking, across Lethe as you would on the wings of the “death-moth” (*i.e.*, become the soul taking leave of the body), but consider how, through the careful ministrations of the dentist or surgeon, the soul will

return unchanged to the body and a deep sleep of forgetfulness need no longer be thought the sleep of oblivion (death).

Still other things may yet have been at play. Augustus Gould, one of Morton's intimates, had been a zoology instructor at Harvard before focusing on entomology and then conchology. Using his knowledge of Latin and Greek, Gould either coined or sought consensus on generic and specific names for novel or redundantly referenced species by the hundreds. Familiar with the seminal work of the entomologists Jacob Hübner (1761–1826) of Germany and Johan(n) Christian Fabricius (1745–1808) of Denmark, he would have been acquainted with the shade-seeking *Lethe* genus of butterfly, several species of which are now considered native to New England. By a short imaginative leap, Gould, the etymologist–entomologist, might easily have reimagined shade-seeking butterflies as shade-seeking souls—men and women, that is, troubled by disease or injury and nervously contemplating surgery, now at last without an expectation of pain unto death but rather the restful dark shade of amnesia offered by the new compound with the winking name of *Letheon*.

Gould in particular might have touched Keats' rather startling imagery with a scientist's hand, alighting on the mention of the “death-moth” and letting his fancy roam. (Fabricius noted, in 1798, the genus *Acherontia lachesis*, the death's-head hawk-moth, of which Keats might or mightn't have been aware; tellingly, *A. lachesis* takes its name in part from Acheron, the underworld River of Pain or Woe noted above.) And any learned punster might have done him one better, recognizing that the Greek *Lēthē* finds a Latin equivalent not only in *lētum* but also in *mors*, *-tis* (which yields, for instance, the English “mortal” and “mortician”). A poetic jocularly attends the recognition that were the Latin root substituted for the Greek, *Letheon* (*Lēthē* + the common suffix *-on*) becomes “Morton” (*mort-* + *-on*). Or perhaps the play worked in reverse, the surname of the eager young dentist suggesting, along classical lines almost too faint to trace, the product name with which to promote the new anodyne gas. As we discuss below (“The Coinage: *Lethe*, *Lethean*, *Letheon*”), the Latin phrase *lucus a non lucendo* (meaning, *via* an imaginative and twisting translation, an “illogic explanation” or “absurd derivation”) was well enough known to the polyglot Holmes in particular to have bounded into view for just enough time to leave its mark.

Lethean in the Lexicon

Morton, whose educational pedigree was not nearly as distinguished as that of the physicians with whom he associated, was probably unfamiliar with etymological niceties, and none but specialists like Gould would have known of the butterfly genus *Lethe*. But all would have recognized the importance of presenting not only a new product but also a name with commercial appeal. If the “*Lethe*” of the poets carried unwanted hints of mortal demise, the adjective

Lethean—fortuitously already alive and abroad—stopped just short of an underworld passage harboring rank oblivion. Definitions of *Lethean* initially drew from both the Greek *Lēthē* and its Latin cognate *lētum* (death). The Anglicized *Lethean* (generally capitalized) likely entered the English vernacular at some point in the 16th or early 17th century.

The earliest dictionaries were little more than bilingual compilations of words with simple definitions. *Medulla Grammaticae [Marrow (Core) of Grammar]* (Pepys Library MS 2002, ca. 1480), carries not only the entry *Lethe*, with a simple comment (“grece an[gl]ice forgettyng[e]”) that translates as “Greek; in English, forgetting”, but also the Latin *Letu[m]* listed with no more than an analogous word “*mors*”. Similarly, *Ortus Vocabulorum [A Garden of Words]*, a Latin-English dictionary first printed in 1500, includes both *Lethe* (“grece. angl'. forgettyng”) and *Letum* (with a notation roughly translating as “equivalent to *mors* which in English means ‘deth.’”). John Withals (d. ca. 1556) produced, in 1553, *A shorte Dictionarie for yonge begynners*, which became a standard instructional work. His note for *Lethargus* translates as “forgetfulness, a disease that compels one to sleep”; our modern word *lethargy* carries the medical connotation even now.

In 1604, Robert Cawdrey (ca.1538 to ca.1604) assembled the first monolingual English dictionary, *A Table Alphabeticall*, providing definitions for *lethall* (“mortall, deadly”) and *lethargie* (“a drowsie and forgetfull disease”) but no related words. A few years later, Randle Cotgrave (ca. 1569–1634?), in his *Dictionarie of the French and English Tongues* (1611), noted the French forms *lethean* (masc.) and *letheanne* (fem.), most likely imported from the French *Les Épithètes [Special Words]* (1571) compiled by Maurice de La Porte (1531–1571). Cotgrave's definition of *Lethean*, the earliest we have found in an English dictionary, was “deadlie, mortall, pestilent, death-inflicting”; his listing included *Lethe* (“death; mortalitie; obliuion”), and the allied words *lethal* (“deadlie, mortall; pestiferous”), *lethargie* (“a drowsie, and forgetfull sicknesse”), and *lethargique* (“sicke of a Lethargie, or of the drowsie ill”).

Thomas Blount (1618–1679), in *Glossographia* (1656), offered “forgetful” as his first definition of *Lethean* (from the Latin *letheus*), and secondarily “deadly, mortal, pestiferous” (from the Latin *Lætheus*). *Lethe* was “a feigned [*i.e.*, imaginary, fictional] River of Hell, the water whereof being drunk, causeth forgetfulness of all that is past; Hence it is used for Oblivion or forgetfulness.” Drawing heavily from Blount, Edward Phillips (1630 to ca.1696), in *The New World of English Words: Or, a General Dictionary* (1658), defined *Lethean* only as “forgetful,” with a note on its derivation “from *Lethe* a River of Hell, which the Poets feign [*i.e.*, imagine] to be of that nature that the water of it being drunk, causeth oblivion or forgetfulness.” A 1706 revision of Phillips' dictionary by John Kersey the younger (b. ca. 1660 – d. in or after 1721), entitled *The New World of Words: Or, Universal English Dictionary*, omitted the word *Lethean*.

By the mid-18th century, Samuel Johnson (1709–1784) would include *lethargick* (“sleepy”), *lethargickness* (“sleepiness; drowsiness”), *lethargy* (“a morbid drowsiness”), *lethargied* (“laid asleep; entranced”), and *lethe* (“oblivion; a draught of oblivion”), but not *Lethean* in his monumental *Dictionary of the English Language* (two vols., 1755). Elsewhere in the dictionary, Johnson quoted sources using the word *Lethean*, among them John Dryden’s translation, published in 1697, of Virgil’s *Aeneid* (“Whole Drowes of Minds are, by the driving God, / Compell’d to drink the deep *Lethæan* Flood”; vi, 1016–17), and Richard Crashaw’s “Sospetto d’Herode” (published in *Steps to the Temple*, 1646), a translation of the first book of a sacred poem by Giovan Battista Marino, with the lines, “the Night’s companion...kindly cheating them / Of all their cares.../ Sealing all breasts in a *Lethæan* band” (verse 49).

Johnson had overlooked *Lethean* but he could assume educated readers would be aware of its meaning. The 1828 revision by Walker and Jameson, a more streamlined one-volume text more handily used by students and others, expanded its list of definitions to include both *Lethean* (“oblivious; causing oblivion”) and *lethiferous* (“deadly; bringing death”). In his encyclopedic 1828 *American Dictionary of the English Language*, Noah Webster (1758–1843), citing Greek and Latin roots, included *Lethean* (“inducing forgetfulness or oblivion”) as well as *lethal* (“deadly; mortal; fatal”) and *lethiferous* (“deadly; mortal; bringing death or destruction”); Joseph E. Worcester (1784–1865) followed suit in compiling *A Universal and Critical Dictionary of the English Language* (1846).

Lethean in the Language of Everyday Life

The word *Lethean* (an adjectival form of *Lethe*) entered the language in the 16th century or early 17th century (probably via the French *lethean*, -anne) as Middle English and Middle French forms were expanded and simplified. By the 19th century, readers would have encountered it as part of the language of everyday life.

As its earliest example, the *Oxford English Dictionary* (1879–1928) cited James Howell (ca. 1594–1666), who in his oft-reprinted *Familiar Letters* (1647) writes, “I did not think *Suffolk* Waters had such a *Lethean* Quality in them as to cause such an *Amnesia* in him of his Friends here upon the *Thames*” (*The Familiar Letters of James Howell*, 1890 reprint, pp. 520–521). An even earlier source is “Holy Sonnet IX” (ca. 1610, first published in 1633 as “Holy Sonnet V”) by John Donne (1572–1631), which implores God to make of the poet’s tears “a heavenly *Lethean* flood” in which to drown his “sinnes blacke memorie.” John Milton (1608–1674), in *Paradise Lost* (1667), speaks of how the damned “ferry over this *Lethean* Sound” in their progress through the underworld (Bk. 2, line 604).

In citing John Dryden (1631–1700) and the 1697 publication of his translation of Virgil’s *Georgics* (“Nine Mornings thence, *Lethean* Poppy bring,” iv. 787) along with

a few more recent examples, the *Oxford English Dictionary* barely hints at how much the word flourished as a favorite with 19th-century writers of all stripes. An unattributed poem in London’s *The Sporting Magazine* (January 1800, Vol. 15, p. 216), speaks ominously of “names ignoble, born to be forgot,” who “Drop one by one, from Frame’s neglecting hand; / *Lethean* gulphs receive them as they fall, / And dark oblivion soon absorbs them all.” An anonymous reflection entitled “The Meditation of an Interesting Moment” in *The Evangelical Magazine* (London, 1806; Vol. 14, p. 27) provides this awful thought: “In Hell they feel again stings which they thought blunted, and are haunted with recollections for which they hoped to have found *Lethean* draughts.” In his lyric “Song,” John Keats (1795–1821) remarks “night’s sleepy eye” that “Closes up, and forgets all its *Lethean* care” (1818, published 1848), while Percy Bysshe Shelley (1792–1822), in the Gothic novel *Zastrozzi* (1810), writes, “A *Lethean* torpor crept upon his senses...a total forgetfulness of every former event of his life swam in his dizzy brain.”

As in England, so in America: John Greenleaf Whittier (1807–1892), one of America’s popular “Fireside Poets,” published his widely disseminated anti-slavery poem, “The Ship-Builders,” in 1846. Reprinted often, Whittier’s poem would have been circulating at the time of Morton’s demonstration and the events occurring soon thereafter. “Speed on the ship!” it commands, “But let her bear / No merchandise of sin, / No groaning cargo of despair / Her roomy hold within; / No *Lethean* drug for Eastern lands, / Nor poison-draught for ours; / But honest fruits of toiling hands / And Nature’s sun and showers.” Edgar Allan Poe (1809–1849), in his poem “Ulalume” (1847), invoked the “*Lethean* peace of the skies,” and Henry David Thoreau (1817–1862), in a lecture entitled “Walking” (first delivered in 1851; published posthumously in *The Atlantic Monthly* in 1862) noted, “The Atlantic is a *Lethean* stream, in our passage over which we have had an opportunity to forget the Old World and its institutions.” Herman Melville (1819–1891) followed with “Into that *Lethean* canal...fell many a poor soul that night; fell, forever forgotten” (*Israel Potter*, 1855; serialized in *Putnam’s Monthly*, 1854–1855). The adjective’s place in the parlance of the day is reflected in its appearance in popular magazines such as *Putnam’s Monthly*, *Godey’s Lady’s Book*, and *The Knickerbocker; Or New-York Monthly Magazine*. The latter had published, for example, the minor but much admired American novelist F.W. Shelton (1814–1881), whose early story, “The Death Bed,” made full use of a classical allusion for a popular audience, drawing on Shelley’s *Zastrozzi* to boot. The narrator notes that for those blessed with Virgil’s *dulcis vita* (“the sweet life”), existence was not “a vulgar sensuality, a *Lethean* torpor” (February 1844, Vol. 23, p. 129).

In another sense entirely, “*Lethean* torpor” was exactly what Morton wished to induce in dental and surgical patients, a fact probably not lost on shrewd readers such

as Gould and Bigelow, who might have given voice to the thought; and all the better if the effect—this “Lethean torpor”—was achieved by the application of something strangely familiar. Though the poet Whittier’s “Lethean drug” probably referred to opium, his phrase, much in the air in 1846, might easily be appropriated and extended.

The Coinage: *Lethe*, *Lethean*, *Letheon*

Gould, Holmes, and Bigelow, all educated at Harvard, were extremely well-versed in Greek and Latin and likely conversant with French and German; they seem gladly to have participated in the search for a new word to name Morton’s “preparation.” Indeed, they were the beneficiaries not only of a rich classical education but also the spirit of an age in which wordplay and language studies were very much in vogue. “But while schoolrooms taught parsing, they also sparked nationwide punning,” writes the noted literary scholar Michael West of the University of Pittsburgh. He explores our forbears’ “curiosity about foreign languages and the ancient, hidden meaning of words” and goes on to describe at length the “linguistic effervescence” of mid-19th-century America, a time when both scholarly and popular enthusiasms “focused attention on the origins of words.”⁹ The title page of Webster’s immense *American Dictionary* (1828) notes that the work was intended to include “The Origin, Affinities and Primary Signification of English Words, as Far as They Have Been Ascertained... [as well as] Accurate and Discriminating Definitions...to Which are Prefixed, an Introductory Dissertation on the Origin, History and Connection of the Languages of Western Asia and of Europe.” The dictionary reflected expansive lexicographical exploration as well as ordinary readers’ wide-ranging enthusiasms. It is hardly a surprise, then, to learn that a small band of accomplished physicians leapt at the opportunity to suggest original, even fanciful names for a novel “preparation” or “nostrum,” that someone like Gould might have been attempting a play on something as unusual as a shade-seeking butterfly, or that they would have favored a name so similar to a word already in circulation, one that might have played well in the popular imagination. “Lethean torpor,” by verbal sleight of hand, becomes “Letheon torpor,” a physiologic imperative if surgery and dentistry were to involve anesthetic insensibility.

For his part, Oliver Wendell Holmes went to some pains to come up with a name, though it was for the change effected in those to whom Morton’s new compound was administered. On November 21, 1846, he wrote what appears a rather straightforward letter to Morton, arguing that the “state” be called *anæsthesia*: “This signifies,” he said, “insensibility—more particularly (as used by Linnæus and Cullen) to objects of touch. (See Good—Nosology, p. 259.)”^{8,10–13} He went on to elaborate, “Thus we might say the state of Anæsthesia, or the anæsthetic state,” before advising Morton that “it might be allowable to say anæsthetic agent, but this admits of question.” And Holmes

didn’t stop there. “The words,” he says, “anti-neuric, aneuric, neuro-leptic, neuro-lepsia, neuro-stasis, etc., seem too anatomical; whereas the change is a physiological one. I throw them out for consideration.” Morton, he must have known, was likely not to parse the language so finely, and Holmes, for all his sobriety of address, might have been having a bit of fun: anyone checking John Mason Good’s *A Physiologic System of Nosology* (1823) would have been greeted by more than 500 pages of taxonomic complexity with language notations not only in English and Latin, but also in Greek, German, French, and Arabic.¹⁴

Just four months earlier, on July 22, 1846, the poet and wit John Godfrey Saxe (1816–1887) had recited a comic satirical poem to the Associated Alumni of Middlebury College. He called the poem “Progress” and dedicated it to none other than his friend Oliver Wendell Holmes for his “fine Poetical Genius” and “His Unequalled Power of Playful Satire”—traits perhaps in evidence in Holmes’ letter to Morton. On October 16, 1846, the day of Morton’s historic demonstration of etherization, one short stanza of Saxe’s long poem appeared by chance in the *Boston Post* under the title, “Ingenious Recipe for making a Science.” Little could Holmes have known that he’d feel the urge, a month hence, to help “make” (or, more precisely, “name”) a science, but that in part is what his letter purported to do. The recipe, joked Saxe, involved combining “three stale ‘truths;’ a dozen ‘facts,’ assumed; / Two known ‘effects,’ and fifty more, presumed; / ‘Affinities’ a score, to sense unknown, / And, just as ‘*lucus*, [a] *non lucendo*’ shown, / Add but a name of pompous Anglo-Greek, / And only not impossible to speak, / The work is done; a ‘science’ stands confest, / And countless welcomes greet the queenly guest.” No stale truths here, but “effects,” those demonstrated as well as those presumed? Yes, indeed: Morton’s compound surely produced effects in need of explanation, in need even of a name.

As announced by Morton, the word *Letheon* (initially printed as “Lethēon” or “Lethéon”), the subject today of much speculation, would at the time have been a revelation—a novelty word perhaps, but also a tribute to imaginative reach. Johnson’s *Dictionary* (rev. 1828), Webster’s (1828, rev. 1848), and Worcester’s *Dictionary* (1846) all include *Lethean* with the stress on the second syllable (“Lethē’an”); in the latter issues of Warren’s *Some Account*, Morton’s new compound is variously printed with the lengthened or accented second “e” (“Lethēon” and “Lethéon”). This perhaps signaled an intended similarity in pronunciation.

We do not know whether the name came easily to Gould or to Bigelow and, given Holmes’ rather extravagant exercise in naming, we might suppose some head-scratching before *Letheon* presented itself ready-made. We have noted that the suggestive verbal similarity to the adjective *Lethean* had a part to play, and that Gould might have gone so far as to consider the shade-seeking *Lethe* genus of butterfly as a corroborative source. Could other factors have been at play?

The mythologic River Lethe commands a first look always, but given the 19th-century educational emphasis on classical forms generally, at least two more possibilities—one from the Latin, another from the Greek—are worth reviewing.

Was *Letheon* Coined Before 1846?

In *The Origins of Anesthesia* (1983), the surgeon and medical historian Sherwin B. Nuland, M.D. (1930–2014), implicitly discarded the Greek root (the river Lethe, *via lēthē*, “oblivion, forgetfulness”) suggested by Nathan P. Rice and adopted a more direct Latin line of descent: “The writers of antiquity,” he wrote, “commonly referred to poppy-induced sleep with a term used by Virgil: *Letheon*.”¹⁵ He repeated the claim in *Doctors: The Biography of Medicine* (1988), colorfully describing how, two weeks after the first pain-free amputation at the Massachusetts General Hospital (the etherization event of November 7, 1846), Morton “met with two representatives of the hospital, Henry Jacob Bigelow and Oliver Wendell Holmes, and gave the name *Letheon* to sulfuric ether.... The term was borrowed, at the suggestion of Holmes, from the writings of Virgil, who had, as noted earlier, applied it to the restful sleep induced by the tears of the poppy plant.”¹⁶ There is, however, no evidence at all that Holmes ever propounded a Virgilian source or that such a meeting ever took place. The distinguished anesthesiologist Norman Bergman, M.D. (1926–1999), in *The Genesis of Surgical Anesthesia* (1998), also attributed the word *Letheon* to Virgil. “The deep sleep,” he wrote, “associated with opium came to be described by many writers using Virgil’s word ‘*letheon*’; a word which was to assume great significance in more modern times.”¹⁷ Bergman, though, cited a 1946 article by G. K. Tallmadge, where we find this: “Poppy was known to produce sleep, to relieve cough, to stop the bowels, and to alleviate pain, and on the last score it was employed medically in very many diseases. The sleep it caused was described by most writers in Virgil’s word, *Lethean*.”¹⁸

Letheon or *Lethean*? Virgil (70 B.C.E.–19 B.C.E.), of course, wrote in Latin, the *Eclogues*, *Georgics*, and the *Aeneid* comprising his major works. In six instances, four in the *Aeneid* and two in the *Georgics*, he employs forms of the adjective *lethaeus*, which translates as *lethan* (“causing forgetfulness, of Lethe, of the Underworld”). No inflected Latin form of *lethaeus* reads as *letheon* (in the neuter singular nominative case, the word is spelled “*lethaeum*,” as it is in the accusative and vocative cases). In the *Georgics*, for example, Bk. 1, line 78 reads in part “*lethaeo perfusa papavera somno*,” which translates as “poppies drenched in *Lethean* sleep.” Ovid (43 B.C.E. to 17/8 C.E.), in his *Metamorphoses* (ca. 8 C.E.), used the word in a similar fashion: the phrase “*Lethaei gramine succi*” (Bk. VII, line 152) translates roughly as “using an herb of *lethan* juice.” Such examples are plentiful. *Letheon*, in fact, is not a Latin form,

nor can we locate any translator who used it to construe anything in Virgil or other writers of the time.

Bergman, consulting Tallmadge, possibly looked past the word *Lethean*, relying on the mind’s eye to supply *Letheon* where it did not exist. *Lethean* was as unusual to late 20th-century scholars as it continues to be today. Nuland, tumbling into and out of an apocryphal story about the naming experience generally, has more to answer for. Both, though, point us to more expansive terrain, that of the classical canon generally and works more familiar to our learned 19th-century counterparts than to most of us today.

By 1846, when Gould, Bigelow, and Holmes joined with Morton in a rather hurried attempt to name his compound, the word *Letheon* had in fact been neatly (if rather quietly) embedded in the French language if not the English for well over a century (fig. 4). Might Gould have heard or read of a mountain or perhaps a high hill named *Letheon*, to which at least three 18th-century French geographers, drawing on the work of master cartographer Abraham Ortelius (1527–1598), had directed their readers? And what possible significance might that outcropping have had as Gould gave some thought to names for Morton’s “preparation”? This Italian mountain, located in the Campania region of Italy, is not found on any map we have been able to locate, though Ortelius gave his readers to think such a place might indeed have existed, at least according to Lycophron (fig. 5). And who, we ask, was Lycophron?

Gould would likely have had an answer. Attributed to the Hellenistic scholar Lycophron of Chalcides (ca. 320 B.C.E. to ca. 280 B.C.E.) are the obscurely riddling 1,474 lines of iambic trimeter comprising *Alexandra*, a poem that had vexed undergraduate readers of Greek for centuries. We can surmise that it was familiar to Gould and his young Harvard contemporaries, who, making their way through the classical canon, might have come across the unusual place-name *Lethaiōn* (a novel lengthened form of *Lēthē* existing nowhere else). Noted by 12th-century commentators (fig. 6), and translated into English by the early 19th century as *Lethæon*, the word identified a spot passed by the wandering Odysseus: “Thence from *Lethæon*’s hills I mark him fare” (Viscount Royston, *Cassandra*, 1806, p. 52, line 819). This *Lethæon*, located near what we know today as Lake Avernus, close to the ancient Greek colony at Cumae, and a cave considered by Virgil as the entrance to the Underworld, shared in a mythology of earthly existence, of the passage between this world and the next. Implicit parallels to the earlier Greek *Lethe* immediately come to mind, especially when “*Lethæon*’s hills” are understood to represent a rare restful stop in a troubled landscape of “hoarse-resounding Acherusian waves; / ...by where Proserpine’s grove / With gloomy foliage sheds infernal night; / By the red waves of fiery Phlegethon... / By black Avernus; by Cocytus’ wave, / Where sobs, and shrieks, and other voice than song / Pierce the dull ear of Night...” (Royston, 1806, lines 810–822). What 19th-century armchair classicists, while helping

a young dentist name a new “preparation,” might have made of this is of course unknown but not, we posit, beyond all conjecture. (For more on this particular line of inquiry, see appendix, “*Letheon*, Lycophron, and the Classical Canon.”)

Recalling the French tradition that finds the word *Letheon* in 18th-century texts, we are perhaps not as surprised as we otherwise might be at a bit of shipping news twelve years before Morton gave the name to his compound. On August 1, 1834, the *Baltimore* [Maryland] *Patriot and Mercantile Advertiser* reported the French brig *Armede* [sic] had cleared the port of Charleston, South Carolina on July 24, having debarked from Senegal, Africa, under Shipmaster or Captain *Letheon*. On August 7, the *New-York Spectator* announced that the same French brig *L'Armide*, under Captain *Letheon*, out of Senegal, Africa, had cleared the port of Savannah, Georgia. Whoever he was—assuming, that is, the newspapers are correct in their spelling—Captain *Letheon* is a mystery to us today.

Reported Dates of the Meeting to Select a Name

Although we now have more insight into the etymology of *Letheon*, the date when Morton adopted the name remains elusive. Although dates ranging from November 2 to November 21 have been suggested by anesthesia historians,

no definitive citations or original documentation were provided to substantiate the various claims. In fact, no date can be adduced with certainty from 19th-century sources. That no one—not Morton himself, not Gould, Bigelow, or Holmes—seems to have memorialized the date remains a quirk of history. At best, Holmes' November 21 letter suggesting “anæsthesia” as a name might flag a period around which Morton solicited suggestions for a name.

Letheon: A Primer for the Present Day

The implication that the name *Letheon* was coined sometime in October 1846 is of course incorrect. Again, the name *Letheon* was not used by Morton on October 16, 1846, and the name did not appear in the Jackson-Morton patent application on October 27, 1846.

A surprisingly large number of anesthesiologists, historians, and authors have been notably slipshod in referring to *Letheon* in various essays and reviews, as the following three examples will illustrate.

F.D. Moore, M.D., reviewing the story of J. C. Warren's “act of conscience” in allowing Morton into the operating theater on November 7, 1846, for a “capital” operation, proceeds carefully enough in telling the story but then muddies the waters: “We realize now that there were two adverse factors at work, two severe problems for Warren to face, over the use of this ‘preparation,’ this ‘invention,’ this ‘*Letheon*’ of Morton's on the morning of Friday, Oct. 16, 1846.”¹⁹ This *Letheon* of Morton's would not be known by that name for well over a month after the October 16 demonstration of surgical etherization.

James Tayloe Gwathmey, M.D., in his textbook *Anesthesia*, noted, “On October 27, 1846, Morton and Jackson sought to patent their anesthetic under the name of ‘*Letheon*.’ From its odor it was soon recognized as ‘sulphuric ether.’”²⁰

The journal *ANESTHESIOLOGY*, announcing in 2017 its first annual “*Letheon*” poetry prize, has this: “in 1846 William Morton shiftily attempted to patent the anesthetic as ‘*letheon*,’ channeling the mystique of classical mythology.”²¹

In a sense, these and others can be forgiven the lapses. The chronology was confused from the outset by careless editors and physician-writers. Very early on, *The Boston Medical and Surgical Journal* (January 20, 1847) published anonymous correspondence under the banner: “The Patent ‘*Letheon*.’”²² Three months later, in an article titled, “The Patent *Letheon*—Jackson and Morton's Specification,” an anonymous correspondent identified only as “S” wrote, “It has been repeatedly said that Dr. Jackson is not concerned in the Patent for the *Letheon*,” before going on to rehearse Jackson's share in the signal discovery.²³

The phrase, “The patent for the *Letheon*,” which confuses discussion to this day, has an obvious appeal to writers old and new. Though a convenient shorthand reference, it does, however, promulgate an historical error. No great harm is done in simplifying what was, at the time, a swirl of both public and private activity. Still, we do well to remember

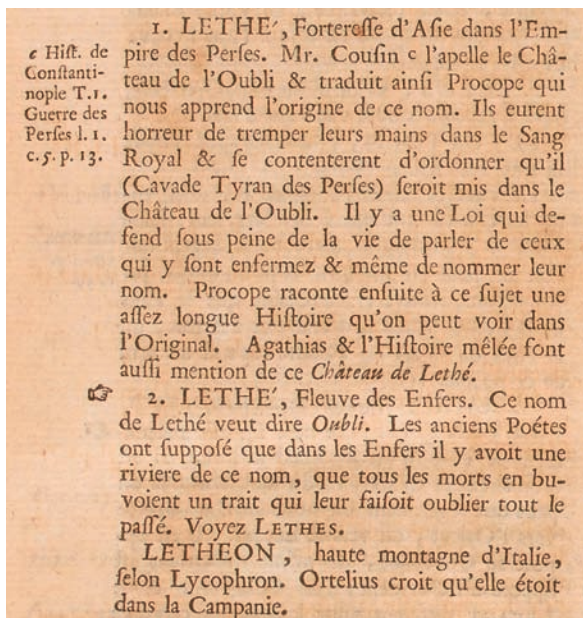
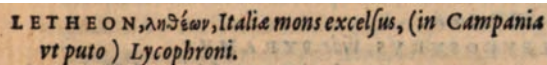
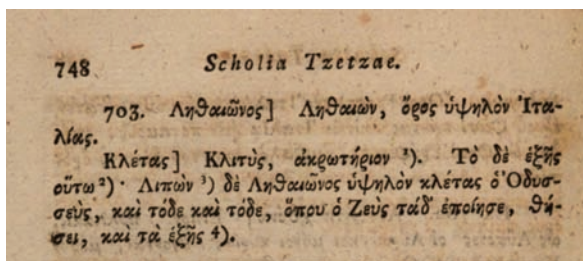


Fig. 4. The name *Letheon* in an 18th-century French dictionary. Translated into English as: “*Letheon*, a high mountain in Italy, according to Lycophron. Ortelius believes it was in Campania.” From: Antoine-Augustin Bruzen la Martinière's *Le Grand Dictionnaire Géographique et Critique. Tome Cinquième. Première Partie. K. L.*, 1735, p. 169. Image source gallica.bnf.fr / Bibliothèque Nationale De France (National Library of France), Paris, France.



LETHEON, ληθέων, Italia mons excelsus, (in Campania ut puto) Lycophroni.

Fig. 5. Abraham Ortelius' note on *Letheon* in *Thesaurus Geographicus* (Antwerp, 1587, unnumbered page): "LETHEON, ληθέων, Italia mons excelsus, (in Campania ut puto) Lycophroni." Ortelius' note translates into English as: "LETHEON, a high mountain in Italy (in Campania, or so I think) [according to] Lycophron." This is the earliest reference we have found in print employing the word *Letheon*. Image reproduced with the permission of Bayerische Staatsbibliothek (Bavarian State Library), Munich, Germany. Call number: Hbks/B 1 a. urn:nbn:de:hbv:12-bsb10801539-7. Image 347.



703. Ληθαίωνος] Ληθαίων, ὄρος ὑψηλὸν Ἰταλίας. Κλέτας] Κλιτύς, ἀκρωτήριον ¹). Τὸ δὲ ἐξ ἧς οὕτω ²). Λιπών ³) δὲ Ληθαίωνος ὑψηλὸν κλέτας ὁ Ὀδυσσεύς, καὶ τότε καὶ τότε, ὅπου ὁ Ζεὺς τὰ δ' ἐποίησε, θάψει, καὶ τὰ ἐξ ἧς ⁴).

Fig. 6. Note on *Ληθαίωνος* (Lethaiōnos) in line 703 of Lycophron's *Alexandra*, in *Scholia Tzetzae* [Commentary of Isaac and Johannes Tzetzes], edited by Christian Gottfried Müller (Liepzig, 1811). *Scholia Tzetzae* reads "Lethaiōnos] Lethaiōn, odos hupselon Italias" ("of Lethaiōn] Lethaiōn, a high path or way in Italy"); hence, by extension, a lofty place, a slope, a hill, as reflected in Hornblower's translation, "the high hill of Lethaiōn," or Royston's "Lethæon's hills." Image source Hathi Trust. Book source Columbia University, New York, New York. Digitized by Google.

that things do slot into place on a timeline that we ought to correct with each new bit of information we find.

Conclusion

Buoyed by the success of his public demonstration of ether anesthesia on October 16, 1846, at the Massachusetts General Hospital, William T. G. Morton undertook to protect his as yet undisclosed "preparation." On October 27, 1846, he joined with Dr. Charles T. Jackson in seeking an American patent. In November, or early December, 1846, Morton enlisted the help of some of Boston's leading physicians regarding a commercial name for his "preparation." He settled on the neologism *Letheon* (as suggested by Augustus Addison Gould, M.D., and Henry Jacob Bigelow, M.D.).

The provenance of the name is conjectural. We have not identified a first-hand account of the coinage of *Letheon*. The primary participants did not leave letters, diaries, or daybooks in which they offered a rationale for the name nor did they reveal any information in their publications

on etherization or in the various affidavits published in Morton's *Statements* volume. Though the word *Letheon* undoubtedly has roots in the Greek *Lēthē* (forgetfulness, oblivion), it may also have stemmed from the common adjective *Lethean* (causing oblivion or forgetfulness), much in use by 19th-century writers. Possibly, too, an element of wordplay common to the era informed the coinage.

Research Support

Support for this study was provided solely from the authors' personal funds.

Competing Interests

The authors declare no competing interests.

Correspondence

Address correspondence to Dr. Haridas: P.O. Box 6278, North Sydney, NSW 2059, Australia. rajesh.haridas@bigpond.com. Information on purchasing reprints may be found at www.anesthesiology.org or on the masthead page at the beginning of this issue. ANESTHESIOLOGY's articles are made freely accessible to all readers, for personal use only, 6 months from the cover date of the issue.

References

1. Warren E: Some Account of the Letheon; Or, Who was the Discoverer? 1st edition. Boston, Dutton and Wentworth, Printers, 1847
2. Warren JC: Etherization; with Surgical Remarks. Boston, William D. Ticknor & Company, 1848, pp 4–6
3. Bigelow HJ: Insensibility during surgical operations produced by inhalation. Boston Med Surg J 1846; 35:309–17
4. Statements, Supported by Evidence, of Wm. T. G. Morton, M.D. on his Claim to the Discovery of the Anaesthetic Properties of Ether, Submitted to the Honorable the Select Committee Appointed by Senate of the United States. Presented at: 32nd Congress, 2nd Session, Washington, D.C., January 21, 1853, pp 400–1, 409–11
5. "Gould, Augustus Addison." In: Complete Dictionary of Scientific Biography, Volume 5. Charles Scribner's Sons, 2008, pp 477–9
6. Morton EW: The discovery of anaesthesia. McClure's Magazine 1896; 7:311–8
7. Pratt LH: Lying and Poetry from Homer to Pindar: Falsehood and Deception in Archaic Greek Poetics. Ann Arbor, MI, University of Michigan Press, 1993, pp 17–24
8. Rice NP: Trials of a Public Benefactor: As Illustrated in the Discovery of Etherization. New York, Putney & Russell, 1859, pp 137–8
9. West M: Transcendental Wordplay: America's Romantic Pundsters & the Search for the Language of Nature. Athens, OH, Ohio University Press, 2000, pp xii, 13, 141

10. Haridas RP: The etymology and use of the word 'anaesthesia': Oliver Wendell Holmes' letter to W.T. G. Morton. *Anaesth Intensive Care* 2016; 44 Suppl:38–44
11. Warren E: Some Account of the Letheon; Or, Who was the Discoverer? 2nd edition. [Second issue] Boston, Dutton and Wentworth, Printers, 1847, p 79
12. Warren E: Some Account of the Lethēon: Or, Who is the Discoverer? 3rd edition. [First issue] Boston, Dutton and Wentworth, Printers, 1847, pp 84–5
13. Warren E: Some Account of the Lethēon: Or, Who is the Discoverer? 3rd edition. [Second issue] Boston, Dutton and Wentworth, Printers, 1847, pp 84–5
14. Good JM: A Physiological System of Nosology; With a Corrected and Simplified Nomenclature. Boston, Wells and Lilly, 1823, p 259
15. Nuland SB: The Origins of Anesthesia. Birmingham, AL, Classics of Medicine Library, 1983, p 3
16. Nuland SB: Doctors: The Biography of Medicine. New York, Alfred A. Knopf, Inc., 1988, pp 267, 292
17. Bergman NA: The Genesis of Surgical Anesthesia. Park Ridge, IL, Wood Library-Museum of Anesthesiology, 1998, p 8
18. Tallmadge GK: Some anesthetics of antiquity. *J Hist Med Allied Sci* 1946; 1:515–20
19. Moore FD: John Collins Warren and his act of conscience: a brief narrative of the trial and triumph of a great surgeon. *Ann Surg* 1999; 229:187–96
20. Gwathmey JT: Anesthesia. New York and London, D. Appleton and Company, 1914, p 16
21. The journal *Anesthesiology*, announcing its first annual "Letheon" poetry prize. Available at: <http://anesthesiology.pubs.asahq.org/ss/letheon.aspx>. Accessed December 1, 2017.
22. Anon [Author identified as "Claudian"]. The patent "Letheon." *Boston Med Surg J* 1847; 35:514
23. Anon [Author identified as "S"]. "The Patent Letheon—Jackson and Morton's Specification. *Boston Med Surg J* 1847; 36:194–8

Appendix: *Letheon*, Lycophron, and the Classical Canon

Augustus A. Gould, Henry J. Bigelow, and Oliver Wendell Holmes were all proficient in Latin and Greek, quizzed since their school days in the classical canon. Perhaps the branding of ether as *Letheon* owed something to such training beyond the simple note that *Lēthē* might be adduced as *Letheon*'s root. We have already remarked on the misguided notion that *Letheon* derives from Virgil's *lethaeus* ("causing forgetfulness"); one overlooked source for *Letheon* is the Greek *Ληθαίων* (*Lethaiōn* or *Lethaion*), a neologism found in the poem *Alexandra*, attributed to the 3rd-century-B.C.E. poet and grammarian Lycophron of Chalcides.

Among the most gifted American students to do postgraduate work at the University of Göttingen in central Germany was Harvard's Edward Everett (1794–1865). After earning his A.B., *summa cum laude*, in 1811 and his A.M. in Divinity Studies in 1814, he took a doctorate at Göttingen, the first American to do so, in 1817. Installed at Harvard in 1815 as the inaugural Eliot Professor of Greek Literature, he had traveled to Göttingen for two years' tutoring under the guidance of the distinguished classicist G. Ludolf Dissen (1784–1837)¹; Everett toured Europe for two additional years, returning to his post at Harvard in 1819. Dissen screened preceptees like Everett with the same intentionally obscure 1,474 lines of lyric Greek poetry with which the poet John Milton had tested himself: *Alexandra*, attributed to Lycophron.²

A daughter of Troy's King Priam, Cassandra (or "Alexandra") was blessed by Apollo with the gift of prophecy but was cursed, after rebuffing him, with universal disbelief of her predictions. She even foresaw that Ajax the Lesser would rape her after dragging her from the temple of the goddess Athena when the Greeks sacked Troy. When Ajax avoided punishment for his crime, an enraged Athena condemned the Grecian fleet, even the ships commanded by Odysseus, to destruction or a trying voyage home. On reaching Mycenae with Cassandra now his concubine, the Greeks' commander-in-chief, Agamemnon, and the hapless

Cassandra were murdered by his wife, Clytemnestra, or Aegisthus, her lover.

Riddled with obscurities, Lycophron's *Alexandra*, a prophetic pronouncement on various fates of Greek and Trojan warriors, is difficult to follow even in English. "The rivers and lakes of the underworld," notes Oxford classicist Simon Hornblower, "conventionally located in Campania, are the subject of some powerfully evocative lines," among them: "He leaves the high hill of Lethaion, / and lake Aornos encircled by a noose, / and the river of Kokytos violently roaring in darkness, / tributary of black Styx..." (lines 703–706).³ The subject of these lines is Odysseus. But where exactly are we, and what of this "high hill of Lethaion," an apparent verbal cousin to a Greek place (a plain, a house, a river) of oblivion?

The Greek text of *Alexandra* contained the hitherto unknown word *Ληθαῖωνος* (*Lethaiōnos*), the genitive (or possessive) case of *Ληθαίων* (*Lethaiōn* or *Lethaion*), a lengthened form of *Lēthē* not found elsewhere in the Greek canon. In an 1811 edition of a standard commentary—that of the Byzantine poet and grammarian Joannes Tzetzes (ca. 1110–1180) and his brother Isaac (d. 1138)—we (as did our 19th-century counterparts) find the word *Lethaiōnos* (meaning "of Lethaiōn"; i.e., the genitive singular of the proper noun) set off by a bracket with the foundational *Lethaiōn* referenced alongside, the latter identified as "a high path or way in Italy" (fig. 6).⁴ Hornblower explains, "Lyk[ophron] wished to mention as many of the rivers of the Underworld as possible, but Lethe, River of Forgetfulness, was post-Homeric (it featured most famously in the Myth of Er, Pl[ato]. *Rep[ublic]*, 621a); so the name, or an enlarged adaptation of it to suit a mountain, could be introduced into the Campanian narrative only by a bold fictional creation."⁵ Lycophron, in effect, imagined the word *Lethaiōn* as the name of a mountain in the Campania region of Italy when he set his story there.

Back now to American students of Göttingen's Professor Dissen. Puzzlement, we might imagine, ruled whenever the *Alexandra* came out. But they had the Tzetzes' commentary for grammatical, geographical, and even thematic help, and it sufficed to a point. They might have been helped as well by a translation by Philip Yorke, Viscount Royston (1784–1808), an 1803 graduate of St. John's College, Cambridge. Prepared while he was an undergraduate, privately printed in 1806 by the Cambridge University Press, and published posthumously in 1816, Viscount Royston's rendering reads in part: "Thence from Lethaion's hills I mark him [*i.e.*, Odysseus] fare / By black Avernus; by Cocytus' wave," and so on. Royston, following Tzetzes, identifies "Lethaion" simply as "a mountain of Italy," but tellingly notes of "Avernus or Aornos" that it is "a lake near the Lucrine, and surrounded with woods, according to Virgil..." (Here Royston notes Virgil's *Aeneid*, Bk. 3, line 442).⁶ In John Dryden's expansive rendering of Virgil's epic poem, the speaker warns the Trojan hero Aeneas, "Arriv'd at Cumæ, when you view the flood / Of black Avernus, and the sounding wood, / The mad prophetic Sibyl you shall find, / Dark in

¹Varg PA: Edward Everett: The Intellectual in the Turmoil of Politics. Selinsgrove, PA, Susquehanna University Press, 1992, pp. 21–2

²Hale JK: Milton's Languages: The Impact of Multilingualism on Style. Cambridge, UK, Cambridge University Press, 1997, pp. 75–6

³Hornblower S: Lycophron's *Alexandra*, Rome, and the Hellenistic World. Oxford, Oxford University Press, 2018, p. 110 and p. 110, n.15

⁴Tzetzes I, Tzetzes J: Isaakiou Kai Ioannou Tou Tzetze Scholia Eis Lykophrona, Volumina Tria [Commentary on Lycophron. In Three Volumes]. Christ[ian] Gottfried Müller, ed. Lipsiae, F.C.G. Vogelii, 1811, p. 748

⁵Hornblower S: Lycophron: *Alexandra*. Greek Text, Translation, Commentary, and Introduction. Oxford, Oxford University Press, 2015, p. 290

⁶Yorke P (Viscount Royston): Cassandra, Translated from the Original Greek of Lycophron, and Illustrated with Notes. The Classical Journal (London) 1816; 14:16–7

a cave, and on a rock reclin'd" (*Aen.* Bk. 3, trans. Dryden, Vol. 13, The Harvard Classics, 1909, p. 145). The reference is to the Cumaean Sibyl, guide to the Underworld, to whom Aeneas applies for assistance in finding the spirit of his dead father. To descend is easy, she tells him, "The gates of hell are open night and day; / Smooth the descent, and easy is the way: / But to return, and view the cheerful skies, / In this the task and mighty labor lies" (*Aen.* Bk. 6, trans. Dryden, 1909, p. 216).

The *Lethaiōn* of the Tzetzes' commentary made its way into at least three 18th-century French geographies, all of which simplified the Latin spelling *Lethæon* to *Letheon*.⁷⁻⁹ The earliest—Antoine-Augustin Bruzen la Martinière's *Le Grand Dictionnaire Géographique et Critique* (1735)—announces: "LETHEON, haute montagne d'Italie, selon Lycophron" (i.e., "Letheon, a high mountain in Italy, according to Lycophron"; fig. 4).⁷ In fact, this might more properly have read, "Letheon, a high mountain in Italy, according to a commentary on Lycophron's *Alexandra*."

Bruzen la Martinière continues, "Ortelius croit qu'elle étoit dans la Campanie" or, fleshing it out a bit, "The Brabantian master cartographer and geographer Abraham Ortelius (1527–1598) believes this Letheon was in Campania." In his *Thesaurus Geographicus* (1587), Ortelius specifically references the place-name *Letheon*, identifying it as "ληθέων, Italia mons excelsus, (in Campania ut puto) Lycophroni" or "Letheon, a high mountain in Italy (in Campania, or so I think), [according to] Lycophron" (fig. 5).¹⁰ The substitution of the accented Greek letter epsilon (έ) for the Greek diphthong *ai* perhaps provides a clue to the rendering in the *Thesaurus* and the simplified spelling thereafter. Whatever the case, we need note only that Ortelius was likely reporting an historical myth;

he probably knew of the Tzetzes' commentary ("Lethaiōn, a high path or way in Italy"), and possibly extrapolated from geographical insights gleaned from Virgil. And as for Bruzen la Martinière, his definition of *Aornos* (Lake Avernus) relies in part on Virgil, who said the Greeks associated the lake with a Cumaean cave that the Roman's knew as the entrance to the Underworld (*Aen.* Bk. 6, line 239). Tellingly, a century hence, a British geography relying not on a poet of antiquity but on observed realities, the *Thesaurus Geographicus. A New Body of Geography: Or, a Compleat Description of the Earth... Collected with great Care from the most approv'd Geographers and Modern Travellers and Discoveries, by several Hands* (London: Printed for Abel Swall and Tim. Child, 1695) makes no mention of a mountain named Letheon in Italy.

We cannot know how much of this someone like Edward Everett would have been aware of. Of Lycophron's *Alexandra* and Virgil's *Aeneid*? Of course. Of a 12th-century commentary, reprinted in a German edition of 1811, that had introduced the word *Lethaiōn*? Yes, more than likely. Of a simplified spelling in French? Possibly. And we cannot know how much of this he imparted to his students, one of whom, Augustus Addison Gould, was a student during Everett's final years at Harvard as Eliot Professor. We can only speculate whether, in 1846, Gould would have remembered Lycophron or Virgil in attempting a name for Morton's "preparation." But *Lēthē*, the name of a river and goddess, doubtless opened onto thoughts of the common adjective *Lethean* and possibly to *Lethæon*, the name of a mythical mountain, a simplified spelling of which Morton would seize on as the commercial name with which to present his preparation to a waiting world. A single verbal thread here ties together the Greek notion of an afterlife as oblivion with the Roman idea of descent into and emergence from a dark place of spirits. And we can only speculate whether, in thinking through the state of insensibility he sought to explain, Gould would have remembered his *Aeneid*, as versified by Dryden (*Aen.* Bk. 6, trans. Dryden, 1909, p. 216): "Smooth the descent... / But to return, and view the cheerful skies, / In this the task and mighty labor lies." A few inhalations of the ethereal gas, and smooth the descent into insensibility, then the physician's fine labor to retrieve the insensible soul so that the cheerful skies should open and a conscious delight be restored.

⁷Bruzen la Martinière [A-A]: *Le Grand Dictionnaire Géographique et Critique*. Tome Cinquième. Première Partie. K. L. [The Great Geographic and Critical Dictionary, Vol. 5, Part 1, K through L.] 1735, p. 169

⁸Sabbathier [F]: *Dictionnaire pour l'Intelligence des Auteurs Classiques, Grecs et Latins, Tant Sacrés que Profanes, Contenant la Géographie, l'Histoire, la Fable, et les Antiquités*. Tome Vingt-Cinquième. [A Dictionary of Things Relating to Greek and Latin Authors, both Sacred and Profane, Containing Geography, History, Folklore, and Fables. Volume 25.] Paris, Chez Delalain, 1778, p. 187

⁹Mentelle [E]: *Encyclopédie Méthodique. Géographie Ancienne*. Tome Second. [Methodical Encyclopedia. Ancient Geography. Volume II.] Paris, Chez Panckoucke, 1789, p. 270

¹⁰Ortelius A. *Thesaurus Geographicus*. Antwerp, Christophori Plantini, 1587

ANESTHESIOLOGY

Population Pharmacodynamics of Propofol and Sevoflurane in Healthy Volunteers Using a Clinical Score and the Patient State Index

A Crossover Study

Merel H. Kuizenga, M.D., Pieter J. Colin, Ph.D.,
Koen M. E. M. Reynjtens, M.D., Daan J. Touw, Ph.D.,
Hasan Nalbat, R.N., Froukje H. Knotnerus, R.N.,
Hugo E. M. Vereecke, M.D., Ph.D.,
Michel M. R. F. Struys, M.D., Ph.D.

ANESTHESIOLOGY 2019; 131:1223–38

EDITOR'S PERSPECTIVE

What We Already Know about This Topic

- Hypnotic drug effects can be assessed as the presence or absence of standard clinical endpoints, such as tolerance to calling the person by name and tolerance to shake and shout
- Antinociceptive drug effects can be assessed as the presence or absence of tolerance to tetanic stimulus
- The Patient State Index is a processed, electroencephalographic-derived index that is considered by some to be a drug-independent representation of the depth of sedation and anesthesia

What This Article Tells Us That Is New

- A four-period randomized sequence crossover study determined the concentration–effect relationships for both propofol and sevoflurane, both with and without remifentanyl coadministration, with effects measured as tolerance to standard stimuli and by the Patient State Index
- The sevoflurane Patient State Index values associated with a 50% probability of tolerance to the standard stimuli were higher for than those for propofol
- Adding a $2 \text{ ng} \cdot \text{ml}^{-1}$ predicted effect-site remifentanyl concentration increased all Patient State Index values associated with a 50% probability of tolerance to the standard stimuli, but $4 \text{ ng} \cdot \text{ml}^{-1}$ produced additional effects only during propofol administration

ABSTRACT

Background: The population pharmacodynamics of propofol and sevoflurane with or without opioids were compared using the endpoints no response to calling the person by name, tolerance to shake and shout, tolerance to tetanic stimulus, and two versions of a processed electroencephalographic measure, the Patient State Index (Patient State Index-1 and Patient State Index-2).

Methods: This is a reanalysis of previously published data. Volunteers received four anesthesia sessions, each with different drug combinations of propofol or sevoflurane, with or without remifentanyl. Nonlinear mixed effects modeling was used to study the relationship between drug concentrations, clinical endpoints, and Patient State Index-1 and Patient State Index-2.

Results: The C_{50} values for no response to calling the person by name, tolerance to shake and shout, and tolerance to tetanic stimulation for propofol ($\mu\text{g} \cdot \text{ml}^{-1}$) and sevoflurane (vol %; relative standard error [%]) were 1.62 (7.00)/0.64 (4.20), 1.85 (6.20)/0.90 (5.00), and 2.82 (15.5)/0.91 (10.0), respectively. The C_{50} values for Patient State Index-1 and Patient State Index-2 were $1.63 \mu\text{g} \cdot \text{ml}^{-1}$ (3.7) and $1.22 \text{ vol } \%$ (3.1) for propofol and sevoflurane. Only for sevoflurane was a significant difference found in the pharmacodynamic model for Patient State Index-2 compared with Patient State Index-1. The pharmacodynamic models for Patient State Index-1 and Patient State Index-2 as a predictor for no response to calling the person by name, tolerance to shake and shout, and tetanic stimulation were indistinguishable, with Patient State Index₅₀ values for propofol and sevoflurane of 46.7 (5.1)/68 (3.0), 41.5 (4.1)/59.2 (3.6), and 29.5 (12.9)/61.1 (8.1), respectively. *Post hoc* C_{50} values for propofol and sevoflurane were perfectly correlated (correlation coefficient = 1) for no response to calling the person by name and tolerance to shake and shout. *Post hoc* C_{50} and Patient State Index₅₀ values for propofol and sevoflurane for tolerance to tetanic stimulation were independent within an individual (correlation coefficient = 0).

Conclusions: The pharmacodynamics of propofol and sevoflurane were described on both population and individual levels using a clinical score and the Patient State Index. Patient State Index-2 has an improved performance at higher sevoflurane concentrations, and the relationship to probability of responsiveness depends on the drug used but is unaffected for Patient State Index-1 and Patient State Index-2.

(ANESTHESIOLOGY 2019; 131:1223–38)

It remains unclear how to quantitatively compare the pharmacodynamics of propofol and sevoflurane in the absence or presence of opioids in a patient during anesthesia. Comparing the concentration–effect relationships for various specific hypnotic–opioid drug combinations might be interesting to clinicians when titrating combined hypnotics during anesthesia or when switching between drugs during a case.^{1,2}

Anesthesia can be considered to be the combination of the hypnotic drug effect producing loss of consciousness and the analgesic drug effect (antinociception) inhibiting

induced noxious stimuli (nociception).¹ Hypnotic drug effects can be measured using clinical endpoints such as no response to calling the person by name or tolerance to shake and shout, derived from the Modified Observer's Assessment of Alertness/Sedation Scale,^{3–5} as seen in table 1. For the assessment of the balance between nociception and antinociception, one can use the relationship between movement in response to a tetanic stimulus and the combined hypnotic–analgesic drug concentrations, expressed as tolerance to tetanic stimulus.^{6–8}

Anesthetic drug effects between and within individuals can also be quantified using processed, electroencephalographic-derived indices.⁹ The Patient State Index (Masimo, USA) is such an index and is calculated by a proprietary algorithm based on a combination of quantitative electroencephalographic parameters and recorded from a four-channel frontal electroencephalographic monitor (SedLine; Masimo).^{10–14} Patient State Index values range between 100 (awake condition) and 0 (full suppression of electroencephalography), with a recommended target range between 25 and 50 for surgical anesthesia conditions. Patient State Index-1 has been clinically available for many years¹⁰ and has been described in various studies.^{10–15} Like most conventional electroencephalographic-based depth of anesthesia monitors, Patient State Index-1 suffers from intermittent electromyographic noise that interferes with the electroencephalography, leading to the need to limit the electroencephalographic frequency band of interest during index calculations,^{16–18} difficulty in calculating an index value with low-power electroencephalography, and significant index variability at baseline that limits the interpretation of the effects of low drug concentrations.^{19,20} Recently, a new generation of the Patient State Index (Patient State Index-2) was introduced to deal with limitations of Patient State Index-1 and characterize electroencephalographic behavior in many different frequency bands. During online electroencephalographic signal processing, raw electroencephalographic waves from the four frontal channels are captured independently, and parallel signal processing engines are applied to

Table 1. Modified Observer's Assessment of Alertness/Sedation (MOAA/S) scale

5	Responds readily to name spoken in normal tone
4	Lethargic response to name spoken in normal tone
3	Responds only after name is called loudly and/or repeatedly
2	Responds only after mild shaking of the shoulder
1	Does not respond to mild shaking of the shoulder but responds to trapezius squeeze
0	Does not respond to a noxious trapezius squeeze

compute an electroencephalographic-derived parameter including Patient State Index that is less influenced by electromyography. Additionally, adaptive signal processing with band-independent features empowers the algorithm during periods of low-power electroencephalography.²¹

The aim of this four-period randomized sequence crossover study was to describe the concentration–effect relationship of four different anesthetic regimens, being propofol and sevoflurane with and without remifentanyl coadministration, as measured by no response to calling the person by name, tolerance to shake and shout, and tolerance to tetanic stimulation and by two different versions of the Patient State Index. To eliminate potential sources of interindividual variability caused by differences in brain structures, each participant was submitted to all drug combinations. The ability of the Patient State Index to predict different levels of responsiveness was also investigated. In addition, we compared the behavior of the Patient State Index-1 *versus* the new Patient State Index-2.

Materials and Methods

Study Design

For this study, data from a previously published trial,²² registered at ClinicalTrials.gov (identifier NCT02043938) and approved by the Institutional Review Board of the University Medical Center Groningen (NL43238.042.13) were reanalyzed. The specific details of the clinical study are described in full elsewhere.²² This manuscript adheres to the applicable Consolidated Standards of Reporting Trials guidelines.

In brief, 36 healthy volunteers (American Society of Anesthesiologists physical status class I), stratified by age, sex, and remifentanyl concentration (table 1 of the Supplemental Digital Content, <http://links.lww.com/ALN/C53>) were included. Written informed consent was obtained from all subjects before inclusion. Exclusion criteria were weight less than 70% or more than 130% of ideal body weight, pregnancy, neurologic disorder, diseases involving the cardiovascular, pulmonary, gastric, and endocrinologic system or recent use of psychoactive medication or intake of more than 20 g of alcohol daily.

Each volunteer was scheduled to receive four sessions of anesthesia with different drug combinations in a random order, with an interval of at least 1 week between

This article is featured in "This Month in Anesthesiology," page 1A. This article is accompanied by an editorial on p. 1199. This article has a related Infographic on p. 17A. This article has an audio podcast. This article has a visual abstract available in the online version. Supplemental Digital Content is available for this article. Direct URL citations appear in the printed text and are available in both the HTML and PDF versions of this article. Links to the digital files are provided in the HTML text of this article on the Journal's Web site (www.anesthesiology.org). Part of this study was presented as a poster titled "Comparison between Two Versions of the Patient State Index® during Propofol and Sevoflurane Anesthesia, with or without Remifentanyl" at Euroanaesthesia, the European Anaesthesiology Congress, June 4, 2017, in Geneva, Switzerland.

Submitted for publication September 13, 2018. Accepted for publication August 2, 2019. From the Departments of Anesthesiology (M.H.K., P.J.C., K.M.E.M.R., H.N., F.H.K., H.E.M.V., M.M.R.F.S.) and Clinical Pharmacy and Pharmacology (D.J.T.), University Medical Center Groningen and the Department of Pharmacy, Section of Pharmacokinetics, Toxicology and Targeting, (D.J.T.), University of Groningen, Groningen, The Netherlands; the Department of Bioanalysis, Faculty of Pharmaceutical Sciences (P.J.C.) and the Department of Basic and Applied Medical Sciences, Faculty of Medicine and Health Sciences (M.M.R.F.S.), Ghent University, Ghent, Belgium; and the Department of Anesthesiology and Reanimation, AZ St.-Jan Brugge-Oostende AV, Brugge, Belgium (H.E.M.V.).

sessions. Randomization was performed before each session by drawing a sealed envelope. Any volunteer withdrawing from the study before finishing all sessions was replaced by a newly recruited volunteer. The four sessions were named “propofol,” “sevoflurane,” “remifentanyl with step-dose propofol,” and “remifentanyl with step-dose sevoflurane.”

An arterial line for blood sampling was placed before any drug was administered. Propofol and remifentanyl were administered through an intravenous line by a Fresenius Base Primea docking station (Fresenius-Kabi, Germany) carrying two Fresenius module dynamic pressure system pumps, controlled by RUGLOOPII software (Demed, Belgium). RUGLOOPII steers the pumps and their infusion rates as target-controlled infusions to achieve desired target concentrations using pharmacokinetic–pharmacodynamic models consisting of three-compartment pharmacokinetic models linked to an effect site compartments. For propofol, the effect-site concentration was predicted by the pharmacokinetic–pharmacodynamic model of Schnider *et al.*^{23,24} For remifentanyl, the pharmacokinetic–pharmacodynamic model published by Minto *et al.*^{25,26} was used to predict the effect-site concentration. Sevoflurane was titrated using the closed-loop algorithm of the Zeus ventilator (software version 4.03.35; Dräger Medical, Germany) to target and maintain a constant end-tidal sevoflurane concentration over time.

Each session followed an identical titration procedure. After 2 min of baseline monitoring, a stepwise infusion of anesthetic drugs was administered. For the propofol group, the initial effect-site concentration was set to $0.5 \mu\text{g} \cdot \text{ml}^{-1}$ followed by consecutive steps to target concentrations of 1, 1.5, 2.5, 3.5, 4.5, 6, and $7.5 \mu\text{g} \cdot \text{ml}^{-1}$. For the sevoflurane group, the initial end-tidal sevoflurane concentration was set to 0.2 vol % followed by consecutive end-tidal sevoflurane concentration of 0.5, 1, 1.5, 2.5, 3.5, 4, and 4.5 vol %. After the predicted effect-site concentration for the propofol group or end-tidal sevoflurane concentration reached the target at each step, an equilibration time of 12 min was maintained to allow optimal equilibration between plasma or end-tidal concentration and the corresponding effect-site concentration. For the sessions with remifentanyl, the same procedure was executed, although 2 min before propofol or sevoflurane was started, an effect-site concentration of 2 or $4 \text{ ng} \cdot \text{ml}^{-1}$ was targeted according to the stratification and maintained during the entire study.

After the 12 min of equilibration time, an additional minute of baseline electroencephalographic and hemodynamic measurements was maintained before assessing subject responsiveness using the Modified Observer’s Assessment of Alertness/Sedation scale (table 1). No response to calling the person by name corresponded to an Observer’s Assessment of Alertness/Sedation score of less than 3 and tolerance to shake and shout corresponded to a score of less than 2. For the analyses, response to the stimulus was considered as 0 and tolerance as 1. After assessing subject responsiveness, an arterial blood sample was obtained for analysis of plasma propofol and/or remifentanyl concentrations.^{22,27} For

sevoflurane, the measured end-tidal sevoflurane concentration at this steady-state condition was recorded. A graphical representation of the sequence of events can be found in the supplemental data of the original study.²² An electrical stimulus was applied for a maximum duration of 30 s, as described before,²² 2 min after assessing subject responsiveness, and tolerance/motor responsiveness to tetanic stimulation was scored, again followed by 2 min to observe a possible response to the stimulus.

In each session, all volunteers started with spontaneous ventilation *via* a tight-fitting face mask connected to an anesthesia ventilator (Zeus, software version 4.03.35; Dräger Medical). End-tidal sevoflurane, carbon dioxide, and oxygen concentrations were monitored using the gas analyzer of the anesthesia ventilator.

When needed, respiratory support was applied to secure an unobstructed airway, adequate oxygenation (oxygen saturation measured by pulse oximetry of more than 92%), and CO_2 (35 to 45 mmHg) homeostasis. Throughout the study, oxygen saturation (measured by pulse oximetry), electrocardiogram, and blood pressure (measured noninvasively at 1-min intervals using a Philips IntelliVue MP50 vital signs monitor, Philips Medizin Systeme, Germany) were monitored.

Patient State Index-1 and Patient State Index-2 were derived from *post hoc* running proprietary software (Masimo) and extracted from raw electroencephalographic-waveforms that were recorded throughout the study using a frontal bilateral electrode (SedLine Sensor; Masimo). The electrode was attached on the forehead according to the manufacturer’s guidelines and connected to a Masimo root monitor (model RDS-7; Masimo) running the SedLine brain function software (Masimo).

Pharmacodynamic Modeling

Nonlinear mixed effects modeling was used to study the relationship between measured concentrations, the two versions of the Patient State Index (Patient State Index-1 and Patient State Index-2) and clinical endpoints (no response to calling the person by name, tolerance to shake and shout, and tolerance to tetanic stimulation). For continuous dependent variables (Patient State Index-1 and Patient State Index-2), models were fitted to the data using the first-order conditional estimation routine in NONMEM (version 7.3; Icon Development Solutions, USA). For binary dependent variables (no response to calling the person by name, tolerance to shake and shout, and tolerance to tetanic stimulation), the LAPLACE estimation routine was used.

A sigmoid E_{max} model, as shown in equation 1, was used to describe the nonlinear relationship between Patient State Index (PSI) and the measured plasma propofol and end-tidal sevoflurane concentrations (C).

$$PSI = PSI_0 - \frac{E_{\text{max}} \times C^\gamma}{C_{50}^\gamma + C^\gamma} \quad (1)$$

In this model, Patient State Index is related to the measured propofol or sevoflurane concentration according to a nonlinear function with γ defining the steepness of the concentration–effect relationship. PSI_0 is the baseline Patient State Index when no drug is present and E_{\max} is the maximum drug effect. The C_{50} is the concentration that produces 50% of the maximal drug effect. The two versions of the Patient State Index, being Patient State Index-1 and Patient State Index-2, were modeled simultaneously.

For the clinical endpoints (no response to calling the person by name, tolerance to shake and shout, and tolerance to tetanic stimulation), the sigmoid E_{\max} model described the probability of observing the respective clinical outcome. These probabilities are naturally bound between 0 and 1; hence the baseline term and the E_{\max} term in equation 1 were *a priori* forced to 0 and 1. In these models C_{50} and Patient State Index₅₀ denote the concentration or the Patient State Index value corresponding to a 50% probability of observing the clinical outcome measure.

Interindividual variability around the population typical parameters was assumed according to a multivariate log normal distribution with mean 0 and variances ω^2 . Correlations between off-diagonal elements were explored. For continuous dependent variables, residual unexplained variability was described using additive error models.

Accounting for the Hypnotic–Opioid Interaction

In our analysis we assumed that differences existed between the remifentanyl groups (0, 2 and 4 ng · ml⁻¹). To account for these differences, we introduced an interaction term on the C_{50} and the Patient State Index₅₀. Equations 2 and 3 illustrate the parameterization for the interaction on C_{50} (the same parameterization applies in the case of Patient State Index₅₀).

$$C50' = C50 \times (1 + INT) \quad (2)$$

$$INT = \theta_1 \times (1 + \theta_2) \quad (3)$$

In these equations, θ_1 and θ_2 are 0 for all volunteers not receiving remifentanyl. θ_1 denotes the proportional difference in C_{50} between the 0 and 2 ng · ml⁻¹ remifentanyl groups. θ_2 denotes the proportional difference in C_{50} between the 2 and 4 ng · ml⁻¹ remifentanyl groups. Both θ_1 and θ_2 are estimated from the data. In case there is a (strong) influence of remifentanyl on the C_{50} or Patient State Index₅₀, the estimate for θ_1 will be significantly different from 0. Moreover, if the influence is different between the volunteers in the 4 ng · ml⁻¹ and those in 2 ng · ml⁻¹ group, θ_2 will be significantly higher than 0.

Testing for Differences between Patient State Index-1 and Patient State Index-2

We tested for potential differences in the estimated parameters derived for both Patient State Index algorithms.

Therefore, as shown in equation 4, additional parameters were added to the model. This doubles the number of parameters to be estimated.

$$TV = TV_{PSI-2} \times (1 + \theta_{\Delta PSI}) \quad (4)$$

In equation 4, a population typical parameter (TV), such as E_{\max} , C_{50} , Patient State Index₅₀, etc., was composed of a parameter denoting the estimate for the Patient State Index-2 model (TV_{PSI-2}) and a parameter describing the proportional difference in the estimate when switching from Patient State Index-2 to Patient State Index-1 ($\theta_{\Delta PSI}$). A $\theta_{\Delta PSI}$ significantly different from 0 indicates a difference between the two versions of the Patient State Index algorithm for that particular estimated parameter.

General Modeling Strategy

First, a full model was constructed. This model accounted for the hypnotic–opioid interaction as described under “Accounting for the Hypnotic–Opioid Interaction.” For the pharmacodynamic models for Patient State Index, the full model also included additional terms to quantify the difference in model parameters between Patient State Index-1 and Patient State Index-2, as described under “Testing for Differences between Patient State Index-1 and Patient State Index-2.” Next, this saturated model was simplified by removing nonsignificant parameters. An increase of the objective function value of less than 3.84, corresponding to a value of $P < 0.05$, was considered nonsignificant and led to the removal of the tested parameter.

All models were fitted to the data using PsN²⁸ and Pirana²⁹ as back and/or front end to NONMEM. The numerical and graphical assessment of the goodness of fit was conducted in R (R Foundation for Statistical Computing, Austria).

Statistical Analysis

To determine an appropriate sample size, the sample of 36 volunteers was based on previous expertise in pharmacokinetic–pharmacodynamic modeling in our group and what has been used by others in similar study conditions considering the population variability on age and sex. Statistical significance was set at $P < 0.05$ unless stated otherwise. All model parameters are reported as typical values with associated relative standard errors.

Results

The Consolidated Standards of Reporting Trials flow diagram of the screening and inclusion methodology of the 36 healthy volunteers included in the analysis is provided elsewhere.²² In total, 107 volunteers were assessed for eligibility. Of these 107 volunteers, 20 did not meet the inclusion criteria, 17 declined to participate, and 2 were excluded for other reasons, leaving 68 volunteers confirmed to be eligible. Of these 68 volunteers, 44 were allocated to the

intervention, but 8 discontinued it because of the commitment/load of the four sessions. In total, 36 volunteers completed the study and were analyzed. There were no missing data from these 36 volunteers. The subject demographics are shown in table 2 of the Supplemental Digital Content (<http://links.lww.com/ALN/C53>).

In total, 891 no response to calling the person by name/tolerance to shake and shout and 781 tolerance to tetanic stimulation observations were included in the analysis. Measured arterial propofol and remifentanyl concentrations and end-tidal sevoflurane concentrations were used as surrogates for their respective effect-site concentrations in the analysis. In total, 655 arterial blood samples were drawn during the step-wise titration procedure. From these samples, 451 propofol and 204 remifentanyl concentrations were measured. From the continuously measured end-tidal sevoflurane concentration, only those exactly matching the timing of the Modified Observer's Assessment of Alertness/Sedation Scale and tolerance to tetanic stimulation observations were retained in the dataset, constituting a total of 440 measurements.

Relation between No Response to Calling the Person by Name, Tolerance to Shake and Shout, Tolerance to Tetanic Stimulation, and Propofol or Sevoflurane Concentrations

Figure 1 shows the raw data of the steady-state, measured plasma propofol and end-tidal sevoflurane concentration *versus* the no observed response to calling the person by name, tolerance to shake and shout, and tolerance to tetanic stimulus. Box plots are used to show the distribution of the measured concentrations in the different groups. The predicted probability of achieving no response to calling the person by name, tolerance to shake and shout, and tolerance to tetanic stimulation at a specific steady-state, measured plasma propofol and end-tidal sevoflurane concentration in the absence or presence of a specific effect-site concentration (remifentanyl) is shown in figure 2. Table 2 describes the parameter estimates (and associated relative standard errors) for the pharmacodynamic model shown in figure 2 relating no response to calling the person by name, tolerance to shake and shout, and tolerance to tetanic stimulation to the steady-state, measured plasma propofol (in $\mu\text{g} \cdot \text{mL}^{-1}$) and end-tidal sevoflurane concentrations (in vol %) and the influence of remifentanyl $2\text{ ng} \cdot \text{mL}^{-1}$ (θ_1) and $4\text{ ng} \cdot \text{mL}^{-1}$ (θ_2) on the estimated C_{50} values. In the propofol + $2\text{ ng} \cdot \text{mL}^{-1}$ remifentanyl group, we found 32.7% (relative standard error, 20.5%), 28.0% (relative standard error, 15.1%), and 72.2% (relative standard error, 7.0%) decreases in the C_{50} for no response to calling the person by name, tolerance to shake and shout, and tolerance to tetanic stimulation, respectively, whereas a target effect-site concentration (remifentanyl) of $4\text{ ng} \cdot \text{mL}^{-1}$ led to decreases in the C_{50} of 66.3% (relative standard error, 49.6%), 84.1% (relative standard error, 27.7%), and 22.4% (relative standard error, 36.6%) for no response to calling the person by name, tolerance to shake and shout, and tolerance to tetanic stimulation, respectively. In contrast to the

results for propofol, the addition of remifentanyl 2 or $4\text{ ng} \cdot \text{mL}^{-1}$ did not significantly affect the C_{50} for no response to calling the person by name during sevoflurane anesthesia. For tolerance to shake and shout and tolerance to tetanic stimulation, effect-site concentration (remifentanyl) $2\text{ ng} \cdot \text{mL}^{-1}$ decreased the C_{50} 26.4% (relative standard error, 21.1%) and 56.0% (relative standard error, 10.6%), respectively. Adding more remifentanyl did not alter these C_{50} values for sevoflurane further. Table 2 also shows the interindividual variability for the various C_{50} values and the correlation between the C_{50} values for no response to calling the person by name, tolerance to shake and shout, and tolerance to tetanic stimulation when giving propofol or sevoflurane. During model building, it was found that the interindividual variability around the population typical C_{50} values for propofol and sevoflurane were highly correlated within an individual for no response to calling the person by name and tolerance to shake and shout, as represented by the value of 1 in table 2. Simplification of the random effects model to a single interindividual variability term for both propofol and sevoflurane lead to a non-significant increase in the model's objective function value, being +0.9 and +2.9 for no response to calling the person by name and tolerance to shake and shout, respectively. On the other hand, for tolerance to tetanic stimulation, we found that interindividual variability in C_{50} values for propofol and sevoflurane were independent within an individual. Removal of the correlation coefficient (ρC_{50}) had a marginal impact on the model's goodness of fit ($\Delta\text{OFV} +2.9$).

Relation between Patient State Index-1 or Patient State Index-2 and Propofol or Sevoflurane Concentrations

The pharmacodynamic relationship between the two versions of Patient State Index for each volunteer and the steady-state, measured plasma propofol and end-tidal sevoflurane concentration for each effect-site concentration (remifentanyl) coadministration are shown in figure 3. The *two left columns* show the individual responses for Patient State Index-1 (*dark gray*) or Patient State Index-2 (*light gray*) and a nonparametric smooth to the data (in *blue* for Patient State Index-1 or *red* for Patient State Index-2). For all propofol groups, increasing propofol concentrations resulted in a monotonically decreasing Patient State Index-1 and Patient State Index-2. For sevoflurane, a clear paradoxical response is observed at higher concentrations for Patient State Index-1. The *two right columns* show the individual *post hoc* expected responses for Patient State Index-1 (*dark gray*) or Patient State Index-2 (*light gray*) and the typical population expectation (in *blue* for Patient State Index-1 or *red* for Patient State Index-2) as calculated by NONMEM using the pharmacodynamic model. The biphasic response at higher sevoflurane concentrations results in a difference between the pharmacodynamic models for Patient State Index-1 and Patient State Index-2. No differences for propofol are observed. Table 3 lists the parameter estimates (and associated relative standard errors) for the

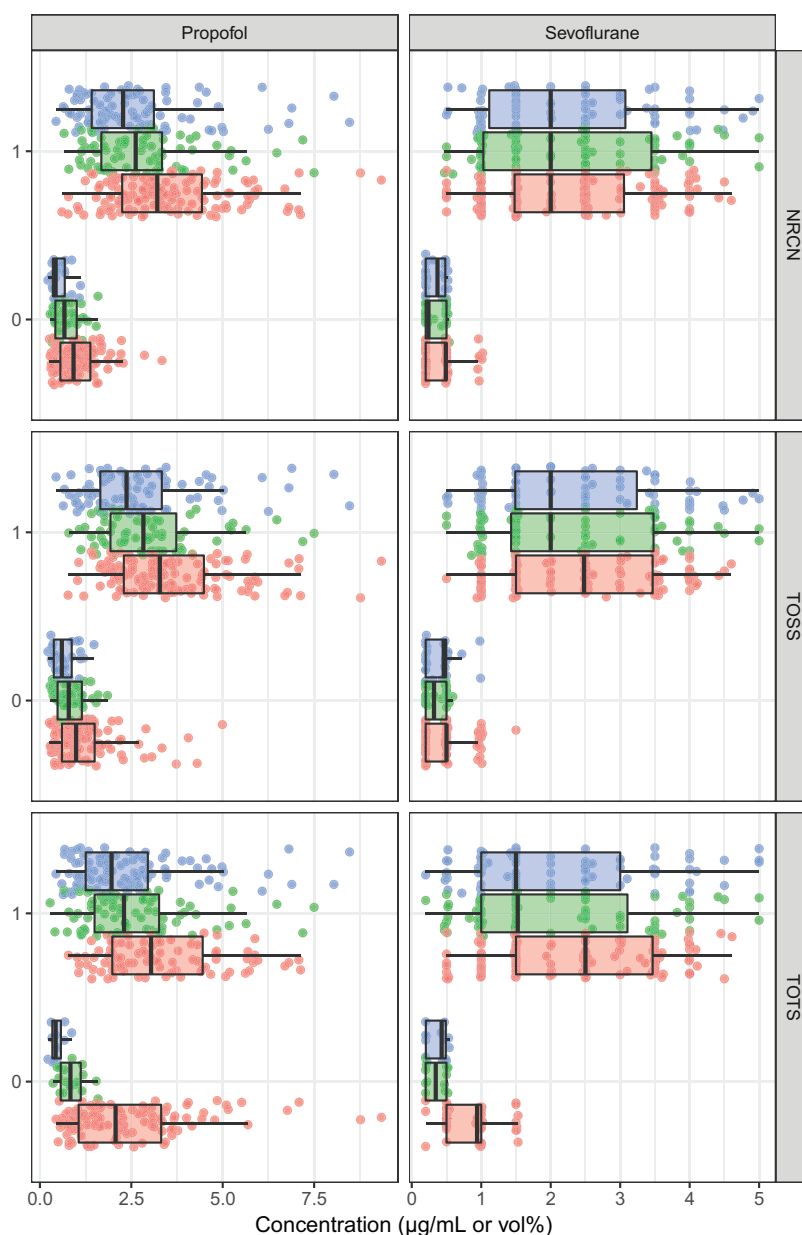


Fig. 1. Steady-state, measured plasma propofol ($\mu\text{g} \cdot \text{mL}^{-1}$) and end-tidal sevoflurane concentration (vol %) *versus* observed response (defined as 0) or no response (defined as 1) to calling the person by name (NRCN), tolerance to shake and shout (TOSS), and tolerance to tetanic stimulation (TOTS). Box plots are used to show measured concentrations in the different remifentanyl groups. Individual observations are shown with circles and are scattered and offset against the y axis to increase visibility. Red, green, and blue are used for the 0, 2, and $4 \text{ ng} \cdot \text{mL}^{-1}$ remifentanyl groups, respectively.

pharmacodynamic models for the Patient State Index-2 and Patient State Index-1 related to the steady-state, measured plasma propofol (in $\mu\text{g} \cdot \text{mL}^{-1}$) and end-tidal sevoflurane concentration (in vol %; C) and the influence of remifentanyl $2 \text{ ng} \cdot \text{mL}^{-1}$ (θ_1) and $4 \text{ ng} \cdot \text{mL}^{-1}$ (θ_2) on the estimated C_{50} values. For propofol, the estimated drug effect parameters were not significantly different between Patient State Index-1 and Patient State Index-2. In contrast, for

sevoflurane, significant differences in the estimated drug effect parameters were obtained for E_{max} and γ . The E_{max} of Patient State Index-1 was 15.2% (relative standard error, 17.1%) lower than the E_{max} of Patient State Index-2. The γ of Patient State Index-1 was 42.2% (relative standard error, 57.4%) higher than that of Patient State Index-2. At baseline (in the awake state), the Patient State Index-1 has a higher interindividual variability and has a higher overall

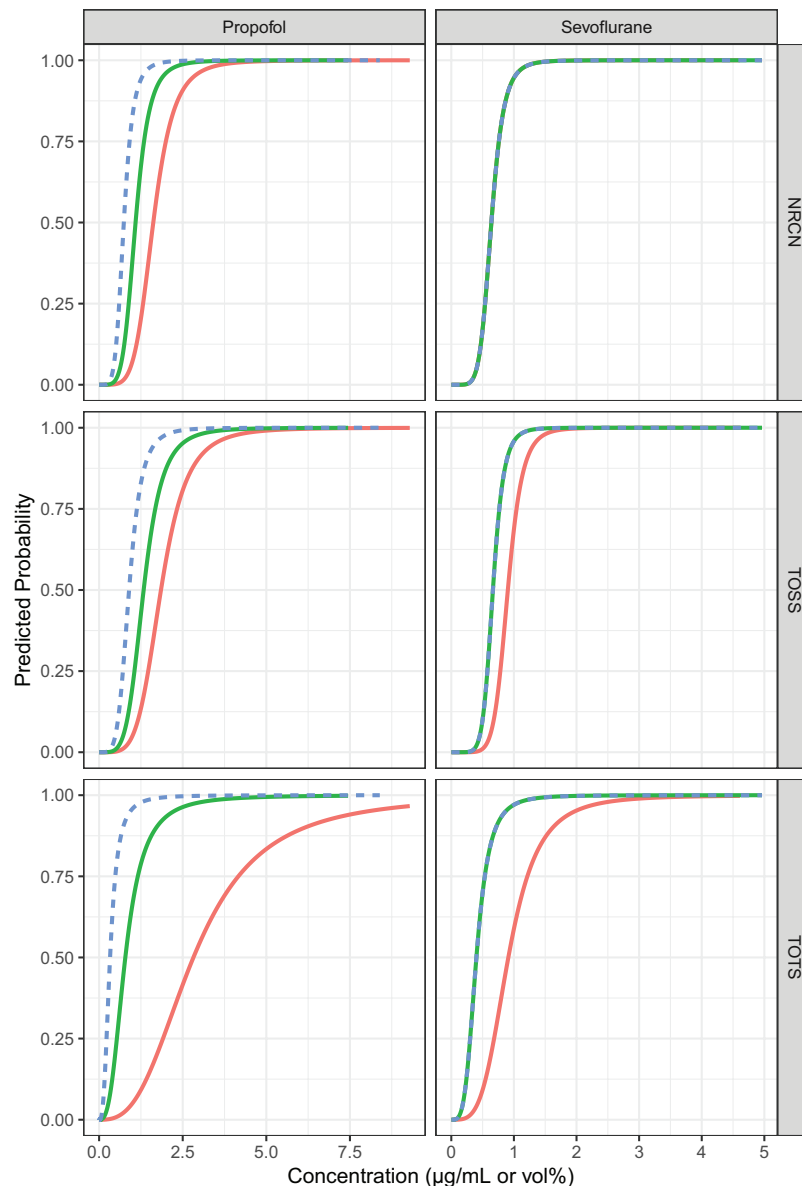


Fig. 2. Steady-state, measured plasma propofol ($\mu\text{g} \cdot \text{mL}^{-1}$) and end-tidal sevoflurane concentration (vol %) versus predicted probabilities for no response to calling the person by name (NRCN), tolerance to shake and shout (TOSS), and tolerance to tetanic stimulation (TOTS). Solid red, solid green, and dashed blue lines are used for the predicted probabilities in the 0, 2, and $4 \text{ ng} \cdot \text{mL}^{-1}$ remifentanyl groups.

residual unexplained variability than Patient State Index-2. The ability of Patient State Index-2 to detect the interaction between hypnotics and opioids is not affected compared with Patient State Index-1. The addition of remifentanyl lowered the C_{50} of propofol significantly for both models to a similar degree. In the propofol + $2 \text{ ng} \cdot \text{mL}^{-1}$ remifentanyl group, we found a 13.5% (relative standard error, 20.8%) decrease in the C_{50} (from 1.63 to $1.41 \mu\text{g} \cdot \text{mL}^{-1}$), whereas a target effect-site concentration (remifentanyl) of $4 \text{ ng} \cdot \text{mL}^{-1}$ led to a decrease in the C_{50} of 81.6% (relative standard error, 62.3%). In contrast to the results for propofol, the addition

of remifentanyl 2 or $4 \text{ ng} \cdot \text{mL}^{-1}$ did not significantly affect the C_{50} of sevoflurane (1.22 vol %) in both Patient State Index-1 and Patient State Index-2 models.

Relation between Patient State Index-2 and No Response to Calling the Person by Name, Tolerance to Shake and Shout, and Tolerance to Tetanic Stimulation for Propofol and Sevoflurane

During model building and using a likelihood ratio test at the 5% level of significance, the estimated model parameters

Table 2. Parameter Estimates for the Pharmacodynamic Models Relating the NRCN, TOSS, and TOTS to the Steady-state, Measured Plasma Propofol and End-tidal Sevoflurane Concentration and the Influence of Remifentanyl on the Model

		NRCN		TOSS		TOTS	
		Propofol	Sevoflurane	Propofol	Sevoflurane	Propofol	Sevoflurane
Drug effect	C_{50}	1.62 (7.00)	0.64 (4.20)	1.85 (6.20)	0.90 (5.00)	2.82 (15.5)	0.91 (10.0)
	γ	5.26 (14.6)	6.40 (16.1)	4.75 (13.1)	7.68 (14.2)	2.82 (10.7)	3.82 (12.7)
Remifentanyl interaction	θ_1	-0.327 (20.5)	NS $P = 0.314$	-0.280 (15.1)	-0.264 (21.1)	-0.722 (7.00)	-0.560 (10.6)
	θ_2	0.663 (49.6)	NS $P = 0.710$	0.841 (27.7)	NS $P = 1.00$	0.224 (36.6)	NS $P = 0.693$
IIV	C_{50}^*	16.8 (71.8)		16.1 (50.8)		71.4 (29.1)	29.5 (43.4)
	ρC_{50}	1		1		NS $P = 0.132$	

The values indicate parameter estimates and associated relative standard error (%). Steady-state, measured plasma propofol in $\mu\text{g} \cdot \text{ml}^{-1}$. End-tidal sevoflurane concentration in vol %. Remifentanyl 2 $\text{ng} \cdot \text{ml}^{-1}$ (θ_1) and 4 $\text{ng} \cdot \text{ml}^{-1}$ (θ_2).

*The P value for the likelihood-ratio test leading to the exclusion of the parameter is included in the table, calculated according to: $\sqrt{e^{\omega} - 1} \cdot 100\%$.

C_{50} , the concentration producing 50% probability of NRCN, TOSS, or TOTS; γ , the steepness/slope of the concentration–effect relationship; IIV, interindividual variability, modeled using a log normal distribution with variance ω^2 ; ρC_{50} , the correlation between the C_{50} values for propofol and sevoflurane; NRCN, no response to calling the person by name; NS, parameter not significant at the 5% level of significance as assessed by likelihood-ratio testing; TOSS, tolerance to shake and shout; TOTS, tolerance to tetanic stimulus.

for Patient State Index-1 and Patient State Index-2 as predictors for no response to calling the person by name, tolerance to shake and shout, and tolerance to tetanic stimulation were indistinguishable. Consequently, both Patient State Index-1 and Patient State Index-2 result in indistinguishable box plots in figure 4, curves in figure 5, and parameter estimates in table 4. As such, only Patient State Index-2 results are shown. Figure 4 shows the raw data of the observed Patient State Index-2 *versus* the no observed response to calling the person by name, tolerance to shake and shout, and tolerance to tetanic stimulus. Box plots are used to show the distribution of Patient State Index-2 in the different groups. The predicted probability of achieving no response to calling the person by name, tolerance to shake and shout, and tolerance to tetanic stimulation at a specific Patient State Index-2 in the absence or presence of a specific effect-site concentration (remifentanyl) is shown in figure 5. Table 4 describes the parameter estimates for the pharmacodynamic model shown in figure 4 relating no response to calling the person by name, tolerance to shake and shout, and tolerance to tetanic stimulation to Patient State Index-2 and the influence of remifentanyl 2 $\text{ng} \cdot \text{ml}^{-1}$ (θ_1) and 4 $\text{ng} \cdot \text{ml}^{-1}$ (θ_2) on the estimated Patient State Index₅₀ values. For no response to calling the person by name, tolerance to shake and shout, and tolerance to tetanic stimulation, a significant decrease in Patient State Index₅₀ was found when coadministering an effect-site concentration (remifentanyl) of 2 $\text{ng} \cdot \text{ml}^{-1}$ with propofol or sevoflurane. Patient State Index₅₀ only decreased further at effect-site concentration (remifentanyl) of 4 $\text{ng} \cdot \text{ml}^{-1}$ for tolerance to shake and shout and tolerance to tetanic stimulation during propofol administration. Table 4 also shows the interindividual variability for the various Patient State Index₅₀ values and the correlation between the Patient State Index₅₀ values for no response to calling

the person by name, tolerance to shake and shout, and tolerance to tetanic stimulation within an individual when giving propofol or sevoflurane. During model building, it was found that within an individual, Patient State Index₅₀ values for propofol and sevoflurane were moderately correlated, as represented by the values of 0.65 and 0.58. In contrast, for tolerance to tetanic stimulation, we found that Patient State Index₅₀ values for propofol and sevoflurane were independent within an individual.

Discussion

Because in this trial the same group of volunteers received four different anesthetic regimens in steady-state conditions, our results offer a unique possibility to directly compare the pharmacodynamics of propofol *versus* sevoflurane with and without remifentanyl coadministration at both a population and an individual level.

Relation between No Response to Calling the Person by Name, Tolerance to Shake and Shout, Tolerance to Tetanic Stimulation, and Propofol or Sevoflurane Concentrations

The pharmacodynamic relation between no response to calling the person by name, tolerance to shake and shout, tolerance to tetanic stimulation, and the steady-state, measured plasma propofol or end-tidal sevoflurane concentration could be described by a classical nonlinear relation. The model parameter values are in agreement with others for no response to calling the person by name and tolerance to shake and shout but mostly lower than others for tolerance to tetanic stimulation.^{7,30–32} However, comparing our C_{50} values with those from other studies is not that relevant, because the results are influenced by observer differences for clinical scores and differences in device and stimulation characteristics for tolerance

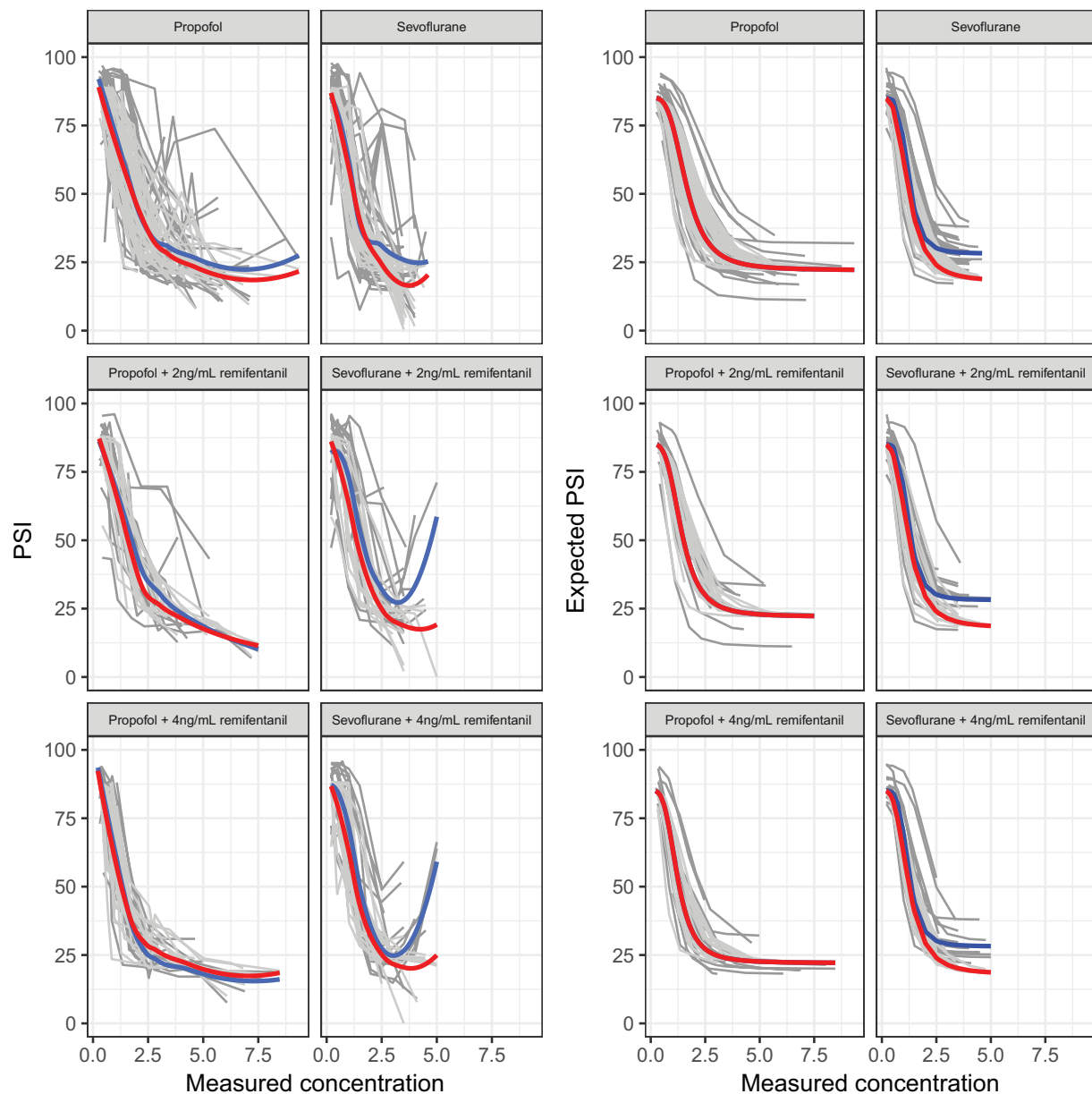


Fig. 3. Relationship between Patient State Index (PSI)-1 or PSI-2 and the steady-state measured plasma propofol ($\mu\text{g} \cdot \text{mL}^{-1}$) or end-tidal sevoflurane (vol %) concentration during various effect-compartment targeted remifentanyl ($\text{ng} \cdot \text{mL}^{-1}$) coadministrations. The *two left columns* show the individual responses for PSI-1 (dark gray) or PSI-2 (light gray) and a nonparametric smooth (in blue for PSI-1 or red for PSI-2). The *two right columns* show the individual *post hoc* expected responses for PSI-1 (dark gray) or PSI-2 (light gray) and the typical population expectation (in blue for PSI-1 or red for PSI-2) as calculated by NONMEM using the pharmacodynamic model.

to tetanic stimulation. Because we used a crossover design, it is much more interesting to quantify the ratio between C_{50} values for no response to calling the person by name, tolerance to shake and shout, and tolerance to tetanic stimulation between propofol and sevoflurane (without remifentanyl), being $1.62 \mu\text{g} \cdot \text{mL}^{-1}/0.64 \text{ vol } \%$, $1.85 \mu\text{g} \cdot \text{mL}^{-1}/0.90 \text{ vol } \%$, and $2.82 \mu\text{g} \cdot \text{mL}^{-1}/0.91 \text{ vol } \%$, respectively. As an example using tolerance to

shake and shout, this means that a clinician can expect tolerance to shake and shout in 50% of his patients when titrating a propofol steady-state concentration of $1.85 \mu\text{g} \cdot \text{mL}^{-1}$ or a steady-state end-tidal concentration of sevoflurane of $0.90 \text{ vol } \%$, resulting in ratio of 2.05. This also means that a clinician titrating the propofol effect at a steady-state concentration of $1.85 \mu\text{g} \cdot \text{mL}^{-1}$ can theoretically produce a similar

Table 3. Final Parameter Estimates for the Pharmacodynamic Model for the PSI-2 and PSI-1 *versus* the Steady-state, Measured Plasma Propofol and End-tidal Sevoflurane Concentration and the Influence of Remifentanyl on the Model

		PSI-2		PSI-1	
		Propofol	Sevoflurane	Propofol	Sevoflurane
Baseline	E_0		85.1 (0.8)		$P = 0.508$
Drug effect	E_{\max}	63.1 (1.9)	67.2 (2.3)	$P = 0.163$	$-0.152^* (17.1)$
	C_{50}	1.63 (3.7)	1.22 (3.1)	$P = 0.952^{\dagger}$	$P = 0.952^{\dagger}$
	γ	3.41 (5.6)	3.23 (6.7)	$P = 0.749$	$0.422^* (57.4)$
Remifentanyl interaction	θ_1	$-0.135 (20.8)$	$P = 1.00$	$P = 0.771$	—
	θ_2	$0.816 (62.3)$	$P = 1.00$	$P = 0.593$	—
IIV	E_0^{\ddagger}		$P = 0.874$		$6.64 (38.6)$
	C_{50}^{\ddagger}	$25.8 (22.2)$	$20.1 (24.3)$	$26.2 (21.9)$	$28.0 (23.1)$
	ρC_{50}		$0.54 (25.5)$		$0.69 (17.1)$
RUV	$\sigma_{\text{Additive}}^{\S}$		$8.54 (5.0)$		$12.7 (5.1)$

The values indicate parameter estimates and associated relative standard error (%). The dash (—) denotes a situation where the difference between PSI-1 and PSI-2 could not be tested because the parameter was already excluded from the PSI-2 model. Steady-state, measured plasma propofol in $\mu\text{g} \cdot \text{ml}^{-1}$. End-tidal sevoflurane concentration in vol %. Remifentanyl 2 $\text{ng} \cdot \text{ml}^{-1}$ (θ_1) and 4 $\text{ng} \cdot \text{ml}^{-1}$ (θ_2).

*Parameters are expressed as relative differences *versus* parameters estimates obtained for PSI-2. † These parameters were removed from the model simultaneously. ‡ Statistical significance was set at $P < 0.05$, calculated according to: $\sqrt{e^{\omega} - 1} \cdot 100\%$. § Expressed as SD.

C_{50} , the concentration which produces 50% of the maximal drug effect; E_0 , the baseline measurement of the pharmacodynamic endpoint when no drug is present; E_{\max} , the maximum drug effect; γ , the steepness/slope of the concentration–effect relationship; IIV, interindividual variability, by assuming a log normal distribution of C_{50} , with η_1 being an individual realization from this distribution with variance ω^2 ; PSI, Patient State Index; ρC_{50} , the correlation between the C_{50} values for propofol and sevoflurane; RUV, the residual unexplained variability (σ_{Additive}).

hypnotic effect as measured with tolerance to shake and shout when switching to a sevoflurane steady-state concentration of 0.90 vol %. As such, these values become clinically useful to help the clinician optimizing drug titration when switching between propofol and sevoflurane. Our propofol and sevoflurane ratios are close to the observations made by Schumacher *et al.*⁷ when studying the interaction between propofol and sevoflurane, being 2.05 and 3.09 for tolerance to shake and shout and tolerance to tetanic stimulation, respectively.

Because of the absence of analgesic properties for propofol, we found a difference between propofol and sevoflurane in the influence of remifentanyl on the C_{50} values for the various clinical endpoints. For propofol, significant decreases in the propofol C_{50} for no response to calling the person by name, tolerance to shake and shout, and tolerance to tetanic stimulation were found at increasing effect-site concentration (remifentanyl) as also found by Kern *et al.*³⁰ For sevoflurane, the influence of remifentanyl on the sevoflurane C_{50} values was variable, ranging from no influence for no response to calling the person by name to an effect of effect-site concentration (remifentanyl) of 2 $\text{ng} \cdot \text{ml}^{-1}$ for tolerance to shake and shout and tolerance to tetanic stimulation without an additional effect when increasing effect-site concentration (remifentanyl) to 4 $\text{ng} \cdot \text{ml}^{-1}$. Heyse *et al.*³² studied the interaction between sevoflurane and remifentanyl and also found differences in the synergy between various clinical endpoints. In addition, Heyse *et al.*³² showed that above a effect-site concentration (remifentanyl) of 4 $\text{ng} \cdot \text{ml}^{-1}$, the interaction no longer increases.

Relation between Patient State Index-1 or Patient State Index-2 and Propofol or Sevoflurane Concentrations

As shown in figure 3, both Patient State Index-1 and Patient State Index-2 decreased with increasing measured plasma propofol or end-tidal sevoflurane concentrations. For propofol, we found no significant differences between Patient State Index-1 and Patient State Index-2 in the model parameters of the concentration–effect relationship, independent of the addition of remifentanyl. In contrast, for sevoflurane with or without remifentanyl, we found an improved monotonic relationship of the concentration–effect curve for Patient State Index-2 compared with Patient State Index-1. This was also reflected in a significant difference between Patient State Index-1 and Patient State Index-2 in two model parameters, E_{\max} and γ , even though the C_{50} values were similar for both indices. In combination with the decreased variability for Patient State Index-2 at baseline (suggesting a better signal-to-noise ratio in awake individuals), our findings indicate that Patient State Index-2 has improved characteristics to serve as a continuous pharmacodynamic measure of cortical electrical activity during both propofol and sevoflurane anesthesia. Paradoxical increases, especially during administration of higher concentrations of inhaled anesthetics, have been described before and must be taken into consideration during processed electroencephalographic algorithm development to avoid incorrect anesthetic management under electroencephalographic monitoring.^{33–35}

We are aware of only two articles that have used pharmacodynamic modeling to compare the concentration–effect relationship between propofol or sevoflurane and the Patient

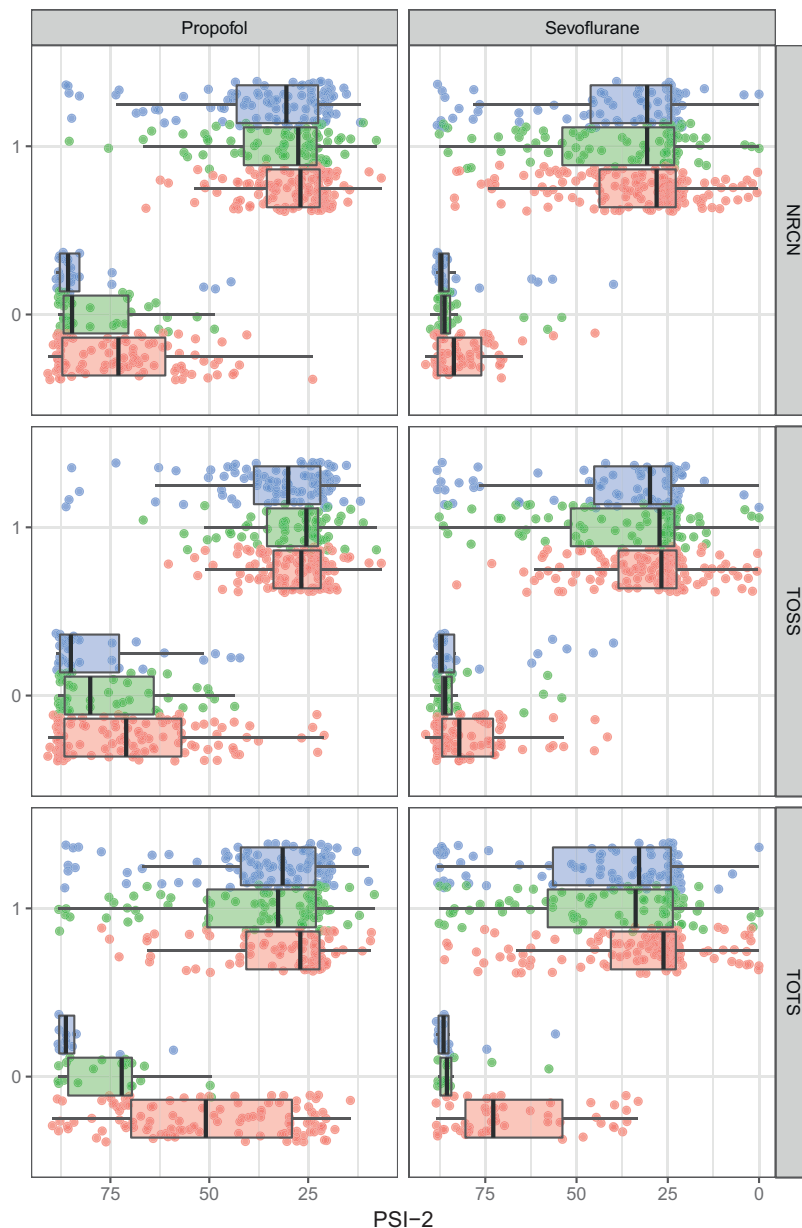


Fig. 4. Patient State Index (PSI)-2 *versus* no observed response to calling the person by name (NRCN), tolerance to shake and shout (TOSS), and tolerance to tetanic stimulation (TOTS) during propofol and sevoflurane administration. Box plots are used to show the distribution of the PSI-2 index in the different remifentanyl groups. Individual observations are shown with *circles* and are scattered and offset against the y axis to increase visibility. *Red, green, and blue* are used for the 0, 2, and 4 ng · ml⁻¹ remifentanyl groups, respectively.

State Index-1. Soehle *et al.*^{13,14} obtained C_{50} values of 1.38 $\mu\text{g} \cdot \text{ml}^{-1}$ and 0.77 vol % for propofol and sevoflurane, respectively, which are considerably lower for sevoflurane compared with our C_{50} values; the difference is probably related to differences in sample selection and methodology. More relevant and similar to the clinical endpoints, we compared C_{50} values for both Patient State Index-1 and Patient State Index-2 between propofol and sevoflurane in the same sample of volunteers on both a population and an individual level.

Relation between Patient State Index-2 and No Response to Calling the Person by Name, Tolerance to Shake and Shout, and Tolerance to Tetanic Stimulation for Propofol and Sevoflurane

We found indistinguishable results in the model parameters for Patient State Index-1 and Patient State Index-2 in relation to no response to calling the person by name, tolerance to shake and shout, and tolerance to tetanic

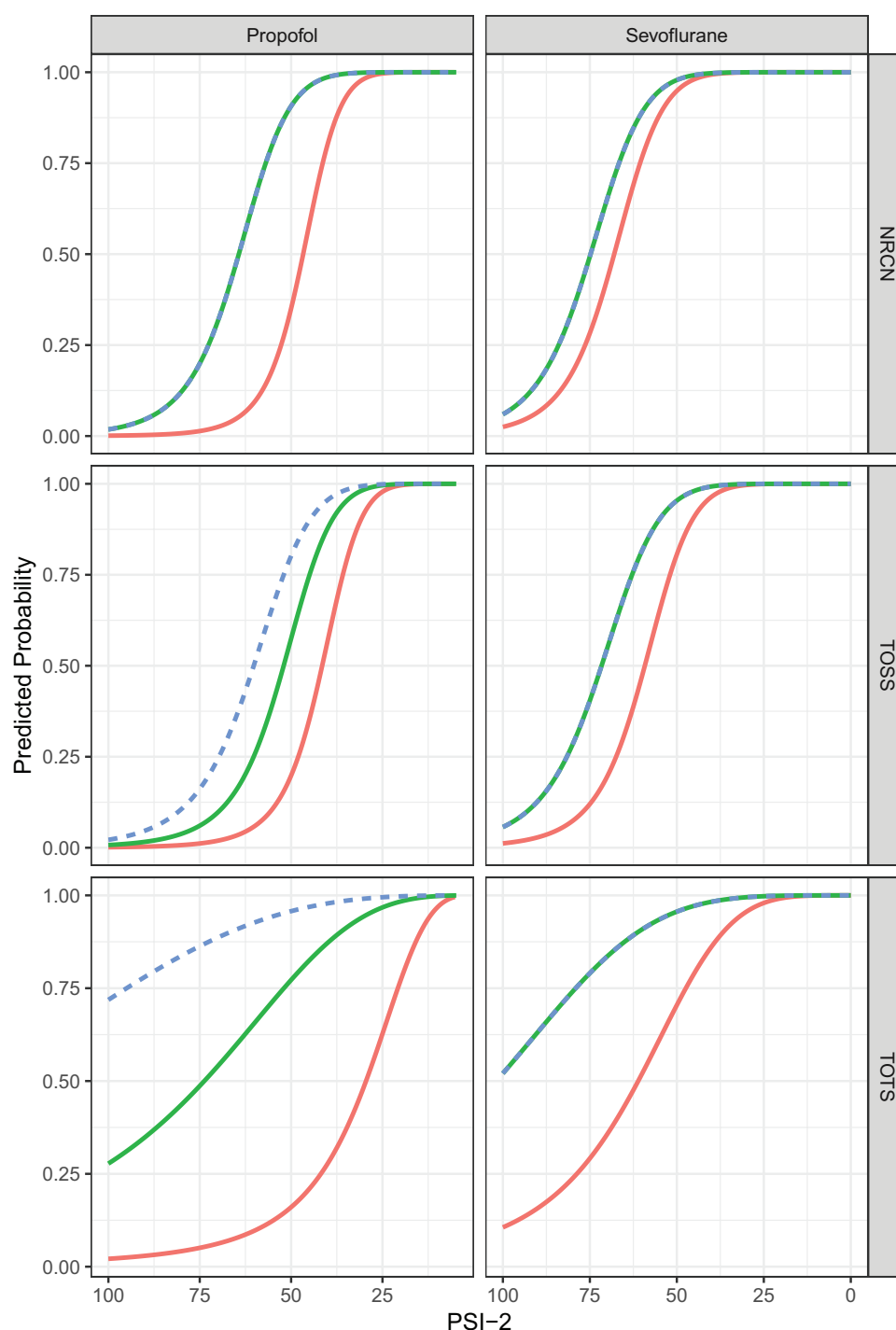


Fig. 5. Patient State Index (PSI)-2 versus predicted probabilities for no response to calling the person by name (NRCN), tolerance to shake and shout (TOSS), and tolerance to tetanic stimulation (TOTS) during propofol and sevoflurane administration. Solid red, solid green, and dashed blue lines are used for the predicted probabilities in the 0, 2, and 4 ng·ml⁻¹ remifentanyl groups.

stimulation, and as such, we only present results for Patient State Index-2. Although improvements in concentration-effect relationship for Patient State Index-2 were observed, particularly for sevoflurane, this did not influence the

correlation between Patient State Index and no response to calling the person by name, tolerance to shake and shout, and tolerance to tetanic stimulation. Therefore, no adaptation is required for the clinician when switching to

Table 4. Parameter Estimates for the Pharmacodynamic Models Relating the NRCN, TOSS, and TOTS to PSI-2 and the Influence of Remifentanyl 2 ng·ml⁻¹ (θ_1) and 4 ng·ml⁻¹ (θ_2) on the Model

		NRCN		TOSS		TOTS	
		Propofol	Sevoflurane	Propofol	Sevoflurane	Propofol	Sevoflurane
Drug effect	PSI ₅₀	46.7 (5.10)	68.0 (3.00)	41.5 (4.10)	59.2 (3.60)	29.5 (12.9)	61.1 (8.10)
	γ	9.04 (19.8)	9.49 (17.8)	7.50 (13.7)	8.42 (14.7)	3.14 (10.5)	4.33 (9.60)
Remi interaction	θ_1	0.377 (21.6)	0.100 (40.4)	0.254 (18.5)	0.210 (25.2)	1.50 (30.2)	0.668 (27.5)
	θ_2	NS $P = 0.063$	NS $P = 0.906$	0.777 (80.1)	NS $P = 1.00$	1.38 (57.5)	NS $P = 0.856$
IIV	PSI ₅₀ *	17.0 (38.9)	10.3 (38.8)	15.2 (39.6)	13.2 (42.4)	55.6 (35.7)	28.2 (19.1)
	ρ PSI ₅₀	0.65 (50.8)		0.584 (40.9)		NS $P = 0.297$	

The values indicate parameter estimates and associated relative standard errors (%).

*The P value for the likelihood-ratio test leading to the exclusion of the parameter is included in the table, calculated according to: $\sqrt{e^{\omega} - 1} * 100\%$.

γ , the steepness/slope of the PSI-2 effect relationship; IIV, interindividual variability, modeled using a log normal distribution with variance ω^2 ; NRCN, no response to calling the person by name; NS, parameter not significant at the 5% level of significance as assessed by likelihood-ratio testing; PSI, Patient State Index; PSI₅₀, the Patient State Index-2 index associated with 50% probability of NRCN, TOSS or TOTS; ρ PSI₅₀, the correlation between the Patient State Index₅₀ values for propofol and sevoflurane; TOSS, tolerance to shake and shout; TOTS, tolerance to tetanic stimulus.

the new Patient State Index-2. Moreover, it seems that our results do not invalidate earlier publications on the relation between Patient State Index and clinical endpoints.^{10–15}

The relationships between Patient State Index-2 and the three clinical endpoints show some fundamental clinical differences between propofol and sevoflurane anesthesia. The Patient State Index-2 values associated with 50% probability (Patient State Index₅₀) of no response to calling the person by name, tolerance to shake and shout, and tolerance to tetanic stimulation are significantly higher for sevoflurane than propofol. Adding remifentanyl 2 ng · ml⁻¹ increased all Patient State Index₅₀ values significantly. However higher effect-site concentration (remifentanyl) values showed an additional effect for tolerance to shake and shout and tolerance to tetanic stimulation only during propofol administration. When maintaining a Patient State Index-2 within the range of 25 to 50 as recommended by the company for general anesthesia, there was still a significant risk that the patient could be responsive to one of the clinical endpoints during propofol administration even in the presence of remifentanyl. Based on our findings presented in figure 5 and table 4, we recommend lowering the upper range limit towards a Patient State Index-2 value of 35 to maintain a safe level of the hypnotic component of anesthesia when using propofol. When using sevoflurane, the recommended Patient State Index-2 range of 50 to 25 is sufficient to ensure a high probability for the hypnotic endpoints no response to calling the person by name and tolerance to shake and shout. The significant difference in Patient State Index₅₀ for tolerance to tetanic stimulation between propofol and sevoflurane also reflects the much higher intrinsic immobilizing capacity of sevoflurane compared with propofol.^{36,37} To obtain a similar probability of immobility to noxious stimulus, propofol should inhibit the cortical electrical activity to a much larger extent compared

with sevoflurane and therefore requires a higher concentration of propofol, resulting in more electroencephalographic suppression and lower Patient State Index-2 values. The addition of a sufficiently effective concentration of remifentanyl during propofol anesthesia is mandatory to ensure immobility after a noxious stimulus.

Originally, Patient State Index-1 was presented as a drug-independent representation of electroencephalographic suppression by some authors.^{12,38} Our study clearly indicates that the Patient State Index-2 needs to be interpreted differently depending on the anesthetic drugs used, as suggested by Purdon *et al.*³⁹ and Schneider *et al.*⁴⁰

Interindividual Variability around C₅₀

Because our study allows direct comparisons between propofol and sevoflurane, we studied variability in C₅₀ values and Patient State Index₅₀ values within an individual during propofol and sevoflurane administration in the absence or presence of remifentanyl. We found that within an individual, C₅₀ values for propofol and sevoflurane are perfectly correlated ($\rho C_{50} = 1$) for no response to calling the person by name and tolerance to shake and shout. This means that an individual having a higher or lower C₅₀ for propofol *versus* the population typical value also has a higher or lower C₅₀ value for sevoflurane. At the same time, this means that the ratio of C₅₀ values for no response to calling the person by name and tolerance to shake and shout between propofol and sevoflurane is identical for all individuals and equal to the population ratios of 1.62 $\mu\text{g} \cdot \text{ml}^{-1}/0.64 \text{ vol } \%$, and 1.85 $\mu\text{g} \cdot \text{ml}^{-1}/0.90 \text{ vol } \%$, respectively.

We also showed that C₅₀ values for propofol and sevoflurane for Patient State Index-1 ($\rho C_{50} = 0.69$) and Patient State Index-2 ($\rho C_{50} = 0.54$) and Patient State Index₅₀ values for no response to calling the person by name ($\rho C_{50} = 0.65$)

and tolerance to shake and shout ($\rho C_{50} = 0.58$) are positively correlated. This means that, on average, individuals having a higher or lower C_{50} or Patient State Index₅₀ for propofol also have a higher or lower C_{50} or Patient State Index₅₀ for sevoflurane. A consequence of the correlation coefficient being less than 1 is that the population typical ratio does not apply to all individuals and that some interindividual variability exists in the ratios. For example, for Patient State Index-2 the population typical ratio is $1.63 \mu\text{g} \cdot \text{ml}^{-1}/1.22 \text{ vol } \%$ with individual (*post hoc*) ratios ranging from $0.85 \mu\text{g} \cdot \text{ml}^{-1}/1.22 \text{ vol } \%$ to $2.06 \mu\text{g} \cdot \text{ml}^{-1}/1.30 \text{ vol } \%$. Similarly, the population typical ratio of Patient State Index₅₀ values for Patient State Index-2 was 0.69 with individual ratios ranging from 0.55 to 0.75 for no response to calling the person by name and tolerance to shake and shout, respectively.

Interestingly, no correlation between C_{50} values and Patient State Index₅₀ values for propofol and sevoflurane was found for tolerance to tetanic stimulation. This means that an individual having a higher C_{50} for propofol (compared with the population typical value) has an equal probability of having a higher or lower C_{50} for sevoflurane. Consequently, individual ratios vary considerably from the population typical ratios of C_{50} and Patient State Index₅₀. The population typical ratios of C_{50} and Patient State Index₅₀ are $2.82 \mu\text{g} \cdot \text{ml}^{-1}/0.91 \text{ vol } \%$ and 0.48 and individual ratios range from $0.91 \mu\text{g} \cdot \text{ml}^{-1}/0.81 \text{ vol } \%$ to $5.13 \mu\text{g} \cdot \text{ml}^{-1}/0.92 \text{ vol } \%$ and from 0.22 to 0.84. These correlations between *post hoc* C_{50} and Patient State Index₅₀ values for propofol and sevoflurane for these hypnotic-related, clinical, and electroencephalographic endpoints, but not for the spinal reaction-related tolerance to tetanic stimulation, are exciting and might offer new insights into mechanisms of action for sevoflurane *versus* propofol.^{41,42}

A limitation of our modeling approach is that we used the predicted effect-site concentrations of remifentanyl instead of the measured concentrations. As such, the between-subject variability in the measured concentrations is not considered. Although parameter estimates on the group level are likely unbiased, this approach could possibly have confounded the estimates for the correlations between the C_{50} values and Patient State Index₅₀ values. Nevertheless, in our opinion this approach is justified because we did not aim at building a surface-response model, and considering the between-subject variability in the measured concentrations would only increase the complexity of the analysis without leading to different conclusions with respect to the pharmacodynamics of propofol and sevoflurane for no response to calling the person by name, tolerance to shake and shout, tolerance to tetanic stimulation, and Patient State Index.

Conclusions

The pharmacodynamics for propofol and sevoflurane with and without remifentanyl coadministration were described on both population and individual levels using clinical scores and Patient State Index. We observed that

the interindividual variability around the population typical C_{50} values and Patient State Index₅₀ during propofol and sevoflurane administration were significantly correlated within an individual for no response to calling the person by name and tolerance to shake and shout, but not for tolerance to tetanic stimulation. Patient State Index-2 has an improved monotonic concentration–effect relationship and descriptive performance at higher sevoflurane concentrations compared with Patient State Index-1. Finally, the probability of responsiveness for no response to calling the person by name, tolerance to shake and shout, and tolerance to tetanic stimulation as a function of Patient State Index is drug- and drug combination-specific but is not affected by the version of Patient State Index used.

Acknowledgments

The authors acknowledge the assistance of R. Spanjersberg, R.N., University Medical Center Groningen, Groningen, The Netherlands, and A. R. Absalom, M.B.Ch.B., F.R.C.A., M.D., University Medical Center Groningen, Groningen, The Netherlands.

Research Support

Supported in part by Masimo (Irvine, California) and in part by departmental and institutional funding.

Competing Interests

Dr. Reyntjens is a member of the Key Opinion Leader group on patient warming and received funding for travel and lectures of the 37°Company (Amersfoort, The Netherlands). Dr. Touw serves as editor for the Journal of Cystic Fibrosis and of Clinical Pharmacokinetics. Dr. Struys's department received grants and funding from The Medicines Company (Parsippany-Troy Hills, New Jersey), Masimo (Irvine, California), Fresenius (Bad Homburg, Germany), Acacia Design (Maastricht, The Netherlands), and Medtronic (Dublin, Ireland); received honoraria from The Medicines Company, Masimo, Fresenius, Baxter (Deerfield, Illinois), Medtronic, and Demed Medical (Temse, Belgium); and serves as a director and editorial board member of the British Journal of Anesthesia. The other authors declare no competing interests.

Reproducible Science

Full protocol available at: m.h.kuizenga@umcg.nl. Raw data available at: m.h.kuizenga@umcg.nl.

Correspondence

Address correspondence to Dr. Kuizenga: University of Groningen, University Medical Center Groningen, Hanzeplein 1, 9713 GZ Groningen, The Netherlands. m.h.kuizenga@umcg.nl. This article may be accessed for personal use at no charge through the Journal Web site, www.anesthesiology.org.

References

1. Glass PS: Anesthetic drug interactions: An insight into general anesthesia: Its mechanism and dosing strategies. *ANESTHESIOLOGY* 1998; 88:5–6
2. Struys MM, Sahinovic M, Lichtenbelt BJ, Vereecke HE, Absalom AR: Optimizing intravenous drug administration by applying pharmacokinetic/pharmacodynamic concepts. *Br J Anaesth* 2011; 107:38–47
3. Chernik DA, Gillings D, Laine H, Hendler J, Silver JM, Davidson AB, Schwam EM, Siegel JL: Validity and reliability of the Observer's Assessment of Alertness/Sedation Scale: Study with intravenous midazolam. *J Clin Psychopharmacol* 1990; 10:244–51
4. Bruhn J, Bouillon TW, Radulescu L, Hoeft A, Bertaccini E, Shafer SL: Correlation of approximate entropy, Bispectral Index, and spectral edge frequency 95 (SEF95) with clinical signs of "anesthetic depth" during coadministration of propofol and remifentanyl. *ANESTHESIOLOGY* 2003; 98:621–7
5. Bouillon TW, Bruhn J, Radulescu L, Andresen C, Shafer TJ, Cohane C, Shafer SL: Pharmacodynamic interaction between propofol and remifentanyl regarding hypnosis, tolerance of laryngoscopy, Bispectral Index, and electroencephalographic approximate entropy. *ANESTHESIOLOGY* 2004; 100:1353–72
6. Rantanen M, Yppärilä-Wolters H, van Gils M, Yli-Hankala A, Huiku M, Kymäläinen M, Korhonen I: Tetanic stimulus of ulnar nerve as a predictor of heart rate response to skin incision in propofol remifentanyl anaesthesia. *Br J Anaesth* 2007; 99:509–13
7. Schumacher PM, Dossche J, Mortier EP, Luginbuehl M, Bouillon TW, Struys MM: Response surface modeling of the interaction between propofol and sevoflurane. *ANESTHESIOLOGY* 2009; 111:790–804
8. Kim TK, Niklewski PJ, Martin JF, Obara S, Egan TD: Enhancing a sedation score to include truly noxious stimulation: The Extended Observer's Assessment of Alertness and Sedation (EOAA/S). *Br J Anaesth* 2015; 115:569–77
9. Fahy BG, Chau DF: The technology of processed electroencephalogram monitoring devices for assessment of depth of anesthesia. *Anesth Analg* 2018; 126:111–7
10. Drover DR, Lemmens HJ, Pierce ET, Plourde G, Loyd G, Ornstein E, Prichep LS, Chabot RJ, Gugino L: Patient State Index: Titration of delivery and recovery from propofol, alfentanil, and nitrous oxide anesthesia. *ANESTHESIOLOGY* 2002; 97:82–9
11. Prichep LS, Gugino LD, John ER, Chabot RJ, Howard B, Merkin H, Tom ML, Wolter S, Rausch L, Kox WJ: The Patient State Index as an indicator of the level of hypnosis under general anaesthesia. *Br J Anaesth* 2004; 92:393–9
12. Drover D, Ortega HR: Patient State Index. *Best Pract Res Clin Anaesthesiol* 2006; 20:121–8
13. Soehle M, Kuech M, Grube M, Wirz S, Kreuer S, Hoeft A, Bruhn J, Ellerkmann RK: Patient State Index *vs.* Bispectral Index as measures of the electroencephalographic effects of propofol. *Br J Anaesth* 2010; 105:172–8
14. Soehle M, Ellerkmann RK, Grube M, Kuech M, Wirz S, Hoeft A, Bruhn J: Comparison between Bispectral Index and Patient State Index as measures of the electroencephalographic effects of sevoflurane. *ANESTHESIOLOGY* 2008; 109:799–805
15. Lee KH, Kim YH, Sung YJ, Oh MK: The Patient State Index is well balanced for propofol sedation. *Hippokratia* 2015; 19:235–8
16. Nasraway SS, Jr., Wu EC, Kelleher RM, Yasuda CM, Donnelly AM: How reliable is the Bispectral Index in critically ill patients?: A prospective, comparative, single-blinded observer study. *Crit Care Med* 2002; 30:1483–7
17. Borjian Boroojeny S: The effect of facial muscle contractions on the cerebral state index in an ICU patient: A case report. *Cases J* 2008; 1:167
18. Aho AJ, Kamata K, Yli-Hankala A, Lyytikäinen LP, Kulkas A, Jäntti V: Elevated BIS and Entropy values after sugammadex or neostigmine: An electroencephalographic or electromyographic phenomenon? *Acta Anaesthesiol Scand* 2012; 56:465–73
19. Bruhn J, Bouillon TW, Hoeft A, Shafer SL: Artifact robustness, inter- and intraindividual baseline stability, and rational EEG parameter selection. *ANESTHESIOLOGY* 2002; 96:54–9
20. Vereecke HE, Vasquez PM, Jensen EW, Thas O, Vandenbroecke R, Mortier EP, Struys MM: New composite index based on midlatency auditory evoked potential and electroencephalographic parameters to optimize correlation with propofol effect site concentration: Comparison with Bispectral Index and solitary used fast extracting auditory evoked potential index. *ANESTHESIOLOGY* 2005; 103:500–7
21. Next Generation SedLine® Brain Function Monitoring, Available at: <http://www.masimo.com/products/continuous/root/root-sedline/>. Accessed April 26, 2019.
22. Kuizenga MH, Colin PJ, Reyntjens KMEM, Touw DJ, Nalbat H, Knotnerus FH, Vereecke HEM, Struys MMRF: Test of neural inertia in humans during general anaesthesia. *Br J Anaesth* 2018; 120:525–36
23. Schnider TW, Minto CE, Gambus PL, Andresen C, Goodale DB, Shafer SL, Youngs EJ: The influence of method of administration and covariates on the pharmacokinetics of propofol in adult volunteers. *ANESTHESIOLOGY* 1998; 88:1170–82
24. Schnider TW, Minto CE, Shafer SL, Gambus PL, Andresen C, Goodale DB, Youngs EJ: The influence of

- age on propofol pharmacodynamics. *ANESTHESIOLOGY* 1999; 90:1502–16
25. Minto CF, Schnider TW, Egan TD, Youngs E, Lemmens HJ, Gambus PL, Billard V, Hoke JF, Moore KH, Hermann DJ, Muir KT, Mandema JW, Shafer SL: Influence of age and gender on the pharmacokinetics and pharmacodynamics of remifentanyl: I. Model development. *ANESTHESIOLOGY* 1997; 86:10–23
 26. Minto CF, Schnider TW, Shafer SL: Pharmacokinetics and pharmacodynamics of remifentanyl: II. Model application. *ANESTHESIOLOGY* 1997; 86:24–33
 27. Koster RA, Vereecke HE, Greijdanus B, Touw DJ, Struys MM, Alfenaar JW: Analysis of remifentanyl with liquid chromatography–tandem mass spectrometry and an extensive stability investigation in EDTA whole blood and acidified EDTA plasma. *Anesth Analg* 2015; 120:1235–41
 28. Lindbom L, Pihlgren P, Jonsson EN, Jonsson N: PsN-Toolkit: A collection of computer intensive statistical methods for non-linear mixed effect modeling using NONMEM. *Comput Methods Programs Biomed* 2005; 79:241–57
 29. Keizer RJ, van Benten M, Beijnen JH, Schellens JH, Huitema AD: Piraña and PCluster: A modeling environment and cluster infrastructure for NONMEM. *Comput Methods Programs Biomed* 2011; 101:72–9
 30. Kern SE, Xie G, White JL, Egan TD: A response surface analysis of propofol-remifentanyl pharmacodynamic interaction in volunteers. *ANESTHESIOLOGY* 2004; 100:1373–81
 31. Johnson KB, Syroid ND, Gupta DK, Manyam SC, Egan TD, Huntington J, White JL, Tyler D, Westenskow DR: An evaluation of remifentanyl propofol response surfaces for loss of responsiveness, loss of response to surrogates of painful stimuli and laryngoscopy in patients undergoing elective surgery. *Anesth Analg* 2008; 106:471–9
 32. Heyse B, Proost JH, Schumacher PM, Bouillon TW, Vereecke HE, Eleveld DJ, Luginbühl M, Struys MM: Sevoflurane remifentanyl interaction: Comparison of different response surface models. *ANESTHESIOLOGY* 2012; 116:311–23
 33. Litscher G, Schwarz G: Is there paradoxical arousal reaction in the EEG subdelta range in patients during anesthesia? *J Neurosurg Anesthesiol* 1999; 11:49–52
 34. Andrzejowski J, Sleigh J: Increasing isoflurane concentration may cause paradoxical increases in the EEG Bispectral Index in surgical patients. *Br J Anaesth* 2000; 85:171–2
 35. Detsch O, Schneider G, Kochs E, Hapfelmeier G, Werner C: Increasing isoflurane concentration may cause paradoxical increases in the EEG Bispectral Index in surgical patients. *Br J Anaesth* 2000; 84:33–7
 36. Antognini JF, Carstens E: *In vivo* characterization of clinical anaesthesia and its components. *Br J Anaesth* 2002; 89:156–66
 37. Rudolph U, Antkowiak B: Molecular and neuronal substrates for general anaesthetics. *Nat Rev Neurosci* 2004; 5:709–20
 38. John ER, Prichep LS, Kox W, Valdés-Sosa P, Bosch-Bayard J, Aubert E, Tom M, di Michele F, Gugino LD, diMichele F: Invariant reversible QEEG effects of anesthetics. *Conscious Cogn* 2001; 10:165–83
 39. Purdon PL, Sampson A, Pavone KJ, Brown EN: Clinical electroencephalography for anesthesiologists: Part I. Background and basic signatures. *ANESTHESIOLOGY* 2015; 123:937–60
 40. Schneider G, Gelb AW, Schmeller B, Tschakert R, Kochs E: Detection of awareness in surgical patients with EEG-based indices: Bispectral Index and Patient State Index. *Br J Anaesth* 2003; 91:329–35
 41. Khan KS, Hayes I, Buggy D: Pharmacology of anaesthetic agents: II. Inhalation anaesthetic agents. *Continuing Education in Anaesthesia, Critical Care and Pain* 2014; 14:106–11
 42. Tang P, Eckenhoff R: Recent progress on the molecular pharmacology of propofol. *F1000Res* 2018; 7:123

ANESTHESIOLOGY

δ -Oscillation Correlates of Anesthesia-induced Unconsciousness in Large-scale Brain Networks of Human Infants

Ioannis Pappas, Ph.D., Laura Cornelissen, Ph.D.,
David K. Menon, M.D., Ph.D., Charles B. Berde, M.D., Ph.D.,
Emmanuel A. Stamatakis, Ph.D.

ANESTHESIOLOGY 2019; 131:1239–53

EDITOR'S PERSPECTIVE

What We Already Know about This Topic

- Electroencephalographic α -oscillations in the frontal cortex do not appear during general anesthesia in infants less than 3 to 4 months old
- In adults, functional connectivity and brain network integration appear to break down during anesthesia but whether this is true in infants is unknown

What This Article Tells Us That Is New

- In infants younger than four months, slow-wave functional connectivity breaks down during general anesthesia and brain networks are less integrated
- Functional disconnections in the cortex might be a common marker of anesthesia-induced unconsciousness in infants and adults

Each year millions of infants and children are administered general anesthesia for surgery.^{1,2} Volatile anesthetic drugs bind to multiple targets at the brain and spinal cord, where they exert their physiologic and functional effects.³ Sevoflurane is one of the most commonly used vapor anesthetics in infants and children and is used for its rapid induction, emergence, and recovery profile. Many clinical studies use noninvasive recordings such as electroencephalography as a way to monitor adult brain function during titration of anesthesia. Although several studies have characterized

ABSTRACT

Background: Functional brain connectivity studies can provide important information about changes in brain-state dynamics during general anesthesia. In adults, γ -aminobutyric acid–mediated agents disrupt integration of information from local to the whole-brain scale. Beginning around 3 to 4 months postnatal age, γ -aminobutyric acid–mediated anesthetics such as sevoflurane generate α -electroencephalography oscillations. In previous studies of sevoflurane-anesthetized infants 0 to 3.9 months of age, α -oscillations were absent, and power spectra did not distinguish between anesthetized and emergence from anesthesia conditions. Few studies detailing functional connectivity during general anesthesia in infants exist. This study's aim was to identify changes in functional connectivity of the infant brain during anesthesia.

Methods: A retrospective cohort study was performed using multichannel electroencephalograph recordings of 20 infants aged 0 to 3.9 months old who underwent sevoflurane anesthesia for elective surgery. Whole-brain functional connectivity was evaluated during maintenance of a surgical state of anesthesia and during emergence from anesthesia. Functional connectivity was represented as networks, and network efficiency indices (including complexity and modularity) were computed at the sensor and source levels.

Results: Sevoflurane decreased functional connectivity at the δ -frequency (1 to 4 Hz) in infants 0 to 3.9 months old when comparing anesthesia with emergence. At the sensor level, complexity decreased during anesthesia, showing less whole-brain integration with prominent alterations in the connectivity of frontal and parietal sensors (median difference, 0.0293; 95% CI, −0.0016 to 0.0397). At the source level, similar results were observed (median difference, 0.0201; 95% CI, −0.0025 to 0.0482) with prominent alterations in the connectivity between default-mode and frontoparietal regions. Anesthesia resulted in fragmented modules as modularity increased at the sensor (median difference, 0.0562; 95% CI, 0.0048 to 0.1298) and source (median difference, 0.0548; 95% CI, −0.0040 to 0.1074) levels.

Conclusions: Sevoflurane is associated with decreased capacity for efficient information transfer in the infant brain. Such findings strengthen the hypothesis that conscious processing relies on an efficient system of integrated information transfer across the whole brain.

(*ANESTHESIOLOGY* 2019; 131:1239–53)

electroencephalography-based dynamics in adults under anesthesia, less is known about the dynamics that occur in the infant brain, particularly during early postnatal development.

Quantifying large-scale functional brain network connectivity reconstructed from neurophysiologic data constitutes a promising method for exploring the brain's complex dynamics during anesthesia.⁴ In that regard, graph theory examines network properties of nodes connected by edges, representing brain regions and their functional connections.⁵

This article is featured in "This Month in Anesthesiology," page 1A. This article is accompanied by an editorial on p. 1202. This article has a video abstract. This article has a visual abstract available in the online version. I.P. and L.C. contributed equally to this article.

Submitted for publication December 4, 2018. Accepted for publication August 15, 2019. From the Division of Anesthesia, Department of Clinical Neurosciences, University of Cambridge, Addenbrooke's Hospital, Cambridge, United Kingdom (I.P., D.K.M., E.A.S.); and the Department of Anesthesiology, Critical Care and Pain Medicine, Boston Children's Hospital, Boston, Massachusetts (L.C., C.B.B.) and Department of Anesthesia, Harvard Medical School, Boston, Massachusetts (L.C., C.B.B.). Current affiliations: Helen Wills Neuroscience Institute, University of California Berkeley, Berkeley, California (I.P.).

Copyright © 2019, the American Society of Anesthesiologists, Inc. All Rights Reserved. *Anesthesiology* 2019; 131:1239–53. DOI: 10.1097/ALN.0000000000002977

General anesthesia modulates functional connectivity networks at the local, meso, and whole-brain network scales.⁶ Several recent studies using electroencephalography, functional magnetic resonance imaging, and transcranial magnetic stimulation indicate that sevoflurane weakens signal correlations or “connectivity” among brain regions that share functionality and specialization during wakefulness.⁷ Specifically, connectivity studies of resting state networks indicate that within- and between-network functional disconnections occur in the default mode and frontoparietal networks, with connectivity of primary sensory networks maintained.^{8,9} These alterations in network connectivity indicate that the brain during anesthesia drastically reorganizes toward a less complex configuration in which the brain’s functional systems are more segregated, thus inhibiting whole-brain integration.¹⁰

Few studies detailing the sevoflurane-induced alterations in functional connectivity in infants have been described. Early studies suggest that the neurophysiologic responses to sevoflurane are different in infants from those of adults and change as a function of age.^{11,12} Age-varying changes in the spectral properties indicate that coherent δ -oscillations (1 to 4 Hz) dominate in the first 3 months of life.¹³ Adult-like features, consisting of a frontal predominance of coherent α -oscillations, emerge in late infancy at ~10 months old.¹⁴ However, less is known about anesthesia-associated changes in functional connectivity at the sensor and source levels during early postnatal development.

The study rationale is to provide a comprehensive analysis of how sevoflurane-induced brain δ -oscillations change during anesthesia at the first months of life. The goal is to understand how the functional organization of the infant brain (birth up to 3.9 months old) changes during deep and relatively lighter levels of anesthesia. We characterized infant brain connectivity during a state of maintenance of general anesthesia (where a subject is unresponsive to a noxious surgical incision), and during emergence from general anesthesia (immediately before a behaviorally responsive state). We hypothesized that infant brain networks during maintenance of general anesthesia would display less complex and more fragmented connectivity because general anesthesia-induced loss of consciousness is associated with altered functional connectivity and disruption of whole-brain integration. These findings can provide valuable clinical insights regarding accurate monitoring of anesthesia in the pediatric operating room with analysis of electroencephalography data.

Materials and Methods

Study Design

The objective of this study was to examine functional connectivity changes in response to different depths of anesthesia in infants aged 0 to 3.9 months old. We analyzed electroencephalography data in 20 infants aged 0 to 3.9 months during administration of sevoflurane general anesthesia for elective surgery. End-tidal anesthetic gas volume and video

recordings of behavioral activity were time-locked to the electroencephalography recordings. Functional connectivity measures were evaluated during the maintenance period and during emergence from sevoflurane general anesthesia. This study was approved by the Boston Children’s Hospital (Boston, Massachusetts) Institutional Review Board (protocol No. P000003544) and classified as a “no more than minimal risk” study. Informed written consent was obtained from the parents or legal guardians before each study.

Participants. Infants who were scheduled for an elective surgical procedure were recruited from the preoperative clinic at Boston Children’s Hospital from December 2011 to August 2016 (under Institutional Review Board P-3544, with written informed consent obtained from parents/legal guardians). Subjects required surgery below the neck, were clinically stable on the day of study, and had American Society of Anesthesiologists’ physical status I or II. Exclusion criteria were (1) born with congenital malformations or other genetic conditions thought to influence brain development, (2) diagnosed with a neurologic or cardiovascular disorder, (3) born at less than 32 weeks postmenstrual age, and (4) postnatal age of 4 months and older. We included all the infants of this cohort that matched the inclusion criteria and were aged 0 to 3.9 months. The summary demographics of subjects included in the analysis are given in table 1.

Anesthetic Management. Each patient received anesthesia induced with sevoflurane alone or with a combination of sevoflurane and nitrous oxide. Nitrous oxide was added at the discretion of the anesthesiologist. Nitrous oxide was discontinued after placement of an endotracheal tube or laryngeal mask. Epochs used for analysis were comprised of sevoflurane administration with air and oxygen, titrated to clinical signs; end-tidal sevoflurane concentration was adjusted per the anesthesiologist’s impression of clinical need, not a preset end-tidal sevoflurane concentration.

Data Acquisition

Electroencephalography Recording. Electroencephalography data were acquired using an electroencephalography cap (WaveGuard electroencephalography cap, Advanced NeuroTechnology, Enschede, The Netherlands). In total, 33 recording electrodes were positioned per the modified international 10/20 electrode placement system. Reference and ground electrodes were located at Fz and AFz, respectively. Electroencephalography activity from 0.1 to 500 Hz was recorded with an Xtek electroencephalography recording system (EMU40EX, Natus Medical Inc., Canada). The signals were digitized at a sampling rate of 1.024 Hz and a resolution of 16 bits.

Clinical Data Collection. Demographics and clinical information were collected from the electronic medical records and from the in-house anesthesia information management system. End-tidal sevoflurane, oxygen, and nitrous oxide concentrations were downloaded from the anesthetic monitoring device (Dräger Apollo, Dräger Medical Inc., USA) to a recording

Table 1. Demographics of the Study Cohort

	All Subjects (0–3.9 Months, n = 20)
Demographics	
Age at birth, weeks (median, IQR)	38.00 (35.84–39.0)
PNA, months (median, IQR)	2.89 (35.84–39.0)
Weight, kg (median, IQR)	5.45 (35.84–39.0)
Male, n (%)	18 (90.0)
Anesthetic management	
Duration of anesthesia, min (median, IQR)	103.00 (35.84–39.0)

IQR, interquartile range; PNA, postnatal age.

computer in real-time using ixTrend software (ixcellence, Germany). The signals were recorded at a 1-Hz sampling rate.

Electroencephalography Analysis

Data Preprocessing. Raw electroencephalography signals were exported and processed using custom-built code in MATLAB (MathWorks Inc., USA). Electrodes at M1 and M2 were removed. For conformity, the same channels were taken from all subjects and used for the analysis. The preprocessing pipeline involved: (1) remontaging to a nearest neighbor Laplacian reference using distances along the scalp surface to weight neighboring electrode contributions; (2) bandpass filter (0.1 to 50 Hz); (3) downsampling to 256 Hz; (4) rejection and interpolation of bad channels using EEGLAB¹⁵ (<https://scn.ucsd.edu/eeqlab/index.php>; accessed February 1, 2019) average channel interpolation was 6 ± 2 channels; (5) cleaning of the data using EEGLAB routines; and (6) visually inspecting the remaining data to ensure that no artifact was present.

Epoch Selection. For each subject, epochs in the electroencephalography recordings were identified based on when the subject was in the maintenance of anesthesia period or in the emergence period. The maintenance of anesthesia (anesthesia) period was defined as a steady state of end-tidal sevoflurane volume $\pm 0.1\%$ required for maintenance of a surgical state of anesthesia. The end-tidal sevoflurane was maintained between 1.8 to 2.5% in all epochs selected (median end-tidal sevoflurane, $1.9 \pm 0.1\%$). The emergence period was defined as the time point in the electroencephalography recording at 2 min before body movement was observed (median end-tidal sevoflurane, $0.3 \pm 0.1\%$). One segment of 100s was selected for maintenance anesthesia and emergence periods. The choice was made because there were a limited number of clean segments corresponding to maintenance of surgical anesthesia with steady sevoflurane concentration.

Electroencephalography Data Processing. Electroencephalography time-frequency decomposition of oscillatory activity into different frequency bands was calculated using multitaper analysis. Multitaper analysis reduces the bias in obtaining the true underlying oscillatory activity caused

by standard Fourier techniques.¹⁶ Multitaper analysis uses tapers of data and calculates the spectrum within each taper separately by using spectral decomposition functions. For a taper of specific time length and for a frequency band of interest (tile of frequency and time), the time-bandwidth product $T \times W$ corresponds to how many such functions will be used in this particular tile of frequency and time. We divided the signal into canonical frequency bands including slow (0.1 to 1 Hz), δ (1 to 4 Hz), θ (4 to 8 Hz), α (8 to 12 Hz), and β (13 to 30 Hz) using a setup of $T \times W = 3$, $K = 5$ tapers as previously reported.^{11,13} Quantification of power for each tile of frequency and time was done using “mtspecgram” function implemented in the Chronux toolbox (<http://chronux.org/>; accessed February 1, 2019).¹⁶

Functional Connectivity. Cross-spectral coherence was calculated by correlating the multitaper spectrums of two sensors i and j . One issue with using cross-spectral coherence relates to the volume conduction problem. This refers to the case when two different electrodes might give spuriously high coherence just because they are measuring the same source.¹⁷ One way to overcome this problem is by keeping only the imaginary part of the coherence.¹⁸ Two sensors measuring the same source cannot give non-zero imaginary coherence.¹⁸ In that regard, we obtained a functional connectivity matrix for each infant where each entry (i, j) represented imaginary coherence between the two channels i and j at the frequency band of interest. Comparing connectivity at the local scale involved statistical comparisons in each pair (i, j) between maintenance of anesthesia and emergence conditions.

Functional Connectivity Networks: Variable 1 Analysis–Complexity. Each δ -specific matrix was converted to network for each infant by thresholding the most important connections. This was conducted within a range 10 to 50% thresholds T at steps of 2%. The limits were chosen to prevent the network from being severely fragmented and from being random by introducing connections. Graph-theoretic indices such as complexity and modularity were estimated in these thresholded networks as an average of the aforementioned range of thresholds T . Functional connectivity complexity was computed by calculating the Shannon entropy of each network's degree distribution. The degree sample of each network was computed by using the BCT toolbox (<https://sites.google.com/site/bctnet/>; accessed February 1, 2019).¹⁹ We used a standard estimator to calculate entropy of the degree sample that utilizes the frequency estimates of the sample. Formally, let $F = (F(1), F(2), \dots)$ the fingerprint of the degree sample of size k , where $F(1)$ is the number of nodes appearing once, $F(2)$ is the number of nodes appearing twice and so on. Degree entropy was then calculated as

$$H = - \sum_{i \in p_i} p_i \log p_i = - \sum_i \frac{i}{k} F(i) \log i / k.^{20}$$

At the network whole-brain scale, δ -oscillation complexity is a measure of richness of the connectivity repertoire across the whole-brain network and is associated with

the brain's ability to balance integration of information coming from different specialized/segregated modules.²¹ Complexity was estimated by calculating the entropy of the degree (number of connections of each node of the network) distribution across all scalp electrodes.

Functional Connectivity Networks: Variable 2 Analysis—Modularity. Functional connectivity was estimated using a modularity index. Modularity is a meso scale graph metric used to calculate the extent to which the nodes of a network can be grouped together in modules.¹⁹ Modularity was calculated using the heuristic Louvain algorithm, and the modularity measure derived was averaged more than 50 repetitions of the algorithm.

Source Reconstruction. One way of linking surface electroencephalography activity to source activity in the cortex is to use source reconstruction methods. The two steps for source reconstruction include forward modeling and its inverse solution. Forward modeling refers to using Maxwell's equations to predict the electromagnetic field produced by the sources at a given electrode or else the "leadfield" matrix. In other words, the leadfield matrix relates the measured activity at the electrode level with the underlying source activity. To calculate the forward model one needs to combine information regarding (1) how electric activity spreads through different tissues (the head model), (2) the position and orientation of different dipoles (the source model), and (3) the electrodes' locations. As far as the head model is concerned, one approach is to use numerical solutions such as the boundary element model,²² in which the brain is compartmentalized into three tissues (brain, skull, and scalp), with each one being covered by a tessellation. To obtain such a geometrical description, one needs anatomical information from the T1 images such as to segment out the brain, scalp, and skull tissues. Because of a lack of individual data, an alternative way is to use predefined templates. Under this framework, it is important to use age-appropriate brain templates and parameters to accurately quantify the localization and time course in each infant.²³ Toward this direction, we used age-specific templates provided by the Richards laboratory (<https://jerlab.sc.edu/projects/neurodevelopmental-mri-database/>; accessed February 1, 2019).²³

In addition to T1 and T2 structural images, scalp, brain, and skull segmentations were also obtained. The specific details are described by Sanchez and colleagues.²⁴

For each template, we used standard conductivity settings and the "bemcp" option in FieldTrip (<http://www.fieldtriptoolbox.org/>; accessed February 1, 2019)²⁵ to obtain a boundary element head model using the tessellation of the three compartments (brain, skull, and scalp). We used a standard number of vertices for the construction of the head model (3,000, 200, and 1,000, respectively).

The next step required realignment of the electrodes' positions with the head model. This was performed manually using FieldTrip's graphical interface. Finally, for the source model, a three-dimensional grid of dipoles with 1-cm resolution was constructed. Electrodes, head model,

and source model were aligned and mapped to the same space. To increase the validity of the forward solution, the alignment between the electrodes, head model, and source model was visually inspected. Following this methodology, we obtained the leadfield matrix for each template.

Inverse solution refers to obtaining the source level activity using the leadfield matrix and the obtained electroencephalography data. One popular method for obtaining the inverse solution encompasses beamforming techniques.²⁵ The basic principle of beamforming lies in obtaining a single source's activity by looking at how it contributes to the measured electroencephalography activity compared with other sources.²⁶ Using the forward solution obtained, alongside the electroencephalography data, we utilized the beamforming technique to obtain the activity of each dipole. We used the FieldTrip toolbox with the option "pcc" to obtain the time course and spectrum of each dipole. We then calculated the $dipole \times dipole$ connectivity matrix using the imaginary coherence as with electrode-based networks. It is worth noting that the data here were remontaged to an average reference before source reconstruction. Because of the way a forward solution is obtained, there is usually a small error associated with each channel. By remontaging the electrodes at an average reference, the model error is averaged out across the electrodes, thus allowing more precise inverse solutions.²⁵

After obtaining the dipole matrices, we wanted to group dipoles based on known cortical regions to assist with interpretation of the results. We used a specific parcellation obtained in the Richards templates to group dipoles into specific regions of interest (<https://jerlab.sc.edu/projects/neurodevelopmental-mri-database/>; accessed February 1, 2019).

The parcellation was based on the macroanatomical Hammers atlas previously used in adult literature.²⁷ We assigned each dipole to a region of interest by overlapping the source model (the dipole positions) and the parcellation image. We then averaged the connectivity values of the dipoles belonging to each region of interest to obtain a region of interest-specific time courses. This resulted in a region of interest \times region of interest connectivity matrix for each infant that was eventually used for the source level graph-theoretic analysis presented in the main text.

We excluded regions corresponding to the cerebellum, brainstem, striatum, corpus callosum, hippocampus, thalamus, amygdala, and insula because of known difficulties in obtaining source signals from subcortical regions using beamforming techniques.²⁸ To assess the validity of source reconstruction, we further examined whether signal was obtained from regions where no signal would be expected, such as the ventricles. To do this, we used the ventricle regions defined in the Hammers atlas, and we observed that no signal could be extracted using these regions as regions of interest. Matrix thresholding was conducted by looking at a range of thresholds 10 to 50% in steps of 2%. Network measures (pairwise connectivity, modularity, and complexity) were calculated in source networks as in the sensor-based networks.

Statistics

Power Analysis. There was no power calculation performed *a priori*. This is a retrospective study with secondary analysis of δ -oscillatory properties in infants aged 0 to 3.9 months. From our large data set of more than 100 infants, we identified a subcohort of infants who were specifically aged 0 to 3.9 months and had acceptable electroencephalography data; this yielded 20 subjects.

General Statistics. Statistics were used for comparing local connectivity changes, changes in modularity and changes in complexity. Statistical analysis was performed using custom-written MATLAB code.

First, for local connectivity changes, statistical comparison between pairs of connections was performed using the Network Based Statistic Toolbox (<http://sites.google.com/site/bctnet/comparison/nbs>; accessed February 1, 2019).²⁹ Because of the mass-univariate testing, Network Based Statistic Toolbox controls the family-wise error rate by identifying “clusters” of suprathreshold statistically significant connections. Each connection is associated with a test statistic quantifying evidence with respect to whether or not it favors the null hypothesis. Then a test statistical threshold is chosen; connections with a test statistic value exceeding this threshold or suprathreshold connections are considered. In turn, if there is a connected component (from a graph perspective) of suprathreshold statistically significant connections, a *P* value is assigned by indexing its size with the null distribution of maximal component size (the latter is derived using permutations at which the group to which each subject belongs is randomly exchanged). We identified statistically significant connections using *t* tests with contrast emergence greater than anesthesia and with a statistical *t* test threshold of 3, a number of permutations of 5,000, and statistical significance level of 0.05 for the permutations. Visualization of the significant edges was produced using the in-built function of the Network Based Statistic Toolbox. The function uses the regions of interest coordinates as input and produces a network with significant edges and how these project in a standard brain template. The results are also presented using the false discovery rate method. The false discovery rate enables rejection of the null hypothesis at the level of individual connections (as opposed to clusters of connections in the way that the Network Based Statistic Toolbox does) and does not require the use of a prespecified statistical threshold.³⁰

Second, within-subject comparisons were performed to evaluate the difference in complexity and in modularity in the maintenance period compared with the emergence period. Normality tests were performed using the Kolmogorov–Smirnov test. Because modularity and complexity data were not normally distributed, we used a paired Wilcoxon signed rank test (two-tailed). A *P* value of less than 0.05 was considered statistically significant. CI values were computed *via* bootstrapping. Specifically we sampled with replacement from the two samples, and we calculated the

difference in the medians. This process was repeated 10,000 times. The naïve 95% CI was calculated using the 25th and 97.5th largest median differences. The box plot data are shown as median values alongside the 1.5 interquartile range.

Results

We used multichannel scalp electroencephalograph recordings in infants undergoing sevoflurane general anesthesia for elective surgery. Continuous multichannel electroencephalography recordings were collected during maintenance of a surgical state of anesthesia and at emergence (first body movement) in 20 subjects aged 0 to 3.9 months old. End-tidal sevoflurane (end-tidal sevoflurane) was between 1.8 to 2.5% during the maintenance phase and 0 to 0.3% during the emergence phase. Electroencephalography functional connectivity was obtained using the cross-spectral coherence between sensor signals or region of interest source-reconstructed signals. For each infant and two conditions (emergence and anesthesia), we obtained a functional connectivity graph or network by keeping the strongest connectivity values between all sensors and regions of interest for sensor and source level analysis respectively. Subject demographics and clinical characteristics are provided in table 1. Details concerning the study design and the relevant methods are given under “Materials and Methods” and in figure 1.

Functional Connectivity at the Sensor and Source Levels

Power spectral analysis indicated that δ power (1 to 4 Hz) was the dominant frequency component during maintenance and emergence from anesthesia in all infants (*n* = 20; fig. 2). During maintenance, peak power was observed at the mean frequency of $1.25 \text{ Hz} \pm 0.62 \text{ Hz}$ (mean \pm SD). During emergence, peak power was observed at $1.08 \text{ Hz} \pm 0.29$. Based on this key feature, δ -oscillation functional connectivity networks properties were evaluated during anesthesia and emergence in subsequent analyses.

At the network local scale, we looked at differences in δ -oscillation connectivity values between maintenance and emergence from anesthesia. Connections that survived statistical significance are presented in figure 3. We observed a decrease between frontal and central/parietal electrodes when comparing anesthesia with emergence (fig. 3A). The full list of edges is presented in table 2. Similar results obtained using the false discovery rate method are presented in table 3. At the source level, we observed decreased connectivity during anesthesia with statistically significant changes in the connectivity within the posterior cingulate with right frontal and parietal regions (fig. 3B). The full list of edges for which connectivity was significantly decreased during anesthesia is presented in table 4. Similar results obtained using the false discovery rate method are presented in table 5.

Modularity at the Sensor and Source Levels

At the network meso scale, δ -oscillation modularity was estimated for the functional connectivity networks at

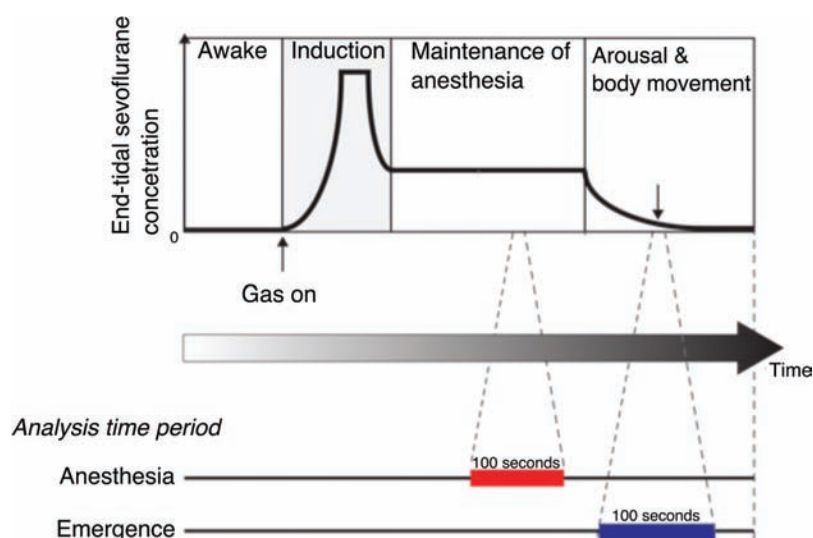


Fig. 1. Study protocol. Schematic time-course of end-tidal sevoflurane concentration during the awake phase, induction, anesthesia, and emergence phases of general anesthesia. From individual recording electrodes, 100-s electroencephalography data were analyzed *post hoc* only for the phases of maintenance anesthesia (shown in red) and emergence from general anesthesia (shown in blue).

anesthesia and emergence. Modularity is a measure of functional segregation, where large values indicate scattering between many communities or networks, and low values indicate high network integration. We found that modularity during anesthesia was increased when compared with emergence (fig. 4A; Wilcoxon signed rank test z value, 2.53; $P = 0.011$; difference in medians, 0.0562; 95% CI, 0.0048 to 0.1298). This suggested that networks became more fragmented during anesthesia, thus increasing segregation between different parts of the brain. Similar results were obtained when we remontaged the data to the average reference (Wilcoxon signed rank test z value, 2.15; $P = 0.032$). This result was confirmed at the source level where we observed that modularity increased during anesthesia compared with emergence (fig. 4B; Wilcoxon signed rank test z value, 2.31; $P = 0.021$; difference in medians, 0.0548; 95% CI, -0.0040 to 0.1074).

Complexity at the Sensor and Source Levels

We then looked at complexity as a global measure of information integration. δ -Oscillation complexity decreased when comparing anesthesia with the emergence phase (fig. 5A). The change in complexity between anesthetic states was statistically significant (Wilcoxon signed rank test z value, 2.01; $P = 0.044$; difference in medians, 0.0293; 95% CI, -0.0016 to 0.0397). Similar results were obtained when we remontaged the data to the average reference (Wilcoxon signed rank test z value, 1.9700; $P = 0.049$).

Complexity was further evaluated for each infant at the source level. δ -Oscillation complexity decreased

during anesthesia compared with emergence corroborating the results observed at the sensor level (fig. 5B; Wilcoxon signed rank test z value, 2.50; $P = 0.012$; difference in medians, 0.0201; 95% CI, -0.0025 to 0.0482). Collectively, functional connectivity was reorganized during maintenance anesthesia, with network connectivity becoming less complex.

Discussion

Summary of Findings

In this study, we described functional connectivity network changes during anesthesia-induced loss of consciousness in early postnatal development. We examined brain state transitions from the maintenance phase of anesthesia to emergence from anesthesia and quantified modulations of connectivity patterns. Our findings indicated that infant general anesthesia is potentially (1) driven by connectivity changes in key default mode network and frontoparietal regions (fig. 3), (2) associated with more segregation (increase in δ -oscillation modularity; fig. 4); and (3) related to reduction in δ -oscillation complexity (fig. 5), at both the sensor and source levels.

Studies of Electroencephalography Functional Connectivity in Adults under General Anesthesia

A growing number of studies have indicated differences in functional connectivity during general anesthesia^{31,32} and also at different stages of brain development.^{33,34} Deeper stages of anesthesia are characterized by reduced functional connectivity in higher-order brain networks such as the

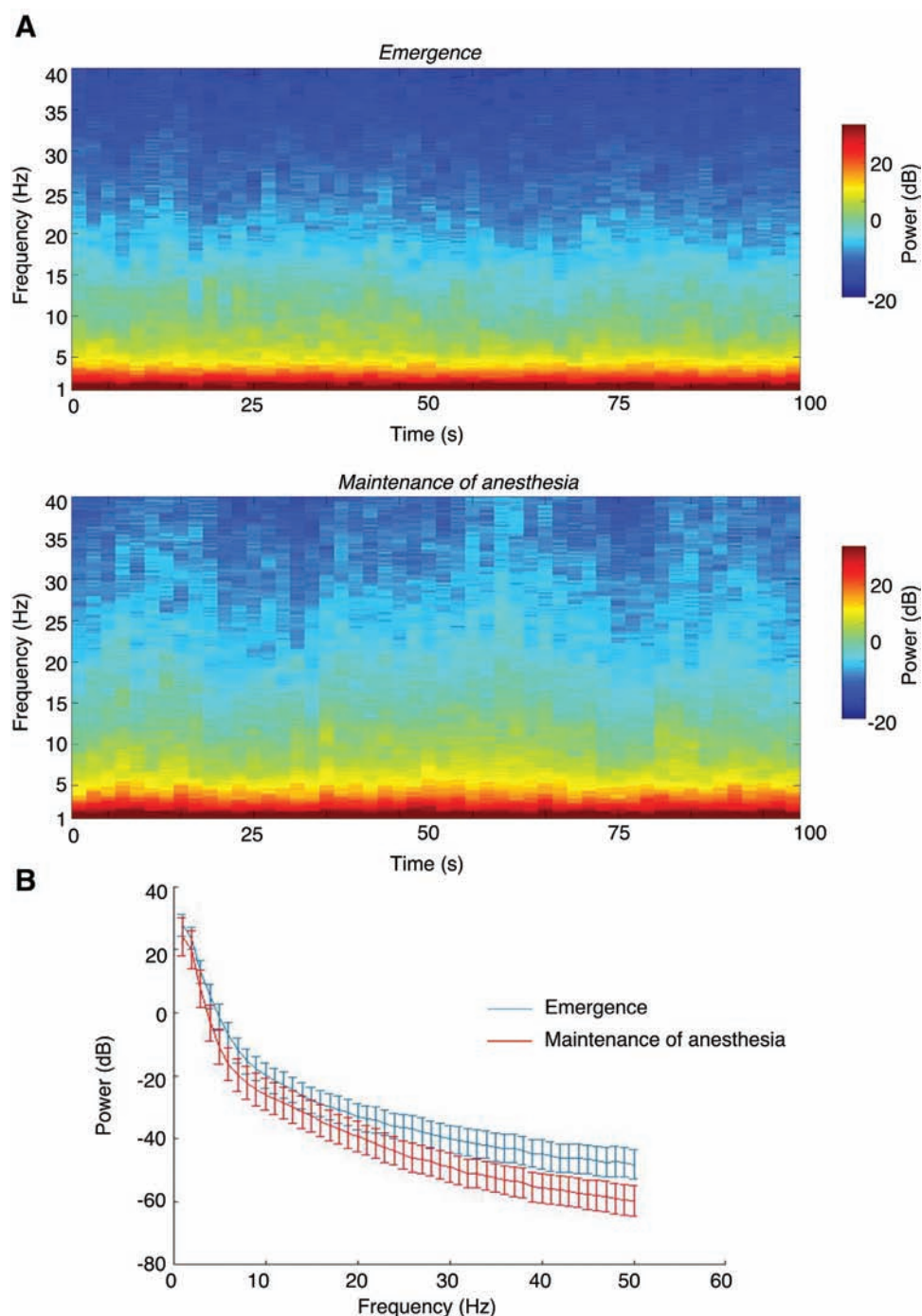


Fig. 2. Power analysis for infants aged 0 to 3.9 months. (A) Median spectral power during maintenance anesthesia (end-tidal sevoflurane range, 1.8 to 2.5%) and emergence (end-tidal sevoflurane range, 0 to 0.3%); $n = 20$. (B) Power in the time domain during maintenance anesthesia and emergence for all infants. Dots represent mean values; lines show standard errors of the mean.

default mode network and the frontoparietal network.^{10,12,35} Crucially, emergence from anesthesia is associated with restoration of functional connectivity between frontoparietal regions and subcortical regions.³⁶

Further evidence for the reconfiguration of functional connectivity in adult anesthesia is evident in studies investigating alterations in graph-theoretic properties. At the local scale, previous studies have shown disruption

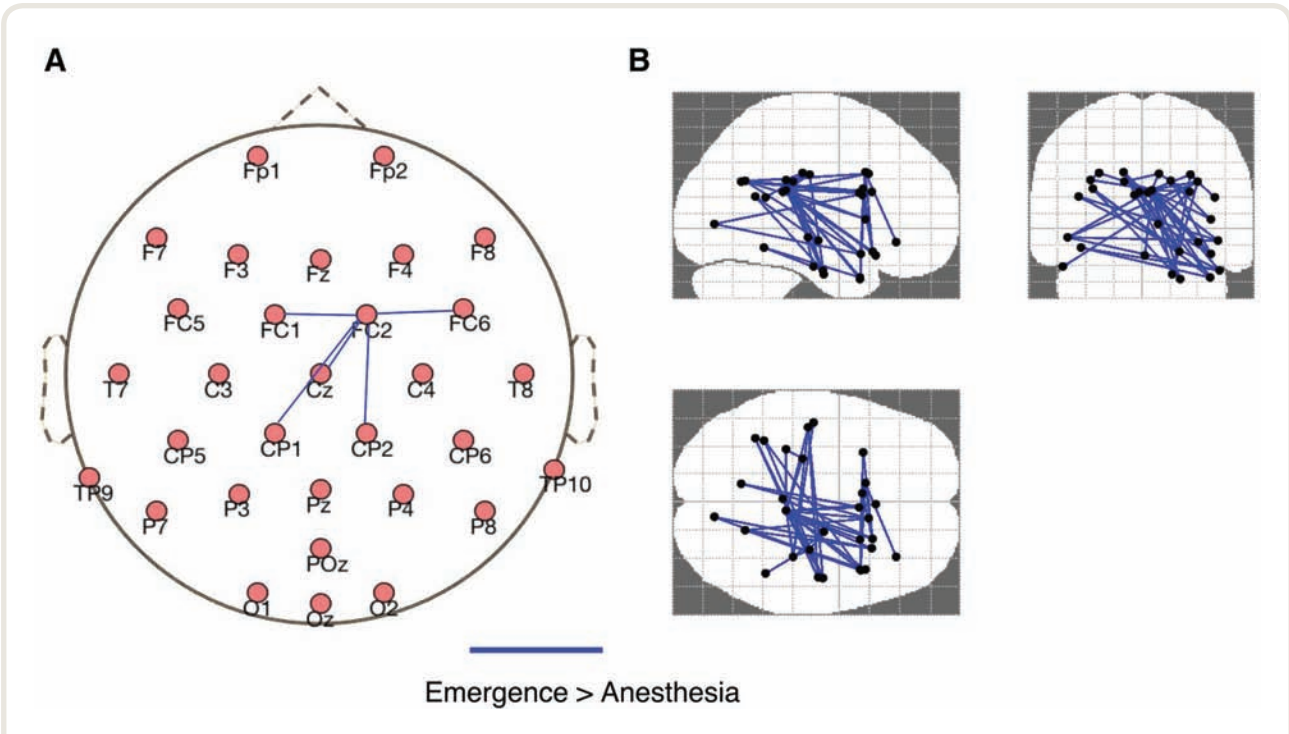


Fig. 3. Sensor and source level functional connectivity differences during maintenance and emergence phases of sevoflurane general anesthesia in infants aged 0 to 3.9 months. (A) Statistically significant connections between different sensors during maintenance anesthesia compared with emergence (blue lines). (B) Sagittal, coronal, and axial views of connections between regions of interest for which connectivity was decreased during maintenance anesthesia compared with emergence. Data comes from n = 20 infants from 100-s epochs. Anesthetic depth range end-tidal sevoflurane was 1.8 to 2.5%, and emergence end-tidal sevoflurane was 0 to 0.3%.

Table 2. Brain Network Edges at the Sensor Level in the Form of Node i and Node j for Which Connectivity Was Significantly Decreased When Comparing Anesthesia with Emergence Using the Network Based Statistic Toolbox Method

Node i	Node j	P Value
FC2	FC1	< 0.001
FC2	Cz	0.0018
FC2	CP1	0.0052
FC2	CP2	0.0009
FC2	FC6	0.0056

The results were obtained using the Network Based Statistic Toolbox. The *t* test threshold was set to 3, the number of permutations was set to 5,000, and the *P* value threshold for the permutations was set to 0.05. The *P* values in the last column represent two-tailed statistical significance of individual connections within the significant network.

Table 3. Brain Network Edges at the Sensor Level in the Form of Node i and Node j for Which Connectivity Was Significantly Decreased When Comparing Anesthesia with Emergence Using the False Discovery Rate Method

Node i	Node j	P Value
FC2	FC1	< 0.001
FC2	CP2	< 0.001

The results were obtained using the Network Based Statistic Toolbox. The number of permutations was set to 5,000, and the *P* value threshold for the permutations was set to 0.05. The *P* values in the last column represent two-tailed statistical significance of individual connections.

of highly connected regions located in the default mode network and frontoparietal networks.^{37,38} At the meso and whole-brain scales, α -based electroencephalography networks in adults during propofol-induced anesthesia were shown to be more fragmented and less efficient.¹⁷ Overall, α -oscillation functional connectivity in the anesthetized adult brain is less globally efficient and more segregated as

a result of attenuated connectivity between higher-order networks.

Studies of Electroencephalography Functional Connectivity of the Infant Brain under General Anesthesia

However, there are few studies describing alterations of functional connectivity in infants. Previous studies analyzing electroencephalography power in infants less than 6 months of age showed no difference in power between anesthesia and

Table 4. Brain Network Edges at the Source Level in the Form of Node i and Node j for Which Connectivity Was Significantly Decreased When Comparing Anesthesia with Emergence Using the Network Based Statistic Toolbox Method

Node i	Node j	P Value
Middle frontal gyrus left	Posterior orbital gyrus right	0.0051
Middle frontal gyrus left	Anterior temporal lobe medial part left	0.0049
Middle frontal gyrus left	Anterior temporal lobe lateral part left	0.0022
Middle frontal gyrus right	Superior parietal gyrus right	0.0042
Middle frontal gyrus right	Cuneus right	0.0045
Middle frontal gyrus right	Cingulate gyrus, posterior part right	0.0045
Precentral gyrus left	Postcentral gyrus left	0.0034
Precentral gyrus left	Cingulate gyrus, posterior part right	0.0063
Precentral gyrus right	Parahippocampal gyrus left	0.0071
Precentral gyrus right	Postcentral gyrus right	0.0061
Precentral gyrus right	Cingulate gyrus, posterior part right	0.0070
Straight gyrus right	Cingulate gyrus, posterior part right	0.0065
Inferior frontal gyrus right	Superior parietal gyrus right	0.0054
Inferior frontal gyrus right	Cingulate gyrus, posterior part right	0.0053
Superior frontal gyrus left	Lateral orbital gyrus right	0.0032
Superior frontal gyrus left	Posterior orbital gyrus right	0.0053
Superior frontal gyrus left	Anterior temporal lobe medial part left	0.0066
Superior frontal gyrus left	Anterior temporal lobe lateral part left	0.0063
Superior frontal gyrus left	Superior temporal gyrus, anterior part right	0.0048
Superior frontal gyrus right	Superior parietal gyrus left	0.0051
Superior frontal gyrus right	Superior parietal gyrus right	0.0028
Superior frontal gyrus right	Cingulate gyrus, posterior part right	0.0037
Posterior orbital gyrus right	Cingulate gyrus, anterior part left	0.0040
Posterior orbital gyrus right	Cingulate gyrus, posterior part left	0.0049
Posterior orbital gyrus right	Cingulate gyrus, posterior part right	0.0068
Anterior temporal lobe medial part left	Cingulate gyrus, posterior part right	0.0059
Anterior temporal lobe lateral part left	Posterior temporal lobe left	0.0060
Anterior temporal lobe lateral part left	Cingulate gyrus, posterior part right	0.0071
Parahippocampal gyrus left	Postcentral gyrus right	0.0056
Parahippocampal gyrus left	Cingulate gyrus, posterior part right	0.0045
Superior temporal gyrus, central left	Superior temporal gyrus, central right	0.0067
Superior temporal gyrus, central left	Remainder of the parietal lobe left	0.0044
Superior temporal gyrus, central left	Cingulate gyrus, posterior part right	0.0021
Superior temporal gyrus, central right	Medial and inferior temporal gyri left	0.0025
Superior temporal gyrus, central right	Postcentral gyrus right	0.0070
Superior temporal gyrus, central right	Cingulate gyrus, posterior part right	0.0033
Superior temporal gyrus, anterior part right	Superior parietal gyrus right	0.0019
Superior temporal gyrus, anterior part right	Cuneus right	0.0019
Superior temporal gyrus, anterior part right	Cingulate gyrus, posterior part right	0.0028
Medial and inferior temporal gyri left	Posterior temporal lobe left	0.0013
Medial and inferior temporal gyri left	Remainder of the parietal lobe left	0.0028
Medial and inferior temporal gyri left	Cingulate gyrus, posterior part right	0.0061
Medial and inferior temporal gyri right	Postcentral gyrus right	0.0067
Postcentral gyrus left	Cingulate gyrus, posterior part right	0.0017
Postcentral gyrus right	Remainder of the parietal lobe right	0.0036
Postcentral gyrus right	Cingulate gyrus, posterior part right	0.0010
Superior parietal gyrus left	Cingulate gyrus, anterior part right	0.0051
Cingulate gyrus, anterior part right	Cingulate gyrus, posterior part right	0.0055

The results were obtained using the Network Based Statistic Toolbox (NBS). The *t* test threshold was set to 3, the number of permutations was set to 5,000, and the *P* value threshold for the permutations was set to 0.05. The *P* values in the last column represent two-tailed statistical significance of individual connections within the significant network. *P* values < 0.002 are represented in bold type.

emergence.^{39,40} Previous studies showed that although δ power was prominent, there were no differences in δ power in infants 0 to 3.9 months when comparing the awake state with anesthesia and between anesthesia and first body movement (a surrogate of emergence).⁴¹ In addition, functional connectivity (coherence) between frontal electrodes was weak in δ frequencies in infants 0 to 3.9 months compared with older infants.¹¹

A Mechanistic Explanation for Loss of Consciousness in the Infant Brain

We thus argue that power cannot discriminate between young infants' brain responses during anesthesia and brain responses during emergence. In contrast, graph-theoretic approaches can provide a holistic representation of how different parts of the brain integrate and how this integration

Table 5. Brain Network Edges at the Source Level in the Form of (Node i, Node j) for Which Connectivity Was Significantly Decreased When Comparing Anesthesia with Emergence Using the False Discovery Rate Method

Node i	Node j	P Value
Superior temporally gyrus central left	Remainder of the parietal lobe left	0.0049
Postcentral gyrus left	Cingulate gyrus posterior part right	0.0010

The results were obtained using the Network Based Statistic Toolbox. The number of permutations was set to 5,000, and the *P* value threshold for the permutations was set to 0.05. The *P* values in the last column represent two-tailed statistical significance of individual connections.

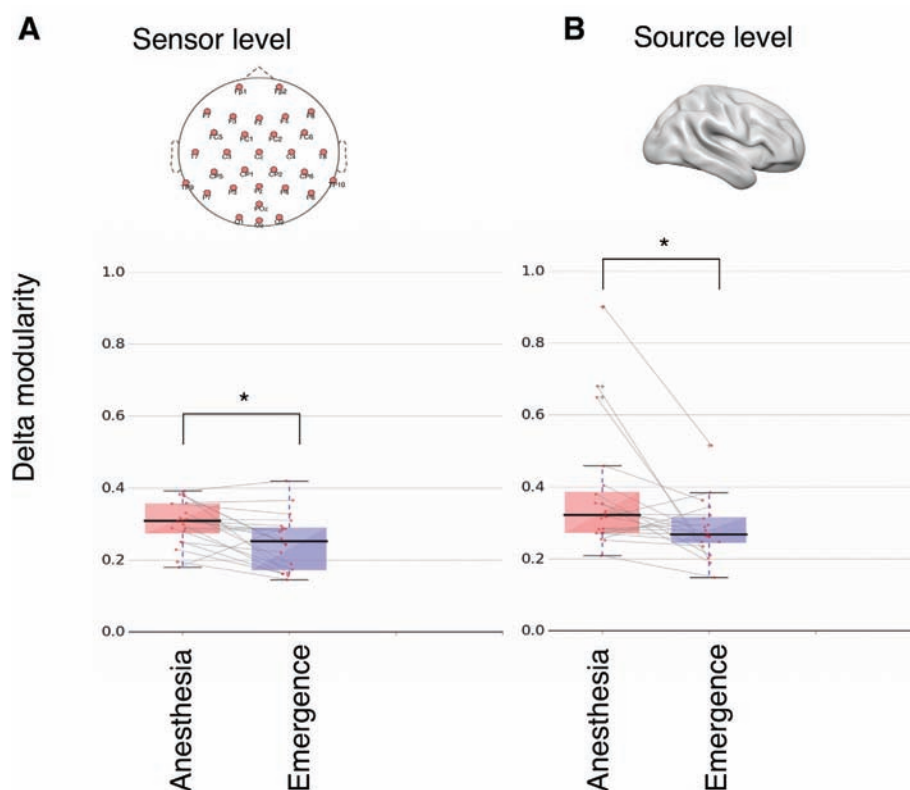


Fig. 4. Sensor and source level δ -oscillation modularity during maintenance and emergence phases of sevoflurane general anesthesia in infants aged 0 to 3.9 months. (A) δ -Oscillation modularity at the sensor level was increased when comparing maintenance anesthesia with emergence. (B) Similar results were observed at the source level. In the box plots, *thick lines* represent median values, and *whiskers* represent 1.5 times the interquartile range. *Gray lines* indicate individual data. Data comes from $n = 20$ infants from 100-s epochs. The average anesthetic depth range end-tidal sevoflurane was 1.8 to 2.5%, and emergence end-tidal sevoflurane was 0 to 0.3%. * $P < 0.05$ using the two-tailed Wilcoxon signed rank test.

is affected by anesthesia.⁹ Motivated by this, we asked whether δ -oscillation whole-brain connectivity would provide more information with respect to the infant brain dynamics. Our results showed that brain connectivity was less complex during anesthesia compared with emergence. Complexity is an aggregate measure of how connectivity is distributed across the brain. It captures the coexistence of hubs and other sparsely connected regions that, together, provide a balance between segregation and global integration.²¹ Reduced complexity implies a more segregated

configuration that promotes local efficiency in communicating information and inhibits global integration.¹⁰ This result was corroborated at the meso scale where we found that infant brain networks during anesthesia were more segregated into clusters compared with emergence.

How does the shifting to a less complex brain network occur? In light of our findings at the local scale, it is possible that such shifting might take place because of reduction in connectivity between default mode network and frontoparietal regions. Frontoparietal connectivity is modulated by anesthetic-induced

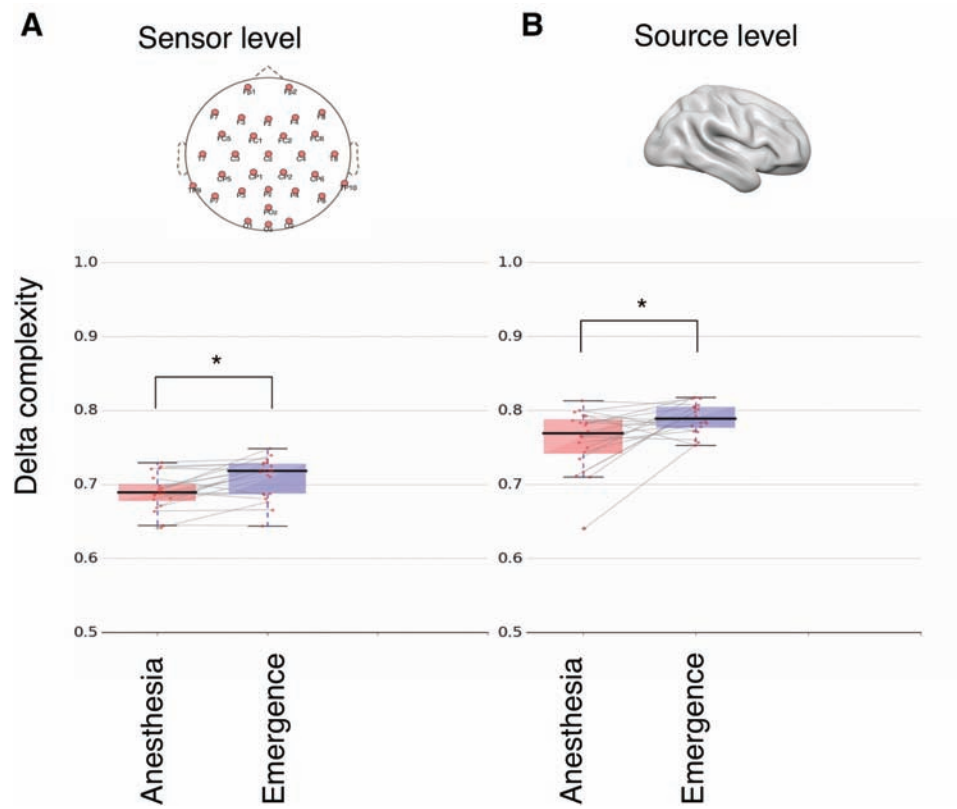


Fig. 5. Sensor and source level δ -oscillation complexity during maintenance and emergence phases of sevoflurane general anesthesia in infants aged 0 to 3.9 months. (A) δ -Oscillation complexity at the sensor level was decreased when comparing anesthesia with emergence. (B) Similar results were observed at the source level. In the box plots, the *thick lines* represent median values, and *whiskers* represent 1.5 times the interquartile range. *Gray lines* indicate individual data. Data comes from $n = 20$ infants from 100-s epochs. The anesthesia end-tidal sevoflurane was 1.8 to 2.5%, and the emergence end-tidal sevoflurane was 0 to 0.3%. * $P < 0.05$ using the two-tailed Wilcoxon signed rank test.

loss of consciousness.³⁶ In addition to its relationship with the anesthetic effect, frontoparietal connectivity is important for loss of consciousness because of its extensive connectivity to the rest of the brain.³⁷ We observed loss of connectivity in frontoparietal regions and distant parts of the brain, most notably the posterior cingulate. In that regard, long-range connections are crucial in communicating information between distant regions, thus increasing global integration in the network. Specifically, long-range connections from the posterior cingulate, a key region of the default mode network, to the frontoparietal regions have been deemed important in regulating communication in the whole brain allowing the cross-talk between different specialized regions.⁴² Therefore, it is possible that impairment of long-range connections could be linked to loss of consciousness in the sense that their alteration causes the whole-brain network to become more disconnected.¹⁰

The Role of δ -Oscillations in Loss of Consciousness

The results reported here were for δ -oscillations based on the limited range of oscillatory frequencies generated in the human infant brain in early postnatal development. There is no clear

consensus as to how δ -oscillations are produced. They can be generated cortically⁴³ or from parts of the thalamus such as the thalamic reticular nucleus.⁴⁴ Electrophysiologic studies in adult rodents show that propofol-induced coherent α - and δ -oscillations develop rapidly at loss of consciousness, appearing to mediate the functional disruption of thalamus and cortex, and disappear in a spatiotemporal sequence during emergence from anesthesia.⁴⁵ However, their role in loss of consciousness in humans is still exploratory. Alterations in δ -oscillations have been shown in intracortical recordings in patients under propofol-induced anesthesia.⁴⁶ In this study, it was conjectured that loss of consciousness would be associated with whole-brain network fragmentation, whereas local network structure would remain intact.⁴⁷ Toward this direction, we have provided evidence for δ -based whole-brain alterations in the infant brain with δ -based connectivity becoming less complex and more fragmented.

Clinical Implications for Brain Monitoring under Anesthesia

General anesthetics and hypnotic agents such as sevoflurane, propofol, ketamine, and dexmedetomidine produce

stereotyped electroencephalography oscillations that relate fundamentally to neural circuit architecture and function in adults.⁴⁸ Spectral features of the electroencephalography can be used to monitor brain activity during anesthesia and guide anesthetic dosing. With respect to this, many academic publications, as well as proprietary algorithms used for Bispectral Index, SedLine, and other commercial monitors, place emphasis on frontal α spectral power to monitor the transitions into and recovery from anesthetic-induced unconsciousness.⁴⁷ Previous studies from our group show an association of α power with an anesthetic state beginning around age 4 to 6 months.^{11,13,49} However, infants 0 to 3.9 months of age show very little α power, with most of the overall power concentrated in the slow frequency range. In this age range, power spectra during a surgical state of anesthesia (e.g., sevoflurane concentration, 1.8 to 2.5%) shows no discernible difference from power spectra around return of gross body movement (sevoflurane concentration less than 0.4%), unlike in older infants and young children.⁴⁹ Conversely, studies of age dependence of minimal alveolar concentration required to prevent response to surgical incision have found very weak dependence on age, at least for 0 to 6 months of age.⁵⁰ It is therefore clinically relevant to determine whether, for infants 0 to 3.9 months of age undergoing surgery, more sophisticated electroencephalography analyses might distinguish features of brain function during a surgical state of anesthesia compared with emergence.

In that regard, combining our results with the literature in infants and adults shows that whole-brain connectivity and its properties at the respective dominant frequencies (for example δ -oscillations for infants and α oscillations for adults and infants) can discriminate between different levels of consciousness. In anesthetized infants, where power is indiscriminable between anesthesia and emergence, a connectivity-based marker might assist perioperatively with monitoring anesthetic depth. With the increased sophistication of hardware and software technology for real-time electroencephalography monitoring of general anesthesia, it is now possible to perform spectral analysis of electroencephalography data online, thus paving the way for real-world application of electroencephalography network-based markers for monitoring infant anesthesia. Similar efforts have begun to emerge in classifying patients with disorders of consciousness,^{51,52} showing that electroencephalography connectivity can directly contribute to consciousness-level dependent brain monitoring.

Study Limitations and Constraints

It is possible that the observed electroencephalography features could have been confounded by systematic age-related differences in drug administration; further studies will need to address this effect. Although challenging to pursue because of the idiosyncratic nature of the experimental setup (anesthetic management was administered according

to the anesthesiologist's discretion, rather than in a controlled, titrated fashion), there is a need for more detailed electroencephalography studies including controlled sevoflurane administration at a wider range of concentrations and over longer periods of time.^{36,53} Limitations regarding source reconstruction methods apply to this study⁵⁴; we attempted to alleviate these by focusing on cortical regions only and using age-matched templates to obtain realistic electrophysiologic models for brain activity in the infant head. Finally, the limited sample size and number of clean segments prevented us from further looking into individual variability across time and anesthetic concentrations; thus, our plan is to generalize the findings using a larger cohort.

Conclusions

General anesthetics modulate functional connectivity and reduce brain network integration. We showed that such a process takes place even in young infants where δ power is dominant. Thus connectivity can become an important tool for assessing anesthetic depth in the very young infant brain even in the absence of α -oscillations.

Acknowledgments

The authors thank the preoperative and operating room staff, Boston Children's Hospital, Boston, Massachusetts, for their assistance during these studies, as well as the families who took part in the study. The authors also thank Ann-Marie Bergin, M.B., Sc.M., M.R.C.P., Department of Neurology, Boston Children's Hospital, for reviewing all electroencephalogram recordings for potential incidental findings.

Research Support

Supported by Downing College, University of Cambridge through a Treherne Studentship (Cambridge, United Kingdom; to Dr. Pappas), Boston Children's Hospital (Boston, Massachusetts; to Dr. Cornelissen), International Anesthesia Research Society Mentored Research Award (San Francisco, California; to Dr. Cornelissen), a Sara Page Mayo Endowment for Pediatric Pain Research and Treatment (Boston, Massachusetts; to Dr. Berde), the National Institute for Health Research through the Cambridge National Institute for Health Research Biomedical Centre and a Senior Investigator Award (Cambridge, United Kingdom; to Dr. Menon), the Canadian Institute for Advanced Research Brain, Mind and Consciousness Program (Toronto, Canada; to Dr. Menon), and a Stephen Erskine Fellowship from the University of Cambridge (Cambridge, United Kingdom; to Dr. Stamatakis).

Competing Interests

The authors declare no competing interests.

Correspondence

Address correspondence to Dr. Pappas: University of Cambridge, Cambridge, United Kingdom. ip322@cam.ac.uk This article may be accessed for personal use at no charge through the Journal Web site, www.anesthesiology.org.

References

- Rabbitts JA, Groenewald CB, Moriarty JP, Flick R: Epidemiology of ambulatory anesthesia for children in the United States: 2006 and 1996. *Anesth Analg* 2010; 111:1011–5
- Sun L: Early childhood general anaesthesia exposure and neurocognitive development. *Br J Anaesth* 2010; 105:i61–82. Brown EN, Lydic R, Schiff ND: General anesthesia, sleep, and coma. *N Engl J Med* 2010; 363:2638–50
- Purdon PL, Pierce ET, Mukamel EA, Prerau MJ, Walsh JL, Wong KF, Salazar-Gomez AF, Harrell PG, Sampson AL, Cimenser A, Ching S, Kopell NJ, Tavares-Stoeckel C, Habeeb K, Merhar R, Brown EN: Electroencephalogram signatures of loss and recovery of consciousness from propofol. *Proc Natl Acad Sci USA* 2013; 110:E1142–51
- Mashour GA, Hudetz AG: Neural correlates of unconsciousness in large-scale brain networks. *Trends Neurosci* 2018; 41:150–60
- Bullmore E, Sporns O: The economy of brain network organization. *Nat Rev Neurosci* 2012; 13:336–49
- Hudetz AG: General anesthesia and human brain connectivity. *Brain Connect* 2012; 2:291–302
- Palanca BJA, Avidan MS, Mashour GA: Human neural correlates of sevoflurane-induced unconsciousness. *Br J Anaesth* 2017; 119:573–82
- Boveroux P, Vanhaudenhuyse A, Bruno MA, Noirhomme Q, Lauwick S, Luxen A, Degueldre C, Plenevaux A, Schnakers C, Phillips C, Bricchant JF, Bonhomme V, Maquet P, Greicius MD, Laureys S, Boly M: Breakdown of within- and between-network resting state functional magnetic resonance imaging connectivity during propofol-induced loss of consciousness. *ANESTHESIOLOGY* 2010; 113:1038–53
- Stamatakis EA, Adapa RM, Absalom AR, Menon DK: Changes in resting neural connectivity during propofol sedation. *PLoS One* 2010; 5:e14224
- Alkire MT, Hudetz AG, Tononi G: Consciousness and anesthesia. *Science* 2008; 322:876–80
- Cornelissen L, Kim SE, Purdon PL, Brown EN, Berde CB: Age-dependent electroencephalogram (EEG) patterns during sevoflurane general anesthesia in infants. *Elife* 2015; 4:e06513
- Purdon PL, Pavone KJ, Akeju O, Smith AC, Sampson AL, Lee J, Zhou DW, Solt K, Brown EN: The ageing brain: Age-dependent changes in the electroencephalogram during propofol and sevoflurane general anaesthesia. *Br J Anaesth* 2015; 115:i46–57
- Akeju O, Pavone KJ, Thum JA, Firth PG, Westover MB, Puglia M, Shank ES, Brown EN, Purdon PL: Age-dependency of sevoflurane-induced electroencephalogram dynamics in children. *Br J Anaesth* 2015; 115:i66–76
- Cornelissen L, Kim SE, Lee JM, Brown EN, Purdon PL, Berde CB: Electroencephalographic markers of brain development during sevoflurane anaesthesia in children up to 3 years old. *Br J Anaesth* 2018; 120:1274–86
- Delorme A, Makeig S: EEGLAB: An open source toolbox for analysis of single-trial EEG dynamics including independent component analysis. *J Neurosci Methods* 2004; 134:9–21
- Mitra P, Bokil H: Observed brain dynamics. New York, Oxford University Press; 2008
- Stam CJ, Nolte G, Daffertshofer A: Phase lag index: Assessment of functional connectivity from multi channel EEG and MEG with diminished bias from common sources. *Hum Brain Mapp* 2007; 28:1178–93
- Nolte G, Bai O, Wheaton L, Mari Z, Vorbach S, Hallett M: Identifying true brain interaction from EEG data using the imaginary part of coherency. *Clin Neurophysiol* 2004; 115:2292–307
- Rubinov M, Sporns O: Complex network measures of brain connectivity: Uses and interpretations. *Neuroimage* 2010; 52:1059–69
- Harris B: The statistical estimation of entropy in the non-parametric case, *Topics in Information Theory*. Edited by Csiszar I. North-Holland, Amsterdam, pp 323–55
- Zamora-López G, Chen Y, Deco G, Kringelbach ML, Zhou C: Functional complexity emerging from anatomical constraints in the brain: The significance of network modularity and rich-clubs. *Sci Rep* 2016; 6:38424
- Mosher JC, Leahy RM, Lewis PS: EEG and MEG: Forward solutions for inverse methods. *IEEE Trans Biomed Eng* 1999; 46:245–59
- Ortiz-Mantilla S, Hämäläinen JA, Benasich AA: Time course of ERP generators to syllables in infants: A source localization study using age-appropriate brain templates. *Neuroimage* 2012; 59:3275–87
- Sanchez CE, Richards JE, Almli CR: Neurodevelopmental MRI brain templates for children from 2 weeks to 4 years of age. *Dev Psychobiol* 2012; 54:77–91
- Oostenveld R, Fries P, Maris E, Schoffelen JM: FieldTrip: Open source software for advanced analysis of MEG, EEG, and invasive electrophysiological data. *Comput Intell Neurosci* 2011; 2011:156869
- Van Veen BD, van Drongelen W, Yuchtman M, Suzuki A: Localization of brain electrical activity via linearly

- constrained minimum variance spatial filtering. *IEEE Trans Biomed Eng* 1997; 44:867–80
27. Hammers A, Allom R, Koepp MJ, Free SL, Myers R, Lemieux L, Mitchell TN, Brooks DJ, Duncan JS: Three-dimensional maximum probability atlas of the human brain, with particular reference to the temporal lobe. *Hum Brain Mapp* 2003; 19:224–47
 28. Krishnaswamy P, Obregon-Henao G, Ahveninen J, Khan S, Babadi B, Iglesias JE, Hämäläinen MS, Purdon PL: Sparsity enables estimation of both subcortical and cortical activity from MEG and EEG. *Proc Natl Acad Sci USA* 2017; 114:E10465–74
 29. Zalesky A, Fornito A, Bullmore ET: Network-based statistic: Identifying differences in brain networks. *Neuroimage* 2010; 53:1197–207
 30. Genovese CR, Lazar NA, Nichols T: Thresholding of statistical maps in functional neuroimaging using the false discovery rate. *Neuroimage* 2002; 15:870–8
 31. Akeju O, Pavone KJ, Westover MB, Vazquez R, Prerau MJ, Harrell PG, Hartnack KE, Rhee J, Sampson AL, Habeeb K, Gao L, Lei G, Pierce ET, Walsh JL, Brown EN, Purdon PL: A comparison of propofol- and dexmedetomidine-induced electroencephalogram dynamics using spectral and coherence analysis. *ANESTHESIOLOGY* 2014; 121:978–89
 32. Mashour GA: Top-down mechanisms of anesthetic-induced unconsciousness. *Front Syst Neurosci* 2014; 8:115
 33. Fransson P, Skiöld B, Horsch S, Nordell A, Blennow M, Lagercrantz H, Aden U: Resting-state networks in the infant brain. *Proc Natl Acad Sci USA* 2007; 104:15531–6
 34. Fransson P, Aden U, Blennow M, Lagercrantz H: The functional architecture of the infant brain as revealed by resting-state fMRI. *Cereb Cortex* 2011; 21:145–54
 35. Schröter MS, Spoormaker VI, Schorer A, Wohlschläger A, Czisch M, Kochs EF, Zimmer C, Hemmer B, Schneider G, Jordan D, Ilg R: Spatiotemporal reconfiguration of large-scale brain functional networks during propofol-induced loss of consciousness. *J Neurosci* 2012; 32:12832–40
 36. Untergerhrer G, Jordan D, Kochs EF, Ilg R, Schneider G: Fronto-parietal connectivity is a non-static phenomenon with characteristic changes during unconsciousness. *PLoS One* 2014; 9:e87498
 37. Cole MW, Repovš G, Anticevic A: The frontoparietal control system: A central role in mental health. *Neuroscientist* 2014; 20:652–64
 38. Betzel RF, Bassett DS: Specificity and robustness of long-distance connections in weighted, interreal connectomes. *Proc Natl Acad Sci USA* 2018; 115:E4880–9
 39. Davidson AJ, Sale SM, Wong C, McKeever S, Sheppard S, Chan Z, Williams C: The electroencephalograph during anesthesia and emergence in infants and children. *Paediatr Anaesth* 2008; 18:60–70
 40. Hayashi K, Shigemitsu K, Sawa T: Neonatal electroencephalography shows low sensitivity to anesthesia. *Neurosci Lett* 2012; 517:87–91
 41. Kaisti KK, Långsjö JW, Aalto S, Oikonen V, Sipilä H, Teräs M, Hinkka S, Metsähonkala L, Scheinin H: Effects of sevoflurane, propofol, and adjunct nitrous oxide on regional cerebral blood flow, oxygen consumption, and blood volume in humans. *ANESTHESIOLOGY* 2003; 99:603–13
 42. Khalsa S, Mayhew SD, Chechacz M, Bagary M, Bagshaw AP: The structural and functional connectivity of the posterior cingulate cortex: Comparison between deterministic and probabilistic tractography for the investigation of structure–function relationships. *Neuroimage* 2014; 102 Pt 1:118–27
 43. Timofeev I, Grenier F, Bazhenov M, Sejnowski TJ, Steriade M: Origin of slow cortical oscillations in deafferented cortical slabs. *Cereb Cortex* 2000; 10:1185–99
 44. Blethyn KL, Hughes SW, Tóth TI, Cope DW, Crunelli V: Neuronal basis of the slow (<1 Hz) oscillation in neurons of the nucleus reticularis thalami *in vitro*. *J Neurosci* 2006; 26:2474–86
 45. Flores FJ, Hartnack KE, Fath AB, Kim SE, Wilson MA, Brown EN, Purdon PL: Thalamocortical synchronization during induction and emergence from propofol-induced unconsciousness. *Proc Natl Acad Sci USA* 2017; 114:E6660–8
 46. Lewis LD, Weiner VS, Mukamel EA, Donoghue JA, Eskandar EN, Madsen JR, Anderson WS, Hochberg LR, Cash SS, Brown EN, Purdon PL: Rapid fragmentation of neuronal networks at the onset of propofol-induced unconsciousness. *Proc Natl Acad Sci USA* 2012; 109:E3377–86
 47. Akeju O, Brown EN: Neural oscillations demonstrate that general anesthesia and sedative states are neurophysiologically distinct from sleep. *Curr Opin Neurobiol* 2017; 44:178–85
 48. Purdon PL, Sampson A, Pavone KJ, Brown EN: Clinical electroencephalography for anesthesiologists: Part I. Background and basic signatures. *ANESTHESIOLOGY* 2015; 123:937–60
 49. Cornelissen L, Bergin AM, Lobo K, Donado C, Soul JS, Berde CB: Electroencephalographic discontinuity during sevoflurane anesthesia in infants and children. *Paediatr Anaesth* 2017; 27:251–62
 50. Lerman J, Sikich N, Kleinman S, Yentis S: The pharmacology of sevoflurane in infants and children. *ANESTHESIOLOGY* 1994; 80:814–24
 51. Sitt JD, King JR, El Karoui I, Rohaut B, Faugeras F, Gramfort A, Cohen L, Sigman M, Dehaene S, Naccache L: Large scale screening of neural

- signatures of consciousness in patients in a vegetative or minimally conscious state. *Brain* 2014; 137:2258–70
52. Chennu S, Annen J, Wannez S, Thibaut A, Chatelle C, Cassol H, Martens G, Schnakers C, Gosseries O, Menon D, Laureys S: Brain networks predict metabolism, diagnosis and prognosis at the bedside in disorders of consciousness. *Brain* 2017; 140:2120–32
 53. Mashour GA, Hudetz AG: Bottom-up and top-down mechanisms of general anesthetics modulate different dimensions of consciousness. *Front Neural Circuits* 2017; 11:44
 54. Song J, Davey C, Poulsen C, Luu P, Turovets S, Anderson E, Li K, Tucker D: EEG source localization: Sensor density and head surface coverage. *J Neurosci Methods* 2015; 256:9–21

ANESTHESIOLOGY REFLECTIONS FROM THE WOOD LIBRARY-MUSEUM

Managing Pain for “Lady President”: Mary Todd Lincoln’s Fall from Chair to Bath



While living abroad, the former First Lady of the United States, Mrs. Mary Todd Lincoln (1818 to 1882) tried to realign a picture hanging in her parlor in Pau, France. Unfortunately, the chair that she was standing upon collapsed, throwing her against a table. Debilitated by the ensuing back pain, Mrs. Lincoln boarded a transatlantic steamer back to New York City in October of 1880. There she was nearly crushed, emotionally and physically, by crowds rushing past her toward fellow passenger, actress Sarah Bernhardt. As the impoverished Mrs. Abraham Lincoln lingered in New York, waiting for congressional supplementation of her widow's stipend, she enjoyed the generosity of Eli Peck Miller, M.D. (1828 to 1912), who boarded her at his “Miller's Hotel.” There the woman that “Honest Abe” had nicknamed “Lady President” found pain relief in the “Turkish, Electric, and Roman Baths” advertised (*above*) on Dr. Miller's trade card. (Copyright © the American Society of Anesthesiologists' Wood Library-Museum of Anesthesiology.)

George S. Bause, M.D., M.P.H., Honorary Curator and Laureate of the History of Anesthesia, Wood Library-Museum of Anesthesiology, Schaumburg, Illinois, and Clinical Associate Professor, Case Western Reserve University, Cleveland, Ohio. UJYC@aol.com.

ANESTHESIOLOGY

Peripheral Nerve Blocks for Ambulatory Shoulder Surgery

A Population-based Cohort Study of Outcomes and Resource Utilization

Gavin M. Hamilton, M.D., M.Sc., Reva Ramlogan, M.D., B.Sc., Anne Lui, M.D., M.Sc., Colin J. L. McCartney, M.B., Ch.B., Ph.D., Faraj Abdallah, M.D., M.Sc., Jason McVicar, M.D., Daniel I. McIsaac, M.D., M.P.H.

ANESTHESIOLOGY 2019; 131:1254–63

Ambulatory surgeries are increasingly common.^{1,2} Compared to inpatient surgery, ambulatory surgery results in lower costs with similar safety.^{3,4} However, despite low incidence of serious complications after ambulatory surgery,⁵ more than 3% of patients require unplanned hospital admission on the day of surgery,⁶ and more than 10% of patients have an emergency department visit in the 30 days after surgery.⁷ Evidence suggest that more than 25% of unanticipated admissions after ambulatory surgery are attributable to anesthesiology care and interventions.⁸

Variations in perioperative anesthesia care for shoulder surgery have been documented.⁹ The majority of ambulatory shoulder surgeries are performed with general anesthesia, although there is wide variation in reported institutional practices regarding provision of peripheral nerve blocks (20 to 86%).^{2,10} This may reflect a lack of comparative effectiveness evidence to guide the choice of optimal perioperative management strategies.¹¹ Recent systematic reviews suggest that nerve blocks provide the highest degree of acute postoperative pain relief in ambulatory shoulder surgery patients; however, high-quality evidence supporting a positive impact of regional anesthesia on longer-term outcomes is lacking.^{12–14} Population-based studies could help to address this lack of data; however, available studies are at risk of bias as they have used exposures and outcomes that have not been

ABSTRACT

Background: Nerve blocks improve early pain after ambulatory shoulder surgery; impact on postdischarge outcomes is poorly described. Our objective was to measure the association between nerve blocks and health system outcomes after ambulatory shoulder surgery.

Methods: We conducted a population-based cohort study using linked administrative data from 118 hospitals in Ontario, Canada. Adults having elective ambulatory shoulder surgery (open or arthroscopic) from April 1, 2009, to December 31, 2016, were included. After validation of physician billing codes to identify nerve blocks, we used multilevel, multivariable regression to estimate the association of nerve blocks with a composite of unplanned admissions, emergency department visits, readmissions or death within 7 days of surgery (primary outcome) and healthcare costs (secondary outcome). Neurology consultations and nerve conduction studies were measured as safety indicators.

Results: We included 59,644 patients; blocks were placed in 31,073 (52.1%). Billing codes accurately identified blocks (positive likelihood ratio 16.83, negative likelihood ratio 0.03). The composite outcome was not significantly different in patients with a block compared with those without (2,808 [9.0%] vs. 3,424 [12.0%]; adjusted odds ratio 0.96; 95% CI 0.89 to 1.03; $P = 0.243$). Healthcare costs were greater with a block (adjusted ratio of means 1.06; 95% CI 1.02 to 1.10; absolute increase \$325; 95% CI \$316 to \$333; $P = 0.005$). Prespecified sensitivity analyses supported these results. Safety indicators were not different between groups.

Conclusions: In ambulatory shoulder surgery, nerve blocks were not associated with a significant difference in adverse postoperative outcomes. Costs were statistically higher with a block, but this increase is not likely clinically relevant.

(*ANESTHESIOLOGY* 2019; 131:1254–63)

EDITOR'S PERSPECTIVE

What We Already Know about This Topic

- The use of peripheral nerve blocks after ambulatory shoulder surgery is increasing
- While short-term pain control is improved by nerve blocks in this context, the relationship with postdischarge outcomes is unclear

What This Article Tells Us That Is New

- Peripheral nerve blocks are associated with a decrease in unplanned admissions after ambulatory shoulder surgery
- There is no associated improvement in other postoperative outcomes such as emergency department visits, readmissions, mortality, or costs

This article has been selected for the Anesthesiology CME Program. Learning objectives and disclosure and ordering information can be found in the CME section at the front of this issue. This article is featured in "This Month in Anesthesiology," page 1A. This article is accompanied by an editorial on p. 1205. Supplemental Digital Content is available for this article. Direct URL citations appear in the printed text and are available in both the HTML and PDF versions of this article. Links to the digital files are provided in the HTML text of this article on the Journal's Web site (www.anesthesiology.org). This article has an audio podcast. This article has a visual abstract available in the online version.

Submitted for publication September 19, 2018. Accepted for publication May 30, 2019. From the Department of Anesthesiology and Pain Medicine (G.M.H., R.R., A.L., C.J.L.M., F.A., J.M., D.I.M.) and School of Epidemiology and Public Health (D.I.M.), University of Ottawa, Ottawa, Canada; The Ottawa Hospital Research Institute, Ottawa, Canada (R.R., A.L., C.J.L.M., F.A., D.I.M.); and the Institute for Clinical Evaluative Sciences (IC/ES), Toronto, Canada (D.I.M.).

Copyright © 2019, the American Society of Anesthesiologists, Inc. All Rights Reserved. *Anesthesiology* 2019; 131:1254–63. DOI: 10.1097/ALN.0000000000002865

previously validated, while postdischarge outcomes have not been comprehensively examined.^{15,16}

Therefore, after validation of a case-ascertainment algorithm to identify nerve blocks in health administrative data (against a clinical reference standard), we hypothesized that receipt of a nerve block would reduce the odds of unplanned day of surgery admissions, emergency department visits, hospital readmissions or deaths within 7 days of surgery (combined as a composite primary outcome). We further hypothesized that nerve blocks would decrease healthcare costs and would not increase the incidence of adverse neurologic issues requiring diagnostic testing or consultation.

Materials and Methods

Design and Setting

After ethics approval by the Ottawa Health Sciences Network Research Ethics Board, Ottawa, Canada (REB #: 20160800-01H), we conducted a population-based historical cohort study in Ontario, Canada, a province of more than 13 million people that provides universal health care coverage to all residents. Written informed consent was legally waived. The administration of Ontario's universal health insurance plan produces population-based health administrative data that are collected using standardized disease classifications, procedural terminologies, and abstraction, which are stored at the Institute for Clinical Evaluative Sciences (IC/ES), Toronto, Canada, an independent research institute. The study period extended from April 2009 to December 2016. The start time was chosen to coincide with the introduction of a specific physician billing code in Ontario to identify the placement of continuous nerve catheters (this code was added in 2008; we elected to use a 1-yr washout period after implementation to promote data consistency). The end time was the latest time at which all datasets were complete.

Data Sources

All data were linked deterministically using encrypted patient-specific identifiers. Datasets used included the Same Day Surgery Database, which records all ambulatory surgical procedures performed (*i.e.*, those with planned hospital stays of less than 24 h) and present on admission diagnoses; the National Ambulatory Care Reporting System, which records all emergency department visits; the Discharge Abstract Database, which records all inpatient hospital admissions and present on admission diagnoses; the Ontario Health Insurance Plan database, which captures physician service claims; the Ontario Drug Benefits Database, which captures prescription drug claims for residents 65 yr and older; and the Registered Persons Database, which captures death dates for residents of Ontario. The analytic dataset was created by a trained data analyst independent from

the study team. Because the analytic data were generated from data normally collected at the IC/ES, no further data processing was required. The analysis was performed by an independent analyst following an analysis plan prespecified by the lead and senior author. The study protocol was registered at clinicaltrials.gov (NCT03544775), and the manuscript is reported per the Strengthening the Reporting of Observational Studies in Epidemiology and the REporting of studies Conducted using Observational Routinely-collected health Data guidelines.^{17,18}

Cohort

We included Ontario residents, aged 18 yr and older, who underwent elective ambulatory shoulder surgery. Participants were identified using the Same Day Surgery Database through application of previously studied Canadian Classification of Interventions codes to identify the following shoulder surgeries: rotator cuff repair, shoulder arthroplasty or joint repair, and other repair of shoulder muscles (see specific codes in Supplemental Digital Content, appendix 1, <http://links.lww.com/ALN/B993>).⁷ We compiled a patient-level cohort by including only the first surgery for any participant in the study period.

Exposure

Our primary exposure was receipt of a nerve block. Before any outcome analysis, we validated the exposure definition by measuring the accuracy and validity of a case ascertainment algorithm to identify receipt of a nerve block in health administrative data (see full description in Supplemental Digital Content, appendix 2, <http://links.lww.com/ALN/B993>). Briefly, our algorithm consisted of physician billing codes in Ontario Health Insurance Plan (G260-major plexus block, G060-major nerve block, G061-minor nerve block, or G279-percutaneous nerve block catheter for continuous infusion analgesia) compared to a reference standard of nested clinical data from a single hospital linked to the IC/ES. Full validation is described in the Supplemental Digital Content, appendix 2 (<http://links.lww.com/ALN/B993>), but briefly, we defined our reference standard from The Ottawa Hospital Data Warehouse, a peer-reviewed central data repository that stores a combination of administrative and clinical data for all patients cared for at The Ottawa Hospital, Ottawa, Canada, and includes all electronic anesthesia medical records (which are the medico-legal standard for anesthesia data collection). The validation data contained all adult ambulatory shoulder surgery patients at The Ottawa Hospital from January 2013 to December 2016. The algorithm was highly accurate (positive likelihood ratio 16.83, negative likelihood ratio 0.03; sensitivity 97%, specificity 94%) for correctly identifying the true presence (or absence) of a nerve block.

For our main outcome study we compared (1) no nerve block (*i.e.*, no physician billing codes) to (2) nerve block (*i.e.*, presence of a nerve block billing code). We also identified any patient who had a continuous catheter inserted to allow for a sensitivity analysis using the billing code G279.

Outcomes

Our primary outcome was a composite including (1) unplanned admissions on the day of surgery (from the Discharge Abstract Database), (2) postdischarge emergency department visits within 7 days of surgery (from National Ambulatory Care Reporting System), (3) readmission within 7 days of surgery (from the Discharge Abstract Database), and (4) death from any cause (from the Registered Persons Database). We included mortality, even though it is a rare after ambulatory surgery, as it is a competing risk.¹⁹ The most responsible diagnosis, as defined by the treating physician, for all emergency department visits was identified. Our secondary outcome was total health system costs from the perspective of the payer (*i.e.*, the Ontario Ministry of Health and Longterm Care, Toronto, Ontario, Canada), calculated from the day of surgery to 7 days after surgery. To calculate these costs, we used standardized patient-level costing algorithms that include all direct health system costs (*i.e.*, those directly attributable to the patient such as physician service claims, diagnostic and laboratory testing, pharmaceuticals, equipment or medical devices, home care) as well as indirect costs (*i.e.*, health system utilization of inpatient and outpatient hospital care, emergency care, inpatient rehabilitation, complex continuing care and long-term-care). The indirect costs are calculated by accounting for an individual's resource intensity weight, case-mix group, and duration of care in each location. This approach does include the cost of surgery, but lacks the granularity to specifically account for materials used in the operating room (such as regional anesthesia supplies), although the fee paid to the anesthesiologist for placing the block is included.²⁰ Costs incurred by the individual patient that are not covered by the health system (*e.g.*, private physiotherapy, custom slings or braces, or opportunity costs such as missed time at work) are not included. Costs were standardized to 2016 Canadian dollars. We also evaluated the composite outcome and health system costs in the 30 days after surgery.

As an indicator of possible nerve injury or complication from the nerve block, we examined the rate of neurology consults (Ontario Health Insurance Plan physician billing code A180-special neurology consultation, A/C188-neurology partial assessment or concurrent care, or A/C385-neurology limited consultation) and nerve conduction studies (code G455-G456-complete electromyography study, both technical/professional component, or G466/G457-limited electromyography study, both technical/professional component) in the 90 days after surgery. A time frame of 90 days was chosen to ensure late presentations of peripheral nerve injuries would not be missed.

Electromyography has improved diagnostic utility if performed more than 3 weeks after injury, which may not have been captured if a shorter time frame was used.²¹

Covariates

Patient demographics, comorbidities, and preoperative patterns of healthcare resource use could confound the association between receipt of a nerve block and outcomes. Therefore, we collected detailed baseline data on all participants: age (restricted cubic spline with five knots), gender (binary), rural residence (binary), neighborhood income quintile (five-level categorical), year of surgery (restricted cubic spline with three knots), validated chronic disease status for asthma²² (binary), chronic obstructive pulmonary disease²³ (binary), diabetes mellitus²⁴ (binary), acute coronary syndrome²⁵ (binary), heart failure²⁶ (binary) and hypertension²⁷ (binary), all Elixhauser comorbidities (using a 3-yr lookback, each as a binary variable),²⁸ American Society of Anesthesiologists score (2 or lower *vs.* 3 or higher), baseline 1-yr mortality risk using the Johns Hopkins Adjusted Clinical Groups score (continuous linear; derived using Adjusted Diagnosis Groups²⁹ from each individuals' inpatient and outpatient contact with the health system). The Johns Hopkins Adjusted Clinical Groups scores were then assigned points to produce a measure of baseline mortality risk that has been validated across the full Ontario population (c-statistic 0.92, well-calibrated across the risk spectrum),³⁰ acute care hospitalization in the previous year (binary), emergency department visits in the previous year (categorical: 0, 1, 2 or greater); and predicted healthcare utilization based on the Johns Hopkins Adjusted Clinical Groups Resource Utilization Band (six-level categorical),²⁹ which accounts for patterns of preoperative inpatient and outpatient health resource use. Last, all prescriptions for oral and transdermal opioids (short- and long-acting) were identified from the Ontario Drug Benefits Database for all people older than 65 yr in the 6 months before surgery.

Data Analysis

The dataset was created, manipulated, and analyzed using SAS version 9.4 (SAS Institute, Cary, North Carolina). After reviewer feedback, absolute standardized differences were used to compare baseline characteristics between exposure groups instead of tests of significance; values greater than 10 are felt to represent substantial differences.³¹

We calculated the unadjusted and adjusted association between nerve blocks and outcomes. Generalized linear mixed models (PROC GLIMMIX) were used to account for clustering of patients within hospitals (which was the highest level of hierarchy in our data)³² using a random intercept term in all adjusted analyses. Dichotomous outcomes (our primary outcome and its components, safety outcomes) were analyzed using logistic regression. Cost data, which are typically skewed, were analyzed using a gamma

distribution and a log link.³³ Adjusted differences in attributable costs were calculated by estimating the predicted adjusted cost from the log-gamma cost model, followed by creation of 1,000 bootstrap samples with replacement. We then calculated the median adjusted cost difference across the bootstrap samples as the effect size and CI using the percentile method.³⁴ All adjusted models included the variables listed in the Covariates section, plus a categorical variable for the specific type of shoulder surgery based on the type of surgery (three-level categorical) and a binary indicator for open *versus* arthroscopic approach (derived from the Canadian Classification of Interventions code). All analyses were conducted using two-tailed hypothesis testing with a *P* value of less than 0.05 as statistically significant. Adjustment for multiple testing was not specified; however, a conservative adjustment for the fact that we had two main primary analyses (*i.e.*, the composite outcome and costs), such as a Bonferroni corrected *P* value of 0.025, would not have changed the significance threshold interpretation for either result.

Sensitivity Analyses

We performed several prespecified sensitivity analyses to test the robustness of our primary analysis. First, we recalculated the adjusted associations for our primary outcome restricting the cohort to people older than 65 yr to evaluate whether addition of preoperative opioid drug data impacted our estimated associations. Next, we tested whether our choice of analytic approach impacted our primary findings. We used a nonparsimonious logistic regression model to assign a propensity score for receipt of a nerve block to each person based on covariates used in the primary analysis. We then matched patients who received a nerve block one-to-one without replacement exactly on the index hospital (to account for clustering), and then using a greedy matching algorithm based on a caliper width of 0.2 times the logit of the SD of the propensity score. Within this propensity score matched cohort, we estimated the impact of nerve blocks on the primary outcome. Finally, to assess the impact of catheters, we reran our primary analysis, but specified our independent variable as a three-level categorical variable (no nerve block, nerve block only, nerve block plus catheter).

Post Hoc Subgroup Analyses

After protocol registration, we identified that there could be effect modification based on (1) the type of surgery performed (shoulder arthroplasty or joint repair *vs.* rotator cuff repair), and (2) surgery being performed before, or after, 2014 (as in 2014, two key systematic reviews of dexamethasone prolonging duration of brachial plexus blocks were published^{35,36}). To test for effect modification, we added a multiplicative interaction term to our primary multi-level multivariable model to test whether the interaction

between nerve block and procedure, or nerve block and time period, was significant ($P < 0.05$).

Reviewer-requested Sensitivity Analyses

During peer review, the following *post hoc* sensitivity analyses were requested: (1) excluding data from 2009 when utilization of nerve blocks was substantially lower, (2) providing an adjusted cost difference, (3) adjusting for procedural risk using the full Canadian Classification of Interventions code, (4) adjusting for hospital-level variation using hospital identifier as a categorical fixed effect, (5) adjusting for the Johns Hopkins Adjusted Clinical Groups score as a five-knot restricted cubic spline, and (6) rerunning our cost analysis after subtracting the physician billing cost of the block (estimated at \$60 of anesthesia time plus \$80 for G260, \$55 for G060, \$30 for G061, \$80 G279). The methods employed and results of these analyses are provided in Supplemental Digital Content, appendix 4 (<http://links.lww.com/ALN/B993>).

Sample Size

This was a population-based cohort, so all eligible participants were included. With more than 6,000 outcomes, we conservatively had 600 degrees of freedom to support logistic regression modeling.³⁷ We did not prespecify a clinically important difference in the primary outcome.

Missing Data

Main outcome and exposure variables were complete for all participants.

Results

We identified 59,644 people who underwent shoulder surgery in Ontario from January 2009 to December 2016 (fig. 1) at one of 118 different hospitals. Overall, nerve blocks were placed in 31,073 patients (52.1%), 1,508 (4.9%) of which were catheters. In the first year of the study, 626 of 6,487 (9.7%) of patients received a nerve block for their shoulder surgery; subsequent years had an increasingly greater proportion of patients who received a nerve block (fig. 2). Patient characteristics are described in table 1.

In the total cohort, 6,234 of 59,644 (10.4%) experienced the primary outcome (no patients died in the 30 days after surgery). Specifically, 4.9% of patients had an unplanned admission after their surgery, 0.3% of patients were readmitted to the hospital within 7 days of their surgery, and 5.9% of patients were seen in the emergency department within 7 days of their surgery.

Primary Outcome

Of people with a nerve block, 2,808 of 31,073 patients (9.0%) had an admission, readmission, or emergency department visit within 7 days of surgery compared to 3,424 of 28,571 patients (12.0%) without a nerve block (unadjusted odds ratio 0.73;

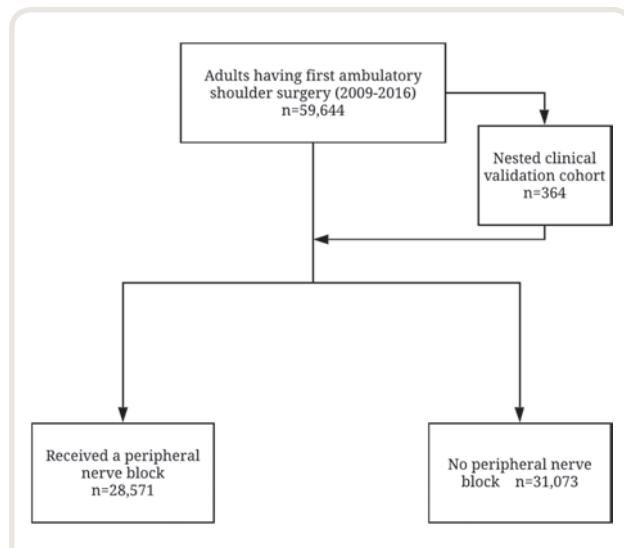


Fig. 1. Flow diagram depicting the creation of the analytical dataset.

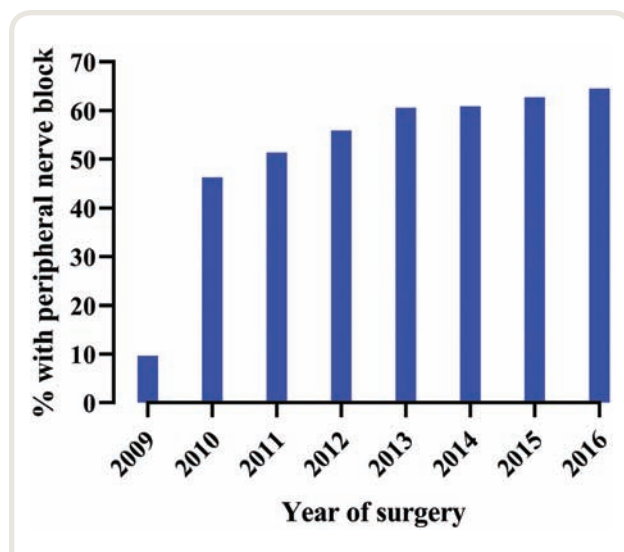


Fig. 2. Graph displaying the number of peripheral nerve blocks placed by year of study.

95% CI 0.69 to 0.77; $P < 0.0001$). After multilevel, multivariable adjustment, no significant difference remained (odds ratio 0.96; 95% CI 0.89 to 1.03; $P = 0.243$). The fully specified model is provided in Supplemental Digital Content, appendix 3 (<http://links.lww.com/ALN/B993>), including the calibration plot, which demonstrated good agreement between observed and expected outcomes across the risk spectrum.

When evaluating the individual components of the composite outcome, there was a significant adjusted decrease in unplanned admissions for patients with a nerve block (adjusted odds ratio 0.88; 95% CI 0.79 to 0.98; $P = 0.020$). There was no significant adjusted difference in

Table 1. Characteristics of the Study Cohort

	No PNB (n = 28,571)	PNB (n = 31,073)	ASD
Demographics			
Age, yr, mean \pm SD	51 \pm 13	52 \pm 12	8.0
Female, %	32.7	33.9	0.9
Rural, %	18.7	13.0	10.7
Neighborhood income quintile, median (IQR)	3 (4–2)	3 (4–2)	0.0
Surgery type, %			
Shoulder arthroplasty or joint repair	40.8	36.5	2.0
Rotator cuff repair	58.0	63.1	2.2
Other shoulder repair	1.2	0.4	8.9
Surgical approach, %			
Arthroscopic	71.1	75.9	5.1
Open	28.9	24.1	
Healthcare resource use, %			
Hospitalization in the last year	5.8	4.9	3.6
Emergency department visit in the last year	43.9	39.2	1.6
Comorbidities			
ACG score, mean \pm SD	8 \pm 3	8 \pm 3	0.0
ASA score, < 3	68.7	64.3	3.1
Cerebrovascular disease, %	0.3	0.3	0.0
Chronic renal disease, %	0.2	0.1	2.6
Dialysis, %	0.1	0.1	0.0
Dementia, %	0	0	N/A
Primary malignancy, %	0.7	0.7	0.0
Metastatic solid tumor, %	0.1	0.0	4.5
Peripheral vascular disease, %	0.2	0.2	0.0
History of peptic ulcer disease, %	0.2	0.1	2.6
Liver disease, %	0.1	0.1	0.0
Rheumatologic disease, %	0.2	0.1	2.6
Hemiplegia or paraplegia, %	0.1	0.0	4.5
Atrial arrhythmia, %	0.4	0.4	0.0
History of venous thromboembolism, %	0.1	0.1	0.0
History of heart failure, %	1.3	1.2	0.9
History of hypertension, %	33.6	36.0	1.5
History of diabetes mellitus, %	14.7	15.6	1.8
Chronic obstructive pulmonary disease, %	12.3	12.2	0.2
Asthma, %	17.8	18.2	0.7
Myocardial infarction, %	1.5	1.6	0.8
Cardiac valvular disease, %	0.1	0.1	0.0
Disease of the pulmonary circulation, %	0.1	0.1	0.0
Coagulopathy, %	0.1	0.1	0.0
Obesity, %	0.5	0.6	1.3
Weight loss, %	0.1	0.0	4.5
Blood loss anemia, %	0.5	0.6	1.3
Deficiency anemia, %	0.0	0.0	N/A
Alcohol abuse, %	0.4	0.3	1.7
Drug abuse, %	0.2	0.1	2.6
Psychosis, %	0.0	0.0	N/A
Depression, %	0.4	0.4	0.0

ACG, Johns Hopkins Adjusted Clinical Groups score; ASD, adjusted standardized difference; ASA, American Society of Anesthesiologists; IQR, interquartile range; N/A, not applicable; PNB, peripheral nerve block.

readmissions or emergency department visits within 7 days between the two groups, although the directional associations for these postdischarge associations did not favor nerve blocks (table 2). Table 3 describes the most common

Table 2. Association of Peripheral Nerve Blocks with Outcomes in Ambulatory Shoulder Surgery (Primary and Secondary)

	No PNB	PNB	Unadjusted Relative Effect* (95% CI)	PValue	Adjusted† Relative Effect‡ (95% CI)	PValue
Primary analysis	n = 28,571	n = 31,073				
Composite outcome (7 days), n (%)	3,424 (12.0)	2,808 (9.0)	0.73 (0.69–0.77)	< 0.0001	0.96 (0.89–1.03)	0.243
Unplanned admission §, n (%)	1,784 (6.2)	1,132 (3.6)	0.57 (0.53–0.61)	< 0.0001	0.88 (0.79–0.98)	0.020
Readmission within 7 days, n (%)	85 (0.3)	98 (0.3)	1.06 (0.79–1.42)	0.693	1.00 (0.73–1.39)	0.987
ED visits within 7 days, n (%)	1,779 (6.2)	1,732 (5.6)	0.89 (0.83–0.95)	< 0.001	1.02 (0.94–1.12)	0.583
Secondary analysis						
Composite outcome (30 days), n (%)	4,400 (15.4)	3,754 (12.1)	0.76 (0.72–0.79)	< 0.0001	0.95 (0.89–1.02)	0.137
Unplanned admission§, n (%)	1,784 (6.2)	1,132 (3.6)	0.57 (0.52–0.61)	< 0.0001	0.88 (0.79–0.98)	0.020
Readmission within 30 days, n (%)	229 (0.8)	207 (0.7)	0.83 (0.69–1.00)	0.053	1.00 (0.73–1.39)	0.987
ED visits within 30 days, n (%)	2,837 (9.9)	2,727 (8.8)	0.87 (0.83–0.92)	< 0.0001	1.00 (0.93–1.07)	0.983
Cost after surgery‡ (7 days)	4,391 (3,910–4,836)	4,681 (4,337–5,066)	1.07 (1.07–1.07)§	< 0.0001	1.06 (1.02–1.10)§	0.005
Cost after surgery‡ (30 days)	4,528 (4,014–5,019)	4,840 (4,451–5,258)	1.07 (1.07–1.08)§	< 0.0001	1.06 (1.02–1.10)§	0.007
Neurology consultations in the 90 days after surgery	74 (0.3)	92 (0.3)	1.14 (0.84–1.55)	0.391	1.04 (0.71–1.53)	0.839
Nerve conduction studies in the 90 days after surgery	235 (0.8)	274 (0.9)	1.07 (0.9–1.28)	0.432	1.02 (0.84–1.24)	0.834

Weighted frequencies of outcomes for the "No PNB" group are presented.

*All relative effect measures represent odds ratios, except for costs which are ratios of means. †Variables included in the model include patient demographics, surgery location, surgery type, healthcare resource use, and comorbidities as outlined in table 1. ‡Cost after surgery includes the day of surgery costs. §Unplanned admission refers to admission on the day of surgery only. || $P < 0.05$ is statistically significant.

ED, emergency department; PNB, peripheral nerve block.

Table 3. Most Common Etiologies of Unplanned Admissions and ED Visits within 7 Days of Surgery

Etiology of ED Visits	No PNB (n = 28,571) n (%)	PNB (n = 31,073) n (%)
Acute pain	302 (1.1)	434 (1.4)
Surgical dressing or suture	168 (0.6)	102 (0.3)
Bleeding	94 (0.3)	69 (0.2)
Pain in joint	50 (0.2)	68 (0.2)
Urinary retention	76 (0.3)	64 (0.2)

ED, emergency department; PNB, peripheral nerve block.

physician-assigned primary diagnoses for patients who presented to the emergency department. When the primary outcome was measured over the 30 days after surgery, findings were similar to the 7-day outcomes (table 2).

Secondary Outcomes

Before adjustment, health system costs on the day of surgery to 7 days after surgery were significantly higher with a nerve block (median cost with a nerve block \$4,681 *vs.* \$4,391 without; ratio of means 1.07; 95% CI 1.07 to 1.07; $P < 0.0001$). After multilevel multivariable adjustment, costs remained significantly higher in those who received a nerve block (ratio of means 1.06; 95% CI 1.02 to 1.10; $P = 0.005$). We found \$325 (95% CI \$316 to \$333) in excess health system costs attributable to provision of a nerve block. A similar cost difference was seen with the

30-day cost data (median cost with a nerve block \$4,840 *vs.* \$4,528 without; adjusted ratio of means 1.06; 95% CI 1.02 to 1.10; $P = 0.007$).

Evaluating safety indicators between the receipt of a nerve block *versus* no nerve block, we found that there were no differences in the odds of either neurology consultations (adjusted odds ratio 1.04; 95% CI 0.71 to 1.53; $P = 0.839$) or nerve conduction studies in the 90 days after surgery (adjusted odds ratio 1.02; 95% CI 0.84 to 1.24; $P = 0.834$).

Sensitivity Analyses

In people more than 65 yr of age ($n = 8,653$ or 15% of total cohort), for whom we could add additional adjustment for receipt of preoperative opioids, there was no difference in the adjusted odds of the composite outcome between nerve blocks compared to those without a nerve block (adjusted odds ratio 0.87; 95% CI 0.75 to 1.03; $P = 0.110$).

The propensity score analysis resulted in successful matching of 12,699 people with a nerve block to 12,699 people without (42.6% of total cohort; characteristics in Supplemental Digital Content, appendix 5, <http://links.lww.com/ALN/B993>). The presence of a nerve block was not associated with a difference in the composite outcome at 7 days (10.8%) compared with those without a nerve block (10.5%; adjusted odds ratio 1.04; 95% CI 0.95 to 1.13; $P = 0.382$).

When we compared no nerve block (reference category) *versus* nerve block with no catheter *versus* nerve block with a catheter, the presence of a catheter was associated with a significant increase in the adjusted odds of the 7-day

composite outcome (odds ratio 1.92; 95% CI 1.55 to 2.38; $P < 0.0001$) compared to no nerve block; there was no difference in the adjusted odds of composite outcome between no nerve block and nerve blocks without a catheter (odds ratio 0.93; 95% CI 0.87 to 1.00; $P = 0.059$).

Subgroup Analyses

There was no evidence of significant effect modification on the multiplicative scale between nerve block receipt and surgery type ($P = 0.067$), or nerve block and time period ($P = 0.314$).

Reviewer-requested Sensitivity Analyses

Results of the requested analyses are provided in Supplemental Digital Content, appendix 4 (<http://links.lww.com/ALN/B993>). No substantive changes in our results were identified for the primary composite outcome or 7-day health system costs. The association of increased costs persisted (although attenuated) after subtracting physician billing charges for block placement (ratio of means 1.03; 95% CI 1.03 to 1.04; $P < 0.001$).

Discussion

In this retrospective study examining nerve blocks in ambulatory shoulder surgery, there was no association between nerve blocks (measured using validated billing codes) and the composite outcome of unplanned admissions or readmissions, emergency department visits, or death within 7 days. These data suggest that the early benefits of decreased pain scores with nerve blocks, proven in randomized trials, may not translate into postdischarge health system benefits. Additionally, nerve blocks were associated with a \$325 increase in health system costs up to 7 postoperative days; however, despite statistical significance, this may not be clinically significant. These findings suggest that pragmatic randomized trials focused on postdischarge patient-reported outcomes, and evaluation of processes, are needed to help extend the early benefits of nerve blocks into the postdischarge phase and to address important knowledge gaps around nerve block use in ambulatory shoulder surgery.

Two previous studies using administrative data have attempted to address health system outcomes associated with nerve blocks for shoulder surgery.^{15,16} However, both studies had significant limitations. Importantly, both lacked a validated exposure measure (*i.e.*, manner to identify true receipt or nonreceipt of a nerve block). This can bias results,^{38,39} as misclassification bias can improperly categorize patients as having had, or not had, a given exposure in unpredictable ways.³⁹ Furthermore, the study by Danninger *et al.*¹⁵ of rotator cuff repairs, which found nerve blocks to be associated with decreased day of surgery admissions, was limited to outcomes happening up to the time of hospital discharge and did not specify whether surgeries were planned as ambulatory or inpatient cases (which could

also misclassify their outcome variable). Ding *et al.*¹⁶ found nerve blocks used in the absence of general anesthesia to be associated with decreased rates of 90-day readmissions compared to general anesthesia (with or without a nerve block). As the study was limited by grouping all people who received general anesthesia (including those with a nerve block) in a single level, outcome differences may not be due to the nerve block altering postoperative pain, but rather an avoidance of general anesthesia. Furthermore, causally relating a block on the day of surgery to 90-day readmissions may be difficult. In contrast, we used a validated nerve block exposure and collected data on a combination of key health system outcomes from surgery to postoperative day 7. Importantly, we captured emergency department visits, which are common after ambulatory surgery but not routinely studied. Using this robust approach, we found no difference associated with receipt of a nerve block and a combination of unplanned admissions, emergency department visits, hospital readmissions, or deaths.

While using a composite outcome allowed us to assess a combination of pertinent outcomes in a manner relevant to patients and the health system, the individual components of the composite outcome warrant closer examination. Unplanned day of surgery admissions were significantly lower in the nerve block group, which is consistent with the trial data demonstrating improved early pain control and shorter postanesthesia care unit stays with nerve blocks.¹³ However, this early benefit did not impact postdischarge outcomes, as emergency department visits and readmissions did not differ between groups. The reasons for emergency department visits may provide some insight into this finding. In the nerve block group, acute pain was more common as the primary emergency department diagnosis (table 3). This could reflect rebound pain, a phenomenon in which profound initial analgesia from a block leads to inadequate oral analgesic consumption as the block wears off.⁴⁰ These findings could inform a possible prevention strategy focusing on greater patient education or process optimization around systemic analgesia as nerve blocks wear off. In people without a block, emergency department diagnoses were more commonly related to surgical issues, which is consistent with previous research.⁴¹ Across both nerve block and no nerve block groups, it is also important to note that approximately 6% of adults having ambulatory shoulder surgery return to the emergency department or are readmitted to hospital within 7 days.

Our sensitivity analyses also provide insights into the relationship between nerve blocks and outcomes. As indication and confounding bias are also important considerations in database research,³⁹ we assessed whether a propensity score match (as opposed to our regression model) would lead to differing results (as matching allows one to estimate the effect of an intervention in the section of the population that is most comparable at baseline, whereas regression provides an estimate of what would happen if the whole population

switched from no block to a block).⁴² However, the results were similar (no significant difference associated with nerve blocks). Unmeasured confounders can also bias results, and in the case of nerve blocks, baseline chronic pain could influence both receipt of a nerve block and risk of an adverse outcome. However, in those older than 65 yr, where prescription opioid data was available, again we found no primary outcome difference. Finally, as an exploratory analysis, we compared no block with isolated blocks or blocks with a catheter. While we found that receipt of a catheter was associated with a 92% relative increase in the odds of unplanned admissions, readmissions, or emergency department visits, caution is needed in interpreting the result of a secondary analysis. There is little published evidence regarding post-discharge outcomes with catheters *versus* single shot nerve blocks.⁴³ This finding could reflect complications specific to the catheter, or patient uncertainty associated with continuous catheters. Unmeasured confounding may contribute to this effect size; however, using the E-value⁴⁴ to estimate how strong a missing variable would need to be to explain away the measured effect suggests that this is unlikely (we estimate that a missing variable would need to have an odds ratio of 3.25 to decrease the association between catheters and adverse outcomes to no effect).

Finally, our analysis also addressed the association of nerve blocks with health system costs and safety indicators. We found a statistically significant association between nerve blocks and a small increase in health system costs on the day of surgery to 7 days afterward (approximately \$325). Some of this cost is attributable to the cost of the physician service in placing the block and the additional anesthesia care time (in Ontario, anesthesiologists are fee-for-service and bill for specific procedures as well as time-based billing); however, even after accounting for these charges, a 3% relative increase in costs remained. Whether these costs represent a clinically important increase is questionable. For example, one must consider whether this increased cost may still represent value in providing a nerve block. While we were unable to identify any valuation data specific to pain avoidance after ambulatory surgery, avoiding postoperative pain has been identified as the third highest priority outcome for patients after surgery, and chronic pain patients have identified that they would be willing to pay \$56 to \$145 per day to avoid pain; therefore, the higher cost associated with nerve block placement may well provide value at the patient level.^{45–47} In terms of safety, we are not aware of validated means to identify nerve injuries in administrative data; however, we did not find any differences between groups in the number of neurologic consultations or nerve conduction studies in the 90 days after surgery. While this outcome can only be considered a proxy for true nerve injury, it is important to note that there was no strong signal that nerve blocks were associated with increased nerve injuries significant enough to require specialist consultation or diagnostic testing.

Limitations

Our findings are at risk of several types of bias. First, there is risk of misclassification bias. We validated our exposure to confirm that blocks were accurately identified, but only know that a block was placed, not how well it worked. Therefore, our findings reflect a pragmatic approach as opposed to an explanatory study.⁴⁸ Confounding bias may influence receipt of specific interventions and outcomes; if unmeasured confounders led to higher risk of adverse events and increased likelihood of a block, our findings would be biased to the null. However, we controlled for prespecified confounders, and results were consistent across all analyses that were prespecified in our protocol. We were unable to measure patient-reported outcomes such as quality of life, quality of recovery, experience/satisfaction, or return to work. Our findings do not preclude benefit, as our 95% CI included values below the null value; however, despite a large sample, we found no statistically significant impact. Cost were captured at the health system level, but were not adequately granular to capture operating room supplies, and partly rely on indirect techniques that could be associated with estimation error. We did not have specifics of each nerve block technique (*e.g.*, ultrasound *vs.* landmark, dose or type of local anesthetic or additives) that may impact nerve block efficacy. Findings may not generalize to all jurisdictions.

Implications

Receipt of a nerve block for ambulatory shoulder surgery was not associated with a difference in unplanned admissions, emergency department visits, readmissions, or deaths in the 7 days after surgery; unplanned admission rates were lower in the presence of a nerve block. Pragmatic randomized trials powered for patient-centered postdischarge outcomes, as well as process evaluation, are needed to understand how the early benefits of blocks may extend after discharge and to fully inform anesthetic care.

Acknowledgments

We would like to acknowledge the assistance of Sascha Davis, B.Sc., Information Specialist (Learning Services, The Ottawa Hospital, Ottawa, Canada) for her assistance in developing and executing our search. Dr. McIsaac acknowledges salary support from The Ottawa Hospital Department of Anesthesiology. This study was also supported by IC/ES, Toronto, Canada, which is funded by an annual grant from the Ontario Ministry of Health and Long-Term Care. The opinions, results and conclusions reported in this paper are those of the authors and are independent from the funding sources. No endorsement by IC/ES or the Ontario Ministry of Health and Long-Term Care is intended or should be inferred. These data sets were held securely in a linked, deidentified form and analyzed at IC/ES. This study used The Johns Hopkins ACG System version 10.

Research Support

The study was funded by a Canadian Anesthesia Society Resident Research Grant. Dr. McIsaac receives salary support from Department of Anesthesiology and Pain Medicine, The Ottawa Hospital, is a Clinical Research Chair at the University of Ottawa, Ottawa, Canada, and is supported by the Canadian Anesthesia Society Career Scientist Award.

Competing Interests

The authors declare no competing interests.

Correspondence

Address correspondence to Dr. McIsaac: Department of Anesthesiology and Pain Medicine, 1053 Carling Ave, Ottawa, Ontario, K1Y 4E9, Canada. dmcisaac@toh.ca. This article may be accessed for personal use at no charge through the Journal Web site, www.anesthesiology.org.

References

1. Ambulatory Surgery in the United States. 2006. Available at: <http://www.cdc.gov/nchs/data/nhsr/nhsr011.pdf>. Accessed April 26, 2019.
2. Jain NB, Higgins LD, Losina E, Collins J, Blazar PE, Katz JN: Epidemiology of musculoskeletal upper extremity ambulatory surgery in the United States. *BMC Musculoskelet Disord* 2014; 15:4
3. Lumsdon K, Anderson HJ, Burke M: New surgical technologies reshape hospital strategies. *Hospitals* 1992; 66:30–6, 38, 40–2
4. Leroux TS, Basques BA, Frank RM, Griffin JW, Nicholson GP, Cole BJ, Romeo AA, Verma NN: Outpatient total shoulder arthroplasty: A population-based study comparing adverse event and readmission rates to inpatient total shoulder arthroplasty. *J Shoulder Elbow Surg* 2016; 25:1780–6
5. Warner MA, Shields SE, Chute CG: Major morbidity and mortality within 1 month of ambulatory surgery and anesthesia. *JAMA* 2010; 304:1437–41
6. Whippey A, Kostandoff G, Paul J, Ma J, Thabane L, Ma HK: Predictors of unanticipated admission following ambulatory surgery: A retrospective case-control study. *Can J Anaesth* 2013; 60:675–83
7. McIsaac DI, Bryson GL, van Walraven C: Impact of ambulatory surgery day of the week on postoperative outcomes: a population-based cohort study. *Can J Anaesth* 2015; 62:857–65
8. Fortier J, Chung F, Su J: Unanticipated admission after ambulatory surgery—A prospective study. *Can J Anaesth* 1998; 45:612–9
9. Cozowicz C, Poeran J, Memtsoudis SG: Epidemiology, trends, and disparities in regional anaesthesia for orthopaedic surgery. *Br J Anaesth* 2015; 115 (suppl 2):ii57–67
10. Hughes MS, Matava MJ, Wright RW, Brophy RH, Smith MV: Interscalene brachial plexus block for arthroscopic shoulder surgery: A systematic review. *J Bone Joint Surg Am* 2013; 95:1318–24
11. Wennberg J, Gittelsohn: Small area variations in health care delivery. *Science* 1973; 182:1102–8
12. Atchabahian A, Schwartz G, Hall CB, Lajam CM, Andrae MH: Regional analgesia for improvement of long-term functional outcome after elective large joint replacement. *Cochrane Database Syst Rev* 2016; 8
13. Warrender WJ, Syed UAM, Hammoud S, Emper W, Ciccotti MG, Abboud JA, Freedman KB: Pain management after outpatient shoulder arthroscopy: A systematic review of randomized controlled trials. *Am J Sports Med* 2017; 45:1676–86
14. Mueller KG, Memtsoudis SG, Mariano ER, Baker LC, Mackey S, Sun EC: Lack of association between the use of nerve blockade and the risk of persistent opioid use among patients undergoing shoulder arthroplasty: Evidence from the Marketscan Database. *Anesth Analg* 2017; 125:1014–20
15. Danninger T, Stundner O, Rasul R, Brummett CM, Mazumdar M, Gerner P, Memtsoudis SG: Factors associated with hospital admission after rotator cuff repair: The role of peripheral nerve blockade. *J Clin Anesth* 2015; 27:566–73
16. Ding DY, Mahure SA, Mollon B, Shamah SD, Zuckerman JD, Kwon YW: Comparison of general *versus* isolated regional anesthesia in total shoulder arthroplasty: A retrospective propensity-matched cohort analysis. *J Orthop* 2017; 14:417–24
17. Elm E von, Altman DG, Egger M, Pocock SJ, Gøtzsche PC, Vandenbroucke JP: Strengthening the Reporting of Observational Studies in Epidemiology (STROBE) statement: Guidelines for reporting observational studies. *BMJ* 2007; 335:806–8
18. Benchimol EI, Smeeth L, Guttmann A, Harron K, Moher D, Petersen I, Sørensen HT, von Elm E, Langan SM; RECORD Working Committee: The REporting of studies Conducted using Observational Routinely-collected health Data (RECORD) statement. *PLoS Med* 2015; 12:e1001885
19. Waterman BR, Dunn JC, Bader J, Urrea L, Schoenfeld AJ, Belmont PJ Jr: Thirty-day morbidity and mortality after elective total shoulder arthroplasty: Patient-based and surgical risk factors. *J Shoulder Elbow Surg* 2015; 24:24–30
20. Wodchis W, Bushmeneva K, Nikitovic M, McKillop I: Guidelines on person level cost using administrative databases in Ontario. *Work Pap Ser* 2013; 1
21. Neal JM, Barrington MJ, Brull R, Hadzic A, Hebl JR, Horlocker TT, Huntoon MA, Kopp SL, Rathmell JP, Watson JC: The Second ASRA Practice Advisory on Neurologic Complications Associated With Regional Anesthesia and Pain Medicine: Executive summary 2015. *Reg Anesth Pain Med* 2015; 40:401–30

22. Gershon AS, Wang C, Guan J: Identifying patients with physician-diagnosed asthma. *COPD J Chronic Obstr Pulm Dis* 2009; 5:388–94
23. Gershon AS, Wang C, Guan J, Vasilevska-Ristovska J, Cicutto L, To T: Identifying individuals with physician diagnosed COPD in health administrative databases. *COPD* 2009; 6:388–94
24. Hux JE, Ivis F, Flintoft V, Bica A: Diabetes in Ontario: Determination of prevalence and incidence using a validated administrative data algorithm. *Diabetes Care* 2002; 25:512–6
25. Tu K, Mitiku T, Guo H, Lee DS, Tu JV: Myocardial infarction and the validation of physician billing and hospitalization data using electronic medical records. *Chronic Dis Can* 2010; 30:141–6
26. Schultz SE, Rothwell DM, Chen Z, Tu K: Identifying cases of congestive heart failure from administrative data: A validation study using primary care patient records. *Chronic Dis Inj Can* 2013; 33:160–6
27. Tu K, Campbell NR, Chen ZL, Cauch-Dudek KJ, McAlister FA: Accuracy of administrative databases in identifying patients with hypertension. *Open Med* 2007; 1:e18–26
28. Quan H, Sundararajan V, Halfon P, Fong A, Burnand B, Luthi JC, Saunders LD, Beck CA, Feasby TE, Ghali WA: Coding algorithms for defining comorbidities in ICD-9-CM and ICD-10 administrative data. *Med Care* 2005; 43:1130–9
29. The Johns Hopkins ACG System: Excerpt from Version 11.0 Technical Reference Guide. 2014. Available at: <https://www.hopkinsacg.org/>. Accessed June 14, 2019.
30. Austin PC, Walraven CV: The mortality risk score and the ADG score: Two points-based scoring systems for the Johns Hopkins aggregated diagnosis groups to predict mortality in a general adult population cohort in Ontario, Canada. *Med Care* 2011; 49:940–7
31. Austin PC: Using the standardized difference to compare the prevalence of a binary variable between two groups in observational research. *Commun Stat Simul Comput* 2009; 38:1228–34
32. Bottomley C, Kirby MJ, Lindsay SW, Alexander N: Can the buck always be passed to the highest level of clustering? *BMC Med Res Methodol* 2016; 16:29
33. Austin PC, Ghali WA, Tu JV: A comparison of several regression models for analysing cost of CABG surgery. *Stat Med* 2003; 22:2799–815
34. Austin PC, Laupacis A: A tutorial on methods to estimating clinically and policy-meaningful measures of treatment effects in prospective observational studies: A review. *Int J Biostat* 2011; 7:6
35. Albrecht E, Kern C, Kirkham KR: A systematic review and meta-analysis of perineural dexamethasone for peripheral nerve blocks. *Anaesthesia* 2015; 70:71–83
36. Choi S, Rodseth R, McCartney CJ: Effects of dexamethasone as a local anaesthetic adjuvant for brachial plexus block: A systematic review and meta-analysis of randomized trials. *Br J Anaesth* 2014; 112:427–39
37. Vittinghoff E, McCulloch CE: Relaxing the rule of ten events per variable in logistic and Cox regression. *Am J Epidemiol* 2007; 165:710–8
38. McIsaac DI, Gershon A, Wijeyesundera D, Bryson GL, Badner N, van Walraven C: Identifying obstructive sleep apnea in administrative data: A study of diagnostic accuracy. *ANESTHESIOLOGY* 2015; 123:253–63
39. Walraven C van, Austin P: Administrative database research has unique characteristics that can risk biased results. *J Clin Epidemiol* 2012; 65:126–31
40. Lavand'homme P: Rebound pain after regional anesthesia in the ambulatory patient. *Curr Opin Anaesthesiol* 2018; 31:6
41. Mezei G, Chung F: Return hospital visits and hospital readmissions after ambulatory surgery. *Ann Surg* 1999; 230:721–7
42. Austin PC: A tutorial and case study in propensity score analysis: An application to estimating the effect of in-hospital smoking cessation counseling on mortality. *Multivariate Behav Res* 2011; 46:119–51
43. Ilfeld BM: Continuous peripheral nerve blocks: An update of the published evidence and comparison with novel, alternative analgesic modalities. *Anesth Analg* 2017; 124:308–35
44. VanderWeele TJ, Ding P: Sensitivity analysis in observational research: Introducing the E-value. *Ann Intern Med* 2017; 167:268–74
45. Liu SS, Strödtbeck WM, Richman JM, Wu CL: A comparison of regional *versus* general anesthesia for ambulatory anesthesia: A meta-analysis of randomized controlled trials. *Anesth Analg* 2005; 101:1634–42
46. Ólafsdóttir T, Ásgeirsdóttir TL, Norton EC: Valuing pain using the Subjective Well-being Method: NBER working paper No. 23649. *Natl Bur Econ Res* 2017. Available at: <https://www.nber.org/papers/w23649>. Accessed June 14, 2019.
47. Macario A, Weinger M, Carney S, Kim A: Which clinical anesthesia outcomes are important to avoid? The perspective of patients. *Anesth Analg* 1999; 89:652–8
48. Koppelaar T, Linmans J, Knottnerus JA, Spigt M: Pragmatic vs. explanatory: An adaptation of the PRECIS tool helps to judge the applicability of systematic reviews for daily practice. *J Clin Epidemiol* 2011; 64:1095–101

ANESTHESIOLOGY

An Automated Software Application Reduces Controlled Substance Discrepancies in Perioperative Areas

Nirav Shah, M.D., Anik Sinha, M.S., Aleda Thompson, M.S., Kevin Tremper, Ph.D., M.D., Arjun Meka, M.D., Sachin Kheterpal, M.D., M.B.A.

ANESTHESIOLOGY 2019; 131:1264–75

Controlled substance diversion and tracking have received increased regulatory focus throughout the United States, in part because of the opioid epidemic. Within our hospitals, efforts to address this focus include many changes to clinical practice and provider workflow to decrease the risk of controlled substance diversion and reduce errors in controlled substance handling. Perioperative care areas have not been spared from these changes, with the management of controlled substances in the perioperative environment coming under increasing scrutiny. Regulatory groups such as The Joint Commission (Oakbrook Terrace, Illinois) and federal agencies such as the Drug Enforcement Administration (Springfield, Virginia) are reviewing how anesthesia providers manage the large amounts of controlled substances are administered to our patients. These entities are interested in ensuring that¹:

1. Chain of custody of a controlled substance is maintained from the time it enters a hospital to the time it is either administered or disposed.
2. Documentation practices are accurate and auditable.
3. Controlled substance documentation in the anesthesia record matches documentation used to manage its dispensing and return.
4. Witnessing and wasting is performed according to hospital policy and tracked.
5. Discrepancies are reviewed systematically and integrated into diversion monitoring systems.

The lack of robust systems to allow providers to meticulously track controlled substances could increase the

ABSTRACT

Background: Perioperative controlled substance diversion and tracking have received increased regulatory focus throughout the United States. The authors' institution developed and implemented an automated web-based software application for perioperative controlled substance management. The authors hypothesized that implementation of such a system reduces errors as measured by missing controlled substance medications, missing controlled substance kits (a package of multiple controlled substance medications), and missing witness signatures during kit return.

Methods: From December 1, 2014 to March 31, 2017, the authors obtained missing controlled substance medication, controlled substance kit, and witness return signature data during the preimplementation, implementation, and study period of the controlled substance management application at a single university hospital. This before and after study was based on a QI project at the authors' institution. The authors included all cases requiring anesthesia services. The primary outcome of this study was the rate of missing controlled substance medications. Secondary outcomes included rates for kits not returned to pharmacy and missing kit return witness signatures.

Results: There were 54,302 cases during the preimplementation period, 57,670 cases during the implementation period, and 65,911 cases during the study period. The number of missing controlled substance medication (difference 0.7 per 1,000 cases; 95% CI, 0.38–1.02; $P < 0.001$) and kit return errors (difference 0.45 per 1,000 cases; 95% CI, 0.24–0.66, $P < 0.001$) declined after implementation of the application. There was no difference in the number of missing witness return signatures (difference 0.09 per 1,000 cases; 95% CI, –0.08 to 0.26, $P = 0.350$). A user survey with 206 of 485 (42%) response rate demonstrated that providers believed the new application managed controlled substances better than the previous system.

Conclusions: A software application that tracks perioperative controlled substance kits with deep integration into the electronic health record and pharmacy systems is associated with a decrease in management errors.

(*ANESTHESIOLOGY* 2019; 131:1264–75)

EDITOR'S PERSPECTIVE

What We Already Know about This Topic

- Controlled substance diversion and tracking have received increased regulatory focus in a perioperative setting in the United States. Although an automated web-based software application for management has the potential to reduce errors, little data are available to support its use.

What This Article Tells Us That Is New

- In a large number of patients studied, a software application that tracks perioperative controlled substance use that is integrated into the electronic health and pharmacy records and database systems is associated with a decrease in management errors.

Part of the work presented in this article has been presented at the American Society of Anesthesiologists Annual Meeting, Boston, Massachusetts, October 3, 2017.

Submitted for publication October 8, 2018. Accepted for publication July 17, 2019. From the Department of Anesthesiology, University of Michigan, Ann Arbor, Michigan.

Copyright © 2019, the American Society of Anesthesiologists, Inc. All Rights Reserved. *Anesthesiology* 2019; 131:1264–75. DOI: 10.1097/ALN.0000000000002957

perception that anesthesia providers may be too casual in how they handle controlled substances, a perception supported by the high rate of controlled substance abuse by anesthesia providers.^{2,3} Our institution experienced issues with both diversion as well as inadequate tracking of controlled substances. Commercially available automated anesthesia drug carts have software to manage controlled substances, but are currently not well integrated with anesthesia information systems resulting in published reports of controlled substance reconciliation error rates of greater than 5%.^{4,5} These systems are unable to provide true real-time notifications on potential controlled substance management errors, which are essential for timely resolution of management issues. Although *post hoc* controlled substance dispensing surveillance systems have been described and evaluated in the literature, there are no data regarding accuracy (or quality) of point-of-care real-time perioperative controlled substance management tools.⁴ Our institution responded to inadequate controlled substance tracking by developing a new software application that addressed the entire perioperative controlled substance management process by integrating both pharmacy and anesthesia systems and enabling real-time error resolution.

We tested the hypothesis that implementation of such an application is associated with a reduction in management errors of an individual controlled substance medication or a package of multiple controlled substance medications used for one or more patients (sometimes known as a kit).

Materials and Methods

The authors followed the Enhancing the Quality and Transparency of Health Research Standards for Quality Improvement Reporting Excellence 2.0 guidelines in the development and structure of this manuscript.⁶

A notice of “not regulated status” (HUM00141108) was received from the Institutional Review Board (University of Michigan Medical School, Ann Arbor, Michigan) for analysis of data from a quality improvement project.⁷ The protocol for this quality improvement study was prespecified and presented at our departmental anesthesia clinical research committee before data extraction and after receiving Institutional Review Board determination of “not regulated status.”

Context

The studied institution is a large, academic, tertiary care center in the United States. Approximately 450 anesthesia providers including residents, fellows, certified registered nurse anesthetists, and attending anesthesiologists, and an additional 30 pharmacy staff participate in more than 85,000 procedures per year, administering more than one million doses of controlled substances annually across six geographically distinct facilities (adult and pediatric inpatient facilities and several ambulatory surgery centers) and more than 100 anesthetizing locations. The management of controlled

substances is a complex process in this setting. Historically, providers were supplied with a kit (defined above as a package of multiple controlled substance medications) for one or more patients that approximated what a provider would need throughout the day for multiple cases—a commonly used “kit per day” model with paper tracking and reconciliation. Ongoing review of controlled substance management practices, combined with unfortunate adverse events related to clinician abuse of substances (both controlled and uncontrolled), led first to change from a “kit per day” to a “kit per case” model still relying on paper tracking of the kits, and then an unsuccessful trial of automated drug dispensing carts in the operating rooms. This trial was deemed unsuccessful because of difficulties in maintaining chain of custody of controlled substances through provider breaks and reliefs and ineffective integration of real-time clinical documentation with drug inventory management.

To implement a more robust system for tracking controlled substances at sites requiring anesthesia care, our institution developed a web-based secure software application for controlled substance management in the perioperative area. This application manages the life cycle of the standardized controlled substance kits assembled by pharmacy staff and used by anesthesia providers, and includes data integration with electronic health record (pre-, intra-, and postoperative anesthesia documentation) and centralized operating room automated pharmacy dispensing and inventory tracking systems (Omnicell, USA).

The Intervention—A Controlled Substance Management Software Application and Workflow

In an attempt to minimize controlled substance management errors, a “kit-per-case” controlled substance management workflow was in place for one year before implementation of the software application; providers had already made the process and documentation changes necessary for the transition from “kit-per-day” to “kit-per-case” using a paper tracking system (appendix 1).

Our intervention was the implementation of the controlled substance management software application (appendix 2). The hospital’s controlled substance oversight committee approved development and implementation of a new perioperative controlled substance management system in March 2015. By September 2015, a pilot rollout was implemented at a free-standing ambulatory surgery center with health system-wide adoption at all anesthetizing locations by December 2015.

A web-based software application that integrated with our commercially available anesthesia information management system (General Electric Healthcare Centricity Anesthesia, USA) and pharmacy system (Omnicell, USA) was developed to track preparation, inventory and distribution, chain of custody, administration, and breakdown of controlled substance kits assigned to a specific case. An alerting module was developed within the application to

notify users when workflow deviated from best controlled substance management practice. Examples of alerts include prompt notification to the anesthesia provider if a discrepancy is discovered, and timely escalation of discrepancies to departmental and hospital staff assigned to address such issues (such as a drug diversion compliance team).⁸ A reporting and discrepancy notification module was created for managers to review and follow up on any important controlled substance discrepancy in real-time. Fundamentally, the software application and workflow was designed to maximize the real-time recognition and alerting of variations from ideal processes rather than retrospective auditing after case completion. Overall cost for the implementation at our institution was approximately \$500,000, and ongoing maintenance and support is about \$50,000 per year across more than 100 anesthetizing sites.

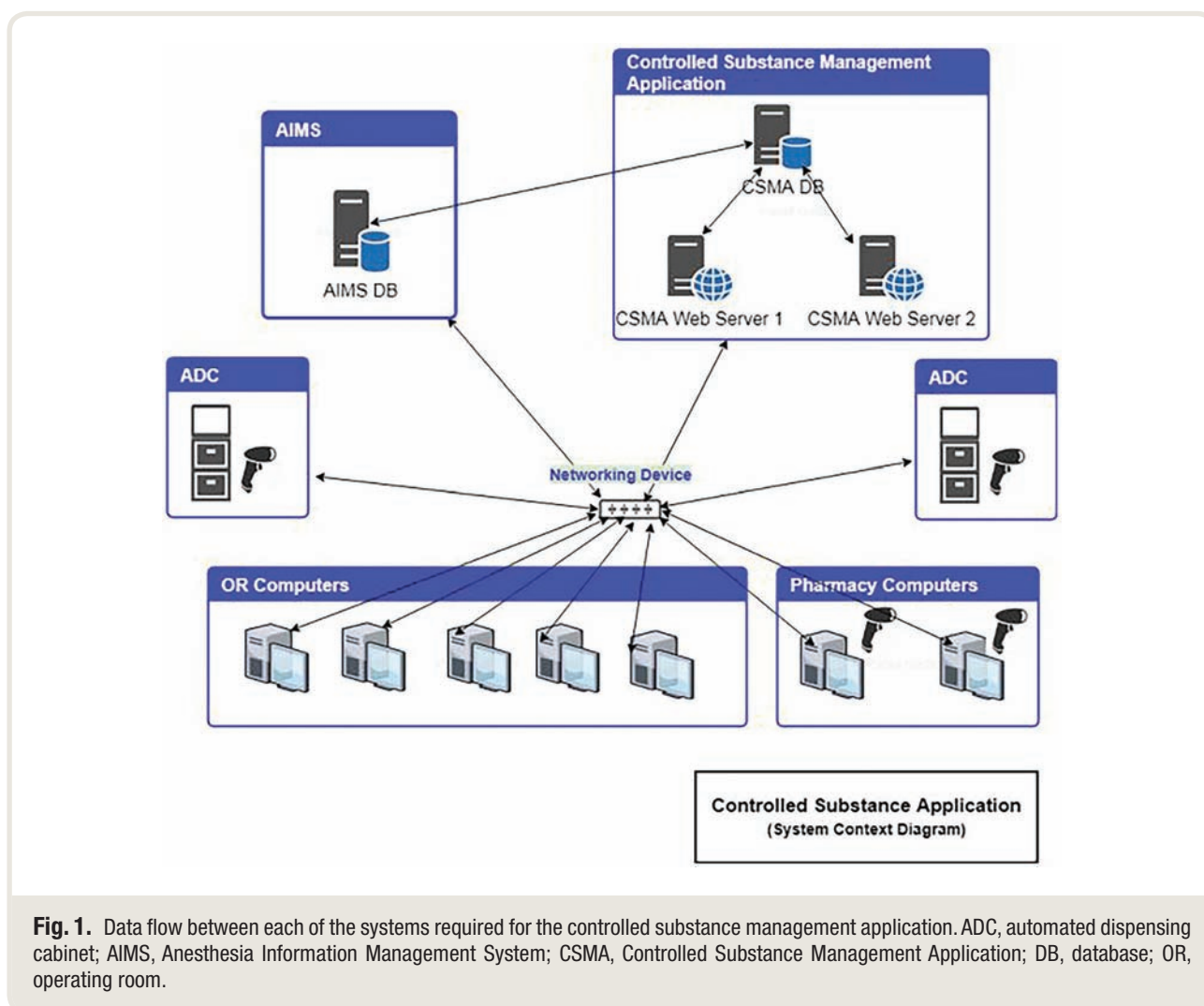
After implementation of this controlled substance management application, a survey was sent to all anesthesia providers and pharmacy staff, asking them to compare the new system and process with the previous one.

Controlled Substance Management Application Technical Infrastructure

The controlled substance management application is a web-based application built in C# with ASP.NET framework (Microsoft Corporation, USA) with interfaces between our anesthesia information management system and pharmacy management system. Anesthesia and pharmacy data are stored within a structured query language server database that is queried in real time (figs. 1 and 2).

Controlled Substance Management Application Workflow

Three distinct controlled substance workflow phases mirror the perioperative clinical workflow. *Preoperatively*, controlled substance kits are assembled on a routine basis and available for distribution to anesthesia providers in the immediate preoperative period. Pharmacy staff barcode scan the kit, and information about the kit (such as kit type and storage location) is stored within the application database. Controlled substance kits are specific by case type (General, Cardiac,



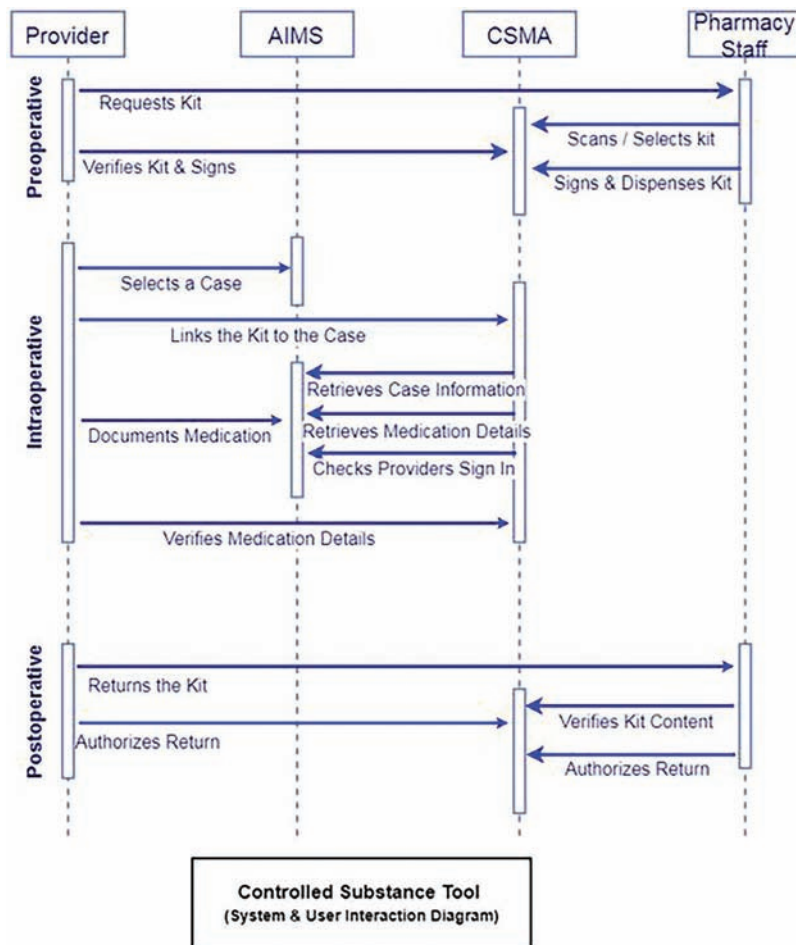


Fig. 2. Process diagram of how users (providers and pharmacy staff) interact with the controlled substance management application and anesthesia information management system during each phase of care. AIMS, Anesthesia Information Management System; CSMA, Controlled Substance Management Application.

Monitored Anesthesia Care, Obstetrics, and Pediatrics), and each kit type has specific quantities of controlled substances such as midazolam, fentanyl, morphine, ketamine, and ephedrine. Anesthesia providers obtain kits either from an operating room pharmacy or from an automated dispensing cabinet depending on location. In either scenario, the application logs this change in custody of the kit (from pharmacy to anesthesia provider), and transfers “ownership” to the anesthesia provider. The provider then assigns or “links” the kit to the anesthetic case the kit will be used for.

Intraoperatively, the application queries the anesthesia information management system for controlled substance administration and progressively decrements controlled substance totals requiring return to pharmacy, as these medications are documented in the anesthesia information management system. In-room provider (resident, fellow, or certified registered nurse anesthetist in our care setting) breaks and relief that occur during a case are noted in the application, and a

transfer-of-care module within the application ensures that chain of custody is maintained from the leaving provider to the incoming provider. At each break or relief, clinicians transfer chain of custody of the controlled substance kit using a user ID and password verification step. To maximize usability, the user ID and password for the application is the same as the provider’s electronic health record credentials using single-sign authentication. Each handover identifies any discrepancies automatically by comparing anesthesia information management system and application calculations for used *versus* remaining controlled substances. If additional controlled substance is required in the middle of the case, then the central pharmacy or central automated drug cabinet dispenses additional vials or syringes of controlled substance to a provider (usually the attending anesthesiologist or other anesthesia provider not assigned to a room). This provider then gives the controlled substance to the in-room provider. Both

interactions are documented with electronic attestation in the automated controlled substance management application.

Postoperatively, after care is handed over to the receiving provider (nurse in recovery room or intensive care unit), the provider will return the kit to the pharmacy, where both the anesthesia and pharmacy staff will jointly verify returned contents of the kit. After hours, when the operating room pharmacy may be closed, another licensed clinician will verify returned kit contents by visually inspecting the syringes and unused vials and electronically attesting in the application, and then the anesthesia provider places the kit in a secure lockbox for later pick-up by pharmacy staff. As per institutional policy, all unused medications must be returned to the in-hospital pharmacy or lockbox, whether in vial or syringe. (fig. 3). Leftover medication is not disposed of by the provider. A random sample of leftover medication is assayed by pharmacy staff and tracked in the application.

Alerts and Real-time Notifications

Throughout the period of anesthesia care, the application sends alerts *via* pages or application screen pop-ups to the anesthesia provider when required practice is not followed. Examples of these alerts include:

1. Failure of timely linking of a controlled substance kit to a case
2. Failure of timely transfer of kit between providers during a documented break or relief
3. Kit not returned to pharmacy within timely fashion after documentation of anesthesia end
4. Controlled substance documented in the anesthesia record not part of kit contents

Discrepancy Notification

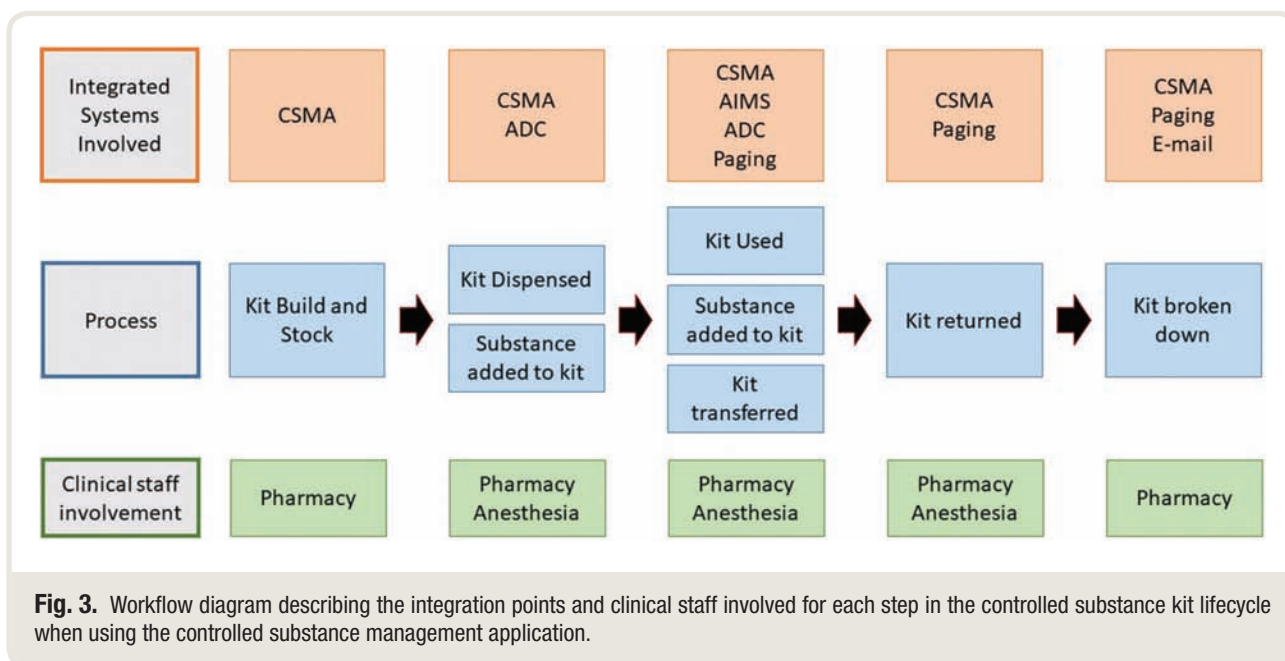
The application also has a discrepancy notification module in which controlled substance quantitative errors detected by the application, anesthesia, or pharmacy staff are logged and notifications are sent *via* email to address the error, escalating to department and hospital compliance leaders if not addressed in a timely fashion. Routine analytical reports are generated for review by controlled substance management committees within the departments and hospital.

Study of the Intervention

We conducted a retrospective before–after analysis of data for missing controlled substances from operating rooms. The preintervention period (consisting of paper tracking of kits) was from December 1, 2014 to August 31, 2015 (9 months). September 1, 2015 to May 31, 2016 (9 months) was the application implementation and user stabilization period across our institution. The study period was from June 1, 2016 to March 31, 2017 (also 9 months). A voluntary electronic survey (Qualtrics, USA) was administered in December 2016 to evaluate provider perceptions (fig. 5).

Measures

The primary outcome of this study was the rate of missing controlled substance medications, defined as any difference between the expected returned amounts of controlled substances *versus* actual returned amount. Secondary outcomes included rates for kits not returned to pharmacy and missing kit return witness signatures. All three of these events are tracked by U.S. Drug Enforcement Administration diversion program officers.



Statistical Analysis

Summary statistics were displayed for both time periods as frequency of event and event rate per 1,000 cases with 95% CI. Additionally, the difference of event proportion between time periods with 95% CI was reported per 1,000 cases. Event rate per 1,000 was calculated as total number of events divided by the total number of cases to allow for consistency in denominator between periods of implementation. Outliers were assessed for all outcomes using box-and-whisker plots, and none were found. Outcome data were assessed for normality using histograms and were found to be normally distributed, therefore data is presented as mean \pm SD. A two-sample independent *t* test for the equality of proportions with continuity correction was used to compare the paper kit discrepancy (preintervention) and application kit discrepancy (study period) event rates for the primary and secondary outcomes. A Joinpoint analysis was conducted to allow for potential nonlinear trend in the number of event counts across time,⁹ and the Bayesian Information Criteria was used to determine the best number of joinpoints to fit the model. Finally, means and SD, and slopes for trend in event counts were compared between the time periods using Student *t* tests and *F* tests, as appropriate. Analyses were conducted using SAS v. 9.4 (SAS Institute, USA) and Joinpoint Regression software (Joinpoint Regression Program, Version 4.5.0.1, June 2017; Statistical Methodology and Applications Branch, Surveillance Research Program, National Cancer Institute, Bethesda, Maryland). Survey responses were evaluated between anesthesia providers (residents, fellows, certified registered nurse anesthetists, anesthesiology faculty) and pharmacy providers (pharmacy technician, pharmacist) using a chi-square or Fisher exact test, as appropriate. Survey responses were collapsed into a binary variable, with *agree* and *strongly agree* in one category and *neither agree nor disagree*, *disagree*, and *strongly disagree* in the other. Survey questions which directly compare the controlled substance management application to the paper-based system (3, 5, 6,

and 7), were analyzed only between those providers who indicated they worked with both reporting systems.

All analyses were conducted using a two-sided hypothesis, and a *P* value less than or equal to 0.05 was considered statistically significant. Because this is a *post hoc* quality improvement study, no prospective power analysis was performed.

Ethical Considerations

Ethical aspects of this implementation included the detailed review of provider administration habits and tracking of practice patterns that this new tool enabled. Our hospital's and department's compliance and Quality Assurance or Quality Improvement committees all agreed that benefits outweighed any potential risks, and that the implementation team would develop a process for feedback and modification of the tool as needed if these issues arose.

Results

During the preintervention (paper tracking of kits) period 53,400 cases were examined, during the implementation period 57,670 cases were examined, and during the study (using the new application) period 65,911 cases were examined. In the preintervention *versus* study period analysis, the study period had significantly lower rates (per 1,000 cases) of missing controlled substance medications (0.42 *vs.* 1.12; difference 0.7, 95% CI: 0.38, 1.02, *P* < 0.001). For the secondary outcomes, we found that rates (per 1,000 cases) of kits not returned was also significantly lower (0.09 *vs.* 0.54; difference 0.45, 95% CI: 0.24, 0.66, *P* < 0.001). There was no statistically significant difference in the number of missing witness return signatures between the two kit tracking periods (0.17 controlled substance management application *vs.* 0.26 paper tracking; difference 0.09; 95% CI, -0.08 to 0.26, *P* = 0.350; table 1).

Joinpoint analysis exhibited different trends during the preintervention, implementation, and study periods. During

Table 1. Errors with Paper *versus* Electronic Tracking of Controlled Substance Kits

	Paper Tracking of Kits Preintervention Period (December 1, 2014–August 31, 2015) n = 53,400 Cases		CSMA Tracking of Kits Study Period (June 1, 2016–March 31, 2017) n = 65,911 Cases		<i>P</i> Value
	Total Errors	Error Rate per 1,000 Cases (95% CI)	Total Errors	Error Rate per 1,000 Cases (95% CI)	
Primary outcome					
Missing medication	60	1.12 (0.86–1.42)	28	0.42 (0.29–0.61)	<0.001
Secondary outcomes					
Kit not returned	29	0.54 (0.37–0.77)	6	0.09 (0.04–0.19)	<0.001
Missing witness signature	14	0.26 (0.15–0.43)	11	0.17 (0.09–0.30)	0.350

ADC, automated dispensing cabinet; AIMS, Anesthesia Information Management System; CSMA, Controlled Substance Management Application.

the preintervention paper tracking period and early implementation period (December 1, 2014 to March 31, 2016), a statistically significant increase in the number of missing controlled substance medication errors was observed at a rate of 0.38 (95% CI, 0.10–0.66) more errors per month ($P = 0.017$, fig. 4A). Near the end of the implementation period, from March 2016 to June 2016, there was a nonstatistically significant decrease in the number of missing controlled substance medication errors, a rate of -2.52 (95% CI, -9.24 to 4.20) fewer errors per month ($P = 0.471$). During the study period, from June 2016 to the March 2017, there was no statistically significant change in the rate of missing controlled substance medication errors ($P = 0.858$). There was a significant mean decrease of -3.87 errors per month in the rate of missing controlled substance medication errors between the preintervention period (mean 6.67 ± 2.60) and the study period (mean 2.80 ± 2.04 errors per month, $P = 0.002$).

A significant decrease in the number of kit not returned errors at a rate of -0.10 fewer cases per month was consistent across the preintervention, implementation, and study periods ($P = 0.032$, fig. 4B). There was a significant mean decrease of -2.62 fewer cases per month in the rate of kit not returned errors between the preintervention paper kit tracking period (mean 3.22 ± 2.49) and the study period (mean 0.60 ± 0.84 , $P = 0.008$).

There were no significant changes in the rate of missing witness signatures errors over the preintervention, implementation, and study periods (slope = -0.03 ; 95% CI, -0.09 to 0.03 ; $P = 0.281$; fig. 4C). Additionally, there was not a significant change in the mean errors per month

of missing witness signature between the preintervention (mean 1.56 ± 1.01 and study periods (mean 1.10 ± 1.37 , $P = 0.160$).

Survey Results

Responses were received from 189 of the 450 anesthesia providers (42%) and 17 of 35 pharmacy staff surveyed (49%, fig. 5). Of the anesthesia provider responses, 176 answered at least one question of interest. Eighty percent of those who completed the survey worked in both the preintervention paper kit period and the study period with the new controlled substance management application. Those who worked at other institutions (72 anesthesia providers and 3 pharmacy staff) said the application was better than or equal to the automated anesthesia dispensing machines and software at other institutions 48 of 75 (64%) of the time.

Those who worked in both the preintervention paper kit period and the study period with the new controlled substance management application (144 anesthesia providers and 14 pharmacy staff) largely agreed that using the new application was less time consuming and overall better than the paper kit system. When comparing anesthesia provider and pharmacy staff responses, significantly fewer anesthesia providers than pharmacy staff agreed or strongly agreed that the new application is less time consuming for controlled substance administration documentation than the paper-based system (108 of 144 [75%] of anesthesia providers *vs.* 13 of 14 [93%] of pharmacy staff, $P = 0.003$), and that overall the new application is better than the previous paper-based system (101 of 143 [71%] *vs.* 14 of 14 [100%],



Fig. 4. Complete survey questions, in order from top to bottom: Survey Question 1: Compared with the paper-based system, the tool enhances controlled substance (CS) management in the operating room. Survey Question 2: Compared with the paper-based system, I feel that the tool maintains a chain of custody of CS better. Survey Question 3: The tool reduces delays in correcting possible discrepancies in record keeping. Survey Question 4: The tool allows both the Anesthesiology and Pharmacy departments to better track CS. Survey Question 5: The tool is effective in notifying CS discrepancies to the provider. Survey Question 6: The tool's witness waste feature reduces the potential for CS diversion. Survey Question 7: I feel the tool helps to create a culture for the safe handling of CS.

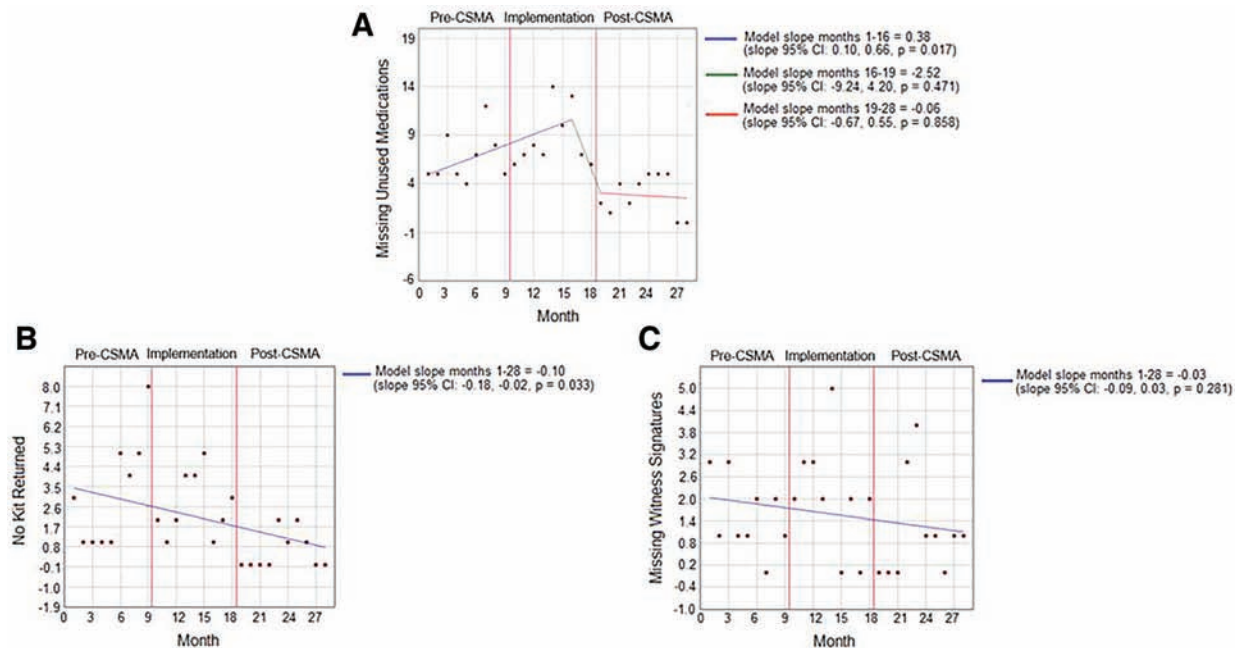


Fig. 5. Joinpoint analysis for (A) missing unused medications (two intercepts and three slopes), (B) no kit returned (zero intercepts and one slope), and (C) missing witness signatures (zero intercepts and one slope). The number of intercepts was determined using the Bayesian Information Criteria values as determined by the Joinpoint software. Transitions between pre-Controlled Substance Management Application (CSMA) period, the implementation period, and the post-CSMA period are indicated with red lines. The slopes for each segment are presented in the figure in units of errors/month.

$P = 0.012$). The question asking whether overall the new application is better than the previous paper-based system was missing one response from the anesthesia providers.

Among all survey participants, significantly fewer anesthesia providers compared with pharmacy providers agreed or strongly agreed that the application's witness waste functionality reduces the potential for controlled substance diversion (70 of 176 [40%] *vs.* 12 of 17 [71%], $P = 0.019$) and that the application helps to create a culture for the safe handling of controlled substances (108 of 176 [61%] *vs.* 17 of 17 [100.0%], $P < 0.001$).

Discussion

We implemented an automated and integrated electronic controlled substance management application and workflow in response to increasing scrutiny of medication handling. We observed a statistically significant reduction in missing controlled substance medications and missing controlled substance kits. This statistical significance is also practically significant because regulatory and governance groups such as the Drug Enforcement Administration and hospital controlled substance committees require that we are able to accurately track and report on the life cycle of every controlled substance, and have a mechanism in place for discrepancy tracking, which we are now able to much

more accurately. These types of software applications can play an important role in improving accounting of controlled substances through the perioperative period.

With the recent rise of opioid addiction and its devastating consequences moving to the forefront of public health challenges, regulatory groups (*e.g.*, The Joint Commission) and enforcement agencies (*e.g.*, Drug Enforcement Administration) are auditing hospitals to ensure that processes and documentation of controlled substances establishes a clear chain of custody, and that errors are captured and followed up in a swift and appropriate manner. Internal and external review at our institution revealed high error rates with paper kit tracking, including paper kit documentation mismatches with anesthesia record drug administration documentation, transfers of controlled substances unable to be tracked, and witness waste processes not completed correctly. Added up, these internal and external reviews determined that close to one-fifth of controlled substance kits with our old paper tracking system had at least one of these errors.

A study at another academic institution described implementation of a controlled substance electronic auditing tool that queried automated drug cabinet transactions and anesthetic information management system drug administration totals and presented to providers as a daily reconciliation report. Drug reconciliation errors decreased from 8.8% to 5.2% with deployment of their near-real-time tool.⁴ We

observed a less than 1% rate of drug reconciliation errors using the controlled substance management application and process changes. Other efforts to manage controlled substance administration include deployment of automated anesthesia drug carts (for example, Pyxis Anesthesia Station or Omnicell Anesthesia Workstation). These devices are increasingly present in operating rooms and can allow for inventory management of drugs and other supplies. Although they also offer software to maintain chain of custody of controlled substances, this software is rarely integrated with anesthesia information management system data or equipped with alerting functionality and therefore unable to provide real-time notifications regarding controlled substance management errors.

An important part of our plan to improve our controlled substance management processes and address these findings was the development of our new software application. Consistent with new American Society of Health-System Pharmacists (Bethesda, Maryland) guidelines, software applications that integrate data, especially drug administration data, from anesthesia information management system and pharmacy systems, and enable anesthesia providers to maintain chain of custody of controlled substances in complex practice environments may reduce institutional and provider risk related to controlled substance management when combined with institutional culture change⁸

Our primary and secondary outcomes (number of missing controlled substance medications, missing kits, and missing witness return signature) were analyzed to determine whether error rate changed over the course of the study. Results from our analysis show a clinically significant change of error rates in missing medications due to the controlled substance management application. The error rate stabilized during the study period, once the application was widely deployed and well-integrated in provider workflow. The alerting functionality built into the system, as well as the heightened awareness of controlled substance accountability within our department, was conducive to a decrease in rates of missing medications between the preintervention paper kit period and the study period.

For kit return errors, joinpoint analysis demonstrated a decreasing linear trend of error rates through all three phases. This suggests that despite a statistically significant difference in kit return error rates between the preimplementation and study period, factors other than implementation of the new application may have led to the decrease in kit return errors. No significant change was found in the error rates of missing witness signatures between the preintervention period and the study period. Further review of data demonstrated that missing signatures largely occurred after hours, when kits were dropped in secure lockboxes for later review by pharmacy staff. Our opinion is that lack of direct pharmacy involvement in the return of controlled substances contributes to documentation errors, especially in after-hour situations where other clinicians able to witness a return (to ensure accuracy) may not be easily available.

At our institution, we learned that meticulous recordkeeping must exist to ensure that chain of custody of controlled substances is maintained from hospital arrival to administration or wasting for bolus and infusion medications. Each transfer of care in a case requires documentation of the transfer of care process for the controlled substances. Discrepancies between the anesthesia record and controlled substance management and reconciliation record must be identified, addressed, and rectified rapidly. Controlled substance management errors must be appropriately escalated to leadership, diversion control experts, and perhaps law enforcement, in a timely and predictable manner. Documented hospital policy must reflect these processes. Finally, if violations of these policies occur, thorough documentation and notification to regulatory bodies (*e.g.*, Drug Enforcement Administration) may be necessary. Our experience is that this will be the minimum standard that sites must adhere to and will be judged against if a regulatory body audit occurs. There is little in the published literature regarding perioperative best practices and standards. In early 2019, the American Society of Health-System Pharmacists published guidelines regarding perioperative controlled substance management services that include recommendations similar to those above. These guidelines were still available online only and not accessible in the peer-reviewed literature as of April 2019.⁸

Survey to Anesthesia Provider and Pharmacy Staff

Results of the survey showed that both anesthesia providers and pharmacy staff perceived that the new application was more effective than both the previous paper tracking system and trial of the automated anesthesia drug carts. Pharmacy staff felt more strongly than anesthesia providers that the controlled substance management application was a better process for controlled substance handling, that controlled substance management was more time efficient with the new application, and that the application creates a culture of safe controlled substance handling. This is not surprising given that pharmacy staff had primary responsibility for managing paper forms with the previous process. Overall, survey results indicated strong user acceptance of our application, but also room for improvement, especially with our witness waste process for anesthesia providers.

Limitations

There are several limitations with this study. First, issues that are known to affect before–after implementation studies limited by historical controls may be present with this project as well.¹⁰ Benefit may be overestimated as we cannot quantitatively account for contemporaneous changes in culture and education regarding the importance of maintaining controlled substance chain of custody. Also, the discrepancy tracking process was far more cumbersome in the old, paper kit tracking process. However, this likely resulted in significant underreporting of discrepancies compared with the new

software-based system. Our observations may be limited to specific processes and cultures at our organization and not generalizable to other organizations. Although there had been several Quality Improvement projects at our institution over the previous years focusing on controlled substance management, the unfortunate adverse events to hospital staff and Drug Enforcement Administration audit certainly were known to providers and may have played a role in the reduction of discrepancies. Heightened press attention to the controlled substance problem may also have led providers to be more vigilant with management of controlled substances. Finally, although this study demonstrates reduction in controlled substance management error, it is fair to state that these types of management and analytical tools, even in their finest form, may not prevent diversion at all. The typical practice pattern of our specialty enables providers who divert to develop systems that may bypass the checks developed by the most sophisticated of these surveillance tools. Further projects need to focus on how to best identify diverters while minimizing disruption to clinical workflow and provider privacy.

Conclusion

The automated controlled substance management application was reliably associated with a statistically significant drop in controlled substance management errors. These types of systems may ensure that appropriate accounting of controlled substances is performed throughout the perioperative period. They enable hospitals to comply with institutional policy and regulatory requirements. They may work synergistically with other programs to prevent diversion, but cannot be relied upon independently to prevent provider abuse of controlled substances. Our providers found the implementation of this application improved controlled substance chain of custody of as well as overall controlled substance management within our institution. Although the new application is unlikely to directly impact drug diversion, the survey results demonstrate that it is more user friendly and joinpoint analysis demonstrates it reduces errors handling controlled substances compared to paper processes. Future studies must evaluate replicability of our single-center observations and evaluate whether these systems actually prevent diversion. These studies could either use the described application which has modular design enabling integration with most anesthesia systems or other commercially available applications as they become available and develop similar functionality.

Research Support

Support for this study was provided solely from institutional and/or departmental sources.

Competing Interests

The authors declare no competing interests. The software evaluated in this study has not been patented or

commercialized but is the property of the Regents of the University of Michigan, Ann Arbor, Michigan.

Correspondence


Address correspondence to Dr. Shah: Department of Anesthesiology, University of Michigan, 1H247 UH, SPC 5048, 1500 East Medical Center Drive, Ann Arbor, Michigan 48109-5048. nirshah@med.umich.edu. Information on purchasing reprints may be found at www.anesthesiology.org or on the masthead page at the beginning of this issue. ANESTHESIOLOGY's articles are made freely accessible to all readers, for personal use only, 6 months from the cover date of the issue.

References

1. Drugs of Abuse DEA Resource Guide. Available at: https://www.dea.gov/sites/default/files/2018-06/drug_of_abuse.pdf. Accessed February 13, 2019.
2. Warner DO, Berge K, Sun H, Harman A, Hanson A, Schroeder DR: Substance use disorder among anesthesiology residents, 1975-2009. *JAMA* 2013; 310:2289-96
3. Bryson EO, Silverstein JH: Addiction and substance abuse in anesthesiology. *ANESTHESIOLOGY* 2008; 109:905-17
4. Epstein RH, Dexter F, Gratch DM, Perino M, Magrann J: Controlled substance reconciliation accuracy improvement using near real-time drug transaction capture from automated dispensing cabinets. *Anesth Analg* 2016; 122:1841-55
5. Vigoda MM, Gencorelli FJ, Lubarsky DA: Discrepancies in medication entries between anesthetic and pharmacy records using electronic databases. *Anesth Analg* 2007; 105:1061-5, table of contents
6. Ogrinc G, Davies L, Goodman D, Batalden P, Davidoff F, Stevens D: SQUIRE 2.0 (Standards for Quality Improvement Reporting Excellence): Revised publication guidelines from a detailed consensus process. *BMJ Qual Saf* 2016; 25:986-92
7. UM Policy Human Research Protection Program Operations Manual Part 4.V.A, 2018
8. ASHP Guidelines on Perioperative Pharmacy Services. Available at: <https://www.ashp.org/-/media/assets/policy-guidelines/docs/guidelines/perioperative-pharmacy-services.ashx?la=en&hash=34AE-96918C1109EE880C9258322C5AA0D1671CE3>. Accessed February 13, 2019.
9. Kim HF, MP; Feuer, EJ; Midthune, DN: Permutation tests for joinpoint regression with applications to cancer rates. *Stat Med* 2000; 19: 335-51
10. Eccles M, Grimshaw J, Campbell M, Ramsay C: Research designs for studies evaluating the effectiveness of change and improvement strategies. *Qual Saf Health Care* 2003; 12:47-52

Appendix 1

Paper Kit Form

UNIVERSITY OF MICHIGAN HOSPITALS & HEALTH CENTERS Department of Anesthesiology Controlled Substances (CS) Form				Serial Number: XXXXXX  123456		
NOT A MEDICAL RECORD DOCUMENT						
		UH General				
Build by: _____ <small>page/ID:</small> _____ <small>Date:</small> _____ Dispensed by: _____ <small>page/ID:</small> _____ <small>Date:</small> _____ Received by: _____ <small>page/ID:</small> _____ <small>Date:</small> _____						
Patient Name	Fentanyl 50mcg/ml 2ml	Midazolam 1mg/ml 2ml	Morphine 10mg/ml 1ml	Ephedrine 50mg/ml 1ml	Ketamine 1mg/ml	Remifentanyl 1mg
MRN	Starting Balance:	2	1	1	—	—
	Administered	mg	mg	mg	mg	mg
	Waste	mg	mg	mg	mg	mg
Count of unopened vials or syringes returned to pharmacy: _____						
Infusion <input type="checkbox"/> transferred or <input type="checkbox"/> received (check appropriate box if applicable) Infusion Drug: _____ Amount present at transfer: _____ Infusion Drug Transferred to/from: _____ <small>page/ID:</small> _____						
KIT Return Anesthesia Signature: _____ <small>page/ID:</small> _____ Reconciler Signature: _____ <small>page/ID:</small> _____ Waste Witness Signature: _____ <small>page/ID:</small> _____						

1. "Received by" signature verifies inventory received
2. Chart all doses in mg or mcg, not by ml/cc
3. Record all waste with witness signature
4. Record remaining vials to be returned to pharmacy
5. Record infusions transferred to or received by another provider during a case
6. Drug amount administered and wasted must be documented for infusions received
7. "Anesthesia Signature" is required prior to returning kit
8. "Reconciler Signature" is required prior to returning to pharmacy drop safe
9. Pharmacist signs "Reconciler Signature" when kit returned directly to Pharmacy

Appendix 2

Controlled Substance Management Application Screenshot

M CONTROLLED SUBSTANCE TOOL
ANESTHESIOLOGY
UNIVERSITY OF MICHIGAN HEALTH SYSTEM

Anesthesia Provider View

[testpr2]

**** Kit is Returned ****

Dashboard

Substance	Dispensed		Used		Returned		
	Count	Amt.	Adm.	Loss	Total Returned	Unused Vials	For Waste
Ephedrine 50mg/ml(1ml)	1	50	0	0	50 mg	1	0 mg
Fentanyl 50mcg/ml(20ml)	1	1000	0	0	1000 mcg	1	0 mcg
Hydromorphone 1mg/ml(1ml)	1	1	0	0	1 mg	1	0 mg
Midazolam 1mg/ml(10ml)	1	10	0	0	10 mg	1	0 mg
Morphine 10mg/ml(1ml)	1	10	0	0	10 mg	1	0 mg

Kit Number	Kit Type	Built By	Location Dispensed
001	Cardiac	testpa	CVC
Returned By	Returned To	Returned Date	Witnessed By
testpr2		10/14/2015 1:21:32 PM	testpr
Return Discrepancy/Comments			

ANESTHESIOLOGY

Drug-selective Anesthetic Insensitivity of Zebrafish Lacking γ -Aminobutyric Acid Type A Receptor $\beta 3$ Subunits

Xiaoxuan Yang, M.D., Ph.D., Youssef Jounaidi, Ph.D., Kusumika Mukherjee, Ph.D., Ryan J. Fantasia, B.S., Eric C. Liao, M.D., Ph.D., Buwei Yu, M.D., Ph.D., Stuart A. Forman, M.D., Ph.D.

ANESTHESIOLOGY 2019; 131:1276–91

EDITOR'S PERSPECTIVE

What We Already Know about This Topic

- $\beta 3$ subunits of the γ -aminobutyric acid type A ($GABA_A$) receptor play a central role in mediating hypnotic and sedative effects of etomidate, propofol, and pentobarbital in mice
- Zebrafish are a vertebrate animal model amenable to high-throughput pharmacologic studies
- The role of $GABA_A$ receptor $\beta 3$ subunits in mediating the effects of anesthetic drugs in zebrafish has not been previously reported

What This Article Tells Us That Is New

- Zebrafish larvae lacking functional $\beta 3$ subunits of the γ -aminobutyric acid type A ($GABA_A$) receptor displayed selective insensitivity to the same anesthetic drugs (etomidate, propofol, and pentobarbital) as transgenic mice with mutated $GABA_A$ receptor $\beta 3$ subunits
- These experiments indicate phylogenetic conservation of $\beta 3$ subunit-containing $GABA_A$ receptors between zebrafish and mice in mediating hypnotic and sedative components of general anesthesia
- These observations also suggest that zebrafish can be a valuable experimental model for mechanisms of anesthesia research

γ -aminobutyric acid type A ($GABA_A$) receptors are the major inhibitory neurotransmitter receptors in mammalian brain. Mammalian genes for 19 subunit iso-types have been identified ($\alpha 1$ –6, $\beta 1$ –3, $\gamma 1$ –3, δ , ϵ , θ , π ,

ABSTRACT

Background: Transgenic mouse studies suggest that γ -aminobutyric acid type A ($GABA_A$) receptors containing $\beta 3$ subunits mediate important effects of etomidate, propofol, and pentobarbital. Zebrafish, recently introduced for rapid discovery and characterization of sedative-hypnotics, could also accelerate pharmacogenetic studies if their transgenic phenotypes reflect those of mammals. The authors hypothesized that, relative to wild-type, $GABA_A$ - $\beta 3$ functional knock-out ($\beta 3^{-/-}$) zebrafish would show anesthetic sensitivity changes similar to those of $\beta 3^{-/-}$ mice.

Methods: Clustered regularly interspaced short palindromic repeats (CRISPR)-Cas9 mutagenesis was used to create a $\beta 3^{-/-}$ zebrafish line. Wild-type and $\beta 3^{-/-}$ zebrafish were compared for fertility, growth, and craniofacial development. Sedative and hypnotic effects of etomidate, propofol, pentobarbital, alphaxalone, ketamine, tricaine, dexmedetomidine, butanol, and ethanol, along with overall activity and thigmotaxis were quantified in 7-day postfertilization larvae using video motion analysis of up to 96 animals simultaneously.

Results: *Xenopus* oocyte electrophysiology showed that the wild-type zebrafish $\beta 3$ gene encodes ion channels activated by propofol and etomidate, while the $\beta 3^{-/-}$ zebrafish transgene does not. Compared to wild-type, $\beta 3^{-/-}$ zebrafish showed similar morphology and growth, but more rapid swimming. Hypnotic EC50s (mean [95% CI]) were significantly higher for $\beta 3^{-/-}$ versus wild-type larvae with etomidate (1.3 [1.0 to 1.6] vs. 0.6 [0.5 to 0.7] μM ; $P < 0.0001$), propofol (1.1 [1.0 to 1.4] vs. 0.7 [0.6 to 0.8] μM ; $P = 0.0005$), and pentobarbital (220 [190 to 240] vs. 130 [94 to 179] μM ; $P = 0.0009$), but lower with ethanol (150 [106 to 213] vs. 380 [340 to 420] mM; $P < 0.0001$) and equivalent with other tested drugs. Comparing $\beta 3^{-/-}$ versus wild-type sedative EC50s revealed a pattern similar to hypnosis.

Conclusions: Global $\beta 3^{-/-}$ zebrafish are selectively insensitive to the same few sedative-hypnotics previously reported in $\beta 3$ transgenic mice, indicating phylogenetic conservation of $\beta 3$ -containing $GABA_A$ receptors as anesthetic targets. Transgenic zebrafish are potentially valuable models for sedative-hypnotic mechanisms research.

(ANESTHESIOLOGY 2019; 131:1276–91)

and $\rho 1$ –3), with each subunit sharing canonical pentameric ligand-gated ion channel topology: a large (~200 amino acid) extracellular domain, a transmembrane domain with four transmembrane helices (M1 through M4), and a variable size intracellular domain between M3 and M4.^{1,2} Most neuronal $GABA_A$ receptors contain two α s and two β s along with γ , δ , or another β .¹ $GABA_A$ receptors are modulated by a variety of general anesthetics, including propofol, etomidate, barbiturates, alphaxalone, halogenated volatile agents, and alcohols.^{3,4} In typical synaptic $\alpha\beta\gamma$ $GABA_A$ receptors, the binding sites for etomidate, propofol, and

This article is featured in "This Month in Anesthesiology," page 1A. Some of the work presented in this article has been presented at the annual meetings of the International Society of Anesthetic Pharmacology and the American Society of Anesthesiologists, Boston, Massachusetts, October 20 to 24, 2017. X.Y. and Y.J. contributed equally to this work.

Submitted for publication January 21, 2019. Accepted for publication July 29, 2019. From the Department of Anesthesiology, Ruijin Hospital, Shanghai Jiaotong University School of Medicine, Shanghai, China (X.Y., B.Y.); the Department of Anesthesia Critical Care and Pain Medicine (X.Y., Y.J., R.J.F., S.A.F.); and the Center for Regenerative Medicine (K.M., E.C.L.), Massachusetts General Hospital, Boston, Massachusetts.

Copyright © 2019, the American Society of Anesthesiologists, Inc. All Rights Reserved. Anesthesiology 2019; 131:1276–91. DOI: 10.1097/ALN.0000000000002963

pentobarbital are formed by portions of the β subunit M1, M2, and M3 transmembrane helices that are 100% conserved among zebrafish, mice, and humans.⁵

Evidence from studies in transgenic mice indicate that major actions of etomidate, propofol, and pentobarbital are mediated by a subset of GABA_A receptors isotypes containing $\beta 3$ subunits. Compared to wild-type animals, global $\beta 3$ knockout ($\beta 3^{-/-}$) mice are resistant to the sedative-hypnotic effects, measured as sleep time, of etomidate and propofol, whereas sensitivity to isoflurane is weakly affected and is unchanged for pentobarbital and ethanol.^{6,7} Additionally, global $\beta 3^{-/-}$ mice are phenotypically characterized by more than 90% neonatal mortality, cleft palate, epilepsy, hyperactivity, and hypersensitivity to stimuli, possibly reflecting anxiety.^{8–11} A pan-neuronal $\beta 3^{-/-}$ mouse line also displays frequent neonatal mortality and resistance to loss-of-righting reflexes after etomidate injection.¹² Another transgenic mouse line harbors the $\beta 3N265M$ point mutation, which obliterates sensitivity to etomidate in molecular studies.^{13–15} Homozygous $\beta 3N265M$ transgenic mice are characterized by normal fertility, morphology, and behavior, with unchanged sensitivity to alphaxalone or alcohol, but resistance to both loss-of-righting reflexes and loss of nociceptive withdrawal actions of etomidate, propofol, and pentobarbital.^{16,17}

Zebrafish have recently been introduced as a vertebrate animal model with advantages for pharmacologic studies of intravenous sedative-hypnotics.^{18,19} Video analysis tools enable simultaneous behavioral assessments of many zebrafish larvae. Larval tissues rapidly equilibrate with aqueous drugs through transdermal and respiratory pathways. Thus, drug effect studies in zebrafish can achieve high-throughput at steady-state, avoiding pharmacodynamic variation due to complex drug pharmacokinetics following intraperitoneal or intravenous drug injections in mice. Moreover, transgenic zebrafish have provided useful models for neurologic diseases, including epilepsies, and craniofacial developmental abnormalities.^{20,21}

For the current study, we established a global $\beta 3^{-/-}$ line of zebrafish and tested its utility as a robust and efficient animal model for studies of anesthetic drug mechanisms. We hypothesized that global $\beta 3^{-/-}$ zebrafish would display a pattern of anesthetic sensitivities similar to those of global $\beta 3^{-/-}$ mice and might share additional phenotypic features. We therefore characterized $\beta 3^{-/-}$ in comparison to wild-type zebrafish for fertility and early survival, craniofacial morphology, motor activity, and sensitivity to both the sedative and hypnotic effects of a panel of anesthetic drugs varying in potency and molecular mechanisms.

Materials and Methods

Animals

Zebrafish (*danio rerio*, Tübingen strain) were used with approval from the Massachusetts General Hospital Institutional Animal Care and Use Committee (Boston,

Massachusetts; protocol No. 2014N000031) in accordance with established protocols.²² Behavioral experiments were performed on larvae at 7 days postfertilization. Sexual differentiation of zebrafish remains indeterminate at this stage of development.²³ Embryos and larvae were maintained in Petri dishes (140-mm diameter) filled with buffered E3 medium (in mM; 5.0 NaCl, 0.17 KCl, 0.33 CaCl₂, 0.33 MgSO₄, 2.0 HEPES; pH 7.2) in a 28.5°C incubator under a 14/10-h light/dark cycle. The density of embryos and larvae was less than 100 per dish. After either use in experiments or at 8 days postfertilization, larvae were euthanized in 0.2% tricaine (also known as MS-222) followed by addition of bleach (1:20 by volume). Adult zebrafish were briefly anesthetized using 0.02% tricaine before being weighted, imaged, or undergoing tailfin clipping.

Female *Xenopus laevis* frogs were used as a source of oocytes with approval from the Massachusetts General Hospital Institutional Animal Care and Use Committee (protocol No. 2010N000002). *Xenopus* care and use has been previously described.²⁴

Sedative-hypnotic Drugs

Etomidate was a gift from Douglas Raines, M.D. (Department of Anesthesia Critical Care and Pain Medicine, Massachusetts General Hospital, Boston, Massachusetts) and was prepared as a 2 mg/ml solution in 35% propylene glycol: water (by volume). Alphaxalone was purchased from Tocris Bioscience (Bristol, United Kingdom) and prepared as a 10 mM stock in dimethyl sulfoxide. Ketamine was purchased from Mylan Pharmaceuticals (USA) as a 10 mg/ml aqueous solution with 0.1 mg/ml benzethonium chloride as a preservative. Dexmedetomidine was purchased from United States Pharmacopeia (USA). Propofol, pentobarbital, ethanol, and n-butanol were purchased from Sigma-Aldrich (USA). Propofol was prepared as a 100 mM stock in dimethyl sulfoxide.

Clustered Regularly Interspaced Short Palindromic Repeats (CRISPR) Gene Modification and Genotyping

The CRISPR guide RNA expression plasmid pDR274 and Cas9 template DNA pT3TS-nCas9n were purchased from Addgene (USA). CRISPR guide RNA target sites in GABRB3 were identified using CHOPCHOP.²⁵ Complementary DNA sequences for targets in GABRB3 exon 7 were synthesized as oligonucleotides by the Massachusetts General Hospital DNA core and cloned into pDR274.²⁶ Guide RNAs were generated by *in vitro* transcription from linearized pDR274 templates and purified. The guide RNA sequence used to generate the transgenic fish line is reported in table 1.

The pT3TS-nCas9n plasmid encoding Cas9 was linearized with XbaI and purified (Wizard SV Gel and PCR Clean-up system; Promega Corp, USA). Capped *cas9* messenger RNA was synthesized *in vitro* (mMESSAGE mMACHINE;

Table 1. CRISPR guide RNA and Primer Sequences

CRISPR guide RNA and Primers	Sequence
CRISPR guide RNA	GGGAGGAGAAACCGCAGTGA
GABRB3 Fluorescence PCR Primer_ Forward	AATGGATCATTACTCTTTGACTGA
GABRB3 Fluorescence PCR Primer_ Reverse	ATGCATCCATAAATTCACGTG
GABRB3 q-RT PCR Primer_ Forward	CAAGCTAAAAAGAAACATCGGC
GABRB3 q-RT PCR Primer_ Reverse	AGCCAAGAAAACAAAGACGAAG
GABRB1 q-RT PCR Primer_ Forward	CAAGCAACATGTCATACGTCAA
GABRB1 q-RT PCR Primer_ Reverse	CGTAAAGGTCCTACCAAGTGAG
GABRB2 q-RT PCR Primer_ Forward	TTCTCAACGACAAGAAGTCCT
GABRB2 q-RT PCR Primer_ Reverse	TACTGCAGGGTGGAGCTATCAT
β -actin q-RT PCR Primer_ Forward	GATGCCCTCGTGCTGTTTTC
β -actin q-RT PCR Primer_ Reverse	TCTCTGTTGGCTTTGGGATTCA

GABRB3 is the gene for the GABAA receptor $\beta 3$ subunit. GABRB1 is the gene for the GABAA receptor $\beta 1$ subunit. GABRB2 is the gene for the GABAA receptor $\beta 2$ subunit.

Thermo Fisher Scientific, USA) on the linearized template and purified (NucAway Spin Columns, Invitrogen). One-cell staged zebrafish embryos were micro-injected in the cytoplasm with 2 nl of a solution containing both guide RNA (50 ng/ μ l) and *cas9* mRNA (200 ng/ μ l).

DNA for genotyping was isolated from either whole zebrafish embryos or tailfin clips from adults (more than 2 months old), using the HotSHOT method.²⁷ Polymerase chain reaction primers flanking the CRISPR target site are reported in table 1. Fluorescent polymerase chain reaction products were synthesized using a forward primer modified with 6-carboxyfluorescein, and sized to determine if insertions and/or deletions were present after CRISPR mutagenesis. To determine the GABRB3 genotype in single adult fish, tail-snip derived target site polymerase chain reaction products were cloned into the pCR2.1-TOPO vector (Invitrogen), which was then amplified and subjected to DNA sequencing.

Quantitative Polymerase Chain Reaction of GABA_A Receptor β Messenger RNAs

Fifteen larvae that were 7 days postfertilization from each zebrafish line (wild-type, $\beta 3^{+/-}$, and $\beta 3^{-/-}$) were euthanized, placed on ice, and homogenized in 1 ml TRIzol (Invitrogen). Total RNA was isolated using phenol-chloroform extraction, treated with DNase I²⁸ and quantified using a NanoDrop spectrophotometer (Thermo Fisher). In triplicate samples, WT, $\beta 3^{+/-}$, and $\beta 3^{-/-}$ messenger RNA (1 μ g) underwent reverse transcription (SMARTScribe Reverse Transcriptase kit; Takara Bio, USA) to produce cDNA. Quantitative real-time polymerase chain reaction to quantify cDNA encoding $\beta 1$, $\beta 2$, and $\beta 3$ was performed on each triplicate sample, using full-length flanking primers (sequences given in table 1) and Platinum SYBR Green qPCR SuperMix-UDG with ROX (Invitrogen) on the StepOne Plus RT-PCR platform (Applied Biosystems/Thermo Fisher). β -actin transcripts were used for normalization and GABRB/ β -actin signal ratios were renormalized

to the average wild-type value. For each subunit, melt curve analysis and gel electrophoresis were consistent with the presence of a single real-time polymerase chain reaction product. Negative controls were performed on samples lacking either reverse transcription or template.

Next-generation Sequencing

To test for the presence of chimerism in $\beta 3^{-/-}$ zebrafish, we isolated genomic DNA from tailfin tissue of three adult $\beta 3^{-/-}$ males and three adult $\beta 3^{-/-}$ females, as described previously. Sequences near the guide RNA target site were amplified using nonfluorescent primers (table 1). The amplicons were submitted to the Massachusetts General Hospital Center for Computational and Integrative Biology (Boston, Massachusetts) DNA Core for massively parallel sequencing of single DNA strands using the Illumina MiSeq platform with V2 chemistry (Illumina Inc., USA). Illumina-compatible adapters with unique DNA barcodes were ligated onto each sample during library construction. Multiplexed sequencing of more than 100,000 single DNA copies were produced for each amplicon. The sequencing error rate is less than 0.003 per base. Next-generation sequencing results were analyzed by the Massachusetts General Hospital Center for Computational and Integrative Biology and reported as the frequency of unique complementary sequence pairs, including clusters of sequences with overlapping ends, from each demultiplexed sample. Sequence pairs occurring less than 100 times were not reported and assumed to be erroneous reads.

Complementary DNA Cloning and Xenopus Oocyte Electrophysiology

We cloned GABA_A $\beta 3$ cDNA from wild-type and $\beta 3^{-/-}$ zebrafish, heterologously expressed the gene products in *Xenopus* oocytes, and used electrophysiology to compare the molecular function phenotypes of the gene products.

To clone cDNA, we isolated messenger RNA from zebrafish brain tissue using TRIzol. RNA was reversed transcribed as described above (see Quantitative Polymerase Chain Reaction of GABA_A Receptor β Messenger RNAs) and $\beta 3$ cDNAs were amplified using Phusion High-Fidelity DNA polymerase (Thermo Fisher) and full-length zebrafish-specific $\beta 3$ cloning primers (forward: AGTTGGTACCGA GCTCGTGCCCCATTTC AAATATTCCGCCTT GG; reverse: ATGCCTCGAGTGCGAGCACGTC CGTA AAGTACATCAGAG). Full-length cDNAs were cloned into pCDNA3.1 plasmids between KpnI and XhoI endonuclease sites. Single clones carrying wild-type or $\beta 3^{-/-}$ were amplified and complete cDNA sequences from the purified plasmids were confirmed by Sanger sequencing at the MGH DNA core. Messenger RNA was prepared using T7 mMESSAGE mMACHINE and polyadenylation kits (both from Ambion—Thermo Fisher), purified, and stored in RNAase-free water at -80°C .

Methods for preparation of *Xenopus* oocytes, injection of mRNA, and two-microelectrode voltage clamp electrophysiology have been previously described.²⁴ We injected oocytes with mRNA (1 ng per oocyte) encoding either wild-type zebrafish $\beta 3$ or the $\beta 3^{-/-}$ gene product. We also tested oocytes injected with mRNA encoding human GABA_A $\beta 3$ subunits as positive controls and uninjected oocytes as negative controls. To test for expression of functional $\beta 3$ homomeric channels, oocytes ($n = 5$ per group) were voltage-clamped at -50 mV and exposed to 10 mM GABA, 100 μ M propofol, and 100 μ M etomidate.^{29,30} In cells producing currents in response to anesthetic applications, we measured the ratio of currents elicited by 100 μ M propofol and 100 μ M etomidate. We also tested a separate group of oocytes expressing zebrafish $\beta 3$ for inhibition of currents by 10 μ M picrotoxin.

Cartilage Staining and Imaging Processing

To analyze the craniofacial skeleton, Alcian blue staining was performed on five wild-type and five $\beta 3^{-/-}$ embryos euthanized at 4.5 days postfertilization, as described previously.³¹ Embryos were mounted in 95% glycerol in 1x phosphate buffered saline with tween 20 and images were obtained at 10x and 40x on a Nikon 80i compound microscope (Nikon Instruments Inc., USA). Images were processed with an NIS-Elements advanced research image acquisition and analysis system (Nikon Instruments), using the maximum intensity projection feature applied to z-stacks. Images for each animal were examined for abnormalities and measurements recorded for palate length and width as well as lower jaw length and width.

Locomotor Activity and Thigmotaxis

Spontaneous locomotor activity of 7 days postfertilization larvae was tracked and quantified by Zebralab v3.2 software (Viewpoint Behavioral Systems, Canada) in tracking mode, using previously described methods.³² Wild-type and $\beta 3^{-/-}$ larvae (48 larvae/ group) were loaded individually into wells on 24-well plates (12 of each genotype per plate). After a 15-min adaptation to the Zebrabox environment with white light level 110 lux, spontaneous movements were tracked for 1h with detection threshold set at 22 (scale 0 to 200). The distance and duration traveled was recorded and analyzed in three speed categories: fast movements: v greater than or equal to 20 mm/s; slow movement: v is less than or equal to 20 mm/s and greater than or equal to 5 mm/s; and nonmoving: v less than 5 mm/s. Tests were performed between 11:00 AM and 6:00 PM, in order to minimize diurnal variation.

Thigmotaxis, a measure of anxiety, is the tendency of animals to remain near the walls of their environment relative to its central area. To assess this, 1-h locomotion tracking videos were analyzed to quantify, for each animal, both time spent and distance traveled within *versus* outside a central circle with area half that of the total circular well.³³

Zebrafish Larvae Sedation and Photomotor Response Assays

Larval zebrafish from both wild-type and $\beta 3^{-/-}$ colonies were tested for sensitivities to both sedative and hypnotic effects of a set of nine compounds across relevant concentration ranges: etomidate (0.03 to 5 μ M), propofol (0.1 to 5 μ M), pentobarbital (20 to 400 μ M), alphaxalone (0.02 to 4 μ M), ketamine (1 to 400 μ M), dexmedetomidine (0.3 nM to 20 μ M), ethyl-3-aminobenzoate methane thiosulfonate (MS-222 or tricaine; 5 to 500 μ M), butanol (0.2 to 40 mM), and ethanol (30 to 400 mM). Both wild-type and $\beta 3^{-/-}$ larvae were tested on the same day on a given drug prepared from the same stock solution. For each genotype, 6 to 18 larvae were studied at each drug concentration plus a negative (no drug) control group. Drug inhibition of both spontaneous motor activity (sedation) and photomotor responses (hypnosis) were assessed in separate groups of animals using previously described methods.¹⁸ Briefly, each larva was loaded into a well of a standard 96-well plate containing 200 μ l of E3 buffer with or without drug. Plates were placed in the dark chamber of a Zebrabox maintained at 28.5°C and incubated for 15 min, for drug equilibration and dark adaptation. Following the adaptation period, spontaneous movements of each larvae were quantified during six sequential 30-s epochs. In photomotor responses assays, four test runs at 3-min intervals were performed and recorded as digitized video. Each test run included a 10-s basal motor activity period followed by a 0.2-s white light stimulus (500 lux) and a 5-s poststimulus period. Motor activity data (Zebralab software v3.2) during all baseline periods for each larva were normalized to 0.2-s epochs and combined to calculate mean \pm SD and 95% CI. The binary photomotor responses in each run for a given larva was considered positive if motor activity during the 0.2-s light flash or the two subsequent 0.2-s epochs exceeded the upper 95% CI for that larva's basal activity. Cumulative photomotor response probabilities for each animal were calculated from the four runs.

Statistical Analyses

Spontaneous movement and thigmotaxis metrics, fertility and embryonic viability, body weight, and body length for groups of wild-type and $\beta 3^{-/-}$ animals were pooled to calculate mean \pm SD. Normality of the data distributions was assessed and confirmed using D'Agostino-Pearson tests and statistical comparisons of these characteristics were based on two tailed unpaired Student's *t* tests. Statistical comparisons of mRNA levels from wild-type, $\beta 3^{+/-}$, and $\beta 3^{-/-}$ fish were performed using ANOVA with Dunnett multiple comparisons tests between wild-type and the others. In oocytes expressing $\beta 3$ homomeric channels, the within-cell ratio of electrophysiologic responses to 100 μ M propofol *versus* 100 μ M etomidate for human *versus* zebrafish ($n = 5$ each) were compared using an unpaired two-tailed Student's *t* test. For drug-dependent inhibition of photomotor

responses probabilities and normalized spontaneous movement, results for all animals in each exposure group were combined and plotted as mean \pm SD against log [drug, M]. Logistic functions (equation 1) were fitted to all independent data points using nonlinear least squares. Sedative and hypnotic EC50s are reported as mean with 95% CIs. EC50 comparisons for wild-type *versus* $\beta 3^{-/-}$ larvae were based on F-tests with $\alpha = 0.05$. Linear least-squares fits and statistical comparisons were performed using Graphpad Prism v7.0 (Graphpad Software, USA).

$$Y = \frac{Max}{1 + 10^{(\log EC50 - \log [ANES]) * nH}} \quad (1)$$

The maximum (*Max*) represents either control photomotor responses probability or normalized control spontaneous movement, [ANES] is the anesthetic concentration, EC50 is the half-effect concentration, and *nH* is the Hill slope.

Results

CRISPR-Cas9 Targeting Zebrafish GABRB3 Exon 7 Creates Frameshifting Insertion that Destabilizes mRNA and Eliminates $\beta 3$ Subunit Function

To establish a zebrafish line lacking functional GABA_A receptor $\beta 3$ subunits, GABRB3 exon 7, which encodes part of the extracellular domain of the $\beta 3$ subunit, was targeted with CRISPR-Cas9 random mutagenesis. The sequences of CRISPR guide RNA and flanking polymerase chain reaction primers are reported in table 1. Approximately 200 one-cell stage embryos were injected with guide RNA and Cas9 messenger RNA. At 24 h postinjection, fluorescent polymerase chain reaction size analysis of pooled DNA from 10 embryos showed the presence of both insertions and deletions near the target sequence. Viable F0 embryos were raised to adulthood (3 months), when individual tail-snip samples were analyzed with fluorescent polymerase chain reaction sizing. Individuals with insertions or deletions were out-crossed with wild-type zebrafish. At 3 months, heterozygous F1 offspring were genotyped at the guide RNA target site (fig. 1A). Fluorescence polymerase chain reaction sizing identified several F1 fish of both sexes containing a 10-bp insertion in the GABRB3 exon 7 coding sequence. Subsequent DNA sequencing identified fish of both sexes with identical 10-bp insertions producing a frameshift and a premature stop codon near the guide RNA target site and predicted by *in silico* translation to truncate $\beta 3$ peptide within the extracellular domain (fig. 1B). One pair of heterozygous F1 siblings carrying this mutation was incrossed. The resulting F2 offspring were genotyped based on tail-snips at age 2 to 3 months, revealing wild-type, heterozygous, and homozygous mutants at approximately 1:2:1 ratios. Homozygous F2 fish were successfully incrossed to maintain the transgenic line (fig. 1A).

To test for possible chimerism in transgenic zebrafish, six individual DNA samples from adults (three males and three

females) were amplified using primers flanking the target sequence and analyzed using massive parallel next-generation sequencing. In all six samples, a single sequence comprising 99.7 to 100% of paired sequence reads (more than 50,000 paired reads per sample) was identified. This sequence contained the extra 10 base sequence identified in F2 genotyping (fig. 1B). Thus, chimerism was definitively ruled out in the $\beta 3^{-/-}$ transgenic line.

Molecular Comparisons of Wild-type and $\beta 3^{-/-}$ Zebrafish

Wild-type ($\beta 3^{+/+}$), $\beta 3^{+/-}$, and $\beta 3^{-/-}$ zebrafish were characterized at 7 days postfertilization for expression of GABRB3 messenger RNA (mRNA), using reverse transcription and quantitative polymerase chain reaction. Negative controls lacking either reverse transcriptase or template produced no detectable signal. Compared to wild-type larvae, GABRB3 mRNA was significantly reduced in $\beta 3^{-/-}$, but not in $\beta 3^{+/-}$ (fig. 1C). The reduced mRNA level in $\beta 3^{-/-}$ larvae is probably due to nonsense-mediated RNA decay triggered by the mutation-induced premature stop codon.³⁴ Quantification of mRNAs for GABRB1 ($\beta 1$) and GABRB2 ($\beta 2$) was also performed in the same triplicate samples. Normalized GABRB1 mRNA levels (mean \pm SD) were: wild-type = 1.00 ± 0.072 ; $\beta 3^{+/-}$ = 1.21 ± 0.088 ; and $\beta 3^{-/-}$ = 1.21 ± 0.16 . Normalized GABRB2 mRNA levels were wild-type = 1.00 ± 0.043 ; $\beta 3^{+/-}$ = 0.92 ± 0.16 ; and $\beta 3^{-/-}$ = 1.18 ± 0.15 . Analysis using ANOVA with Dunnett comparison tests indicated no significant differences in GABRB1 or GABRB2 levels between wild-type and $\beta 3^{+/-}$ or $\beta 3^{-/-}$ animals.

We used expression in *Xenopus* oocytes and electrophysiology to compare function of the wild-type and $\beta 3^{-/-}$ GABRB3 gene products. All tested oocytes injected with mRNA encoding the wild-type zebrafish $\beta 3$ subunit (*n* = 5) expressed ion channels that produced small (less than 50 nA) currents when exposed to 10 mM GABA, and much larger currents when exposed to 100 μ M propofol (range, 0.4 to 1.6 μ A) or 100 μ M etomidate (range, 1.9 to 5.6 μ A; fig. 1D). Picrotoxin (10 μ M) inhibited small basal leak currents and etomidate-elicited currents in five separate oocytes expressing zebrafish $\beta 3$ channels. Similar electrophysiologic characteristics were found in oocytes injected with mRNA encoding human GABA_A $\beta 3$ subunits. The within-oocyte current ratios elicited with propofol and etomidate for human *versus* zebrafish $\beta 3$ channels (*n* = 5 each) were similar (fig. 1E). In contrast, none of the tested oocytes injected with $\beta 3^{-/-}$ mRNA (*n* = 5) produced currents that could be distinguished from background noise. Voltage clamp recordings from these oocytes were similar to those from uninjected negative control oocytes (fig. 1D). These results confirm that the mutated GABRB3 gene in $\beta 3^{-/-}$ zebrafish encodes a nonfunctional peptide, presumably because the premature stop codon results in truncated subunits lacking the transmembrane domains that form ion channels.

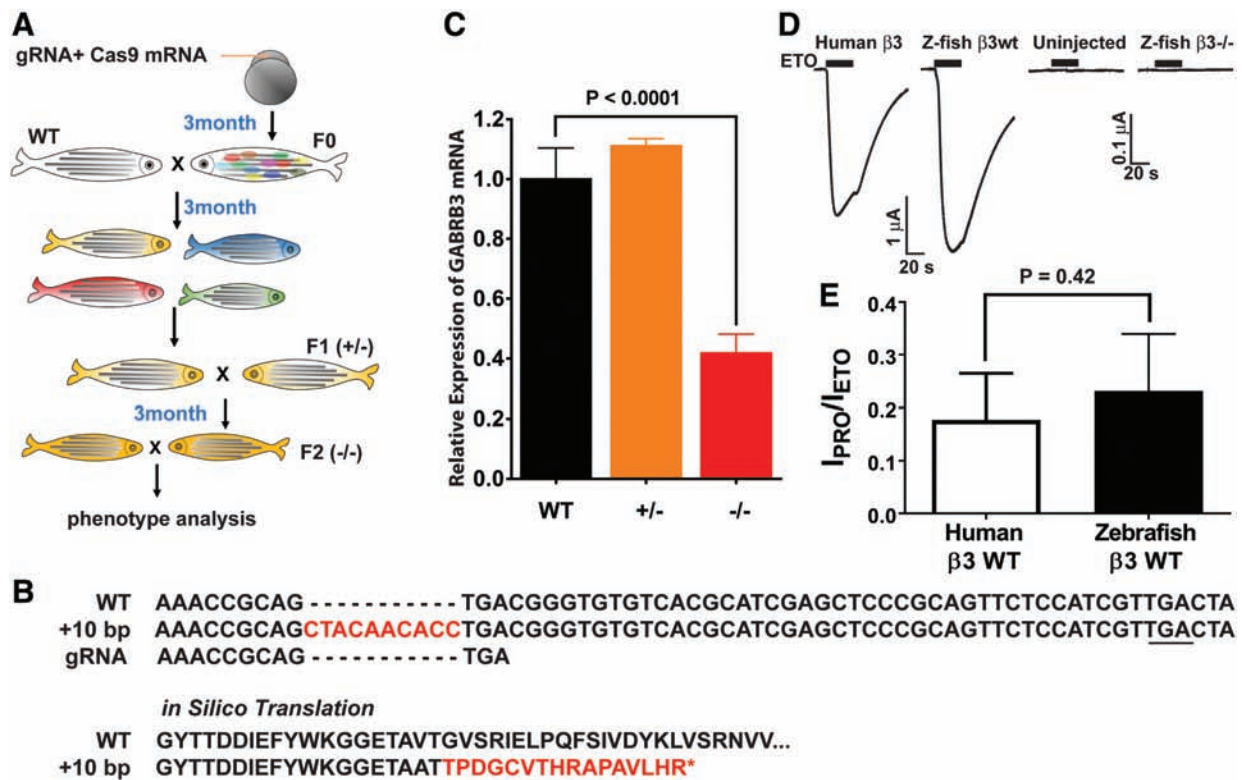


Fig. 1. Generation and genotype of $\beta 3^{-/-}$ mutant zebrafish. (A) A flowchart depicting the generation of a zebrafish germline mutation. CRISPR guide RNA (gRNA) and Cas9 mRNA was injected into one-cell stage embryos. The injected embryos were raised and outcrossed with wild-type (WT) to generate heterozygous F1 fish. Mutant fish were identified by fluorescence polymerase chain reaction and Sanger sequencing. F1 siblings carrying the same mutation were then crossed to generate F2 progeny, and phenotype–genotype correlations were done using F2 embryos. (B) DNA sequencing at the target sequence revealed a 10-bp insertion that is predicted by *in silico* translation to cause a frameshift and a premature stop codon (underlined sequence) downstream of CRISPR guide RNA target site, truncating the protein within the extracellular domain (*). (C) Real-time quantitative polymerase chain reaction revealed that *GABRB3* mRNA in homozygotes was significantly degraded. Bar graphs summarize normalized results (mean \pm SD) of triplicate measures with 15 pooled larvae per group. (D) Examples of current traces recorded from voltage-clamped oocytes exposed to 100 μ M etomidate (ETO; application indicated by bars over traces). Oocytes injected with WT zebrafish (z-fish) $\beta 3$ mRNA produce large currents, while oocytes injected with mRNA derived from the mutated $\beta 3^{-/-}$ gene produce no current (note tenfold amplified current scale). Traces from an oocyte injected with human $\beta 3$ mRNA and from an uninjected oocyte are shown for comparison. (E) Columns represent the ratios of voltage-clamp currents elicited with 100 μ M propofol (I_{PRO}) and 100 μ M etomidate (I_{ETO}) recorded in the same oocyte expressing either zebrafish or human $\beta 3$ subunits ($n = 5$ each). The P value is based on unpaired two-tailed Student's t test.

Comparison of Growth and Gross Morphology in Wild-type and $\beta 3^{-/-}$ Zebrafish

Neonatal mortality is high and cleft palate is common in global $\beta 3^{-/-}$ mice.⁸ Mating adult (3 month to 1 yr old) $\beta 3^{-/-}$ zebrafish pairs produced viable embryos in 7 of 19 (24%) trials, compared with 15 of 19 (79%) successful wild-type matings ($P < 0.0001$ by Student's t test). On average, 30% fewer $\beta 3^{-/-}$ than WT embryos were produced per successful mating and the fraction of viable embryos surviving to 7 days postfertilization was also 30% lower. However, at 3 months of age, no significant differences were evident between wild-type and $\beta 3^{-/-}$ in gross morphology, body weight, or body length of either sex (fig. 2). Comparisons

of 4.5 days postfertilization zebrafish (wild-type vs. $\beta 3^{-/-}$; mean \pm SD; $n = 5$ per group; P values from unpaired Student's t tests) for palatal length (410 ± 16 vs. 410 ± 15 μ m; $P = 0.97$), palatal width (400 ± 9.2 vs. 380 ± 16 μ m; $P = 0.17$), lower jaw length (400 ± 11 vs. 400 ± 13 μ m; $P = 0.84$), and lower jaw width (379 ± 5.9 vs. 377 ± 9.2 μ m; $P = 0.78$) identified no differences in craniofacial morphology (fig. 3).

$\beta 3^{-/-}$ Zebrafish Are More Active than Wild-type

Motor hyperactivity was observed in both global and neuron-selective $\beta 3^{-/-}$ mice.^{8,12} The locomotor activity of wild-type versus $\beta 3^{-/-}$ zebrafish at 7 days postfertilization

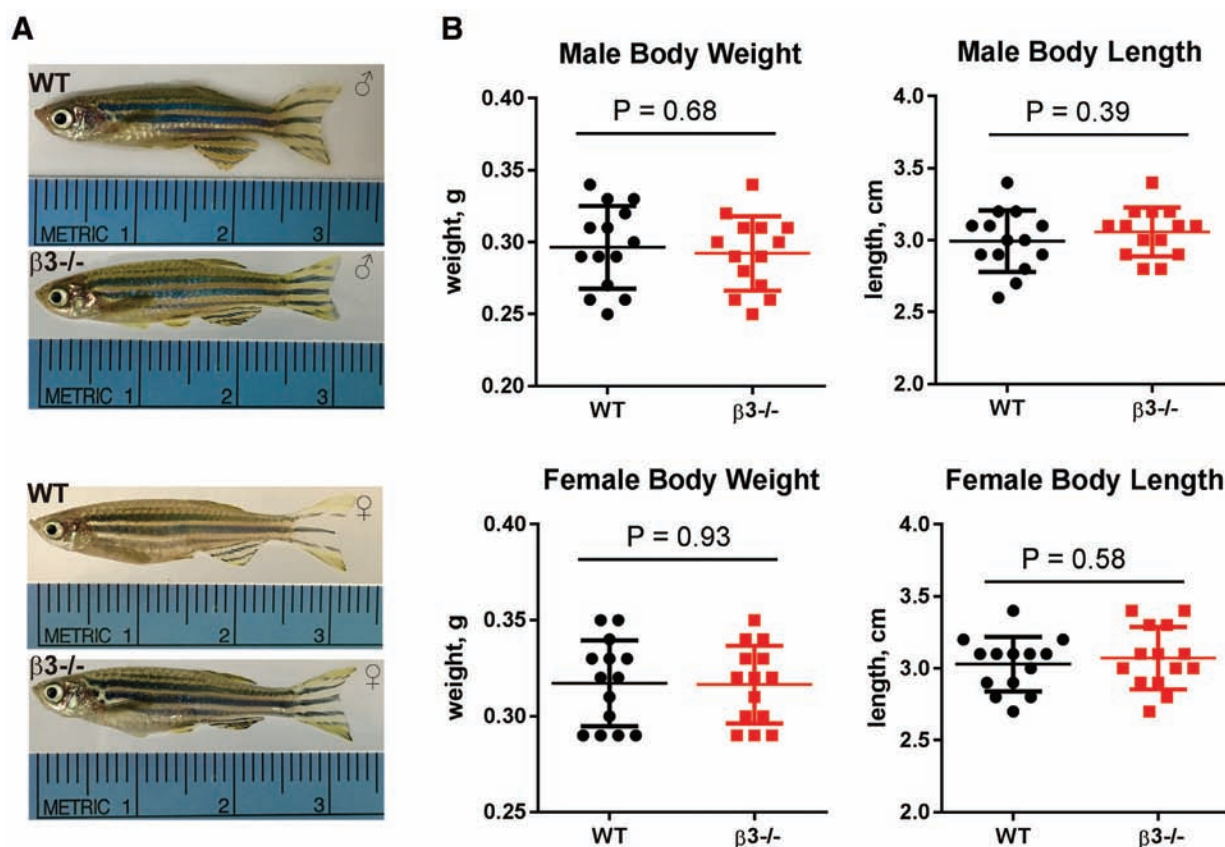


Fig. 2. Comparative morphology of 3-month postfertilization wild-type (WT) and $\beta 3^{-/-}$ zebrafish. (A) Representative images of WT and GABA_A receptor $\beta 3^{-/-}$ males (top) and females (bottom), showing that the mutants have normal overall morphology. Scales are in cm. (B) Comparisons of body weight and body length by sex. Black circles are WT, red squares are mutants, and each data point represents an individual fish. Mean \pm SD ($n = 14$ per group) are indicated by horizontal lines through data. P values were calculated based on two-tailed Student's t tests.

was assessed for both swimming speed and distance during 1 h. Tracking analysis (fig. 4A) showed that $\beta 3^{-/-}$ larvae swam about 15% farther than wild-type larvae (fig. 4B; Total Distance). This difference was largely accounted for by increased fast swimming (fig. 4B; Fast Distance).

Anxiety is another phenotypic feature of global $\beta 3^{-/-}$ mice.³⁵ Thigmotaxis, defined as maintenance of contact with the environmental periphery and the avoidance of open areas, is an index of anxiety, which is evolutionarily conserved in a wide range of species, including fish, rodents, and humans.^{33,36,37} Using measures of both percentage distance and time spent in the central half of their individual wells, both WT and $\beta 3^{-/-}$ zebrafish larvae displayed similar preferences for swimming near walls (fig. 4C).

$\beta 3^{-/-}$ Zebrafish Show Reduced Sensitivity to Specific Sedative-hypnotic Drugs

Sensitivities to nine different sedative-hypnotic drugs, ranging widely in potency and molecular effects, were compared in 7 days postfertilization wild-type and

$\beta 3^{-/-}$ zebrafish larvae. Drug-induced hypnosis was measured as reduced photomotor response probability (fig. 5) and sedation was measured as reduced spontaneous activity (fig. 6). Pooled control photomotor response probabilities for all control wild-type (mean \pm SD = 0.79 ± 0.23 ; $n = 111$) and $\beta 3^{-/-}$ (0.72 ± 0.23 ; $n = 112$) larvae did not differ significantly ($P = 0.06$ by two-tailed unpaired Student's t test). Concentration-response relationships for photomotor responses inhibition by etomidate (fig. 5A), propofol (fig. 5B), and pentobarbital (fig. 5C) differed significantly between wild-type and $\beta 3^{-/-}$ larvae, with $\beta 3^{-/-}$ larvae exhibiting EC₅₀s about twofold higher than those for wild-type (table 2). In contrast, concentration-dependent photomotor responses inhibition in wild-type and $\beta 3^{-/-}$ larvae displayed similar EC₅₀s (table 2) for alfaxalone (fig. 3D), ketamine (fig. 5E), butanol (fig. 5F), MS-222 (tricaine, fig. 5G), and dexmedetomidine (fig. 5H). Interestingly, the EC₅₀ for photomotor responses inhibition by ethanol in $\beta 3^{-/-}$ larvae was lower than that for wild-type (fig. 5I).

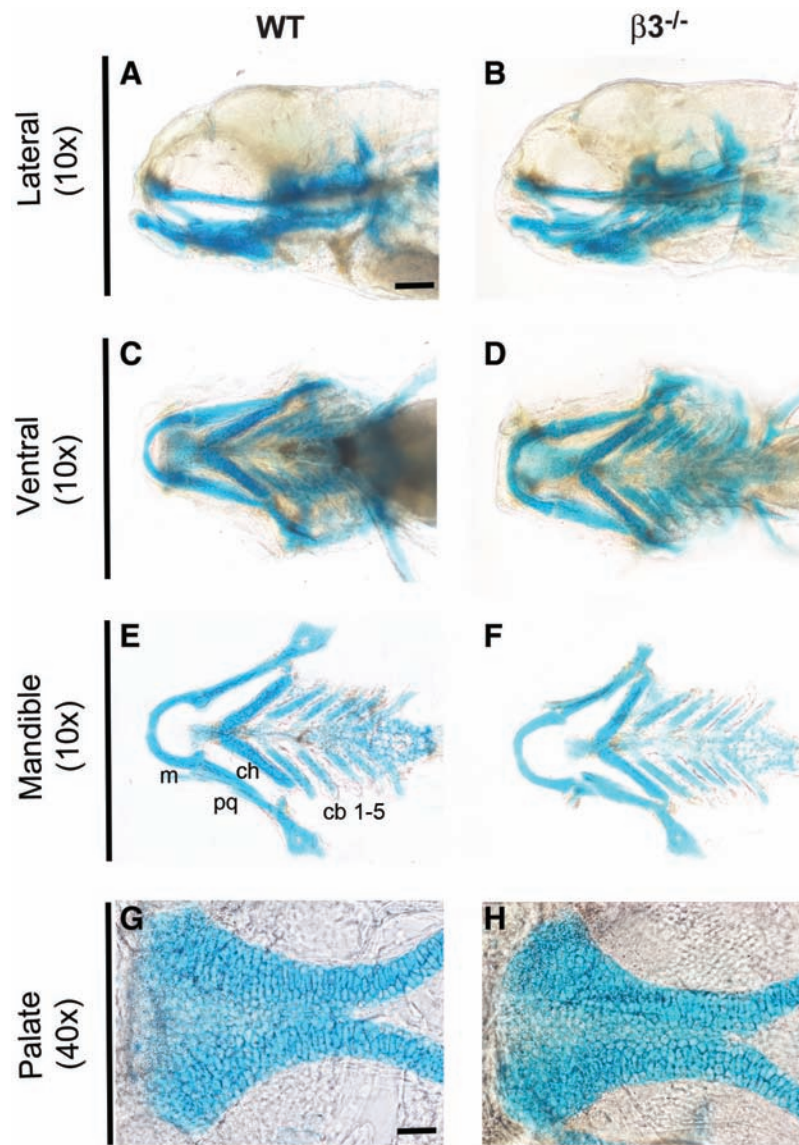


Fig. 3. Craniofacial cartilage in wild-type (WT) and $\beta 3^{-/-}$ zebrafish at 4.5 days postfertilization. Cartilage was stained using Alcian blue. Craniofacial structures (A, B, lateral; C, D, ventral), flat mount of the mandible (E, F) and the dissected palate (G, H) are shown. WT (A, C) and $\beta 3^{-/-}$ mutants (B, D) show comparable craniofacial cartilage structures with no difference in the mandible (E, F) or the palate (G, H). Scale is 200 μ m for A to F; 65 μ m for G to H. cb, ceratobranchial; ch, ceratohyal; m, Meckel cartilage; pq, palatoquadrate.

Inhibition of spontaneous motor activity (sedation) was evident at lower concentrations than photomotor responses inhibition (hypnosis) for all tested drugs, except ethanol in both wild-type and $\beta 3^{-/-}$ larvae (fig 6; table 3). Comparing sedative concentration-responses in the two zebrafish lines showed a similar pattern to that for photomotor responses inhibition. Sedative EC50s for etomidate (fig. 6A), propofol (fig. 6B), and pentobarbital (fig. 6C) were higher for $\beta 3^{-/-}$ than for wild-type, did not change for alphaxalone (fig. 6D), ketamine (fig. 6E), butanol (fig. 6F), MS-222 (tricaine, fig. 6G), and dexmedetomidine (fig. 6H), and was reduced for ethanol (fig. 6I).

Discussion

In this study, we aimed to establish whether $\beta 3^{-/-}$ zebrafish share pharmacogenetic and other phenotypes with $\beta 3$ transgenic mice. Several transgenic $\beta 3$ mouse lines have been used to investigate the neurobiologic roles of $\beta 3$, including in general anesthetic actions. These are a global $\beta 3^{-/-}$ line,⁸ two neuron-specific $\beta 3^{-/-}$ lines,¹² and $\beta 3$ N265M knock-in mice¹⁶ harboring a mutation that impairs receptor modulation by drugs that act through some of the multiple modulator sites on GABA_A receptors.⁵ However, mice are poorly

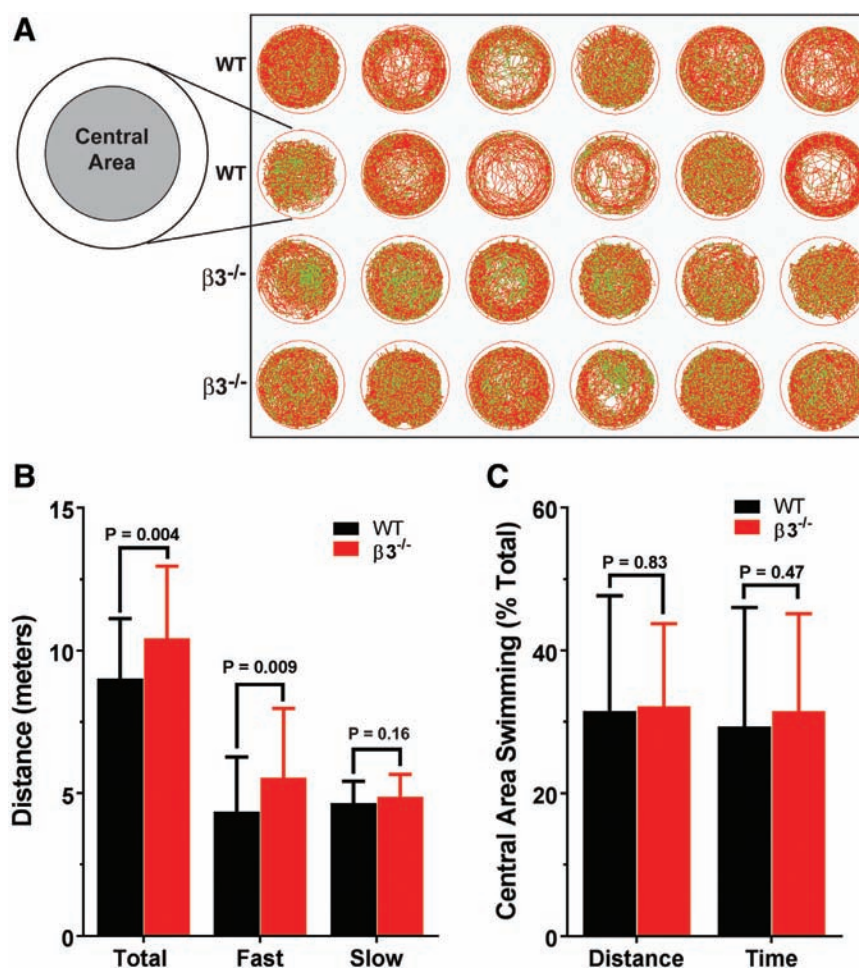


Fig. 4. Comparison of spontaneous movement in $\beta 3^{-/-}$ and wild-type (WT) zebrafish larvae. (A) Swimming trajectories of 7 days postfertilization larvae during 1 h. Red, trajectories in v are greater than or equal to 20 mm/s; green, trajectories in v are less than 20 mm/s and greater than or equal to 5 mm/s. The insert panel shows how the central area is defined, the area of the inner circle corresponded to half of the total area of each well. (B) Bars represent mean \pm SD for 1 h swimming distances ($n = 48$ larvae per group). (C) Bars represent mean \pm SD for distance or time spent in the central half of the circular well during 1 h, expressed as a percentage of the total ($n = 48$ larvae per group). Statistical comparisons were based on two-tailed unpaired Student's t tests.

suit for pharmacodynamic studies of intravenous anesthetics. Interindividual variations in drug absorption, distribution, and metabolism after intravenous or intraperitoneal anesthetic injections increase the variation in drug-induced mouse behavioral effects. Consequently, few intravenous anesthetics, each at only a few doses, have been tested in $\beta 3$ transgenic mice. Among the drugs tested in multiple transgenic $\beta 3$ mouse lines, inconsistent results were reported for pentobarbital (table 4).

Zebrafish larvae represent another vertebrate species for assessing the role of $\beta 3$ -containing GABA_A receptors in anesthetic mechanisms, while providing important advantages over mice. Zebrafish are amenable to high-throughput studies quantifying both sedative and hypnotic effects under conditions of steady-state drug exposure.¹⁸ In the current

study, we assessed the effects of nine drugs, each at seven or more concentrations, in up to 18 animals per condition, in both wild-type and $\beta 3^{-/-}$ zebrafish, providing statistically robust EC50 comparisons.

Similarities and Differences between $\beta 3^{-/-}$ Zebrafish and Transgenic Mice

Fertility, Survival, and Growth. The $\beta 3^{-/-}$ zebrafish showed reduced fertility and 30% lower survival at 7 days postfertilization compared to wild-type. For comparison, neonatal mortality was frequent ($\sim 90\%$) in global $\beta 3^{-/-}$ mice and 61% in neuron-specific $\beta 3^{-/-}$ mice, but infrequent in $\beta 3N265M$ knock-ins. Neonatal mortality in $\beta 3^{-/-}$ mice was not strongly linked to cleft palate, but possibly to poor maternal care for pups.¹² Moreover, $\beta 3^{-/-}$ mice that survived

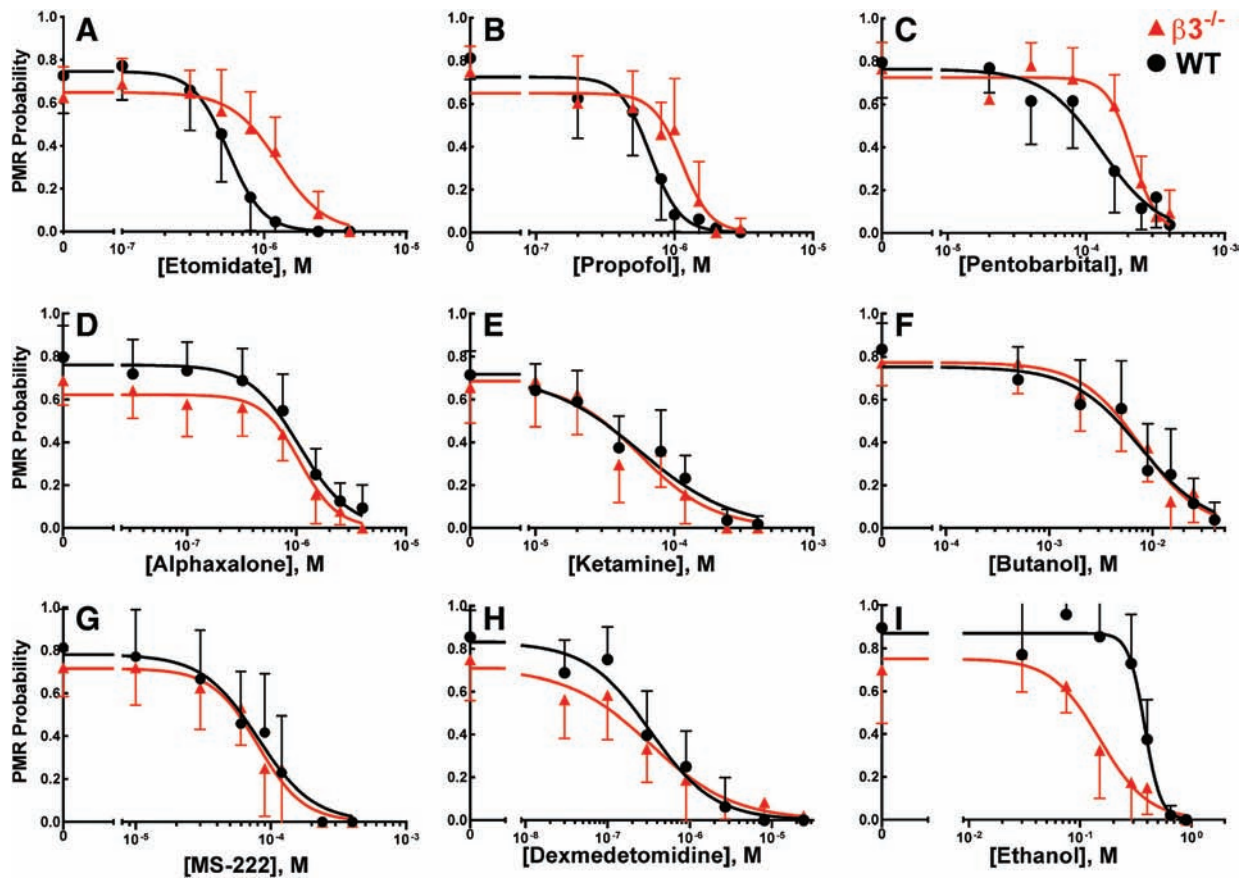


Fig. 5. Hypnotic potencies of anesthetic drugs in wild-type (WT) versus $\beta 3^{-/-}$ zebrafish larvae. Photomotor response probabilities were assessed using video analysis of between 88 and 128 larvae per experiment. Plotted symbols represent mean \pm 95% CI ($n = 8$ to 16 larvae per point; error bars are symmetrical; unidirectional error bars were drawn for clarity). WT is black circles; $\beta 3^{-/-}$ is red triangles. Lines through data represent logistic fits, colored to match symbols. Results of logistic fits are reported in table 2. Significant differences in fitted EC50s for wild-type versus $\beta 3^{-/-}$ larvae were found with etomidate (A), propofol (B), pentobarbital (C), and ethanol (I). M, molar; MS-222, tricaine; PMR, photomotor response.

Table 2. Hypnotic Potencies in Wild-type versus $\beta 3^{-/-}$ Zebrafish Larvae

Anesthetics	Wild-type			$\beta 3^{-/-}$			P Value (EC50s)
	EC50 Mean (95% CI)	Hill Slope	N*	EC50 Mean (95% CI)	Hill Slope	N*	
Etomidate	0.6 μ M (0.5–0.7)	–3.5	88	1.3 μ M (1.0–1.6)	–2.6	96	<0.0001
Propofol	0.7 μ M (0.6–0.8)	–4.0	96	1.1 μ M (1.0–1.4)	–4.2	96	0.0005
Pentobarbital	130 μ M (94–179)	–2.1	101	220 μ M (190–240)	–4.7	127	0.0009
Alphaxalone	1.1 μ M (0.9–1.5)	–2.0	128	1 μ M (0.8–1.3)	–2.6	128	0.47
Ketamine	50 μ M (35–85)	–1.6	128	60 μ M (40–89)	–1.3	112	0.77
Butanol	7 mM (4.1–11.8)	–1.6	103	8 mM (5.7–11.6)	–1.2	96	0.66
Tricaine (MS-222)	80 μ M (56–111.0)	–2.1	96	80 μ M (64–105)	–2.6	64	0.86
Dexmedetomidine	0.4 μ M (0.2–0.6)	–1.2	96	0.3 μ M (0.1–0.6)	–0.8	96	0.56
Ethanol	380 mM (340–420)	–6.0	96	150 mM (106–213)	–2.0	79	<0.0001

Hypnosis was assessed as probability of photomotor responses.

P values are based on F-tests comparing EC50s in wild-type versus $\beta 3^{-/-}$. *N is the total number of larvae used in a concentration–response experiment at eight different drug concentrations, including a no-drug control.

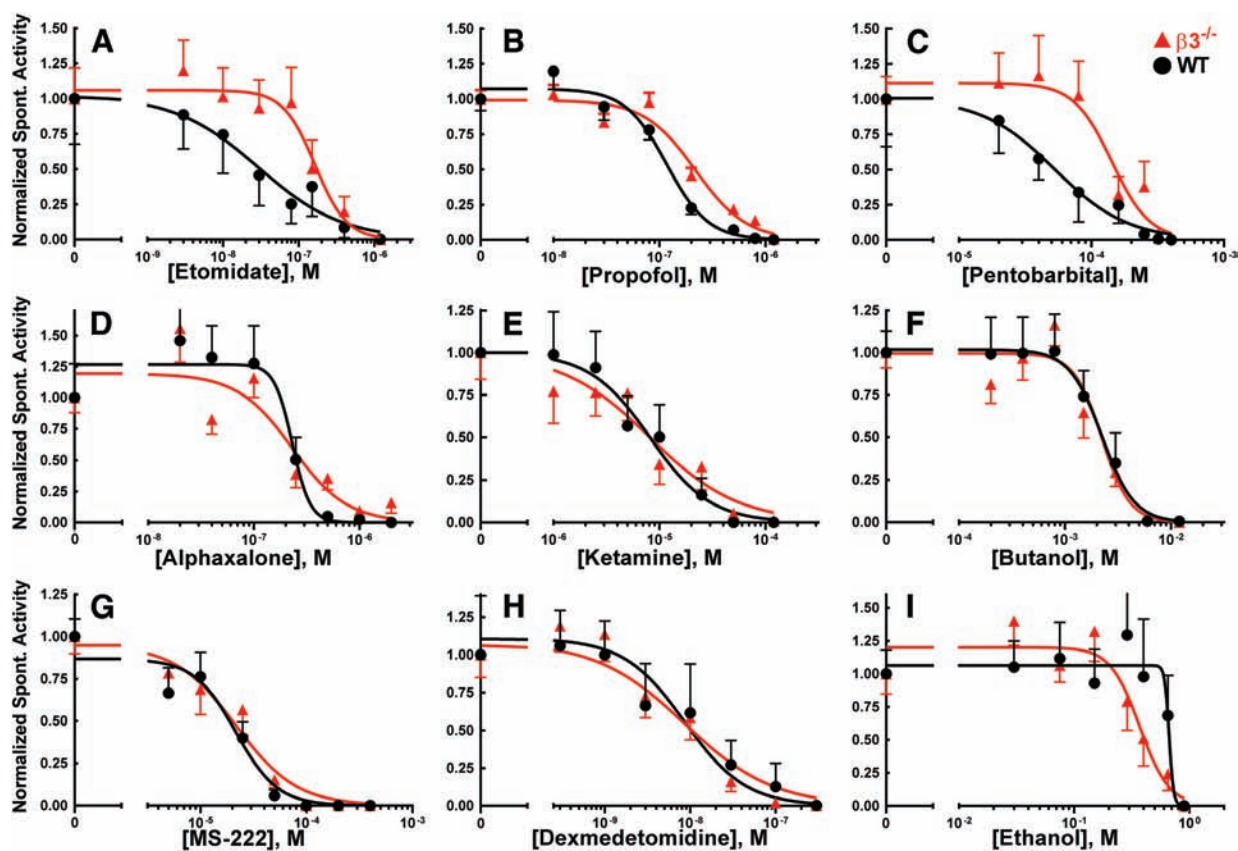


Fig. 6. Sedative potencies of anesthetic drugs on wild-type (WT) *versus* $\beta 3^{-/-}$ zebrafish larvae. Spontaneous movement was assessed using video analysis (72 to 144 larvae per experiment) and normalized to the no-drug control group result for each drug. Plotted symbols represent mean \pm 95% CI ($n = 9$ to 18 larvae per point); *error bars* are symmetrical; *unidirectional error bars* were drawn for clarity. WT is *black circles*; $\beta 3^{-/-}$ is *red triangles*. Lines through data represent logistic fits, colored to match symbols. Results of logistic fits are reported in table 3. Significant differences in fitted EC₅₀s for WT *versus* $\beta 3^{-/-}$ larvae were found with etomidate (A), propofol (B), pentobarbital (C), and ethanol (I). M, molar; MS-222, tricaine; Spont., spontaneous.

Table 3. Sedative Potencies in Wild-type *versus* $\beta 3^{-/-}$ Zebrafish Larvae

Anesthetics	Wild-type			$\beta 3^{-/-}$			P Value (EC ₅₀ s)
	EC ₅₀ Mean (95% CI)	Hill Slope	N*	EC ₅₀ Mean (95% CI)	Hill Slope	N*	
Etomidate	30 nM (12–73)	–0.8	72	160 nM (121–223)	–2.1	96	0.0016
Propofol	120 nM (104–132)	–2.2	120	220 nM (196–244)	–1.8	120	<0.0001
Pentobarbital	50 μ M (36–78)	–1.6	72	140 μ M (119–176)	–3.0	72	<0.0001
Alphaxalone	230 nM (186–287)	–5.1	144	230 nM (178–302)	–1.7	144	0.98
Ketamine	8 μ M (5.7–11.6)	–1.5	96	8 μ M (6.1–10.7)	–1.0	96	0.98
Butanol	2 mM (1.9–2.9)	–2.9	120	2 mM (1.8–2.4)	–3.3	120	0.52
Tricaine (MS-222)	20 μ M (17–25)	–2.0	96	23 μ M (18.1–29.5)	–1.6	72	0.62
Dexmedetomidine	10 nM (4–26)	–0.9	144	8 nM (5.7–11.5)	–1.2	144	0.69
Ethanol	670 mM (270–1630)	–22.9	96	370 mM (324–424)	–3.4	96	<0.0001

Sedation was assessed as spontaneous motor activity normalized to no-drug control groups.

P values are based on F-tests comparing EC₅₀s in wild-type *versus* $\beta 3^{-/-}$. *N is the total number of larvae used in a concentration–response experiment at eight different drug concentrations, including a no-drug control.

Table 4. Summary of Phenotypic Features of $\beta 3$ Transgenic Mice and Zebrafish

Phenotype (Relative to WT)	Transgenic Mouse Type			Zebrafish
	Global $\beta 3^{-/-}$	Neuronal $\beta 3^{-/-}$	$\beta 3N265M$	Global $\beta 3^{-/-}$
Neonatal mortality	$\uparrow\uparrow$	\uparrow	—	\uparrow
Craniofacial abnormalities	\uparrow	—	—	—
Hyperactivity	$\uparrow\uparrow$	$-\uparrow^{\dagger}$	—	\uparrow
Epilepsy	\uparrow	$-\uparrow^{\dagger\dagger}$	—	ND
Sensitivity to sedation, LoRR, or Nociception				
Etomidate	\downarrow	\downarrow	\downarrow	\downarrow
Propofol	ND	ND	\downarrow	\downarrow
Pentobarbital	—	ND	\downarrow	\downarrow
Ethanol	—	—	—	\uparrow
Alphaxalone	ND	ND	—	—
Tricaine (MS-222)	ND	ND	ND	—
Ketamine	ND	ND	ND	—
Dexmedetomidine	ND	ND	ND	—
Butanol	ND	ND	ND	—
References	6,8,35	12	16,17,42	

Cell contents indicate changes in $\beta 3$ transgenic animal phenotypes relative to wild-type.

† Hyperactivity was not reported in pan-neuronal $\beta 3^{-/-}$ mice, but was observed in forebrain-selective $\beta 3^{-/-}$ mice. †† Seizures were not observed in pan-neuronal $\beta 3^{-/-}$ mice, but were observed in forebrain-selective $\beta 3^{-/-}$ mice.

—, no change; LoRR, loss-of-righting reflexes; ND, no data. Up arrows indicate increases and down arrows indicate decreases. Two arrows indicate large changes.

to weaning subsequently grew normally. While zebrafish survive for 7 days on yolk, $\beta 3^{-/-}$ zebrafish that survived to 3 months of age were morphologically indistinguishable from wild-type, suggesting that any postlarval developmental effects of the genotype were negligible.

Behavior. Our studies demonstrated modestly increased spontaneous motor activity in $\beta 3^{-/-}$ zebrafish larvae compared with wild-type (fig. 4). Overt hyperactivity was also reported in both global and forebrain $\beta 3^{-/-}$ mice (table 4). Hypersensitivity to handling and stimuli was also reported in these transgenic mice, but in zebrafish, baseline photomotor responses probabilities were similar in wild-type and $\beta 3^{-/-}$ larvae, implying normal reactivity to stimuli.

In both global and forebrain $\beta 3^{-/-}$ mice, overt seizures were observed and electroencephalography confirmed abnormal brain activity in global knock-outs (table 4). Could the excess motor activity of $\beta 3^{-/-}$ zebrafish be due to seizures? The hyperactivity we observed in $\beta 3^{-/-}$ zebrafish was attributable to increased rapid swimming (fig. 4B), which is also increased by exposure to convulsant drugs.³⁸ Thus, $\beta 3^{-/-}$ zebrafish could experience epilepsy, but we cannot rule out a simple increase in normal fast swimming without convulsions. High-speed videography and specialized behavioral analyses or electroencephalography will be needed to detect whether intermittent seizures are occurring.³⁹

Craniofacial Morphology. Craniofacial abnormalities observed in global $\beta 3^{-/-}$ mice were not evident in $\beta 3^{-/-}$ zebrafish at 4.5 days postfertilization, when bony structures are established (fig. 3). Interestingly, cleft palate is not

evident in neuron-specific $\beta 3^{-/-}$ mice, and it appears that nonneuronal $\beta 3$ $GABA_A$ receptors influence murine palate development.⁴⁰ Significant linkage disequilibrium has been reported between the human GABRB3 gene and cleft lip and/or palate.⁴¹ The lack of such linkage in zebrafish illustrates the limitations inherent in animal models.

Sensitivities to Sedative-Hypnotics. Both global $\beta 3^{-/-}$ mice and zebrafish larvae share one pharmacogenetic characteristic: insensitivity to etomidate (table 4). However, the $\beta 3^{-/-}$ genotype in mice *versus* zebrafish is associated with divergent sensitivities for pentobarbital and ethanol. After either pentobarbital or ethanol exposure, global $\beta 3^{-/-}$ and wild-type mice sleep for similar durations, while $\beta 3^{-/-}$ zebrafish displayed lower sensitivity to pentobarbital and higher sensitivity to ethanol in comparison to wild-type.

The drug sensitivity profile of $\beta 3^{-/-}$ zebrafish larvae more closely resembles that of $\beta 3N265M$ mice (table 4). In comparison to the respective wild-type controls, both $\beta 3^{-/-}$ zebrafish and $\beta 3N265M$ mice displayed reduced sensitivities to etomidate, propofol, and pentobarbital, but similar sensitivity to alphaxalone. The only notable difference among drug sensitivities is for ethanol. While $\beta 3^{-/-}$ zebrafish larvae exhibited hypersensitivity to ethanol in assays for both sedation and hypnosis, wild-type and $\beta 3N265M$ mice displayed similar sensitivities to ethanol-induced loss-of-righting reflexes (hypnosis).⁴²

At the molecular level, $\beta 3N265M$ mutations impair $GABA_A$ receptor modulation by etomidate and propofol, drugs that bind in the two $\beta +/\alpha -$ outer transmembrane intersubunit sites in typical synaptic $\alpha\beta\gamma$ receptors.⁵ Importantly, $\alpha\beta 3N265M\gamma$ receptors retain sensitivity to

alphaxalone, which binds at distinct β +/ α - interfacial sites that are adjacent and intracellular to etomidate/propofol sites.^{13,43} The case of pentobarbital is more complex. Pentobarbital inhibits photolabeling by both etomidate analogs (in β +/ α - sites) and a potent barbiturate, R-5-allyl-1-methyl-5-(*m*-trifluoromethyl-diazirinyphenyl) barbituric acid, that selectively binds in α +/ β - and γ +/ β - transmembrane sites.⁴⁴ Pentobarbital effects in β 3 homomers, but not in α 1 β 3 heteromeric receptors are reduced by β 3N265S mutations,³⁰ while the effect of β 3N265M on pentobarbital modulation of α β γ receptors remains unknown. However, β 3N265M modestly reduces R-mTFD-MPAB modulation of α 1 β 3 γ 2L receptors⁴⁵ and β 3N265M mice exhibit normal sensitivity to hypnosis induced by R-5-allyl-1-methyl-5-(*m*-trifluoromethyl-diazirinyphenyl) barbituric acid injections.⁴⁶

The pharmacogenetic phenotype of β 3^{-/-} zebrafish larvae both confirms and extends inferences drawn from previous molecular and transgenic animal studies. Our results confirm that β 3-containing GABA_A receptors mediate important behavioral effects of etomidate, propofol, and pentobarbital. We observed no reduction in sensitivity to tricaine, ketamine, or dexmedetomidine in β 3^{-/-} larvae, consistent with evidence that these anesthetics minimally modulate GABA_A receptors while affecting other molecular targets.⁴ While ethanol, butanol, and other alcohols modulate GABA_A receptors and multiple other anesthetic targets, our current results indicate that β 3-containing GABA_A receptors are not important mediators of their sedative-hypnotic effects. At present, we have no basis for speculating on why the β 3^{-/-} genotype differentially affects ethanol sensitivity in fish *versus* mice. The normal sensitivity of β 3N265M mice to alphaxalone was previously interpreted as reflecting the unaltered molecular sensitivity of β 3N265M receptors to neuroactive steroids.¹⁶ However, our β 3^{-/-} zebrafish studies suggest that alphaxalone effects are mediated through mechanisms entirely independent of the β 3 subunit. Other transgenic mouse studies implicate GABA_A receptors containing δ subunits, which are usually extra-synaptic, in anesthetic actions of neurosteroids.⁴⁷

Limitations of This Study

One limitation in comparing our results with those in transgenic mice is the lack of tests for nociceptive responses. Manual methods for this outcome in zebrafish have been reported.¹⁹ High throughput methods using electric shock or photo-switchable irritant chemicals may be employed for this purpose.⁴⁸ We did not test zebrafish sensitivities to volatile anesthetics, which are readily studied at steady-state in mice. Modification of zebrafish test equipment may extend our experimental repertoire to accommodate metered anesthetic gas exposure. Additionally, we have not tested drug sensitivities in more mature wild-type and β 3^{-/-} zebrafish, which could differ from those in larvae. Our high-throughput testing approach is not amenable to studies of mature adult zebrafish.

Animals may compensate for gene knock-outs by over-expressing similar gene products. We tested β 3^{-/-} zebrafish for compensation by quantifying β 1 and β 2 mRNAs. In

wild-type zebrafish, levels of mRNA for β 2 are around threefold higher than for β 3, so compensatory overexpression of β 2 may be difficult to detect.⁴⁹ Zebrafish also possess another gene for a GABA_A receptor β 4 subunit. We aim to determine whether silencing other β subunits affect zebrafish sensitivity to intravenous anesthetics. Another strategy that minimizes genetic compensation is to incorporate point mutations like β 3N265M that selectively alter anesthetic sensitivity of GABA_A receptors. Creating knock-ins in zebrafish with CRISPR-Cas9 has proven extremely difficult, and reliable strategies are being sought.⁵⁰

Summary and Conclusions

Global β 3^{-/-} zebrafish and mice display more differences than similarities among the morphologic, behavioral, and pharmacodynamic phenotypes that we assessed (table 4). Unexpectedly, the phenotype for β 3^{-/-} zebrafish most closely resembles that of homozygous β 3N265M knock-in mice, which are characterized by normal growth and neuromotor behavior, while displaying insensitivity to specific general anesthetics including etomidate, propofol, and pentobarbital.

Several other transgenic mouse lines have provided information on molecular targets mediating important anesthetic actions in vertebrates.^{3,47,51} However, because of limitations discussed above, few intravenous anesthetics have been tested in these mouse lines. Development of additional transgenic zebrafish could help determine the molecular targets that mediate anesthetic drug actions.

Our current results, along with other recent studies,^{18,19} show how transgenic zebrafish may accelerate both drug discovery and mechanisms research related to general anesthesia. A direct extension of this current work is identification of novel sedative-hypnotics that depend on β 3-containing GABA_A receptors. Zebrafish also represent a model for studying neural circuit activity, and experiments in transgenic fish may help reveal where specific targets in specific neural circuits mediate key anesthetic actions.

Acknowledgments

The authors thank Helen Hoyt, B.S. (Department of Anesthesia, Critical Care, and Pain Medicine, Massachusetts General Hospital, Boston, Massachusetts), for assistance with zebrafish fertility and embryo survival experiments. The authors thank the Center for Computational and Integrative Biology (Massachusetts General Hospital) for expert support in performance and analysis of next-generation sequencing experiments.

Research Support

This work was supported by a grant from the National Institute of General Medical Science (Bethesda, Maryland; grant No. R01-GM128989; to Dr. Forman) and by grants from Shanghai Jiaotong University School of Medicine, Shanghai, China, and the Chinese Medical Association, Beijing, China

(to Dr. Yang). The Department of Anesthesia, Critical Care, and Pain Medicine, Massachusetts General Hospital (Boston, Massachusetts) supported this work through a Research Scholars Award and an Innovation Grant (to Dr. Forman).

Competing Interests

The authors declare no competing interests.

Correspondence

Address correspondence to Dr. Forman: Department of Anesthesia, Critical Care, and Pain Medicine, Jackson 444, Massachusetts General Hospital, Boston, Massachusetts 02114. saforman@mgh.harvard.edu. Information on purchasing reprints may be found at www.anesthesiology.org or on the masthead page at the beginning of this issue. ANESTHESIOLOGY's articles are made freely accessible to all readers, for personal use only, 6 months from the cover date of the issue.

References

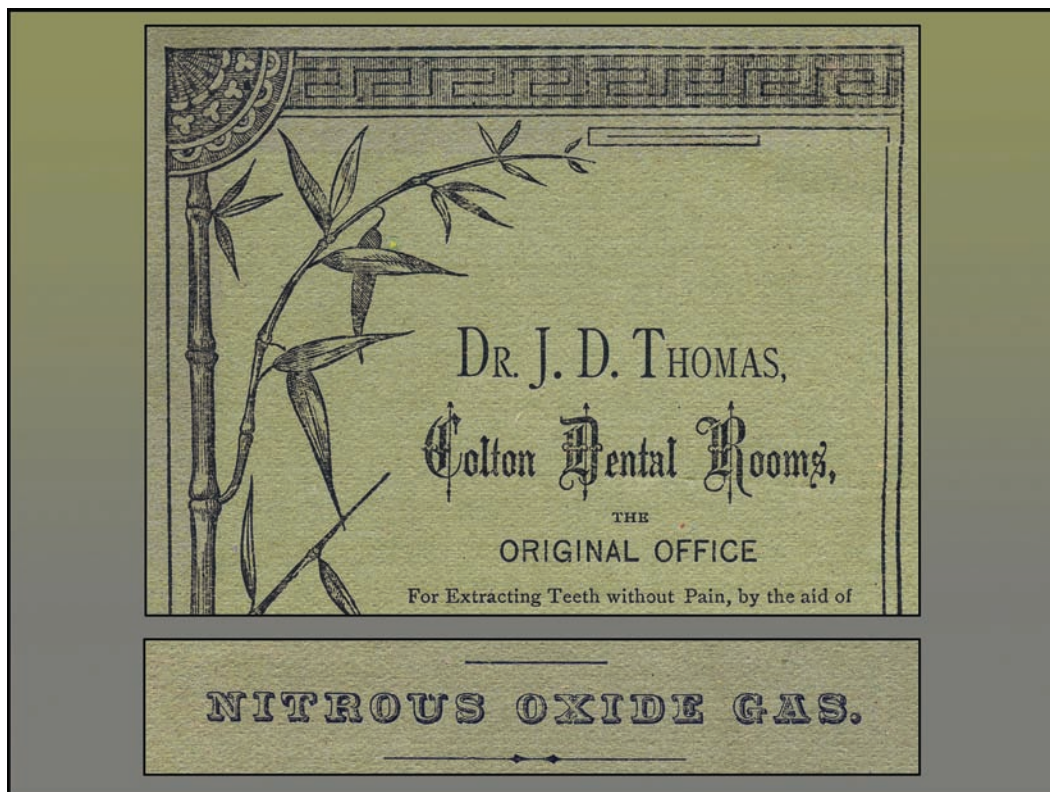
- Olsen RW, Sieghart W: GABA A receptors: Subtypes provide diversity of function and pharmacology. *Neuropharmacology* 2009; 56:141–8
- Phulera S, Zhu H, Yu J, Claxton DP, Yoder N, Yoshioka C, Gouaux E: Cryo-EM structure of the benzodiazepine-sensitive $\alpha 1\beta 1\gamma 2S$ tri-heteromeric GABAA receptor in complex with GABA. *Elife* 2018; 7. pii: e39383. doi: 10.7554/eLife.39383
- Rudolph U, Antkowiak B: Molecular and neuronal substrates for general anaesthetics. *Nat Rev Neurosci* 2004; 5:709–20
- Franks NP: General anaesthesia: From molecular targets to neuronal pathways of sleep and arousal. *Nat Rev Neurosci* 2008; 9:370–86
- Forman SA, Miller KW: Mapping general anesthetic sites in heteromeric γ -aminobutyric acid type A receptors reveals a potential for targeting receptor subtypes. *Anesth Analg* 2016; 123:1263–73
- Quinlan JJ, Homanics GE, Firestone LL: Anesthesia sensitivity in mice that lack the $\beta 3$ subunit of the γ -aminobutyric acid type A receptor. *ANESTHESIOLOGY* 1998; 88:775–80
- Liao M, Sonner JM, Jurd R, Rudolph U, Borghese CM, Harris RA, Laster MJ, Eger EI II: $\beta 3$ -containing γ -aminobutyric acidA receptors are not major targets for the amnesic and immobilizing actions of isoflurane. *Anesth Analg* 2005; 101:412–8
- Homanics GE, DeLorey TM, Firestone LL, Quinlan JJ, Handforth A, Harrison NL, Krasowski MD, Rick CE, Korpi ER, Mäkelä R, Brilliant MH, Hagiwara N, Ferguson C, Snyder K, Olsen RW: Mice devoid of γ -aminobutyrate type A receptor $\beta 3$ subunit have epilepsy, cleft palate, and hypersensitive behavior. *Proc Natl Acad Sci USA* 1997; 94:4143–8
- Culiat CT, Stubbs LJ, Woychik RP, Russell LB, Johnson DK, Rinchik EM: Deficiency of the $\beta 3$ subunit of the type A γ -aminobutyric acid receptor causes cleft palate in mice. *Nat Genet* 1995; 11:344–6
- Ugarte SD, Homanics GE, Firestone LL, Hammond DL: Sensory thresholds and the antinociceptive effects of GABA receptor agonists in mice lacking the $\beta 3$ subunit of the GABA(A) receptor. *Neuroscience* 2000; 95:795–806
- DeLorey TM, Handforth A, Anagnostaras SG, Homanics GE, Minassian BA, Asatourian A, Fanselow MS, Delgado-Escueta A, Ellison GD, Olsen RW: Mice lacking the $\beta 3$ subunit of the GABAA receptor have the epilepsy phenotype and many of the behavioral characteristics of Angelman syndrome. *J Neurosci* 1998; 18:8505–14
- Ferguson C, Hardy SL, Werner DE, Hileman SM, DeLorey TM, Homanics GE: New insight into the role of the $\beta 3$ subunit of the GABAA-R in development, behavior, body weight regulation, and anesthesia revealed by conditional gene knockout. *BMC Neurosci* 2007; 8:85
- Sieghart W, Jurd R, Rudolph U: Molecular determinants for the action of general anesthetics at recombinant $\alpha 2\beta 3\gamma 2$ γ -aminobutyric acid(A) receptors. *J Neurochem* 2002; 80:140–8
- Belelli D, Lambert JJ, Peters JA, Wafford K, Whiting PJ: The interaction of the general anesthetic etomidate with the γ -aminobutyric acid type A receptor is influenced by a single amino acid. *Proc Natl Acad Sci USA* 1997; 94:11031–6
- Desai R, Ruesch D, Forman SA: γ -amino butyric acid type A receptor mutations at $\beta 2N265$ alter etomidate efficacy while preserving basal and agonist-dependent activity. *ANESTHESIOLOGY* 2009; 111:774–84
- Jurd R, Arras M, Lambert S, Drexler B, Sieghart W, Crestani F, Zaugg M, Vogt KE, Ledermann B, Antkowiak B, Rudolph U: General anesthetic actions *in vivo* strongly attenuated by a point mutation in the GABA(A) receptor $\beta 3$ subunit. *FASEB J* 2003; 17:250–2
- Zeller A, Arras M, Jurd R, Rudolph U: Identification of a molecular target mediating the general anesthetic actions of pentobarbital. *Mol Pharmacol* 2007; 71:852–9
- Yang X, Jounaidi Y, Dai JB, Marte-Oquendo F, Halpin ES, Brown LE, Trilles R, Xu W, Daigle R, Yu B, Schaus SE, Porco JA Jr, Forman SA: High-throughput screening in larval zebrafish identifies novel potent sedative-hypnotics. *ANESTHESIOLOGY* 2018; 129:459–76
- Du WJ, Zhang RW, Li J, Zhang BB, Peng XL, Cao S, Yuan J, Yuan CD, Yu T, Du JL: The locus coeruleus modulates intravenous general anesthesia of zebrafish via a cooperative mechanism. *Cell Rep* 2018; 24:3146–3155.e3

20. Sakai C, Ijaz S, Hoffman EJ: Zebrafish models of neurodevelopmental disorders: Past, present, and future. *Front Mol Neurosci* 2018; 11:294
21. Duncan KM, Mukherjee K, Cornell RA, Liao EC: Zebrafish models of orofacial clefts. *Dev Dyn* 2017; 246:897–914
22. Westerfield M: *The Zebrafish Book. A Guide for the Laboratory Use of Zebrafish (Danio rerio)*, 5th Edition, University of Oregon Press, Eugene, Oregon, 2007
23. von Hofsten J, Olsson PE: Zebrafish sex determination and differentiation: involvement of FTZ-F1 genes. *Reprod Biol Endocrinol* 2005; 3:63
24. Nourmahnad A, Stern AT, Hotta M, Stewart DS, Ziemba AM, Szabo A, Forman SA: Tryptophan and cysteine mutations in M1 helices of $\alpha 1\beta 3\gamma 2L$ γ -aminobutyric acid type A receptors indicate distinct intersubunit sites for four intravenous anesthetics and one orphan site. *ANESTHESIOLOGY* 2016; 125:1144–58
25. Labun K, Montague TG, Gagnon JA, Thyme SB, Valen E: CHOPCHOP v2: A web tool for the next generation of CRISPR genome engineering. *Nucleic Acids Res* 2016; 44(W1):W272–6
26. Talbot JC, Amacher SL: A streamlined CRISPR pipeline to reliably generate zebrafish frameshifting alleles. *Zebrafish* 2014; 11:583–5
27. Meeker ND, Hutchinson SA, Ho L, Trede NS: Method for isolation of PCR-ready genomic DNA from zebrafish tissues. *Biotechniques* 2007; 43:610, 612, 614
28. Li EB, Truong D, Hallett SA, Mukherjee K, Schutte BC, Liao EC: Rapid functional analysis of computationally complex rare human IRF6 gene variants using a novel zebrafish model. *PLoS Genet* 2017; 13:e1007009
29. Woollorton JR, Moss SJ, Smart TG: Pharmacological and physiological characterization of murine homomeric beta3 GABA(A) receptors. *Eur J Neurosci* 1997; 9:2225–35
30. Cestari IN, Min KT, Kulli JC, Yang J: Identification of an amino acid defining the distinct properties of murine beta1 and beta3 subunit-containing GABA(A) receptors. *J Neurochem* 2000; 74:827–38
31. Walker MB, Kimmel CB: A two-color acid-free cartilage and bone stain for zebrafish larvae. *Biotech Histochem* 2007; 82:23–8
32. Colwill RM, Creton R: Locomotor behaviors in zebrafish (*Danio rerio*) larvae. *Behav Processes* 2011; 86:222–9
33. Schnörr SJ, Steenbergen PJ, Richardson MK, Champagne DL: Measuring thigmotaxis in larval zebrafish. *Behav Brain Res* 2012; 228:367–74
34. Hentze MW, Kulozik AE: A perfect message: RNA surveillance and nonsense-mediated decay. *Cell* 1999; 96:307–10
35. Liljelund P, Ferguson C, Homanics G, Olsen RW: Long-term effects of diazepam treatment of epileptic GABAA receptor beta3 subunit knockout mouse in early life. *Epilepsy Res* 2005; 66:99–115
36. Simon P, Dupuis R, Costentin J: Thigmotaxis as an index of anxiety in mice. Influence of dopaminergic transmissions. *Behav Brain Res* 1994; 61:59–64
37. Treit D, Fundytus M: Thigmotaxis as a test for anxiolytic activity in rats. *Pharmacol Biochem Behav* 1988; 31:959–62
38. Winter MJ, Redfern WS, Hayfield AJ, Owen SF, Valentin JP, Hutchinson TH: Validation of a larval zebrafish locomotor assay for assessing the seizure liability of early-stage development drugs. *J Pharmacol Toxicol Methods* 2008; 57:176–87
39. Baraban SC, Taylor MR, Castro PA, Baier H: Pentylentetrazole induced changes in zebrafish behavior, neural activity and c-fos expression. *Neuroscience* 2005; 131:759–68
40. Hagiwara N, Katarova Z, Siracusa LD, Brilliant MH: Nonneuronal expression of the GABA(A) beta3 subunit gene is required for normal palate development in mice. *Dev Biol* 2003; 254:93–101
41. Scapoli L, Martinelli M, Pezzetti F, Carinci F, Bodo M, Tognon M, Carinci P: Linkage disequilibrium between GABRB3 gene and nonsyndromic familial cleft lip with or without cleft palate. *Hum Genet* 2002; 110:15–20
42. Sanchis-Segura C, Cline B, Jurd R, Rudolph U, Spanagel R: Etomidate and propofol-hyposensitive GABAA receptor beta3(N265M) mice show little changes in acute alcohol sensitivity but enhanced tolerance and withdrawal. *Neurosci Lett* 2007; 416:275–8
43. Ziemba AM, Szabo A, Pierce DW, Haburcak M, Stern AT, Nourmahnad A, Halpin ES, Forman SA: Alphaxalone binds in inner transmembrane $\beta + / \alpha$ -interfaces of $\alpha 1\beta 3\gamma 2$ γ -Aminobutyric acid type A receptors. *ANESTHESIOLOGY* 2018; 128:338–51
44. Chiara DC, Jayakar SS, Zhou X, Zhang X, Savechenkov PY, Bruzik KS, Miller KW, Cohen JB: Specificity of intersubunit general anesthetic-binding sites in the transmembrane domain of the human $\alpha 1\beta 3\gamma 2$ γ -aminobutyric acid type A (GABAA) receptor. *J Biol Chem* 2013; 288:19343–57
45. Szabo A, Nourmahnad A, Halpin E, Forman SA: Monod-Wyman-Changeux allosteric shift analysis in mutant $\alpha 1\beta 3\gamma 2L$ GABAA receptors indicates selectivity and crosstalk among intersubunit transmembrane anesthetic sites. *Mol Pharmacol* 2019; 95:408–17
46. Amlong CA, Perkins MG, Houle TT, Miller KW, Pearce RA: Contrasting effects of the γ -aminobutyric acid type A receptor $\beta 3$ subunit N265M mutation on loss of righting reflexes induced by etomidate and the novel anesthetic barbiturate R-mTFD-MPAB. *Anesth Analg* 2016; 123:1241–6
47. Mihalek RM, Banerjee PK, Korpi ER, Quinlan JJ, Firestone LL, Mi ZP, Lagenaur C, Tretter V, Sieghart W,

- Anagnostaras SG, Sage JR, Fanselow MS, Guidotti A, Spigelman I, Li Z, DeLorey TM, Olsen RW, Homanics GE: Attenuated sensitivity to neuroactive steroids in gamma-aminobutyrate type A receptor delta subunit knock-out mice. *Proc Natl Acad Sci USA* 1999; 96:12905–10
48. Kokel D, Cheung CY, Mills R, Coutinho-Budd J, Huang L, Setola V, Sprague J, Jin S, Jin YN, Huang XP, Bruni G, Woolf CJ, Roth BL, Hamblin MR, Zylka MJ, Milan DJ, Peterson RT: Photochemical activation of TRPA1 channels in neurons and animals. *Nat Chem Biol* 2013; 9:257–63
 49. Cocco A, Rönnerberg AM, Jin Z, André GI, Vossen LE, Bhandage AK, Thörnqvist PO, Birnir B, Winberg S: Characterization of the γ -aminobutyric acid signaling system in the zebrafish (*Danio rerio* Hamilton) central nervous system by reverse transcription-quantitative polymerase chain reaction. *Neuroscience* 2017; 343:300–21
 50. Zhang Y, Qin W, Lu X, Xu J, Huang H, Bai H, Li S, Lin S: Programmable base editing of zebrafish genome using a modified CRISPR–Cas9 system. *Nat Commun* 2017; 8:118
 51. Chen X, Shu S, Bayliss DA: HCN1 channel subunits are a molecular substrate for hypnotic actions of ketamine. *J Neurosci* 2009; 29:600–9

ANESTHESIOLOGY REFLECTIONS FROM THE WOOD LIBRARY-MUSEUM

Dr. John D. Thomas's Advertising Folder: 154,000 Nitrous-Oxide Anesthetics



From the Wood Library–Museum’s Ben Z. Swanson Collection, the images above were extracted from a folder advertising the anesthetic prowess of John D. Thomas, D.D.S. (1850 to 1931). Dr. Thomas had assumed command of Philadelphia’s “Colton Dental Rooms” after his dental preceptor and older brother, Frank, had passed away suddenly in 1875. That “original office” was on Walnut Street in Philadelphia. The main purpose of this one-sheet, four-page folder was to trumpet Dr. Thomas’s claim that he had administered 154,000 nitrous-oxide anesthetics “without a single failure or accident.” (Copyright © the American Society of Anesthesiologists’ Wood Library–Museum of Anesthesiology.)

George S. Bause, M.D., M.P.H., Honorary Curator and Laureate of the History of Anesthesia, Wood Library–Museum of Anesthesiology, Schaumburg, Illinois, and Clinical Associate Professor, Case Western Reserve University, Cleveland, Ohio. UJYC@aol.com.

ANESTHESIOLOGY

Hydrocortisone Compared with Placebo in Patients with Septic Shock Satisfying the Sepsis-3 Diagnostic Criteria and APROCCHSS Study Inclusion Criteria

A *Post Hoc* Analysis of the ADRENAL Trial

Balasubramanian Venkatesh, M.D., Simon Finfer, M.D., Jeremy Cohen, M.D., Ph.D., Dorrilyn Rajbhandari, R.N., Yaseen Arabi, M.D., Rinaldo Bellomo, M.D., Laurent Billot, M.Sc., Parisa Glass, Ph.D., Christopher Joyce, M.D., Ph.D., Qiang Li, M.Biostat., Colin McArthur, M.D., Anders Perner, M.D., Ph.D., Andrew Rhodes, M.D., Kelly Thompson, R.N., M.P.H., Steve Webb, M.D., Ph.D., John Myburgh, M.D., Ph.D.

ANESTHESIOLOGY 2019; 131:1292–300

EDITOR'S PERSPECTIVE

What We Already Know about This Topic

- Definitions and management strategies for septic shock continue to be updated as defined in Sepsis-2, Sepsis-3, and other guidelines
- Recent randomized controlled trials of corticosteroids in septic shock report different treatment effects on 90-day mortality but use different inclusion criteria

What This Article Tells Us That Is New

- In a *post hoc* analysis of the Adjunctive Glucocorticoid Therapy in Patients with Septic Shock (ADRENAL) trial, in participants who fulfilled either the Sepsis-3 or -2 inclusion criteria or those with severe septic shock, a continuous infusion of hydrocortisone did not result in a lower 90-day mortality than placebo

ABSTRACT

Background: Two recent randomized controlled trials (Adjunctive Glucocorticoid Therapy in Patients with Septic Shock [ADRENAL] and Activated Protein C and Corticosteroids for Human Septic Shock [APROCCHSS]) of corticosteroids in patients with septic shock reported different treatment effects on 90-day mortality. Both trials enrolled patients who met the criteria for septic shock using the second international consensus definitions for sepsis and septic shock (Sepsis-2), but the APROCCHSS trial mandated a greater severity of shock as an inclusion criterion.

Methods: The authors conducted *post hoc* sensitivity analyses of the ADRENAL trial to determine the effects of hydrocortisone *versus* placebo in subgroups selected using third international consensus definitions for sepsis and septic shock (Sepsis-3) diagnostic criteria or APROCCHSS inclusion criteria.

Results: There were 1,950 subjects (973 hydrocortisone and 977 placebo) who met the Sepsis-3 criteria (ADRENAL–Sepsis-3 cohort) and 905 patients (455 hydrocortisone and 450 placebo) who met the APROCCHSS criteria (ADRENAL–APROCCHSS cohort). At 90 days after randomization, in the ADRENAL–Sepsis-3 cohort, 312 of 963 (32.4%) and 337 of 958 (35.2%) patients assigned to hydrocortisone and placebo, respectively, had died (odds ratio, 0.86; 95% CI, 0.70 to 1.06; $P = 0.166$). The corresponding figures for the ADRENAL–APROCCHSS cohorts were 187 of 453 (41.3%) and 200 of 445 (44.9%), respectively (odds ratio, 0.84; 95% CI, 0.60 to 1.17; $P = 0.303$). There was no statistically significant difference in the time to death between the groups during the 90 days after randomization (hazard ratio = 0.87; 95% CI, 0.75 to 1.02; $P = 0.082$ for ADRENAL–Sepsis-3; and hazard ratio = 0.86; 95% CI, 0.71 to 1.06; $P = 0.156$ for ADRENAL–APROCCHSS cohorts). In both cohorts, patients assigned to hydrocortisone had faster resolution of shock. In the ADRENAL–Sepsis-3 cohort, patients assigned to hydrocortisone had an increase in the number of days alive and free of mechanical ventilation (57.0 ± 37.2 vs. 53.7 ± 38.2 days; 95% CI, 0.40 to 7.04; $P = 0.028$) and the number of days alive and free of the intensive care unit (54.3 ± 36.0 vs. 51.0 ± 37.1 ; 95% CI, 0.82 to 7.24; $P = 0.014$).

Conclusions: In a *post hoc* analysis of the ADRENAL trial participants who fulfilled either the Sepsis-3 or the APROCCHSS inclusion criteria, a continuous infusion of hydrocortisone did not result in a lower 90-day mortality than placebo in septic shock.

(ANESTHESIOLOGY 2019; 131:1292–300)

Two recent large randomized controlled trials (Adjunctive Glucocorticoid Therapy in Patients with Septic Shock [ADRENAL] and Activated Protein C and Corticosteroids for Human Septic Shock [APROCCHSS]) have added substantial new data to inform opinion regarding the use of corticosteroids in patients with septic shock.^{1,2} The ADRENAL trial (N = 3,800) investigated the role of 200 mg per day of hydrocortisone by infusion for 7 days compared with placebo and reported no significant difference between groups with

This article is featured in "This Month in Anesthesiology," page 1A. This article has a visual abstract available in the online version. Supplemental Digital Content is available for this article. Direct URL citations appear in the printed text and are available in both the HTML and PDF versions of this article. Links to the digital files are provided in the HTML text of this article on the Journal's Web site (www.anesthesiology.org).

Copyright © 2019, the American Society of Anesthesiologists, Inc. All Rights Reserved. Anesthesiology 2019; 131:1292–300. DOI: 10.1097/ALN.0000000000002955

respect to 90-day mortality (27.9% *vs.* 28.8%), but patients assigned to hydrocortisone had earlier shock reversal and liberation from mechanical ventilation.¹ The trial used the second international consensus definitions for sepsis and septic shock (Sepsis-2)³ and additionally mandated a minimum duration of 4 h of vasopressor therapy and the need for mechanical ventilation to be eligible for enrollment.

In 2016, subsequent to the commencement of the ADRENAL trial, a third international task force provided an updated consensus definition of sepsis and septic shock, termed Sepsis-3.⁴ It is unclear whether the use of Sepsis-3 criteria for enrolling patients into the ADRENAL trial would have influenced the trial results and resulted in different conclusions.

The APROCCHSS trial² (N = 1,241) examined the effect of 200 mg per day of hydrocortisone administered in divided doses, combined with oral fludrocortisone compared with placebo in patients with severe septic shock and reported improved 90-day mortality in the steroid group (43.0% *vs.* 49.1%), coupled with earlier shock reversal and liberation from mechanical ventilation. The two trials differed with respect to trial design, inclusion–exclusion criteria, mode of administration of hydrocortisone (infusion *vs.* bolus), and use of fludrocortisone. Attention has focused on the inclusion criteria of the two trials and whether the different treatment effect was because of a sicker cohort of patients in the APROCCHSS group.

We hypothesized that hydrocortisone may have beneficial effects on mortality in the sicker cohort of patients with septic shock. We therefore conducted *post hoc* subgroup analyses of the ADRENAL trial to determine whether the application of the Sepsis-3 or the APROCCHSS inclusion criteria to the study population would have resulted in different treatment effects between the hydrocortisone and the placebo groups.

Materials and Methods

Study Design and Research

We conducted a *post hoc* analysis of the ADRENAL database to identify patient cohorts who met Sepsis-3

criteria (ADRENAL–Sepsis-3) for septic shock or the APROCCHSS (ADRENAL–APROCCHSS) inclusion criteria. A detailed description of the study methods, outcomes, statistical analysis, and the results for the ADRENAL trial has already been published.⁵ In brief, the ADRENAL trial enrolled mechanically ventilated patients with septic shock who required a minimum duration of 4 h of vasopressor therapy. The APROCCHSS trial enrolled patients with septic shock with organ failure criteria and who required a minimum duration of 6 h of vasopressor therapy and doses of norepinephrine of $0.25 \mu\text{g} \cdot \text{kg}^{-1} \cdot \text{min}^{-1}$. The key aspects of and the differences in the inclusion–exclusion criteria and interventions for the ADRENAL and APROCCHSS trials are listed in Supplemental Digital Content 1 (<http://links.lww.com/ALN/C48>). To identify patients for inclusion in the analyses, we performed two separate interrogations of the ADRENAL database as outlined below.

ADRENAL–Sepsis-3 Analysis. Patients were selected using the following criteria: subjects who had (1) a mean arterial pressure (MAP) of less than 65 mmHg in the 24 h preceding randomization and (2) a plasma lactate concentration of more than 2 mmol.

ADRENAL–APROCCHSS Analysis. Patients were selected using the following criteria: patients receiving (1) more than $0.25 \mu\text{g} \cdot \text{kg}^{-1} \cdot \text{min}^{-1}$ of catecholamines at baseline and (2) any one of the following criteria for organ failure: partial pressure of arterial oxygen tension/fraction of inspired oxygen concentration ratio less than 200, or platelets less than $50 \times 10^9/\text{l}$, or bilirubin more than $102 \mu\text{mol/l}$, or creatinine of more than $300 \mu\text{mol/l}$.

Statistical Analysis and Outcome Measures

Of the original cohort of 3,800 patients, 1,950 met the Sepsis-3 criteria, and 905 met the APROCCHSS criteria. We determined that a sample size of 1,950 in the ADRENAL–Sepsis-3 cohort provided 90% power to detect an absolute difference of 7% and 80% power to detect an absolute difference of 6%, assuming 35% mortality rate in control group. In the ADRENAL–APROCCHSS cohort, a sample size of 905 provided 90% power to detect an absolute difference of 11% and 80% power to detect an absolute difference of 9%, assuming a baseline mortality of 45%. We applied the same statistical methods as described in the original ADRENAL trial and used the same set of primary and secondary outcomes. For the primary outcome of mortality at day 90, to account for stratification variables, the main analysis was performed using logistic regression with treatment allocation and admission type (medical or surgical) as fixed effects and trial site as a random effect. For secondary binary and continuous outcomes, logistic regression and linear regression were used, respectively, depending on the type of outcomes, including treatment allocation and admission type as fixed effect and site as a random effect. These were described in detail in a statistical analysis plan published before database lock of the ADRENAL trial.⁵ All

Submitted for publication February 1, 2019. Accepted for publication July 16, 2019. From the George Institute for Global Health, Sydney, New South Wales, Australia (B.V., S.F., D.R., L.B., P.G., Q.L., K.T., J.M.); Princess Alexandra Hospital, University of Queensland, Brisbane, Queensland, Australia (B.V., C.J.); Wesley Hospital, Brisbane, Queensland, Australia (B.V.); University of New South Wales, Sydney, New South Wales, Australia (B.V., S.F., J.M.); Sydney Medical School, University of Sydney, Sydney, New South Wales, Australia (S.F.); Royal North Shore Hospital, Sydney, New South Wales, Australia (S.F.); Royal Brisbane and Women's Hospital, University of Queensland, Brisbane, Queensland, Australia (J.C.); King Abdulaziz Medical City, King Saud Bin Abdulaziz University for Health Sciences, Riyadh, Saudi Arabia (Y.A.); Austin and Repatriation Medical Center, Melbourne, Victoria, Australia (R.B.); the Department of Critical Care Medicine, Auckland City Hospital, Auckland, New Zealand (C.M.); Rigshospitalet, Copenhagen, Denmark (A.P.); St. George's Hospital, London, United Kingdom (A.R.); Royal Perth Hospital, Perth, Western Australia, Australia (S.W.); University of Western Australia, School of Medicine and Pharmacology, Perth, Western Australia (S.W.); and St. George Hospital, University of New South Wales, Sydney, New South Wales (J.M.).

tests were conducted with statistical significant level of 0.05 (type 1 error), and significant test results are hypothesis-generating. No adjustments for multiplicity of testing were applied, but significant test results were interpreted in light of the multiple comparisons made.

We also applied the analytical methods as reported in the APROCCHSS article⁶ on the ADRENAL–APROCCHSS cohort to assess the treatment effect on the primary outcome, using relative risk without adjustment of stratification factor and trial site. We also performed survival analysis of time to death using same approach as described for the ADRENAL trial. Time to death was reported using Kaplan–Meier plots with differences in survival tested using a Cox proportional hazard model⁷ including the randomized treatment arm, admission type, and a random-center effect. Proportional hazard assumptions were tested by adding the interaction term between time and treatment in the Cox regression model. We used SAS Enterprise Guide 7.15 software for statistical analysis (SAS institute, Australia).

Results

Of the original cohort of 3,800 patients in ADRENAL, there were 1,950 (51.3%) subjects who met the Sepsis-3 criteria: 973 assigned to hydrocortisone and 977 assigned to placebo. Of these subjects, 905 (23.8%) patients met the APROCCHSS criteria: 455 assigned to hydrocortisone and 450 assigned to placebo. The patient flow chart is shown in Supplemental Digital Content 2 (<http://links.lww.com/ALN/C49>).

The baseline characteristics of all ADRENAL participants as well as the cohorts meeting Sepsis-3 and APROCCHSS criteria are reported in table 1. The three groups were similar at baseline with respect to demographic characteristics, admission diagnoses, sources of sepsis, baseline interventions, and illness severity. Patients in the ADRENAL–Sepsis-3 and ADRENAL–APROCCHSS cohorts had higher mean baseline plasma lactate concentration than the original ADRENAL cohort. There was higher proportion of medical admissions and more patients treated with renal replacement therapy at baseline in the ADRENAL–APROCCHSS cohort than in the ADRENAL cohort.

Outcomes

Primary Outcome. At 90 days after randomization, in the ADRENAL–Sepsis-3 cohort, 312 of 963 (32.4%) of the patients assigned to hydrocortisone and 337 of 958 (35.2%) of the patients assigned to placebo had died (odds ratio, 0.86; 95% CI, 0.70 to 1.06; $P = 0.166$; table 2). The corresponding figures for the ADRENAL–APROCCHSS cohorts were 187 of 453 (41.3%) and 200 of 445 (44.9%), respectively, for hydrocortisone and the placebo groups (odds ratio, 0.84; 95% CI, 0.60 to 1.17; $P = 0.303$). We conducted an additional *post hoc* analysis of the primary outcome in the ADRENAL–APROCCHSS cohort who were randomized after 6 h of vasopressor therapy. Of the 905

patients in the ADRENAL–APROCCHSS, 730 patients were randomized after 6 h of pressor therapy (365 in each group). The 90-day mortality rates were 42% (153 of 365) and 46.1% (168 of 365) in the hydrocortisone and placebo groups, respectively (odds ratio, 0.83; 95% CI, 0.60 to 1.16; $P = 0.306$). When the original ADRENAL data and the ADRENAL–APROCCHSS cohorts were analyzed using the APROCCHSS approach as rate ratios, there were no statistically significant differences in the primary outcome between the treatment groups (Supplemental Digital Content 1, <http://links.lww.com/ALN/C48>). There was no statistically significant difference in the time to death between the groups during the 90 days after randomization (hazard ratio = 0.87; 95% CI, 0.75 to 1.02; $P = 0.082$ for the ADRENAL–Sepsis-3 cohort; and hazard ratio = 0.86; 95% CI, 0.71 to 1.06; $P = 0.156$ for the ADRENAL–APROCCHSS cohort; figs. 1 and 2).

Secondary Outcomes.

ADRENAL–Sepsis-3. There was a statistically significant difference in day-28 mortality between the two groups 26.7% (259 of 969) *versus* 31% (300 of 968) in the hydrocortisone and placebo groups, respectively (odds ratio, 0.80; 95% CI, 0.64 to 0.99; $P = 0.042$). Patients assigned to hydrocortisone had faster resolution of shock (median [interquartile range], 3 [2 to 6] *vs.* 5 [3 to 12] days; hazard ratio = 1.36; 95% CI, 1.23 to 1.50; $P < 0.0001$), a higher frequency of recurrence of shock (22.1% [214 of 970] *vs.* 17.4% [170 of 977]; odds ratio, 1.35; 95% CI, 1.08 to 1.69; $P = 0.009$), an increase in the number of days alive and free of mechanical ventilation (57.0 ± 37.2 *vs.* 53.7 ± 38.2 days; 95% CI, 0.40 to 7.04; $P = 0.028$), an increase in the number of days alive and free of renal replacement therapy (60.9 ± 38.2 *vs.* 57.2 ± 39.6 days; 95% CI, 0.57 to 7.43; $P = 0.022$), and an increase in the number of days alive and free of the intensive care unit (54.3 ± 36.0 *vs.* 51.0 ± 37.1 ; 95% CI, 0.82 to 7.24; $P = 0.014$). There were no significant differences with respect to the development of new onset bacteremia or fungemia, in the proportions of patients requiring blood transfusions, in days alive and out of hospital, or in time to hospital discharge between the groups.

ADRENAL–APROCCHSS. There was no statistically significant difference in day-28 mortality between the two groups (36.6% [166 of 454] *vs.* 40.3% [181 of 449] in the hydrocortisone and placebo groups, respectively; odds ratio, 0.84; 95% CI, 0.62 to 1.13; $P = 0.251$). Patients assigned to hydrocortisone had a faster resolution of shock (median [interquartile range], 4 [3 to 41] *vs.* 7 [3 to unavailable value] days; hazard ratio = 1.27; 95% CI, 1.09 to 1.48; $P = 0.002$) but a higher frequency of recurrence of shock (23.3% [106 of 455] *vs.* 16.2% [73 of 450]; odds ratio, 1.57; 95% CI, 1.12 to 2.18; $P = 0.008$).

There were no statistically significant differences with respect to the number of days alive and free of

Table 1. Baseline Patient Characteristics

Characteristic	ADRENAL		ADRENAL (Sepsis-3)		ADRENAL-APROCHSS		APROCHSS	
	Hydrocortisone (N = 1,853)	Placebo (N = 1,860)	Hydrocortisone (N = 973)	Placebo (N = 977)	Hydrocortisone (N = 455)	Placebo (N = 450)	Hydrocortisone (N = 614)	Placebo (N = 627)
Age, yr	62 ± 15	63 ± 15	62 ± 15	64 ± 15	63 ± 14	62 ± 15.0	66 ± 14	66 ± 15
Male sex	1,119/1,853 (60.4)	1,140/1,860 (61.3)	558/973 (57.3%)	577/977 (59.1%)	271/455 (59.6%)	266/450 (59.1%)	402/614 (65.5%)	424/626 (67.7%)
Weight, kg	85.8 ± 26.6	85.6 ± 26.3	84.9 (26.58)	84.4 (25.59)	79.9 ± 22.4	78.7 ± 22.1	74 ± 19	75 ± 20
Admission type								
Medical	1,273/1,849 (68.8)	1,266/1,857 (68.2)	676/973 (69.5%)	657/977 (67.2%)	355/455 (78.0%)	342/450 (76.0%)	495/601 (75.5%)	499/616 (81%)
Surgical	576/1,849 (31.2)	591/1,857 (31.8)	297/973 (30.5%)	320/977 (32.8%)	100/455 (22.0%)	108/450 (24.0%)	106/601 (24.5%)	117/616 (19%)
APACHE II (median IQR)	24.0 (19.0 to 29.0)	23.0 (18.0 to 29.0)	25.0 (20.0 to 30.0)	25.0 (20.0 to 30.0)	27.0 (22.0 to 31.0)	26.0 (22.0 to 31.0)	N/A	N/A
Baseline therapies								
Mechanical ventilation	1,845/1,849 (99.8)	1,855/1,857 (99.9)	970/973 (99.7%)	976/977 (99.9%)	454/455 (99.8%)	450/450 (100%)	567/614 (91.3%)	569/623 (92.3%)
Inotropes/vasopressors								
Norepinephrine	1,823/1,853 (98.4)	1,821/1,860 (97.9)	958/973 (98.5%)	962/977 (98.5%)	454/455 (99.8%)	450/450 (100%)	534/590 (90.5%)	552/595 (92.8%)
Vasopressin	280/1,853 (15.1)	321/1,860 (17.3)	196/973 (20.1%)	234/977 (24.0%)	120/455 (26.4%)	155/450 (34.4%)	0/577 (0.0%)	1/580 (0.2%)
Epinephrine	134/1,853 (7.2)	113/1,860 (6.1)	109/973 (11.2%)	94/977 (9.6%)	62/455 (13.6%)	51/450 (11.3%)	53/585 (9.1%)	58/582 (10.0%)
Others	157/1,853 (8.5)	173/1,860 (9.3)	85/973 (8.7%)	113/977 (11.6%)	47/455 (10.3%)	55/450 (12.2%)	86/584 (14.7%)	100/584 (17.1%)
Antimicrobials	1,817/1,848 (98.3)	1,821/1,857 (98.1)	956/972 (98.4%)	962/977 (98.5%)	446/454 (98.2%)	445/450 (98.9%)	595/614 (96.9%)	602/626 (96.2%)
Renal replacement therapy	228/1,849 (12.3)	242/1,857 (13.0)	136/973 (14.0%)	159/977 (16.3%)	97/455 (21.3%)	90/450 (20.0%)	161/596 (27.0%)	168/598 (28.1%)
Physiologic variables								
Heart rate, beats/min	96.0 ± 21.6	95.0 ± 20.9	100.2 ± 21.67	98.0 ± 21.63	105.5 ± 23	101.5 ± 21.6	N/A	N/A
MAP, mmHg	72.5 ± 8.2	72.2 ± 8.3	71.6 ± 8.4	71.0 ± 8.2	71.0 ± 8.6	71.0 ± 8.8	N/A	N/A
CVP, mmHg	12.0 ± 5.2	12.1 ± 5.3	12.1 ± 5.3	12.6 ± 5.5	12.6 ± 5.5	12.8 ± 5.5	N/A	N/A
Lowest MAP	57.3 ± 8.5	57.1 ± 9.1	53.9 ± 7.6	53.4 ± 8.4	55.4 ± 8.6	54.6 ± 9.8	N/A	N/A
Highest lactate, mmol/l	3.8 ± 3.2	3.8 ± 3.1	5.2 ± 3.4	5.0 ± 3.2	5.2 ± 4.0	5.2 ± 3.7	4.4 ± 5.2	4.3 ± 4.6
Highest bilirubin, mg/dl	1.7 ± 2.4	1.7 ± 2.4	2.0 ± 2.7	1.9 ± 2.9	1.9 ± 2.2	2.05 ± 3.3	N/A	N/A
Highest creatinine, mg/dl	2.2 ± 2.0	2.1 ± 1.7	2.3 ± 1.9	2.3 ± 1.6	2.7 ± 2.3	2.5 ± 2.0	N/A	N/A
Lowest PaO ₂ /FiO ₂	164.6 ± 91.3	166.4 ± 91.9	157.9 ± 89.2	160.1 ± 90.6	122.0 ± 60.6	126.3 ± 66.0	190 ± 100	197 ± 102
Highest white cell count, 10 ⁹ /l	17.4 ± 11.4	17.8 ± 14.7	17.5 ± 12.0	17.7 ± 15.9	17.2 ± 13.2	17.6 ± 19.9	N/A	N/A
Primary site of infection								
Pulmonary	623/1,844 (33.8)	677/1,854 (36.5)	289/970 (29.8%)	324/976 (33.2%)	169/453 (37.3%)	179/450 (39.8%)	373/614 (60.7%)	363/626 (58.0%)
Abdominal	477/1,844 (25.9)	467/1,854 (25.2)	221/970 (22.8%)	225/976 (23.1%)	83/453 (18.3%)	96/450 (21.3%)	74/614 (12.1%)	68/626 (10.9%)
Blood	316/1,844 (17.1)	325/1,854 (17.5)	185/970 (19.1%)	188/976 (19.3%)	93/453 (20.5%)	83/450 (18.4%)	225/614 (36.6%)	229/626 (36.6%)
Skin/soft tissue	137/1,844 (7.4)	116/1,854 (6.3)	72/970 (7.4%)	59/976 (6.0%)	21/453 (4.6%)	21/450 (4.7%)	23/626 (3.7%)	29/614 (4.7%)
Urinary	146/1,844 (7.9)	133/1,854 (7.2)	83/970 (8.6%)	74/976 (7.6%)	41/453 (9.1%)	27/450 (6.0%)	N/A	N/A
Others	145/1,844 (7.9)	136/1,854 (7.3)	52/970 (5.4%)	47/976 (4.8%)	21/453 (4.6%)	22/450 (4.9%)	11/614 (1.8%)	18/626 (2.9%)
ICU admission to randomization, h	26.1 ± 70.7	28.9 ± 72.8	20.0 ± 32.2	23.3 ± 51.4	19.8 ± 31.4	23.0 ± 36.6	72 ± 312	72 ± 312
Shock to randomization, h	20.9 ± 91.9	21.2 ± 83.4	21.5 ± 110.94	20.3 ± 83.3	24.0 ± 124.9	21.8 ± 102.3	N/A	N/A

Plus-minus values represent means ± standard deviations. The proportions are presented as numbers of subjects/denominator (percentage). Surgical admissions were defined as patients admitted to the ICU from the operating room or the recovery room. For the ADRENAL, ADRENAL-Sepsis-3, and ADRENAL-APROCHSS cohorts: (1) heart rate, MAP, and CVP values represent the most recent value preceding randomization; (2) lowest values for MAP and the ratio between arterial and inspired oxygen tension (PaO₂/FiO₂) and highest values for lactate, bilirubin, creatinine, and white blood cell counts were measured during 24 h before randomization; and (3) baseline therapies denote the value in the 24 h before randomization. The data from APROCHSS were those reported in the main article or in Supplemental Digital Content 1 (<http://links.lww.com/ALN/C48>). No significant differences between the groups were observed at baseline. To convert values for bilirubin to μmol/l, multiply by 17.1. To convert values for creatinine to μmol/l, multiply by 88.4.

ADRENAL, Adjuvant Glucocorticoid Therapy in Patients with Septic Shock trial; APROCHSS, Activated Protein C and Corticosteroids for Human Septic Shock trial; CVP, central venous pressure; ICU, intensive care unit; IQR, interquartile range; MAP, mean arterial pressure; N/A, not available (value not reported in the article and hence not available); Sepsis-3, third international consensus definitions for sepsis and septic shock.

Table 2. Primary Outcome Comparison: ADRENAL, ADRENAL–Sepsis-3 cohort, ADRENAL–APROCCHSS cohort, and APROCCHSS original

	Hydrocortisone	Placebo	Odds or Rate Ratio	95% CI	P Value
ADRENAL (original)	511/1,832 (27.9)	526/1,826 (28.8)	0.95*	0.82 to 1.10	0.504
ADRENAL–Sepsis-3	312/963 (32.4)	337/958 (35.2)	0.86*	0.70 to 1.06	0.166
ADRENAL–APROCCHSS	187/453 (41.3)	200/445 (44.9)	0.84*	0.60 to 1.17	0.303
APROCCHSS (original)	264/614 (43.0)	308/627 (49.1)	0.88†	0.78 to 0.99	0.03

The primary outcome was 90-day mortality (%) reported as odds ratios (using the statistical analytical methods described in the ADRENAL article^{1,5}). The proportions are presented as number of subjects/denominator (percentage). The analysis of mortality at day 90 reported in this table, adjusted for stratification variables is a logistic regression including treatment and admission type as fixed effects and study site as a random effect.

*Odds ratios. †Rate ratios.

mechanical ventilation, the number of days alive and free of renal replacement therapy, the number of days alive and free of the intensive care unit, the development of new onset bacteremia or fungemia, in the proportions of patients requiring blood transfusions, the number of days alive and out of hospital, or the time to hospital discharge between the groups. A comparison of the secondary outcomes of the Sepsis-3 and the APROCCHSS cohorts with those of the original ADRENAL and the APROCCHSS trial participants is outlined in table 3.

Discussion

In the subsets of patients from the ADRENAL trial who met the Sepsis-3 or APROCCHSS inclusion criteria, there was a higher overall mortality rate at day 90, but the administration of hydrocortisone did not result in a significantly lower mortality as compared with placebo. This is in line with the original trial results.

There was also concordance between the three cohorts in some of the secondary outcomes: earlier time to reversal

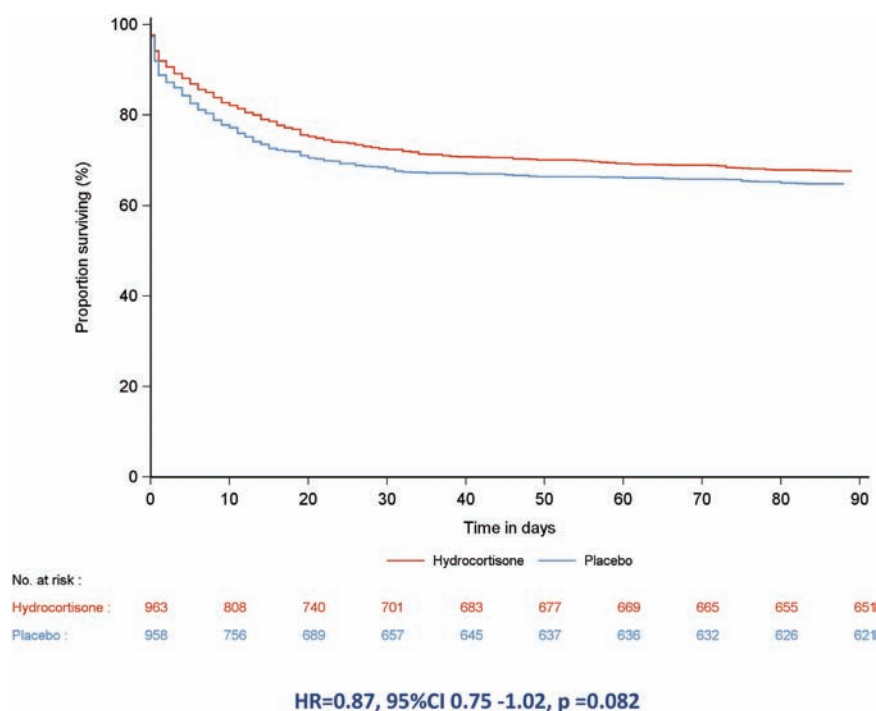


Fig. 1. Adjunctive Glucocorticoid Therapy in Patients with Septic Shock (ADRENAL) Sepsis-3: Probability of survival and risk of death at 90 days, according to subgroup. Shown are the Kaplan–Meier estimates of the probability of survival for patients receiving either hydrocortisone or placebo. The *P* value was calculated using a Cox proportional hazard model including the randomized treatment arm, admission type, and a random-center effect. HR, hazard ratio.

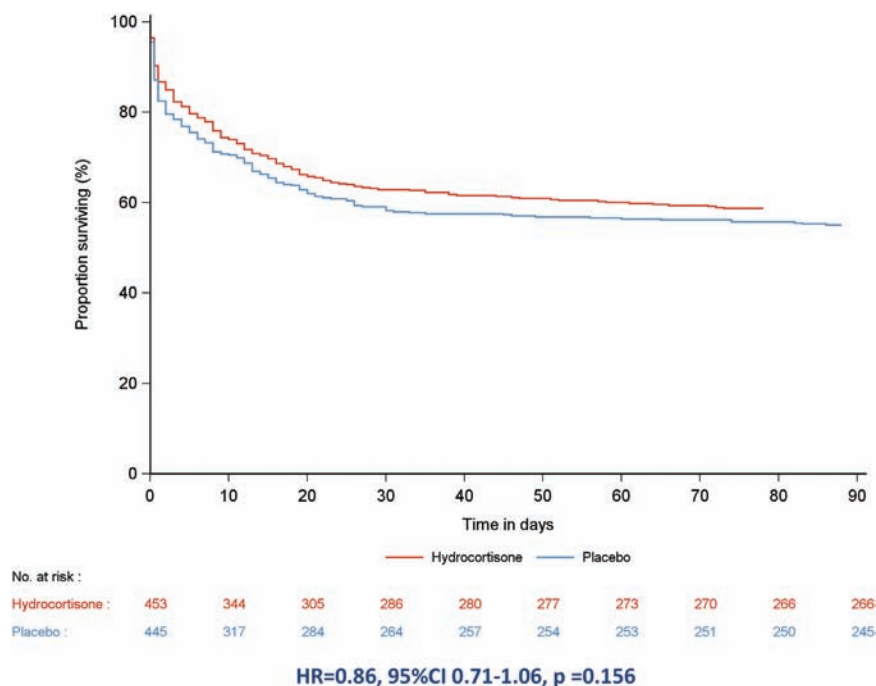


Fig. 2. Adjunctive Glucocorticoid Therapy in Patients with Septic Shock (ADRENAL)—Activated Protein C and Corticosteroids for Human Septic Shock (APROCCHSS): Probability of survival and risk of death at 90 days, according to subgroup. Shown are the Kaplan–Meier estimates of the probability of survival for patients receiving either hydrocortisone or placebo. The *P* value was calculated using a Cox proportional hazard model including the randomized treatment arm, admission type, and a random-center effect. HR, hazard ratio.

of shock with hydrocortisone, rate of recurrence of mechanical ventilation, days alive and out of hospital, and the rate of new-onset bacteremia or fungemia. In contrast to the original trial, patients in both subsets who received hydrocortisone had a higher rate of recurrence of shock, but there was no differential treatment effect on the blood transfusion rates. In patients meeting the Sepsis-3 criteria, those assigned to hydrocortisone had reduced 28-day mortality, an increase in the number of days alive and free of mechanical ventilation and renal replacement therapy, and an increase in the number of days alive and out of the intensive care unit.

Comparisons of Mortality among ADRENAL, ADRENAL–Sepsis-3, and ADRENAL–APROCCHSS

The day-90 mortality in the ADRENAL–Sepsis-3 cohort was 33.8% (about 4 percentage points higher than the original ADRENAL cohort) but substantially lower than that predicted by the task force.⁴ Of note, all the patients in the ADRENAL–Sepsis-3 cohort were mechanically ventilated, suggesting a higher degree of organ failure. Although a number of *post hoc* analyses of randomized controlled trials and registry data report mortality rates greater than 40% when Sepsis-3 criteria are applied,^{8–10} other data sets have also found lower than predicted mortality rates when applying the Sepsis-3 criteria.^{11–13}

The mortality rates for day 90 were comparable between the ADRENAL–APROCCHSS cohort and the original APROCCHSS cohort, although there was no different treatment effect between hydrocortisone and placebo in the ADRENAL. The other major difference between the ADRENAL and APROCCHSS was the use of fludrocortisone in the latter. It is unclear whether the use of fludrocortisone would be sufficient to explain the difference in survival. The only trial comparing hydrocortisone alone *versus* hydrocortisone plus fludrocortisone lacked adequate statistical power to identify a difference in mortality.¹⁴ There are several reasons to doubt that the addition of fludrocortisone to the treatment regime would confer any additional benefit. Because the mineralocorticoid receptor has an equal affinity for both mineralocorticoids and glucocorticoids, a daily dose of 50 mg or more of hydrocortisone is equivalent to 0.1 mg of fludrocortisone.¹⁵ Furthermore, the short plasma half-life (1.4 h) of fludrocortisone suggests that a single daily dose may not be optimal,¹⁶ and there is evidence to suggest that its oral absorption is impaired in critically ill patients.¹⁷

In both cohorts, similar to the original trial, shock reversal occurred earlier in the hydrocortisone group, but at variance with the original ADRENAL trial results was the observation that recurrence of shock was higher in the hydrocortisone group. This finding was not reported in either of the primary studies, is an observation

Table 3. Secondary Outcomes Comparison: ADRENAL, ADRENAL–Sepsis-3 Cohort, ADRENAL–APROCCCHSS Cohort, and APROCCCHSS Original

	Hydrocortisone	Placebo	Odds Ratio, Hazard Ratio, Rate Ratio, or Absolute difference	95% CI	P Value
28-day mortality					
ADRENAL (original)	410/1,841 (22.3)	448/1,840 (24.3)	0.89*	0.76 to 1.03	0.125
ADRENAL–Sepsis-3	259/969 (26.7%)	300/968 (31.0%)	0.80*	0.64 to 0.99	0.042
ADRENAL–APROCCCHSS	166/454 (36.6%)	181/449 (40.3%)	0.84*	0.62 to 1.13	0.251
APROCCCHSS (original)	207/614 (33.7)	244/627 (38.9)	0.87	0.75 to 1.01	0.06
Time to reversal of shock (days); median (IQR)					
ADRENAL (original)	3 (2–5)	4 (2–9)	1.32†	1.23 to 1.41	< 0.0001
ADRENAL–Sepsis-3	3 (2–6)	5 (3–12)	1.36†	1.23 to 1.50	< 0.0001
ADRENAL–APROCCCHSS	4.0 (3.0 to 41.0)	7.0 (3.0 to N/A)	1.27†	1.09 to 1.48	0.002
APROCCCHSS (original)	N/A	N/A	N/A	N/A	N/A
Recurrence of shock					
ADRENAL (original)	365/1,853 (19.7)	343/1,860 (18.4)	1.07*	0.94 to 1.22	0.319
ADRENAL–Sepsis-3	214/970 (22.1%)	170/977 (17.4%)	1.35	1.08 to 1.69	0.009
ADRENAL–APROCCCHSS	106/455 (23.3%)	73/450 (16.2%)	1.57	1.12 to 2.18	0.008
APROCCCHSS (original)	N/A	N/A	N/A	N/A	N/A
Days alive and free of ICU					
ADRENAL (original)	58.2 ± 34.8	56.0 ± 35.4	2.26‡	0.04 to 4.49	0.047
ADRENAL–Sepsis-3	54.3 ± 36.0	51.0 ± 37.1	4.03‡	0.82 to 7.24	0.014
ADRENAL–APROCCCHSS	45.9 ± 37.7	42.3 ± 37.7	4.20‡	−0.66 to 9.07	0.090
APROCCCHSS (original)	42 ± 38	38 ± 38	N/A	N/A	0.05
Days alive and free of hospital					
ADRENAL (original)	40.0 ± 32.0	38.6 ± 32.4	1.45‡	−0.59 to 3.49	0.164
ADRENAL–Sepsis-3	36.3 ± 31.9	34.8 ± 32.6	1.68	−1.16 to 4.52	0.245
ADRENAL–APROCCCHSS	31.6 ± 31.5	28.3 ± 31.1	3.67‡	−0.36 to 7.70	0.074
APROCCCHSS (original)	31 ± 33	29 ± 33	N/A	N/A	0.27
Days alive and free of mechanical ventilation					
ADRENAL (original)	61.2 ± 35.6	59.1 ± 36.1	2.18‡	−0.11 to 4.46	0.062
ADRENAL–Sepsis-3	57.0 ± 37.2	53.7 ± 38.2	3.72‡	0.40 to 7.04	0.028
ADRENAL–APROCCCHSS	48.5 ± 39.2	45.4 ± 39.1	3.78‡	−1.28 to 8.84	0.143
APROCCCHSS (original)	45 ± 39	40 ± 39	N/A	N/A	0.04
Recurrence of mechanical ventilation					
ADRENAL (original)	180/1,842 (9.8)	154/1,850 (8.3)	1.18*	0.96 to 1.45	0.113
ADRENAL–Sepsis-3	93/967 (9.6%)	71/974 (7.3%)	1.36*	0.98 to 1.88	0.063
ADRENAL–APROCCCHSS	38/455 (8.4%)	31/447 (6.9%)	1.22*	0.74 to 2.0	0.432
APROCCCHSS (original)	N/A	N/A	N/A	N/A	N/A
Days alive and free of RRT					
ADRENAL (original)	42.6 ± 39.1	40.4 ± 38.5	2.37‡	−2.00 to 6.75	0.294
ADRENAL–Sepsis-3	60.9 ± 38.2	57.2 ± 39.6	4.00‡	0.57 to 7.43	0.022
ADRENAL–APROCCCHSS	51.5 ± 40.6	49.5 ± 40.9	2.54‡	−2.73 to 7.82	0.344
APROCCCHSS (original)	N/A	N/A	N/A	N/A	N/A
Use of RRT					
ADRENAL (original)	567/1,853 (30.6)	609/1,860 (32.7)	0.94*	0.86 to 1.03	0.178
ADRENAL–Sepsis-3	350/969 (36.1%)	389/973 (40.0%)	0.83*	0.69 to 1.00	0.049
ADRENAL–APROCCCHSS	239/454 (52.6%)	217/447 (48.5%)	1.16*	0.89 to 1.52	0.275
APROCCCHSS (original)	N/A	N/A	N/A	N/A	N/A
New bacteremia or fungemia					
ADRENAL (original)	262/1,853 (14.1)	262/1,860 (14.1)	1.00*	0.86 to 1.16	0.957
ADRENAL–Sepsis-3	143/969 (14.8%)	135/972 (13.9%)	1.07*	0.82 to 1.39	0.616
ADRENAL–APROCCCHSS	66/455 (14.5%)	60/448 (13.4%)	1.13*	0.75 to 1.70	0.560
APROCCCHSS (original)	49/614 (8.0%)	48/626 (7.7%)	1.04	0.71 to 1.53	0.86
Blood transfusion					
ADRENAL (original)	683/1,848 (37.0)	773/1,855 (41.7)	0.82*	0.72 to 0.94	0.004
ADRENAL–Sepsis-3	393/973 (40.4%)	424/977 (43.4%)	0.89*	0.74 to 1.07	0.212
ADRENAL–APROCCCHSS	224/455 (49.2%)	205/450 (45.6%)	1.17*	0.90 to 1.52	0.246
APROCCCHSS (original)	N/A	N/A	N/A	N/A	N/A
180-day mortality					
ADRENAL (original)	571/1,812 (31.5%)	574/1,803 (31.8%)	0.99*	0.86 to 1.13	0.834
ADRENAL–Sepsis-3	349/959 (36.4%)	367/952 (38.6%)	0.89*	0.76 to 1.10	0.239
ADRENAL–APROCCCHSS	199/448 (44.4%)	211/441 (47.8%)	0.84*	0.64 to 1.11	0.220
APROCCCHSS (original)	285/611 (46.6%)	328/625 (52.5%)	0.89*	0.79 to 0.99	0.04

Plus-minus values represent means ± standard deviations. The proportions are presented as numbers of subjects/denominator (percentage). Median (IQR) values are presented for not normally distributed variables. The analysis of mortality at days 28 and 180 reported in this table, adjusted for stratification variables, is a logistic regression including treatment and admission type as fixed effects and study site as a random effect.

*Odds ratios; †Hazard ratios; ‡Mean absolute differences.

ADRENAL, Adjunctive Glucocorticoid Therapy in Patients with Septic Shock trial; APROCCCHSS, Activated Protein C and Corticosteroids for Human Septic Shock trial; ICU, intensive care unit; IQR, interquartile range; N/A, not available (value not reported in the main article or in the Supplemental Digital Content 1 [http://links.lww.com/ALN/C48] of the APROCCCHSS publication and hence not available); RRT, renal replacement therapy; Sepsis-3, third international consensus definitions for sepsis and septic shock.

originating from *post hoc* analyses, and may be regarded as hypothesis-generating.

Limitations

The Sepsis-3 task force stipulated three criteria for the diagnosis of septic shock: MAP of less than 65 mmHg, lactate of more than 2 mmol/L, and absence of hypovolemia. Volume status is difficult to assess in critically ill patients. Baseline filling pressures assessed by the central venous pressure was within normal limits in the Sepsis-3 cohort, and this was used as a surrogate for euvolemia. Our study was limited to patients who required a minimum of 4 h of vasopressor therapy and mechanical ventilator support, neither of which are required to meet the Sepsis-3 criteria for septic shock. Therefore, the number of eligible patients who would have met Sepsis-3 criteria may have been underestimated. Because a number of patients who were deemed to be in danger of imminent death or in whom death was deemed inevitable during the admission were excluded (which were not exclusions in the original Sepsis-3 validation cohort), the mortality in our cohort of patients meeting Sepsis-3 criteria may have been underestimated. Matching of the ADRENAL trial participants with the APROCCHSS cohort may not have been precise, because there were different duration requirements for pressor therapy for entry into the study. The APROCCHSS trial used 6 h of pressor therapy, as opposed to only 4 h in the ADRENAL trial. However, this is mitigated by the baseline equivalence of patients between the ADRENAL–APROCCHSS and original APROCCHSS trials. Moreover, the analysis of primary outcome in the cohort of patients in the ADRENAL–APROCCHSS group who were randomized after 6 h did not reveal a treatment effect. Another key difference between the two trials was the exclusion of patients who had received etomidate, a known adrenal suppressant, in the ADRENAL trial. Although the impact of this exclusion criterion could not be evaluated in this analysis, it is well recognized that the use of etomidate was a significant confounder in the interpretation of the results of two earlier trials of low dose steroids in septic shock.^{18,19} The absolute risk reduction of 3.6% in mortality in favor of hydrocortisone observed in the ADRENAL–APROCCHSS cohort may be considered as clinically significant, especially in the context of a safe and an inexpensive intervention, but the interpretation is limited by the lack of statistical significance, the *post hoc* nature of the analysis, and the reduced power due to the smaller sample size.

Conclusions

In the ADRENAL trial participants who fulfilled either the Sepsis-3 or the APROCCHSS inclusion criteria, a continuous infusion of hydrocortisone did not result in a significantly lower 90-day mortality than placebo in septic shock.

Research Support

Supported by National Health and Medical Research Council of Australia (Canberra, Australia) project grant Nos. 1004108 and 1124926 and Health Research Council of New Zealand (Auckland, New Zealand) project grant No. 12/206 to the ADRENAL study, which received indirect funding from the National Institute of Health Research (London, United Kingdom) after being adopted onto their research portfolio. Supported by a Practitioner Fellowship from Medical Research Future fund (Canberra, Australia; to Dr. Venkatesh) by Practitioner Fellowships from the National Health and Medical Research Council of Australia (to Drs. Bellomo, Finfer, and Myburgh).

Competing Interests

The authors declare no competing interests.

Correspondence

Address correspondence to Dr. Venkatesh: George Institute for Global Health, Sydney, New South Wales 2042, Australia. bvenkatesh@georgeinstitute.org.au. This article may be accessed for personal use at no charge through the Journal Web site, www.anesthesiology.org.

References

1. Venkatesh B, Finfer S, Cohen J, Rajbhandari D, Arabi Y, Bellomo R, Billot L, Correa M, Glass P, Harward M, Joyce C, Li Q, McArthur C, Perner A, Rhodes A, Thompson K, Webb S, Myburgh J; ADRENAL Trial Investigators and the Australian–New Zealand Intensive Care Society Clinical Trials Group: Adjunctive glucocorticoid therapy in patients with septic shock. *N Engl J Med* 2018; 378:797–808
2. Annane D, Renault A, Brun-Buisson C, Megarbane B, Quenot JP, Siami S, Cariou A, Forceville X, Schwebel C, Martin C, Timsit JF, Misset B, Ali Benali M, Colin G, Souweine B, Asehnoune K, Mercier E, Chimot L, Charpentier C, François B, Boulain T, Petitpas F, Constantin JM, Dhonneur G, Baudin F, Combes A, Bohé J, Loriferne JF, Amathieu R, Cook F, Slama M, Leroy O, Capellier G, Dargent A, Hissem T, Maxime V, Bellissant E; CRICS-TRIGGERSEP Network: Hydrocortisone plus fludrocortisone for adults with septic shock. *N Engl J Med* 2018; 378:809–18
3. Bone RC, Balk RA, Cerra FB, Dellinger RP, Fein AM, Knaus WA, Schein RM, Sibbald WJ: Definitions for sepsis and organ failure and guidelines for the use of innovative therapies in sepsis. *Chest* 1992; 101:1644–55
4. Shankar-Hari M, Phillips GS, Levy ML, Seymour CW, Liu VX, Deutschman CS, Angus DC, Rubenfeld GD, Singer M; Sepsis Definitions Task Force: Developing a new definition and assessing new clinical criteria for septic shock: For the third international consensus

- definitions for sepsis and septic shock (Sepsis-3). *JAMA* 2016; 315:775–87
5. Billot L, Venkatesh B, Myburgh J, Finfer S, Cohen J, Webb S, McArthur C, Joyce C, Bellomo R, Rhodes A, Perner A, Arabi Y, Rajbhandari D, Glass P, Thompson K, Correa M, Harward M: Statistical analysis plan for the Adjunctive Corticosteroid Treatment in Critically Ill Patients with Septic Shock (ADRENAL) trial. *Crit Care Resusc* 2017; 19:183–91
 6. Annane D, Buisson CB, Cariou A, Martin C, Misset B, Renault A, Lehmann B, Millul V, Maxime V, Bellissant E; APROCCHSS Investigators for the TRIGGERSEP Network: Design and conduct of the activated protein C and corticosteroids for human septic shock (APROCCHSS) trial. *Ann Intensive Care* 2016; 6:1–13
 7. Ripatti S, Palmgren J: Estimation of multivariate frailty models using penalized partial likelihood. *Biometrics* 2000; 56:1016–22
 8. Rygård SL, Holst LB, Wetterslev J, Johansson PI, Perner A; TRISS trial group; Scandinavian Critical Care Trials Group: Higher vs. lower haemoglobin threshold for transfusion in septic shock: Subgroup analyses of the TRISS trial. *Acta Anaesthesiol Scand* 2017; 61:166–75
 9. Demiselle J, Wepler M, Hartmann C, Radermacher P, Schortgen F, Meziani F, Singer M, Seegers V, Asfar P; HYPER2S investigators: Hyperoxia toxicity in septic shock patients according to the Sepsis-3 criteria: A post hoc analysis of the HYPER2S trial. *Ann Intensive Care* 2018; 8:90
 10. Shankar-Hari M, Harrison DA, Rubenfeld GD, Rowan K: Epidemiology of sepsis and septic shock in critical care units: Comparison between sepsis-2 and sepsis-3 populations using a national critical care database. *Br J Anaesth* 2017; 119:626–36
 11. Peake SL, Delaney A, Bailey M, Bellomo R; ARISE Investigators: Potential impact of the 2016 consensus definitions of sepsis and septic shock on future sepsis research. *Ann Emerg Med* 2017; 70:553–61.e1
 12. Sterling SA, Puskarich MA, Glass AF, Guirgis F, Jones AE: The impact of the Sepsis-3 septic shock definition on previously defined septic shock patients. *Crit Care Med* 2017; 45:1436–42
 13. Ryoo SM, Kang GH, Shin TG, Hwang SY, Kim K, Jo YH, Park YS, Choi SH, Yoon YH, Kwon WY, Suh GJ, Lim TH, Han KS, Choi HS, Chung SP, Kim WY; Korean Shock Society (KoSS) Investigators: Clinical outcome comparison of patients with septic shock defined by the new sepsis-3 criteria and by previous criteria. *J Thorac Dis* 2018; 10:845–53
 14. Annane D, Cariou A, Maxime V, Azoulay E, D'Honneur G, Timsit JF, Cohen Y, Wolf M, Fartoukh M, Adrie C, Santre C, Bollaert PE, Mathonet A, Amathieu R, Tabah A, Clec'h C, Mayaud J, Lejeune J, Chevret S: Corticosteroid treatment and intensive insulin therapy for septic shock in adults: A randomized controlled trial. *JAMA* 2010; 303:341–8
 15. Charmandari E, Kino T, Chrousos GP: *Glucocorticoids, Neonatal and Pediatric Pharmacology*, 4th edition. Edited by Yaffe SJ, Aranda JV. Philadelphia, Pennsylvania, Lippincott Williams and Wilkins; 2010, pp 760–72
 16. Hamitouche N, Comets E, Ribot M, Alvarez JC, Bellissant E, Laviolle B: Population pharmacokinetic–pharmacodynamic model of oral fludrocortisone and intravenous hydrocortisone in healthy volunteers. *AAPS J* 2017; 19:727–35
 17. Polito A, Hamitouche N, Ribot M, Polito A, Laviolle B, Bellissant E, Annane D, Alvarez JC: Pharmacokinetics of oral fludrocortisone in septic shock. *Br J Clin Pharmacol* 2016; 82:1509–16
 18. Annane D, Sébille V, Charpentier C, Bollaert PE, François B, Korach JM, Capellier G, Cohen Y, Azoulay E, Troché G, Chaumet-Riffaut P, Chaumet-Riffaut P, Bellissant E: Effect of treatment with low doses of hydrocortisone and fludrocortisone on mortality in patients with septic shock. *JAMA* 2002; 288:862–71
 19. Sprung CL, Annane D, Keh D, Moreno R, Singer M, Freivogel K, Weiss YG, Benbenishty J, Kalenka A, Forst H, Laterre PF, Reinhart K, Cuthbertson BH, Payen D, Briegel J; CORTICUS Study Group: Hydrocortisone therapy for patients with septic shock. *N Engl J Med* 2008; 358:111–24

ANESTHESIOLOGY

Sevoflurane Promotes Bactericidal Properties of Macrophages through Enhanced Inducible Nitric Oxide Synthase Expression in Male Mice

Thomas J. Gerber, M.D., Valérie C. O. Fehr, M.Med.,
Suellen D. S. Oliveira, Ph.D., Guochang Hu, M.D., Ph.D.,
Randal Dull, M.D., Ph.D., Marcelo G. Bonini, Ph.D.,
Beatrice Beck-Schimmer, M.D., Richard D. Minshall, Ph.D.

ANESTHESIOLOGY 2019; 131:1301–15

EDITOR'S PERSPECTIVE

What We Already Know about This Topic

- Sevoflurane has antiinflammatory properties, but less is known about effects on infectious inflammation
- Sevoflurane effects on macrophage function in inflammation are not well understood

What This Article Tells Us That Is New

- In a lipopolysaccharide model of inflammation, sevoflurane increased mouse macrophage nitric oxide synthase activity and bacteria phagocytosis *in vitro* and *in vivo*
- These effects were abolished by pharmacologically inhibiting nitric oxide synthase expression
- In endotoxemia in mice, sevoflurane had bactericidal effects

Modern volatile anesthetics such as sevoflurane have been shown to be protective in scenarios of ischemia-reperfusion injury in various organs including the heart,¹ kidney,² and liver.³ Furthermore, sevoflurane is known to have antiinflammatory properties as it reduces the inflammatory response associated with alveolar epithelial cells^{4,5} and decreases the activation of nuclear factor- κ B.^{6–12}

ABSTRACT

Background: Sevoflurane with its antiinflammatory properties has shown to decrease mortality in animal models of sepsis. However, the underlying mechanism of its beneficial effect in this inflammatory scenario remains poorly understood. Macrophages play an important role in the early stage of sepsis as they are tasked with eliminating invading microbes and also attracting other immune cells by the release of proinflammatory cytokines such as interleukin-1 β , interleukin-6, and tumor necrosis factor- α . Thus, the authors hypothesized that sevoflurane mitigates the proinflammatory response of macrophages, while maintaining their bactericidal properties.

Methods: Murine bone marrow–derived macrophages were stimulated *in vitro* with lipopolysaccharide in the presence and absence of 2% sevoflurane. Expression of cytokines and inducible NO synthase as well as uptake of fluorescently labeled *Escherichia coli* (*E. coli*) were measured. The *in vivo* endotoxemia model consisted of an intraperitoneal lipopolysaccharide injection after anesthesia with either ketamine and xylazine or 4% sevoflurane. Male mice ($n = 6$ per group) were observed for a total of 20 h. During the last 30 min fluorescently labeled *E. coli* were intraperitoneally injected. Peritoneal cells were extracted by peritoneal lavage and inducible NO synthase expression as well as *E. coli* uptake by peritoneal macrophages was determined using flow cytometry.

Results: *In vitro*, sevoflurane enhanced lipopolysaccharide-induced inducible NO synthase expression after 8 h by 466% and increased macrophage uptake of fluorescently labeled *E. coli* by 70% compared with vehicle-treated controls. Inhibiting inducible NO synthase expression pharmacologically abolished this increase in bacteria uptake. *In vivo*, inducible NO synthase expression was increased by 669% and phagocytosis of *E. coli* by 49% compared with the control group.

Conclusions: Sevoflurane enhances phagocytosis of bacteria by lipopolysaccharide-challenged macrophages *in vitro* and *in vivo* via an inducible NO synthase–dependent mechanism. Thus, sevoflurane potentiates bactericidal and antiinflammatory host-defense mechanisms in endotoxemia.

(ANESTHESIOLOGY 2019; 131:1301–15)

Nuclear factor- κ B, a well-known nuclear transcription factor, is seen as one of the key regulators for initiating an immune response toward inflammation. Inhalation of sevoflurane also appears to be beneficial during acute lung injury.^{13,14} Less is known about the effects of sevoflurane on infectious inflammation. Animal studies suggest favorable influences as sevoflurane improved survival in bacterial sepsis.^{15,16} This finding is particularly interesting because propofol, another commonly used anesthetic agent, showed adverse effects in infectious conditions, as exposure to

Part of the work presented in this article has been presented at the Swiss Society of Anesthesiology and Resuscitation Annual Conference in Basel, Switzerland, November 4, 2016; the College of Medicine Research Forum, University of Illinois at Chicago, Chicago, Illinois, November 18, 2016; and the International Anesthesia Research Society Annual Conference in Montreal, Quebec, Canada, May 21, 2019. T.J.G. and V.C.O.F. as first authors as well as B.B.S. and R.D.M. as last authors contributed equally to this article.

Submitted for publication December 6, 2018. Accepted for publication August 19, 2019. From the Departments Anesthesiology (T.J.G., V.C.O.F., S.D.S.O., G.H., R.D., B.B.-S., R.D.M.), Medicine (M.G.B.), and Pharmacology (R.D.M.), University of Illinois at Chicago, Chicago, Illinois; and Institute of Anesthesiology (V.C.O.F., B.B.-S.) and the Institute of Physiology and Zurich Center for Integrative Human Physiology (T.J.G., V.C.O.F., B.B.-S.), University of Zurich, Zurich, Switzerland.

Copyright © 2019, the American Society of Anesthesiologists, Inc. All Rights Reserved. Anesthesiology 2019; 131:1301–15. DOI: 10.1097/ALN.0000000000002992

propofol increased bacterial burden of infected animals¹⁷ and decreased survival in sepsis.¹⁶

Sevoflurane interacts with immune cells like neutrophils and decreases their adhesion to the endothelium^{18,19} as well as transmigration,²⁰ and reduces apoptosis.²¹ Only a few studies have investigated the effects of sevoflurane on other immune cells. Macrophages, as part of the innate immune system, are among the first to interact with microbial invaders and defend the host against pathogens. They are recruited to the site of infection and attract other immune cells by releasing proinflammatory cytokines such as interleukin-1 β , interleukin-6, and tumor necrosis factor- α .²² Invading microorganisms are eradicated when macrophages engulf them *via* phagocytosis, whereas bactericidal proteins such as inducible NO synthase are upregulated, leading to increased expression of NO.^{22,23} Antigens from eradicated pathogens are then presented to the adaptive immune system and a specific immune response can be initiated.^{24,25} Thus, macrophages play a pivotal role in restoring tissue homeostasis and overcoming inflammation.²³

We hypothesized that sevoflurane prevents macrophages from eliciting an exaggerated immune response by attenuating the expression of nuclear factor- κ B-dependent gene products, thereby contributing to sevoflurane's overall beneficial effect in severe inflammation. The first aim was thus to assess the inflammatory response of murine macrophages on stimulation with bacterial lipopolysaccharide in the presence and absence of sevoflurane. The second aim was to evaluate macrophage function under the influence of sevoflurane *in vitro* as well as *in vivo* in a lipopolysaccharide-induced endotoxemia model in mice.

Materials and Methods

Cell Culture

All cell culture procedures were conducted under sterile conditions in a laminar flow cabinet, with reagents warmed to 37°C before use, if not stated otherwise. Abelson murine leukemia virus-transformed macrophages from BALB/c mice (RAW) 264.7 cells (ATCC TIB-71), were cultured under standard cell culture conditions (37°C, 80% relative humidity and 5% carbon dioxide [CO₂]) in Dulbecco's Modified Eagle's Medium with 10% heat-inactivated fetal bovine serum (Gemini Bio-Products, USA), 1 U/ml penicillin, 100 μ M/ml streptomycin, and 1 mM sodium pyruvate (all from Thermo Fisher Scientific, USA). RAW 264.7 macrophages were used for nitrate measurement and degradation of nuclear factor- κ B inhibitor- α . All other *in vitro* experiments were conducted with murine bone marrow-derived macrophages.

Animals

After approval by the institutional ethical board, all animal procedures and experiments were conducted in accordance with the guidelines of the University of Illinois at Chicago Institutional Animal Care and Use Committee and Office

of Laboratory Animal Welfare (Chicago, Illinois). C57BL/6 mice were purchased from Jackson Laboratory (USA) and used in all experiments. Male C57BL/6 mice, 8–12 weeks old with a target weight of 25–30 g, were used. We only used male animals because hormonal changes occurring during the menstrual cycle could possibly have an impact on the experimental setup. Four animals were housed per cage. Animals had free access to food and water and were subjected to a 12-hr day and night cycle. Experiments were performed in the animal facility at the University of Illinois at Chicago. Anesthesia was either induced with an intraperitoneal injection of ketamine (100 mg/kg bodyweight, Hospira Inc., USA) and xylazine (10 mg/kg bodyweight, AKORN Animal Health, USA) or with 4% sevoflurane (Baxter, USA), corresponding to a 1.2 minimum alveolar concentration (MAC) in mice.¹⁵

Isolation of Murine Bone Marrow-derived Macrophages

Bone marrow-derived macrophages were isolated and differentiated as previously described.²⁶ After induction of anesthesia with ketamine/xylazine, mice were euthanized *via* exsanguination and removal of the heart. Thereafter, bone marrow cells from the femur and tibia were isolated and differentiated for 5–7 days in Roswell Park Memorial Institute containing 10% heat-inactivated fetal bovine serum (Gemini Bio-Products, West Sacramento, USA), 1% (volume/volume) Antibiotic-Antimycotic, 1 mM sodium pyruvate (both from Thermo Fisher Scientific, USA), and 10 to 15% L929 conditioned cell culture medium. For experimental procedures in six-well plates, macrophages were differentiated in the same plate. For experiments in other plates, bone marrow-derived macrophages were removed after 5–7 days with 5 mM EDTA (Sigma-Aldrich, USA) in Dulbecco's phosphate buffered saline and reseeded into the appropriate cell culture dish.

Experimental Exposure *In Vitro*

Cells were incubated with bacterial lipopolysaccharide from *Escherichia coli* (*E. coli*) serotype 055:B5 (Sigma-Aldrich, USA) at a concentration of 100 ng/ml for up to 24 h. Sevoflurane (Baxter, USA) was vaporized with a Penlon (USA) Sigma Elite vaporizer, and the cells were incubated in an airtight Oxoid chamber (Pratteln, Switzerland) for the entire time of lipopolysaccharide exposure. This time varied according to the endpoint (inflammatory mediators interleukin-1 β , interleukin-6, and tumor necrosis factor- α : mRNA 0–24 h, protein: 4–24 h; inducible NO synthase mRNA 0–24 h; inducible NO synthase protein 4 and 8 h; nitrite 24 h; nuclear factor- κ B inhibitor- α 0–90 min; extracellular signal-regulated kinase 8 h; bone marrow-derived macrophage *E. coli* uptake: *in vitro* 8 h *in vivo* experiments 20 h). A schematic illustration of the experimental setting is shown in figure 1.

For inducible NO synthase inhibition, the selective inducible NO synthase inhibitor 1400W (Calbiochem, USA) was used at a final concentration of 1 μ M. Sevoflurane

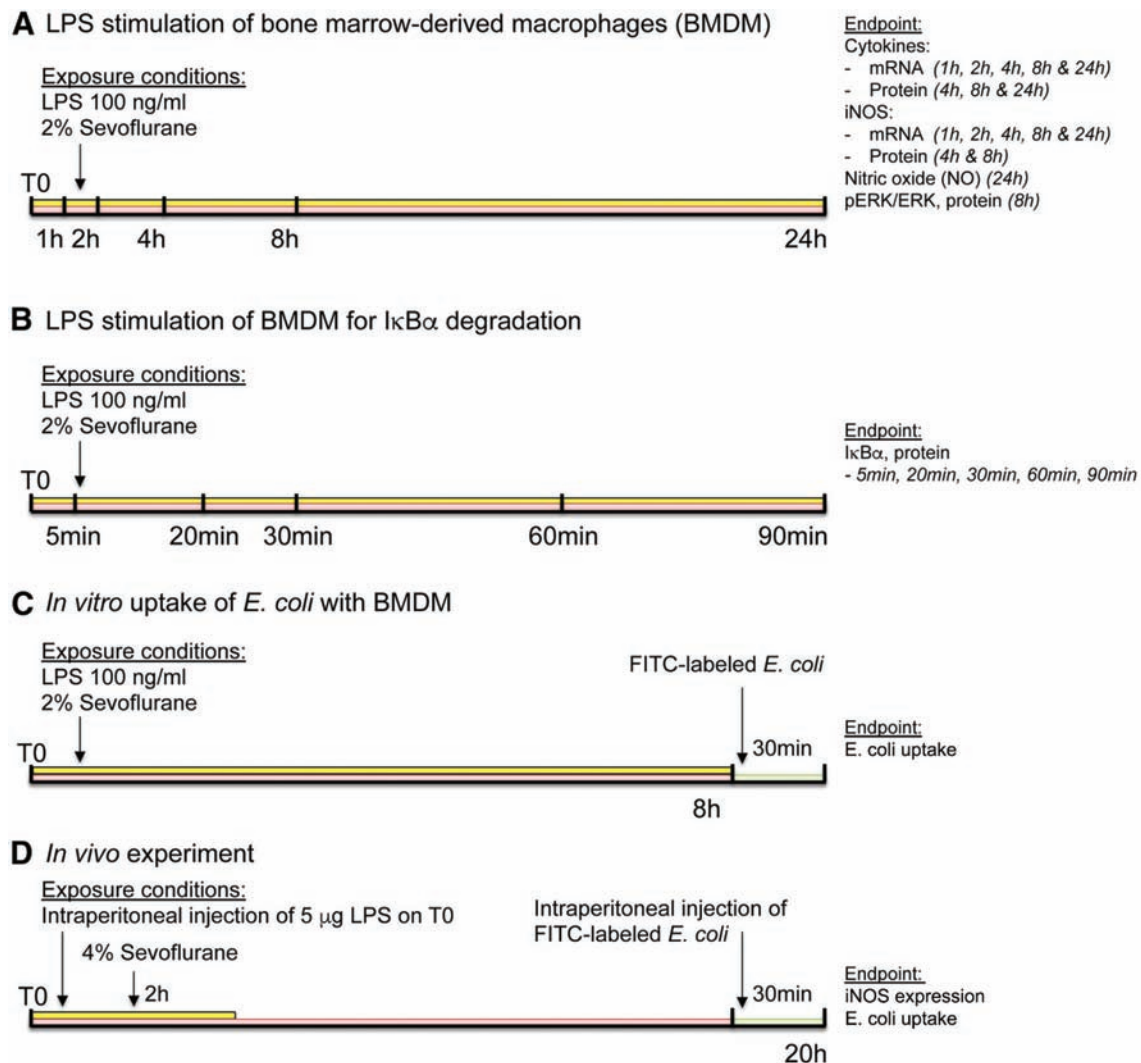


Fig. 1. Schematic illustration of the experimental setting. (A) Stimulation of bone marrow-derived macrophages (BMDM) with lipopolysaccharide (LPS) in the presence and absence of 2% sevoflurane. (B) Experimental setup for degradation of nuclear factor- κ B inhibitor- α (I κ B α). (C) *In vitro* uptake of fluorescein isothiocyanate (FITC)-labeled *Escherichia coli* (*E. coli*). (D) *In vivo* inducible NO synthase (iNOS) expression and uptake of FITC-labeled *E. coli* by murine peritoneal macrophages.

concentration in the outflowing air from the airtight chamber was measured with an E-CAiO gas analyzer and displayed on a CARESCAPE Monitor B650, both from GE Healthcare (USA). Sevoflurane was vaporized in synthetic air with 5% CO₂ (21% O₂, 74% N₂, and 5% CO₂).

Quantitative Real-time Polymerase Chain Reaction Analysis

Total RNA was isolated from bone marrow-derived macrophages with TRIzol reagent (Invitrogen, USA) following the manufacturer's protocol. After RNA purification, 1 μg RNA was used to produce cDNA using the high-capacity cDNA reverse transcription kit (Applied Biosystems, USA). Quantitative real-time polymerase chain reaction was performed with Fast SYBR green master mix (Applied

Biosystems, USA) on a ViiA 7 real-time polymerase chain reaction system (Applied Biosystems). The following primers were used: interleukin-1 β forward primer 5'-TTC CCA TTA GAC AAC TGC ACT AC-3' and reverse primer 5'-GTC GTT GCT TGG TTC TCC TT-3'; interleukin-6 forward primer 5'-CAC AAG TCC GGA GAG GAG AC-3' and reverse primer 5'-TTC TGC AAG TGC ATC ATC GT-3'; glyceraldehyde 3-phosphate dehydrogenase forward primer 5'-GGG TGT GAA CCA CGA GAA ATA-3' and reverse primer 5'-GTC ATG AGC CCT TCC ACA AT-3'; inducible NO synthase forward primer 5'-CAG CTG GGC TGT ACA AAC CTT-3' and reverse primer 5'-CAT TGG AAG TGA AGC GTT TCG-3'; tumor necrosis factor- α forward primer 5'-AGT TCT ATG GCC CAG ACC CT-3' and reverse primer 5'-CAC TTG GTG GTT TGC TAC GA-3'. Cycle threshold

(Ct) values were transformed (2^{-Ct}) and normalized to corresponding glyceraldehyde 3-phosphate dehydrogenase values for each sample. Graphs show fold the change compared with controls at time point 0 min.

Enzyme-linked Immunosorbent Assay

The concentrations of murine interleukin-1 β and interleukin-6 were determined in the supernatant by enzyme-linked immunosorbent assay, according to the manufacturer's manual (ELISA DuoKits, R&D Systems, USA). Optical density at 450 nm with a wavelength correction of 540 nm was measured on the Tecan (Switzerland) GENios Pro microplate reader.

Nitrite Measurement

NO release by macrophages was measured indirectly by determination of nitrite production. Nitrite level reflects the total NO production as it forms immediately on oxidation of NO, and also is more stable than NO which has a half-life of a few seconds.²⁷ RAW 264.7 cells (9×10^5 per well) were seeded into six-well plates and stimulated for 24 h. Nitrite concentrations in the supernatant were measured with the Griess reagent measurement kit (Cell Signaling, USA) according to the manufacturer's protocol.

Western Blot

Cells were rinsed one time with ice-cold Dulbecco's phosphate buffered saline (Cellgro, USA) and then lysed with RIPA buffer (Boston Bioproducts, USA) containing phosphatase and proteinase inhibitors (both from Sigma-Aldrich, USA). Thereafter, the lysate was scraped from the cell culture plate and left on ice for 30 min, followed by centrifugation at 4°C and 12,000g for 20 min. Total protein was measured using a detergent compatible protein assay (Bio-Rad, USA) using albumin as the protein standard (Thermo Fisher, USA). The supernatant was stored at -80°C until further analysis, at which time equal amounts of protein were diluted using Laemmli buffer (Bio-Rad) plus beta-mercaptoethanol (Bio-Rad) and boiled for 5 min at 95°C. Proteins were separated by sodium dodecyl sulfate-polyacrylamide gel electrophoresis and transferred to a nitrocellulose membrane. After blocking for 1 h with either 5% milk or 5% bovine serum albumin in tris-buffered saline with 0.1% Tween20, membranes were washed three times and probed with primary antibody overnight at 4°C. After washing with tris-buffered saline with 0.1% Tween20, membranes were probed with a secondary antibody (KPL, USA) and chemiluminescent signal was detected using supersignal chemiluminescence substrate (Thermo Fisher, USA) and an Odyssey Fc imager (Li-cor, USA). Digital images were analyzed with ImageJ 1.49v software (National Institutes of Health, Bethesda, MD). For protein phosphorylation, membranes were exposed to stripping buffer (100 mmol/l glycine, 1% sodium dodecyl sulfate, 0.1% NP-40, pH 2 in H₂O) and reprobed with antibodies as previously described.

Glyceraldehyde 3-phosphate dehydrogenase or β -actin were used as loading controls. The following primary antibodies were used: β -actin from BD Bioscience (USA); total and phosphorylated (pThr202/pTyr204) extracellular signal-regulated kinases from Cell Signaling (USA); glyceraldehyde 3-phosphate dehydrogenase and nuclear factor- κ B inhibitor- α from Santa Cruz Biotechnology (USA); inducible NO synthase from EMD Millipore (USA).

Measurement of Uptake of Fluorescently Labeled *E. coli*

Macrophage-mediated uptake of heat inactivated *E. coli* was performed as previously described.²⁸ Bone marrow-derived macrophages (10^5 per well) were seeded in a black, clear-bottom 96-well plate (Corning, USA) and pretreated for 8 h with or without 100 ng/ml lipopolysaccharide in the presence or absence of 2% sevoflurane. Thereafter, the medium was removed and replaced with medium containing approximately 10^8 fluorescein isothiocyanate-labeled heat-inactivated *E. coli* and incubated for 30 min. The fluorescent signal of extracellular *E. coli* was quenched with Trypan blue (Sigma-Aldrich, USA), as previously described,^{28–30} and the cells were then fixed in 4% paraformaldehyde (Electron Microscopy Science, USA) and stained with 4',6-diamidino-2-phenylindole (Molecular Probes, USA). The fluorescent signal from fluorescein isothiocyanate ($\lambda_{\text{Excitation}}$ 494 nm/ $\lambda_{\text{Emission}}$ 518 nm) and 4',6-diamidino-2-phenylindole ($\lambda_{\text{Excitation}}$ 364 nm/ $\lambda_{\text{Emission}}$ 454 nm) were obtained using a Synergy H4 fluorescent microplate reader (BioTek, USA). Uptake of heat-inactivated fluorescein isothiocyanate-labeled *E. coli* was calculated as: Uptake = (fluorescein isothiocyanate signal-background)/ (4',6-diamidino-2-phenylindole signal). Uptake was normalized to bone marrow-derived macrophages that were exposed to medium without additives.

Lipopolysaccharide-induced Endotoxemia Model

Animals were randomly assigned to the following groups: (1) Sham, (2) Sevoflurane/Sham, (3) lipopolysaccharide, and (4) Sevoflurane/lipopolysaccharide. Endotoxemia was induced by intraperitoneal injection of 5 μ g lipopolysaccharide, Serotype O111:B4 (Sigma-Aldrich, USA) in 200 μ l of sterile prewarmed saline.³¹ Experiments were always initiated at the same time of day (start at 2 PM). To ensure solubilization the suspension was sonicated for 10 min prior to injection. Mice were anesthetized either with ketamine/xylazine (Sham and lipopolysaccharide) or with sevoflurane (Sevoflurane/Sham and Sevoflurane/lipopolysaccharide). The goal was to reach a group size of six, resulting in a total of 24 animals based on previous experiments, respecting replacement, refinement, or reduction of animals in research (3R) without sample size calculation. Animals were randomly assigned to one of the groups without blinding. Sevoflurane-treated animals were exposed to 4% sevoflurane for 2 h after injection of lipopolysaccharide. Sevoflurane concentration was used as previously

described.^{15,32} For the last 30 min (at 19.5 h), 10^7 fluorescein isothiocyanate-labeled heat-inactivated *E. coli* in 500 μ l prewarmed phosphate-buffered saline were injected intraperitoneally. After a total of 20 h, the anesthetized mice were euthanized by cervical dislocation.³¹ Subsequently, peritoneal lavage with 6 ml ice-cold phosphate-buffered saline was performed.³³ The lavage was centrifuged for 5 min at 300g and the cell pellet resuspended in 1 ml ice-cold FACS buffer (phosphate-buffered saline and 0.5% bovine serum albumin). Before initiation of the experiments outcomes were defined. The primary outcome was uptake of *E. coli* by peritoneal macrophages; the secondary outcome was inducible NO synthase expression by peritoneal macrophages.

Flow Cytometry

Before staining, the cells were treated with anti-CD16/CD32 monoclonal antibody (BD Bioscience, USA) according to the manufacturer's recommendation to block Fc γ RII/III receptors. If not stated otherwise, all stainings were conducted on ice and protected from light. First, surface staining with the following antibodies was performed for 30 min: PerCP Cy5-5 labeled Ly6C, Pacific Blue labeled Ly6G, APCy7 labeled CD11b, Brilliant Violet 510 labeled CD11c and PE labeled F4/80 (all from Biolegend, USA). Thereafter, the cell suspension was washed in phosphate-buffered saline and

stained for dead cells with fixable viability dye eFluor 660 (eBioscience, USA) for 15 min. To prepare the cells for the intracellular inducible NO synthase staining, they were fixed and permeabilized with a kit (eBioscience) according to the manufacturer's protocol. This step was followed by intracellular staining with PE Cy7 labeled inducible NO synthase antibody, which was performed for 20 min at room temperature. For compensation, Ultracomp eBeads (Invitrogen, USA) were stained with 0.5 μ l of each dye for 20 min. The cells and beads were analyzed with a BD LSR Fortessa flow cytometer. For analysis, FlowJo v10 (FlowJo, LCC, USA) software was used; fluorescence minus one controls were used to set the gates.

Statistical Analysis

Values are shown as means \pm SD. Data analysis and graphical presentations were performed using GraphPad Prism version 7.0 and 8.0 (GraphPad, USA). Normal distribution was visually analyzed using Q-Q plots. Comparisons between two groups were performed by an unpaired two-tailed *t* test, and for three or more groups using one-way ANOVA with Bonferroni's *post hoc* comparison. In experiments with one single time point analysis, comparison of one-way ANOVA was used. To assess the effect of the treatment and time an ordinary two-way ANOVA (no repeated measures) with

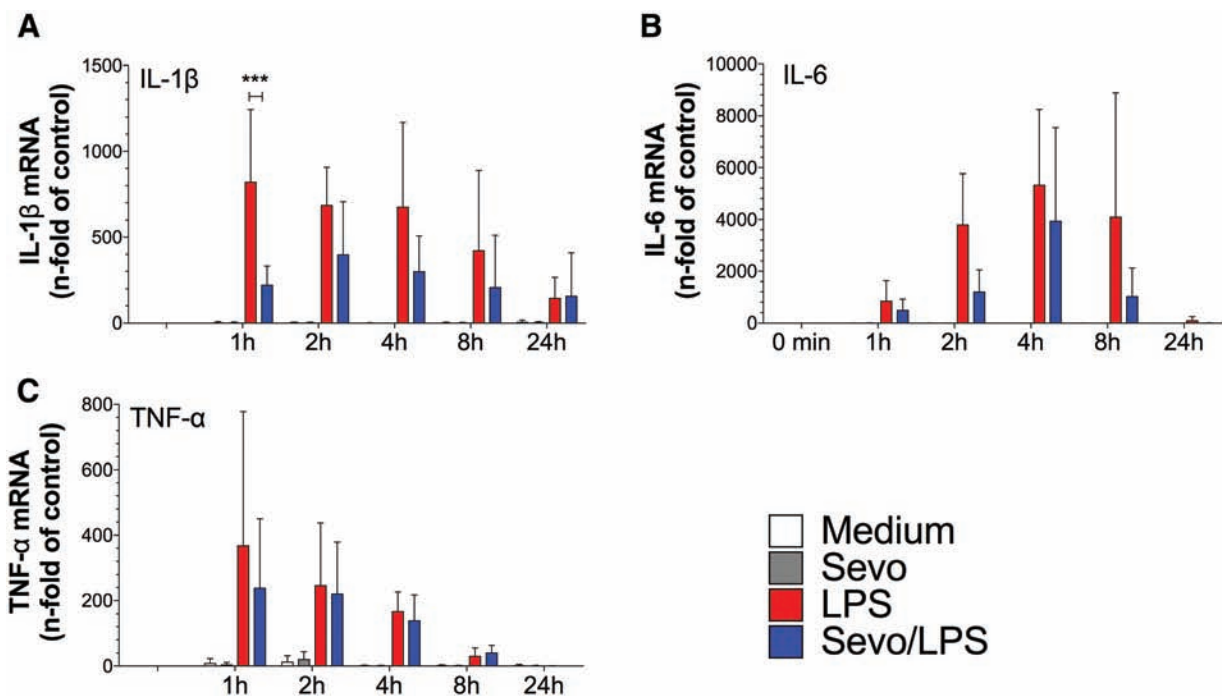


Fig. 2. mRNA cytokine expression in bone marrow-derived macrophages. Cells were exposed to lipopolysaccharide in the presence of absence of 2% sevoflurane (Sevo) for 0, 1, 2, 4, 8, and 24 h. RNA was extracted and quantitative real-time polymerase chain reaction was performed. mRNA expression of the proinflammatory mediators interleukin-1 β (IL-1 β ; **A**), interleukin-6 (IL-6; **B**) and tumor necrosis factor- α (TNF- α ; **C**). Values represent means \pm SD; $n \geq 3$ –6, two-way ANOVA (group and time interaction). *** $P = 0.0006$.

Bonferroni's *post hoc* test was used with time and treatment as factors to be evaluated. No statistical power analysis was conducted prior to the study. The sample size was based on previous experience with the experimental design(s). There was no exclusion of outliers. A *P* value of less than 0.05 was considered statistically significant. All experimental procedures were performed at least three times.

Sevoflurane Suppresses Lipopolysaccharide-induced Expression and Production of Proinflammatory Cytokines in Bone Marrow–derived Macrophages

Expression of the proinflammatory cytokines interleukin-1 β , interleukin-6, and tumor necrosis factor- α in bone marrow–derived macrophages after lipopolysaccharide stimulation was determined using quantitative real-time polymerase chain reaction. As expected, we observed a time-dependent increase in the expression of proinflammatory cytokines after stimulation with lipopolysaccharide as compared with control (t_{0min} ; fig. 2, A–C). Lipopolysaccharide-induced interleukin-1 β expression in bone marrow–derived macrophages was reduced by sevoflurane at 1 h ($P = 0.0006$; fig. 2A), whereas no difference was observed in the expression of tumor necrosis factor- α at any of the observed time points (fig. 2C).

To evaluate whether reduced interleukin-1 β and interleukin-6 mRNA expression was associated with a decrease in protein level, the concentration of these cytokines was measured in the supernatant from lipopolysaccharide-treated bone marrow–derived macrophages using enzyme-linked immunosorbent assay. Stimulation with lipopolysaccharide increased the release of both interleukin-1 β and interleukin-6 at 4 h, 8 h, and 24 h (fig. 3, A and B). The release of interleukin-1 β on lipopolysaccharide stimulation at 24 h (546 ± 346 ng/ml [mean \pm SD]) was reduced in the presence of 2% sevoflurane to a value of 145 ± 155 ng/ml ($P < 0.0001$; fig. 3A). Similarly, after lipopolysaccharide stimulation there was a time-dependent increase in interleukin-6 protein concentration over time to a value of ($9,006 \pm 5,817$ ng/ml) at 24 h, while sevoflurane reduced lipopolysaccharide-induced interleukin-6 release to $4,183 \pm 2,797$ ng/ml; $P < 0.0001$; fig. 3B).

Sevoflurane Differentially Modulates Inducible NO Synthase Expression on Lipopolysaccharide Stimulation

We also assessed the effect of sevoflurane on another classic nuclear factor- κ B–dependent inflammatory mediator, namely inducible NO synthase. Lipopolysaccharide stimulation promoted a time-dependent increase in inducible NO synthase mRNA expression, which peaked at 4 h (fig. 4A). The effect of sevoflurane on lipopolysaccharide stimulated inducible NO synthase expression level, however, differed over the 24-hr time course as compared with other proinflammatory cytokines. Sevoflurane increased inducible NO synthase gene expression at 4 h ($P < 0.0001$). At 8 h,

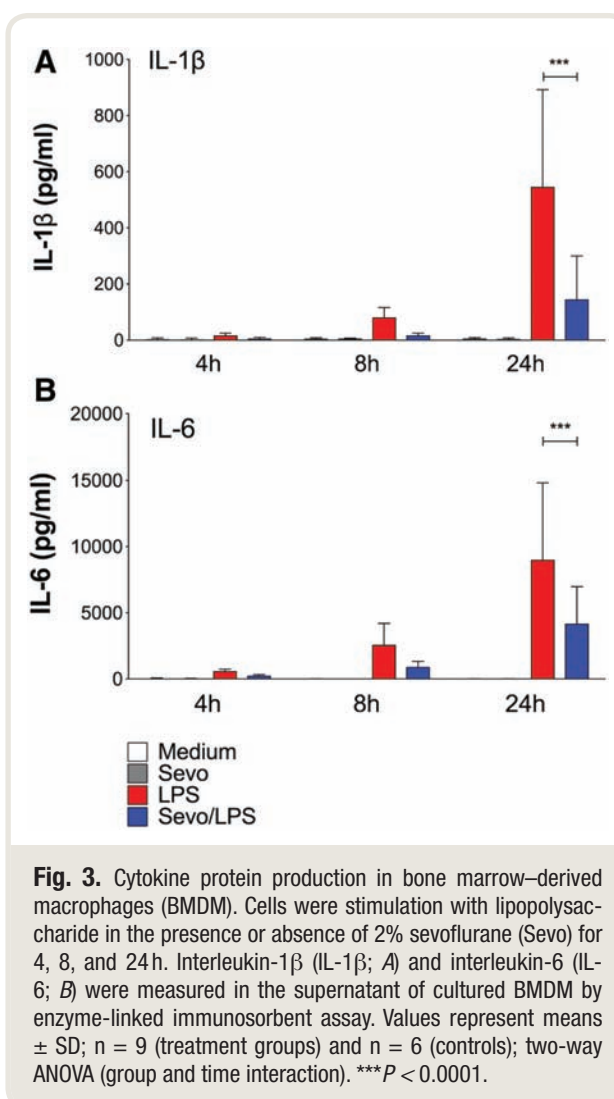


Fig. 3. Cytokine protein production in bone marrow–derived macrophages (BMDM). Cells were stimulation with lipopolysaccharide in the presence or absence of 2% sevoflurane (Sevo) for 4, 8, and 24 h. Interleukin-1 β (IL-1 β ; A) and interleukin-6 (IL-6; B) were measured in the supernatant of cultured BMDM by enzyme-linked immunosorbent assay. Values represent means \pm SD; $n = 9$ (treatment groups) and $n = 6$ (controls); two-way ANOVA (group and time interaction). *** $P < 0.0001$.

inducible NO synthase expression did not differ ($P = 0.099$) in sevoflurane-treated cells compared with cells exposed to air only (fig. 4A). Effects of sevoflurane on inducible NO synthase protein levels mirrored the changes observed by quantitative real-time polymerase chain reaction. At 4 h of lipopolysaccharide stimulation, sevoflurane reduced inducible NO synthase expression by 41% compared with bone marrow–derived macrophages treated with lipopolysaccharide alone ($P = 0.0005$; fig. 4B) and sevoflurane increased inducible NO synthase expression by 466% at 8 h compared with lipopolysaccharide alone ($P = 0.0012$; fig. 4C).

Sevoflurane Enhances Nitrite Production during Lipopolysaccharide Stimulation

To assess whether the increase in inducible NO synthase protein resulted correspondingly in enhanced NO production, we measured nitrite concentration in the culture media. As expected, lipopolysaccharide stimulation led to an increase in nitrite production by macrophages compared with

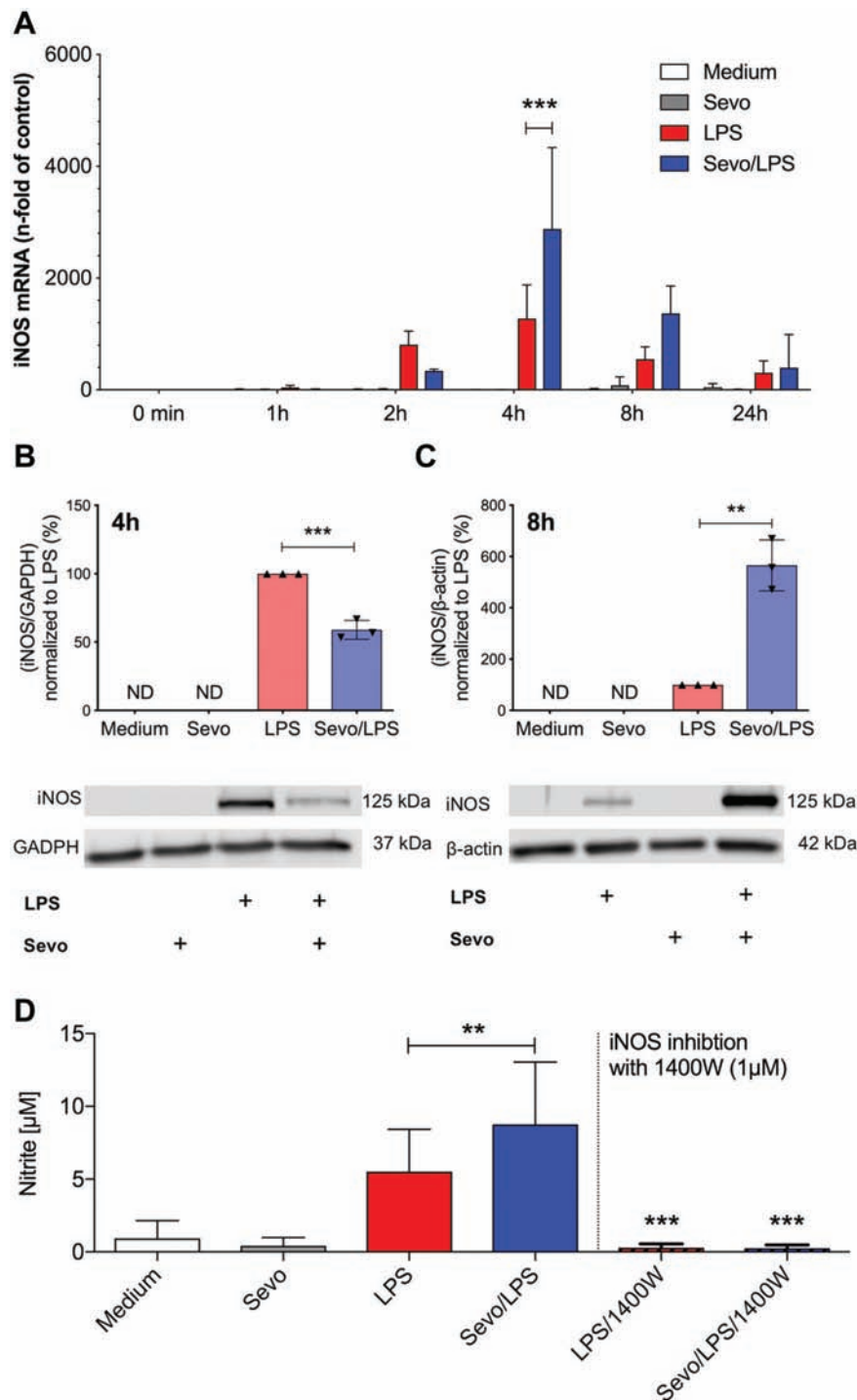


Fig. 4. Inducible NO synthase (iNOS) gene expression and NO production in bone marrow-derived macrophages. (A) Cells were exposed to lipopolysaccharide (LPS) in the presence and absence of 2% sevoflurane (Sevo) for 0, 1, 2, 4, 8, and 24 h. RNA was extracted and quantitative real-time PCR was performed to determine iNOS mRNA. Values represent means \pm SD; $n = 4$, two-way ANOVA (group and time interaction). *** $P < 0.0001$. (B and C) Protein levels of iNOS were determined after 4 h or 8 h of LPS stimulation in the presence or absence of 2% sevoflurane. Whole-cell lysates were used for Western blot analysis. Representative Western blots are shown. Values represent means \pm SD; $n = 3$; unpaired two-tailed t test; ** $P = 0.0012$, *** $P = 0.0005$. (D) NO production in bone marrow-derived macrophages after 24-h stimulation with LPS in the presence or absence of 2% sevoflurane was measured indirectly by determination of nitrite production using Griess reagent. To inhibit iNOS production 1400W was added for the entire incubation. Values represent means \pm SD; $n = 15$ samples without 1400W, $n = 6$ samples with 1400W; one-way ANOVA; LPS versus Sevo/LPS ** $P = 0.009$, Sevo/LPS versus Sevo/LPS/1400W *** $P = 0.0005$.

unstimulated controls ($P < 0.0001$; fig. 4D). The nitrite production after 24 h of lipopolysaccharide stimulation ($5.5 \pm 2.9 \mu\text{M}$ [mean \pm SD]) was enhanced when cells were coexposed to sevoflurane ($8.8 \pm 4.3 \mu\text{M}$; $P = 0.009$). Furthermore, lipopolysaccharide-induced increase in nitrite concentration was completely abolished in cells treated with the inducible NO synthase specific inhibitor 1400W ($1 \mu\text{M}$; lipopolysaccharide *vs.* lipopolysaccharide 1400W, $P = 0.0007$; Sevoflurane/lipopolysaccharide *vs.* Sevoflurane/lipopolysaccharide/1400W, $P = 0.0005$), confirming increased nitrate level is promoted by inducible NO synthase activation.

Sevoflurane Decreases Lipopolysaccharide-induced Extracellular Signal-regulated Kinase Phosphorylation Whereas Nuclear Factor- κB Inhibitor- α Degradation Is Not Altered

As proinflammatory genes in macrophages were observed to be differentially modulated by sevoflurane, we next assessed potential molecular mechanisms by interrogating

signaling proteins associated with the various inflammatory pathways. As the data indicated sevoflurane promotes a decrease in the expression of nuclear factor- κB -dependent genes, such as proinflammatory cytokines interleukin-1 β and interleukin-6, we next assessed whether degradation of nuclear factor- κB inhibitor- α , which suppresses nuclear factor- κB activation, would play a role in the reduced expression of interleukin-1 β and interleukin-6. Because this step is found at the very beginning of the inflammatory cascade, early time points (0, 5, 20, 30, 60, and 90 min) were chosen.³⁴ Lipopolysaccharide led to a time-dependent degradation of nuclear factor- κB inhibitor- α , which peaked at 20 min ($P = 0.004$ compared with medium), which was still reduced at 30 min ($P = 0.002$ compared with medium), and finally returned to baseline at 60 min ($P > 0.999$ compared with controls). In the presence of sevoflurane, lipopolysaccharide-induced degradation of nuclear factor- κB inhibitor- α was not affected ($P > 0.999$; fig. 5, A and B).

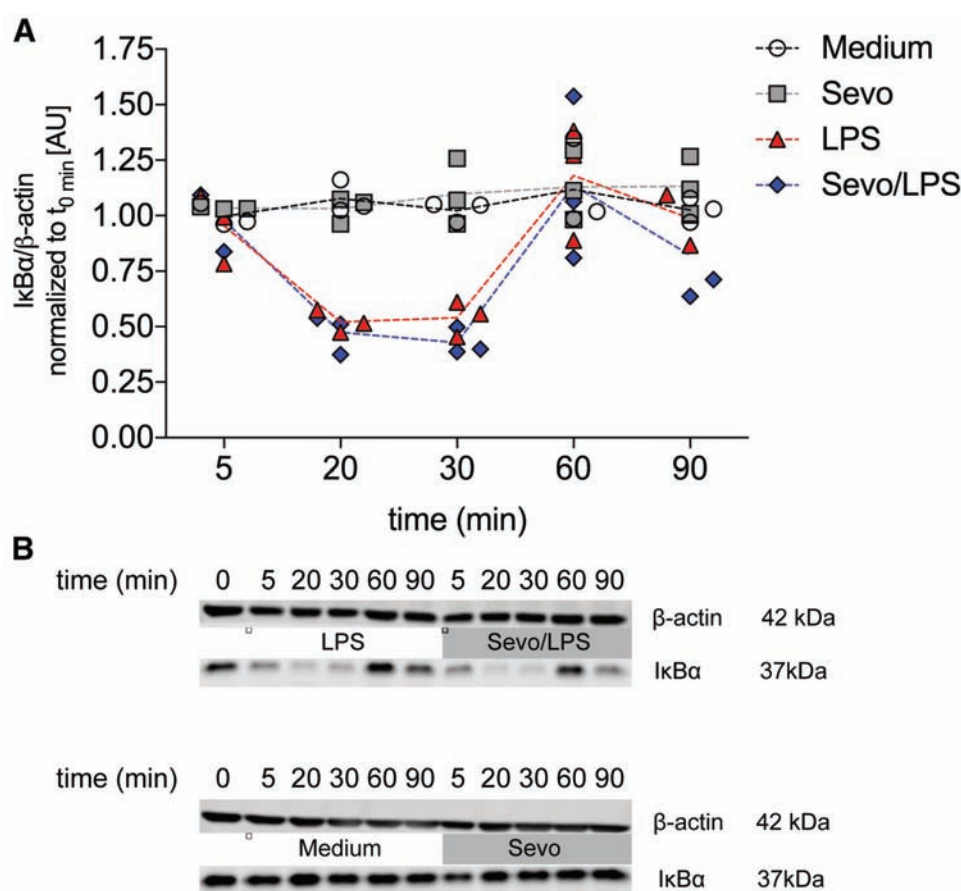


Fig. 5. Degradation of the nuclear factor- κB inhibitor $\text{I}\kappa\text{B}\alpha$ in bone marrow-derived macrophages. (A) Cells were exposed to lipopolysaccharide (LPS) in the presence and absence of 2% sevoflurane (Sevo) for 0, 5, 20, 30, 60, and 90 min, followed by Western blot analysis. Scatter plot with actual values and the connecting line representing the mean; $n = 3$, two-way ANOVA (group and time interaction). (B) Representative Western blots.

Next, mitogen-activated protein kinase pathways were explored. Extracellular signal-regulated kinase, which is part of the mitogen-activated protein kinase pathway, is activated by phosphorylation at Thr202/Tyr204 by MEK1. Phosphorylated extracellular signal-regulated kinase then influences the activity of several transcription factors. After 8 h of lipopolysaccharide stimulation, extracellular signal-regulated kinase phosphorylation increased (control *vs.* lipopolysaccharide, $P > 0.0001$; control *vs.* Sevoflurane/lipopolysaccharide $P = 0.0004$) and sevoflurane decreased lipopolysaccharide-induced extracellular signal-regulated kinase phosphorylation ($P = 0.036$) compared with lipopolysaccharide alone (fig. 6).

Sevoflurane Increases Uptake of Fluorescently Labeled Heat-inactivated *E. coli* by Macrophages *In Vitro* and *In Vivo*

To test whether enhanced inducible NO synthase expression affects phagocytosis by macrophages, following exposure to medium alone, lipopolysaccharide or lipopolysaccharide and sevoflurane for 8 h, bone marrow–derived macrophages were incubated with fluorescein isothiocyanate-labeled heat-inactivated *E. coli* for 30 min. All samples were normalized to bone marrow–derived macrophages pretreated with medium without additional additives. There was no difference between bone marrow–derived macrophages pretreated with medium ($100\% \pm 32.4\%$ [mean \pm SD]) and lipopolysaccharide ($99.8\% \pm 29.6\%$; $P > 0.999$).

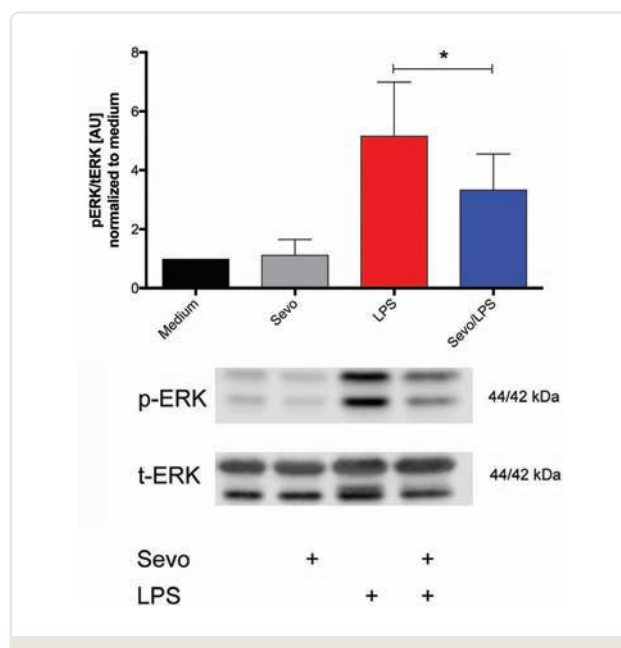


Fig. 6. Expression of extracellular signal-regulated kinase (ERK) phosphorylation (p-ERK) in bone marrow–derived macrophages normalized by total ERK (t-ERK). Cells were stimulated for 8 h with lipopolysaccharide (LPS) in the presence or absence of 2% sevoflurane (Sevo), followed by Western blot analysis. Representative Western blots are shown below. Values represent means \pm SD; $n = 7$, one-way ANOVA. * $P = 0.036$.

However, in lipopolysaccharide/Sevoflurane treated bone marrow–derived macrophages, we observed a statistically significant increase in the uptake of fluorescein isothiocyanate-labeled *E. coli* ($169.9\% \pm 79.2\%$, $P = 0.004$). In addition, in the presence of the inducible NO synthase inhibitor 1400W, the increase in *E. coli* uptake induced by sevoflurane was abolished (fig. 7A), indicating *E. coli* uptake in the presence of sevoflurane was mediated by inducible NO synthase.

Finally, we assessed whether results obtained *in vitro* can be observed *in vivo*. Six animals per group were evaluated of a total number of 31 animals included. In each group, cell count or assessment was not possible in two animals (in the sham group only one animal) because of severe blood contamination of the lavage or technical difficulties when performing cell harvest and analysis. The average weight was 27.4 g. Using the lipopolysaccharide model of endotoxemia, macrophage inducible NO synthase expression and *E. coli* uptake in the peritoneal cavity was determined. Macrophages were identified as CD11c⁺ CD11b⁺ F4/80⁺ cells.^{31,35} Data showed that inducible NO synthase expression was very low in all three control groups (Sham mean fluorescence intensity equals 1,813, lipopolysaccharide mean fluorescence intensity equals 6,736, Sevoflurane/Sham mean fluorescence intensity equals 6,757). In the Sevoflurane/lipopolysaccharide group, inducible NO synthase expression was markedly increased by 669% (mean fluorescence intensity equals 51,768) compared with the lipopolysaccharide group ($P = 0.0003$; fig. 7B). To quantify the number of bacteria internalized by macrophages, we analyzed the mean fluorescence intensity of fluorescein isothiocyanate-labeled *E. coli*. Consistent with results of our *in vitro* study, we detected an increase in *E. coli* uptake by 49% in the Sevoflurane/lipopolysaccharide treated group compared with lipopolysaccharide alone (lipopolysaccharide mean fluorescence intensity equals 6,756, Sevoflurane/lipopolysaccharide mean fluorescence intensity equals 10,068; $P = 0.006$; fig. 7C), demonstrating that the increased uptake of *E. coli* by macrophages after exposure to sevoflurane is also occurring *in vivo*.

Discussion

The present findings demonstrate that sevoflurane differentially modulates proinflammatory genes in murine macrophages. Whereas sevoflurane suppressed the expression of proinflammatory cytokines, it enhanced the expression of inducible NO synthase. Furthermore, sevoflurane increased the uptake of *E. coli* in an inducible NO synthase–dependent manner *in vitro* and *in vivo*.

This study demonstrates that endotoxin-induced release of proinflammatory cytokines in murine macrophage can be reduced by sevoflurane, as shown previously in other cell types.^{4,5,10,36,37} Because nuclear factor- κ B is the primary mechanism associated with the regulation of proinflammatory genes, we assumed that sevoflurane would reduce the activation of nuclear factor- κ B in bone marrow–derived

macrophages, as described in other cells.^{6–12} As we did not observe a difference in the degradation of nuclear factor- κ B inhibitor- α in presence of sevoflurane, we concluded that sevoflurane might be interacting directly with nuclear factor- κ B. Boost *et al.*⁶ postulated that sevoflurane decreases nuclear factor- κ B inhibitor- α degradation on tumor necrosis factor- α stimulation, but because lipopolysaccharide stimulates Toll-like receptor 4 we concluded that it affects the Toll-like receptor 4 pathway differently than the tumor necrosis factor- α pathway, the latter with involvement of tumor necrosis factor receptors, tumor necrosis factor receptor type 1–associated death domain and tumor necrosis factor receptor–associated factor 2.

Interestingly, we observed that sevoflurane affected lipopolysaccharide-induced expression of nuclear factor- κ B–dependent genes differentially. Sevoflurane promoted the expression of inducible NO synthase, which is in agreement with previous findings.^{3,5} Because sevoflurane differentially modulates proinflammatory genes in murine macrophages, we concluded that different inflammatory pathways may be involved. Our data showed that sevoflurane affected the mitogen-activated protein kinase pathway by decreasing extracellular signal-regulated kinase phosphorylation. This may be a potential mechanism by which sevoflurane promotes inducible NO synthase expression in murine macrophages. Further, other groups reported decreased levels of extracellular signal-regulated kinase phosphorylation in the presence of sevoflurane^{38–40} and that inhibition of extracellular signal-regulated kinase phosphorylation was associated with enhanced inducible

NO synthase expression.⁴¹ Because reduced extracellular signal-regulated phosphorylation was observed at later time points, and decreased expression of nuclear factor- κ B–dependent genes was found as early as 1 h of stimulation, we postulate that sevoflurane-induced downregulation of inducible NO synthase at the early time point may be attributable to decreased activation of nuclear factor- κ B during the initial phase. A question remains: Which transcription factor is involved in the increase in inducible NO synthase expression? A possible explanation is that reduced extracellular signal-regulated kinase phosphorylation leads to increased nuclear factor- κ B activation. Bhatt *et al.* showed reduced extracellular signal-regulated kinase phosphorylation on stimulation of the Toll-like receptor 2 pathway enhances nuclear factor- κ B activation.⁴¹ However, it remains unclear whether the same mechanism occurs with the Toll-like receptor 4 pathway or whether a different transcription factor is involved.

This is the first study to investigate the effect of sevoflurane on uptake of heat-inactivated *E. coli* by murine macrophages. We observed increased uptake of *E. coli* after exposure to sevoflurane, and the mechanism appears to be linked to the activity of inducible NO synthase as enhanced uptake was abolished when inducible NO synthase was pharmacologically inhibited. It has been shown that NO donors increase phagocytosis⁴² and that inhibiting NO release with L-N_G-Nitroarginine methyl ester reduces bacterial uptake and bacterial killing.⁴³ However, the role of inducible NO synthase in bacterial clearance remains controversial, as there is a report showing higher

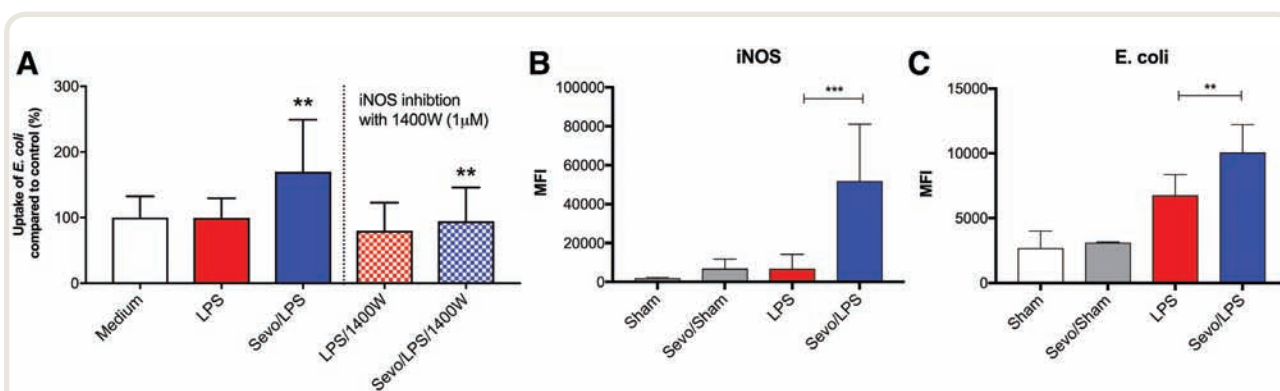


Fig. 7. (A) Bone marrow–derived macrophages: uptake of fluorescein isothiocyanate (FITC)-labeled heat-inactivated *Escherichia coli* (*E. coli*). Cells were exposed to lipopolysaccharide (LPS) in the presence or absence of 2% sevoflurane (Sevo) for 8 h. Thereafter, the cells were exposed to *E. coli* for an additional 30 min. Fluorescence was determined using a fluorescence microplate reader. The same experiments were performed in the presence or absence of 1400W, an inhibitor of the inducible NO synthase (iNOS), which was added for the entire incubation. Values represent means \pm SD; $n = 15$ samples without 1400W and $n = 9$ samples with 1400W; one-way ANOVA; LPS versus Sevo/LPS $**P = 0.004$, Sevo/LPS versus Sevo/LPS/1400W $**P = 0.009$. (B) Mice were exposed to intraperitoneally applied LPS for a total of 20 h. Mice in the sevoflurane group received 2-hr anesthesia with 4% sevoflurane, whereas control animals were anesthetized with ketamine/xylazine. Thirty minutes before collection of peritoneal macrophages for analysis, FITC-labeled *E. coli* were injected intraperitoneally. Mean fluorescence intensity (MFI) of iNOS, after staining with fluorescently-labeled antibody, was measured using flow cytometry. (C) MFI of FITC-labeled *E. coli* using flow cytometry. Exposition as just described. For B, and C, values represent means \pm SD; $n = 6$, one-way ANOVA $**P = 0.006$ LPS versus Sevo/LPS, $***P = 0.0003$ LPS versus Sevo/LPS.

bacterial clearance and resistance to bacterial meningitis in inducible NO synthase-deficient newborn mice.⁴⁴ These findings are in contrast with the current data. Furthermore, various groups have observed that inducible NO synthase knockout animals exhibit an increase in mortality induced by different sepsis models,^{26,45–48} consistent with the idea that reactive nitrogen species play a significant role in host defense against microbes.^{49,50}

Inducible NO synthase is an important mediator in the inflammatory response to lipopolysaccharide stimulation. Although inducible NO synthase protein levels are decreased in the Sevoflurane/lipopolysaccharide group compared with lipopolysaccharide alone shortly after initiating endotoxin stimulation, inducible NO synthase expression in the Sevoflurane/lipopolysaccharide group exceeds the lipopolysaccharide values at later time points. With regard to inducible NO synthase expression, sevoflurane appears to be most likely interacting with at least two different inflammatory pathways, with opposed effects on inducible NO synthase expression. This is consistent with the findings that exposure to sevoflurane leads to decreased proinflammatory cytokine expression while enhancing bactericidal properties.

Obviously, the effect of sevoflurane upregulating inducible NO synthase can be evoked by using varying exposure times to sevoflurane. This becomes evident when comparing *in vitro* with *in vivo* results (*in vitro*: 8 h, *in vivo*: 2 h). However, *in vitro* scenarios are for sure not comparable with *in vivo* experimental setups, the latter being more complex with many different cell types over time involved. Moreover, it is known from previous studies that sevoflurane preconditioning increases nitric oxide release,⁵¹ and that conditioning with a volatile anesthetic for a short time provides long-term protection.^{3,15,52–54}

We observed markedly increased inducible NO synthase expression on lipopolysaccharide stimulation when animals were exposed to sevoflurane. Additionally, we demonstrated that exposure to sevoflurane increased the uptake of *E. coli* by peritoneal macrophages *in vivo* in mice. However, because the impact of sex on inducible NO synthase expression and uptake of *E. coli* was not evaluated, conclusions have to be drawn in a careful way.

Erol *et al.*⁵⁵ reported that the phagocytic function of human polymorphonuclear leukocytes was not altered by sevoflurane when compared with desflurane and propofol, whereas another study showed reduced phagocytic function of human granulocytes after exposure to sevoflurane.⁵⁶ Interestingly, this reduction was observed for granulocytes but not in monocytes,⁵⁶ implying that the effects of sevoflurane on phagocytic function may be different between granulocytes and cells of monocyte-macrophage lineage.

Considering these data, we provide a possible mechanism by which sevoflurane increases bacterial uptake and survival in animal models of endotoxemia/sepsis^{15,16} (fig. 8). Stimulation of the Toll-like receptor 4 pathway with lipopolysaccharide leads to a well-understood inflammatory

response. After stimulation of Toll-like receptor 4 in the plasma membrane, a signal transduction cascade is initiated which culminates in the phosphorylation of nuclear factor- κ B inhibitor- α . Once nuclear factor- κ B inhibitor- α is phosphorylated, it is degraded and nuclear factor- κ B is no longer inhibited, enabling it to translocate to the nucleus to increase transcription of dependent genes. Because sevoflurane did not affect lipopolysaccharide-induced nuclear factor- κ B inhibitor- α degradation, we assume that sevoflurane may directly interact with the translocation of nuclear factor- κ B into the nucleus or reduce transcription of nuclear factor- κ B-dependent genes as highlighted in figure 8. At later time points, sevoflurane reduced extracellular signal-regulated kinase phosphorylation, and this effect may be associated with an increase in inducible NO synthase expression through a mechanism that is not yet understood.

This study demonstrates that sevoflurane differentially modulates proinflammatory genes in murine bone marrow-derived macrophages. Whereas sevoflurane reduced lipopolysaccharide-induced release of proinflammatory cytokines, it enhanced the production of anti-microbial inducible NO synthase. Sevoflurane also increased macrophage uptake of heat-inactivated *E. coli* by a mechanism that seems to be linked to the activity of inducible NO synthase. These observations made *in vitro* were corroborated by *in vivo* studies that demonstrated sevoflurane promotes inducible NO synthase expression and bacterial uptake by peritoneal macrophages in the murine model of endotoxemia. These results provide an explanation, at least in part, for increased survival of septic rodents exposed to sevoflurane.^{15,16} It remains unclear whether results observed in rodents will hold true in higher mammals such as humans.

Acknowledgments

The authors kindly thank lab manager Maricela Castellon, M.S. (Department of Anesthesiology, University of Illinois at Chicago, Chicago, Illinois), Zhenlong Chen, Ph.D. (Department of Anesthesiology, University of Illinois at Chicago), Chenxia He, Ph.D. (Department of Medicine, University of Illinois at Chicago), and André L. de Abreu, Ph.D. (Department of Medicine, University of Illinois at Chicago), for technical support.

Research Support

This study was supported by National Institutes of Health, Heart, Lung, and Blood Institute grant Nos. HL60678 and HL125356 (Bethesda, Maryland; to Dr. Minshall); the Swiss National Science Foundation, project No. 320030_160283 (Bern, Switzerland; to Dr. Beck-Schimmer), including a mobility grant for Dr. Gerber; an award from the American Heart Association (Dallas, Texas) and the Circle of Service Foundation (Chicago, Illinois) award no. 18POST34020037 (to Dr. Oliveira); and by the Masikini Foundation (Triesen, Liechtenstein) and the Uniscientia Foundation (Vaduz, Liechtenstein).

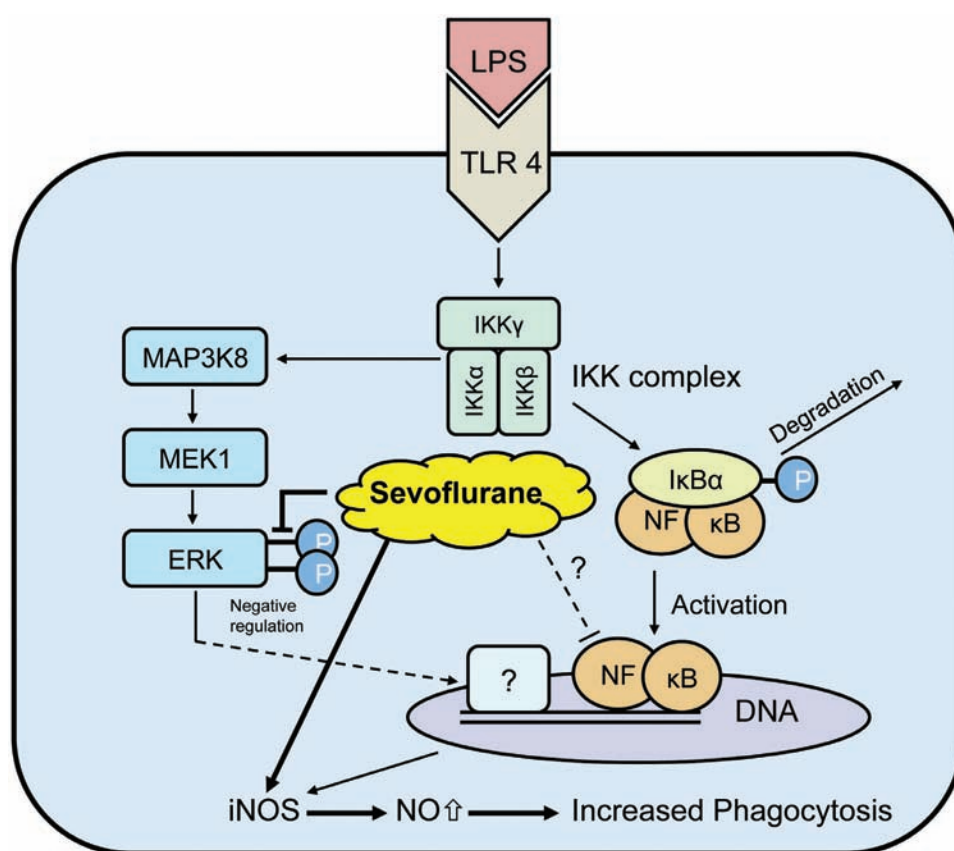


Fig. 8. Schematic illustration of proposed antiinflammatory mechanism of action of sevoflurane. Exposure to lipopolysaccharide (LPS) leads to activation of Toll-like receptor 4 (TLR4) and initiates proinflammatory cascade. Degradation of nuclear factor- κ B inhibitor- α (I κ B α) was not altered by sevoflurane and thus sevoflurane may directly interact with nuclear factor- κ B (NF- κ B; highlighted with '?'). Sevoflurane reduces phosphorylation of extracellular signal-regulated kinases (ERK) that may cause enhanced expression of inducible NO synthase (iNOS) and increased macrophage-mediated bacterial clearance.

Competing Interests

Dr. Beck-Schimmer received a grant from Baxter AG (Opfikon, Switzerland), not related to this work; was a participant of an Advisory Board Meeting of Baxter AG, not related to this topic; chaired a session (Satellite Symposium on “General Anaesthesia and its effect on organ function – What do we know?”) at Euroanaesthesia 2013, organized by Baxter AG; received a speaker's fee from Abbvie (Baar, Switzerland; Pro/cons of volatile anaesthetics) for a Grand Round talk at Kantonsspital Chur (Chur, Switzerland); and has a patent: 04/10/14 – 20140100278: Injectable formulation for treatment and protection of patients having an inflammatory reaction or an ischemia-reperfusion event – M. Urner, L. K. Limbach, I. K. Herrmann, W. J. Stark, B. Beck-Schimmer, applied as Patent Cooperation Treaty (internationally), July 2009.

Correspondence

Address correspondence to Dr. Beck-Schimmer: Institute of Physiology and Zurich Center for Integrative

Human Physiology, University of Zurich, Institute of Anesthesiology, University Hospital Zurich, Raemistrasse 100, CH-8091 Zurich, Switzerland. beatrice.beckschimmer@uzh.ch. Information on purchasing reprints may be found at www.anesthesiology.org or on the masthead page at the beginning of this issue. ANESTHESIOLOGY's articles are made freely accessible to all readers, for personal use only, 6 months from the cover date of the issue.

References

1. De Hert SG, Van der Linden PJ, Cromheecke S, Meeus R, Nelis A, Van Reeth V, ten Broecke PW, De Blier IG, Stockman BA, Rodrigus IE: Cardioprotective properties of sevoflurane in patients undergoing coronary surgery with cardiopulmonary bypass are related to the modalities of its administration. *ANESTHESIOLOGY* 2004; 101:299–310
2. Lee HT, Ota-Setlik A, Fu Y, Nasr SH, Emala CW: Differential protective effects of volatile anesthetics

- against renal ischemia-reperfusion injury *in vivo*. *ANESTHESIOLOGY* 2004; 101:1313–24
3. Beck-Schimmer B, Breitenstein S, Urech S, De Conno E, Wittlinger M, Puhon M, Jochum W, Spahn DR, Graf R, Clavien PA: A randomized controlled trial on pharmacological preconditioning in liver surgery using a volatile anesthetic. *Ann Surg* 2008; 248:909–18
 4. Suter D, Spahn DR, Blumenthal S, Reyes L, Booy C, Z'graggen BR, Beck-Schimmer B: The immunomodulatory effect of sevoflurane in endotoxin-injured alveolar epithelial cells. *Anesth Analg* 2007; 104:638–45
 5. Yue T, Roth Z'graggen B, Blumenthal S, Neff SB, Reyes L, Booy C, Steurer M, Spahn DR, Neff TA, Schmid ER, Beck-Schimmer B: Postconditioning with a volatile anaesthetic in alveolar epithelial cells *in vitro*. *Eur Respir J* 2008; 31:118–25
 6. Boost KA, Leipold T, Scheiermann P, Hoegl S, Sadik CD, Hofstetter C, Zwissler B: Sevoflurane and isoflurane decrease TNF- α -induced gene expression in human monocytic THP-1 cells: Potential role of intracellular I κ B α regulation. *Int J Mol Med* 2009; 23:665–71
 7. Lee HT, Chen SW, Doetschman TC, Deng C, D'Agati VD, Kim M: Sevoflurane protects against renal ischemia and reperfusion injury in mice via the transforming growth factor- β 1 pathway. *Am J Physiol Renal Physiol* 2008; 295:F128–36
 8. Lee HT, Kim M, Jan M, Emala CW: Antiinflammatory and antinecrotic effects of the volatile anesthetic sevoflurane in kidney proximal tubule cells. *Am J Physiol Renal Physiol* 2006; 291:F67–78
 9. Lee HT, Kim M, Song JH, Chen SW, Gubitosa G, Emala CW: Sevoflurane-mediated TGF- β 1 signaling in renal proximal tubule cells. *Am J Physiol Renal Physiol* 2008; 294:F371–8
 10. Sun XJ, Li XQ, Wang XL, Tan WF, Wang JK: Sevoflurane inhibits nuclear factor- κ B activation in lipopolysaccharide-induced acute inflammatory lung injury via toll-like receptor 4 signaling. *PLoS One* 2015; 10:e0122752
 11. Watanabe K, Iwahara C, Nakayama H, Iwabuchi K, Matsukawa T, Yokoyama K, Yamaguchi K, Kamiyama Y, Inada E: Sevoflurane suppresses tumour necrosis factor- α -induced inflammatory responses in small airway epithelial cells after anoxia/reoxygenation. *Br J Anaesth* 2013; 110:637–45
 12. Zhong C, Zhou Y, Liu H: Nuclear factor kappaB and anesthetic preconditioning during myocardial ischemia-reperfusion. *ANESTHESIOLOGY* 2004; 100:540–6
 13. Schläpfer M, Leutert AC, Voigtsberger S, Lachmann RA, Booy C, Beck-Schimmer B: Sevoflurane reduces severity of acute lung injury possibly by impairing formation of alveolar oedema. *Clin Exp Immunol* 2012; 168:125–34
 14. Kellner P, Müller M, Piegeler T, Eugster P, Booy C, Schläpfer M, Beck-Schimmer B: Sevoflurane abolishes oxygenation impairment in a long-term rat model of acute lung injury. *Anesth Analg* 2017; 124:194–203
 15. Herrmann IK, Castellon M, Schwartz DE, Hasler M, Urner M, Hu G, Minshall RD, Beck-Schimmer B: Volatile anesthetics improve survival after cecal ligation and puncture. *ANESTHESIOLOGY* 2013; 119:901–6
 16. Schläpfer M, Piegeler T, Dull RO, Schwartz DE, Mao M, Bonini MG, Z'graggen BR, Beck-Schimmer B, Minshall RD: Propofol increases morbidity and mortality in a rat model of sepsis. *Crit Care* 2015; 19:45
 17. Visvabharathy L, Xayarath B, Weinberg G, Shilling RA, Freitag NE: Propofol increases host susceptibility to microbial infection by reducing subpopulations of mature immune effector cells at sites of infection. *PLoS One* 2015; 10:e0138043
 18. Kowalski C, Zahler S, Becker BF, Flaucher A, Conzen PF, Gerlach E, Peter K: Halothane, isoflurane, and sevoflurane reduce postischemic adhesion of neutrophils in the coronary system. *ANESTHESIOLOGY* 1997; 86:188–95
 19. Möbert J, Zahler S, Becker BF, Conzen PF: Inhibition of neutrophil activation by volatile anesthetics decreases adhesion to cultured human endothelial cells. *ANESTHESIOLOGY* 1999; 90:1372–81
 20. Müller-Edenborn B, Frick R, Piegeler T, Schläpfer M, Roth-Z'graggen B, Schlicker A, Beck-Schimmer B: Volatile anaesthetics reduce neutrophil inflammatory response by interfering with CXCR2 receptor-2 signaling. *Br J Anaesth* 2015; 114:143–9
 21. Tyther R, O'Brien J, Wang J, Redmond HP, Shorten G: Effect of sevoflurane on human neutrophil apoptosis. *Eur J Anaesthesiol* 2003; 20:111–5
 22. Wynn TA, Chawla A, Pollard JW: Macrophage biology in development, homeostasis and disease. *Nature* 2013; 496:445–55
 23. Murray PJ, Wynn TA: Protective and pathogenic functions of macrophage subsets. *Nat Rev Immunol* 2011; 11:723–37
 24. Janeway C.A. Jr, Travers P, Walport M, Shlomchik MJ: Immunobiology: The Immune System in Health and Disease. 5th edition. New York, Garland Science, 2001
 25. Junt T, Moseman EA, Iannaccone M, Massberg S, Lang PA, Boes M, Fink K, Henrickson SE, Shayakhmetov DM, Di Paolo NC, van Rooijen N, Mempel TR, Whelan SP, von Andrian UH: Subcapsular sinus macrophages in lymph nodes clear lymph-borne viruses and present them to antiviral B cells. *Nature* 2007; 450:110–4
 26. Baig MS, Zaichick SV, Mao M, de Abreu AL, Bakhshi FR, Hart PC, Saqib U, Deng J, Chatterjee S, Block ML, Vogel SM, Malik AB, Consolaro ME, Christman JW, Minshall RD, Gantner BN, Bonini MG: NOS1-derived nitric oxide promotes NF- κ B transcriptional activity through inhibition of suppressor of cytokine signaling-1. *J Exp Med* 2015; 212:1725–38
 27. Kelm M, Feelisch M, Deussen A, Schrader J, Strauer BE: The role of nitric-oxide in the control of coronary vascular tone in relation to partial oxygen-pressure,

- perfusion–pressure, and flow. *J Cardiovasc Pharmacol* 1991; 17: S95–S99
28. Ninkovic J, Roy S: High throughput fluorometric technique for assessment of macrophage phagocytosis and actin polymerization. *J Vis Exp* 2014; e52195
 29. Hed J: Methods for distinguishing ingested from adhering particles. *Methods Enzymol* 1986; 132:198–204
 30. Scott AJ, Woods JP: Monitoring internalization of *Histoplasma capsulatum* by mammalian cell lines using a fluorometric microplate assay. *Med Mycol* 2000; 38:15–22
 31. Ghosn EE, Cassado AA, Govoni GR, Fukuhara T, Yang Y, Monack DM, Bortoluci KR, Almeida SR, Herzenberg LA, Herzenberg LA: Two physically, functionally, and developmentally distinct peritoneal macrophage subsets. *Proc Natl Acad Sci USA* 2010; 107:2568–73
 32. Redel A, Stumpner J, Tischer-Zeit T, Lange M, Smul TM, Lotz C, Roewer N, Kehl F: Comparison of isoflurane-, sevoflurane-, and desflurane-induced pre- and postconditioning against myocardial infarction in mice *in vivo*. *Exp Biol Med (Maywood)* 2009; 234:1186–91
 33. Ray A, Dittel BN: Isolation of mouse peritoneal cavity cells. *J Vis Exp* 2010; 35: 1488
 34. Cruz MT, Duarte CB, Gonalo M, Carvalho AP, Lopes MC: LPS induction of I kappa B-alpha degradation and iNOS expression in a skin dendritic cell line is prevented by the janus kinase 2 inhibitor, Tyrphostin b42. *Nitric Oxide* 2001; 5:53–61
 35. Johnson TE, Michel BA, Meyerett C, Duffy A, Avery A, Dow S, Zabel MD: Monitoring immune cells trafficking fluorescent prion rods hours after intraperitoneal infection. *J Vis Exp* 2010; 45:2349
 36. Rodr guez-Gonz lez R, Baluja A, Veiras Del R o S, Rodr guez A, Rodr guez J, Taboada M, Brea D,  lvarez J: Effects of sevoflurane postconditioning on cell death, inflammation and TLR expression in human endothelial cells exposed to LPS. *J Transl Med* 2013; 11:87
 37. Steurer M, Schl pfer M, Steurer M, Z’graggen BR, Booy C, Reyes L, Spahn DR, Beck-Schimmer B: The volatile anaesthetic sevoflurane attenuates lipopolysaccharide-induced injury in alveolar macrophages. *Clin Exp Immunol* 2009; 155:224–30
 38. Kim SH, Li M, Pyeon TH, So KY, Kwak SH: The volatile anesthetic sevoflurane attenuates ventilator-induced lung injury through inhibition of ERK1/2 and Akt signal transduction. *Korean J Anesthesiol* 2015; 68:62–9
 39. Wiklund A, Gustavsson D, Ebber yd A, Sundman E, Schulte G, Jonsson Fagerlund M, Eriksson LI: Prolonged attenuation of acetylcholine-induced phosphorylation of extracellular signal-regulated kinase    following sevoflurane exposure. *Acta Anaesthesiol Scand* 2012; 56:608–15
 40. Yufune S, Satoh Y, Akai R, Yoshinaga Y, Kobayashi Y, Endo S, Kazama T: Suppression of ERK phosphorylation through oxidative stress is involved in the mechanism underlying sevoflurane-induced toxicity in the developing brain. *Sci Rep* 2016; 6:21859
 41. Bhatt KH, Sodhi A, Chakraborty R: Role of mitogen-activated protein kinases in peptidoglycan-induced expression of inducible nitric oxide synthase and nitric oxide in mouse peritoneal macrophages: Extracellular signal-related kinase, a negative regulator. *Clin Vaccine Immunol* 2011; 18:994–1001
 42. De Boo S, Kopecka J, Brusa D, Gazzano E, Matera L, Ghigo D, Bosia A, Riganti C: iNOS activity is necessary for the cytotoxic and immunogenic effects of doxorubicin in human colon cancer cells. *Mol Cancer* 2009; 8:108
 43. Tsai WC, Strieter RM, Zisman DA, Wilkowski JM, Bucknell KA, Chen GH, Standiford TJ: Nitric oxide is required for effective innate immunity against *Klebsiella pneumoniae*. *Infect Immun* 1997; 65:1870–5
 44. Mittal R, Gonzalez-Gomez I, Goth KA, Prasadara NV: Inhibition of inducible nitric oxide controls pathogen load and brain damage by enhancing phagocytosis of *Escherichia coli* K1 in neonatal meningitis. *Am J Pathol* 2010; 176:1292–305
 45. MacMicking JD, Nathan C, Hom G, Chartrain N, Fletcher DS, Trumbauer M, Stevens K, Xie QW, Sokol K, Hutchinson N: Altered responses to bacterial infection and endotoxic shock in mice lacking inducible nitric oxide synthase. *Cell* 1995; 81:641–50
 46. MacMicking JD, North RJ, LaCourse R, Mudgett JS, Shah SK, Nathan CF: Identification of nitric oxide synthase as a protective locus against tuberculosis. *Proc Natl Acad Sci USA* 1997; 94:5243–8
 47. Mastroeni P, Vazquez-Torres A, Fang FC, Xu Y, Khan S, Hormaeche CE, Dougan G: Antimicrobial actions of the NADPH phagocyte oxidase and inducible nitric oxide synthase in experimental salmonellosis. II. Effects on microbial proliferation and host survival *in vivo*. *J Exp Med* 2000; 192:237–48
 48. Miki S, Takeyama N, Tanaka T, Nakatani T: Immune dysfunction in endotoxemia: Role of nitric oxide produced by inducible nitric oxide synthase. *Crit Care Med* 2005; 33:716–20
 49. Fang FC: Antimicrobial reactive oxygen and nitrogen species: Concepts and controversies. *Nat Rev Microbiol* 2004; 2:820–32
 50. Flannagan RS, Cos o G, Grinstein S: Antimicrobial mechanisms of phagocytes and bacterial evasion strategies. *Nat Rev Microbiol* 2009; 7:355–66
 51. Novalija E, Fujita S, Kampine JP, Stowe DF: Sevoflurane mimics ischemic preconditioning effects on coronary flow and nitric oxide release in isolated hearts. *ANESTHESIOLOGY* 1999; 91:701–12
 52. Liu PT, Stenger S, Li H, Wenzel L, Tan BH, Krutzik SR, Ochoa MT, Schaubert J, Wu K, Meinken C, Kamen DL, Wagner M, Bals R, Steinmeyer A, Z gel U, Gallo RL, Eisenberg D, Hewison M, Hollis BW, Adams JS, Bloom

- BR, Modlin RL: Toll-like receptor triggering of a vitamin D-mediated human antimicrobial response. *Science* 2006; 311:1770–3
53. Yamada Y, Laube I, Jang JH, Bonvini JM, Inci I, Weder W, Beck Schimmer B, Jungraithmayr W: Sevoflurane preconditioning protects from posttransplant injury in mouse lung transplantation. *J Surg Res* 2017; 214:270–7
 54. Zhao J, Wang F, Zhang Y, Jiao L, Lau WB, Wang L, Liu B, Gao E, Koch WJ, Ma XL, Wang Y: Sevoflurane preconditioning attenuates myocardial ischemia/reperfusion injury via caveolin-3-dependent cyclooxygenase-2 inhibition. *Circulation* 2013; 128(11 Suppl 1):S121–9
 55. Erol A, Reisli R, Reisli I, Kara R, Otelcioglu S: Effects of desflurane, sevoflurane and propofol on phagocytosis and respiratory burst activity of human polymorphonuclear leucocytes in bronchoalveolar lavage. *Eur J Anaesthesiol* 2009; 26:150–4
 56. Fahlenkamp AV, Coburn M, Rossaint R, Stoppe C, Haase H: Comparison of the effects of xenon and sevoflurane anesthesia on leucocyte function in surgical patients: a randomized trial. *Br J Anaesth* 2014; 112:272–80

ANESTHESIOLOGY

Superior Trunk Block Provides Noninferior Analgesia Compared with Interscalene Brachial Plexus Block in Arthroscopic Shoulder Surgery

RyungA Kang, M.D., Ph.D., Ji Seon Jeong, M.D., Ph.D., Ki Jinn Chin, M.B.B.S., F.R.C.P.C., Jae Chul Yoo, M.D., Ph.D., Jong Hwan Lee, M.D., Ph.D., Soo Joo Choi, M.D., Ph.D., Mi Sook Gwak, M.D., Ph.D., Tae Soo Hahm, M.D., Ph.D., Justin Sangwook Ko, M.D., Ph.D.

ANESTHESIOLOGY 2019; 131:1316–26

EDITOR'S PERSPECTIVE

What We Already Know about This Topic

- Interscalene nerve block is commonly used for shoulder surgery for anesthesia and postoperative analgesia
- Unfortunately, interscalene blocks commonly result in hemidiaphragmatic paralysis

What This Article Tells Us That Is New

- When interscalene block was compared with superior trunk block, less frequent hemidiaphragmatic paralysis was seen in the superior trunk block group
- Superior trunk block was noninferior to interscalene block in terms of pain scores for up to 24 h postoperatively, and superior trunk block patients were no less satisfied

The conventional ultrasound-guided interscalene brachial plexus block involves injection directly around the C5 and C6 nerve roots. Although it provides highly effective postoperative analgesia after arthroscopic shoulder surgery,^{1,2} it almost always results in hemidiaphragmatic paresis.^{3,4} Other

ABSTRACT

Background: Interscalene brachial plexus block of the C5–C6 roots provides highly effective postoperative analgesia after shoulder surgery but usually results in hemidiaphragmatic paresis. Injection around the superior trunk of the brachial plexus is an alternative technique that may reduce this risk. The authors hypothesized that the superior trunk block would provide noninferior postoperative analgesia compared with the interscalene block and reduce hemidiaphragmatic paresis.

Methods: Eighty patients undergoing arthroscopic shoulder surgery were randomized to receive a preoperative injection of 15 ml of 0.5% ropivacaine and 5 $\mu\text{g} \cdot \text{ml}^{-1}$ epinephrine around either (1) the C5–C6 nerve roots (interscalene block group) or (2) the superior trunk (superior trunk block group). The primary outcome was pain intensity 24 h after surgery measured on an 11-point numerical rating score; the prespecified noninferiority limit was 1. Diaphragmatic function was assessed using both ultrasonographic measurement of excursion and incentive spirometry by a blinded investigator before and 30 min after block completion.

Results: Seventy-eight patients completed the study. The pain score 24 h postoperatively (means \pm SDs) was 1.4 ± 1.0 versus 1.2 ± 1.0 in the superior trunk block ($n = 38$) and interscalene block ($n = 40$) groups, respectively. The mean difference in pain scores was 0.1 (95% CI, -0.3 to 0.6), and the upper limit of the 95% CI was lower than the prespecified noninferiority limit. Analgesic requirements and all other pain measurements were similar between groups. Hemidiaphragmatic paresis was observed in 97.5% of the interscalene block group versus 76.3% of the superior trunk block group ($P = 0.006$); paresis was complete in 72.5% versus 5.3% of the patients, respectively. The decrease in spirometry values from baseline was significantly greater in the interscalene block group.

Conclusions: The superior trunk block provided noninferior analgesia compared with interscalene brachial plexus block for up to 24 h after arthroscopic shoulder surgery and resulted in significantly less hemidiaphragmatic paresis.

(ANESTHESIOLOGY 2019; 131:1316–26)

concerns include the risk of intraneural injection into the relatively unprotected roots^{5,6} and injury to the dorsal scapular nerve or long thoracic nerve.^{7,8} The superior trunk block was described by Burckett-St. Laurent *et al.*⁹ as a refinement of the conventional interscalene block technique that addresses these limitations. The superior trunk is formed by the fusion of C5 and C6 nerve roots, and therefore local anesthetic injection around the superior trunk should produce similar analgesia of the shoulder because all the terminal nerves innervating the shoulder arise distal to the superior trunk. Moreover, the site of injection is further away from the phrenic nerve, and this should theoretically reduce the risk of hemidiaphragmatic

This article has been selected for the Anesthesiology CME Program. Learning objectives and disclosure and ordering information can be found in the CME section at the front of this issue. This article is featured in "This Month in Anesthesiology," page 1A. This article is accompanied by an editorial on p. 1207. This article has a visual abstract available in the online version. Part of the work presented in this article has been presented at the 95th Annual Scientific Meeting of the Korean Society of Anesthesiologists in Seoul, Korea, November 8–10, 2018. R.A.K. and J.S.J. contributed equally to this article.

Submitted for publication February 1, 2019. Accepted for publication July 6, 2019. From the Departments of Anesthesiology and Pain Medicine (R.A.K., J.S.J., J.H.L., S.J.C., M.S.G., T.S.H., J.S.K.) and of Orthopedics (J.C.Y.), Samsung Medical Center, Sungkyunkwan University School of Medicine, Seoul, Korea; and the Department of Anesthesia, Toronto Western Hospital, Toronto, Canada (K.J.C.).

Copyright © 2019, the American Society of Anesthesiologists, Inc. All Rights Reserved. Anesthesiology 2019; 131:1316–26. DOI: 10.1097/ALN.0000000000002919

paresis. However, the analgesic efficacy of the superior trunk block and the associated incidence of hemidiaphragmatic paresis have yet to be systematically investigated in clinical trials. We therefore designed the present randomized, double-blinded, noninferiority clinical trial to test the hypothesis that the superior trunk block would provide noninferior postoperative analgesia to the interscalene brachial plexus block while reducing hemidiaphragmatic paresis in patients undergoing arthroscopic shoulder surgery.

Materials and Methods

Study Participants

After receiving approval by the Samsung Medical Center Research Ethics Board (Seoul, Korea; SMC 2018-02-006-001), this trial was prospectively registered on the Clinical Trial Registry of Korea (Seoul, Korea; KCT0002802 with principal investigator Justin Sangwook Ko) on April 16, 2018. Written informed consent was obtained from all participants. We enrolled 80 adult patients with American Society of Anesthesiologists (ASA) Physical Status classification I to III scheduled for elective unilateral arthroscopic shoulder surgery between April 16, 2018 to September 1, 2018 at Samsung Medical Center, Seoul, Korea. All operations were performed by a single surgeon. Eligible patients were identified from the surgeon's operating list and contacted the day before their surgery to inform them of the study protocol. We excluded patients who refused to participate in the study and those with a history of cardiac, renal, or hepatic disease; preexisting neurologic deficits or neuropathy affecting the brachial plexus; contraindications to peripheral nerve block; preexisting operative respiratory dysfunction; or allergy to local anesthetics. Patients undergoing revision, planned open, or irrigation and debridement procedures were also excluded.

Randomization and Blinding

A member of the Samsung Medical Center who was not otherwise involved in the study performed computer-generated block randomization in a 1:1 ratio to an interscalene brachial plexus block group ($n = 40$) and a superior trunk block group ($n = 40$). Allocation of patients to each study group was concealed in an opaque envelope, which was only opened by the block practitioner just before block performance. To eliminate performance bias, all blocks were performed by a single experienced regional anesthesiologist (J.S.K.) together with a single assistant nurse. They were not involved in any other aspect of the conduct of the study. All other research personnel, outcome assessors, and caregivers were blinded to group allocation. Patient blinding was maintained by standardizing the perceptible elements of block performance between both groups: positioning, ultrasound probe placement, needle insertion site, use of neurostimulation, and local anesthetic injection volume.

Brachial Plexus Block Performance

Patients received no premedication before arrival in a dedicated block room, where the brachial plexus block was performed. After applying standard ASA monitoring and supplemental oxygen, IV midazolam (1 to 1.5 mg) was administered for anxiolysis. Before performing the block, a prescan was performed to identify the presence of long thoracic and dorsal scapular nerves and blood vessels around the brachial plexus, using a 6 to 15 MHz high-frequency linear array transducer (X-Porte, Sonosite, USA). The C5 and C6 nerve roots were located within the interscalene groove and traced distally to where they coalesced into the superior trunk. After sterile skin preparation and skin infiltration with 1 ml of 1% lidocaine, an ultrasound-guided interscalene block or superior trunk block was performed according to group allocation using a 22-gauge 50-mm insulated stimulating needle (UniPlex Nanoline, Pajunk, Germany). The interscalene block was performed using the posterior in-plane extraplexus approach.¹ Briefly, the block needle was advanced in-plane to the ultrasound beam at the level of the cricoid cartilage in a lateral-to-medial direction through the middle scalene muscle. The dorsal scapular nerve and long thoracic nerve were identified within the middle scalene muscle and avoided, using a combination of ultrasonographic visualization and neurostimulation with an initial current of 2.0 mA, pulse width of 100 ms, and a frequency of 2 Hz. Once the needle tip was in proximity to the brachial plexus, the current was decreased to 0.5 mA, and a contraction of the biceps or deltoid was sought.⁷ The final needle tip position was immediately lateral to the brachial plexus sheath and adjacent to C5 and C6 nerve roots,¹⁰ whereupon 15 ml of 0.5% ropivacaine with $5 \mu\text{g} \cdot \text{mL}^{-1}$ epinephrine was injected.

The superior trunk block was performed according to the method described by Burckett-St. Laurent *et al.*⁹ The superior trunk was visualized distal to the convergence of the C5 and C6 nerve roots but proximal to the take-off of the suprascapular nerve.⁹ The block needle was advanced in-plane to the ultrasound beam in a lateral-to-medial direction under the deep cervical fascia and superficial to the middle scalene muscle, until the needle tip was immediately adjacent to the lateral border of the superior trunk (fig. 1).¹¹ The same neurostimulation protocol was used to maintain patient blinding, and an identical volume and concentration of local anesthetic was injected.

After block completion, sensory and motor blockade was assessed every 5 min for 30 min. Motor block was evaluated by asking the patient to make a fist and squeeze the assessor's fingers. Motor function was graded on a three-point scale (2 = normal; 1 = weakness; and 0 = complete loss of power). Sensory block was evaluated in the C5 and C6 dermatomes, and the extent of sensory loss was graded on a three-point scale (2 = normal; 1 = loss of sensation to pinprick; and 0 = loss of sensation to light touch). Block success was defined as a sensory score of 0 within 30 min

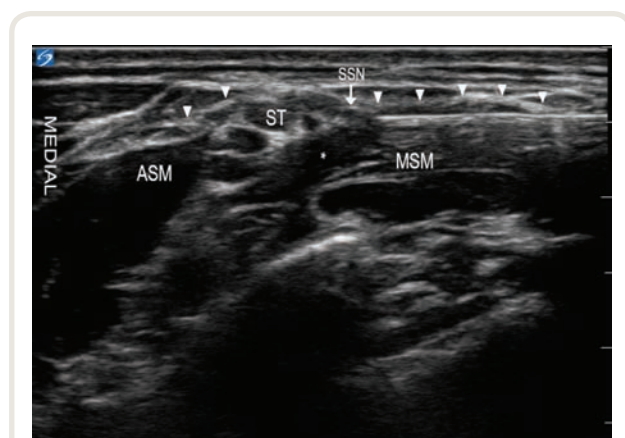


Fig. 1. Ultrasongraphic image of the superior trunk block. At the level of the superior trunk, the suprascapular nerve (SSN, arrow) is visible in this individual on the lateral side of the superior trunk. The block needle was advanced in-plane in the lateral-to-medial direction until the needle tip was just adjacent to the lateral boarder of the superior trunk. Local anesthetic (*) was injected around the superior trunk. ASM, anterior scalene muscle; MSM, middle scalene muscle; ST, superior trunk. White down-pointing triangles indicate the deep cervical fascia.

of local anesthetic injection. The block was also considered a failure if the resting pain score equaled or exceeded the threshold for intense pain, defined as 6 of 10 on an 11-point numerical rating scale (0 = no pain; and 10 = worst pain imaginable), within 3 h after initiation of block.

Assessment of Diaphragmatic Movement and Pulmonary Function

Ipsilateral diaphragmatic excursion was assessed using ultrasound imaging before (baseline) and 30 min after block completion in all patients by a single anesthesiologist (R.A.K.) who was experienced in the technique¹² and who was blinded to group allocation. Diaphragmatic excursion was assessed using M-mode ultrasonography with the patient in the sitting position.⁴ A 5 to 2 MHz curvilinear transducer (X-Porte, Sonosite) was placed under the lowest rib at the anterior or midaxillary line, and the liver or spleen was used as an acoustic window. Diaphragmatic excursion between full inspiration and expiration was measured in centimeters. Each test was performed three times, and the values were averaged. The severity of hemidiaphragmatic paresis was measured by the decrease in diaphragmatic excursion (calculated as a percentage difference) between baseline and 30 min after block completion (fig. 2). Complete hemidiaphragmatic paresis was defined as a 75 to 100% decrease or the occurrence of paradoxical movement. Partial and absent hemidiaphragmatic paresis were defined as 25 to 75% decrease and a less than 25% decrease in diaphragmatic excursion, respectively.¹³ Overall, we considered

hemidiaphragmatic paresis to be present if partial or complete paresis occurred.¹² Pulmonary function was evaluated before and 30 min after block completion using a bedside spirometer (COPd-6, Vitalograph, Ireland) with the patient in the sitting position. The forced expiratory volume at 1 s and forced expiratory volume at 6 s were measured three times, and the values were averaged. We used forced expiratory volume at 6 s as a surrogate for forced vital capacity.¹⁴

Intraoperative Management

After completion of postblock assessments, all patients underwent general anesthesia with tracheal intubation using IV propofol (1.5 to 2.0 mg · kg⁻¹), rocuronium (0.6 to 0.8 mg · kg⁻¹), and IV remifentanyl (0.05 to 0.1 µg · kg⁻¹ · min⁻¹). Anesthesia was maintained with sevoflurane in an air-oxygen mixture. A continuous infusion of remifentanyl (0.01 to 0.1 µg · kg⁻¹ · min⁻¹) was used as needed to maintain the heart rate and mean blood pressure within 20% of preinduction values. No additional intraoperative analgesics were given.

Postoperative Management

After surgery, all patients were transferred to the postanesthesia care unit, where they remained until they met the discharge criteria.¹⁵ Patients were then transferred to the surgical ward for further care. Pain in the shoulder at rest was measured using an 11-point numerical rating scale. Postoperative supplemental analgesia was standardized as follows. At the first report of pain at the surgical site (pain score of higher than 0 of 10), in either the postanesthesia care unit or the surgical ward, IV patient-controlled analgesia (PCA) with fentanyl was initiated by a nurse who was blinded to group allocation. The IV fentanyl PCA pump was programmed to deliver a continuous infusion of 15 µg · h⁻¹ and a bolus dose of 15 µg on demand with a lockout interval of 15 min. Both the start time of the IV PCA and cumulative fentanyl dose were recorded automatically by the pump (Gemster, Hospira, Inc., USA), and these data were later downloaded for analysis. Once oral intake was tolerated, all patients received multimodal analgesia consisting of oral acetaminophen 650 mg every 8 h, oral celecoxib 200 mg every 12 h, and oral Targin (oxycodone hydrochloride 10 mg/naloxone hydrochloride 5 mg; Mundipharma, Korea) 1 tablet every 12 h. Patients with persistent pain scores of higher than 4 of 10 despite this regimen received rescue analgesia with either IV morphine 10 mg (if not tolerating oral intake) or oral oxycodone 5 mg. The IV PCA was discontinued on postoperative day 2. All patients remained in the hospital for 3 days after surgery and were followed up at the outpatient clinic on postoperative day 14.

Outcome Measures

The primary outcome was the pain score at rest 24 h postoperatively. Secondary outcomes included resting pain

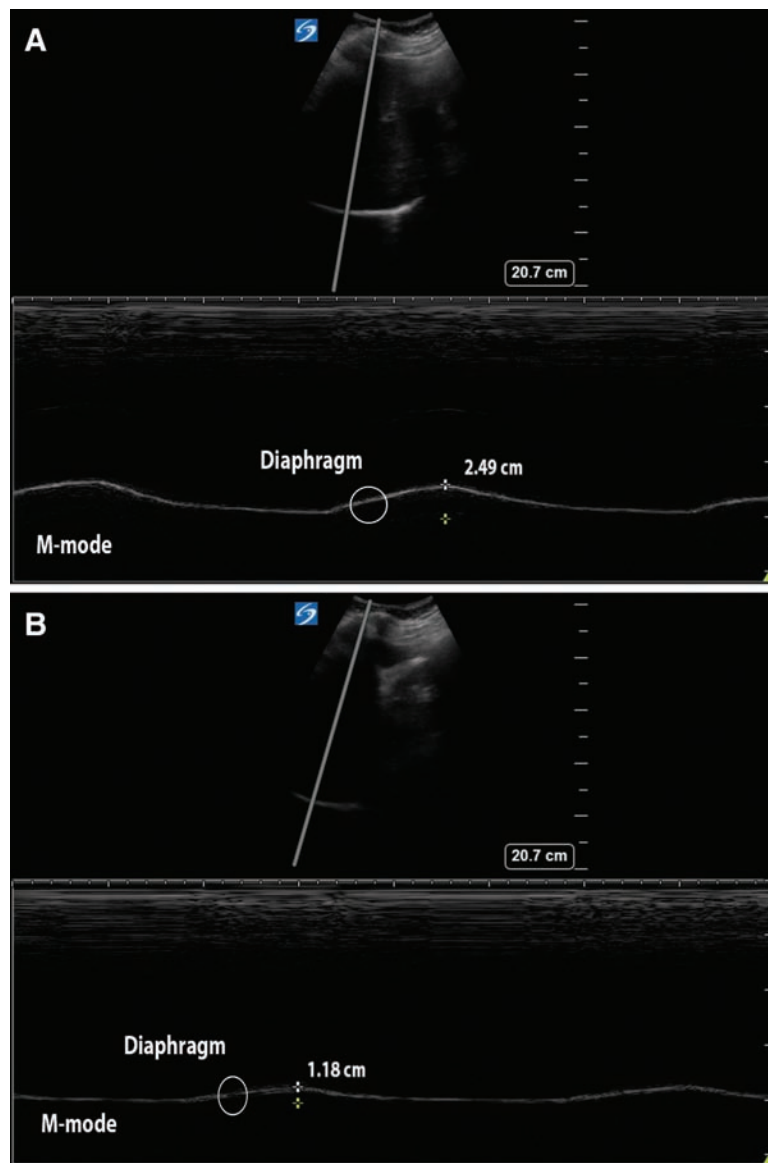


Fig. 2. Curvilinear transducer ultrasound image of the right diaphragm using the liver as an acoustic window in two-dimensional B-mode and M-mode. (A) Preblock (baseline) diaphragmatic excursion was checked on deep breathing in M-mode (2.49 cm). (B) Postblock assessment of diaphragmatic excursion. Reduced diaphragmatic excursion was seen in M-mode (1.18 cm); the decrease in diaphragmatic excursion was 52.6%, indicating partial hemidiaphragmatic paresis.

scores at 6, 12, and 18 h, area under the 24-h pain curve, maximum pain score during the first 24 h, the incidence and severity of hemidiaphragmatic paresis, cumulative postoperative opioid consumption at 24 h postoperatively (reported as IV morphine equivalents¹⁶), duration of analgesia (time between block completion and initiation of IV PCA) and motor block (time between block completion and return to presurgical hand grip strength), patient satisfaction with analgesia at 24 h, and quality of sleep on the first night. Patient satisfaction at 24 h, and quality of sleep were measured using a Likert scale (1 = very dissatisfied, 2 =

dissatisfied, 3 = neutral, 4 = satisfied, and 5 = very satisfied). Residual block-related neurologic symptoms (persistent numbness, paresthesia, or weakness) were also measured at 24 h, 48 h, and 14 days postoperatively. All assessments and data collection were performed by research personnel blinded to group allocation.

Sample Size Considerations

The sample size was calculated based on the primary endpoint according to the noninferiority hypothesis.¹⁷ The predetermined noninferiority limit (δ) was set to 1 point on

the 11-point visual analogue score scale.¹⁸ Based on a preliminary analysis (unpublished), an SD of 1.48 was assumed for the pain scores distribution. With $\alpha = 0.05$ and power of 90%, 38 patients were required in each group. Assuming a 5% dropout rate, we decided to enroll 40 patients per group. Primary outcome was analyzed according to the noninferiority approach.¹⁹ The noninferiority hypothesis for the primary outcome was tested using the one-sided *t* test (null hypothesis that the difference in pain scores was at least 1 point *vs.* the alternative hypothesis that the difference in pain scores was less than 1 point) under a significance level of 2.5%. The two-sided 95% CI values,²⁰ the upper limit of which was equivalent to the upper limit of the one-sided 97.5% CI of the mean difference in pain scores by treatment, are presented in relation to the predefined noninferiority limit and null effect.

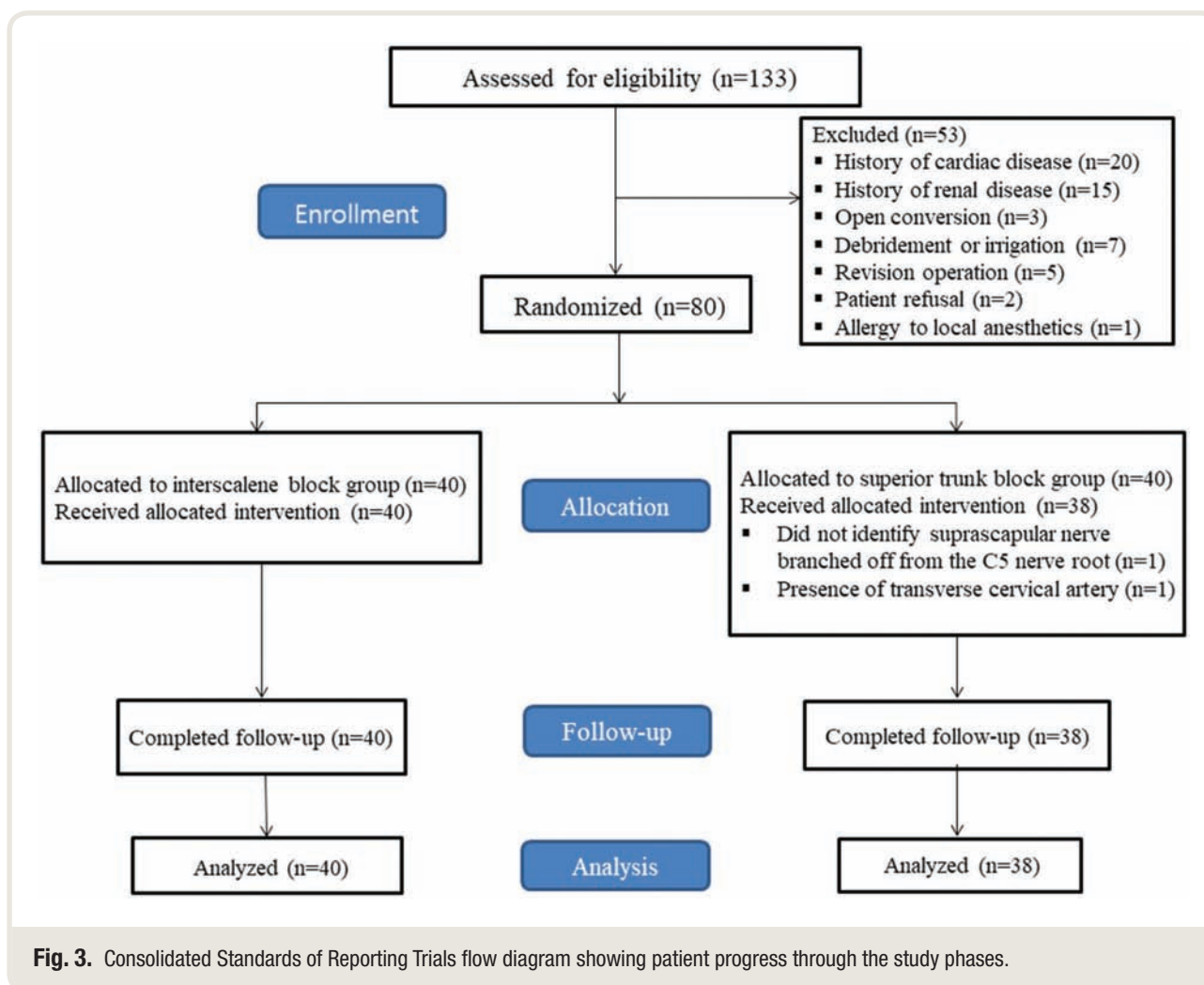
Statistical Analysis

After confirming the normality of data distribution using the Shapiro–Wilk test, descriptive statistics and other secondary outcome variables were compared using the *t* test

or Mann–Whitney test for continuous variables and the chi-square test or Fisher exact test for categorical variables. Continuous variables are presented as means \pm SDs with 95% CI or median and interquartile range as appropriate. Categorical variables are presented as numbers and percentages. Two-sided tests were used, except for the one-sided *t* test of noninferiority. Comparison of area under the curve for pain data to assess cumulative or average pain within the first 24 h used linear interpolation between time points. A Bonferroni correction was used for multiple comparisons. Data analysis was performed using SPSS software (version 25.0, SPSS Inc., USA). For all analyses, $P < 0.05$ was taken to indicate significance. The full trial protocol used during this study is available from the corresponding author on request.

Results

From April 16, 2018 to September 1, 2018, 133 patients scheduled for arthroscopic shoulder surgery were assessed for eligibility, and 53 patients who did not meet the inclusion criteria were excluded (fig. 3). All enrolled patients ($n = 80$)



were randomly assigned to one of the two treatment groups ($n = 40$ each). Two patients allocated to the superior trunk block group were excluded after the preblock ultrasound scan revealed the transverse cervical artery overlying the superior trunk in one patient, and the suprascapular nerve could not be identified branching off from the C5 nerve root in the other patient. Both these patients received interscalene brachial plexus block and did not participate further in the study. A total of 78 patients (interscalene block group [$n = 40$] and superior trunk block group [$n = 38$]) completed the study and were included in the final analysis. The baseline patient and surgical characteristics are shown in table 1. All blocks met the criteria for success at 30 min after block completion, and none of the patients required supplemental analgesia or IV PCA initiation in the postanesthesia care unit.

The mean pain score at 24 h postoperatively was 1.4 ± 1.0 in the superior trunk block group (95% CI, 1.0 to 1.7) and 1.2 ± 1.0 in the interscalene block group (95% CI, 0.9 to 1.5). The mean treatment difference (superior trunk block group–interscalene block group) in the pain score at 24 h between the two groups was 0.1 (95% CI, -0.3 to 0.6). Because the upper limit of the 95% CI was lower than the prespecified noninferiority margin ($\delta = 1$), noninferiority was established ($P < 0.001$; fig. 4). There was no significant difference in the 24-h area under the curve for pain scores between the two groups (superior trunk block group *vs.* interscalene block group; 2.1 ± 1.0 *vs.* 2.1 ± 1.1 ; $P = 0.963$). Pain scores at each time point 6, 12, 18, or 24 h postoperatively were also similar between both groups ($P > 0.522$; fig. 5). There was no significant difference in the reported maximum pain score during the first 24 h postoperatively (superior trunk block group *vs.* interscalene block group; 4.7 ± 1.9 *vs.* 4.8 ± 1.8 ; $P = 0.361$). Duration of analgesia, duration of motor block, incidence of need for rescue analgesics, and cumulative opioid consumption at 24 h were similar between both groups (table 2). There were no significant differences between groups in the quality of sleep

on the first postoperative night or satisfaction with analgesia at 24 h (table 2).

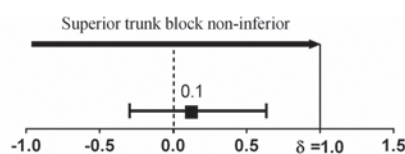
Baseline diaphragmatic excursion on deep breathing was similar in both groups before block performance (table 3). At 30 min after block completion, the mean reduction in diaphragmatic excursion was significantly less in the superior trunk block group compared with interscalene block group ($42.2 \pm 21.9\%$ *vs.* $79.5 \pm 21.1\%$, $P < 0.001$). The incidence of complete or partial hemidiaphragmatic paresis was significantly lower in the superior trunk block group than in the interscalene block group (29 [76.3%] *vs.* 39 [97.5%] patients; $P = 0.006$). There were significantly more patients with complete hemidiaphragmatic paresis in the interscalene block group (2 [5.3%] *vs.* 29 [72.5%] patients; $P < 0.001$). Twenty-seven patients (71.1%) in the superior trunk block group and ten patients (25%) in the interscalene block group showed partial hemidiaphragmatic paresis. There was no evidence of hemidiaphragmatic paresis at 30 min after the blockade in nine patients (23.7%) and one patient (2.5%) in the superior trunk block and interscalene block groups, respectively. The superior trunk block group had smaller mean reductions in forced expiratory volume at 1 s and forced expiratory volume at 6 s compared with the interscalene group (table 3).

One patient in each of the treatment groups developed symptomatic dyspnea without desaturation after surgery in the postanesthetic care unit. After reassuring the patients, we assessed the diaphragmatic excursion with ultrasound and obtained chest radiographs to exclude pneumothorax. Both patients had complete hemidiaphragmatic paresis. Their symptoms subsided with administration of oxygen in the sitting position and resolved within 12 h. Two and four patients in the interscalene block group and superior trunk block group, respectively, reported numbness in the distal fingers at 24 h, but this resolved spontaneously within 48 h. Four patients in the interscalene block group reported persistent weakness of hand grip at 24 h that resolved within 48 h. None of the patients in the superior trunk block

Table 1. Patient Characteristics

Parameter	Interscalene Block Group (n = 40)	Superior Trunk Block Group (n = 38)
Age, yr	59 [44–64]	56 [42–62]
Sex, male/female	20/20	23/15
Body mass index, kg · m ⁻²	25.7 ± 3.5	25.5 ± 3.3
ASA status, I/II/III	22/18/0	20/17/1
Duration of surgery, min	81 [70–98]	78 [68–89]
Surgical procedure		
Arthroscopy + rotator cuff repair	28	30
Arthroscopy + Bankart repair	5	3
Arthroscopy + superior labrum from anterior to posterior repair	3	3
Arthroscopy + Latarjet	4	2

The values are means ± SDs, median [interquartile range], or number as appropriate. ASA, American Society of Anesthesiologists.



Pain scores differences (superior trunk group-interscalene block group) at 24 h

Fig. 4. Noninferiority diagram of numerical rating scale pain score differences in superior trunk block group and interscalene block group at 24 h postoperatively. The *solid line* indicates a noninferiority margin (δ) of 1. *Squares* indicate mean pain score differences, and *error bars* indicate the 95% CIs of the difference between groups. $P < 0.05$ was taken to indicate statistical significance.

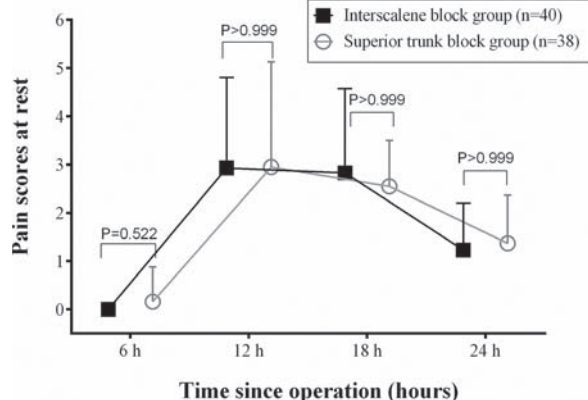


Fig. 5. The numerical rating scale pain scores at rest during the first 24 h after surgery. *Symbols* indicate the means, and *whiskers* indicate SDs. The individual P values result from a Bonferroni correction for multiple comparisons. $P < 0.05$ was taken to indicate statistical significance.

group reported motor weakness at 24 h. No other significant adverse events occurred in either group.

Discussion

The ultrasound-guided superior trunk block has only been described in two case reports,^{9,21} and this study is the first randomized controlled trial to evaluate the technique in comparison with the conventional ultrasound-guided interscalene brachial plexus block. In this noninferiority clinical trial, we demonstrated that the superior trunk block provided postoperative shoulder analgesia equivalent to that of the interscalene brachial plexus block, as demonstrated by similar pain scores and area under the pain curve up to 24 h postoperatively. In addition, the duration of analgesia and 24-h opioid consumption were similar with both techniques.

It is notable that patients who received a superior trunk block had less deterioration in diaphragmatic excursion and respiratory function compared with interscalene brachial plexus block. The first report on superior trunk block described effective shoulder analgesia without hemidiaphragmatic paresis, and this was attributed to the more distal site of injection.⁹ The phrenic nerve and C5 nerve root are anatomically separated by a distance of 1.8 to 2.0 mm in adults at the level of the cricoid cartilage, and the distance between them increases by an additional 3 mm for every centimeter as the phrenic nerve courses more medially into the root of the neck.²² The likelihood of local anesthetic spread to the phrenic nerve or its origins from the C3–C5 roots is therefore reduced with the superior trunk block, and this hypothesis is supported by our results. Although healthy individuals with transient hemidiaphragmatic paresis are usually asymptomatic,⁴ our findings may have important implications for the choice of regional anesthesia technique in patients with compromised respiratory function undergoing shoulder surgery. The incidence of hemidiaphragmatic paresis after conventional interscalene brachial plexus block is as high as 100% with local anesthetic volumes of 20 ml or more.^{3,23} Although this incidence can be reduced up to 45% by decreasing local anesthetic volume to 5 to 10 ml,^{3,24} this is accompanied by a clinically significant reduction in the duration and potency of perioperative analgesia²⁵ and may also carry a significant risk of block failure in less-experienced hands. For this reason, it is standard practice in our institution to use 15 ml of 0.5% ropivacaine for interscalene brachial plexus blockade in patients undergoing arthroscopic shoulder surgery.^{1,2} This is also consistent with the reported practice in other centers.²⁶ We believe the significance and generalizability of our findings are strengthened by the use of a pragmatic local anesthetic dose in both treatment groups.

There are other potential advantages of the superior trunk block that we did not formally evaluate in this study. The aim in regional anesthesia of the shoulder is to block the nerves derived from the C5 and C6 nerve roots. The ultrasound-guided interscalene brachial plexus block is therefore generally performed at the level of the cricoid cartilage, where the C5 and C6 roots are located within the groove between the anterior and middle scalene muscles.⁹ However, this technique can sometimes be technically challenging. The enveloping fascial layer around the hypoechoic C5 and C6 roots is very thin, which not only makes it difficult to discern the boundaries of the hypoechoic C5 and C6 roots but also increases the risk of subepineurial injection and injury from needle-nerve contact.⁶ Anatomical variation in the course of the C5 and C6 roots is common and can further contribute to difficulties with identification. For example, the C5 nerve root may be found within the anterior scalene muscle rather than the interscalene groove,²⁷ and the C6 nerve root almost always splits into two hypoechoic rootlets that

Table 2. Postoperative Clinical Parameters between the Interscalene Block Group and Superior Trunk Block Group

Outcomes	Interscalene Block Group (n = 40)	Superior Trunk Block Group (n = 38)	P Value*
Duration of analgesia: Time to first pain at surgical site, h	10 ± 3	9 ± 2	0.321
Duration of motor blockade, h	14 ± 4	13 ± 5	0.136
Cumulative opioid consumption at 24 h, mg	60.9 ± 10.2	58.5 ± 9.1	0.281
Patients who received rescue analgesics, n (%)	26 (65)	11 (28.9)	0.488
Quality of sleep on the first night (Likert scale; 1 to 5 [†])	2 [2–2]	2 [1–2]	0.911
Patient satisfaction with pain relief at 24 h (Likert scale; 1 to 5 [†])	3 [2–3]	3 [2–3]	0.697
Complications			
Symptomatic dyspnea at postanesthesia care unit/24 h	1/0	1/0	> 0.999
Numbness at fingers at 24 h/48 h/14 days	2/0/0	4/0/0	0.425
Motor weakness at 24 h/48 h/14 days	4/0/0	0/0/0	0.116

The values are means ± SDs, median [interquartile range], or number (percentages) as appropriate.

*The *P* value for the *t* test, Mann–Whitney U test, and Fisher exact test is set at 0.05. [†]Likert scale where 1 = very dissatisfied, 2 = dissatisfied, 3 = neutral, 4 = satisfied, and 5 = very satisfied.

Table 3. Outcomes of Diaphragmatic Movement and Pulmonary Function between the Interscalene Block Group and Superior Trunk Block Group

Outcomes	Interscalene Block Group (n = 40)	Superior Trunk Block Group (n = 38)	P Value*
Incidence of hemidiaphragmatic paresis, n (%)	39 (97.5)	29 (76.3)	0.006
Absent/partial/complete paresis, n	1/10/29	9/27/2	< 0.001
Diaphragmatic excursions, cm			
At baseline	4.1 ± 1.5	4.0 ± 1.3	0.835
At 30 min after blockade	0.8 ± 0.7	2.4 ± 1.1	< 0.001
Decrease in diaphragmatic excursion, %	79.5 ± 21.1	42.2 ± 21.9	< 0.001
Pulmonary function test			
FEV ₁ at baseline, l	2.4 ± 0.9	2.2 ± 0.9	0.327
FEV ₁ at 30 min after blockade, l	1.3 ± 0.8	1.4 ± 0.9	0.496
Decreases in FEV ₁ , %	44.7 ± 22.8	33.2 ± 20.5	0.021
Forced expiratory volume at 6 s at baseline, l	2.8 ± 1.0	2.7 ± 1.2	0.570
Forced expiratory volume at 6 s at 30 min after blockade, l	1.7 ± 1.0	2.0 ± 1.1	0.166
Decreases in forced expiratory volume at 6 s, %	41.5 ± 23.0	24.9 ± 16.6	< 0.001

The values are means ± SDs or number (percentages) as appropriate.

*The *P* value for the *t* test and the Fisher exact test is set at 0.05.

FEV₁, forced expiratory volume at 1 s.

can be mistaken for two separate roots (C6 and C7), leading to unintended intraneural injection.⁵ However, the C5 root and C6 nerve rootlets inevitably unite to form the superior trunk regardless of the variations in root anatomy proximal to this point, and thus anatomical variation is inconsequential to the superior trunk block.^{9,21} In addition, unlike the C5 and C6 roots, the superior trunk is surrounded by a clearly visible and well defined connective sheath. This not only facilitates target visualization and identification but also enhances resilience to needle–nerve contact.⁵ Injury to the dorsal scapular nerve and long thoracic nerves is another concern with the posterior in-plane approach to conventional ultrasound-guided interscalene brachial plexus block, because these two nerves run within the middle scalene muscle

and thus lie within the needle path.^{7,8,28} However, the needle path in superior trunk block does not traverse the middle scalene muscle, instead passing between the deep cervical fascia and middle scalene muscle, thus minimizing the risk of inadvertent needle trauma to these nerves.⁹

There are two points we would like to highlight regarding technical performance of the superior trunk block. First, it is important to perform the block at a level proximal to the take-off of the suprascapular nerve. This can usually be identified as a small hypoechoic circle at the most lateral aspect of the superior trunk, which separates and runs laterally under the omohyoid muscle in the supraclavicular region.²⁹ In the present study we excluded one patient in the superior trunk block group because we could not confidently identify the suprascapular nerve, which may

have been due to anatomical variation in the size and location of the suprascapular nerve or the presence of several suprascapular nerves.^{29,30} This was mandated by our study protocol; however, it is not a significant issue in clinical practice, because local anesthetic can simply be injected at the point where the C5 and C6 roots coalesce into the superior trunk, which will reliably anesthetize the suprascapular nerve without the need to specifically identify it. Second, the practitioner must be aware that the transverse cervical artery and dorsal scapular artery cross over the brachial plexus and can overlies the superior trunk.³¹ The transverse cervical artery and dorsal scapular arteries are usually readily identified by careful observation for pulsatile hypoechoic structures and the use of color Doppler. In the present study, we excluded one patient in the superior trunk block group because of the presence of a transverse cervical artery in the planned needle trajectory. However, in practice, it is usually possible to select a transverse plane for needle advancement that avoids these vessels.

The main limitation of our study was that we defined our primary outcome as the pain score at 24 h postoperatively. On hindsight, this may not reflect the true effect of each technique because the block would, in all probability, have worn off by then. Nevertheless, the other analgesic outcomes, including the 24-h area under the curve for pain, time to first analgesic request, and cumulative opioid requirements, strongly support analgesic equivalence of the superior trunk block and interscalene brachial plexus block. Another limitation is that all blocks were performed by a single experienced anesthesiologist in one center. Although this reduces performance bias and increases study validity, it does limit the generalizability of our findings. Based on our experience as clinicians and educators, however, we believe the superior trunk block is no more difficult to perform than the interscalene brachial plexus block and may in fact be easier for the reasons outlined above. Additional studies would be needed to confirm this. Research is also warranted to determine whether lower volumes of local anesthetic may further decrease the incidence and severity of hemidiaphragmatic paresis with the superior trunk block and whether this has any impact on analgesic effect and duration. Finally, in this study, the superior trunk block was administered for perioperative analgesia and not surgical anesthesia. Although in theory it should work as well as an interscalene block with appropriate local anesthetic dosing, this has yet to be formally proven.

In conclusion, the results of our noninferiority trial demonstrated that the superior trunk block provides similar postoperative shoulder analgesia to conventional interscalene brachial plexus block in patients undergoing arthroscopic shoulder surgery. Moreover, the superior trunk block was superior in preserving diaphragmatic and respiratory function. Based on these findings, the superior trunk block may be considered a viable alternative to the

interscalene block, especially in patients at high risk of respiratory complications.

Acknowledgments

The authors thank Seonwoo Kim, Ph.D., from the Statistics and Data Center of the Samsung Medical Center, Seoul, Korea, for providing comments regarding the statistical analysis.

Research Support

Support was provided solely from institutional and/or departmental sources.

Competing Interests

The authors declare no competing interests.

Reproducible Science

Full protocol available at: jsko@skku.edu. Raw data available at: jsko@skku.edu.

Correspondence

Address correspondence to Dr. Ko: Samsung Medical Center, 81 Irwon ro, Gangnam gu, Seoul 06351, Korea. jsko@skku.edu. This article may be accessed for personal use at no charge through the Journal Web site, www.anesthesiology.org.

References

1. Kang R, Jeong JS, Yoo JC, Lee JH, Choi SJ, Gwak MS, Hahm TS, Huh J, Ko JS: Effective dose of intravenous dexmedetomidine to prolong the analgesic duration of interscalene brachial plexus block: A single-center, prospective, double-blind, randomized controlled trial. *Reg Anesth Pain Med* 2018; 43:488–95
2. Kang RA, Jeong JS, Yoo JC, Lee JH, Gwak MS, Choi SJ, Hahm TS, Cho HS, Ko JS: Improvement in postoperative pain control by combined use of intravenous dexamethasone with intravenous dexmedetomidine after interscalene brachial plexus block for arthroscopic shoulder surgery: A randomised controlled trial. *Eur J Anaesthesiol* 2019; 36:360–8
3. Riazi S, Carmichael N, Awad I, Holtby RM, McCartney CJ: Effect of local anaesthetic volume (20 vs. 5 ml) on the efficacy and respiratory consequences of ultrasound-guided interscalene brachial plexus block. *Br J Anaesth* 2008; 101:549–56
4. El-Boghdadly K, Chin KJ, Chan VWS: Phrenic nerve palsy and regional anesthesia for shoulder surgery: Anatomical, physiologic, and clinical considerations. *ANESTHESIOLOGY* 2017; 127:173–91
5. Franco CD, Williams JM: Ultrasound-guided interscalene block: Reevaluation of the “stoplight” sign and

- clinical implications. *Reg Anesth Pain Med* 2016; 41:452–9
6. Orebaugh SL, McFadden K, Skorupan H, Bigeleisen PE: Subepineurial injection in ultrasound-guided interscalene needle tip placement. *Reg Anesth Pain Med* 2010; 35:450–4
 7. Kim YD, Yu JY, Shim J, Heo HJ, Kim H: Risk of encountering dorsal scapular and long thoracic nerves during ultrasound-guided interscalene brachial plexus block with nerve stimulator. *Korean J Pain* 2016; 29:179–84
 8. Thomas SE, Winchester JB, Hickman G, DeBusk E: A confirmed case of injury to the long thoracic nerve following a posterior approach to an interscalene nerve block. *Reg Anesth Pain Med* 2013; 38:370
 9. Burckett-St. Laurent D, Chan V, Chin KJ: Refining the ultrasound-guided interscalene brachial plexus block: The superior trunk approach. *Can J Anaesth* 2014; 61:1098–102
 10. Albrecht E, Bathory I, Fournier N, Jacot-Guillarmod A, Farron A, Brull R: Reduced hemidiaphragmatic paresis with extrafascial compared with conventional intrafascial tip placement for continuous interscalene brachial plexus block: A randomized, controlled, double-blind trial. *Br J Anaesth* 2017; 118:586–92
 11. Neuts A, Stessel B, Wouters PF, Dierickx C, Cools W, Ory JP, Dubois J, Jamaer L, Arijis I, Schoorens D: Selective suprascapular and axillary nerve block versus interscalene plexus block for pain control after arthroscopic shoulder surgery: A noninferiority randomized parallel-controlled clinical trial. *Reg Anesth Pain Med* 2018; 43:738–44
 12. Kang RA, Chung YH, Ko JS, Yang MK, Choi DH: Reduced hemidiaphragmatic paresis with a “corner pocket” technique for supraclavicular brachial plexus block: Single-center, observer-blinded, randomized controlled trial. *Reg Anesth Pain Med* 2018; 43:720–4
 13. Renes SH, Rettig HC, Gielen MJ, Wilder-Smith OH, van Geffen GJ: Ultrasound-guided low-dose interscalene brachial plexus block reduces the incidence of hemidiaphragmatic paresis. *Reg Anesth Pain Med* 2009; 34:498–502
 14. Swanney MP, Jensen RL, Crichton DA, Beckert LE, Cardno LA, Crapo RO: FEV(6) is an acceptable surrogate for FVC in the spirometric diagnosis of airway obstruction and restriction. *Am J Respir Crit Care Med* 2000; 162:917–9
 15. Aldrete JA: The post-anesthesia recovery score revisited. *J Clin Anesth* 1995; 7:89–91
 16. Fishman SM, Ballantyne, Jane C. Rathmell, James P: Opioid analgesics, Bonica's Management of Pain, 4th edition. Philadelphia, Pennsylvania, Lippincott Williams & Wilkins, 2010, pp. 1172–87
 17. D'Agostino RB Sr, Massaro JM, Sullivan LM: Non-inferiority trials: Design concepts and issues: The encounters of academic consultants in statistics. *Stat Med* 2003; 22:169–86
 18. Auyong DB, Hanson NA, Joseph RS, Schmidt BE, Slee AE, Yuan SC: Comparison of anterior suprascapular, supraclavicular, and interscalene nerve block approaches for major outpatient arthroscopic shoulder surgery: A randomized, double-blind, noninferiority trial. *ANESTHESIOLOGY* 2018; 129:47–57
 19. Piaggio G, Elbourne DR, Altman DG, Pocock SJ, Evans SJ, CONSORT Group: Reporting of noninferiority and equivalence randomized trials: An extension of the CONSORT statement. *JAMA* 2006; 295:1152–60
 20. Walker E, Nowacki AS: Understanding equivalence and noninferiority testing. *J Gen Intern Med* 2011; 26:192–6
 21. Lin JA, Chuang TY, Yao HY, Yang SF, Tai YT: Ultrasound standard of peripheral nerve block for shoulder arthroscopy: A single-penetration double-injection approach targeting the superior trunk and supraclavicular nerve in the lateral decubitus position. *Br J Anaesth* 2015; 115:932–4
 22. Kessler J, Schafhalter-Zoppoth I, Gray AT: An ultrasound study of the phrenic nerve in the posterior cervical triangle: Implications for the interscalene brachial plexus block. *Reg Anesth Pain Med* 2008; 33:545–50
 23. Urmey WF, Talts KH, Sharrock NE: One hundred percent incidence of hemidiaphragmatic paresis associated with interscalene brachial plexus anesthesia as diagnosed by ultrasonography. *Anesth Analg* 1991; 72:498–503
 24. Lee JH, Cho SH, Kim SH, Chae WS, Jin HC, Lee JS, Kim YI: Ropivacaine for ultrasound-guided interscalene block: 5 mL provides similar analgesia but less phrenic nerve paralysis than 10 mL. *Can J Anaesth* 2011; 58:1001–6
 25. Fredrickson MJ, Abeysekera A, White R: Randomized study of the effect of local anesthetic volume and concentration on the duration of peripheral nerve blockade. *Reg Anesth Pain Med* 2012; 37:495–501
 26. Rohrbach M, Kentor ML, Orebaugh SL, Williams B: Outcomes of shoulder surgery in the sitting position with interscalene nerve block: A single-center series. *Reg Anesth Pain Med* 2013; 38:28–33
 27. Sakamoto Y: Spatial relationships between the morphologies and innervations of the scalene and anterior vertebral muscles. *Ann Anat* 2012; 194:381–8
 28. Hanson NA, Auyong DB: Systematic ultrasound identification of the dorsal scapular and long thoracic nerves during interscalene block. *Reg Anesth Pain Med* 2013; 38:54–7
 29. Siegenthaler A, Moriggl B, Mlekusch S, Schliessbach J, Haug M, Curatolo M, Eichenberger U:

Ultrasound-guided suprascapular nerve block, description of a novel supraclavicular approach. *Reg Anesth Pain Med* 2012; 37:325–8

30. Wiegel M, Moriggl B, Schwarzkopf P, Petroff D, Reske AW: Anterior suprascapular nerve block versus interscalene brachial plexus block for shoulder surgery in the outpatient setting: A randomized controlled

patient- and assessor-blinded trial. *Reg Anesth Pain Med* 2017; 42:310–8

31. Murata H, Sakai A, Hadzic A, Sumikawa K: The presence of transverse cervical and dorsal scapular arteries at three ultrasound probe positions commonly used in supraclavicular brachial plexus blockade. *Anesth Analg* 2012; 115:470–3

ANESTHESIOLOGY REFLECTIONS FROM THE WOOD LIBRARY-MUSEUM

Dr. E. W. Remsberg's Anesthetic as the "Safest...Brought to Light": Somnoforme



As a 1903 dental graduate of the University of Maryland, Elmer W. Remsberg, D.D.S. (1889 to 1936), had to compete with more established dentists after arriving in Newville, Pennsylvania. Rather than administering "chloroform...cocaine or some other dangerous medium" of anesthetic, Dr. Remsberg advertised his use of "Somnoforme," a volatile French mixture of ethyl chloride, methyl chloride, and ethyl bromide. Touting Somnoforme on his ca. 1907 trade card (*above*) as "the Ideal Anaesthetic," the dentist reminded Newville's citizens that he had "recently installed electric light" and that, day or night, they no longer needed to travel the 11 miles to Carlisle or the 38 miles to Harrisburg for "modern anesthesia." (Copyright © the American Society of Anesthesiologists' Wood Library-Museum of Anesthesiology.)

George S. Bause, M.D., M.P.H., Honorary Curator and Laureate of the History of Anesthesia, Wood Library-Museum of Anesthesiology, Schaumburg, Illinois, and Clinical Associate Professor, Case Western Reserve University, Cleveland, Ohio. UJYC@aol.com.

ANESTHESIOLOGY

Analgesic and Respiratory Depressant Effects of R-dihydroetorphine

A Pharmacokinetic–Pharmacodynamic Analysis in Healthy Male Volunteers

Erik Olofsen, Ph.D., Merel Boom, M.D., Ph.D.,
Elise Sarton, M.D., Ph.D., Monique van Velzen, Ph.D.,
Paul Baily, B.Sc., Kevin J. Smith, Ph.D.,
Alexander Oksche, M.D., Ph.D.,
Albert Dahan, M.D., Ph.D., Marieke Niesters, M.D., Ph.D.

ANESTHESIOLOGY 2019; 131:1327–39

EDITOR'S PERSPECTIVE

What We Already Know about This Topic

- Opioid agonists acting at the nociception/orphanin FQ, δ -opioid, and κ -opioid receptors may counteract respiratory depression induced by activation of the μ -opioid receptor
- R-dihydroetorphine is an opioid with full agonism and high affinity for the μ -opioid, κ -opioid, and δ -opioid receptors and low affinity for the nociception/orphanin FQ receptor

What This Article Tells Us That Is New

- The effects of four R-dihydroetorphine doses (12.5, 75, 125, and 150 ng/kg) on isohypercapnic ventilation and antinociception were studied in 40 healthy male volunteers
- Over the dose range tested, an apparent maximum in respiratory depression to 33% of baseline ventilation was identified, but a maximum in antinociception was not reached
- At an R-dihydroetorphine effect-site concentration of 20 pg/ml, the probability of analgesia was 60%, while the probability of analgesia without respiratory depression was 45%
- The probability of analgesia increased to 95% at 100 pg/ml, but the probability of analgesia without respiratory depression was reduced to 20%

Despite their many side effects, opioids are the cornerstone of contemporary treatment of moderate to severe pain in patients with cancer and perioperative patients.¹ Respiratory depression is one of the more serious

ABSTRACT

Background: There is an ongoing need for potent opioids with less adverse effects than commonly used opioids. R-dihydroetorphine is a full opioid receptor agonist with relatively high affinity at the μ -, δ - and κ -opioid receptors and low affinity at the nociception/orphanin FQ receptor. The authors quantified its antinociceptive and respiratory effects in healthy volunteers. The authors hypothesized that given its receptor profile, R-dihydroetorphine will exhibit an apparent plateau in respiratory depression, but not in antinociception.

Methods: The authors performed a population pharmacokinetic–pharmacodynamic study (Eudract registration No. 2009-010880-17). Four intravenous R-dihydroetorphine doses were studied: 12.5, 75, 125, and 150 ng/kg (infused more than 10 min) in 4 of 4, 6 of 6, 6 of 6, and 4 of 4 male subjects in pain and respiratory studies, respectively. The authors measured isohypercapnic ventilation, pain threshold, and tolerance responses to electrical noxious stimulation and arterial blood samples for pharmacokinetic analysis.

Results: R-dihydroetorphine displayed a dose-dependent increase in peak plasma concentrations at the end of the infusion. Concentration–effect relationships differed significantly between endpoints. R-dihydroetorphine produced respiratory depression best described by a sigmoid E_{max} -model. A 50% reduction in ventilation in between baseline and minimum ventilation was observed at an R-dihydroetorphine concentration of 17 ± 4 pg/ml (median \pm standard error of the estimate). The maximum reduction in ventilation observed was at 33% of baseline. In contrast, over the dose range studied, R-dihydroetorphine produced dose-dependent analgesia best described by a linear model. A 50% increase in stimulus intensity was observed at 34 ± 11 pg/ml.

Conclusions: Over the dose range studied, R-dihydroetorphine exhibited a plateau in respiratory depression, but not in analgesia. Whether these experimental advantages extrapolate to the clinical setting and whether analgesia has no plateau at higher concentrations than investigated requires further studies.

(*ANESTHESIOLOGY* 2019; 131:1327–39)

opioid side effects. Commonly used opioids, such as morphine and fentanyl, produce respiratory depression *via* activation of μ -opioid receptors expressed on pontine respiratory neurons with the cessation of breathing activity (apnea) at high doses.^{2,3} Until recently, few studies addressed the (positive or negative) contribution of the other opioid receptors, such as κ - and δ -opioid receptors, to respiratory depression. We previously showed both in rodents and humans that buprenorphine, a partial agonist at the μ -opioid receptor, antagonist at κ -opioid receptor, and agonist at the nociception/orphanin FQ receptor, produces an apparent maximum in respiratory effect, even at full μ -opioid receptor occupancy.^{4,5} This may be a major advantage over other opioids and suggests some protective effect at high dose. The molecular mechanism of this phenomenon (also

This article is featured in "This Month in Anesthesiology," page 1A.

Submitted for publication February 27, 2019. Accepted for publication August 19, 2019. From the Department of Anesthesiology, Leiden University Medical Center, Leiden, The Netherlands (E.O., M.B., E.S., M.V., A.D., M.N.); Mundipharma Research Limited, Cambridge, United Kingdom (P.B., K.J.S., A.O.); and Rudolf-Buchheim-Institut für Pharmakologie (Rudolph-Buchheim Institute for Pharmacology), University of Giessen, Giessen, Germany (A.O.). Current affiliations: Sosei Heptares, Cambridge, United Kingdom (P.B.).

Copyright © 2019, the American Society of Anesthesiologists, Inc. All Rights Reserved. *Anesthesiology* 2019; 131:1327–39. DOI: 10.1097/ALN.0000000000002991

called “ceiling” or “plateau” effect) has not yet been elucidated. Animal data suggest that apart from partial agonism at the μ -opioid receptor, the apparent maximum in respiratory depression may be related to the activation of the nociception/orphanin FQ receptor.⁶ On the other hand, there are data to suggest that activation of δ -opioid and/or κ -opioid receptors has some respiratory protective effect.⁷ For example, DPI-125, a mixed agonist acting at μ -opioid, δ -opioid, and κ -opioid receptors, has a high respiratory safety profile in rodents (as measured by the ratio carbon dioxide concentration increase/ED50, where ED50 is the dose causing an increase in antinociception by 50%), which is attributed to high δ -opioid receptor potency;⁸ and the κ -opioid receptor agonist U50,488H antagonizes μ -opioid receptor-induced respiratory depression in the rat.⁹ These findings suggest that opioid agonists acting at nociception/orphanin FQ, δ -opioid, and κ -opioid receptors may counteract, at least in part, the respiratory depression induced by the activation of the μ -opioid receptor.

In this study in healthy volunteers, we assessed the respiratory and analgesic effects of R-7,8-dihydro-7 α -[1-(R)-hydroxy-1-methylbutyl]-6,14-*endo*-ethanotetrahydro-orphavine (R-dihydroetorphine; fig. 1), an opioid with full agonism and high affinity for the μ -opioid (K_i 0.10 nM), κ -opioid (K_i 0.74 nM), and δ -opioid receptors (K_i 1.5 nM), and low affinity for the nociception/orphanin FQ receptor (K_i 120 nM; Mundipharma Research Ltd., unpublished observation).¹⁰ We performed a population pharmacokinetic–pharmacodynamic modeling study, which allowed us to construct concentration–effect relationships for the wanted and adverse effects of the drug and construct safety or utility surfaces, which give information on the probability of drug harm in the light of its benefit.^{11–13} Given the R-dihydroetorphine receptor affinity profile, we hypothesize that R-dihydroetorphine has an apparent maximum in respiratory effect and a favorable utility surface compared to full μ -opioid receptor agonists, such as fentanyl.^{11–13} Although R-dihydroetorphine is currently not available in the western world for human clinical use, this specific opioid may serve as an example of the influence of combined μ -opioid, κ -opioid, and δ -opioid receptor agonism

on ventilatory control. Additionally, it may become available in the near future given its possible advantageous over other “classical” opioids.

Materials and Methods

Ethics

This study was performed in the Anesthesia and Pain Research Unit of the Department of Anesthesiology of the Leiden University Medical Center (Leiden, The Netherlands) from March 2011 until November 2011. The protocol was approved by the Institutional Review Board (Commissie Medische Ethiek) and the Central Committee on Research Involving Human Subjects in The Hague. The study was registered at the EU Clinical Trials register identification No. 2009-010880-17 on January 25, 2010. Before enrollment and after being informed about the study, all participants gave written informed consent. All study procedures were conducted according to good clinical practice guidelines and adhered to the tenets of the Declaration of Helsinki. The study protocol consisted of experiments on R-dihydroetorphine, fentanyl, and placebo, and was performed in 92 volunteers. The descriptive results of the complete data set have been published before without disclosure of the nature of the opioid.¹⁴ Here, we present the R-dihydroetorphine pharmacokinetic–pharmacodynamic analysis.

Subjects

Forty healthy male volunteers successfully completed the R-dihydroetorphine part of the study. Inclusion criteria were: age, 18 to 45 yr; weight, 60 to 100 kg; body mass index, 18 to 30 kg/m²; forced expired lung volume in 1 s, greater than 85% of predicted; and no history of major medical disease, alcohol abuse, or illicit drug use. The use of medication was not allowed in the 7 days before the study (including vitamins); the use of opioids was not allowed in the 3 months before the study. The volunteers were asked to fast for 8 h before drug administration. The volunteers were recruited by the study team using flyers distributed on the university campus. Subjects were enrolled after passing a physical examination performed by an independent physician. Following screening (and passing the physical examination), all subjects were familiarized with the experimental setup and some test runs were performed.

Study Design

After arrival in the research unit at 8:00 AM, the subject received a venous line in the arm or hand (for drug infusion) and an arterial line in the radial artery of the non-dominant arm (for blood sampling). Twenty subjects participated in the respiratory part of the study, twenty others in the analgesia part. Each subject participated once in the study in which he received one of four possible R-dihydroetorphine (Mundipharma Research Ltd.,

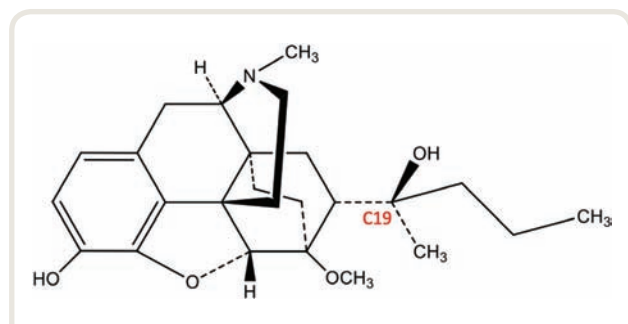


Fig. 1. The chemical structure of dihydroetorphine with a chiral center at C19.

Cambridge, United Kingdom) doses: 12.5 ng/kg ($n = 4$ in the respiratory study, 4 others in the analgesia study), 75 ng/kg ($n = 6$ and 6 others), 125 ng/kg ($n = 6$ and 6), and 150 ng/kg ($n = 4$ and 4). After obtaining baseline data, R-dihydroetorphine was infused during 10 min using a syringe pump (Beckton Dickinson, St. Etienne, France).

Randomization and Allocation. The study was randomized and double blind. Randomization was done by the pharmacy using a computer-generated randomization list. The subjects were randomized 4:6:6:4 (R-dihydroetorphine dose 12.5, 75, 125, and 150 ng/kg) and allocated on the day before the experiment. The pharmacy prepared the study medication. On the morning of the experiment, the study team received a 50-ml syringe with the study drug that was marked with just the subject randomization number. All study personnel and data analysts remained blinded until the data collection was complete and an independent monitor indicated that all data entries were correct and complete.

Ventilation Measurements. In 20 subjects, isohypercapnic ventilation was measured from 5 to 10 min before and for 70 min after the start of the 10-min drug infusion. To maintain isohypercapnia and collect ventilation data, we used the dynamic end-tidal forcing technique, which is described in detail elsewhere.^{15,16} In brief, subjects breathed through a facemask that was attached to a pneumotachograph and pressure transducer system (#4813; Hans Rudolph Inc., USA) and to a set of mass flow controllers (Bronkhorst High Tech, The Netherlands) for the delivery of oxygen, carbon dioxide, and nitrogen. The mass flow controllers were controlled by a computer running RESREG/ACQ software (Leiden University Medical Center, The Netherlands) that steers end-tidal gas concentrations by varying the inspired concentrations and captures ventilatory data. The inspired and expired oxygen and carbon dioxide concentrations were measured at the mouth using a capnograph (Datex Capnomac, Finland); arterial oxygen saturation was measured by pulse oximetry (Masimo Corporation, USA). In the pharmacokinetic–pharmacodynamic analysis, we used 1-min ventilation averages.

Pain Measurements. In 20 subjects, the response to activation of cutaneous nociceptors was measured.^{11,17} Using a computer-controlled constant current stimulator (Leiden University Medical Center), a 0.1-ms stimulus at 20 Hz was applied to the skin over the tibial bone. The stimulus train increased by 0.5 mA per second from 0 mA to a maximum of 128 mA. The subject was instructed to press a button on a control box at the first sensation of pain (*i.e.*, pain threshold) and end the stimulus train by pressing another button when pain reached the level of tolerance (*i.e.*, pain tolerance). Four pain threshold and tolerance values were obtained in the 30 min prior to drug infusion. These values were averaged and served as baseline value. Further measurements were obtained at $t = 10, 15, 30, 45, 60, 75, 90, 105, 120, 150, 180, 210, 240, 300, 360, 420$, and

480 min after the start of drug infusion ($t = 0$ is the start of drug infusion; $t = 10$ min is end of infusion).

Blood Sampling and R-dihydroetorphine Assay

Before (baseline sample), during, and after drug infusion (drug infusion from 0 to 10 min), 2 to 3 ml blood were drawn from the arterial line for measurement of R-dihydroetorphine concentrations in plasma. In the first hour, samples were obtained at $t = 2, 5, 8, 10, 12, 15, 18, 20, 25, 30, 40$, and 60 min, followed in the subsequent hours by samples obtained at $t = 1.5, 2, 3, 4, 5, 12$, and 24 h. Plasma was separated within 30 min of blood collection and stored at -20°C until analysis. Concentrations of R-dihydroetorphine were determined in human plasma samples using a validated analytical methodology by LGC Ltd. (Fordham, United Kingdom) by liquid chromatography or tandem mass spectrometric method, with stable isotope labeled internal standard incorporating deuterium atoms to distinguish the standard by mass. Chromatographic separation was by ultrahigh performance liquid chromatography using a reverse phase analytical column (100 mm \times 2.1 mm, 1.7 μm internal diameter, C18) with a gradient elution using 0.1% (volume/volume %) acetic acid in acetonitrile and water. Samples were analyzed, following precipitation with acetonitrile, using a Sciex API 5000 triple quadrupole mass spectrometer (Sciex, USA) using electrospray ionization. Single specific multiple reaction transitions were monitored for both R-dihydroetorphine and internal standard. The validated analytical range of this assay was 5.00 to 2500 pg/ml with 5.00 pg/ml being the lowest limit of quantification. The interassay precision, as measured by coefficient of variation, at 5.00 pg/ml, 15.0 pg/mL, 100 pg/ml, and 2000 pg/ml was 10.5%, 5.2%, 5.3%, and 6.1%, respectively. The intra-assay accuracy, as measured by relative error, was less than 2.4% and the interassay accuracy was less than 8.8%.

Pharmacokinetic–Pharmacodynamic Analysis

The pharmacokinetic–pharmacodynamic data were analyzed with the mixed-effects modeling software package NONMEMVII (Nonlinear Mixed Effects Modeling; ICON Development Solutions, USA) using a population approach. A two-stage analysis was chosen. From the first stage (pharmacokinetic analysis), individual empirical Bayesian estimates of the pharmacokinetic parameters were obtained and were applied in the second stage (pharmacodynamic analysis; analgesic and respiratory data were analyzed separately). To eliminate the hysteresis between the estimated R-dihydroetorphine concentrations and effect, an effect compartment was postulated. This effect compartment equilibrates with the plasma compartment with rate constant k_{e0} . To obtain the “best” pharmacokinetic model, two and three compartment models were fitted to the R-dihydroetorphine pharmacokinetic data. The number of compartments in the model was determined by the magnitude of the decrease

in the minimum objective function value (χ^2 -test, $P < 0.01$ considered significant). Weight and body mass index were considered as covariates.

Ventilation Data. The 1-min ventilation averages were modeled as follows:^{11,12}

$$\text{Ventilation}(t) = V_B + [V_{\text{MIN}} - V_B] \times [(C_e(t)/C_{50})^\gamma \times (1 + [C_e(t)/C_{50}]^\gamma)^{-1}] + \text{TR} \times t \quad (1)$$

where V_B is (predrug) baseline ventilation, V_{MIN} minimum ventilation, $C_e(t)$ R-dihydroetorphine effect-site concentration, and C_{50} the effect-site or steady-state concentration causing 50% of the effect between V_B and minimum ventilation (an estimated value of zero for minimum ventilation indicates that at high drug concentrations apnea will occur). γ is a shape parameter and TR a linear trend term. The trend term describes a possible increase in ventilation over time. Such an increase has been observed previously by several research groups and is related to the presence of isohypercapnia.^{15,18,19} For example, Dahan *et al.*¹⁵ observed a trend of 30 to 100 ml/min² during 15 to 20 min of isohypercapnia. This effect is most prominent during the first hour of isohypercapnia after which no further increase in ventilation is observed.¹⁸ The rise in ventilation is possibly related to slow central neuronal dynamics in response to central chemoreceptor activation.¹⁹ Most μ -opioid receptor agonists tend to inactive central neuronal dynamics with no need for incorporating a trend term when modeling their effect on ventilation.^{5,11} However, in the current study we did observe a trend in the ventilation data, and indication that R-dihydroetorphine does not impair central neuronal dynamics.

Pain Data. The threshold and pain responses were analyzed simultaneously as follows:^{11,12}

$$\text{Pain Response}(t) = \text{Baseline} \times [1 + 0.5 \times (C_e(t)/C_{50})^\gamma] \quad (2)$$

where Pain Response (t) is the stimulus intensity at which the subjects pressed the control button to indicate his pain threshold or tolerance, Baseline is the predrug stimulus intensity at which pain threshold and tolerance were reported, $C_e(t)$ the R-dihydroetorphine effect-site concentration, C_{50} the effect-site or steady-state concentration at which a 50% increase in stimulus intensity results in a response (pain threshold or tolerance), and γ is a shape parameter.

Model parameters were assumed to be log-normally distributed, except V_B , minimum ventilation and C , which were assumed to be normally distributed. Residual error was assumed to have both an additive and a relative error for concentrations and only an additive error for all effect parameters. Covariance between random effects (η 's) for the three pharmacodynamic end-points were explored using \$OMEGA BLOCKs. P values less than 0.01 were considered significant.

To allow a visual predictive check of the final pharmacokinetic or pharmacodynamic models, we estimated the

normalized prediction discrepancies in NONMEM.^{20,21} To that end, we performed 300 Monte Carlo simulations that were based on the final model considering the distributions of the fixed and random effects. Next, we counted the number of times an observation is greater than the model prediction. The normalized prediction discrepancies are the counts divided by 300, transformed *via* the inverse normal distribution. Under the null hypothesis that the model is correct, the normalized prediction discrepancies should have a normal distribution. It was visually checked that the normalized prediction discrepancies *versus* time showed no trends, heteroscedasticity, or both.

Utility Surface. For a detailed explanation of the step-by-step construction of the utility surfaces, see Boom *et al.*¹¹ and Roozkrans *et al.*¹² In brief, we developed utility surfaces that give information on four possible conditions: (1) probability of adequate analgesia without serious respiratory depression, (2) probability of serious respiratory depression without analgesia, (3) probability of absence of respiratory depression and absence of adequate analgesia, and (4) probability of adequate analgesia with serious respiratory depression. The threshold values for adequate analgesia was $P(A) > 0.25$ and $P(A) > 0.5$, or the probability of a 25% (A+) or 50% (A++) increase in tolerated electrical current, and for serious respiratory depression $P(R) > 0.5$ or a reduction in minute ventilation by more than 50% (R+). Additionally, we calculated the probability of less than 25% analgesia (A−, or no analgesia) and less than 50% respiratory depression (R−, no respiratory depression). To obtain these surfaces, we simulated 10,000 pharmacodynamic profiles as function of time (for doses 12.5, 75, 125, and 150 ng/kg) and steady-state or effect-site concentration (from 0 to 100 pg/ml), according to the typical model parameter estimates and the interindividual variances (ω^2), as derived from the final pharmacokinetic–pharmacodynamic analyses. Probabilities were calculated from the distribution of occurrence of specific conditions (1 to 4). This process yields iso-utility lines that describe the conditions 1 to 4. By giving specific colors to these four conditions (for example, dark red for the least desirable condition [condition 2] and green for most desirable condition [condition 1]), transitions in-between conditions are depicted by transitions between colors and result in a continuum of probabilities.

Results

The 40 subjects were 23 ± 2 (mean \pm SD; range, 18 to 44) yr old, had a body weight of 78 ± 8 (65 to 98) kg, and a body mass index of 23 ± 2 (19 to 23) kg/m². All subjects completed the protocol without serious or unexpected adverse effects. All reported side effects are given in table 1.

We observed a dose-dependent increase in (mean \pm SD) plasma R-dihydroetorphine concentrations with peak concentrations (occurring at the end of the 10-min infusion)

Table 1. Adverse Effects Observed during and after R-dihydroetorphine Dosing

Symptoms	R-dihydroetorphine Dose			
	12.5 ng/kg (n = 8)	75 ng/kg (n = 12)	125 ng/kg (n = 12)	150 ng/kg (n = 8)
Sedation	2 (25%)	7 (58%)	4 (33%)	4 (50%)
Headache	3 (38%)	2 (17%)	2 (17%)	3 (38%)
Nystagmus	0	1 (8%)	3 (25%)	0
Blurred vision	0	0	3 (25%)	4 (50%)
Nausea	0	3 (25%)	0	2 (25%)
Vomiting	0	2 (17%)	0	0
Euphoria	0	2 (17%)	3 (25%)	3 (38%)
Dysphoria	0	0	0	0
Pruritis	0	0	1 (8%)	3 (38%)
Hiccups	0	0	0	1 (13%)
Chest heaviness	0	0	1 (8%)	1 (13%)
Flushing	0	1 (8%)	0	5 (63%)
Total events	5	18	17	26

Events per subject (n, %) and total events counted.

of 44.8 ± 5.7 , 214.2 ± 20.1 , 371.1 ± 30.7 , and 454.4 ± 42.1 pg/ml at doses 12.5, 75, 125, and 150 ng/kg, respectively (fig. 2). After the termination of the infusion the plasma concentrations dropped rapidly, with a more than 50% decrease in plasma concentrations within 2 min. The final pharmacokinetic model consisted of a conventional three-compartment model with one central (V_1) and two peripheral compartments (V_2 and V_3) that was superior to a two-compartment model with just one peripheral compartment (minimum objective function value = 3,120.368 *vs.* 3,314.316, $P < 0.001$). No effect of weight or body mass index was observed on any of the model parameters, most probably due to the fact that we had a homogenous sample of healthy young males weighing 78 ± 8 kg with a body mass index of 23 ± 2 kg/m². Best, median and worst fits are given in figure 3 and goodness of fit plots in figure 4. Inspection of the data fits and all three diagnostic plots (individual predicted *vs.* measured data, individual weighted residuals *vs.* time, and normalized prediction discrepancies) indicate that the three-compartment pharmacokinetic model adequately described the data. The pharmacokinetic parameter estimates, given in table 2, show the relatively small value of V_1 (7.7 l), the large clearance from compartment 1 (68 l/h) and equally large intercompartmental clearances. There were significant covariances between clearances 1 and 2 ($\omega^2 \pm$ standard error of the estimate = 0.05 ± 0.3), 1 and 3 (0.09 ± 0.03), and 2 and 3 (0.14 ± 0.06).

The ventilation and pain responses were adequately fitted by the pharmacodynamic model (see figs. 3 and 4 for best, medium and worst fits and three goodness-of-fit plots, and table 2 for model parameter estimates). Over the dose range tested, an apparent maximum in respiratory depression greater than zero was identified (minimum ventilation = 6.5 l/min or 33% of baseline ventilation). The pharmacodynamic

model with an apparent maximum in ventilation was statistically superior to the model with maximum effect at apnea (minimum ventilation = 0 l/min) with minimum objective function values of 2,243.965 *versus* 2,354.407 ($P < 0.001$), respectively.

In contrast, a maximum in antinociception was not reached at the maximum R-dihydroetorphine dose tested. However, the pharmacodynamic model with and without an apparent maximum did not differ in terms of minimum objective function values (values of model without an apparent maximum 1,969.526 and with an apparent maximum 1,967.408, $P = 0.150$), indicative that we cannot exclude that at higher doses than tested by us an apparent maximum in the analgesic response may occur.

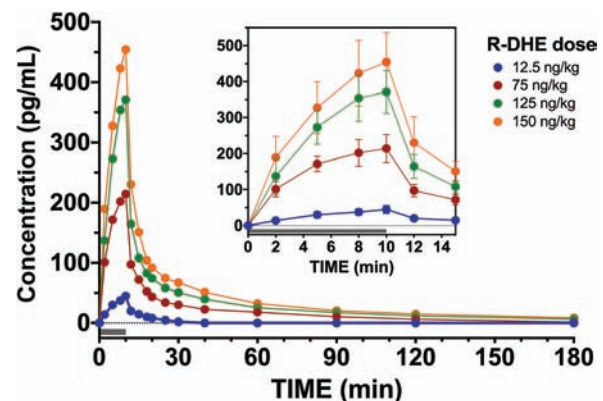


Fig. 2. Plasma R-dihydroetorphine (R-DHE) concentrations following 12.5 (blue symbol), 75 (red), 125 (green) and 150 (orange) ng/kg. The drug was infused more than 10 min. Error bars in the insert are 95% CI.

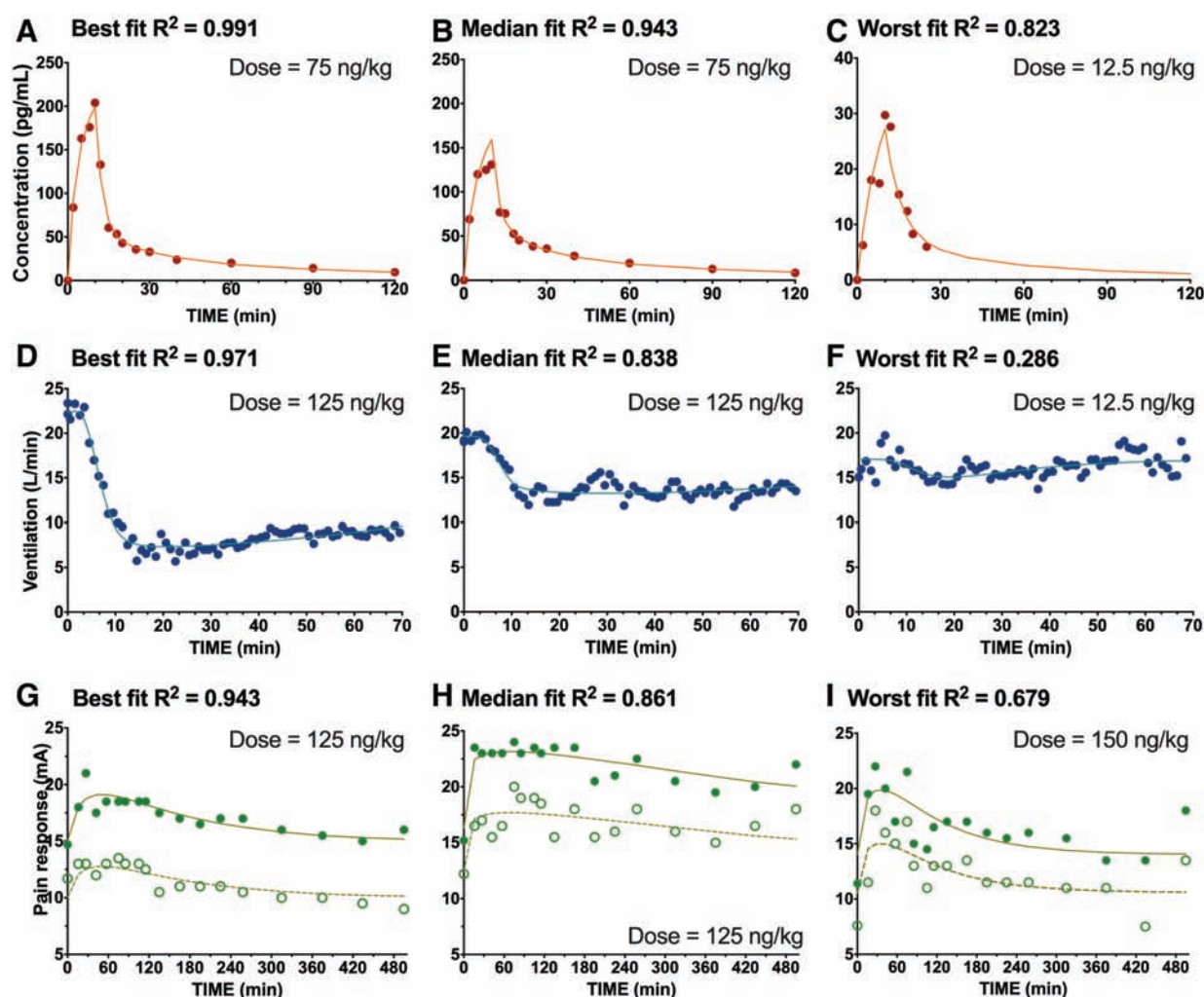


Fig. 3. Best, median and worst data fits as determined by R^2 . (A to C) Pharmacokinetic data. (D to F) Ventilation data. (G to I) Pain responses (the tolerance and threshold data were fitted simultaneously; pain tolerance, closed circles, pain threshold, open circles). Symbols are the measured data, the lines the predicted data.

The delay between plasma concentration and effect ($t_{1/2k_{e0}}$) differed between the two end-points by a factor of 2 (ventilation 0.95 ± 0.20 h *vs.* pain relief 2.19 ± 0.49 h). The ventilation potency parameter ($C_{50,V}$) or the effect-site or steady-state concentration causing 50% of the effect between baseline ventilation and minimum ventilation was 17 ± 4 pg/ml (at this R-dihydroetorphine concentration the ventilation level was 67% of baseline ventilation; the R-dihydroetorphine concentration causing 50% decrease of baseline ventilation was 40% higher, *i.e.*, 27 pg/ml). The analgesia potency parameter ($C_{50,A}$) was 34 ± 11 pg/ml; at this concentration the pain threshold and tolerance responses occurred at a 50% increase relative to pre-drug baseline values. We observed a significant covariance between pain threshold and tolerance with $\omega^2 = 0.08 \pm 0.04$. The steady-state relationships

between R-dihydroetorphine plasma concentration and effects are given in figure 5 (ventilation red line; pain relief blue line).

The constructed utility surfaces or the continuum of probabilities of R-dihydroetorphine analgesia in the presence or absence of respiratory depression are shown in figures 6 and 7. In figure 6A the probabilities are plotted as function of R-dihydroetorphine effect-site concentration (with the iso-utility lines in fig. 6B). The different conditions that may co-exist are depicted by colors that correspond with analgesia and respiratory thresholds. The colors range from deep green (A++/R- or at least 50% analgesia/no respiratory depression) to green (A+/R- or at least 25% analgesia/no respiratory depression), to yellow (A-/R- or no analgesia/no respiratory depression), and from deep red (A-/R+ or no analgesia/serious respiratory

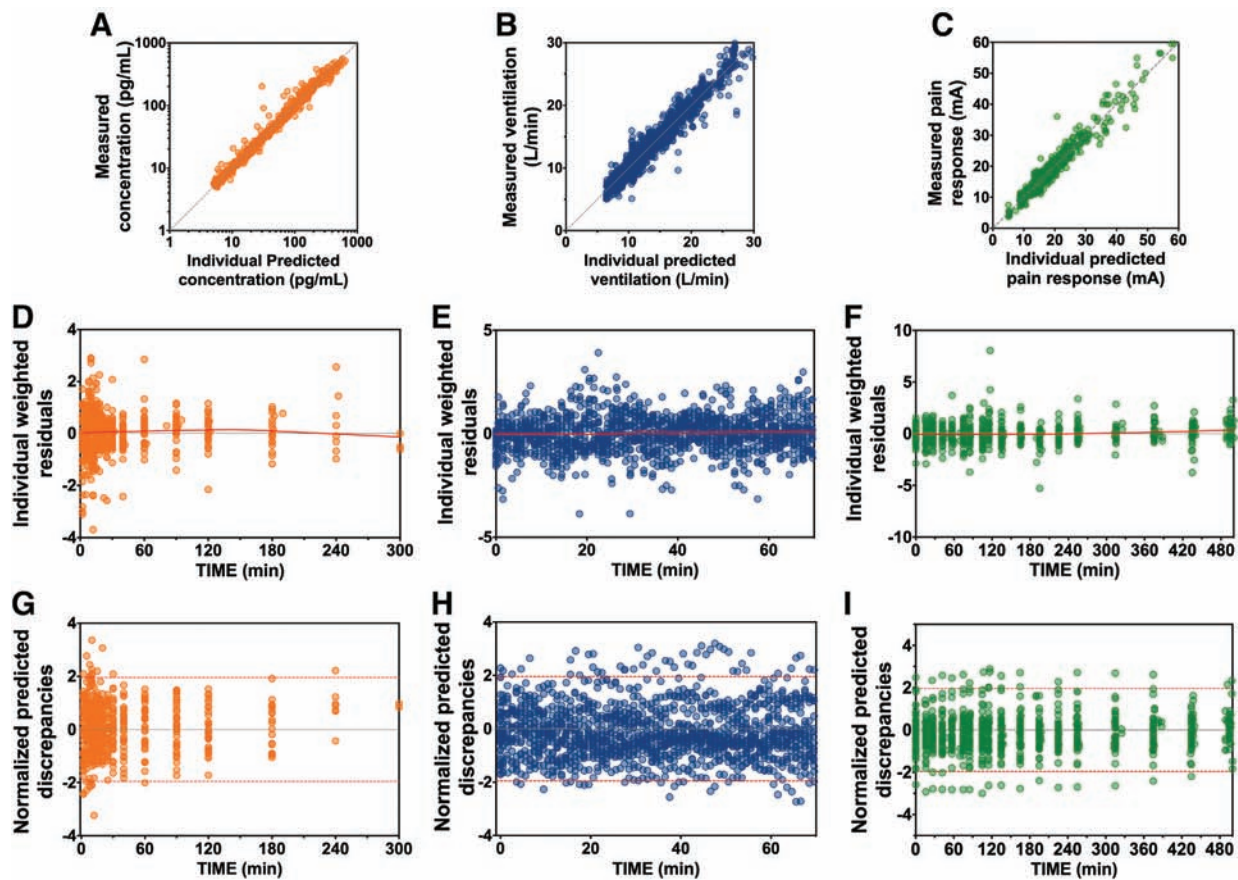


Fig. 4. Goodness of fit plots. (A to C) Measured data versus individual predicted (I_{pred}) data. (D to F) Individual weighted residuals (IWRES) versus time. A smoothed line is plotted through the data points (red line). (G to I) Normalized predicted discrepancies (NPD) versus time. The grey lines are the medians, the red dotted lines are 95% CI. Pharmacokinetic data are orange (A, D, and G), ventilation data is blue (B, E, and H), and pain responses are green (C, F, and I).

depression) to dark orange (A+/R+ or at least 25% analgesia/serious respiratory depression) and to orange (A++/R+ or at least 50% analgesia/serious respiratory depression). At an R-dihydroetorphine effect-site concentration of 20 pg/ml, the probability of analgesia was 60%, while the probability analgesia *without* respiratory depression was 45%. At increasing R-dihydroetorphine effect-site concentrations the probability of analgesia increased toward 95% at 100 pg/ml, but the probability of analgesia without respiratory depression was reduced to 20%. The probabilities as function of time for the four doses administered in the study (12.5, 75, 125, and 150 ng/kg; simulated infusion duration is 90s, enabling comparison with earlier studies)^{11,12} are given in figure 6. At all doses, the probability of respiratory depression without analgesia was 5 to 10% (dark red surfaces). The ratio between green and orange surfaces decreased at increasing R-dihydroetorphine doses: 12.5 ng/kg 469%, 75 ng/kg 205%, 125 ng/kg 151%, and 150 ng/kg 133%.

Discussion

Dihydroetorphine is a six-ring semisynthetic opioid alkaloid (fig. 1), first synthesized in 1967 by Reckitt and Sons Ltd. in England.²² It is a derivative of thebaine like morphine, hydromorphone, and oxycodone (all five-ring opioid molecules), but like buprenorphine it is a six-ring opioid due to a 6,14-endo-ethano-bridge. In etorphine, another six-ring opioid, the 6,14-endo-ethano-bridge is oxidized to a 6,14-endo-etheno-bridge. Six-ring opioids are characterized by high affinity to opioid receptors (K_i in the nanomolar range).²³ Importantly, the dihydroetorphine molecule has a chiral center at C19 and consequently exists in R- and S-configurations.²³ Studies in the rabbit show that R-dihydroetorphine is a potent analgesic, about 6,000 to 12,000 times more potent than morphine when administered parenterally and with an improved respiratory depression/analgesia ratio compared to morphine.²⁴ Also, human studies indicate that R-dihydroetorphine has high analgesic potency with only mild side effects.¹⁰ Since

Table 2. Pharmacokinetic and Pharmacodynamic Parameter Estimates

Parameter	Typical Value \pm SEE	$\omega^2 \pm$ SEE
Pharmacokinetics		
V_1 (l)	7.68 \pm 0.70	0.17 \pm 0.08
V_2 (l)	19.7 \pm 1.35	—
V_3 (l)	61.3 \pm 4.81	—
CL_1 (l/h)	67.9 \pm 2.89	0.07 \pm 0.01
CL_2 (l/h)	76.3 \pm 6.09	0.14 \pm 0.05
CL_3 (l/h)	33.2 \pm 3.27	0.25 \pm 0.07
σ (pg/ml)	0.18 \pm 0.01	—
Ventilation		
V_B (l/min)	19.6 \pm 0.63	7.0 \pm 1.9
V_{MIN} (l/min)	6.9 \pm 1.1	11.7 \pm 3.7
$C_{50,V}$ (pg/ml)	16.9 \pm 4.1	0.26 \pm 0.10
$t_{1/2,k_{e0,V}}$ (h)	0.95 \pm 0.20	—
γ_V	2.5 \pm 0.29	—
TR (ml/min ²)	88 \pm 12	93 \pm 22
σ (pg/ml)	1.2 \pm 0.1	—
Pain Responses		
Baseline threshold (mA)	11.5 \pm 0.90	0.10 \pm 0.05
Baseline tolerance (mA)	17.0 \pm 1.21	0.10 \pm 0.04
$C_{50,A}$ (pg/ml)	34.0 \pm 11.2	1.08 \pm 0.62
$t_{1/2,k_{e0,A}}$ (h)	2.19 \pm 0.49	0.30 \pm 0.17
γ	Fixed to 1	1.06 \pm 0.44
σ threshold (pg/ml)	1.90 \pm 0.24	—
σ tolerance (pg/ml)	1.99 \pm 0.42	—

—, not estimable; γ , a shape parameter; σ , SD of the residual error; ω^2 the variance of the model parameter across the population (in the log domain); $C_{50,A}$, effect-site plasma R-dihydroetorphine concentration causing a 50% increase in pain response; $C_{50,V}$, effect-site R-dihydroetorphine concentration causing a 50% reduction in ventilation in between V_B and V_{MIN} ; CL , clearance; $t_{1/2,k_{e0,V}}$ and $t_{1/2,k_{e0,A}}$ the blood-effect site equilibration half-life for ventilation and pain response, respectively; SEE, standard error of the estimate; TR, trend term; V , volume; V_B , baseline ventilation; V_{MIN} , estimated minimum ventilation.

1992, R-dihydroetorphine is registered in mainland China for the treatment of severe pain, including labor pain, and anesthesia induction,^{10,25} but it is not used clinically in the Western world. To better understand its respiratory effects in relation to its analgesic effects, we studied the effect of four R-dihydroetorphine doses on isohypercapnic ventilation and antinociception in healthy volunteers.

Over the dose range tested (12.5 to 150 ng/kg), we observed an apparent plateau in respiratory depression but not in analgesia. This suggests that R-dihydroetorphine has advantages over other opioids that do not display any plateau in respiratory depression and produce respiratory instability or apnea at high dose (e.g., morphine, fentanyl). However, this is a first and relatively small ($n = 40$) study on R-dihydroetorphine performed in healthy volunteers under highly-controlled experimental conditions. Whether the apparent plateau is also sustained at higher doses (greater than 150 ng/kg), is present in specific patient populations with a high risk of opioid-induced respiratory depression, or occurs at more intense clinical pain requires further testing. The plateau effect observed at the current R-dihydroetorphine doses is similar to that of other opioids, such as buprenorphine, that shares certain pharmacologic characteristics with R-dihydroetorphine (see two paragraphs below).^{4,5}

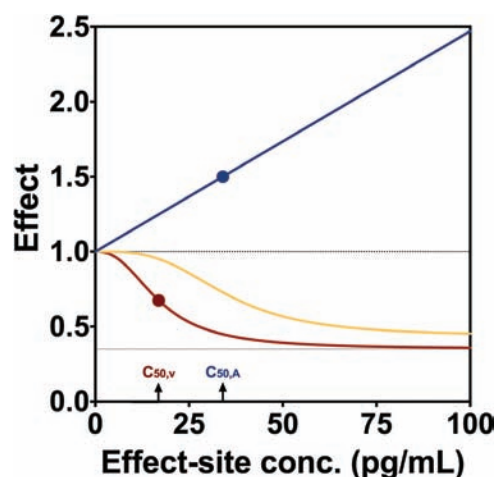


Fig. 5. Steady-state relationship between R-dihydroetorphine plasma or effect-site concentration (conc.) and effect (effect = 1 is pre-drug baseline effect). Pain relief: blue line; ventilation: red line. The red and blue dots are the C_{50} values: $C_{50,V}$ is the R-dihydroetorphine concentration causing a 50% reduction in ventilation in between baseline ventilation and the apparent minimum ventilation (V_{MIN} , grey line), and $C_{50,A}$ the R-dihydroetorphine concentration causing a 50% increase in current intensity at which a pain response is reported. The yellow line the concentration-ventilation response curve modeled by equation 1 (in the Pharmacokinetic-pharmacodynamic Analysis section) without trend term C.

In order to determine the respiratory effect of R-dihydroetorphine relative to its analgesic effect, we constructed utility surfaces (figs. 6 and 7) rather than calculating the therapeutic ratio (which assumes a similar dose-response relationship with just differences in potency between endpoints).^{11–13,26} Since our analysis shows that the two endpoints differ in their concentration-effect curves and C_{50} s (fig. 5), our approach is more suitable to integrate wanted and unwanted end-points into one function.^{26,27} The utility surfaces are based on utility functions that describe the opioids effect in terms of probability of benefit (analgesia) and probability of harm (respiratory depression). For R-dihydroetorphine, we showed a larger probability of analgesia without respiratory depression (green surfaces) than the phenylpiperidines that we tested previously using the same experimental paradigm.^{11–13} Based on the utility surfaces that we constructed, R-dihydroetorphine seems an opioid analgesic with a greater benefit than harm, although this has to be considered in light of the current experimental paradigm and requires replication in clinical studies. Still, we argue that it is important to obtain a library of utility surfaces for all clinically available opioids and determine whether such characterizations correlate with clinical observations of opioid-induced respiratory depression and opioid-related fatalities. Our current approach of constructing utility functions is complex as it requires population pharmacokinetic and pharmacodynamic analyses. To

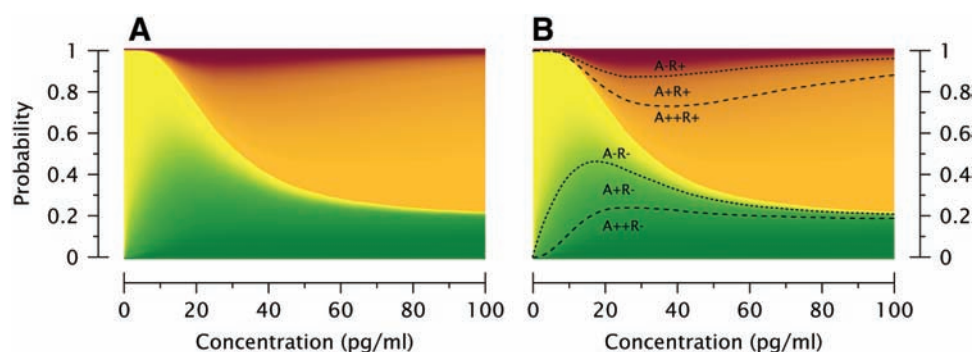


Fig. 6. R-dihydroetorphine response surface; continuum of probabilities of R-dihydroetorphine-induced analgesia and respiratory depression as function of R-dihydroetorphine effect-site concentration (*A* and *B*). The color shading (green to yellow and red to orange) represents the context dependency of the utility functions on the postulated threshold for analgesia. The iso-utility lines in *B* represent the border in between areas of at least 50% analgesia (A++), at least 25% analgesia (A+), no analgesia (A–), at least 50% respiratory depression (R+), and no respiratory depression (R–). At 20 pg/ml, the probability of analgesia without any respiratory depression (green surface) is about 40% as depicted by the dotted line (A+/R–), while at 60 pg/ml and higher concentrations, this same probability remains steady at 20%. This then indicates that at 20 pg/ml, the probability of respiratory depression (irrespective of the presence of analgesia) is 60%, while at concentration greater than 60 pg/ml, this probability remains steady at 80% (as depicted by the area above the dotted line A+/R–).

simplify matters, we recently proposed a more pragmatic method that enables the construction of utility surfaces without the need for pharmacokinetic data.¹³

Our protocol was not designed to clarify the mechanism of the apparent respiratory plateau. However, we believe that this is an important issue that deserves some discussion, and the receptor profile of R-dihydroetorphine, in comparison to that of other opioids (e.g., buprenorphine), may help us identify possible mechanisms. For buprenorphine, the apparent plateau in ventilatory depression is considered related to partial agonism at the μ -opioid receptor (restricting respiratory effect despite full receptors occupancy) and/or full agonism at the nociception/orphanin FQ receptor (with nociception/orphanin FQ receptor activity reducing the respiratory effect from μ -opioid receptor activation).^{4–6,28} Since R-dihydroetorphine is a full agonist at the μ -opioid receptor, the first mechanism seems highly improbable. The nociception/orphanin FQ receptor activation may be a possible mechanism for the reduced R-dihydroetorphine respiratory effect at high dose (see for example, Dahan *et al.* and Linz *et al.* on the combined μ -opioid and nociception/orphanin FQ receptor agonist cebranopadol).^{29,30} However, although R-dihydroetorphine has some affinity for the nociception/orphanin FQ receptor, its affinity is much lower than for the μ -opioid receptor (K_i 0.1 nM *vs.* 120 nM). Whether such low nociception/orphanin FQ receptor affinity is sufficient to cause profound respiratory protection is questionable. Another possible mechanism may be related to the relatively high affinity of R-dihydroetorphine for the κ -opioid and δ -opioid receptors. Notably, when assessing functional activity of μ -opioid, κ -opioid and δ -opioid receptors, following R-dihydroetorphine receptor activation, μ -opioid and κ -opioid receptors have essentially similar IC_{50} -values for inhibition of cyclic adenosine monophosphate

formation, while the IC_{50} -value for δ -opioid receptors is one tenth of that for the μ -opioid receptor (Mundipharma Research Ltd., unpublished observation). There is evidence that κ -opioid and δ -opioid receptor agonists may selectively antagonize μ -opioid receptor agonistic effects, including respiratory depression.^{7–9} Finally, other proposed mechanisms involve the intracellular regulatory protein β -arrestin or off-target activity, such as activation of toll-like receptor 4 or the σ_1 -receptor.^{31–34} Opioid receptors belong to the 7-transmembrane G-protein-coupled receptors that, upon activation, bind to intracellular G-proteins and β -arrestin proteins.^{31,32} Based on prolonged morphine-induced analgesia in β -arrestin-2 knockout mice, it was suggested that analgesic efficacy is driven by G-protein activation and side effects such as constipation and tolerance are mediated by β -arrestin.^{35,36} However, the β -arrestin effect was limited to morphine and was not observed for fentanyl.³⁶ Further, R-dihydroetorphine is biased toward the β -arrestin pathway; this contradicts the notion that β -arrestin bias results in increased adverse effects such as respiratory depression (Mundipharma Research Ltd., unpublished observation). As mentioned, some opioid side effects could be mediated by off-target effects such as toll-like receptor 4 activation, which has been described for several opioids, including morphine, fentanyl, buprenorphine, and oxycodone.³³ For example, remifentanyl-induced hyperalgesia depends on toll-like receptor 4 in mice, and toll-like receptor 4 antagonist TAK-242 attenuated morphine-induced suppression of colonic motility in mice.^{37,38} In summary, the mechanisms involved in compound-related differences of tolerability and (respiratory) safety still remain elusive, but appear to be mediated by several factors such as β -arrestin bias, opioid receptor profile and off-target activity. Identifying compounds that show

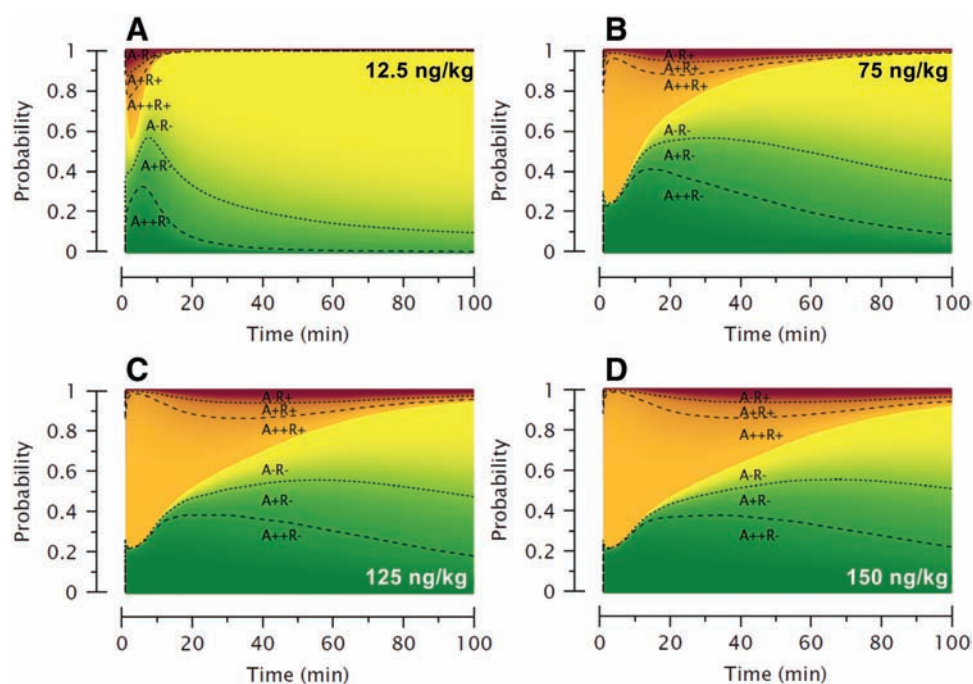


Fig. 7. R-dihydroetorphine response surface; continuum of probabilities of R-dihydroetorphine-induced analgesia and respiratory depression as function of time after 12.5 ng/kg (A), 75 ng/kg (B), 125 ng/kg (C), and 150 ng/kg (D) R-dihydroetorphine. The color shading (green to yellow and red to orange) represents the context dependency of the utility functions on the postulated threshold for analgesia: *deep green* equals A++/R- or at least 50% analgesia/no respiratory depression; *green* equals A+/R- or at least 25% analgesia/no respiratory depression; *yellow* equals A-/R- or no analgesia/no respiratory depression; *deep red* equals A-/R+ or no analgesia/serious respiratory depression; *dark orange* equals A++/R+ or at least 25% analgesia/serious respiratory depression; *orange* equals A+/R+ or at least 50% analgesia/serious respiratory depression. The ratio between *green* and *orange* surfaces is 469% (12.5 ng/kg), 205% (75 ng/kg), 151% (125 ng/kg), and 133% (150 ng/kg).

improved safety and tolerability profile will require careful testing of different end-points (such as gastrointestinal motility, immune cells activation and respiratory depression) and assess a favorable utility based on analgesic activity.

We included a trend term in the pharmacodynamic model to account for the observation that at 12.5 ng/kg, R-dihydroetorphine some respiratory stimulation during the 70 min measurement period occurred. As stated in the Methods section, sustained hypercapnia may activate central neuronal dynamics causing some respiratory stimulation.^{15,18,19} Due to the inclusion of the trend term, we may have underestimated the respiratory protective effects of R-dihydroetorphine somewhat. Analysis without parameter C is given in figure 6 (*yellow line*) and yielded a $C_{50,V}$ of 35 pg/ml and minimum ventilation of 8.9 l/min (44% of baseline), albeit at a significantly higher objective function than the model with trend term. κ -opioid receptor agonists have been associated with dysphoria.³⁹ Interestingly, in our study, during a 24-h observation period, no significant dysphoric effects were observed from R-dihydroetorphine (table 1). We tested only men in the current study. Since men and women quantitatively differ in their opioid analgesic and respiratory depressive effects,^{40–43} future studies should compare the R-dihydroetorphine effects in women and men.

The final question that remains is whether our experimental observations can be extrapolated to the clinical setting, and whether the use of R-dihydroetorphine would lead to less respiratory events in treated patients compared to other commonly used opioids. This is a highly relevant topic as there has been a recent increase in the number of fatalities from misuse or abuse of legally prescribed opioids. While a reduced respiratory effect (especially at high dose) and favorable utility surface are certainly advantages over other opioids that lack such a profile, it is important to realize that in real life comedication, underlying respiratory, cardiac and/or renal disease, genetics, overdosing, sex, and age, among others, play an important role as well.⁴⁴ Still, our observation that R-dihydroetorphine (greater than the dose-range tested) has favorable pharmacodynamics and utility surface gives this analgesic an advantage over other commonly used analgesics such as fentanyl. For example, when comparing the utility surfaces of R-dihydroetorphine (fig. 6A) and fentanyl (fig. 8),¹² it is obvious that R-dihydroetorphine has a much greater green surface, indicative of a high probability of analgesia without respiratory depression, even at high effect-site concentrations. In future studies, we will quantify opioid respiratory and antinociceptive effects in individuals with identified risk factors for respiratory depression. Given the above, it is imperative not to infer clinical utility from our results. The

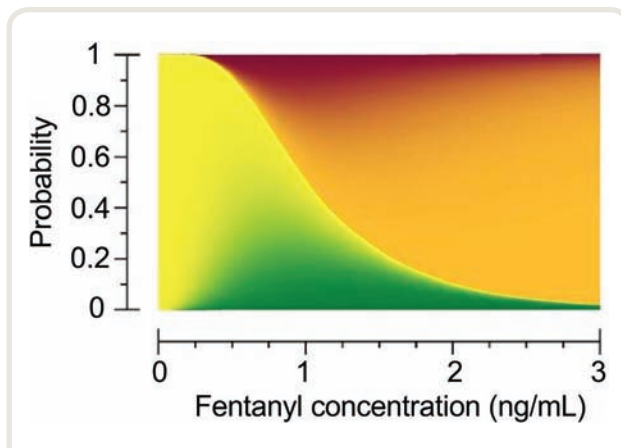


Fig. 8. Fentanyl utility surface as a function of effect-site or steady-state concentration. Data are from Roozekrans *et al.*¹² The color shading (green to yellow and red to orange) represents the context dependency of the utility functions on the postulated threshold for analgesia: *deep green* equals A++/R– or at least 50% analgesia/no respiratory depression; *green* equals A+/R– or at least 25% analgesia/no respiratory depression; *yellow* equals A–/R– or no analgesia/no respiratory depression; *deep red* equals A–/R+ or no analgesia/serious respiratory depression; *dark orange* equals A+/R+ or at least 25% analgesia/serious respiratory depression; *orange* equals A++/R+ or at least 50% analgesia/serious respiratory depression.

utility function is an experimental tool that is developed to compare opioids under artificial study conditions, with preset definitions of pain and respiratory depression. In future studies, we plan to validate the clinical use of the utility functions.

In conclusion, over the dose-range tested, R-dihydroetorphine exhibited an apparent plateau in respiratory depression but not in analgesia.

Research Support

This trial was sponsored by Mundipharma Research Ltd. (Cambridge, United Kingdom) and supported by departmental and institutional funds.

Competing Interests

At the time the study was conducted, Mr. Baily and Dr. Smith were employees of Mundipharma Research Ltd., Cambridge, United Kingdom. Dr. Oksche is an employee of Mundipharma Research Ltd., Cambridge, United Kingdom. The other authors declare no competing interests.

Reproducible Science

Full protocol available at: a.dahan@lumc.nl. Raw data available at: a.dahan@lumc.nl.

Correspondence

Address correspondence to Dr. Dahan: Department of Anesthesiology, Leiden University Medical Center,

H5-22, Albinusdreef 2, 2333 ZA Leiden, The Netherlands. a.dahan@lumc.nl. Information on purchasing reprints may be found at www.anesthesiology.org or on the masthead page at the beginning of this issue. ANESTHESIOLOGY's articles are made freely accessible to all readers, for personal use only, 6 months from the cover date of the issue.

References

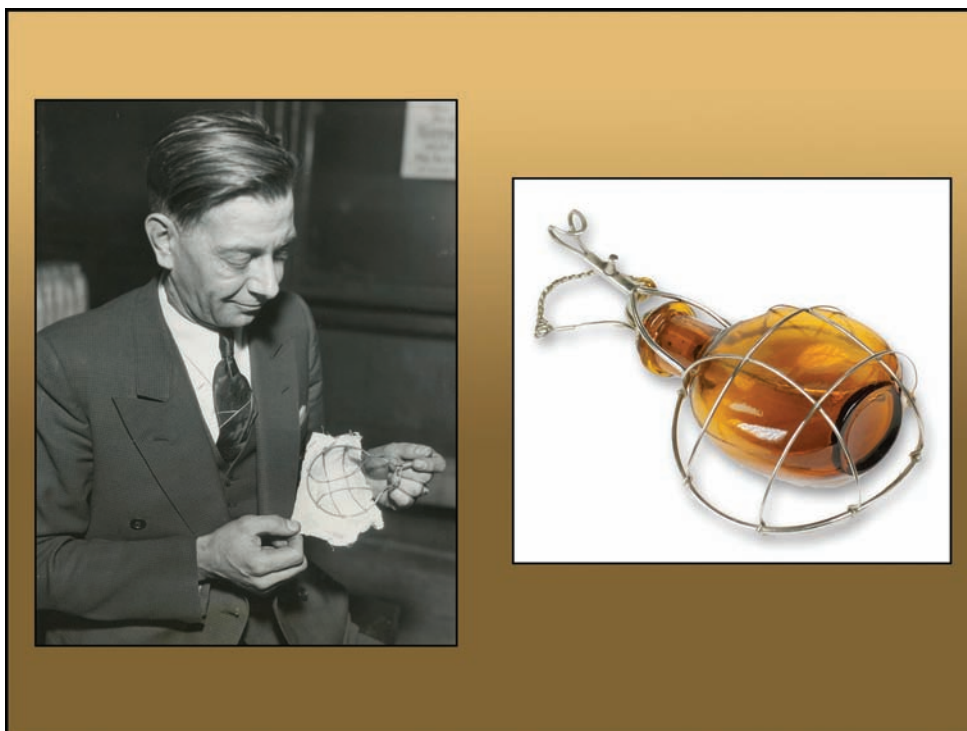
1. Dahan A, Niesters M, Smith T, Overdyk F: Opioids. In: Barash PG, Cullen BF, Stoelting RK, Cahalan MK, Stock MC, Ortega R, Sharar SR, Holt NF eds. *Clinical Anesthesia*, 8th edition. Philadelphia: Wolters Kluwer, 2017; 505–26
2. Pattinson KT: Opioids and the control of respiration. *Br J Anaesth* 2008; 100:747–58
3. Gray PA, Rekling JC, Bocchiaro CM, Feldman JL: Modulation of respiratory frequency by peptidergic input to rhythmogenic neurons in the preBötzinger complex. *Science* 1999; 286:1566–8
4. Dahan A, Yassen A, Bijl H, Romberg R, Sarton E, Teppema L, Olofsen E, Danhof M: Comparison of the respiratory effects of intravenous buprenorphine and fentanyl in humans and rats. *Br J Anaesth* 2005; 94:825–34
5. Yassen A, Olofsen E, Romberg R, Sarton E, Teppema L, Danhof M, Dahan A: Mechanism-based PK/PD modeling of the respiratory depressant effect of buprenorphine and fentanyl in healthy volunteers. *Clin Pharmacol Ther* 2007; 81:50–8
6. Lutfy K, Eitan S, Bryant CD, Yang YC, Saliminejad N, Walwyn W, Kieffer BL, Takeshima H, Carroll FI, Maidment NT, Evans CJ: Buprenorphine-induced antinociception is mediated by mu-opioid receptors and compromised by concomitant activation of opioid receptor-like receptors. *J Neurosci* 2003; 23:10331–7
7. Günther T, Dasgupta P, Mann A, Miess E, Kliever A, Fritzwanker S, Steinborn R, Schulz S: Targeting multiple opioid receptors – Improved analgesics with reduced side effects? *Br J Pharmacol* 2018; 175:2857–68
8. Yi SP, Kong QH, Li YL, Pan CL, Yu J, Cui BQ, Wang YF, Wang GL, Zhou PL, Wang LL, Gong ZH, Su RB, Shen YH, Yu G, Chang KJ: The opioid receptor triple agonist DPI-125 produces analgesia with less respiratory depression and reduced abuse liability. *Acta Pharmacol Sin* 2017; 38:977–89
9. Dosaka-Akita K, Tortella FC, Holaday JW, Long JB: The kappa opioid agonist U-50,488H antagonizes respiratory effects of mu opioid receptor agonists in conscious rats. *J Pharmacol Exp Ther* 1993; 264:631–7
10. Ohmori S, Morimoto Y: Dihydroetorphine: a potent analgesic: Pharmacology, toxicology, pharmacokinetics, and clinical effects. *CNS Drug Rev* 2002; 8:391–404
11. Boom M, Olofsen E, Neukirchen M, Fussen R, Hay J, Groeneveld GJ, Aarts L, Sarton E, Dahan A: Fentanyl

- utility function: A risk-benefit composite of pain relief and breathing responses. *ANESTHESIOLOGY* 2013; 119:663–74
12. Roozkrans M, van der Schrier R, Aarts L, Sarton E, van Velzen M, Niesters M, Dahan A, Olofsen E: Benefit *versus* severe side effects of opioid analgesia: Novel Utility functions of probability of analgesia and respiratory depression. *ANESTHESIOLOGY* 2018; 128:932–42
 13. Olesen AE, Broens S, Olesen O, Niesters M, van Velzen M, Drewes AM, Dahan A, Olofsen E: A pragmatic utility function to describe the risk-benefit composite of opioid and non-opioid analgesic medication. *J Pharmacol Exp Ther* 2019 2018 Nov 15. pii: jpet.118.253716. doi: 10.1124/jpet.118.253716. [Epub ahead of print]
 14. Boom MCA: Opioid therapy: A trade-off between opioid analgesia and opioid-induced respiratory depression. PhD thesis. Leiden University, 2013
 15. Dahan A, DeGoede J, Berkenbosch A, Olievier IC: The influence of oxygen on the ventilatory response to carbon dioxide in man. *J Physiol* 1990; 428:485–99
 16. Dahan A, Nieuwenhuijs D, Teppema L: Plasticity of central chemoreceptors: Effect of bilateral carotid body resection on central CO₂ sensitivity. *PLoS Med* 2007; 4:e239
 17. Olofsen E, Romberg R, Bijl H, Mooren R, Engbers F, Kest B, Dahan A: Alfentanil and placebo analgesia: No sex differences detected in models of experimental pain. *ANESTHESIOLOGY* 2005; 103:130–9
 18. Tansley JG, Pedersen ME, Clar C, Robbins PA: Human ventilatory response to 8 h of euoxic hypercapnia. *J Appl Physiol* (1985) 1998; 84:431–4
 19. Dahan A. The ventilatory response to carbon dioxide and oxygen: Methods and implications. PhD thesis, Leiden University, 1990, pp 68–70 (available at a.dahan@lumc.nl)
 20. Comets E, Brendel K, Mentre F: Model evaluation in nonlinear mixed effect models, with application to pharmacokinetics. *J Soc Franc Stat* 2010; 151:106e27
 21. Jonkman K, van Rijnsoever E, Olofsen E, Aarts L, Sarton E, van Velzen M, Niesters M, Dahan A : Esketamine counters opioid-induced respiratory depression. *Br J Anaesth* 2018; 120:1117–27
 22. Lewis JW, Husbands SM: The orvinols and related opioids—high affinity ligands with diverse efficacy profiles. *Curr Pharm Des* 2004; 10:717–32
 23. Bentley KW, Hardy DG: Novel analgesics and molecular rearrangements in the morphine-thebaine group. 3. Alcohols of the 6,14-endo-ethenotetrahydrooripavine series and derived analogs of N-allylnormorphine and -norcodeine. *J Am Chem Soc* 1967; 89:3281–92
 24. Mao H, Noyi Q: Analgesic and other CNS depressive effects of dihydroetorphine. *Acta Pharmacol Sin* 1982; 3: 9–13
 25. Li E, Weng L: Influence of dihydroetorphine hydrochloride and tramadol on labor pain and umbilical blood flow. *Zhongguo Yao Li Xue Bao* (Chin J Obstet Gyn) 1995; 16:137–40
 26. Kharasch ED, Rosow CE: Assessing the utility of the utility function. *ANESTHESIOLOGY* 2013; 119:504–6
 27. Henthorn TK, Mikulich-Gilbertson SK: μ -Opioid receptor agonists: Do they Have utility in the treatment of acute pain? *ANESTHESIOLOGY* 2018; 128:867–70
 28. Cremeans CM, Gruley E, Kyle DJ, Ko MC: Roles of μ -opioid receptors and nociceptin/orphanin FQ peptide receptors in buprenorphine-induced physiological responses in primates. *J Pharmacol Exp Ther* 2012; 343:72–81
 29. Dahan A, Boom M, Sarton E, Hay J, Groeneveld GJ, Neukirchen M, Bothmer J, Aarts L, Olofsen E: Respiratory effects of the nociceptin/orphanin FQ peptide and opioid receptor agonist, cebranopadol, in healthy human volunteers. *ANESTHESIOLOGY* 2017; 126:697–707
 30. Linz K, Schröder W, Frosch S, Christoph T: Opioid-type respiratory depressant side effects of cebranopadol in rats are limited by its nociceptin/orphanin FQ peptide receptor agonist activity. *ANESTHESIOLOGY* 2017; 126:708–15
 31. Manglik A, Lin H, Aryal DK, McCorvy JD, Dengler D, Corder G, Levit A, Kling RC, Bernat V, Hübner H, Huang XP, Sassano ME, Giguère PM, Löber S, Da Duan, Scherrer G, Kobilka BK, Gmeiner P, Roth BL, Shoichet BK: Structure-based discovery of opioid analgesics with reduced side effects. *Nature* 2016; 537:185–90
 32. Schmid CL, Kennedy NM, Ross NC, Lovell KM, Yue Z, Morgenweck J, Cameron MD, Bannister TD, Bohn LM: Bias Factor and Therapeutic Window Correlate to Predict Safer Opioid Analgesics. *Cell* 2017; 171:1165–1175.e13
 33. Hutchinson MR, Zhang Y, Shridhar M, Evans JH, Buchanan MM, Zhao TX, Slivka PF, Coats BD, Rezvani N, Wieseler J, Hughes TS, Landgraf KE, Chan S, Fong S, Phipps S, Falke JJ, Leinwand LA, Maier SE, Yin H, Rice KC, Watkins LR: Evidence that opioids may have toll-like receptor 4 and MD-2 effects. *Brain Behav Immun* 2010; 24:83–95
 34. Chien CC, Pasternak GW: Selective antagonism of opioid analgesia by a sigma system. *J Pharmacol Exp Ther* 1994; 271:1583–90
 35. Raehal KM, Walker JK, Bohn LM: Morphine side effects in beta-arrestin 2 knockout mice. *J Pharmacol Exp Ther* 2005; 314:1195–201
 36. Raehal KM, Bohn LM: The role of beta-arrestin2 in the severity of antinociceptive tolerance and physical dependence induced by different opioid pain therapeutics. *Neuropharmacology* 2011; 60:58–65
 37. Aguado D, Bustamante R, Gómez de Segura IA: Toll-like receptor 4 deficient mice do not develop remifentanyl-induced mechanical hyperalgesia: An experimental randomised animal study. *Eur J Anaesthesiol* 2018; 35:505–10
 38. Beckett EAH, Staikopoulos V, Hutchinson MR: Differential effect of morphine on gastrointestinal transit, colonic contractions and nerve-evoked relaxations

- in Toll-Like Receptor deficient mice. *Sci Rep* 2018; 8:5923
39. Carr GV, Mague SD: p38: The link between the kappa-opioid receptor and dysphoria. *J Neurosci* 2008; 28:2299–300
 40. Dahan A, Sarton E, Teppema L, Olivier C: Sex-related differences in the influence of morphine on ventilatory control in humans. *ANESTHESIOLOGY* 1998; 88:903–13
 41. Kest B, Sarton E, Dahan A: Gender differences in opioid-mediated analgesia: animal and human studies. *ANESTHESIOLOGY* 2000; 93:539–47
 42. Sarton E, Olofsen E, Romberg R, den Hartigh J, Kest B, Nieuwenhuijs D, Burm A, Teppema L, Dahan A: Sex differences in morphine analgesia: An experimental study in healthy volunteers. *ANESTHESIOLOGY* 2000; 93:1245–54; discussion 6A
 43. Niesters M, Dahan A, Kest B, Zacny J, Stijnen T, Aarts L, Sarton E: Do sex differences exist in opioid analgesia? A systematic review and meta-analysis of human experimental and clinical studies. *Pain* 2010; 151:61–8
 44. Khanna A, Buhre W, Saager L, Si Stefano P, Weingarten T, Dahan A, Brazzi L, Overdyk F: Derivation and validation of a novel opioid-induced respiratory depression risk prediction tool (Abstract). *Crit Care Med* 2019; 47:18

ANESTHESIOLOGY REFLECTIONS FROM THE WOOD LIBRARY-MUSEUM

Insuring Rheta Wynekoop's Gunshot Demise: Telltale Chloroform Burns from Her Murderous Mother-in-Law

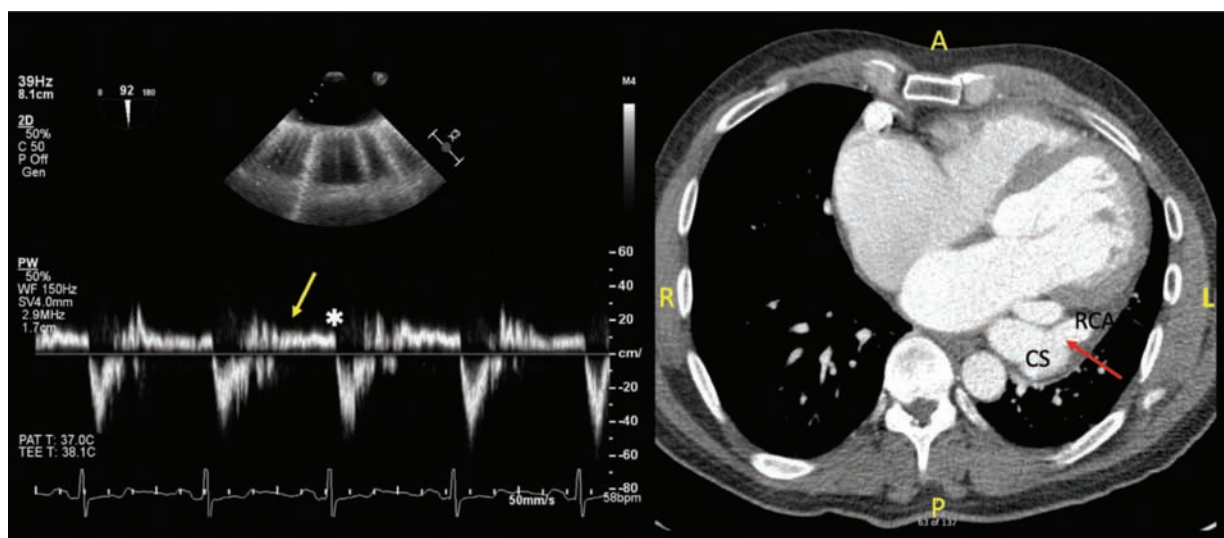


Police officer Charles Thomas (*left*) examines an Esmarch chloroform mask (similar to the museum example, *right*) found in November of 1933 alongside the dead body of Chicagoan Rheta Wynekoop. As the latter's philandering husband rode a train out of town, his cash-strapped mother, physician Alice Wynekoop (1871 to 1955), confirmed that she had already taken out extra life insurance on Rheta. When Rheta complained of abdominal pain, her mother-in-law chloroformed her "for the examination." Panicking when Rheta appeared to have dropped dead, Dr. Wynekoop tried to cover up the medical mishap by shooting her daughter-in-law in the back to stage a "murder by intruder." However, spilled chloroform had already burned Rheta's face and that led to a 25-yr jail sentence for the murderous mother-in-law. (Copyright © the American Society of Anesthesiologists' Wood Library-Museum of Anesthesiology.)

George S. Bause, M.D., M.P.H., *Honorary Curator and Laureate of the History of Anesthesia, Wood Library-Museum of Anesthesiology, Schaumburg, Illinois, and Clinical Associate Professor, Case Western Reserve University, Cleveland, Ohio. UJYC@aol.com.*

Holodiastolic Flow Reversal in Descending Aorta with Right Coronary Artery to Coronary Sinus Fistula

Zahid Merchant, M.D., Andrej Alfirevic, M.D.



A pulsed-wave Doppler spectral profile can be used as a modality to objectively assess flows in the descending thoracic aorta.¹ The normal profile reveals systolic antegrade flow; however, a small amount of retrograde diastolic flow is physiologic and increases with age and decreasing aortic compliance. The image on the left reveals holodiastolic flow reversal and increased end-diastolic velocity, as seen with the yellow arrow and asterisk, revealing continuous retrograde flow in the descending thoracic aorta. Both increased velocities and holodiastolic reversal correlate with increasing severity of aortic insufficiency, large arteriovenous fistula, patent ductus arteriosus, and systemic to pulmonary artery communications such as Blalock-Taussig shunt.¹ A computed tomographic angiography scan, right image, reveals a markedly dilated right coronary artery (RCA) extending in a serpiginous fashion laterally and along the undersurface of the heart. In this plane, the right coronary artery is cut along its short axis revealing a severely dilated coronary sinus (CS) communicating with the right coronary artery *via* fistula, marked by the red arrow. The continuous pressure gradient from the arterial (high pressure) to venous (low pressure) system explains the flow reversal pattern in the descending aorta while hemodynamically responsible for the decreased diastolic forward flow and left-to-right shunting. The consequences of a significantly increased shunt-flow include

volume overload, pulmonary hypertension, and heart failure.² The fistulous communication with the venous system is responsible for diverting oxygenated blood, leading to myocardial ischemia. Anesthetic management includes avoiding hemodynamic fluctuations as anesthesia-induced hypotension decreases coronary perfusion and potentiates myocardial ischemia while hypertension increases the risk of rupturing a dilated coronary artery.³

Competing Interests

The authors declare no competing interests.

Correspondence

Address correspondence to Dr. Merchant: midzmerchant@gmail.com

References

1. Zoghbi WA, Adams D, Bonow RO, Enriquez-Sarano M, Foster E, Grayburn PA, Hahn RT, Han Y, Hung J, Lang RM, Little SH, Shah DJ, Shernan S, Thavendiranathan P, Thomas JD, Weissman NJ: Recommendations for noninvasive evaluation of native valvular regurgitation: A report from the American Society of Echocardiography developed in collaboration

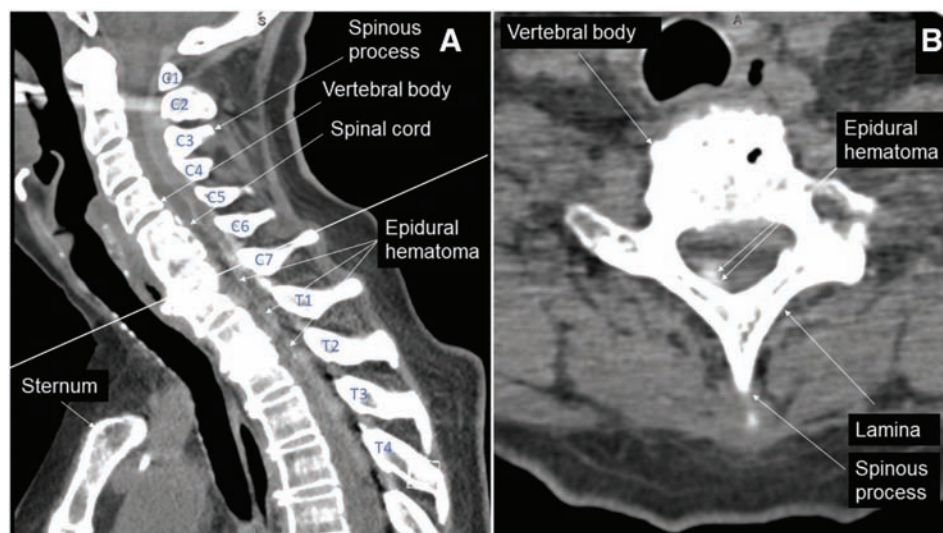
From the Department of Cardiothoracic Anesthesiology, Cleveland Clinic Health System, Cleveland, Ohio.

Copyright © 2019, the American Society of Anesthesiologists, Inc. All Rights Reserved. Anesthesiology 2019; 131:1340–1. DOI: 10.1097/ALN.0000000000002917

- with the Society for Cardiovascular Magnetic Resonance. *J Am Soc Echocardiogr* 2017; 30:303–71
2. Marino M, Frangopoulos C, Kumar PA, Bhatia M: Unusual echolucency seen after bacterial endocarditis. *J Cardiothorac Vasc Anesth* 2018; 32:1087–9
 3. Sawai T, Nakahira J, Minami T: Usefulness of intraoperative transesophageal echocardiography for evaluation of circumflex coronary artery fistula with ruptured aneurysm draining into coronary sinus. *J Anesth* 2015; 29:962–6

Spinal Epidural Hematoma after Interlaminar Cervical Epidural Steroid Injection

Ratan K. Banik, M.D., Ph.D., Clark C. Chen, M.D., Ph.D.



The exact incidence of spinal epidural hematoma after cervical epidural steroid injection is unknown, but the incidence of epidural hematoma after epidural block in obstetric patients is estimated to be ~1:200,000.¹ The computed tomography images above demonstrate an epidural hematoma in an 80-yr-old woman after C7–T1 epidural injection performed under moderate sedation. Thirty minutes after the procedure, she developed acute onset of neck pain, which progressed shortly to numbness down to her mid-sternum, 0/5 strengths in the bilateral elbows, wrists, and lower extremities, and loss of patellar-reflexes. The image was taken ~3 h after the onset of symptoms. Image A is a sagittal computed tomography image, which is notable for hyperdense collection of blood within the spinal canal extending from C2–T4. Image B is a cross-sectional view at the level of C7, which shows a biconvex-shaped hyperdense lesion within the spinal canal suggestive of epidural hematoma. The patient's localized neck pain, quadriplegia, loss of reflexes, numbness, sudden onset of symptoms, and computed tomography findings are characteristic of acute cord compression.

Surgical laminectomy and decompression is the standard intervention for epidural hematoma, and early detection and intervention are necessary to prevent permanent deficits. A previous study has shown that

patients with the same preoperative neurologic status (measured with numerical Frankel-grade: 1 equals complete motor and sensory loss, 5 equals no motor or sensory abnormalities) taken to surgery less than 12 h from the onset of symptoms had higher complete recovery rates than those taken to surgery more than 12 h from the onset of symptoms.² In stable patients, magnetic resonance imaging is the diagnostic modality of choice. The risk factors for bleeding in this case included trazodone³ (selective serotonin reuptake inhibitors have been associated with bleeding) and older age.⁴

Acknowledgments

The authors thank Michael Todd, M.D., Department of Anesthesiology, University of Minnesota, Minneapolis, Minnesota, for his comments. This report is also accepted for presentation at the 2019 Annual Meeting of the American Society of Anesthesiologists.

Research Support

This work was supported by the Department of Anesthesiology, University of Minnesota and Fairview Medical Center, Minneapolis, Minnesota.

From the Department of Anesthesiology (R.K.B.) and Department of Neurosurgery (C.C.C.), University of Minnesota, Minneapolis, Minnesota.

Copyright © 2019, the American Society of Anesthesiologists, Inc. All Rights Reserved. *Anesthesiology* 2019; 131:1342–3. DOI: 10.1097/ALN.0000000000002896

Competing Interests

The authors declare no competing interests.

Correspondence

Address correspondence to Dr. Banik: rkbanik@umn.edu

References

1. D'Angelo R, Smiley RM, Riley ET, Segal S: Serious complications related to obstetric anesthesia: The serious complication repository project of the Society for Obstetric Anesthesia and Perinatology. *ANESTHESIOLOGY* 2014;120:1505–12
2. Lawton MT, Porter RW, Heiserman JE, Jacobowitz R, SonntagVK, Dickman CA: Surgical management of spinal epidural hematoma: Relationship between surgical timing and neurologic outcome. *J Neurosurg* 1995; 83:1–7
3. De Abajo FJ: Effects of selective serotonin reuptake inhibitors on platelet function: Mechanisms, clinical outcomes and implications for use in elderly patients. *Drugs Aging* 2011; 28:345–67
4. Cowman J, Dunne E, Oglesby I, Byrne B, Ralph A, Voisin B, Müllers S, Ricco AJ, Kenny D: Age-related changes in platelet function are more profound in women than in men. *Sci Rep* 2015; 5:12235

Drug Label Ribbons to Improve Patient Safety in Low-resource Environments

Meghan Prin, M.D., M.S., Clare Evans Algeo, M.D., Lucy Kalonga, C.O., Christophe Mkwezalamba, C.O.



These images demonstrate the operating room medication labeling system of a public referral hospital in Malawi (*left image*) and a new system being piloted by the authors in a district hospital of Malawi (*right image*).

Many systems have been developed to prevent medication administration errors, including standardized color-coded labels, two-person verification, operating room pharmacists, and adverse event reporting systems.¹ However, very few of these are feasible in low-resource settings. Even color-coded tape is often unavailable or unaffordable. As demonstrated in the far-right of the *left image*, the underlying tray labels are often relied on and the syringes themselves may remain unlabeled. In most low-income countries, adverse event reporting systems are absent, which limits the ability to monitor errors. A recent meta-analysis of medication errors in anesthesia practice in sub-Saharan Africa found only five case reports and seven studies.² Most reported errors are substitution errors, and the most common causes are syringe swapping or mislabeled syringes.^{1,3}

Although the actual number of adverse events related to syringe labeling is unknown in the index hospital, we nonetheless pursued quality improvement efforts. We sought to develop a medication labeling system that is affordable, easy to apply, and sustainable in low-resource settings. Color-coded ribbon labels can be made at low cost in almost any setting and can be reused to limit expense. Since January

2019, we have found these ribbons to be an easy, durable, and effective tool, and we are working toward widespread implementation and evaluation of this concept.

Competing Interests

The authors declare no competing interests.

Correspondence

Address correspondence to Dr. Prin: meghan.prin@gmail.com

References

1. Wahr JA, Abernathy JH III, Lazarra EH, Keebler JR, Wall MH, Lynch I, Wolfe R, Cooper RL: Medication safety in the operating room: Literature and expert-based recommendations. *Br J Anaesth* 2017; 118:32–43
2. Kunle R, Godwin AA, Kehinde O, Abraham D: Medication administration error in anaesthetic practice: A review of the African experience. *IOSR Journal of Pharmacy and Biologic Sciences* 2014; 9(6): 62–7
3. Llewellyn RL, Gordon PC, Wheatcroft D, Lines D, Reed A, Butt AD, Lundgren AC, James MF: Drug administration errors: A prospective survey from three South African teaching hospitals. *Anaesth Intensive Care* 2009; 37:93–8

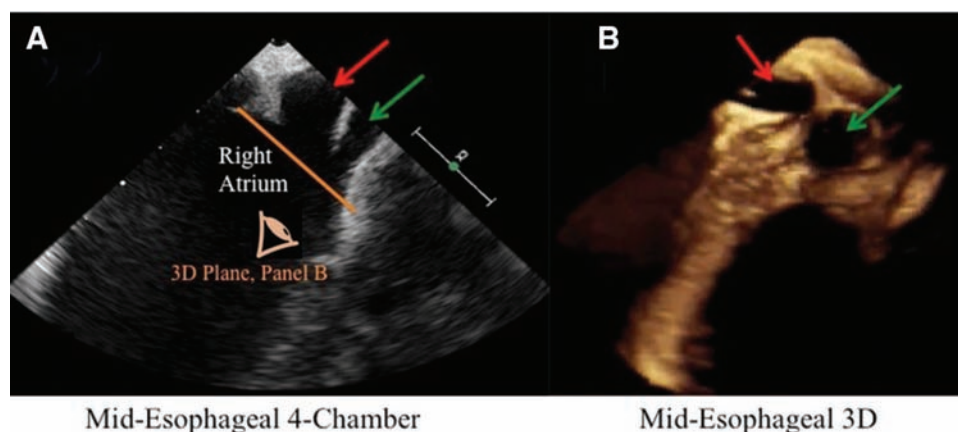
From the Department of Anesthesiology (M.P.) and the Department of Obstetrics and Gynecology (C.E.A., L.K., C.M.), Baylor College of Medicine, Houston, Texas.

Copyright © 2019, the American Society of Anesthesiologists, Inc. All Rights Reserved. *Anesthesiology* 2019; 131:1344. DOI: 10.1097/ALN.0000000000002918

Seeing Double

The Clinical Conundrum of the Double-barrel Coronary Sinus

Samuel J. Hankins, M.D.



The accompanying modified mid-esophageal four-chamber transesophageal echocardiography image shows two coronary sinuses emptying into the right atrium where normally there is one. As shown in *panel A*, both sinuses run parallel in the AV groove inferior to the left atrium (Supplemental Digital Content, <https://links.lww.com/ALN/C43>). This rare anomaly, referred to as “double-barrel coronary sinus,” was discovered during a coronary artery bypass graft procedure in which retrograde cardioplegia was planned. Double-barrel coronary sinus arises when the great cardiac vein fails to combine with the left horn of the sinus venosus during the 10th week of development, and is described in full elsewhere.^{1–3} Despite the obvious perils of cannulating the “false” sinus, criteria for determining the “true” coronary sinus by transesophageal echocardiography have not yet been published.²

Panel B shows both sinuses *en face* from the right atrium, with the cephalad sinus (*red arrow*) appearing slit-like, as described previously.² The caudad sinus (*green arrow*) appeared larger in diameter, and its color Doppler flow was greater. Because the “true” coronary sinus should drain a larger myocardial territory and thus have the larger caliber and flow, the retrograde cardioplegia catheter was guided

into the caudad sinus with good result. In cases of double-barrel coronary sinus, the authors suggest larger vessel caliber (preferably assessed by three-dimensional imaging in an *en face* view) and greater Doppler flow to be important determinants of the “true” sinus.

Competing Interests

The author declares no competing interests.

Correspondence

Address correspondence to Dr. Hankins: samuel.hankins@va.gov

References

1. Williams V, Bartanuszova M, Rahimi OB, Moore CM: A rare variant of the great cardiac vein. *Int J Anat Var* 2013; 6:112–4
2. Bardia A, Owais K, Khabbaz KR, O’Gara B, Mahmood F: Coronary sinus and another sinus: Which one to cannulate? *J Cardiothorac Vasc Anesth* 2015; 29:824–6
3. Marhefka GD, Pavri BP: Double-barrel coronary sinus. *J Cardiovasc Electrophysiol* 2008; 19:102

Supplemental Digital Content is available for this article. Direct URL citations appear in the printed text and are available in both the HTML and PDF versions of this article. Links to the digital files are provided in the HTML text of this article on the Journal’s Web site (www.anesthesiology.org).

From the Department of Anesthesiology, Michael E. DeBakey Veterans Affairs Medical Center, Houston, Texas.

Copyright © 2019, the American Society of Anesthesiologists, Inc. All Rights Reserved. *Anesthesiology* 2019; 131:1345. DOI: 10.1097/ALN.0000000000002931

ANESTHESIOLOGY

Artificial Intelligence and Machine Learning in Anesthesiology

Christopher W. Connor, M.D., Ph.D.

ANESTHESIOLOGY 2019; 131:1346–59

The human mind excels at estimating the motion and interaction of objects in the physical world, at inferring cause and effect from a limited number of examples, and at extrapolating those examples to determine plans of action to cover previously unencountered circumstances. This ability to reason is backed by an extraordinary memory that subconsciously sifts events into those experiences that are pertinent and those that are not, and is also capable of persisting those memories even in the face of significant physical damage. The associative nature of memory means that the aspects of past experiences that are most pertinent to the current circumstance can be almost effortlessly recalled to conscious thought. However, set against these remarkable cerebral talents are fatigability, a cognitive laziness that presents as a tendency to short-cut mental work, and a detailed short-term working memory that is tiny in scope. The human mind is slow and error-prone at performing even straightforward arithmetic or logical reasoning.¹

In contrast, an unremarkable desktop computer in 2019 can rapidly retrieve and process data from 32 gigabytes of internal memory—a quarter of a trillion discrete bits of information—with absolute fidelity and tirelessness, given an appropriately constructed program to execute. The greatest progress in artificial intelligence has historically been in those realms that can most easily be represented by the manipulation of logic and that can be rigorously defined and structured, known as classical or symbolic artificial intelligence. Such problems are quite unlike the vagaries of the interactions of objects in the physical world. Computers are not good at coming to decisions—indeed, the formal definition of the modern computer arose from the proof that certain propositions

ABSTRACT

Commercial applications of artificial intelligence and machine learning have made remarkable progress recently, particularly in areas such as image recognition, natural speech processing, language translation, textual analysis, and self-learning. Progress had historically languished in these areas, such that these skills had come to seem ineffably bound to intelligence. However, these commercial advances have performed best at single-task applications in which imperfect outputs and occasional frank errors can be tolerated.

The practice of anesthesiology is different. It embodies a requirement for high reliability, and a pressured cycle of interpretation, physical action, and response rather than any single cognitive act. This review covers the basics of what is meant by artificial intelligence and machine learning for the practicing anesthesiologist, describing how decision-making behaviors can emerge from simple equations. Relevant clinical questions are introduced to illustrate how machine learning might help solve them—perhaps bringing anesthesiology into an era of machine-assisted discovery.

(*ANESTHESIOLOGY* 2019; 131:1346–59)

are logically undecidable²—and classical approaches to artificial intelligence do not easily capture the idea of a “good enough” solution.

For most of human history, the practice of medicine has been predominantly heuristic and anecdotal. Traditionally, quantitative patient data would be relatively sparse, decision making would be based on clinical impression, and outcomes would be difficult to relate with much certainty to the quality of the decisions made. The transition to evidence-based practice³ and Big Data is a relatively recent occurrence. In contrast, anesthesiologists have long relied on personalized streams of quantified data to care for their unconscious patients, and advances in monitoring and the richness of that data have underpinned the dramatic improvements in patient safety in the specialty.⁴ Anesthesiologists also practice at the sharper end of cause and effect: decisions usually cannot be postponed, and errors in judgment are often promptly and starkly apparent.

The general question of artificial intelligence and machine learning in anesthesiology can be stated as follows:

1. There is some outcome that should be either attained or avoided.
2. It is not certain what factors lead to that outcome, or a clinical test that predicts that outcome cannot be designed.

This article is featured in “This Month in Anesthesiology,” page 1A.

Submitted for publication September 2, 2018. Accepted for publication February 21, 2019. From the Department of Anesthesiology, Perioperative and Pain Medicine, Brigham and Women’s Hospital; and the Department of Physiology and Biophysics, Boston University, Boston, Massachusetts.

Copyright © 2019, the American Society of Anesthesiologists, Inc. All Rights Reserved. *Anesthesiology* 2019; 131:1346–59. DOI: 10.1097/ALN.0000000000002694

3. Nevertheless, a body of patient data is available that provides at least circumstantial evidence as to whether the outcome will occur. The data are plausibly, but not definitively, related.
4. The signal, if it is present in the patient data, is too diffuse across the data set for it to be learned reliably from the number of cases that an anesthesiologist might personally encounter, or the clinical decision-making relies upon a subconscious judgment that the anesthesiologist cannot elucidate.
5. Can an algorithm, derived from the given data and outcomes, provide insight in order to improve patient management and the decision-making process?

This form of machine learning might be termed machine-assisted discovery.

This article takes the form of an integrative review,⁵ defined as “a review method that summarizes past empirical or theoretical literature to provide a more comprehensive understanding of a particular phenomenon or healthcare problem.” The article therefore introduces the theory underlying classical and modern approaches to artificial intelligence and machine learning, and surveys current empirical and clinical areas to which these techniques are being applied. Concepts in the fundamentals of artificial intelligence and machine learning are introduced incrementally:

1. Beginning with classical or symbolic artificial intelligence, a logical representation of the problem is crafted and then searched for an optimal solution.
2. Model fitting of physiologic parameters to an established physiologic model is shown as an extension of search.
3. Augmented linear regression is shown to allow certain nonlinear relationships between outcomes and physiologic variables to be discerned, even in the absence of a defined physiologic model. It requires sufficient expertise about which combinations of nonphysiologic transformations of the variables might be informative.
4. Neural networks are shown to provide a mechanism to establish a relationship between input variables and an output without defining a logical representation of the problem or defining transformations of the inputs in advance. However, this flexibility comes at considerable computational cost and a final model with a behavior that may be hard to comprehend.

Numerous other theoretical and computational approaches do exist, and these may have practical advantages depending on the nature of the problem and the structure of the desired outputs.⁶

The literature search for an integrative review should be transparent and reproducible, comprehensive but focused and purposive. A literature search was performed using PubMed for articles published since 2000 using the following terms: “artificial intelligence anesthesiology” (543 matches), “computerized analysis anesthesiology” (353

matches), “machine learning anesthesiology” (91 matches), and “convolutional neural network anesthesiology” (1 match). Matches were reviewed for suitability, and augmented with references of historical significance. The specialty of anesthesiology features a broad history of attempts to apply computational algorithms, artificial intelligence, and machine learning to tasks in an attempt to improve patient safety and anesthesia outcomes (table 1). Recent significant and informative empirical advances are reviewed more closely.

Classical Artificial Intelligence and Searching

Creating a classical artificial intelligence algorithm begins with the three concepts of a bounded solution space, an efficient search, and termination criteria.

First, using what is known about the problem, a set of possible solutions that the algorithm can produce is defined. The algorithm will be allowed to choose one of these possible solutions, and so the solution set must be created in such a way that it is reasonably certain that the best possible solution is among the choices available. The algorithm will never be able to think outside of this “box,” and in that sense the solution space is bounded. In the game of tic-tac-toe, for example, the set of solutions is those squares that have not yet been taken. The best solution is the one that most diminishes the opponent’s ability to win, ideally until victory is achieved (*i.e.*, minimax).⁷ In real life problems, however, it can be difficult to define a bounded set of solutions or even say explicitly what “best” means.

Second, the possible solutions are progressively evaluated and searched, trying to find the best one. In designing and programming the search strategy, anything else of worth that is known about the problem should be incorporated, such as how to value one solution *versus* another, ways to search efficiently by focusing on areas of the solution space that are more likely to be productive,⁸ and intermediate results that might allow certain subsets of the solution space to be excluded from further evaluation (*i.e.*, pruning). Sometimes the knowledge and understanding of the underlying problem might be quite weak, and then in the worst case it may be necessary to fall back on an exhaustive and computationally intensive brute-force search of all the possible solutions.

Third, the algorithm must terminate and present a result. Given enough time, eventually the algorithm should ideally find and select the optimum solution. Depending on the structure of the problem and the search algorithm, it may be possible to guarantee through theory that the algorithm will terminate with the optimal solution within a constrained amount of time. A weaker theoretical guarantee would be that the algorithm will at least improve its solution with each search iteration. However, in the general case and if no such theoretical guarantee is possible, the algorithm might only select the best good-enough solution found within an

allowed time limit, or perhaps issue an error message that no sufficiently satisfactory solutions were identified.

Search-based classical artificial intelligence has obvious applications to practical problems such as wayfinding on road maps, in which a route must be chosen that is connected by legal driving maneuvers and arrives in the shortest time. Less obviously, this same logic can be applied to real-world problems such as locating a lost child in a supermarket. According to the order of operations above, the first step is to create a bounded solution set: by covering the exit, the location of the child is reasonably bounded to be somewhere within the supermarket. Second, a search is begun. A naive approach might be to walk up and down every aisle in turn until the child is found but, from insight, far better search strategies for this problem can be easily identified. The most efficient search strategy is clearly to walk along the ends of the aisles: this allows whole aisles to be scanned and excluded (*i.e.*, pruned) rapidly. Third, the search terminates either on finding the child, or on determining that additional resources must be employed if the child cannot be found within a certain time.

Designing classical artificial intelligence algorithms is not a turnkey mathematical task; it is heavily dependent on the human expertise of the designer. In classical artificial intelligence, the role of the computer is to contribute its immense power of calculation to evaluate the relative merits of a large number of possible solutions, which the designer provides. This division of labor can be dated back to Ada Lovelace's 1843 description of the conception of the modern computer: "The Analytical Engine has no pretensions whatever to originate anything. It can do whatever we know how to order it to perform. It can follow analysis; but it has no power of anticipating any analytical relations or truths. Its province is to assist us in making available what we are already acquainted with."⁹

In 1997, the IBM supercomputer Deep Blue defeated the then world champion, Garry Kasparov, at chess. It had been a longstanding goal for a machine to be able to play chess at levels unattainable by humans.¹⁰ The rules of chess are clear and unambiguous, and the actions take place within the confines of the board. The state of play is completely apparent and known to both players. It is possible to list all the available legal moves, all responses to those moves, all responses to those responses, and so on—the solution space is bounded. In principle, it is not even particularly difficult to write a program that can play chess flawlessly. The program simply tries out (*i.e.*, searches) all possible moves and all possible responses until the game is either won or lost. However, a computer program that tried to evaluate every possible move and all of its consequences would not be able to make its first move, so immense is the search space.¹¹ Deep Blue's success rested on two pillars. First, its search algorithm possessed an evaluation function to approximate the relative value of a position. This function was crafted from the distilled, programed, strategic wisdom of human

chess experts, and allowed the search algorithm to ignore choices that were likely to be unproductive. Second, this search algorithm was supported by brute-force computing power capable of evaluating two hundred million moves per second. These techniques proved sufficient for Deep Blue to achieve superhuman mastery of a game with approximately 10^{47} possible board positions—an immense but bounded space. In many ways, however, mastery of chess was classical artificial intelligence's triumph but also its swansong. The division of labor remains the same as in Lovelace's original description, and the human strategic understanding of the game was not outdone but instead overwhelmed by the indefatigability of the machine's tactical evaluation of millions and millions of positions. The computer did what it was told, but it did not learn.

In anesthesiology practice, the closest example is open-loop target-controlled infusion. Pharmacokinetic models describe the forwards relationship from a drug administration schedule $D(t)$ to an effect site concentration $e(t)$. However, it is the inverse solution that is required: for a requested $e(t)$, some $D(t)$ should be produced, perhaps subject to limits on administration rate or plasma concentration.¹² An open-loop target-controlled infusion pump will perform a search for a drug administration schedule that brings the predicted concentration of the medication within the body toward this goal, subject to the given constraints. The underlying equations are concise and effective,¹³ but the device cannot become more proficient at its task. It follows the algorithms that it is given.

Model Fitting as a Form of Searching

Anesthesiologists take particular interest in objective patient outcomes, and whether these good or bad outcomes can be predicted from the data that are available. Lacking a direct test for the desired outcome (in which case prognosis would be straightforward), the research question becomes whether the patient's outcome is in some way imprinted upon and foreshadowed by the imperfectly informative data that are available. An approach is to seek to fit models to the data in order to try to make more reliable predictions, and therefore potentially discover previously unappreciated but useful relationships within the data. This approach requires a large enough body of data and patient outcomes on which model fitting can be performed, and this large body of data cannot reasonably be analyzed by hand.

A model is created using an example set for which the data and outcomes are known—*i.e.*, the training data. The essence of a useful model is that it should be able to make useful predictions about data it has not previously seen, *i.e.*, that it is generalizable. An overly complicated model may become overfit to its training data, such that its predictions are not generalizable. Figure 1 shows examples of this. Each figure shows a population of green circles, representing notionally favorable outcomes, and red crosses, representing notionally

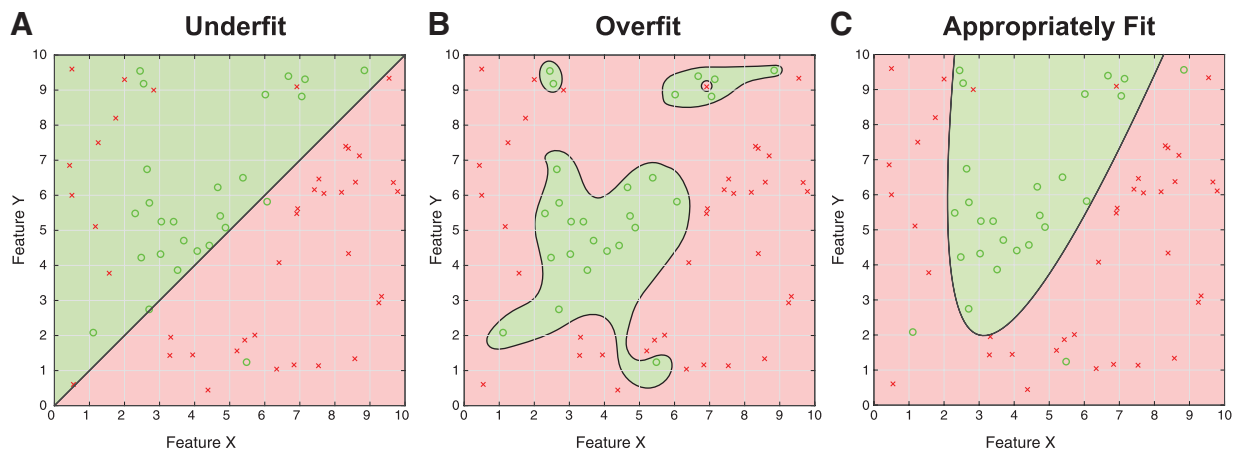


Fig. 1. Examples of model fitting to data. The data are synthetic, for the purposes of illustration only. (A) An underfit representation of the data. Although the linear discriminator captures most of the *green circles*, numerous *red crosses* are misclassified. The linear model is too simple. (B) The discriminator is overfit to the data. Although there are no classification errors for the example data, the model will not generalize well when applied to new data that arrives. (C) A parabola discriminates the data appropriately with only a few errors. This is the best parsimonious classification.

unfavorable outcomes. The question is whether the two available items of data, Feature X and Feature Y, can predict the outcome. Three models are fit to the exact same training data, to produce a black line (known as the discriminant) that separates the figure into prediction regions, shaded either green or red, accordingly. An item of training data is correctly classified when its symbol falls in a region that is shaded the same color, and is misclassified when it does not (*i.e.*, when it lies on the wrong side of the discriminant).

Figure 1A shows a model that is underfit. Although most of the symbols are correctly classified, there are several misclassified red crosses on the left of the figure, and the simple linear discriminant has no way to capture these. A decision algorithm based on this model would have high specificity (green circles are almost all correctly classified), but a lower sensitivity (several bad outcomes are erroneously predicted as good). The decision performance is therefore somewhat reminiscent of the Mallampati test,¹⁴ which also demonstrates high specificity but low sensitivity.¹⁵ The discriminant in figure 1A would function better if it could assume a more complex form. Figure 1B, in contrast, shows a model that is overfit. Although all the training data are correctly classified, the unwieldy discriminant is governed too much by the satisfaction of individual data points rather than the overall structure of the problem. This model is unlikely to generalize well to new data, as it is overly elaborate. Figure 1C shows a model that is appropriately fit to the data (indeed, the data were created to illustrate this point). The discriminant is complex enough to capture the distribution of the outcomes, but it is also parsimonious in that the shape of the discriminant is described by only a few parameters. In practice, of course, the true underlying

distribution is not known in advance, so the performance of the discriminant must be tested statistically. The discriminant in figure 1C has fewer degrees of freedom than the discriminant in figure 1B, so its performance is statistically more likely to represent the true nature of the underlying process even though it has more misclassifications than the overfit discriminant. Model fitting is therefore a form of search in which the choices are the parameters admitted to the model and their relative weights, in order to find models that are statistically most likely to represent the underlying process based upon the training data that are available.

Discovering Nonlinear Relationships in Clinical Medicine

Many judgments in anesthesiology are based on absolute thresholds or linear combinations of variables. A patient with a heart rate above 100 is tachycardic, and one with a temperature above 38°C is febrile. A man whose ECG features an R wave in lead aVL and an S wave in lead V₃ that combined exceed 28 mm has left-ventricular hypertrophy.¹⁶

Logistic regression is useful when fitting a weighted combination of variables to an outcome. Logistic regression defines an error function that measures the extent to which the current weighted combination of variables tends to misclassify outcomes. These weights are subsequently modified in order to improve the classification rate. The regression algorithm determines the changes in the weightings that would most improve the current classification, and then repeats the process until an optimum weighting is settled upon. The regression algorithm therefore performs a gradient descent on the error function; one can

picture an imaginary ball rolling down a landscape defined by the error function until a lowest, optimum point is reached such that the best linear combination of the input variables is determined. Logistic regression is a powerful machine-learning technique that works quickly and is also convex, meaning essentially that the “ball” can roll down to the optimum solution from any starting point (for almost all well-posed problems). However, many outcome problems in anesthesiology and critical care clearly do not depend on linear criteria. For example, intensive care unit outcomes that may depend on a patient’s potassium level, or glucose level, or airway positive end-expiratory pressure are more likely to be Goldilocks problems: the best outcomes require an amount that is neither too big, nor too small, but just right. Figure 2A illustrates such a situation, in which the good outcomes are clustered around a point in the feature space, and deviations from that point result in poor outcomes. As a clinical correlate, one might imagine that the outcomes are timely intensive care unit discharges,¹⁷ and the data K and G represent well-controlled levels of potassium and glucose, although the data shown here are purely artificial and created solely for this example. The data show a clear clustering of the outcomes, but an algorithm that is only capable of producing a discriminant based on a linear combination of K and G would not be able to capture that separation. Rather than performing a nonlinear regression

over the two variables K and G, a solution lies in transforming the data by calculating the squares of K and G (*i.e.*, K^2 , G^2) and their cross-term KG, and then performing an augmented linear logistic regression over the five variables K, G, K^2 , G^2 , and KG.

As shown in figure 2B, a linear discriminant in the K^2 , G^2 plane will perfectly separate the outcomes. This discriminant, given by $(K^2) + (G^2) - 9 = 0$, is exactly the same as a circle of radius 3 in figure 2A, demonstrating that nonlinear boundaries can be discovered. Although it may seem clinically bizarre to talk about the squared value of the serum potassium (K^2), it is easy to write a quadratic function that has clinical meaning. For example, the function $35 - 17K - 2K^2$ is positive if the value of K lies between 3.5 and 5.0, but turns negative for any more hypokalemic or hyperkalemic value outside that range. This simple example underscores the ways in which the outputs from machine-learning algorithms can seem inscrutable or black box. To a computer, the two definitions are essentially equivalent: one is no more meaningful or better than the other. It takes human effort to explain numerical results in a clinically meaningful way.¹⁸

Augmenting the variable space with quadratic terms allows a linear algorithm to define nonlinear features like islands (as in fig. 2A) and open curves (as in fig. 1B), but the technique can be extended further by using higher polynomial terms. Augmentation can also be performed with

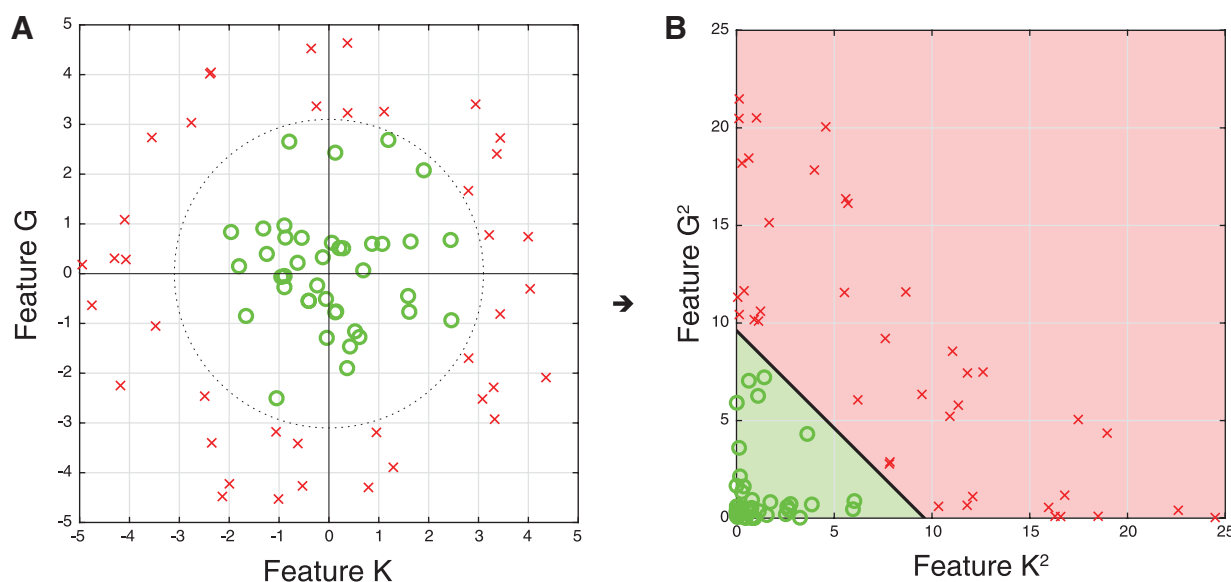


Fig. 2. Examples of model fitting using augmented variables. The data are synthetic, for the purposes of illustration only. (A) An example of a model-fitting problem in which desirable outcomes (represented by green circles) are clustered around a mean point, and adverse outcomes (represented by red crosses) are associated with deviations from that point. For clinical correlation, one might imagine that the data represent favorable or unfavorable intensive care unit outcomes based on rigorous control of potassium (Feature K) and glucose (Feature G). (B) Rather than attempting to fit outcomes solely to the variables K and G, the variable space can be augmented by also fitting to K^2 and G^2 . This example demonstrates that the fitting of a perimeter around a mean value is easily accomplished by a linear fitting within the augmented space of K^2 and G^2 . The linear discriminant of $(K^2) + (G^2) - 9 = 0$ as shown produces a circular boundary of radius 3 in the K,G space.

reciprocal powers such as K^{-1} (*i.e.*, $1/K$), which would in principle allow the machine-learning algorithm to discern useful relationships based on ratios. Common such clinical examples include the following:

- The Shock Index¹⁹ (heart rate / systolic blood pressure), which rises in response to the combined increase in heart rate and decrease in blood pressure associated with hypovolemia.
- The Rapid Shallow Breathing Index²⁰ (respiratory frequency / tidal volume) which rises in response to the fast, small, panting breaths associated with respiratory failure.
- The Body Mass Index (weight / height²), which represents obesity as excess weight distributed over an insufficiently sized physical frame.

A downside to augmenting the variable space is that the number of input variables can increase dramatically, which can overwhelm the size of the available training data and lead to a significant risk of overfitting. One challenge is that the input variables and the augmented combinations that are to be considered must be fully defined in advance. Only nonlinear relationships that can be approximated from a linear combination of the variables that are supplied can be found. For real-world problems in medicine and biology, considerable expertise is required in order to define a meaningful and informative set of inputs. Human insight must also be applied to determine what problem should be solved and what outputs are useful. When only limited knowledge is available about the best way to frame a problem numerically, modern artificial intelligence and neural networks provide an alternative approach.

Modern Artificial Intelligence

The limitations of classical artificial intelligence were particularly apparent in attempts to produce programs capable of playing Go. Go is, at least in terms of its rules, a simpler game than chess. Two players take turns to place a stone, white or black, on a 19×19 board. Plays in Go take place at the intersections of the grid lines, rather than on the squares as in chess. Once a stone is placed, it does not subsequently move. Briefly, the game is won by whoever manages to corral the largest total space on the board. However, in play, Go is a much more complex game than chess, with approximately 10^{170} board positions compared to 10^{47} . It is hard to overstate the magnitude of these combinatoric numbers. There are about 10^{80} atoms in the universe, so if each individual atom were actually another universe in its own right, then that would still represent only a total of 10^{160} atoms. Even the best classical artificial intelligence approaches to Go seemed unable to accomplish anything better than amateurish play.

In March 2016, a computer program, AlphaGo, defeated a human player of the highest professional caliber, the world number two Lee Sedol, in a head-to-head five-game series

of Go. This was the first time that a computer program had beaten a player of that level of skill without handicaps. Although AlphaGo featured an algorithm to choose moves that was somewhat guided by the design of its developers, its evaluation function was composed of a neural network that had been trained against a database of recorded games and outcomes.²¹ In chess, a crude valuation of a position can be made from the strength of the pieces remaining to the player and their ability to move freely. In Go, the stones do not have an equivalent individual worth and the valuation of a Go position instead depends on the relative spatial interplay of the player's stones and the opponent's stones. Where classical artificial intelligence algorithms were unable to discern this strategic posture, AlphaGo's neural network approach was successful.

Neural Networks

Figure 3A illustrates the simplest feasible fully connected feed-forward neural network, taking two inputs and returning one outcome. The network is composed of the inputs, an input layer, a hidden layer, an output layer, and the output. Each layer is fully connected to the next, meaning there is path from each node (*i.e.*, neuron) to every node in the following layer. Each path has an associated weight, which describes how much the signal traveling along that path is amplified or attenuated or inverted. At each node, the weighted inputs are added together and then applied to an activation function. Each of the nodes illustrated here uses a sigmoid activation function, which is the most basic of the standard activation functions as shown in figure 3B. The general idea is that a node, in a manner reminiscent of a biologic neuron, will remain "off" until a suitable degree of excitation is reached, at which point it will quickly turn "on." The first node in the input layer, for example, receives inputs from Features S and T. These inputs are weighted by $w_{fs,il}$ and $w_{ft,il}$ respectively, so the total input z to the first input node is given by $z = w_{fs,il}S + w_{ft,il}T$. The total input is then applied to the sigmoid function, producing an output

from this node of $\frac{1}{1+e^{-z}}$. This output feeds forward to the next, hidden layer along with the other weighted contributions from the input layer, and so forth until an output is produced. The output of the sigmoid activation function is always between 0 and 1, so if the outcomes are classified as 0 (*e.g.*, red crosses) and 1 (*e.g.*, green circles), the performance of the network can be assessed by how closely it predicts the various outcomes in the training data.

The behavior of the network depends on the values of the various weights w , and so the general idea of machine learning in a neural network is to adjust these weights until satisfactory performance is achieved. To begin, the weights are set to random values and so the initial performance of the network will usually be poor. However, for each error in prediction that is output, a degree of blame can

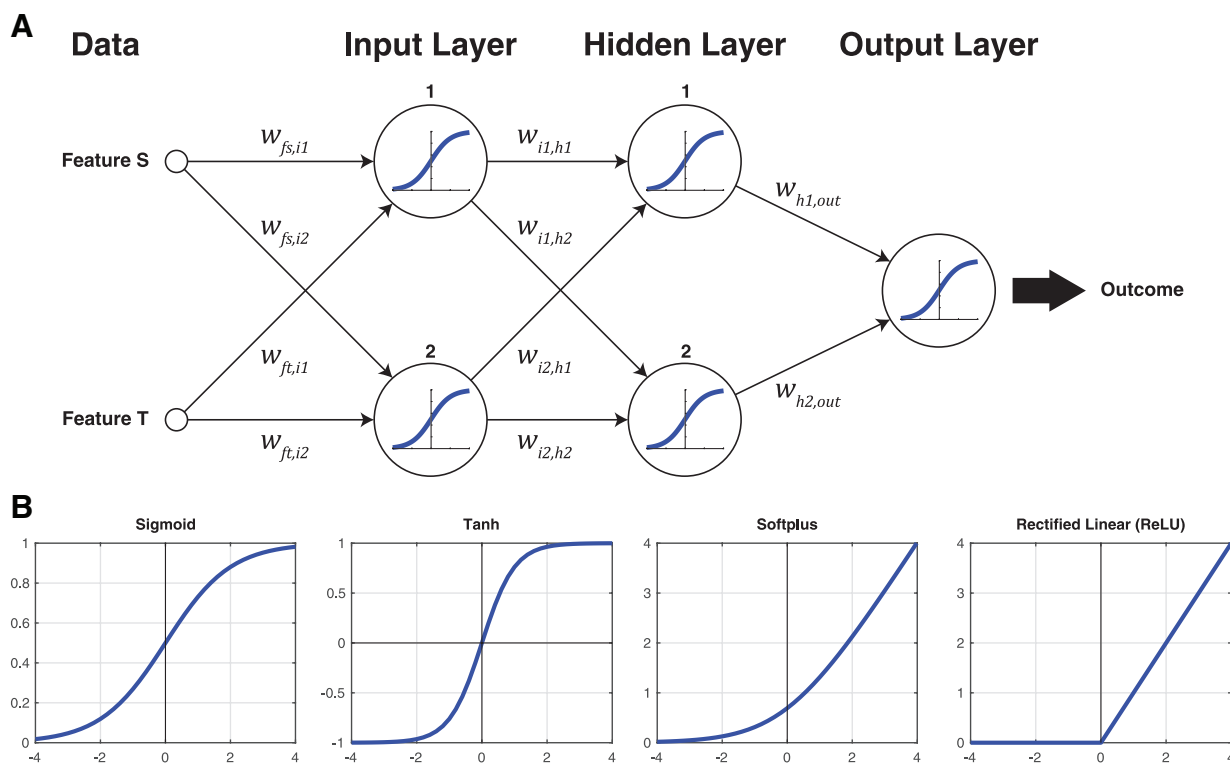


Fig. 3. (A) The simplest fully connected neural network from two input features to one output. The *weights* for each connection are illustrated, and each neuron in the network uses the sigmoid activation function to relate the sum of its weighted inputs, z , to its output. The sigmoid function is $\sigma(z) = (1 + e^{-z})^{-1}$. (B) Other biologically inspired activation functions are possible and have practical benefits beyond the original sigmoid. Further evolutions are the Tanh function (essentially two sigmoids arranged symmetrically), the Softplus (the integral of the sigmoid), and the Rectified Linear Unit (a nonsmooth variant of the Softplus).

be apportioned over the weights that contributed to it, and these weights can then be adjusted accordingly. This process is called back propagation,²² and it is the process by which the network learns to improve from its mistakes. Data are fed forward through the weights and nodes to produce output predictions, and then the errors in these predictions are propagated backward through the network to readjust the weights. This process is continued until, hopefully, the network settles to some form in which it is able to model the outputs satisfactorily based upon the input data. Beyond this basic description, of course, there are extraordinary implementational details and subtleties. For example, even in the rudimentary neural network shown in figure 3A, there are already 10 different weights that can be adjusted. The number of parameters in any practical network will be very large, and a great deal of care is required in the handling of the training data in order to avoid immediate overfitting. Additionally, the error function for neural networks is not globally convex, so there is no guarantee that the learning process will converge upon the optimum solution, and it may instead settle on some less ideal

solution. In the gradient descent analogy described earlier, this would be like the imaginary ball becoming stuck in a small divot and failing to roll down to the valley below. Two ways around this problem are either to survey the landscape by starting from a selection of different locations, or to occasionally give the ball (or the landscape) some sort of shake (*i.e.*, stochastic gradient descent²³). Nevertheless, the process remains very computationally intensive and slow, despite technical advances in repurposing the hardware of three-dimensional graphics cards (*i.e.*, Graphics Processing Units [GPUs]) to parallelize the calculations.²⁴

The primary reason to take on the burden of training neural networks is that they possess the new property of universality.²⁵ Universality means that, given an adequately large number of nodes in the respective layers, the weights of a neural network can be configured to approximate any other continuous function to within any desired level of accuracy.²⁵ This leads to two immediate and important benefits.

1. The property of universality stipulates that the neural network can, in principle, represent any continuous function to any desired degree of accuracy. The idea

of a function is very broad—it does not just mean the transformation of one numerical value into another. It incorporates any transformation of input data into an output, such as a Go board position into a verdict into whether that position is winning or losing,²¹ or determining the location of a lesion on a three-dimensional magnetic resonance image of the brain.²⁶ A function can be any transformation, even if its mathematical form is not known in advance.

2. The behavior of the network is dependent on the weights. The network learns the appropriate weights solely from the training data that it is given. Therefore, the network can learn the functional relationship between the outcome and the data even if there is no preexisting knowledge about what that relationship might be. However, it can be extraordinarily difficult to reverse this process to determine an efficient statement of the functional relationship that is described by the fitted weights. This leads to the well-known criticism that the operation of a neural network is particularly hard to characterize and therefore hard to validate.

As shown in figure 4 therefore, it is possible, at least in the abstract, for a neural network to take a preoperative image of a patient and produce a prediction about how difficult that patient's intubation might be. The proposed function is a transformation from the pixel values of the image to an estimated Cormack–Lehane view,²⁷ but it is hard to intuit in advance what the form of that underlying function might turn out to be. While the picture alone is very unlikely to contain sufficient information to produce a reliable prediction, it is plausible that it is in some way informative as to

the outcome. Although a fully connected neural network is shown, the universality theorem only demonstrates that a fully connected network with a single hidden layer can represent any function. It does not guarantee that the network contains a reasonably tractable number of nodes, nor that the inputs are informative as to the output, nor that convergence to a satisfactory answer can occur within a feasible amount of time. The current state of the art in computer science therefore involves finding network topologies that use a more efficient number of nodes and can be trained in a reasonable period of time. Two examples of these alternative network connection patterns are deep convolutional neural networks,²⁸ in which there are several hidden layers but many weights are constrained to have the same set of values, and residual neural networks,²⁹ in which additional paths with a weight of one skip over intervening hidden layers. Both of these approaches derive plausible justification from analogous arrangements of neurons in the mammalian brain, such as visual field maps for convolutional networks and pyramidal projection neurons for residual networks.

Evolution in Time

Each of the feed-forward neural network tasks illustrated so far make their predictions based solely on the input data available at that immediate time. They are stateless, *i.e.*, they have no temporal relationship to any measurement taken before or after. If a neural network is intended to make intraoperative decisions about patient management, then the network will require some way to base its decision-making

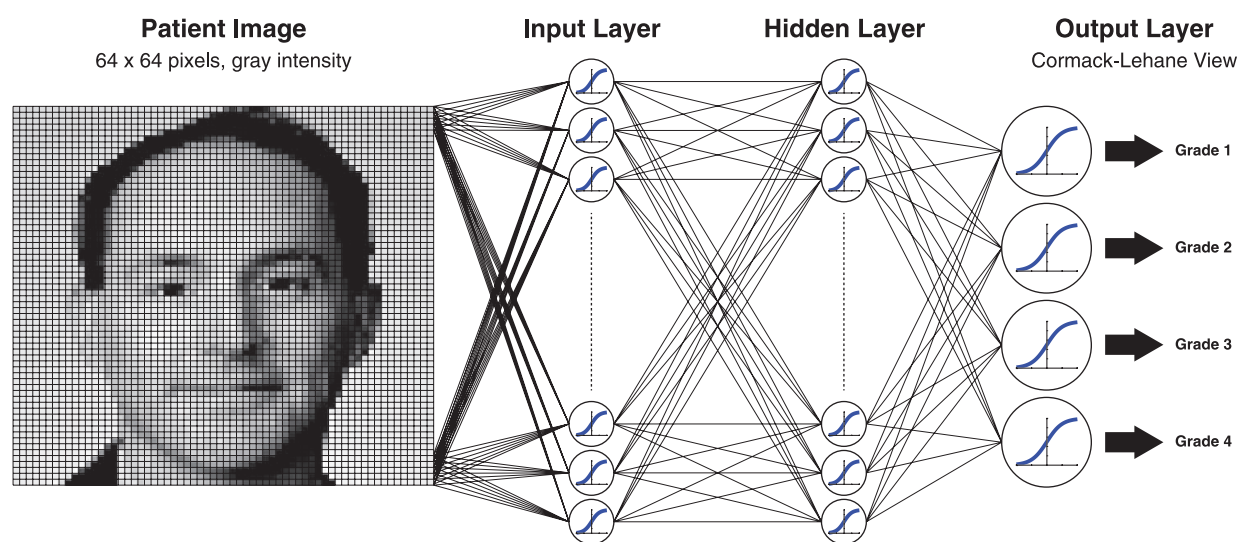


Fig. 4. The property of universality means that neural networks can represent any continuous function. The neural network shown here represents a hypothetical system to take a photographic image of a patient and render a prediction of their Cormack–Lehane view at intubation. (Not all nodes and connections are illustrated, as the input and hidden layers would each contain several thousand nodes. More pragmatic network topologies can be applied to visual recognition problems than the general case shown here.)

on memories of evolving trends. Figure 5 illustrates an Elman network,³⁰ with three inputs and one output. In this topology, weighted paths project from the outputs of the hidden layer to a context layer, and then further weighted paths return from the context layer to the inputs of the hidden layer. An Elman network is the simplest example of a recurrent neural network that can evaluate changes in data over time. For example, the output might be a decision whether to transfuse or not,³¹ and the inputs might be the clinically observable parameters heart rate (R), blood pressure (P), and estimated blood loss (B). The context layer would allow the network to discern and respond to trends in these inputs.

Practical Approaches to Machine Learning in Anesthesiology

Advances in technology and monitoring can change the impetus for machine learning. For example, a neural network developed to detect esophageal intubation from flow-loop parameters³² is obviated by continuous capnography.^{33,34} In this instance, a reliable clinical test has made readily apparent what was once an insidious and devastating complication. A machine-learning model to predict

difficult intubation from patient appearance³⁵ must now be tempered by the convenience and ubiquity of video laryngoscopy. Advances in airway management technology have broadened the range of outcomes of laryngeal visualization that can be accepted. Anesthesiologists have long considered the possibility of an algorithm that might autonomously control depth of anesthesia based on electroencephalogram recordings^{36,37} since the 1950s—yet this concept remains very much a topic of current research.³⁸

Two papers from 2018 illustrate the theoretical concepts covered. The first paper, by Hatib *et al.*,³⁹ uses a very highly augmented data set in conjunction with logistic regression to produce an algorithmic model that can, in *post hoc* analysis, detect the incipient onset of hypotension up to 15 min before hypotension actually occurs. For model training, the authors employed a database of 545,959 min of high-fidelity (100 Hz) arterial waveform recordings acquired from the records of 1,334 patients, internally validated against the records of 350 additional patients that were held back. The training data set included 25,461 episodes of hypotension. The model itself is derived from 51 base variables assembled from significant features extracted from the processing of arterial waveforms obtained by the Edwards FloTrac device (Edwards Lifesciences, USA).⁴⁰ Each variable was

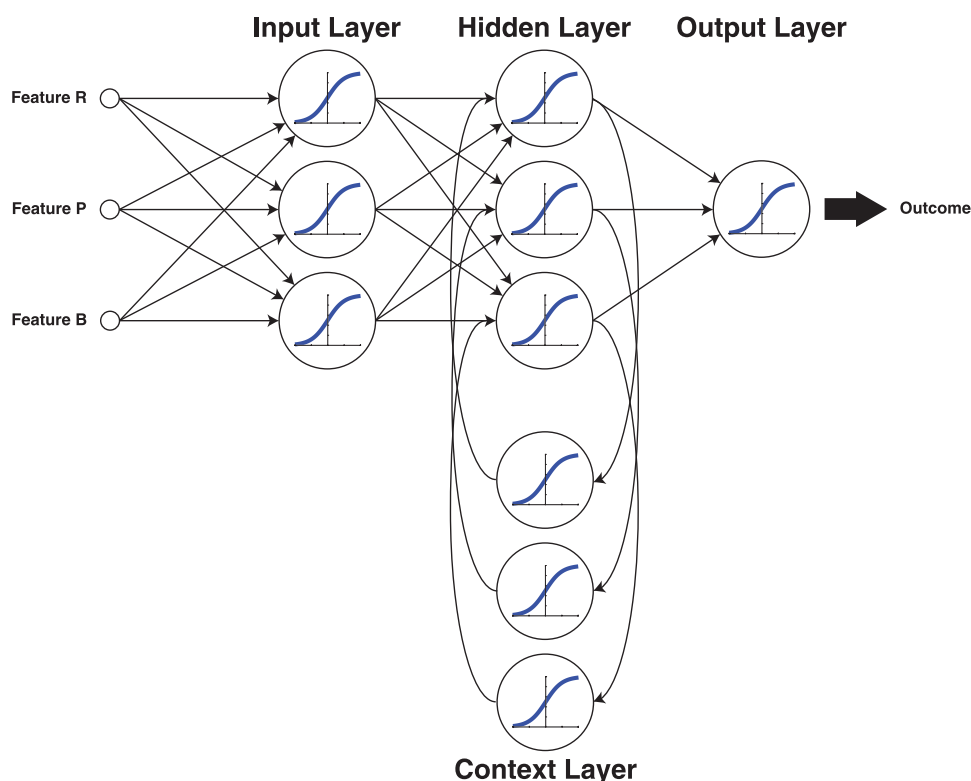


Fig. 5. Recurrent Neural Networks employ feedback such that the output of the system is dependent on both the current input state and also the preceding inputs, enabling the network to respond to trends that evolve over time. In the Elman network arrangement shown here, the context layer feeds from and to the hidden layer.

Table 1. Results of a Survey of the Primary Literature for Articles on the Application of Artificial Intelligence and Machine Learning to Clinical Decision-making Processes in Anesthesiology

Topic	References
ASA score and preoperative assessment	35,59,60
Depth of anesthesia and EEG processing	61–65
PK/PD and control theory	41,66–73
Blood pressure homeostasis and euvoolemia	6,31,39,74–76
Surgical complications and trauma	77–81
Postoperative care	82–84
Acute pain management and regional anesthesia	85–91
ICU sedation, ventilation, and morbidity	17,92–97

ASA, American Society of Anesthesiologists; EEG, electroencephalogram; ICU, intensive care unit; PK/PD, pharmacokinetics/pharmacodynamics.

augmented with its squared term and their reciprocals (*i.e.*, X , X^2 , X^{-1} , X^{-2}), and then every combination of these variables was generated to produce an overall input set of 2,603,125 parameters. The authors chose two clearly separated outcomes: hypotension defined as mean arterial pressure less than 65 mmHg (*e.g.*, notionally red crosses), and nonhypotension defined as mean arterial pressure greater than 75 mmHg (*e.g.*, notionally green circles), but did not consider the “gray zone” between these outcomes. Despite the large number of available parameters and the risk of overfitting, the authors were nevertheless able to use a parsimonious parameter selection process to produce a final model that depended on only 23 of the 2.6 million available inputs (Maxime Cannesson, M.D., Ph.D., Department of Anesthesiology, UCLA Medical Center, Santa Monica, California. Electronic personal communication, June 13, 2018). The study did have some limitations, notably that it did not include any episodes in which hypotension was caused by surgical intervention, all model fitting and assessments were retrospective and offline, and the algorithm made no recommendations as to whether an intervention should be performed. Nevertheless, the authors demonstrated an algorithm that was apparently able to foresee episodes of hypotension in operative patients up to 15 min in advance of the onset of the event itself with an area under the curve of 0.95.

The second paper, by Lee *et al.*,⁴¹ describes a neural network approach to predicting the Bispectral Index (BIS) based upon the infusion history of propofol and remifentanyl. This paper is particularly noteworthy because a strongly theoretical approach to this question already exists in the target-controlled infusion literature. The classical approach is to model the pharmacokinetics of propofol⁴² and remifentanyl⁴³ in the body independently, based upon the infusion history. The effect site concentration of each drug is then combined in a response surface model,⁴⁴ producing an estimate of the BIS. These classical pharmacokinetic models

are well established and have been used to demonstrate closed-loop target-controlled infusion control of anesthetized patients.⁴⁵ In contrast, Lee *et al.* created a neural network comprised of two stages. The first stage receives the infusion history of propofol and remifentanyl over the preceding 30 min with a resolution of 10 s (*i.e.*, 180 inputs for each medication). The inputs for each medication are fed to two separate eight-node recurrent neural networks. Rather than using an Elman³⁰ arrangement, as seen in figure 5, the paper made use of a newer configuration known as a Long Short Term Memory.⁴⁶ Simple recurrent neural networks such as Elman have difficulty recalling or learning events that happen over a long timeframe as their training error gradients become too small to be adaptive. The Long Short Term Memory is a more robust memory topology that also includes pathways that explicitly cause the network to reinforce or forget remembered states. The output from the Long Short Term Memory layer is applied directly to a simple fully connected feed-forward neural network with 16 nodes of the type shown in figures 2 and 3. A single output node emits a scaled BIS estimation. The network was developed from a database of 231 patient cases (101 cases used for training, 30 for validation, and 100 for final testing), and comprised a total of around 2 million data points. In *post hoc* analysis, the classical pharmacokinetic/pharmacodynamic models were able to predict the BIS value with a root-mean-square error of 15 over all phases of the anesthetic. Despite being naive to all existing theory, the neural network comfortably outperformed the best current models with an root-mean-square error of 9—a remarkable victory for modern artificial intelligence over existing classical pharmacokinetic/pharmacodynamic expert systems⁴⁷ that might lead us to question the ongoing utility of classical response surface models.⁴⁸

Future Directions

The most exciting recent advance in machine learning has been the development of AlphaGo Zero,⁴⁹ a system capable of learning how to play board games without any human guidance, solely through self-play alone. It performs at a level superior to all previous algorithms and human players in chess, Go, and shogi. This learning approach requires that the system be able to play several lifetimes' worth of simulated games against itself. Although anesthesia simulators exist, they do not currently simulate patient physiology with the fidelity with which a simulated chess game matches a real chess game.

The most plausible route to the introduction of artificial intelligence and machine learning into anesthetic practice is that the routine intraoperative management of patients will begin to be handed off to closed-loop control algorithms. Maintaining a stable anesthetic is a good first application because the algorithms do not necessarily have to be able to render diagnoses, but rather to detect if the patient has

begun to drift outside the control parameters that have been set by the anesthesiologist.⁵⁰ In this regard, such systems would be like an autopilot, maintaining control but alarming and disconnecting if conditions outside the expected performance envelope were encountered—hardly a threat to the clinical autonomy of the anesthesiologist.⁵¹ A closed-loop control system need not necessarily have any learning capability itself, but it provides the means to collect a large amount of physiologic data from many patients with high fidelity, and this is an essential precursor for machine learning. Access to large volumes of high-quality data will enable more machine-learning successes, such as the offline *post hoc* prediction of BIS⁴¹ and hypotension³⁹ discussed above. For now, finding algorithms that provide good clinical predictions in real time should be emphasized. Management of all the parameters of a stable anesthetic is not a simple problem,⁵² but embedding⁵³ the machine in the care of the patient is a good way to begin.⁵⁴

For further reading, the following books provide accessible introductions to decision making by humans¹ and algorithms,⁵⁵ neural networks,⁵⁶ information theory,⁵⁷ and the early history of computer science.⁵⁸

Research Support

Supported by National Institutes of Health (Bethesda, Maryland) grant No. R01 GM121457.

Competing Interests

Dr. Connor holds the following patents pertinent to the subject matter: U.S. Patent 8460215, Systems and methods for predicting potentially difficult intubation of a subject; U.S. Patent 9113776, Systems and methods for secure portable patient monitoring; U.S. Patent 9549283, Systems and methods for determining the presence of a person.

Correspondence

Address correspondence to Dr. Connor: Department of Anesthesiology, Perioperative and Pain Medicine, 75 Francis Street, CWN-L1, Boston, Massachusetts 02115. cconnor@bwh.harvard.edu. Information on purchasing reprints may be found at www.anesthesiology.org or on the masthead page at the beginning of this issue. ANESTHESIOLOGY's articles are made freely accessible to all readers, for personal use only, 6 months from the cover date of the issue.

References

1. Kahneman D: Thinking, Fast and Slow, 1st pbk. edition. New York, Farrar, Straus and Giroux, 2013
2. Turing AM: On computable numbers, with an application to the Entscheidungsproblem. Proceedings of the London Mathematical Society 1937; 2:230–65
3. Evidence-Based Medicine Working G: Evidence-based medicine. A new approach to teaching the practice of medicine. JAMA 1992; 268:2420–5
4. Eichhorn JH, Cooper JB, Cullen DJ, Maier WR, Philip JH, Seeman RG: Standards for patient monitoring during anesthesia at Harvard Medical School. JAMA 1986; 256:1017–20
5. Whittemore R, Knafl K: The integrative review: Updated methodology. J Adv Nurs 2005; 52:546–53
6. Kendale S, Kulkarni P, Rosenberg AD, Wang J: Supervised machine-learning predictive analytics for prediction of postinduction hypotension. ANESTHESIOLOGY 2018; 129:675–88
7. Maschler M, Solan E, Zamir S, Hellman Z, Borns M: Game theory, Cambridge, Cambridge University Press, 2013
8. Hart PE, Nilsson NJ, Raphael B: A formal basis for the heuristic determination of minimum cost paths. IEEE Trans Syst Sci Cybern 1968; 4:100–7
9. Lovelace A: Notes on L. Menabrea's 'Sketch of the Analytical Engine Invented by Charles Babbage, Esq.' Taylor's Scientific Memoirs 1843; 3:666–731
10. Shannon CE: XXII. Programming a computer for playing chess. The London, Edinburgh, and Dublin Philosophical Magazine and Journal of Science 1950; 41:256–75
11. Newell A, Shaw JC, Simon HA: Chess-playing programs and the problem of complexity. IBM J Res Dev 1958; 2:320–35
12. Van Poucke GE, Bravo LJ, Shafer SL: Target controlled infusions: Targeting the effect site while limiting peak plasma concentration. IEEE Trans Biomed Eng 2004; 51:1869–75
13. Shafer SL, Gregg KM: Algorithms to rapidly achieve and maintain stable drug concentrations at the site of drug effect with a computer-controlled infusion pump. J Pharmacokinet Biopharm 1992; 20:147–69
14. Mallampati SR, Gatt SP, Gugino LD, Desai SP, Waraksa B, Freiburger D, Liu PL: A clinical sign to predict difficult tracheal intubation: A prospective study. Can Anaesth Soc J 1985; 32:429–34
15. Shiga T, Wajima Z, Inoue T, Sakamoto A: Predicting difficult intubation in apparently normal patients: A meta-analysis of bedside screening test performance. ANESTHESIOLOGY 2005; 103:429–37
16. Carey MG, Pelter MM: Cornell voltage criteria. Am J Crit Care 2008; 17:273–4
17. Desautels T, Das R, Calvert J, Trivedi M, Summers C, Wales DJ, Ercole A: Prediction of early unplanned intensive care unit readmission in a UK tertiary care hospital: A cross-sectional machine learning approach. BMJ Open 2017; 7:e017199
18. Connor CW, Segal S: The importance of subjective facial appearance on the ability of anesthesiologists to predict difficult intubation. Anesth Analg 2014; 118:419–27

19. Birkhahn RH, Gaeta TJ, Terry D, Bove JJ, Tloczkowski J: Shock index in diagnosing early acute hypovolemia. *Am J Emerg Med* 2005; 23:323–6
20. Yang KL, Tobin MJ: A prospective study of indexes predicting the outcome of trials of weaning from mechanical ventilation. *N Engl J Med* 1991; 324:1445–50
21. Silver D, Huang A, Maddison CJ, Guez A, Sifre L, van den Driessche G, Schrittwieser J, Antonoglou I, Panneershelvam V, Lanctot M, Dieleman S, Grewe D, Nham J, Kalchbrenner N, Sutskever I, Lillicrap T, Leach M, Kavukcuoglu K, Graepel T, Hassabis D: Mastering the game of Go with deep neural networks and tree search. *Nature* 2016; 529:484–9
22. LeCun YA, Bottou L, Orr GB, Müller K-R: Efficient Backprop. *Neural Networks: Tricks of the Trade*, New York, Springer, 2012, pp 9–48
23. Mei S, Montanari A, Nguyen PM: A mean field view of the landscape of two-layer neural networks. *Proc Natl Acad Sci USA* 2018; 115:E7665–71
24. Peker M, Şen B, Gürüler H: Rapid automated classification of anesthetic depth levels using GPU based parallelization of neural networks. *J Med Syst* 2015; 39:18
25. Cybenko G: Approximation by superpositions of a sigmoidal function. *Math Control Signals Syst* 1989; 2:303–14
26. Kamnitsas K, Ledig C, Newcombe VFJ, Simpson JP, Kane AD, Menon DK, Rueckert D, Glocker B: Efficient multi-scale 3D CNN with fully connected CRF for accurate brain lesion segmentation. *Med Image Anal* 2017; 36:61–78
27. Cormack RS, Lehane J: Difficult tracheal intubation in obstetrics. *Anaesthesia* 1984; 39:1105–11
28. Gulshan V, Peng L, Coram M, Stumpe MC, Wu D, Narayanaswamy A, Venugopalan S, Widner K, Madams T, Cuadros J, Kim R, Raman R, Nelson PC, Mega JL, Webster DR: Development and validation of a deep learning algorithm for detection of diabetic retinopathy in retinal fundus photographs. *JAMA* 2016; 316:2402–10
29. He K, Zhang X, Ren S, Sun J: Deep residual learning for image recognition. *Proc IEEE Comput Soc Conf Comput Vis Pattern Recognit* 2016, pp 770–8
30. Elman JL: Finding structure in time. *Cogn Sci* 1990; 14:179–211
31. Etchells TA, Harrison MJ: Orthogonal search-based rule extraction for modelling the decision to transfuse. *Anaesthesia* 2006; 61:335–8
32. León MA, Räsänen J: Neural network-based detection of esophageal intubation in anesthetized patients. *J Clin Monit* 1996; 12:165–9
33. American Society of Anesthesiologists: Standards for Basic Anesthetic Monitoring. Park Ridge, IL, American Society of Anesthesiologists, 1986.
34. Cheney FW: The American Society of Anesthesiologists Closed Claims Project: What have we learned, how has it affected practice, and how will it affect practice in the future? *ANESTHESIOLOGY* 1999; 91:552–6
35. Connor CW, Segal S: Accurate classification of difficult intubation by computerized facial analysis. *Anesth Analg* 2011; 112:84–93
36. Bickford RG: Use of frequency discrimination in the automatic electroencephalographic control of anesthesia (servo-anesthesia). *Electroencephalogr Clin Neurophysiol* 1951; 3:83–6
37. Bellville JW, Attura GM: Servo control of general anesthesia. *Science* 1957; 126:827–30
38. Pasin L, Nardelli P, Pintauro M, Greco M, Zambon M, Cabrini L, Zangrillo A: Closed-loop delivery systems versus manually controlled administration of total IV anesthesia: A meta-analysis of randomized clinical trials. *Anesth Analg* 2017; 124:456–64
39. Hatib F, Jian Z, Buddi S, Lee C, Settels J, Sibert K, Rinehart J, Cannesson M: Machine-learning algorithm to predict hypotension based on high-fidelity arterial pressure waveform analysis. *ANESTHESIOLOGY* 2018; 129:663–74
40. Pratt B, Roteliuk L, Hatib F, Frazier J, Wallen RD: Calculating arterial pressure-based cardiac output using a novel measurement and analysis method. *Biomed Instrum Technol* 2007; 41:403–11
41. Lee HC, Ryu HG, Chung EJ, Jung CW: Prediction of Bispectral Index during target-controlled infusion of propofol and remifentanyl: A deep learning approach. *ANESTHESIOLOGY* 2018; 128:492–501
42. Schnider TW, Minto CE, Shafer SL, Gambus PL, Andresen C, Goodale DB, Youngs EJ: The influence of age on propofol pharmacodynamics. *ANESTHESIOLOGY* 1999; 90:1502–16
43. Minto CE, Schnider TW, Egan TD, Youngs E, Lemmens HJ, Gambus PL, Billard V, Hoke JF, Moore KH, Hermann DJ, Muir KT, Mandema JW, Shafer SL: Influence of age and gender on the pharmacokinetics and pharmacodynamics of remifentanyl. I. Model development. *ANESTHESIOLOGY* 1997; 86:10–23
44. Bouillon TW, Bruhn J, Radulescu L, Andresen C, Shafer TJ, Cohane C, Shafer SL: Pharmacodynamic interaction between propofol and remifentanyl regarding hypnosis, tolerance of laryngoscopy, Bispectral Index, and electroencephalographic approximate entropy. *ANESTHESIOLOGY* 2004; 100:1353–72
45. Liu N, Chazot T, Hamada S, Landais A, Boichut N, Dussaussoy C, Trillat B, Beydon L, Samain E, Sessler DI, Fischler M: Closed-loop coadministration of propofol and remifentanyl guided by Bispectral Index: A randomized multicenter study. *Anesth Analg* 2011; 112:546–57
46. Hochreiter S, Schmidhuber J: Long short-term memory. *Neural Comput* 1997; 9:1735–80
47. Gambus P, Shafer SL: Artificial intelligence for everyone. *ANESTHESIOLOGY* 2018; 128:431–3

48. Liou JY, Tsou MY, Ting CK: Response surface models in the field of anesthesia: A crash course. *Acta Anaesthesiol Taiwan* 2015; 53:139–45
49. Silver D, Schrittwieser J, Simonyan K, Antonoglou I, Huang A, Guez A, Hubert T, Baker L, Lai M, Bolton A, Chen Y, Lillicrap T, Hui F, Sifre L, van den Driessche G, Graepel T, Hassabis D: Mastering the game of Go without human knowledge. *Nature* 2017; 550:354–9
50. Harrison MJ, Connor CW: Statistics-based alarms from sequential physiological measurements. *Anaesthesia* 2007; 62:1015–23
51. Cannesson M, Rinehart J: Closed-loop systems and automation in the era of patients safety and perioperative medicine. *J Clin Monit Comput* 2014; 28:1–3
52. Yang P, Dumont G, Ford S, Ansermino JM: Multivariate analysis in clinical monitoring: Detection of intraoperative hemorrhage and light anesthesia. *Conf Proc IEEE Eng Med Biol Soc* 2007; 2007:6216–9
53. Brooks RA: Elephants don't play chess. *Robot Auton Syst* 1990; 6:3–15
54. Alexander JC, Joshi GP: Anesthesiology, automation, and artificial intelligence. *Proc (Bayl Univ Med Cent)* 2018; 31:117–9
55. Koerner TW: Naive Decision Making: Mathematics Applied to the Social World. Cambridge, Cambridge University Press, 2008
56. Rashid T: Make Your Own Neural Network: A Gentle Journey through the Mathematics of Neural Networks, and Making Your Own Using the Python Computer Language, CreateSpace, Charleston, SC, 2016
57. MacKay DJC: Information Theory, Inference, and Learning Algorithms. Cambridge, Cambridge University Press, 2004
58. Padua S: The Thrilling Adventures of Lovelace and Babbage. New York, Pantheon Books, 2015
59. Sobrie O, Lazouni MEA, Mahmoudi S, Mousseau V, Pirlot M: A new decision support model for preanesthetic evaluation. *Comput Methods Programs Biomed* 2016; 133:183–93
60. Zhang L, Fabbri D, Lasko TA, Ehrenfeld JM, Wanderer JP: A system for automated determination of perioperative patient acuity. *J Med Syst* 2018; 42:123
61. Ortolani O, Conti A, Di Filippo A, Adembri C, Moraldi E, Evangelisti A, Maggini M, Roberts SJ: EEG signal processing in anaesthesia. Use of a neural network technique for monitoring depth of anaesthesia. *Br J Anaesth* 2002; 88:644–8
62. Ranta SO, Hynynen M, Räsänen J: Application of artificial neural networks as an indicator of awareness with recall during general anaesthesia. *J Clin Monit Comput* 2002; 17:53–60
63. Jeleazcov C, Egner S, Bremer F, Schwilden H: Automated EEG preprocessing during anaesthesia: New aspects using artificial neural networks. *Biomed Tech (Berl)* 2004; 49:125–31
64. Lalitha V, Eswaran C: Automated detection of anesthetic depth levels using chaotic features with artificial neural networks. *J Med Syst* 2007; 31:445–52
65. Shalhaf R, Behnam H, Sleight JW, Steyn-Ross A, Voss LJ: Monitoring the depth of anesthesia using entropy features and an artificial neural network. *J Neurosci Methods* 2013; 218:17–24
66. Lin CS, Li YC, Mok MS, Wu CC, Chiu HW, Lin YH: Neural network modeling to predict the hypnotic effect of propofol bolus induction. *Proc AMIA Symp* 2002: 450–3
67. Laffey JG, Tobin E, Boylan JF, McShane AJ: Assessment of a simple artificial neural network for predicting residual neuromuscular block. *Br J Anaesth* 2003; 90:48–52
68. Santanen OA, Svartling N, Haasio J, Paloheimo MP: Neural nets and prediction of the recovery rate from neuromuscular block. *Eur J Anaesthesiol* 2003; 20:87–92
69. Nunes CS, Mahfouf M, Linkens DA, Peacock JE: Modelling and multivariable control in anaesthesia using neural-fuzzy paradigms. Part I. Classification of depth of anaesthesia and development of a patient model. *Artif Intell Med* 2005; 35:195–206
70. Nunes CS, Amorim P: A neuro-fuzzy approach for predicting hemodynamic responses during anaesthesia. *Conf Proc IEEE Eng Med Biol Soc* 2008; 2008: 5814–7
71. Moore BL, Quasny TM, Doufas AG: Reinforcement learning versus proportional-integral-derivative control of hypnosis in a simulated intraoperative patient. *Anesth Analg* 2011; 112:350–9
72. Moore BL, Doufas AG, Pyeatt LD: Reinforcement learning: A novel method for optimal control of propofol-induced hypnosis. *Anesth Analg* 2011; 112:360–7
73. El-Nagar AM, El-Bardini M: Interval type-2 fuzzy neural network controller for a multivariable anesthesia system based on a hardware-in-the-loop simulation. *Artif Intell Med* 2014; 61:1–10
74. Lin CS, Chiu JS, Hsieh MH, Mok MS, Li YC, Chiu HW: Predicting hypotensive episodes during spinal anesthesia with the application of artificial neural networks. *Comput Methods Programs Biomed* 2008; 92:193–7
75. Lin CS, Chang CC, Chiu JS, Lee YW, Lin JA, Mok MS, Chiu HW, Li YC: Application of an artificial neural network to predict postinduction hypotension during general anesthesia. *Med Decis Making* 2011; 31:308–14
76. Reljin N, Zimmer G, Malyuta Y, Shelley K, Mendelson Y, Blehar DJ, Darling CE, Chon KH: Using support vector machines on photoplethysmographic signals to discriminate between hypovolemia and euvoolemia. *PLoS One* 2018; 13:e0195087

77. Aleksic M, Luebke T, Heckenkamp J, Gawenda M, Reichert V, Brunkwall J: Implementation of an artificial neuronal network to predict shunt necessity in carotid surgery. *Ann Vasc Surg* 2008; 22:635–42
78. Peng SY, Peng SK: Predicting adverse outcomes of cardiac surgery with the application of artificial neural networks. *Anaesthesia* 2008; 63:705–13
79. Thottakkara P, Ozrazgat-Baslanti T, Hupf BB, Rashidi P, Pardalos P, Momcilovic P, Bihorac A: Application of machine learning techniques to high-dimensional clinical data to forecast postoperative complications. *PLoS One* 2016; 11:e0155705
80. Fritz BA, Chen Y, Murray-Torres TM, Gregory S, Ben Abdallah A, Kronzer A, McKinnon SL, Budelier T, Helsten DL, Wildes TS, Sharma A, Avidan MS: Using machine learning techniques to develop forecasting algorithms for postoperative complications: Protocol for a retrospective study. *BMJ Open* 2018; 8:e020124
81. Kuo PJ, Wu SC, Chien PC, Rau CS, Chen YC, Hsieh HY, Hsieh CH: Derivation and validation of different machine-learning models in mortality prediction of trauma in motorcycle riders: A cross-sectional retrospective study in southern Taiwan. *BMJ Open* 2018; 8:e018252
82. Kim WO, Kil HK, Kang JW, Park HR: Prediction on lengths of stay in the postanesthesia care unit following general anesthesia: Preliminary study of the neural network and logistic regression modelling. *J Korean Med Sci* 2000; 15:25–30
83. Traeger M, Eberhart A, Geldner G, Morin AM, Putzke C, Wulf H, Eberhart LH: [Prediction of postoperative nausea and vomiting using an artificial neural network]. *Anaesthesist* 2003; 52:1132–8
84. Knorr BR, McGrath SP, Blike GT: Using a generalized neural network to identify airway obstructions in anesthetized patients postoperatively based on photoplethysmography. *Proceedings of the 28th IEEE EMBS Annual International Conference, New York, New York, Aug 30–Sept 3, 2006*. pp. 6765–8
85. Tighe P, Laduzenski S, Edwards D, Ellis N, Boezaart AP, Aytug H: Use of machine learning theory to predict the need for femoral nerve block following ACL repair. *Pain Med* 2011; 12:1566–75
86. Hu YJ, Ku TH, Jan RH, Wang K, Tseng YC, Yang SF: Decision tree-based learning to predict patient controlled analgesia consumption and readjustment. *BMC Med Inform Decis Mak* 2012; 12:131
87. Tighe PJ, Lucas SD, Edwards DA, Boezaart AP, Aytug H, Bihorac A: Use of machine-learning classifiers to predict requests for preoperative acute pain service consultation. *Pain Med* 2012; 13:1347–57
88. Tighe PJ, Harle CA, Hurley RW, Aytug H, Boezaart AP, Fillingim RB: Teaching a machine to feel postoperative pain: Combining high-dimensional clinical data with machine learning algorithms to forecast acute postoperative pain. *Pain Med* 2015; 16:1386–401
89. Hetherington J, Lessoway V, Gunka V, Abolmaesumi P, Rohling R: SLIDE: Automatic spine level identification system using a deep convolutional neural network. *Int J Comput Assist Radiol Surg* 2017; 12:1189–98
90. Dawes TR, Eden-Green B, Rosten C, Giles J, Governo R, Marcelline F, Nduka C: Objectively measuring pain using facial expression: Is the technology finally ready? *Pain Manag* 2018; 8:105–13
91. Lötsch J, Sipilä R, Tasmuth T, Kringel D, Estlander AM, Meretoja T, Kalso E, Ultsch A: Machine-learning-derived classifier predicts absence of persistent pain after breast cancer surgery with high accuracy. *Breast Cancer Res Treat* 2018; 171:399–411
92. Wong LS, Young JD: A comparison of ICU mortality prediction using the APACHE II scoring system and artificial neural networks. *Anaesthesia* 1999; 54:1048–54
93. Gottschalk A, Hyzer MC, Geer RT: A comparison of human and machine-based predictions of successful weaning from mechanical ventilation. *Med Decis Making* 2000; 20:160–9
94. Ganzert S, Guttmann J, Kersting K, Kuhlen R, Putensen C, Sydow M, Kramer S: Analysis of respiratory pressure-volume curves in intensive care medicine using inductive machine learning. *Artif Intell Med* 2002; 26:69–86
95. Perchiazzi G, Giuliani R, Ruggiero L, Fiore T, Hedenstierna G: Estimating respiratory system compliance during mechanical ventilation using artificial neural networks. *Anesth Analg* 2003; 97:1143–8, table of contents
96. Nagaraj SB, Biswal S, Boyle EJ, Zhou DW, McClain LM, Bajwa EK, Quraishi SA, Akeju O, Barbieri R, Purdon PL, Westover MB: Patient-specific classification of ICU sedation levels from heart rate variability. *Crit Care Med* 2017; 45:e683–90
97. Perchiazzi G, Rylander C, Pellegrini M, Larsson A, Hedenstierna G: Monitoring of total positive end-expiratory pressure during mechanical ventilation by artificial neural networks. *J Clin Monit Comput* 2017; 31:551–9

MIND TO MIND

Creative writing that explores the abstract side of our profession and our lives

Stephen T. Harvey, M.D., Editor

So Many

Mary Dowd

“—as many as the leaves that fall in the woods...” *Book VI, Aeneid*

It's not just the dead that rattle like dry leaves
across stone cold ground, moving at the wind's will.
The living, too, blown by chance and choice,
scrape along the pavement. Men, mostly,
thirty, forty, fifty, most don't make sixty.

Never got the hang of it, work, wife, family.
Had a job once, had several.
Had a girl once, had several,
had a truck, a car, a flatscreen. Good money,
roofing, paving, lobstering.

Then came the accident, the back ache,
the break-up, the heart ache,
the not showing up on time, one time too many.
And everything returned to the dust from which it came,
scattered in the wind, never to reassemble.

Then beer became the boon companion,
whiskey, a shelter, hundred proof,
against empty days and sleepless nights,
against racing thoughts, sweaty palms,
against boredom, loss, loneliness.

This poem is one of the finalists of ANESTHESIOLOGY's 2018 annual creative writing competition, The Letheon. mdownmd@yahoo.com

Permission to reprint granted to the American Society of Anesthesiologists, Inc. by copyright author/owner. Anesthesiology 2019; 131:1360–1. DOI: 10.1097/ALN.0000000000002997

Downloaded from /anesthesiology/issue/131/6 by guest on 16 April 2024

So it begins, the wandering,
like dry leaves blown in autumn,
from shelter to ER to detox,
from library to park to soup kitchen.
Until it ends in an alley, in a ditch,
in a room at Motel 6.

So many moving at the wind's will
across stone cold ground,
gathered like sighs on the shore,
waiting for the boatman to carry them over
the river of forgetting,

Only to begin again.

MIND TO MIND

Creative writing that explores the abstract side of our profession and our lives

Stephen T. Harvey, M.D., Editor

Ganesh Furtado, M.D., ... My Cat

Inês F. Furtado, M.D., Ganesh Furtado, M.D.

Ganesh is not just a cat, but already a doctor, and in a couple of months he will be a senior anesthesiologist. He may be considered as being mostly theoretical, but at the same time he is sensitive and romantic, even philosophical. He is also clever and he strikes without warning.

Doctor Ganesh Furtado (Ganesh to his friends) is a 10-year-old European male cat. His fur is black with symmetrical white spots in the abdomen and neck. His eyes are green and he weighs 7 kg.

Doctor Ganesh had been abandoned on the street, he was probably just around 4 months old when I took him home with me. At the time, I was a third-year medical student, and in my company Ganesh quickly took up the challenge of becoming a doctor.

It required studying a lot, which he handled with pride. Anatomy, however, proved to be his main flaw, as it was a first-year discipline of mine, so one we never studied together. To this day, he still struggles in regional anesthesia... But he could keep up the pace in biochemistry and physiology, to the point of becoming a real pro in ventilation mechanics.

When we sit together to study, he likes to lie on my lap or over my books, so he can have a closer look at all contents. Sometimes he falls asleep, but I believe he knows that sleep enhances neural plasticity and contributes to consolidate his acquired knowledge (fig. 1).

From Almada, Portugal.

Accepted for publication April 10, 2019.

Permission to reprint granted to the American Society of Anesthesiologists, Inc. by copyright author/owner. *Anesthesiology* 2019; 131:1362–5. DOI: 10.1097/ALN.0000000000002796

Downloaded from /anesthesiology/issue/131/6 by guest on 16 April 2024



Fig. 1. Ganesh consolidating his acquired knowledge.

When he is bored, he plays with the pens and pencils lying on the desk, but when he is stressed because of exams and long hours of studying, he attacks people.

Ganesh's "work" was first cited in my first-year anesthesiology trainee examination. I was struggling to write my annual report, when I noticed that everybody else's report opened with a handsome epigraph by some famous author. Most of them were by well-known authors, and many of them were not even related to medicine, they were inspirational cheesy sentences, trivial, even futile. I found myself refusing to adopt such an attitude and style. However, it hit me, this represented the chance to share the thoughts and the written work of my favorite friend and doctor, Ganesh, my cat.

So, the opening quote of my first-year internship report read: *"it started with method, hypnotized by the end, where sleep awaits, where there is no time, no beginning and no end, only the calm of Morpheus"* Ganesh said (in a pretentious tone). And the examiners took it, even loved it! From then on, every single year as a trainee, Ganesh was there for me, providing the thoughts and sentences that added some meaning to the numbers on my reports. But Ganesh became present beyond my reports. Answering challenging theoretical questions in my annual exams, when I could not recall the name of some famous author of some important studies, I found myself claiming Doctor Ganesh as responsible for those amazing results and accomplishments.

My cat thus swiftly became accepted as a medical researcher, as well as a quotable and respectable author. I acknowledge and congratulate him for such a remarkable achievement. Why this happened is the question.

To answer this I must tell you that by no means is my cat a pioneer in this field. The first (known) animal to be quoted was Chester Willard, back in 1975,¹ as co-author of a peer-reviewed physics paper “Two-, Three-, and Four-Atom Exchange Effects in bcc ^3He ,” published in *Physical Review Letters*, a paper describing helium-3 isotope exchanges with temperatures.² Jack H. Hetherington, a professor of physics at Michigan State University, and his cat are still quoted today for “their” important findings.

I think Doctors Ganesh and Chester are a good connection, illustrating what I believe medical writing is turning into nowadays, and the direction I fear it is currently taking. As I am about to complete my five-year training in anesthesiology, I realize that the obligation of publication in our career makes scientific writing “look easy” and even meaningless. When I open a scientific journal, even a good one, frequently a paid-for-publishing one, I struggle to find a good paper. By that I mean something that will bring innovation to my daily practice, or that will make me think about some subject, or even that will show some negative data about something (the absence of negative trials is, on its own, one of the main problems in scientific publication).³ I mean simply free, honest, and good quality information.

After my first published article in a peer-reviewed journal,⁴ I started to receive daily emails from *Dermatology Kanquestan Journal*, *American Journal of Meaningless Stuff*, even *Orthopedic Distant Land Journal*, and the list goes on, calling for article submissions. They want anything, everything. But is this science, I wonder. In my opinion, this is science being taken over by consumer society and the ethos of productivity indicators.

We are led to think that our medical careers are only complete with publications. This is what leads to medical misinformation, to doubt, to bad practices, to mortality.

This made me think... why doesn't the American Society of Anesthesiology apply the principle of the American Physical Society that, a few years ago, announced it extended the benefits of open access to feline and canine authors?⁵ If my work is innovative, what's the difference if my cat is the fifth author? It's just a name, the unseen face of the publication, he will be there for science and, by the same token, for everyone's wallets. He would be the door for free information. Why not use comedy and our pets in the name of science?

I'm sure, that in this publishing industry, someday, there will be a place for free papers with the highest scientific quality by the best anesthesiologist of all times, Doctor Ganesh Furtado, my cat!

References

1. https://en.wikipedia.org/wiki/E._D._C._Willard. Accessed February 26, 2019.
2. Hetherington J, Willard C: Two-, three-, and four-atom exchange effects in bcc^3He . *Phys. Rev. Lett.* 1975;35:1442
3. Jones N: Half of US clinical trials go unpublished. *Nature News* 2013; Dec 3
4. Furtado I, Linda F, Pica S, Monteiro M: Anesthetic management of late pressure angioedema. *Rev Bras Anesthesiol* 2017; 67:422–5
5. <https://journals.aps.org/2014/04/01/aps-announces-a-new-open-access-initiative> Accessed February 26, 2019.

Preload Dependence and Microcirculation Relationship: Comment

To the Editor:

A well-performed study by Bouattour *et al*¹ concluded that preload dependence was associated with reduced sublingual microcirculation during major abdominal surgery. Fluid administration successfully restored microvascular perfusion. This finding suggests immediate correction of preload dependence to avoid reduced microcirculation. In the future, microvascular sublingual parameters could serve as additional indicators when deciding to administer fluids.

By this conclusion, the authors suggest that the presence of preload responsiveness might be associated with impaired sublingual microcirculatory perfusion and thus an abnormal microcirculatory perfusion might be an indicator of vascular volume. In this conclusion, however, we miss two important aspects. First, in general, fluid responsiveness is a normal physiological state² accompanied by a normal sublingual microcirculation.³ When from this state cardiac output is decreased by decreasing venous return either by tamponade, sepsis, or lower body negative pressure, the sublingual microcirculatory perfusion will deteriorate,^{3–5} and restoration of venous return, in these contexts, will improve sublingual microcirculatory perfusion.^{3–5} In the context of sepsis there is no real hypovolemia, but rather a decrease in venous return due to increased vascular capacitance of the venous circulation (unstressed volume). This is frequently referred to, clinically, as relative hypovolemia. In absolute hypovolemia (*e.g.*, hemorrhage) the decrease in venous return results from an absolute loss of intravascular volume. In both these cases, sublingual microcirculatory perfusion will improve after fluid resuscitation. From this, it's clear that an improvement in sublingual microcirculatory perfusion is not indicative of hypovolemia, but rather decreased venous return resulting from decreased stressed volume (mean systemic filling pressure). To further complicate the picture, after initial resuscitation in sepsis, patients' fluid responsiveness can be associated with normal sublingual microcirculatory perfusion.⁶ In the study by Bouattour *et al*,¹ the context of the patient is not clear, as the patients most likely started the procedure in a state of fluid responsiveness and normal

microcirculation. The response of the microcirculation to fluid resuscitation in this context doesn't necessarily clarify this, as both increased vasodilation during the surgery and bleeding will decrease venous return where fluid resuscitation is likely to improve microcirculatory perfusion.

Competing Interests

The authors declare no competing interests.

Jan Bakker, M.D., Ph.D., Glenn Hernandez, M.D., Ph.D.
Erasmus MC University Medical Center, Rotterdam, The Netherlands (J.B.). jan.bakker@erasmusmc.nl

DOI: 10.1097/ALN.0000000000002995

References

1. Bouattour K, Teboul JL, Varin L, Vicaut E, Duranteau J: Preload dependence is associated with reduced sublingual microcirculation during major abdominal surgery. *ANESTHESIOLOGY* 2019; 130:541–9
2. Komatsu T, Shibutani K, Okamoto K, Kumar V, Kubal K, Sanchala V, Lees DE: Critical level of oxygen delivery after cardiopulmonary bypass. *Crit Care Med* 1987; 15:194–7
3. Bartels SA, Bezemer R, Milstein DM, Radder M, Lima A, Cherpanath TG, Heger M, Karemaker JM, Ince C: The microcirculatory response to compensated hypovolemia in a lower body negative pressure model. *Microvasc Res* 2011; 82:374–80
4. van Genderen ME, Klijn E, Lima A, de Jonge J, Sleeswijk Visser S, Voorbeijtel J, Bakker J, van Bommel J: Microvascular perfusion as a target for fluid resuscitation in experimental circulatory shock. *Crit Care Med* 2014; 42:e96–e105
5. van Genderen ME, Bartels SA, Lima A, Bezemer R, Ince C, Bakker J, van Bommel J: Peripheral perfusion index as an early predictor for central hypovolemia in awake healthy volunteers. *Anesth Analg* 2013; 116:351–6
6. Klijn E, van Velzen MH, Lima AP, Bakker J, van Bommel J, Groeneveld AB: Tissue perfusion and oxygenation to monitor fluid responsiveness in critically ill, septic patients after initial resuscitation: A prospective observational study. *J Clin Monit Comput* 2015; 29:707–12

(Accepted for publication August 27, 2019.)

Preload Dependence and Microcirculation Relationship: Reply

In Reply:

I would like to thank the authors of the letter for reminding us that the notion of preload dependence is not synonymous with hypovolemia. As mentioned in the article,¹ preload dependence is defined as a state in which increases in right ventricular and/or left ventricular end-diastolic volume result in an increase in stroke volume.² Changes in preload could be due to hypovolemia and/or a decrease in venous tone with increased venous capacity. Having a preload dependence does not give any indication of the state of the microcirculation. Indeed, microcirculation can be preserved up to a certain level of venous return decline, but can then be altered if the venous return decline is greater. For this reason, it is essential to have an assessment of microcirculation in order to titrate perioperative fluid and correctly administrate vasopressors.

With this in mind, our study highlights that the occurrence of preload dependence was associated with reduced sublingual microcirculation during major abdominal surgery. This shows that decreases in venous return during anesthesia for major abdominal surgery, regardless of cause, are sufficient to alter sublingual microcirculation. In these circumstances, sublingual microcirculation was not protected by self-regulatory mechanisms during venous return decreases. This should encourage us to correct the preload dependency episodes that may occur during surgery in order to avoid these microvascular alterations. As mentioned in the article,¹ the fact that fluid challenge was able to restore microcirculatory alterations pleads for hypovolemia. Fluid administration may have corrected an absolute hypovolemia due to a loss of blood volume or a relative hypovolemia due to a decrease in venous tone. In any case, correcting preload dependency remains a priority considering the risk of failure to treat an alteration of the microcirculation. Static (pulmonary artery occlusion pressure, central venous pressure, global end-diastolic volume, flow time of aortic flow) and dynamic (pulse pressure variation, stroke volume variations, vena cava diameter variations) hemodynamic variables have their own limits and their gray zone to guide fluid administration. Especially, pulse pressure variations cannot be used during arrhythmia, when tidal volumes are less than 8 ml/kg of ideal body weight, when spontaneous breathing occurs, or when pulse pressure variation value is in the gray zone (between 9 and 13%). Microvascular sublingual measurements could be an additional tool in the

future to support the decision to administer fluids or vasopressors. It is clear that we must continue to develop techniques to analyze the behavior of microcirculation because the ultimate goal of hemodynamic optimization is the optimization of microcirculation and tissue oxygenation.

Competing Interests

The author declares no competing interests.

Jacques Duranteau, M.D., Ph.D. Department of Anaesthesia and Intensive Care, University Hospitals of Paris-Sud, Paris, France. jacques.duranteau@aphp.fr

DOI: 10.1097/ALN.0000000000002996

References

1. Bouattour K, Teboul JL, Varin L, Vicaut E, Duranteau J: Preload dependence is associated with reduced sublingual microcirculation during major abdominal surgery. *ANESTHESIOLOGY* 2019; 130:541–9
2. Monnet X, Marik PE, Teboul JL: Prediction of fluid responsiveness: An update. *Ann Intensive Care* 2016; 6:111

(Accepted for publication August 27, 2019.)

IV Fluids for Major Surgery: Comment

To the Editor:

The review article of perioperative fluid therapy by Miller and Myles¹ provides new recommendations for fluid administration during major surgery. Many studies performed during the past 15 yr show that a restrictive strategy consisting of 3 to 5 ml⁻¹ · kg⁻¹ · h⁻¹ of crystalloid fluid during surgery provides a better outcome in comparison with 10 to 12 ml⁻¹ · kg⁻¹ · h⁻¹. The authors now swing the pendulum once again and recommend the larger amount. The basis for their recommendation consists of only two retrospective studies and their own prospective study, the RELIEF (Restrictive Versus Liberal Fluid Therapy in Major Abdominal Surgery) trial.²

We believe that the patient's preoperative fluid status should be considered when giving recommendations of this kind. Miller and Myles encourage unrestricted intake of

fluids until 2 h before elective surgery,¹ but in the RELIEF trial patients had fasted for a median of 9 h, and 25% of them even for 12 h or more, before surgery.² Moreover, 36% of their patients received bowel preparation, which causes fluid depletion. Therefore, many of the patients in the RELIEF trial were probably dehydrated, or even hypovolemic, when surgery started. Finally, the postoperative fluid administration in the restrictive group in the RELIEF trial amounted to only $0.8 \text{ ml}^{-1} \cdot \text{kg}^{-1} \cdot \text{h}^{-1}$, which is less than the recommended minimum water intake of 1.0 to $1.2 \text{ ml}^{-1} \cdot \text{kg}^{-1} \cdot \text{h}^{-1}$ in conscious healthy humans. Therefore, the higher incidence of postoperative creatinine elevation in the restrictive group might be an expected result of the trial.

The issues we mention may even explain the discrepancy between the RELIEF trial and previous studies in this area which, with few exceptions, favor a restrictive strategy. The new recommendations¹ are probably correct for patients with various degrees of preoperative dehydration attributable to lengthy preoperative fasting and bowel preparation, which have fallen out of practice in most parts of the world.^{3,4} However, we question this liberal approach in patients who are euhydrated before surgery.

Competing Interests

The authors declare no competing interests.

Hans Bahlmann, M.D., Ph.D., Robert G. Hahn, M.D., Ph.D.
Södertälje Hospital, Södertälje, Sweden (R.G.H.).
r.hahn@telia.com

DOI: 10.1097/ALN.0000000000003002

References

1. Miller TE, Myles PS: Perioperative fluid therapy for major surgery. *ANESTHESIOLOGY* 2019; 130:825–32
2. Myles P BR, Corcoran T, Forbes A, Wallace S, Peyton P, Christophi C, Story D, Leslie K, Serpell J, McGuinness S, Parke R; Australian and New Zealand College of Anaesthetists Clinical Trials Network, and the Australian and New Zealand Intensive Care Society Clinical Trials Group: Restrictive versus liberal fluid therapy for major abdominal surgery. *N Engl J Med* 2018; 378:2263–74
3. Leenen JPL, Hentzen JEKR, Ochijsen HDL: Effectiveness of mechanical bowel preparation versus no preparation on anastomotic leakage on colorectal surgery: A systematic review and meta-analysis. *Updates Surg* 2019; 71:227–36
4. Feldheiser A, Aziz O, Baldini G, Cox BPBW, Fearon KCH, Feldman LS, Gan TJ, Kennedy RH, Ljungqvist O, Lobo DN, Miller T, Radtke FF, Ruiz Garces T, Schricker T, Scott MJ, Thacker JK, Ytrebo LM, Carli F: Enhanced recovery after surgery (ERAS) for gastrointestinal surgery, part 2: Consensus statement for anaesthesia practice. *Acta Anaesthesiol Scand* 2016; 60:289–334

(Accepted for publication September 3, 2019.)

IV Fluids for Major Surgery: Reply

In Reply:

Drs. Bahlmann and Hahn mention the existence of some published studies supporting a restrictive approach to perioperative IV fluid therapy, but do not mention others (aside from the RELIEF [Restrictive Versus Liberal Fluid Therapy in Major Abdominal Surgery] trial¹) that identified possible harms or at least no measurable benefit.^{2–4} The RELIEF trial clearly identified an increased risk of acute kidney injury when a more restrictive zero-balance approach was used.

We agree with Drs. Bahlmann and Hahn that any unnecessary preoperative fasting should be avoided, and that clinicians should encourage unrestricted intake of fluids until 2 h before elective surgery as a standard of care. This was one of our recommendations.⁵ Although unnecessarily lengthy preoperative fasting times will create a state of relative dehydration, it is quite usual for most people to not drink between the late evening hours and morning (8 to 10 h period of fasting), so this duration is very unlikely to induce dehydration. More importantly, the RELIEF trial investigators analyzed and reported their results for acute kidney injury according to fasting times and the adverse effect of the restrictive zero-balance approach remained. That is, the risk of acute kidney injury occurred in those with short, intermediate, and longer fasting times (*P* value for interaction equals 0.47; see fig. S8 in the supplementary material of Myles *et al.*¹). A similarly consistent finding was observed in those who did or did not receive bowel preparation (*P* value for interaction equals 0.55).

Recent guidelines from others had recommended a zero-balance approach to perioperative IV fluid therapy.^{6–8} This implies that fluid balance should be zero at the end of surgery and over the ensuing 24 h. This is what was tested in the RELIEF trial and the results not only failed to identify any meaningful reduction in complications or hospital length of stay, but there was a higher incidence of acute kidney injury and surgical site infections. It is for this reason

that we recommended a moderately liberal IV fluid strategy for major surgery. That is what the evidence is telling us.

Research Support

The RELIEF (Restrictive Versus Liberal Fluid Therapy in Major Abdominal Surgery) trial was supported by grants from the Australian National Health and Medical Research Council (NHMRC, ID1043755, Canberra, Australia); the Australian and New Zealand College of Anaesthetists (Melbourne, Australia); Monash University (Melbourne, Australia); the Health Research Council of New Zealand (ID 14/222), and the UK National Institute of Health Research. Paul Myles is supported by an Australian NHMRC Practitioner Fellowship.

Competing Interests

Dr. Myles was the principal investigator of the RELIEF (Restrictive Versus Liberal Fluid Therapy in Major Abdominal Surgery) trial. Dr. Miller declares no competing interests.

Paul S. Myles, M.B., B.S., M.P.H., D.Sc., F.A.N.Z.C.A., Timothy E. Miller, M.B., Ch.B., F.R.C.A. Alfred Hospital and Monash University, Melbourne, Australia (P.S.M.). p.myles@alfred.org.au

DOI: 10.1097/ALN.0000000000003003

References

1. Myles P BR, Corcoran T, Forbes A, Wallace S, Peyton P, Christophi C, Story D, Leslie K, Serpell J, McGuinness S, Parke R; Australian and New Zealand College of Anaesthetists Clinical Trials Network, and the Australian and New Zealand Intensive Care Society Clinical Trials Group: Restrictive versus liberal fluid therapy for major abdominal surgery. *N Engl J Med* 2018; 378:2263–74
2. Kabon B, Akca O, Taguchi A, Nagele A, Jebadurai R, Arkilic CF, Sharma N, Ahluwalia A, Galandiuk S, Fleshman J, Sessler DI, Kurz A: Supplemental intravenous crystalloid administration does not reduce the risk of surgical wound infection. *Anesth Analg* 2005; 101:1546–53
3. MacKay G, Fearon K, McConnachie A, Serpell MG, Molloy RG, O'Dwyer PJ: Randomized clinical trial of the effect of postoperative intravenous fluid restriction on recovery after elective colorectal surgery. *Br J Surg* 2006; 93:1469–74
4. Vermeulen H, Hofland J, Legemate DA, Ubbink DT: Intravenous fluid restriction after major abdominal surgery: A randomized blinded clinical trial. *Trials* 2009; 10:50
5. Miller TE, Myles PS: Perioperative fluid therapy for major surgery. *ANESTHESIOLOGY* 2019; 130:825–32
6. Gustafsson UO, Scott MJ, Schwenk W, Demartines N, Roulin D, Francis N, McNaught CE, MacFie J, Liberman AS, Soop M, Hill A, Kennedy RH, Lobo DN, Fearon K, Ljungqvist O: Guidelines for perioperative care in elective colonic surgery: Enhanced Recovery After Surgery (ERAS(R)) Society recommendations. *Clin Nutr* 2012; 31: 783–800
7. Feldheiser A, Aziz O, Baldini G, Cox BP, Fearon KC, Feldman LS, Gan TJ, Kennedy RH, Ljungqvist O, Lobo DN, Miller T, Radtke FF, Ruiz Garces T, Schricker T, Scott MJ, Thacker JK, Ytrebo LM, Carli F: Enhanced recovery after surgery (ERAS) for gastrointestinal surgery, part 2: Consensus statement for anaesthesia practice. *Acta Anaesthesiol Scand* 2016; 60:289–334
8. Ljungqvist O, Scott M, Fearon KC: Enhanced recovery after surgery: A review. *JAMA Surg* 2017; 152:292–8

(Accepted for publication September 3, 2019.)

The Editor-in-Chief and the Editors of *Anesthesiology* would like to thank the following individuals for their participation in the editorial review process. Their contributions are sincerely appreciated.

Sanjib Das Adhikary, M.D.
 Ozan Akca, M.D., F.C.C.M.
 Oluwaseun Akeju, M.D.
 Richard K. Albert, M.D.
 David Amar, M.D.
 Thomas Anthony Anderson, Ph.D., M.D.
 Martin S. Angst, M.D.
 Joseph F. Antognini, M.D., M.B.A.
 James M. Anton, M.D.
 Richard L. Applegate II, M.D.
 Karim Asehnoune, M.D., Ph.D.
 Frederic Aubrun, M.D., Ph.D.
 Michael S. Avidan, M.B., B.Ch.,
 F.C.A.S.A
 Michael F. Aziz, M.D.
 Keith Baker, M.D., Ph.D.
 Matthew I. Banks, Ph.D.
 Michael J. Barrington, Ph.D., M.B.B.S.,
 F.A.N.Z.C.A.
 Melissa E. B. Bauer, D.O.
 Jan H. Baumert, M.D., Ph.D., D.E.A.A.
 Mark G. Baxter, Ph.D.
 Honorio T. Benzoni, M.D.
 Lorenzo Berra, M.D.
 James M. Berry, M.D.
 Andrew Bersten, M.D.
 Mark Bicket, M.D.
 Philip E. Bickler, M.D., Ph.D.
 Luca M. Bigatello, M.D.
 Manfred Blobner, M.D.
 Zeljko J. Bosnjak, Ph.D.
 Dale Bratzler, D.O., M.P.H.
 Emery N. Brown, M.D., Ph.D.
 Charles H. Brown IV, M.D.
 Christian S. Bruells, M.D.
 Sorin J. Brull, M.D., F.C.A.R.C.S.I. (Hon)
 Dario Bugada, M.D.
 Alexander J. Butwick, M.B.B.S.,
 F.R.C.A., M.S.
 Wesley G. Byerly, Pharm.D.
 Javier H. Campos, M.D.
 Kenneth D. Candido, M.D.
 Maxime Cannesson, M.D., Ph.D.
 Xavier Capdevila, M.D., Ph.D.
 Brendan Carvalho, M.B.B.Ch., F.R.C.A.
 Davide Cattano, M.D., Ph.D., F.A.S.A.,
 C.M.Q.
 Maurizio Cereda, M.D.
 George Chalkiadis, M.D.
 George F. Chamoun, B.S.
 Lucy Chen, M.D.
 Jianguo Cheng, M.D., Ph.D.
 Sreekanth Cheruku, M.D.
 Hovig Chitilian, M.D.
 Meera Chitlur, M.D.
 Davide Chiumello, M.D.
 Frances Chung, M.B.B.S., F.R.C.P.C.
 Edmond Cohen, M.D.
 Joshua B. Cohen, M.D.
 Pieter Colin, Pharm.D., Ph.D.
 Douglas Colquhoun, M.B., Ch.B., M.Sc.,
 M.P.H.

Jean M. Connors, M.D.
 Isabelle Constant, Ph.D., M.D.
 Jeffrey B. Cooper, Ph.D.
 Laura Cornelissen, Ph.D.
 Eduardo Leite Vieira Costa, M.D., Ph.D.
 Joseph F. Cotten, M.D., Ph.D.
 Robin G. Cox, M.B., B.S.
 Lester A. H. Critchley, M.D.,
 F.F.A.R.C.S.I., F.H.K.A.M.
 Edward T. Crosby, M.D., F.R.C.P.C.,
 F.A.A.P.
 Gregory Crosby, M.D.
 Marie E. Csete, M.D., Ph.D.
 Ashraf A. Dahaba, M.D., Ph.D., M.Sc.
 Jurgen C. de Graaff, M.D., Ph.D.
 Stefan G. De Hert, M.D., Ph.D.
 Nicolas de Prost, M.D., Ph.D.
 Jesus De Vicente, M.D., Ph.D., M.B.A.
 Jan De Witte, M.D.
 Patch Dellinger, M.D.
 Alexandre Demoule, M.D., Ph.D.
 Mark Dershwitz, M.D., Ph.D.
 Franklin Dexter, M.D., Ph.D.
 Wulf Dietrich, M.D., Ph.D.
 James Anthony DiNardo, M.D.
 Karen B. Domino, M.D., M.P.H.
 Anthony G. Doufas, M.D., Ph.D.
 Matthew T. Drake, M.D., Ph.D.
 John C. Drummond, M.D., F.R.C.P.C.
 Richard P. Dutton, M.D., M.B.A.
 Roderic G. Eckenhoff, M.D.
 Per K. Eide, M.D., Ph.D.
 James C. Eisenach, M.D.
 John E. Ellis, M.D.
 Milo Engoren, M.D.
 William E. Evans, Pharm.D.
 Alex S. Evers, M.D.
 Lisa W. Faberowski, M.D.
 Ludwik Fedorko, Ph.D., M.D., F.R.C.P.C.
 John R. Feiner, M.D.
 Carlos Ferrando, M.D., Ph.D.
 John E. Fiadjoe, M.D.
 Dennis M. Fisher, M.D.
 Michael Gerald Fitzsimons, M.D.
 Pamela Flood, M.D.
 Patrice Forget, M.D., Ph.D.
 Stuart A. Forman, M.D., Ph.D.
 Steven M. Frank, M.D.
 Geoff P. Frawley, M.B.B.S., F.A.N.Z.C.A.
 Gyorgy Frendl, M.D.
 Robert Edward Freundlich, M.D., M.S.
 Patrick Friederich, M.D.
 Dietmar Fries, M.D.
 Emmanuel Futier, M.D.
 Jeffrey Gadsden, M.D., F.R.C.P.C.,
 F.A.N.Z.C.A.
 Marcelo Gama de Abreu, M.D., M.Sc.,
 Ph.D., D.E.S.A.
 Paul S. Garcia, M.D., Ph.D.
 Sailaja Ghanta, M.D.
 Tony Gin, M.D.
 David B. Glick, M.D., M.B.A.

Susan M. Goobie, M.D., F.R.C.P.C.
 Allan Gottschalk, M.D., Ph.D.
 Giacomo Grasselli, M.D.
 John J. Greer, Ph.D.
 Michael A. Gropper, M.D., Ph.D.
 Eric R. Gross, M.D., Ph.D.
 Oliver Grottke, M.D., Ph.D.
 Matthias Gruenewald, M.D.
 Yun Guan, M.D., Ph.D.
 Nicole Renee Guinn, M.D.
 Dhanesh Kumar Gupta, M.D.
 Jacob Gutsche, M.D.
 Thorsten Haas, M.D.
 Guy S. Haller, M.D., Ph.D.
 Michael F. Haney, M.D., Ph.D.
 Samuel Hankins, M.D.
 Gregory M. T. Hare, M.D., Ph.D.
 Richard E. Harris, Ph.D.
 Afton Hassett, Psy.D.
 Bishr Haydar, M.D.
 David William Healy, M.D., F.R.C.A.,
 M.R.C.P.
 Goran Hedenstierna, M.D.
 Hugh C. Hemmings, M.D., Ph.D.
 Thomas K. Henthorn, M.D.
 David L. Hepner, M.D., M.P.H.
 Douglas L. Hester, M.D.
 Charles W. Hogue, M.D.
 Philip M. Hopkins, M.D., F.R.C.A.
 Takafumi Horishita, M.D., Ph.D.
 Cyrill Hornuss, M.D.
 Kimberly Howard-Quijano, M.D., M.S.
 Han Huang, M.D.
 Anthony G. Hudetz, D.B.M., Ph.D.
 Andrew Hudson, M.D., Ph.D.
 Beverley J. Hunt, F.R.C.P., F.R.C.Path.,
 M.D.
 William E. Hurford, M.D.
 Adrienne Huxtable, Ph.D.
 Toshiaki Iba, M.D.
 James William Ibinson, M.D., Ph.D.
 Jeffrey Iliff, M.D.
 Peter B. Imrey, Ph.D.
 Caleb Ing, M.D., M.S.
 Teruhiko Ishikawa, M.D.
 Craig Jabaley, M.D.
 Allison M. Janda, M.D.
 Bechir Jarraya, M.D., Ph.D.
 Marc G. Jeschke, M.D., Ph.D.
 Alexandre Joosten, M.D., Ph.D.
 Max B. Kelz, M.D., Ph.D.
 Samir Kendale, M.D.
 Rebecca Yasmin Klinger, M.D., M.S.
 W. Andrew Kofke, M.D., M.B.A.
 Daniel S. Kohane, M.D., Ph.D.
 Aaron F. Kopman, M.D.
 Andreas Koster, M.D., Ph.D.
 Yoshifumi Kotake, M.D., Ph.D.
 Matthias Kreuzer, Ph.D.
 Dinesh Kurian, M.D.
 Andrea Kurz, M.D.
 Karim Shiraz Ladha, M.D., M.Sc.

- Arthur M. Lam, M.D., F.R.C.P.C.
 Kathryn K. Lauer, M.D.
 Yannick Le Manach, M.D., Ph.D.
 Jean-Yves Lefrant, M.D., Ph.D.
 Claude Lentschener, M.D.
 Marc Leone, M.D., Ph.D.
 Adam I. Levine, M.D.
 J. Lance Lichtor, M.D.
 Philipp Lirk, M.D., Ph.D.
 Ronald S. Litman, D.O., M.L.
 Andreas W. Loepke, M.D., Ph.D.
 Jeffrey Loh, M.D.
 Federico Longhini, M.D.
 Dan Longrois, M.D., Ph.D.
 Torsten Loop, M.D.
 Martin Luginbühl, M.D., Ph.D.
 Trine Meldgaard Lund, Ph.D.
 Haoxiang Luo, M.D.
 Grant C. Lynde, M.D., M.B.A.
 Alex Macario, M.D., M.B.A.
 M. Bruce MacIver, M.Sc., Ph.D.
 Aman Mahajan, M.D., Ph.D.
 Kamal Maheshwari, M.D., M.P.H.
 Jihad Mallat, M.D.
 Shobha Malviya, M.D.
 Jordi Mancebo, M.D.
 John J. Marini, M.D.
 Thomas J. Martin, Ph.D.
 J. A. Jeevendra Martyn, M.D., F.R.C.A.,
 F.C.C.M.
 Anatoly E. Martynyuk, Ph.D., D.Sc.
 Patti Massicotte, M.D., M.H.Sc.
 Kenichi Masui, M.D., Ph.D.
 Joseph P. Mathew, M.D., M.H.Sc., M.B.A.
 Michael R. Mathis, M.D.
 Michael A. Matthey, M.D.
 Bryan G. Maxwell, M.D., M.P.H.
 C. David Mazer, M.D., F.R.C.P.C.
 Mary Ellen McCann, M.D., M.P.H.
 Colin McCartney, M.B.Ch.B., Ph.D.,
 F.R.C.A., F.F.A.R.C.S.I., F.R.C.P.C.
 Patrick J. McCormick, M.D., M.Eng.
 Timothy J. McCulloch, M.B.B.S.,
 B.Sc.(Med.), F.A.N.Z.C.A.
 Daniel I. McIsaac, M.D., M.P.H.,
 F.R.C.P.C.
 Shirley H. J. Mei, Ph.D., M.Sc.
 Christian Sahlholt Meyhoff, M.D., Ph.D.
 Jill M. Mhyre, M.D.
 Wolfram Miekisch, Ph.D.
 Rebecca D. Minehart, M.D., M.S.H.P.Ed.
 Cyrus David Mintz, M.D., Ph.D.
 Karen E. Moe, Ph.D.
 Manuel Ignacio Monge García, M.D.
 Michael Montana, M.D., Ph.D.
 Bernardo Marinheira Monteiro Bollen
 Pinto, M.D.
 Phil G. Morgan, M.D.
 Hiroshi Morimatsu, Ph.D., M.D.
 Kendall Morris, Ph.D.
 Gabriel Casulari Motta Ribeiro, D.Sc.
 Wallis Taylor Muhly, M.D.
 Glenn S. Murphy, M.D.
 David J. Murray, M.D.
 Olubukola Olugbenga Nafiu, M.D.,
 F.R.C.A., M.S.
 Mohamed Naguib, M.B., B.Ch., M.Sc.,
 F.C.A.R.C.S.I., M.D.
 Matthew D. Neal, M.D.
 Sonia Nhieu, M.D.
 Detlef Obal, M.D., Ph.D., D.E.S.A.
 Michael F. O'Connor, M.D.
 Fredrick K. Orkin, M.D., M.B.A., S.M.
 Gail Otulakowski, Ph.D.
 Dinesh Pal, Ph.D.
 Ben Julian A. Palanca, M.D., Ph.D., M.Sc.
 Arvind Palanisamy, M.B.B.S., M.D.,
 F.R.C.A.
 Peter H. Pan, M.D.
 Carlo Pancaro, M.D.
 Oliver P. F. Panzer, M.D.
 Piyush M. Patel, M.D., F.R.C.P.C.
 Matthew Pearn, M.D.
 Paolo Pelosi, M.D.
 Gaetano Perchiazzi, M.D., Ph.D.
 Tjorvi E. Perry, M.D., M.M.Sc.
 Christopher Michael Peters, Ph.D.
 James Peyton, M.B.Ch.B.
 Philip J. Peyton, M.D., Ph.D., M.B.B.S.,
 F.A.N.Z.C.A.
 Paul Picton, M.D.
 Richard M. Pino, M.D., Ph.D.
 Michael R. Pinsky, M.D.
 Jashvant Poeran, M.D., M.Sc., Ph.D.
 David Mark Polaner, M.D., F.A.A.P.
 Karen L. Posner, Ph.D.
 Catherine C. Price, Ph.D.
 Richard C. Prielipp, M.D., M.B.A.,
 F.C.C.M.
 Alexander Proekt, M.D., Ph.D.
 Kane O. Pryor, M.D.
 Michael Puglia II, M.D., Ph.D.
 Jennifer Anne Rabbitts, M.B.Ch.B.
 Oliver Christian Radke, M.D., Ph.D.,
 D.E.A.A.
 Johan Raeder, M.D., Ph.D.
 Douglas E. Raines, M.D.
 Jessica Raper, Ph.D.
 Jacob Raphael, M.D.
 Lars S. Rasmussen, M.D., Ph.D.
 Laura J. Rasmussen-Torvik, Ph.D.
 Aeyal Raz, M.D., Ph.D.
 David L. Reich, M.D.
 Amanda Rhee, M.D., M.S.
 Bernhard Riedel, M.B.Ch.B., F.C.A.,
 F.A.H.A., F.A.N.Z.C.A., M.Med.,
 M.B.A., Ph.D.
 Bruno Riou, M.D., Ph.D.
 Patricia R. M. Rocco, M.D., Ph.D.
 G. Alec Rooke, M.D., Ph.D.
 Henry Rosenberg, M.D.
 Steven Roth, M.D., F.A.R.V.O.
 Jean-Jacques Rouby, M.D., Ph.D.
 James L. Rudolph, M.D., S.M.
 Kurt Ruetzler, M.D.
 Michael J. Rutter, M.D.
 Siavosh Saatee, M.D.
 Nada Sabourdin, M.D.
 Daniel Saddawi-Konefka, M.D., M.B.A.
 Robert D. Sanders, B.Sc., M.B.B.S.,
 Ph.D., F.R.C.A.
 Bernd Saugel, M.D.
 Jörn Schäper, M.D.
 Andreas Schibler, M.D.
 Thomas Schilling, M.D., Ph.D., D.E.A.A.
 Robert B. Schonberger, M.D., M.A.
 Kristin Schreiber, M.D., Ph.D.
 Rebecca A. Schroeder, M.D.
 Mark A. Schumacher, Ph.D., M.D.
 Stephan K. W. Schwarz, M.D., Ph.D.,
 F.R.C.P.C.
 David A. Scott, M.B., B.S., Ph.D.
 Phillip E. Scuderi, M.D.
 Eva Sellden, M.D., Ph.D.
 Muhammad I. Shaikh, M.D., Ph.D.
 Amy Shanks, Ph.D.
 Milad Sharifpour, M.D., M.S.
 Anshuman Sharma, M.D., M.B.A.
 Beth Shaz, M.D.
 Edward R. Sherwood, M.D., Ph.D.
 Sasha Shillcutt, M.D., F.A.S.E.
 Timothy G. Short, M.D.
 Peter D. Slinger, M.D.
 Richard M. Smiley, M.D., Ph.D.
 J. Robert Sneyd, M.D., F.R.C.A.
 Michael J. Souter, M.B., Ch.B., F.R.C.A.,
 F.N.C.S.
 Claudia Spies, M.D.
 Bruce D. Spiess, M.D.
 Anne Kathrine Staehr-Rye, M.D.
 Randolph H. Steadman, M.D., M.S.
 Benjamin E. Steinberg, M.D., Ph.D.,
 F.R.C.P.C.
 Robert D. Stevens, M.D.
 David A. Story, M.B.B.S., B.Med.Sci.,
 M.D., F.A.N.Z.C.A.
 Gary R. Strichartz, Ph.D.
 Balachundhar Subramaniam, M.D.,
 M.P.H., F.A.S.A.
 Louise Y. Sun, M.D., S.M., F.R.C.P.C.
 Takahiro Suzuki, M.D., Ph.D.
 Madhav Swaminathan, M.D., M.M.Ci.,
 F.A.S.E., F.A.H.A.
 Erik R. Swenson, M.D.
 Peter Szmuk, M.D.
 Magnus Knut Teig, M.B., Ch.B.
 Richard Teplick, M.D.
 Niccolo Terrando, Ph.D.
 Oliver M. Theusinger, M.D.
 Slobodan M. Todorovic, M.D., Ph.D.
 Daniel A. Tolpin, M.D.
 Kevin K. Tremper, Ph.D., M.D.
 Susan Treves, Ph.D.
 Ban C. H. Tsui, M.Sc., M.D.
 Alparslan Turan, M.D.
 Kanji Uchida, M.D., Ph.D.
 Guillermo Umpierrez, M.D.
 Albert Urwyler, M.D.
 Wilton A. van Klei, M.D., Ph.D.
 Bruno van Swinderen, Ph.D.
 Judith Anne Rolanda van Waes, M.D.
 Robert A. Veselis, M.D.
 Francis Veyckemans, M.D.
 Emmanuel Vivier, M.D.
 Phillip Vlisides, M.D.
 Keith Vogt, M.D., Ph.D.
 Gebhard Wagener, M.D.
 Joyce Wahr, M.D.

ACKNOWLEDGMENT

Irving W. Wainer, Ph.D.
Suellen M. Walker, M.B., B.S., Ph.D.,
F.A.N.Z.C.A.
Jonathan P. Wanderer, M.D., M.Phil.
David O. Warner, M.D.
Matthew B. Weinger, M.D., M.S.
Richard B. Weiskopf, M.D.
Fletcher A. White, B.A., M.S., Ph.D.

Elizabeth L. Whitlock, M.D., M.Sc.
Robert A. Whittington, M.D.
Jeanine P. Wiener-Kronish, M.D.
Matthew Willsey, M.D.
Tilo Winkler, Ph.D.
Cynthia A. Wong, M.D.
Jean Wong, M.D., F.R.C.P.C.
Hermann Wrigge, M.D., Ph.D.

Zhongcong Xie, M.D., Ph.D.
N. Xirouchaki, M.D.
Shingo Yasuhara, M.D., Ph.D.
Mark Yazer, M.D.
Nadir Yehya, M.D.
Jie Zhou, M.D., M.B.A., M.S.
Zhiyi Zuo, M.D., Ph.D.

A Population-based Comparative Effectiveness Study of Peripheral Nerve Blocks for Hip Fracture Surgery: Erratum

In the November 2019 issue, the article “A Population-based Comparative Effectiveness Study of Peripheral Nerve Blocks for Hip Fracture Surgery” (Hamilton GM, Lalu MM, Ramlogan R, Bryson GL, Abdallah FW, McCartney CJL, McIsaac DI: *ANESTHESIOLOGY* 2019; 131:1025–35. doi: 10.1097/ALN.0000000000002947), costs reported in the results section of the abstract were incorrect. In the sentence “Costs were lower with a nerve block (adjusted difference, −\$1,421; 95% CI, −\$11,579 to −\$11,289 [Canadian dollars]), but no difference in mortality (adjusted odds ratio, 0.99; 95% CI, 0.89 to 1.11) or pneumonia (adjusted odds ratio, 1.01; 95% CI, 0.88 to 1.16) was observed” the costs “−\$11,579 to −\$11,289” should read “−\$1,579 to −\$1,289.” The correct sentence reads: “Costs were lower with a nerve block (adjusted difference, −\$1,421; 95% CI, −\$1,579 to −\$1,289 [Canadian dollars]), but no difference in mortality (adjusted odds ratio, 0.99; 95% CI, 0.89 to 1.11) or pneumonia (adjusted odds ratio, 1.01; 95% CI, 0.88 to 1.16) was observed.”

The publisher regrets this error. The article has been corrected online and in the PDF.

DOI: 10.1097/ALN.0000000000003023

Reference

Hamilton GM, Lalu MM, Ramlogan R, Bryson GL, Abdallah FW, McCartney CJL, McIsaac DI: A population-based comparative effectiveness study of peripheral nerve blocks for hip fracture surgery. *ANESTHESIOLOGY* 2019; 131:1025–35. doi: 10.1097/ALN.0000000000002947

Hypoxemia, Bradycardia, and Multiple Laryngoscopy Attempts during Anesthetic Induction in Infants: Erratum

In the October 2019 issue, the article “Hypoxemia, Bradycardia, and Multiple Laryngoscopy Attempts during Anesthetic Induction in Infants” (Gálvez JA, Acquah S, Ahumada L, Cai L, Polanski M, Wu L, Simpao AF, Tan JM, Wasey J, Fiadjoe JE: *ANESTHESIOLOGY* 2019; 131:830–9. doi: 10.1097/ALN.0000000000002847) contains an error in table 1. In the first row of the first column, the unit for “Age (yr)” should be “Age (months).”

The authors regret the error. The online version and PDF of the article have been corrected.

DOI: 10.1097/ALN.0000000000003024

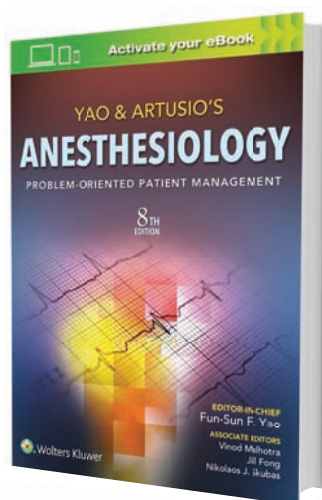
Reference

Gálvez JA, Acquah S, Ahumada L, Cai L, Polanski M, Wu L, Simpao AF, Tan JM, Wasey J, Fiadjoe JE: Hypoxemia, bradycardia, and multiple laryngoscopy attempts during anesthetic induction in infants. *ANESTHESIOLOGY* 2019; 131:830–9. doi: 10.1097/ALN.0000000000002847

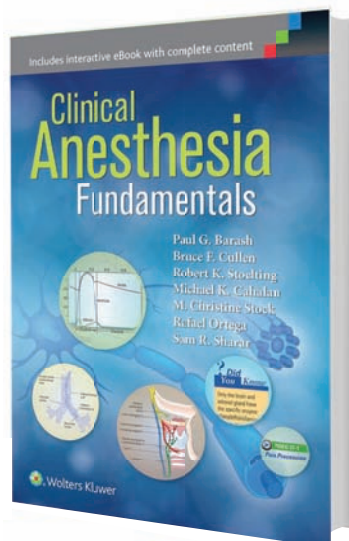


Find the answers you need to ensure the highest standards of anesthetic practice

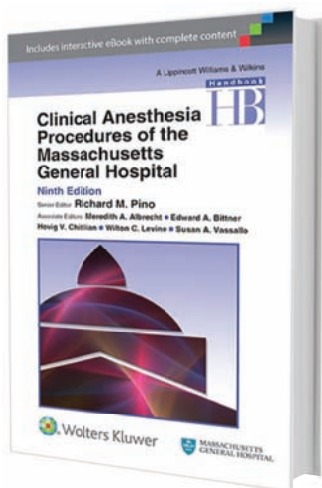
Anesthesiology:
Problem-Oriented
Patient Management,
8th Edition
ISBN: 978-1-4963-1170-2
1,248 pages



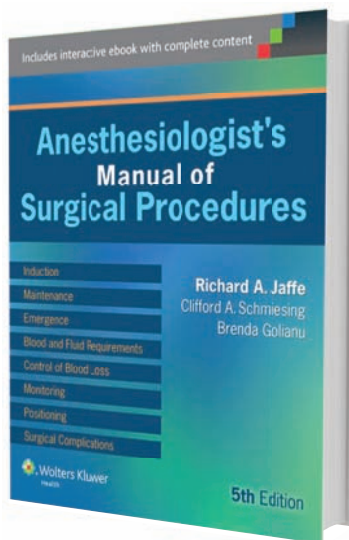
Clinical
Anesthesia
Fundamentals
6th Edition
ISBN: 978-1-4511-9437-1
912 pages



Clinical
Anesthesia
Procedures of the
Massachusetts
General Hospital
9th Edition
ISBN: 978-1-4511-9515-6
768 pages



Anesthesiologist's
Manual of Surgical
Procedures
5th Edition
ISBN: 978-1-4511-7660-5
1,720 pages



Save 20% on today's leading
Anesthesia resources

Visit www.com/anesthesia
and use promo code WEA103AL to save when ordering

Careers & Events

Marketing solutions for Career, Education and Events advertisers.



Wolters Kluwer

Lippincott
Williams & Wilkins

LWW's All Access Recruitment bundle offers advertisers access to the strongest portfolio of print journals, and online advertising in medical media. Build and deploy a powerful and targeted campaign to raise awareness and drive results anytime, anywhere and across all platforms. Contact an LWW Sales Specialist to learn more.

For rates and dealines, visit:
advertising.lww.com

Contact

Dave Wiegand
Wolters Kluwer Health
Two Commerce Square
2001 Market Street
Philadelphia, PA 19103
847-361-6128
dave.wiegand@wolterskluwer.com



ACUTE PAIN & REGIONAL ANESTHESIA FELLOWSHIP

The Department of Anesthesiology & Perioperative Medicine at University of Texas MD Anderson Cancer Center seeks candidates for the Regional Anesthesia and Acute Pain Medicine (RAAPM) Anesthesia Fellowship Program that have completed a U.S. or Canada accredited residency in Anesthesiology and must be board-eligible or board-certified to practice.

The purpose of the RAAPM Fellowship is to provide supervised training to board-certified or board-eligible anesthesiologists in the practice of acute pain management and medical consultation for the full spectrum of injuries, surgical, and other invasive procedures that produce acute pain in the hospital setting. This 12-month program will also teach the fellow how to manage acute pain with minimal opioids.

Required application materials include:

- ◆ Curriculum vitae
- ◆ Statement of Intent: Goals and reason for pursuing an Acute Pain Medicine & Regional Anesthesia
- ◆ Three Letters of Recommendation (LORs): If currently in a program, one letter must be from the Program Director.
- ◆ Letter of Good Standing for current residents that indicates trainee standing and expected completion date from the program.

Post-acceptance materials include:

- ◆ USMLE, COMLEX, FLEX scores report
- ◆ Original medical transcripts
- ◆ Medical diploma: copy
- ◆ Certificate of training completion – copy for each certification

Contact Information: Barbra Bryce Speer, D.O., Fellowship Program Director
Email: BSpeer@mdanderson.org

APPLY ONLINE:

<https://www.mdanderson.org/education-training/clinical-research-training/graduate-medical-education/residencies-fellowships/acute-pain-regional-anesthesia.html>



OPPORTUNITIES FOR ANESTHESIOLOGIST SPECIALIZING IN CRITICAL CARE, NEUROANESTHESIA, REGIONAL, GENERAL AND CARDIAC ANESTHESIA

The Department of Anesthesiology at the University of Wisconsin Madison has openings for several anesthesiology specialties: critical care, neuroanesthesia, regional, general, and cardiac anesthesiologist, at the level of Assistant Professor (CHS), Associate Professor (CHS), or Professor (CHS); or Clinical Assistant Professor, Clinical Associate Professor, or Clinical Professor. These positions will be a dual appointment with UW Madison and UW Medical Foundation.

Requirements: Wisconsin medical license or eligible for Wisconsin license. Board eligible or certified by the American Board of Anesthesiology. Subspecialty training preferred for specific subspecialty as appropriate to position.

Duties: Provision of clinical anesthetic care to patients, and specific subspecialty area (working in the OR, plus call) in an anesthesia team model or personally performed. Teaching responsibilities for residents, fellows, and medical student in the OR, and didactic sessions. For critical care candidates, the above duties also include the provision of critical care coverage to the UWMC Surgical, Medical, Cardio-thoracic, and/or Neuro ICUs, including ICU call coverage, dependent upon training and need.

Apply at <https://jobs.hr.wisc.edu/en-us/listing/>.

In the "Search Jobs" field, search for the type of position which you qualify by entering either "critical care anesthesiologist", "neuroanesthesiologist", or "cardiac anesthesiologist".

Unless confidentiality is requested in writing, information regarding applicants and nominees must be released upon request. Finalists cannot be guaranteed confidentiality. The UW-Madison is an EO and AAE. Wisconsin Caregiver Law applies.



Join A World Class Team!

Critical Care Faculty Positions

The Department of Anesthesiology at Weill Cornell Medical College and NewYork Presbyterian Hospital is seeking Critical Care Anesthesiologists for our 20-bed Cardiothoracic Intensive Care Unit, caring for patients undergoing procedures including CABG, valve repair/replacement, ventricular assist devices, and ECMO. Our faculty provide medical leadership in the Post-Anesthesia Care Unit, participate in the staffing of the Neuro-ICU, SICU, and MICU, and are actively involved in our critical care fellowship and all aspects of resident education. NewYork Presbyterian Hospital is ranked #5 on the Best Hospital Honor Roll of the U.S. News and World Report, and #1 in New York City for the 17th year in a row. We are ranked #4 in Cardiology and Cardiac Surgery.

All candidates must be ABA BC/BE, eligible for medical licensure in New York State and board eligible/certified in Critical Care Anesthesiology. Additional fellowship training in Cardiothoracic Anesthesiology or Basic or Advanced TEE certification from the National Board of Echocardiography are highly desired, but not required. Candidates should send a personal statement and curriculum vitae, and request three letters of reference to: Hugh C. Hemmings, Jr. M.D., Ph.D., Chair, Department of Anesthesiology anes-criticalcare@med.cornell.edu EOE/M/F/D/V



Division Head Regional Anesthesia and Acute Pain Medicine

The Department of Anesthesiology, Pain Management & Perioperative Medicine at the Henry Ford Health System (HFHS) is seeking an accomplished academic anesthesiologist to serve as its Division Head of Regional Anesthesia and Acute Pain Medicine. The division head will bring to the division a vision for enhancing the subspecialty clinical care, the overall patient experience, and strong leadership skills suitable for academic medicine.

Division Head Role

The division head will be responsible for advancing our tripartite mission: clinical care, education, and research. These responsibilities include:

- ◆ Leading regional anesthesiology and acute pain medicine clinical operations to ensure consistently high quality patient care with efficient and innovative utilization of clinical and material resources.
- ◆ Promoting effective collaboration among divisional faculty, other clinical personnel and research scientists across the HFHS.
- ◆ Facilitating undergraduate and graduate medical education in regional anesthesiology and acute pain medicine.
- ◆ Recruitment of new faculty to the division and support of their career development.
- ◆ Leading innovative scholarship in regional anesthesiology and acute pain medicine.
- ◆ Facilitate the application for an ACGME accredited Regional Anesthesiology and Acute Pain Medicine Fellowship

Resources

- ◆ Competitive salary and benefits package.
- ◆ Protected administrative time to support goal-directed, division-related professional development.
- ◆ Opportunity to participate in the development and refinement of simulation models for graduate and postgraduate education in regional anesthesiology and acute pain medicine.
- ◆ Active clinical research program, including participation in multi-center trials.
- ◆ Robust clinical population to challenge inquisitive thinking and progressive clinical procedures.

Candidates must hold an MD, DO, or equivalent degree and be eligible for licensure in Michigan. Candidates must be board-certified or board eligible in anesthesiology. Qualified candidates must show successful completion of an approved fellowship program in regional anesthesiology or demonstrate sufficient clinical and academic experience to support an ACGME approved fellowship program.

For more information, please contact:

Adam Ullman, RN, MPA, FASPR, CMSR
Senior Recruiter, Physician and Advance Practice
Practitioner Recruitment

Henry Ford Health System
One Ford Place 2E
Detroit, MI 48202

Email- aullman1@hfhs.org | Office (313) 587-7094



Critical Care Anesthesiology CARDIOTHORACIC INTENSIVE CARE

Yale School of Medicine Department of Anesthesiology seeks a board certified, fellowship trained critical care anesthesiologist with experience in critical care management of cardiothoracic patients. The candidate should:

- ◆ Fellowship trained in both cardiac anesthesia and ICU medicine
- ◆ Be eligible for appointment as an Assistant or an Associate Professor at the Yale School of Medicine
- ◆ Possess organizational and interpersonal skills to work collaboratively with all members of the cardiothoracic critical care team
- ◆ Have strong teaching skills that will be integral to residents, advance practice providers, nurses and fellow's education
- ◆ Clinical duties will be in both CT-ICU and OR environment
- ◆ Opportunities for J-1 visa candidates are available.

The Department of Anesthesiology faculty provide clinical and administrative leadership in the adult cardiothoracic ICU. The 20 bed unit cares for patients undergoing a wide variety of cardiac procedures including CABG, valves, assist devices, ECMO and transplantation. The faculty are also actively involved in fellowship training for both the cardiac and ICU fellowships; as well as participation in all aspects of resident education.

Interested candidates should apply at <http://apply.interfolio.com/49447>. Questions specific to this position may be sent to manuel.fontes@yale.edu. Review of applications will begin immediately and continue until the position is filled.

Yale University is an Affirmative Action/Equal Opportunity Employer. Women and persons with disabilities, protected veterans and members of under-represented minority groups are encouraged to apply.

HAVE SOMETHING IMPORTANT TO SAY?

Deliver your message in
**THE SOURCES
PHYSICIANS TRUST**

Visit for more information advertising.lww.com

Wolters Kluwer

Lippincott Williams & Wilkins
PhysiciansJobsPLUS
The Health Career Authority
www.physiciansjobsplus.com



Faculty Position in the Division of Neuroanesthesia

Yale School of Medicine Department of Anesthesiology seeks a board certified, fellowship trained (or equivalently experienced) anesthesiologist for a faculty position in the Division of Neuroanesthesia. The candidate should:

- ▶ be eligible for appointment as a faculty member at the Yale School of Medicine
- ▶ possess clinical and interpersonal skills to work collaboratively with all members of the neuroanesthesia team both clinically and academically
- ▶ have strong teaching interests that will be integral to resident and fellow education
- ▶ have an interest or experience in clinical research or be willing to work with others to develop skills in clinical research design and conduct

The Division of Neuroanesthesia provides care for over 1,000 patients annually in a variety of clinical settings, including Yale New Haven Hospital OR's, MRI, CT scan, interventional radiology, and pain management. The state-of-the-art neuro operating rooms enable intraoperative MRI scanning and advanced interventional radiology procedures. There is an established neuroanesthesia fellowship training program as well as multiple clinical and educational opportunities for anesthesia residents. There are robust clinical/translational research groups within the department including opportunities in T-32 and National Clinical Scholar Physicians programs and for participation in international collaborations. The Division of Neuroanesthesia works with active and clinically advanced neurological and neurosurgical services and a dedicated neurointensive care team.

Please send specific inquiries regarding this position to Roberta.Hines@yale.edu.
Please apply to the position at apply.interfolio.com/48850.

*Yale University is an Affirmative Action/Equal Opportunity Employer.
Women, persons with disabilities, protected veterans, and members of underrepresented minority groups are encouraged to apply.*

EXCEPTIONAL CARE DEDICATED TEACHING GROUNDBREAKING RESEARCH

Anesthesiologists: Join Top-Rated Medical Center

Banner University Medical Group (BUMG) and Banner University Medical Center – Tucson (BUMC-T) Department of Anesthesiology is seeking **Anesthesiologists** to provide anesthesia services as well as supervise CRNA's. We're seeking physicians who have the ability to work with diverse populations and have experience with a variety of teaching methods and curricular perspectives. Positions primarily involve clinical anesthesia teaching of anesthesia residents, fellows and medical students.

- Desirable candidates will have completed subspecialty training in: Critical Care, Pediatrics, OB, Vascular, and General OR
- Board Certified/Board Eligible in Anesthesiology
- Experienced physicians and new fellows are welcome to apply

Qualified candidates will have a faculty appointment at the University of Arizona commensurate with their academic credentials.

Banner Health and University of Arizona Health Network have come together to form Banner – University Medicine, a health system anchored in Phoenix and Tucson that makes the highest level of care accessible to Arizona residents. At the heart of this partnership is academic medicine – research, teaching and patient care – across three academic medical centers. **The Department of Anesthesiology is led by Randall Dull, MD, PhD, Professor and Chair.**

- Salary base plus incentives
- Sign on bonus
- Paid malpractice
- Relocation assistance
- 401k retirement plan with 4% match after one year of service
- Paid CME plus allowance

SUBMIT YOUR CV FOR CONSIDERATION TO: doctors@bannerhealth.com For questions, please contact **Andrea Hawkins, Sourcing Strategist**, at: 970-810-2302; Website: www.bannerdocs.com As an equal opportunity and affirmative action employer, Banner University Medical Group (BUMG) recognizes the power of a diverse community and encourages applications from individuals with varied experiences and backgrounds. BUMG is an EEO/AA - M/W/D/V Employer.

DISCOVER IT ALL AT BANNER HEALTH



**Banner
University Medical Center
Tucson**

Ready to up your game?

The University of Iowa Department of Anesthesia seeks talented academic anesthesiologists to take our clinical, educational and research missions to the next level. If you have the skills and the mindset to provide **exceptional** patient care, **inspired** teaching, and **innovative** scholarship, we want you on our team.

Think you have what it takes to be a team captain? Try out for our Division Chief positions in General, Neuro, and Regional Anesthesia. Learn more at jobs.uiowa.edu, (requisition #73494 for general anesthesiologist, #71620 for Division Chief), or send your CV and letter of interest to:

Cynthia A. Wong, MD
Professor, Chair & DEO
Email: cynthia-wong@uiowa.edu
Web: medicine.uiowa.edu/anesthesia

The University of Iowa is an equal opportunity/affirmative action employer. All qualified applicants are encouraged to apply and will receive consideration for employment free from discrimination on the basis of race, creed, color, national origin, age, sex, pregnancy, sexual orientation, gender identity, genetic information, religion, associational preference, status as a qualified individual with a disability, or status as a protected veteran.



Chief, Section of Pediatric Anesthesia

Yale School of Medicine Department of Anesthesiology seeks a board certified, fellowship trained anesthesiologist as Chief of the Section of Pediatric Anesthesia. The candidate should:

- ▶ be eligible for appointment as an associate or full professor at the Yale School of Medicine
- ▶ possess organizational and interpersonal skills to work collaboratively with all members of the Pediatric Anesthesia team both clinically and administratively
- ▶ have strong teaching skills that will be integral to resident and fellow education
- ▶ be experienced with the relevant administrative and regulatory issues
- ▶ have participated in and published clinical research and be able to mentor others in clinical research design and conduct

The section of Pediatric Anesthesia provides care for over 8,500 children in a variety of clinical settings and services including: Yale New Haven Children's Hospital OR's, MRI, CT scan, interventional cardiology/radiology, radiation oncology and pain management. There is an established pediatric fellowship training program as well as dedicated clinical and educational opportunities for anesthesiology residents. There are robust clinical/translational research programs within the department including opportunities for T-32 and National Clinical Scholar Physicians. The section of Pediatric Anesthesia comprises a dozen faculty members, all with board certification and fellowship training in pediatric anesthesiology.

The section chief will join the senior leadership team in the department and the Children's Hospital at Yale New Haven. This individual will also serve as the departmental representative on all committees and related activities at Yale New Haven Children's Hospital.

Please send a letter of interest along with your CV and 3 letters of recommendation
 to roberta.hines@yale.edu.

Yale University is an Affirmative Action/Equal Opportunity Employer.
 Women, persons with disabilities, protected veterans, and members of underrepresented minority groups are encouraged to apply.

Join Us at UF Health

The University of Florida College of Medicine, part of the UF Health system headquartered in Gainesville, FL is searching for the best and brightest full-time assistant/associate/full professors on tenure and clinical tracks in all anesthesiology subspecialties.

Our 87 faculty teach and practice at UF Health Shands Hospital, Shands Children's Hospital, Shands Cancer Hospital and UF Health Heart, Vascular, and Neuromedicine Hospitals at the University of Florida, a quaternary care teaching facility located in Gainesville, FL (Level 1 Trauma/Highrisk Ob/Comprehensive Stroke Center/Congenital Heart Center/Solid Organ Transplantation/Cancer Center). Abundant opportunities exist to develop independent and collaborative research as well as innovative education models.

Department anesthesiologists practice alongside 89 residents, 22 fellows, and 72 CRNA/CAAS. University employment benefits include 403(b) plan, 457 plan, individual and family health insurance, domestic partner benefits, own occ disability insurance, Baby Gator childcare, sovereign immunity malpractice status, and lots of sunshine.

1,232
LICENSED BEDS

55,320
ADMISSIONS

61
ORs

49,646
CASES



☎ 352-273-8909
✉ bvidal@anest.ufl.edu
www.anest.ufl.edu
📍 1600 SW Archer Road
Gainesville, FL 32608



Assistant, Associate, or Full Professor of Anesthesiology Lexington, Kentucky

The Department of Anesthesiology at the University of Kentucky seeks Board-certified or Board-eligible anesthesiologists in the areas of pediatric and general anesthesia. These positions are open to all ranks.

UK HealthCare has undergone a sustained and remarkable growth trajectory for a decade. Clinical volumes have doubled in the past 6 years and the acuity of patient care is high. UK HealthCare's Albert B. Chandler Hospital was named No. 1 in Kentucky in the U.S. News & World Report's Best Hospitals rankings. The Department of Anesthesiology is a collegial group that is well-respected in the medical center. The residency program is strong and nationally recognized. The enterprise financially supports the academic and the clinical mission of the Department of Anesthesiology.

Please include a CV along with application. Applications will be reviewed immediately and will continue until the position is filled.

Completion of residency in Anesthesiology
Fellowship training is required within subspecialty positions
Current license to practice medicine in the state of Kentucky, or eligibility for licensure
Board-certified or Board-eligible in Anesthesiology
Eligibility for ABA subspecialty certification is required within subspecialty positions

Contact Information robert.gaiser@uky.edu
<http://www.wildcatanesthesia.com/>



Join A World Class Team!

Open Faculty Positions in New York City

The Department of Anesthesiology at Weill Cornell Medical College and NewYork Presbyterian Hospital is actively recruiting qualified candidates for faculty positions with expertise in the subspecialty fields of Obstetric Anesthesiology, Pediatric Anesthesiology, and Regional Anesthesiology. We are one of the nation's top five hospitals, located on the lovely Upper East Side of Manhattan. We are expanding to provide services to our growing ambulatory care center and a new women's and newborns' hospital opening in 2020. We are seeking motivated and highly qualified individuals who demonstrate a strong academic commitment and a genuine interest in developing clinical research or educational programs. The department has ACGME-accredited fellowships in Obstetric Anesthesiology and Regional and Acute Pain.

All candidates must be ABA BC/BE and eligible for medical licensure in New York State, with additional board certification or eligibility within the related subspecialty. Academic rank and compensation will be commensurate to qualifications. Please send an electronic letter of intent, curriculum vitae, and three references to: Hugh C. Hemmings, Jr., M.D., Ph.D. Chair, Department of Anesthesiology anes-search@med.cornell.edu EOE/M/F/D/V

THE WOOD LIBRARY-MUSEUM *of* ANESTHESIOLOGY

Exciting Opportunity!

THE WLM FELLOWSHIP

will provide recipients with **financial support** for one to two weeks of scholarly historical research at the Wood Library-Museum.

The Board of Trustees of the Wood Library-Museum invites applications from anesthesiologists, residents in anesthesiology, physicians in other disciplines, historians and other individuals with a developed interest in library, museum and archival research in anesthesiology.

For further information, contact:
Director, Wood Library-Museum
of Anesthesiology at
(847) 825-5586, or visit our website
at: www.WoodLibraryMuseum.org.

Completed proposals must be received by **January 31, 2020**, for consideration. The Wood Library-Museum serves the membership of ASA and the anesthesiology community.

WOOD LIBRARY-MUSEUM *of* ANESTHESIOLOGY

1061 American Lane
Schaumburg, IL 60173-4973
(847) 825-5586

wlm@asahq.org

woodlibrarymuseum.org



Faculty (Open Rank)

Due to expanding clinical volume, Yale University School of Medicine, the Department of Anesthesiology is actively recruiting faculty (open rank) with a commitment to excellence in clinical care, education and/or research. Several opportunities are currently available but faculty are particularly desired in the subspecialty areas of liver transplant, pediatric cardiac anesthesia and neuro anesthesia. Fellowships in the subspecialty areas are preferred. Candidate must be ABA Board eligible/certified and be able to qualify for a Connecticut license. Opportunities for J-1 visa candidates are available.

Interested candidates should apply at apply.interfolio.com/48850. Questions specific to this position may be sent to Roberta.hines@yale.edu.

Yale University is an Affirmative Action/Equal Opportunity Employer. Women and persons with disabilities, protected veterans and members of under-represented minority groups are encouraged to apply.

ANESTHESIOLOGY

The Journal of the American Society of Anesthesiologists, Inc. • anesthesiology.org

Volume 131, Number 6, December 2019

Advertiser Index

Edwards Lifesciences	C2
Masimo	A4
Careers & Events	A19-A24
Masimo	C4

For more information about advertising and the next available issue, contact your sales managers:

Account Manager

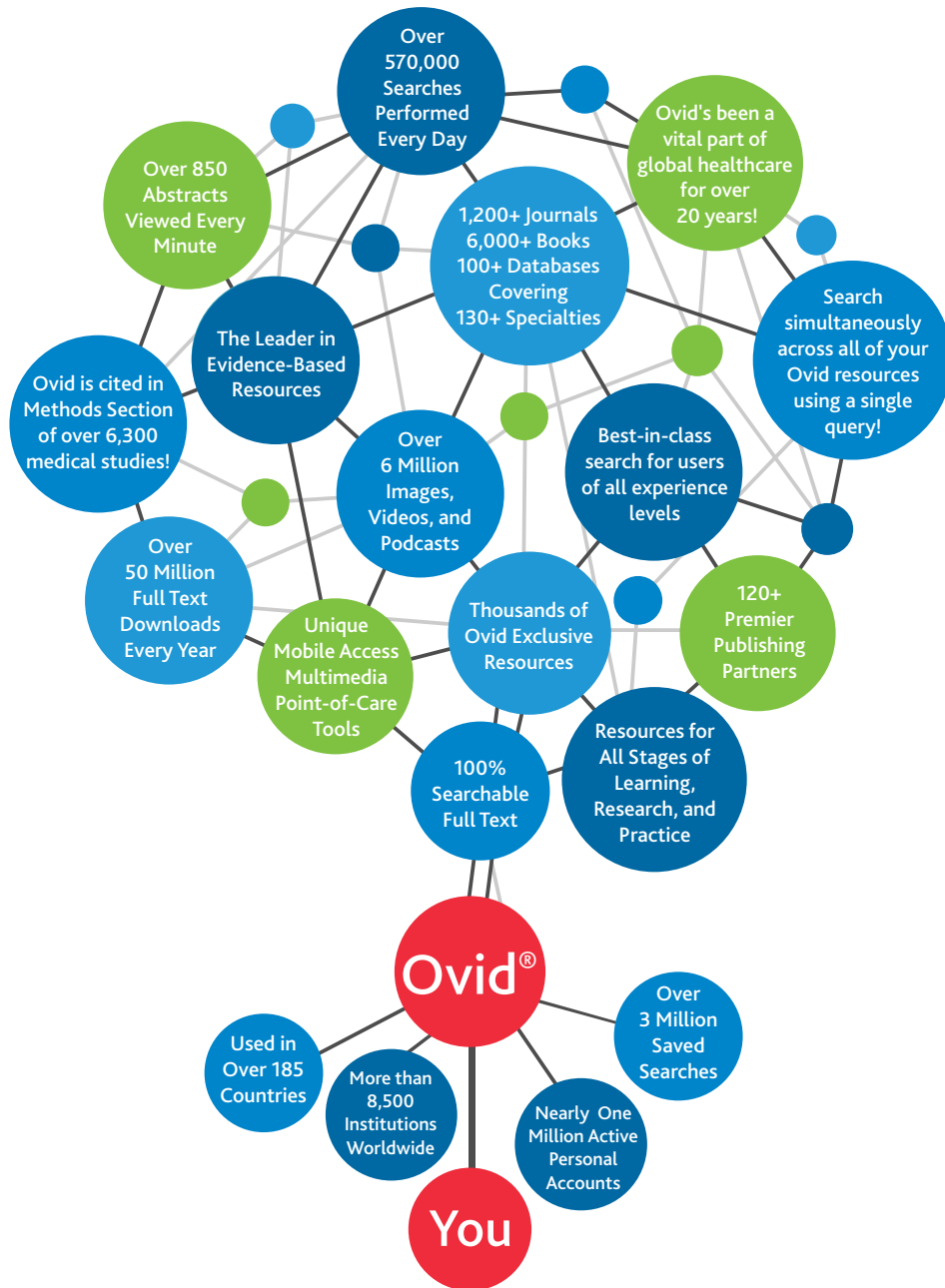
Hilary Druker, 609-304-9187

Careers & Events Advertising Sales Manager

Dave Wiegand, 847-361-6128

Ovid®

The world's most trusted medical research platform.



Make Ovid the source for all of your medical, nursing, and healthcare research needs.

VISIT YOUR LIBRARY - ASK A LIBRARIAN - EXPLORE OVID



Article Reprints

LWW authors can order up to 500 copies of their articles at a special rate. In addition to print, article ePrints are also available.

LWW Article Reprints are:

- Professional, high-quality documents
- Printed on premium paper
- Inclusive of images, charts, graphs, and graphics
- Available with covers (optional)

Order today!

To place your order, visit

www.LWWonline.com/reprints

or call 1-866-903-6951.

 **Lippincott
Williams & Wilkins**
a Wolters Kluwer business

A6Q921CF



Time for a career check-up?

Make an appointment with **PhysiciansJobsPlus.com** to:

- Post your resume
- Sign up for job alerts
- Search our selective job listings
- Apply today! Find a job that provides the respect and advancement you've been looking for.
- Experience a site from a name you know and trust, **Lippincott Williams & Wilkins.**

Plus, the site is easy to use and features comprehensive information for each listing.

Join other career-minded physicians who visit **PhysiciansJobsPlus.com** each month!

PhysiciansJobsPlus
Lippincott Williams & Wilkins
The Health Career Authority



Wolters Kluwer
Health

Lippincott Williams & Wilkins

Global Research – Open for All



Wolters Kluwer's publishing program offers peer-reviewed, open access options to meet the needs of authors and maximize article visibility.



wkopenhealth.com



Wolters Kluwer



A Journal for ALL Healthcare Providers

Journal
Impact
Factor:
2.028*

Medicine®

*2017 Journal Citation Reports (Clarivate Analytics, 2018)



Wolters Kluwer

www.md-journal.com

With its foundation in publishing established over 200 years ago, Lippincott Williams & Wilkins remains rock solid when it comes to delivering premier medical content. Focused on health care and dedicated to progress, LWW continues to feature the latest advances in medicine and pioneer innovation in publishing, fostering the ongoing success of medical professionals worldwide.

Visit www.LWW.com

Rock Solid Medical Content



Wolters Kluwer | Lippincott
Health Williams & Wilkins



As a health professional, you're in demand.

Explore your numerous career options at HealthProfessionsJobsPlus.com today.
You'll be able to:

- Post your resume
- Sign up for job alerts
- Search our selective job listings
- Apply today! Find a job that provides the respect and advancement you've been looking for.
- Experience a site from a name you know and trust, **Lippincott Williams & Wilkins**

Plus, the site is easy to use and features comprehensive information for each listing. Visit **HealthProfessionsJobsPlus.com** and begin exploring your options today.

Join other career-minded health professionals who visit **HealthProfessionsJobsPlus.com** each month!

HealthProfessions **JOBSPLUS**
Lippincott Williams & Wilkins

The Health Career Authority



Wolters Kluwer
Health

Lippincott Williams & Wilkins

EDITORIALS

- 531 The anaesthetists' role in perioperative infection control: what is the action plan?
R. W. Loftus and J. H. Campos
- 534 What's in a name? On the nuance of language in patient safety
G. Brattebø, J. Bergström and C. Neuhaus
- 536 Slow magnetic resonance oscillations diagnose chronic low back pain
J. Kurata
- 539 Nutritional neurobiology and central nervous system sensitisation: missing link in a comprehensive treatment for chronic pain?
J. Nijls, Ö. Elma, S. T. Yilmaz, P. Mullie, L. Vanderweeën, P. Clarys, T. Deliëns, I. Coppieters, N. Weltens, L. Van Oudenhove and A. Malfliet
- 543 'Plus ça change' for the future of sepsis?
D. C. Bryden and A. J. Pittard
- 545 Emergency front-of-neck airway: strategies for addressing its urgency
K. B. Greenland and R. S. Sommerville
- 548 Perioperative ST-elevation myocardial infarction: with time of the essence, is there a case for guidelines?
F. M. Ratcliffe, R. Kharbanda and P. Foëx
- 554 Use of the GRADE approach in systematic reviews and guidelines
A. Granholm, W. Alhazzani and M. H. Møller
- 559 Anaesthesiology in China: present and future
Q. Yang, K. Xie and L. Xiong

CARDIOVASCULAR

- 565 Preoperative coronary angiography in vascular surgery patients with asymptomatic elevated high-sensitivity troponin T: a case series
K. H. J. M. Mol, S. E. Hoeks, N. M. van Mieghem, H. J. M. Verhagen, E. Boersma, R. J. Stalker and F. van Lier

CLINICAL PRACTICE

- 570 Redefining the perioperative stress response: a narrative review
V. Manou-Stathopoulou, M. Korbonits and G. L. Ackland

CRITICAL CARE

- 584 Early remote ischaemic preconditioning leads to sustained improvement in allograft function after live donor kidney transplantation: long-term outcomes in the REal Protection Against Ischaemia-Reperfusion in transplantation (REPAIR) randomised trial
K. V. Veighey, J. M. Nicholas, T. Clayton, R. Knight, S. Robertson, N. Dalton, M. Harber, C. J. E. Watson, J. W. De Fijter, S. Loukogeorgakis and R. MacAllister

NEUROSCIENCE AND NEUROANAESTHESIA

- 592 Electroencephalographic slow wave dynamics and loss of behavioural responsiveness induced by ketamine in human volunteers
J. Sleigh, R. M. Pullon, P. E. Vlissides and C. E. Warnaby
- 601 Noble gas neuroprotection: xenon and argon protect against hypoxic-ischaemic injury in rat hippocampus *in vitro* via distinct mechanisms
M. Koziakova, K. Harris, C. J. Edge, N. P. Franks, I. L. White and R. Dickinson
- 610 Propranolol protects cerebral autoregulation and reduces hippocampal neuronal cell death through inhibition of interleukin-6 upregulation after traumatic brain injury in pigs
W. M. Armstead and M. S. Vavilala

PAEDIATRIC ANAESTHESIA

- 618 Impact of preoperative hyponatraemia on paediatric perioperative mortality
H. A. Benzon, A. Bobrowski, S. Suresh, N. R. Wasson and E. C. Cheon

PAIN

- 627 Preventing opioid prescription after major surgery: a scoping review of opioid-free analgesia
J. F. Fiore Jr., G. Olleik, C. El-Kefraoui, B. Verdolin, A. Kouyoumdjian, A. Alldrit, A. G. Figueiredo, S. Valanci, J. A. Marquez-GdeV, M. Schulz, D. Moldoveanu, P. Nguyen-Powanda, G. Best, A. Banks, T. Landry, N. Pecorelli, G. Baldini and L. S. Feldman

- 637 Pain regulation by gut microbiota: molecular mechanisms and therapeutic potential
R. Guo, L.-H. Chen, C. Xing and T. Liu
- 655 Trends in chronic opioid use and association with five-year survival in South Korea: a population-based cohort study
T. K. Oh, Y.-T. Jeon and J. W. Choi

QUALITY AND PATIENT SAFETY

- 664 Systematic review and consensus definitions for the Standardised Endpoints in Perioperative Medicine initiative: patient-centred outcomes
S. R. Moonesinghe, A. I. R. Jackson, O. Boney, N. Stevenson, M. T. V. Chan, T. M. Cook, M. Lane-Fall, C. Kalkman, M. D. Neuman, U. Nilsson, M. Shulman and P. S. Myles on behalf of the Standardised Endpoints in Perioperative Medicine-Core Outcome Measures in Perioperative and Anaesthetic Care (StEP-COMPAC) Group
- 671 Days alive and out of hospital after fast-track total hip and knee arthroplasty: an observational cohort study in 16 137 patients
C. C. Jørgensen, P. B. Petersen and H. Kehlet on behalf of the Lundbeck Foundation Center for Fast-track Hip and Knee Replacement Collaborative Group
- 679 Anaesthesia provider volume and perioperative outcomes in total joint arthroplasty surgery
S. G. Memtsoudis, L. A. Wilson, J. Bekeris, J. Liu, L. Poultsides, M. Fiasconaro and J. Poeran
- 688 Deep-learning model for predicting 30-day postoperative mortality
B. A. Fritz, Z. Cui, M. Zhang, Y. He, Y. Chen, A. Kronzer, A. Ben Abdallah, C. R. King and M. S. Avidan

RESPIRATION AND THE AIRWAY

- 696 Performance of emergency surgical front of neck airway access by head and neck surgeons, general surgeons, or anaesthetists: an *in situ* simulation study
P. Groom, L. Schofield, N. Hettiarachchi, S. Pickard, J. Brown, J. Sanders and B. Morton

CORRESPONDENCE

- e515 Reverse Takotsubo cardiomyopathy after intravenous glycopyrrolate administration postpartum
N. R. Haslam, N. George, G. Cubas, C. Trainer and A. S. Herrey
- e517 A pilot study of neural correlates of perioperative executive function associated with noncardiac surgery in the elderly
R. Mohanty, H. Lindroth, S. Twadell, V. A. Nair, V. Prabhakaran and R. D. Sanders
- e518 Response to 'Learning from death' (*Br J Anaesth* 2019;123: 12–14)
A. Meaklim
- e520 Improving awareness of chlorhexidine allergy by anaesthesiologists in China
L. Che, X. Li, X. H. Zhang, H. Gao, Y. L. Zhang and Y. G. Huang
- e521 Anaesthesiology in China. Response to *Br J Anaesth* 2019;123: 559–64
D. G. Lambert
- e522 Predictors of post-anaesthesiology residency research productivity: preliminary report
E. S. Haight, F. Chen, P. Tanaka, J. G. Brock-Utne, A. Macario, E. C. Sun and V. L. Tawfik

BOOK REVIEW

- 704 Spinal injection techniques
A. Macfarlane and P. Paisley

PUBLISHER'S NOTE

- 706 Publisher's note